

SM-47004

N70-35956

FACILITY FORM 602	(ACCESSION NUMBER)	(THRU)
	410	1
	(PAGES)	(CODE)
	CR-110075	31
	(NASA CR OR TMY OR AD NUMBER)	(CATEGORY)

SATURN S-IVB-501 STAGE FLIGHT EVALUATION REPORT

VOLUME I

APRIL 1968




SATURN S-IVB-501 STAGE
FLIGHT EVALUATION REPORT

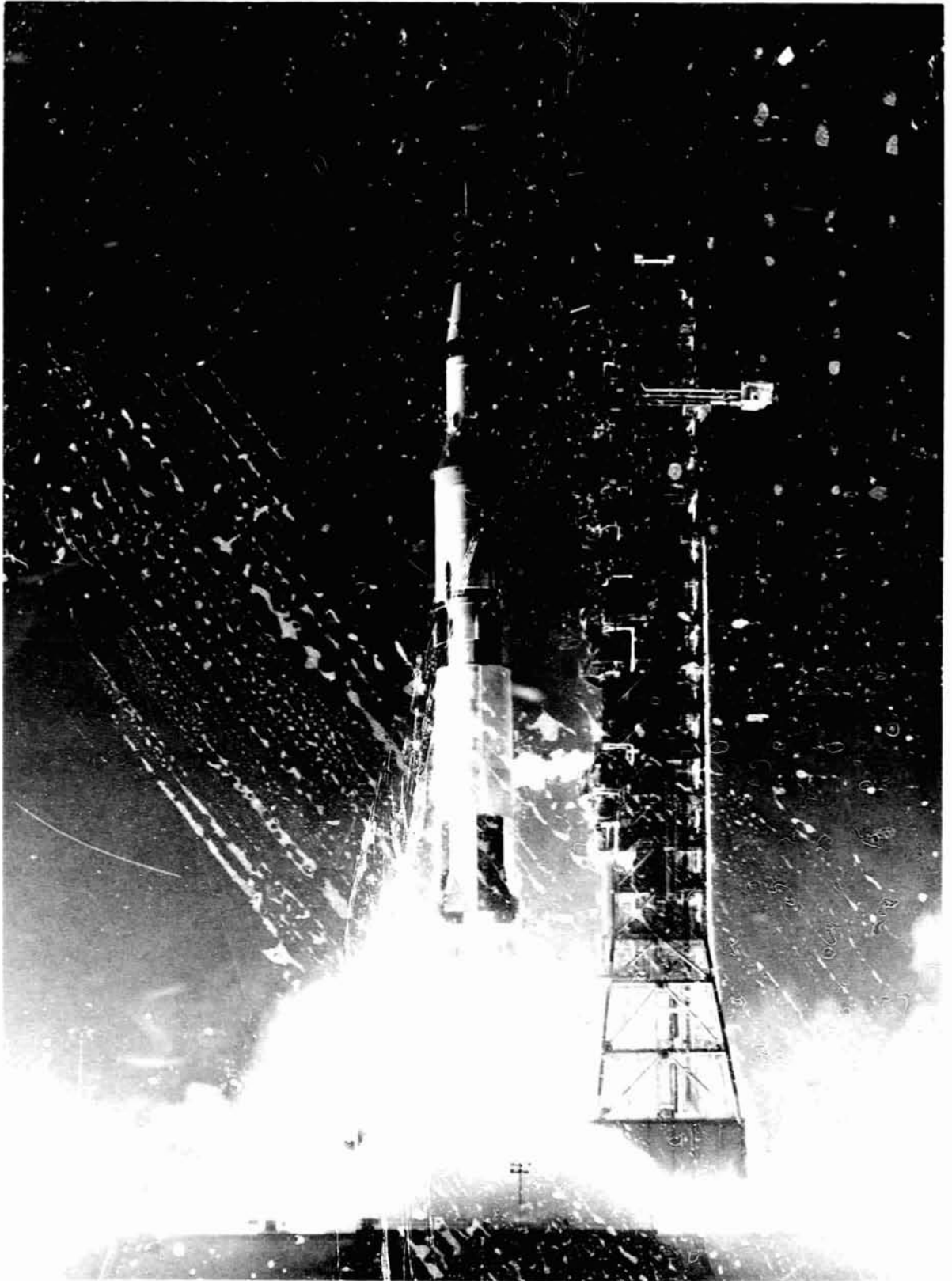
VOLUME I

DOUGLAS REPORT SM-47004
APRIL 1968

PREPARED BY:
SATURN S-IVB TEST PLANNING AND
EVALUATION COMMITTEE AND
COORDINATED BY: J. A. TORIAS
PROJECT OFFICE - FLIGHT TEST
SACRN DEVELOPMENT ENGINEERING

PREPARED FOR:
NATIONAL AERONAUTICS AND
SPACE ADMINISTRATION
UNDER NASA CONTRACT NAS7-107


APPROVED BY: A. P. O'NEAL
DIRECTOR, HUNTINGTON BEACH DEVELOPMENT/
ENGINEERING - SATURN/APOLLO PROGRAM



SATURN AS-501 VEHICLE LIFTOFF

ABSTRACT

This report, prepared in two volumes, presents the evaluation results of the prelaunch countdown, powered flight, and orbital phase of the S-IVB-501 stage which was launched on 9 November 1967 as the third stage of the Saturn AS-501 vehicle.

Volume I contains the first 15 sections of the report; Volume II contains the remaining 10 sections and 6 appendixes of the report.

All flight objectives were satisfied and the stage and ground support equipment functioned as anticipated.

The report is a contractual document as outlined in NASA Report MSFC-DRL-021, Contract Data Requirements, Saturn S-IVB Stage and GSE, dated 1 February 1968, Revision A. It was prepared by the Saturn S-IVB Test Planning and Evaluation Committee and coordinated by the Saturn S-IVB Project Office of the Douglas Aircraft Company, Missile and Space Systems Division.

DESCRIPTORS

data evaluation	S-IVB-501
flight test	Saturn AS-501 vehicle
Saturn V	countdown

PREFACE

The purpose of this report is to present the evaluation results of the prelaunch countdown, powered flight, and orbital phase of the S-IVB-501 stage which was launched on 9 November 1967 as the third stage of the Saturn AS-501 vehicle.

Volume I contains the first 15 sections of the report; Volume II contains the remaining 10 sections and 6 appendixes of the report.

This report was prepared in compliance with the National Aeronautics and Space Administration Contract NAS7-101, is published in accordance with NASA Report MSFC-DRL-021, Contract Data Requirements, Saturn S-IVB Stage and GSE, dated 1 February 1968, Revision A, which delineates the data required from the Douglas Aircraft Company.

This document was prepared by the Saturn S-IVB Test Planning and Evaluation Committee and coordinated by the Saturn S-IVB Project Office of the Douglas Aircraft Company, Missile and Space Systems Division.

PRECEDING PAGE BLANK NOT FILMED.
TABLE OF CONTENTS

<u>Section</u>		<u>Page</u>
1.	INTRODUCTION	1-1
2.	SUMMARY	2-1
	2.1 Countdown Operations	2-1
	2.2 Cost Plus Incentive Fee	2-1
	2.3 Trajectory	2-1
	2.4 Mass Characteristics	2-2
	2.5 Engine System	2-2
	2.6 Solid Rockets	2-2
	2.7 Oxidizer System	2-2
	2.8 Fuel System	2-3
	2.9 Auxiliary Propulsion System	2-3
	2.10 Pneumatic Control and Purge	2-3
	2.11 Propellant Utilization	2-3
	2.12 S-II/S-IVB Separation Dynamics	2-4
	2.13 Data Acquisition System	2-4
	2.14 Electrical System	2-5
	2.15 Range Safety System	2-5
	2.16 Flight Control	2-5
	2.17 Hydraulic System	2-6
	2.18 Stage Structure and Environment	2-7
	2.19 Forward Skirt Thermoconditioning System	2-7
	2.20 Acoustic and Vibration Environment	2-7
	2.21 Aero/Thermodynamic	2-8
3.	TEST CONFIGURATION	3-1
	3.1 Stage Configuration	3-1
	3.2 Stage Modifications	3-4
	3.3 Ground Support Equipment Modifications	3-12
4.	SEQUENCE OF EVENTS	4-1
	4.1 Predicted and Monitored Times	4-1
	4.2 Time Bases	4-2
	4.3 Ground Commands	4-3
	4.4 Ground Sequence of Events	4-3
5.	COUNTDOWN OPERATIONS	5-1
	5.1 Propulsion System Checkouts	5-1
	5.2 Launch Vehicle Tests	5-1
	5.3 APS Preparations	5-3
	5.4 Launch Countdown	5-5
	5.5 Environmental Control Systems	5-8
	5.6 Redline Limits	5-9
	5.7 Countdown Problems	5-10
	5.8 Atmospheric Conditions	5-11

Table of Contents

TABLE OF CONTENTS (Continued)

<u>Section</u>		<u>Page</u>
6.	COST PLUS INCENTIVE FEE	6-1
6.1	Flight Mission Accomplishment	6-1
6.2	Telemetry Performance	6-1
7.	TRAJECTORY	7-1
7.1	Comparison Between Actual and Preflight Predicted Trajectories	7-1
7.2	Postflight Predicted Trajectory Evaluation	7-3
7.3	Analysis of Special Areas of Concern	7-10
8.	MASS CHARACTERISTICS	8-1
8.1	Mass Characteristics Summary	8-1
8.2	Mass Properties Dispersion Analysis	8-1
8.3	Third Flight Stage Best Estimate Ignition and Cutoff Masses	8-1
9.	ENGINE SYSTEM	9-1
9.1	Engine Chillydown and Conditioning	9-2
9.2	Start Sphere Performance	9-4
9.3	Engine Control Sphere Performance	9-7
9.4	Engine Performance	9-10
9.5	Component Operation	9-20
9.6	Engine Sequencing	9-23
9.7	Flight Simulation Analysis	9-23
10.	SOLID ROCKET PERFORMANCE	10-1
10.1	Retrorockets	10-1
10.2	Ullage Rockets	10-1
11.	OXIDIZER SYSTEM	11-1
11.1	Pressurization Control	11-1
11.2	Pressurization System Conditions During Orbit	11-4
11.3	LOX Pump Chillydown	11-10
11.4	Engine LOX Supply	11-12
12.	FUEL SYSTEM	12-1
12.1	Pressurization Control	12-1
12.2	Pressurization System Conditions During Orbit	12-4
12.3	LH2 Pump Chillydown	12-7
12.4	Engine LH2 Supply	12-12
13.	AUXILIARY PROPULSION SYSTEM	13-1
13.1	APS Flight Operation	13-1
13.2	APS Module No. 1	13-2
13.3	APS Module No. 2	13-4
13.4	Engine Performance	13-6

TABLE OF CONTENTS (Continued)

<u>Section</u>		<u>Page</u>
14.	PNEUMATIC CONTROL AND PURGE SYSTEM	14-1
	14.1 Ambient Helium Supply	14-1
	14.2 Pneumatic System Leakage	14-2
15.	PROPELLANT UTILIZATION	15-1
	15.1 PU System Calibration	15-2
	15.2 Propellant Mass History	15-3
	15.3 PU System Response	15-10
	15.4 PU System Induced Thrust Variations	15-17

For sections 16 through 26 and appendixes 1 through 6 of this report, see table of contents in Volume II.

LIST OF TABLES

<u>Table</u>		
3-1	S-IVB-501 Stage and GSE Flight Orifices	3-14
3-2	Pressure Switch Checkout Data	3-16
4-1	Flight Sequence of Events	4-4
4-2	Ground Sequence of Events	4-47
5-1	Launch Vehicle Tests	5-12
5-2	APS Loading Data	5-13
5-3	S-IVB Stage Propellant Loading Data	5-14
5-4	Sphere Pressurization Data	5-15
6-1	Mission Accomplishment (PCF)	6-2
6-2	Mission Accomplishment (ECF)	6-3
6-3	Flight Telemetry Performance Summary	6-4
7-1	Trajectory Conditions at Significant Event Times	7-11
8-1	Mass Summary	8-4
8-2	Best Estimate Program Input Values	8-5
9-1	Control Sphere	9-25
9-2	Engine Control Sphere Temperature Data	9-25
9-3	Engine Control Sphere Helium Mass Summary	9-26
9-4	Fuel Lead Conditions	9-26
9-5	Comparison of Computer Programs Results	9-27
9-6	Data Inputs to Computer Programs	9-28
9-7	J-2 Engine Start Transients	9-28
9-8	J-2 Engine Steady-State Performance	9-29
9-9	Engine Performance Prediction	9-30
9-10	Thrust Oscillation Summary	9-31
9-11	J-2 Engine Cutoff Transients	9-31
9-12	501 Flight Engine Sequence - First Burn	9-32

Table of Contents

LIST OF TABLES (Continued)

<u>Table</u>		<u>Page</u>
9-13	J-2 Flight Engine Sequence - Second Burn	9-34
10-1	Retrorocket Performance	10-3
10-2	Ullage Rocket Performance	10-4
11-1	LOX Tank Prepressurization Data	11-15
11-2	LOX Tank Pressurization Data	11-16
11-3	Cold Helium Supply Data	11-17
11-4	J-2 Heat Exchanger Performance Data	11-18
11-5	LOX Chilldown System Performance Data	11-19
11-6	LOX Pump Inlet Condition Data	11-20
12-1	LH2 Tank Prepressurization Data	12-14
12-2	LH2 Tank Pressurization Data	12-15
12-3	LH2 Tank Repressurization Data	12-16
12-4	LH2 Chilldown System Performance Data	12-17
12-5	LH2 Pump Inlet Condition Data	12-18
13-1	APS Propellant Usage During Flight	13-13
13-2	AS-501/S-IVB Auxiliary Propulsion System (Yaw/Roll) Engine Thrust Characteristics	13-14
14-1	Pneumatic Control and Purge System Data	14-5
15-1	Propellant Mass History	15-20
15-2	Propellant Loading Summary	15-21
15-3	Level Sensor and Volumetric PU Mass	15-22
15-4	Propellant Residuals Summary	15-23
15-5	Thrust Variations	15-24

For sections 16 through 26 and appendixes 1 through 6 of this report, see table of contents in Volume II.

LIST OF ILLUSTRATIONS

<u>Figure</u>		
3-1	Propulsion System and Instrumentation	3-17
3-2	Propulsion Major Components Locations	3-19
3-3	Facility Propellant and Pneumatic Loading Systems	3-20
5-1	GSE Performance During Engine Start Sphere Chilldown and Loading - First Burn	5-16
5-2	GSE Performance During Engine Control Sphere Loading - First Burn	5-17
5-3	GSE Performance During LOX and LH2 Prepressurization - First Burn	5-18
5-4	GSE Performance During Thrust Chamber Chilldown - First Burn	5-19
7-1	S-IC/S-II Stage Flight Altitude History	7-14
7-2	S-IC/S-II Stage Flight Range History	7-14
7-3	S-IC/S-II Stage Flight Crossrange Position History	7-15
7-4	S-IC/S-II Stage Flight Crossrange Velocity History	7-15

LIST OF ILLUSTRATIONS (Continued)

<u>Figure</u>		<u>Page</u>
7-5	S-IC/S-II Stage Flight Inertial Velocity History	7-16
7-6	S-IC/S-II Stage Flight Axial Acceleration History	7-16
7-7	S-IC/S-II Stage Inertial Flight Path Elevation Angle History	7-17
7-8	S-IC/S-II Stage Inertial Flight Path Azimuth Angle History	7-17
7-9	S-IC/S-II Stage Flight Dynamic Pressure History	7-18
7-10	S-IC Stage Flight Angles of Attack	7-18
7-11	S-IVB Stage Flight Altitude History - First Burn	7-19
7-12	S-IVB Stage Flight Range History - First Burn	7-19
7-13	S-IVB Stage Flight Crossrange Position History - First Burn	7-20
7-14	S-IVB Stage Flight Crossrange Velocity History - First Burn	7-20
7-15	S-IVB Stage Flight Inertial Velocity History - First Burn	7-21
7-16	S-IVB Stage Flight Axial Acceleration History - First Burn	7-21
7-17	S-IVB Stage Inertial Flight Path Elevation Angle History - First Burn	7-22
7-18	S-IVB Stage Inertial Flight Path Azimuth Angle History - First Burn	7-22
7-19	S-I*/S-IVB Stage Pitch Attitude Angles - First Burn	7-23
7-20	S-II/S-IVB Stage Yaw Attitude Angles - First Burn	7-23
7-21	S-II/S-IVB Stage Roll Attitude Angles - First Burn	7-24
7-22	Parking Orbit Attitude History	7-24
7-23	Parking Orbit Inertial Velocity History	7-25
7-24	Parking Orbit Inertial Flight Path Elevation Angle History	7-25
7-25	Parking Orbit Inertial Flight Path Azimuth Angle History	7-26
7-26	S-IVB Stage Flight Altitude History - Second Burn	7-26
7-27	S-IVB Stage Flight Ground Range History - Second Burn	7-27
7-28	S-IVB Stage Flight Crossrange Position History - Second Burn	7-27
7-29	S-IVB Stage Flight Crossrange Velocity History - Second Burn	7-28
7-30	S-IVB Stage Flight Inertial Velocity History - Second Burn	7-29
7-31	S-IVB Stage Flight Axial Acceleration History - Second Burn	7-29
7-32	S-IVB Stage Inertial Flight Path Elevation Angle History - Second Burn	7-30
7-33	S-IVB Stage Inertial Flight Path Azimuth Angle History - Second Burn	7-30
7-34	S-IVB Stage Pitch Attitude Angles - Second Burn	7-31
7-35	S-IVB Stage Yaw Attitude Angles - Second Burn	7-31
7-36	S-IVB Stage Roll Attitude Angles - Second Burn	7-32
7-37	Comparison of Actual and Postflight Predicted Attitude	7-32
7-38	Comparison of Actual and Postflight Predicted Ground Range	7-33
7-39	Comparison of Actual and Postflight Predicted Inertial Velocity	7-33
7-40	Comparison of Actual and Postflight Predicted Earth-Fixed Crossrange Velocity	7-34
7-41	First Burn Trajectory Reconstruction Simulation Deviations from Observed Mass Point Trajectory	7-34
7-42	Second Burn Trajectory Reconstruction Simulation Deviations from Observed Mass Point Trajectory	7-35

Table of Contents

LIST OF ILLUSTRATIONS (Continued)

<u>Figure</u>		<u>Page</u>
7-43	Flight Simulated First Burn Engine Steady-State Performance	7-36
7-44	Flight Simulated Second Burn Engine Steady-State Performance	7-36
7-45	AS-501 Parking Orbit Actual and Predicted Continuous Vent System Thrust	7-37
7-46	AS-501 Parking Orbit Difference Between Actual and Simulated Orbit Attitude	7-37
7-47	Iterative Guidance Response to Second Burn Thrust Profile	7-38
8-1	Third Flight Stage Vehicle Mass - First Burn	8-6
8-2	Third Flight Stage Vehicle Mass - Second Burn	8-6
8-3	Third Flight Stage Vehicle Horizontal Center of Gravity - First Burn	8-7
8-4	Third Flight Stage Vehicle Horizontal Center of Gravity - Second Burn	8-7
8-5	Third Flight Stage Vehicle Roll Moment of Inertia - First Burn	8-8
8-6	Third Flight Stage Vehicle Roll Moment of Inertia - Second Burn	8-8
8-7	Third Flight Stage Vehicle Pitch Moment of Inertia - First Burn	8-9
8-8	Third Flight Stage Vehicle Pitch Moment of Inertia - Second Burn	8-9
8-9	Third Flight Stage Final Best Estimate Masses - First Burn	8-10
8-10	Third Flight Stage Final Best Estimate Masses - Second Burn	8-10
9-1	J-2 Engine System and Instrumentation	9-36
9-2	Oxidizer Pump Discharge Pressure Versus Temperature	9-37
9-3	Propellant Inlet Operation Requirements for Engine Using Restartable Ignition Detector Probe	9-37
9-4	Fuel Lead - First Engine Start	9-38
9-5	Fuel Lead - Second Engine Start	9-39
9-6	GH2 Start Sphere Critical Limits at Liftoff	9-40
9-7	Engine Start and Control Sphere Performance - First Burn	9-41
9-8	Start Sphere Refill Performance - First Burn	9-42
9-9	Start Sphere Refill - Second Burn	9-43
9-10	Start Tank Recharge Capability	9-44
9-11	Start Sphere Orbital Conditions	9-45
9-12	Engine Start and Control Sphere Performance During Second Burn	9-46
9-13	Start Sphere Refill Performance - Second Burn	9-47
9-14	Engine Start Sequence - First Burn	9-48
9-15	Engine Start Sequence - Second Burn	9-49
9-16	Engine Control Sphere Pressure History	9-50
9-17	Engine Control Sphere Conditions	9-51
9-18	Engine Control Sphere Temperature During Orbital Coast	9-51
9-19	Start Transient Thrust Profiles	9-52
9-20	Total S-IVB Axial Thrust	9-52
9-21	Engine Start Transient Characteristics - First Burn	9-53
9-22	Engine Start Transient Characteristics - Second Burn	9-53
9-23	Flowrate and Pump Speed During First Burn Start Transient	9-54

LIST OF ILLUSTRATIONS (Continued)

<u>Figure</u>		<u>Page</u>
9-24	Flowrate and Pump Speed During Second Burn Start Transient	9-54
9-25	J-2 Engine Chamber Pressure - First Burn	9-55
9-26	PU Valve Operation - First Burn	9-55
9-27	J-2 Engine Pump Flowrates - First Burn	9-56
9-28	J-2 Engine Pump Operating Characteristics - First Burn	9-56
9-29	J-2 Engine Injector Supply Conditions - First Burn	9-57
9-30	Turbine Inlet Operating Conditions - First Burn	9-57
9-31	J-2 Engine Chamber Pressure - Second Burn	9-58
9-32	PU Valve Operation - Second Burn	9-58
9-33	J-2 Engine Pump Flowrates - Second Burn	9-59
9-34	J-2 Engine Pump Operating Conditions - Second Burn	9-59
9-35	J-2 Engine Injector Supply Conditions - Second Burn	9-60
9-36	Turbine Inlet Operating Conditions - Second Burn	9-60
9-37	Engine Tag Values at Standard Altitude Conditions	9-61
9-38	Specific Impulse Versus Engine Mixture Ratio	9-63
9-39	Thrust and Specific Impulse Characteristics at Standard Altitude Conditions	9-64
9-40	Engine Steady-State Performance - First Burn	9-64
9-41	Thrust Variation - First Burn	9-66
9-42	Engine Steady-State Performance - Second Burn	9-67
9-43	Expanded Pre-cutoff data - Measured	9-68
9-44	Expanded Pre-cutoff Data - Calculated	9-69
9-45	Change in Velocity due to Tailoff Impulse - First Burn	9-69
9-46	Change in Velocity due to Tailoff Impulse - Second Burn	9-70
9-47	Engine Cutoff Transient Characteristics - First Burn	9-70
9-48	Engine Cutoff Transient Characteristics - Second Burn	9-71
9-49	Cutoff Transient Thrust Profiles	9-71
9-50	Main Oxidizer Valve Position - First Burn	9-72
9-51	Main Oxidizer Valve Position - Second Burn	9-73
9-52	LH2 Pump Performance During Engine Start	9-73
9-53	Gas Generator Performance - First Burn	9-74
9-54	Gas Generator Performance - Second Burn	9-74
10-1	Retrorocket Performance	10-5
10-2	Ullage Rocket Performance	10-5
11-1	LOX Tank Pressurization System	11-21
11-2	LOX Tank Conditions During Prepressurization and Boost - First Burn	11-22
11-3	LOX Tank Pressurization System Performance - First Burn	11-23
11-4	Cold Helium Supply - First Burn	11-24
11-5	J-2 Heat Exchanger Performance - First Burn	11-25
11-6	LOX Tank Conditions During Repressurization Period - Second Burn	11-26
11-7	LOX Tank Pressurization System Performance - Second Burn	11-27
11-8	Cold Helium Supply - Second Burn	11-28

Table of Contents

LIST OF ILLUSTRATIONS (Continued)

<u>Figure</u>		<u>Page</u>
11-9	J-2 Heat Exchanger Performance - Second Burn	11-29
11-10	LOX Tank Temperatures During First and Second Orbits	11-30
11-11	LOX Tank Ullage Pressure During First and Second Orbits	11-31
11-12	LOX Tank Ullage Pressure During Third Orbit	11-32
11-13	LOX Tank Temperatures During Third Orbit	11-33
11-14	Cold Helium Sphere Conditions During Orbit	11-34
11-15	LOX Pump Chilldown System Performance - First Burn	11-35
11-16	LOX Pump Chilldown System Operation - First Burn	11-36
11-17	LOX Pump Chilldown System Performance - Second Burn	11-37
11-18	LOX Pump Chilldown System Operation - Second Burn	11-38
11-19	LOX Chilldown Pump Differential Pressure and Flowrate - Second Burn	11-39
11-20	LOX System Schematic	11-40
11-21	LOX Pump Inlet Conditions During Firing - First Burn	11-41
11-22	LOX Pump Interface Conditions During Firing - First Burn	11-42
11-23	Effect of LOX Mass Level on LOX Pump Inlet Temperature	11-43
11-24	LOX Pump Inlet Conditions During Firing - Second Burn	11-44
11-25	LOX Pump Interface Conditions During Firing - Second Burn	11-45
12-1	LH2 Tank Pressurization System	12-19
12-2	LH2 Tank Pre-pressurization System Performance	12-20
12-3	LH2 Tank Pressurization System Performance - First Burn	12-21
12-4	LH2 Tank Repressurization System Performance - Second Burn	12-22
12-5	LH2 Tank Pressurization System Performance - Second Burn	12-23
12-6	LH2 Tank Continuous Vent System Operation During Restart and Second Burn	12-24
12-7	LH2 Tank Continuous Vent System Operation During Orbital Coast	12-25
12-8	LH2 Tank Continuous Vent System Performance During Orbital Coast	12-26
12-9	LH2 Pump Chilldown Characteristics - First Burn	12-27
12-10	LH2 Pump Chilldown - First Burn	12-28
12-11	LH2 Pump Chilldown Characteristics - Second Burn	12-29
12-12	LH2 Pump Chilldown - Second Burn	12-30
12-13	S-IVB-501/201 LH2 Orbital Chilldown Comparison - Second Burn	12-31
12-14	S-IVB-501/202 Heat Input Rate	12-32
12-15	S-IVB-501/203 Mass of LH2 Entering Chilldown System	12-33
12-16	LH2 Supply System	12-34
12-17	LH2 Pump Inlet Conditions - First Burn	12-35
12-18	LH2 Pump Inlet Conditions During Firing - First Burn	12-36
12-19	Effect of LH2 Mass Level on LH2 Pump Inlet Temperature	12-37
12-20	LH2 Pump Inlet Conditions - Second Burn	12-38
12-21	LH2 Pump Inlet Conditions During Firing - Second Burn	12-39
13-1	Auxiliary Propulsion System and Instrumentation	13-15
13-2	Helium Bottle Conditions	13-16

LIST OF ILLUSTRATIONS (Continued)

<u>Figure</u>		<u>Page</u>
13-3	APS Propellant Conditions	13-17
13-4	Module 1 Engine Anomaly Correlation	13-18
13-5	APS Thrust	13-19
13-6	Chamber Pressure Anomalies	13-20
13-7	APS Total Impulse per Pulse	13-21
14-1	Pneumatic Control and Purge System	14-7
14-2	Pneumatic Control and Purge System Performance During Boost and First Burn	14-8
14-3	Pneumatic Control System Conditions During Orbital Coast	14-8
14-4	Pneumatic Control and Purge System Performance - Second Burn	14-9
14-5	Pneumatic Control and Purge System Performance During Third Orbit	14-9
14-6	Control Helium Pressure Transient Response Characteristics	14-10
14-7	Clary Actuation Control Module	14-10
15-1	Total Tank-to-Sensor Correction for Indicated Flight Mass	15-25
15-2	PU Mass Sensor Corrections Due to Center-of-Gravity Offset	15-26
15-3	PU Mass Sensor Correction Due to Tank Deflection	15-27
15-4	Propellant Intank Bulk Temperature Histories	15-28
15-5	Propellant Intank Bulk Density Histories	15-29
15-6	Comparison of Level Sensor and Volumetric PU Mass at Level Sensor Activation	15-30
15-7	PU Valve Position History	15-31
15-8	PU System Deviation Effects on Second Burn PU Valve History	15-32
15-9	Total PU System Tank-to-Sensor Nonlinearities Normalized to Flight Consumed Mass	15-33
15-10	Volumetric Tank-to-Sensor Nonlinearities Normalized to Flight Consumed Mass	15-34
15-11	Capillary Effects on Mass Sensor Signal Prior to Second Burn	15-35
15-12	PU Indicated Fine Mass Data Following Second Engine Start Command	15-36
15-13	Effect of Capillary Action on PU Valve Position History	15-36
15-14	Propellant Utilization System Error Signal	15-37
15-15	Thrust Variations	15-38
15-16	Engine Response to PU Valve Positions	15-39

For sections 16 through 26 and appendixes 1 through 6 of this report, see table of contents in Volume II.

1. INTRODUCTION

1.1 General

This report presents the results of analyses that were performed by Douglas personnel on the countdown, launch, and flight of the Saturn S-IVB-501 stage.

Also described are tests conducted at Kennedy Space Center (KSC), and pertinent modifications made to the S-IVB stage and related ground support equipment.

This report is authorized by NASA Contract NAS7-101 and is the final report on the S-IVB-501 stage by the Douglas S-IVB Test Planning and Evaluation Committee of the Missile and Space Systems Division (MSSD), Huntington Beach, California.

1.2 History

The S-IVB-501 stage was assembled and its systems were checked out at MSSD before it was shipped to the Sacramento Test Center (STC) on 11 March 1966. It arrived there on 15 March 1966. Following preliminary tests, which consisted of manual and automatic subsystem checkouts, integrated system tests, a simulated acceptance firing, and an automatic propellant loading test, it underwent a successful acceptance firing 26 May 1966. The acceptance firing consisted of a first burn, a simulated coast period and a second burn. Its two auxiliary propulsion system (APS) modules, shipped from the Douglas Santa Monica facility, were confidence fired at the STC Gamma Complex on 6 and 13 May 1966.

During these tests, all stage and APS module test objectives presented in Douglas Report No. SM-47377, Saturn S-IVB-501 Stage Acceptance Firing Test Plan were satisfactorily completed and the integrity of the stage and its systems was verified.

On 12 August 1966 the stage was shipped to KSC. It arrived there on 14 August 1966 and was installed in the low bay of the vehicle assembly building and subjected to post transportation receiving inspections.

Section 1
Introduction

After installation of the aft interstage, the stage was transferred to the high bay and mated to the AS-501 space vehicle. The AS-501 space vehicle was transferred to Launch Complex 39A on 26 August 1967 and successfully launched 9 November 1967. After successfully completing its mission objectives, the stage re-entered the earth's atmosphere and splashed down in the Pacific Ocean. No recovery was planned.

2. SUMMARY

The AS-501 space vehicle was launched at 1200:01 GMT from Launch Complex 39A on 9 November 1967. The overall performance of the S-IVB-501 stage was satisfactory during all phases of the countdown and flight.

2.1 Countdown Operations

The AS-501 launch countdown was nearly flawless and was conducted with no holds other than those that were built into the countdown program. No significant S-IVB stage or equipment problems occurred during the countdown activity, and Douglas ground support equipment (GSE) sustained no significant damage during liftoff.

2.2 Cost Plus Incentive Fee

The incentive evaluation of the S-IVB-501 flight performance includes flight mission accomplishment and telemetry performance. Performance of the S-IC and S-II stages provided preconditions of flight at S-II/S-IVB Separation Command that were within allowable tolerances. Trajectory end conditions of flight at waiting orbit insertion were within tolerance. All flight values of attitude errors and rates were within allowable tolerances, all received command signals were recognized and all end condition command signals were given. It was concluded for purposes of incentive achievement, therefore, that all PCF and ECF were achieved. The telemetry system operated at 99.1 percent efficiency during the telemetry performance evaluation period (TPEP) phase I and 97.6 percent efficiency during the TPEP phase II.

2.3 Trajectory

The actual trajectory of the AS-501 flight was close to that predicted. At S-II/S-IVB separation the trajectory was characterized as slow, high, long, and south of the intended path. This slower than predicted velocity was the primary cause of a longer than predicted S-IVB stage first burn. The first burn trajectory can be summarized as slow, high and long.

Section 2 Summary

The parking orbit phase of the flight was very close to that predicted. At S-IVB restart the actual trajectory was slower, higher and further downrange than predicted. S-IVB second burn engine cutoff occurred 13.83 sec earlier than predicted. This early cutoff was mainly caused by a late propellant mixture ratio shift and corresponding high S-IVB thrust early in flight which in turn caused a higher than predicted velocity and acceleration. At second burn engine cutoff conditions were fast, low, and short but almost on the desired orbit.

2.4 Mass Characteristics

At first burn ignition, the mass of the 501 stage was 353,145 \pm 460 lbm. This was within 148 lbm of the data presented at liftoff +1 day using the propellant utilization volumetric system. Cutoff mass was 279,038 \pm 404 lbm. At second burn ignition, the mass was 275,730 \pm 433 lbm, and the cutoff mass was 136,365 \pm 280 lbm.

2.5 Engine System

The engine system performance of the S-IVB was satisfactory during both burns of the AS-501 mission. The thrust chamber condition was not as required for the first burn start but did not adversely affect engine operation. Several performance shifts were noted during the second burn which exceeded the contractor end item specification for engine mixture ratio but did not handicap the ability of the engine to complete the mission. The modifications made to guarantee a reliable second start were successful and there was no evidence of over heating in the gas generator and turbine system.

2.6 Solid Rockets

The solid rocket motors on the S-II and S-IVB stages performed satisfactorily and accomplished their intended purpose. The S-II was separated from the S-IVB stage by the retrorockets, and the S-IVB propellants were settled prior to engine ignition by the ullage rockets.

2.7 Oxidizer System

The oxidizer system performed adequately, supplying LOX to the engine

pump inlet within the specified operating limits throughout both periods of J-2 engine operation. The available NPSP at the LOX pump inlet exceeded the engine manufacturer's minimum requirement at all times.

2.8 Fuel System

The fuel system supplied LH2 to the engine, as designed, with the available NPSP exceeding the engine manufacturer's requirements throughout both burns except at second burn engine start command.

2.9 Auxiliary Propulsion System

The two APS modules operated adequately to fulfill the attitude control, maneuvering, and ullaging requirements of the mission. The chamber pressure data indicated low performance of the roll/yaw engines of module 1. Engine 1-1 chamber pressure exhibited abnormal oscillations during one portion of the mission, and engine 1-3 chamber pressure indicated a significant loss of performance near the end of the mission. The ullage engine of module 1 exhibited an excessively long chamber pressure decay at the termination of both ullage engine firings. The performance of module 2 was as expected.

2.10 Pneumatic Control and Purge System

The pneumatic control and purge system performed satisfactorily throughout the flight. The helium supply was adequate to complete the mission requirements and to accomplish all purges, although a system leak developed during orbital coast and eventually depleted the pneumatic supply during the third orbit. Since the pneumatic operations were complete long before this depletion, the mission was not affected.

2.11 Propellant Utilization

The propellant utilization system successfully accomplished the requirements associated with propellant loading and management during burn. The best estimate propellant mass values at liftoff were 194,395 lbm LOX and 41,173 lbm LH2 as compared to desired mass values or 193,273 lbm LOX and 41,222 lbm LH2. These values were well within

Section 2
Summary

required loading accuracies. The best estimate third flight stage liftoff mass was 353,011 lbm.

Extrapolation of propellant residuals to depletion indicated that a LOX depletion would have occurred approximately 38 sec after second burn velocity cutoff with a usable LH2 residual of 154 lbm. This yielded a PU efficiency of 99.93 percent.

S-IVB-501 is the first flight evaluation in which the volumetric mass analysis has been employed.

2.12 S-II/S-IVB Separation Dynamics

S-II/S-IVB separation was accomplished satisfactorily within the desired period.

Separation was initiated at R0 +520.528 sec; it was completed 1.044 sec later.

Small S-II and S-IVB angular velocities and lateral accelerations utilized 1.9 in. of the available 83 in. of lateral clearance. S-II pitch, yaw, and roll rates remained between 0.0 and -0.7 deg/sec, and the S-IVB rotational rates remained between 0.0 and -0.2 deg/sec during stage separation.

2.13 Data Acquisition System

Data acquisition system performance during the mission was excellent and there were no malfunctions.

System performance is summarized as follows:

Measurements assigned	592
Measurements monitored by S-II	4
Measurements inoperative due to stage configuration	1
Checkout measurements	11
Measurements deleted prior to flight	1

Measurements active for flight	575
Phase I (launch) measurement failures	5
Phase I measurement efficiency	99.1%
Phase II (restart) measurement failure	11
Phase II measurement efficiency	97.0%

During S-IC/S-II separation flame attenuation caused a 1 sec RF blackout, however, no blackout occurred at S-II/S-IVB separation.

Tape recorder performance was very good. It recorded all analog data on fast record, PCM data on slow record, and played it back on command.

2.14 Electrical System

The electrical control system and the electrical power system performed satisfactorily. All responses to switch selector commands were satisfactory. All event measurements verified that the engine control system had responded properly to the Engine Start and Engine Cutoff Commands for both burns. A review of the event and pressure measurements verified that each control pressure switch functioned properly. The APS electrical control system performed within prescribed limitations. All batteries performed within expected limits. The chilldown inverters performed satisfactorily for both engine ignitions. Both 5 v excitation modules performed satisfactorily. The static inverter-converter operated within design limits throughout the flight.

2.15 Range Safety System

The range safety system was not required for propellant dispersion during the flight. All indications were that the system was operating properly and would have properly executed its function had it been called upon to do so.

2.16 Flight Control

The thrust vector control system responded satisfactorily to instrument unit attitude command signals and provided pitch and yaw control during both first and second burn periods. Transients during S-II/S-IVB

Section 2 Summary

separation, J-2 engine restart, and guidance mode changes were within the capabilities of the control system. Body bending did not noticeably affect the control system during first and second burn periods.

The auxiliary attitude control system provided satisfactory roll stabilization during first and second burns; also, satisfactory pitch, yaw, and roll control during orbit. All orbital maneuvers were accomplished as planned and vehicle attitude control was verified until R0 +6 hr 57 min 3 sec.

LH2 and LOX propellant sloshings were well damped during S-IC, S-II, and S-IVB burn periods. Sloshing during second burn appeared normal, however, amplitudes (particularly LOX) increased after large guidance commands beginning at R0 +11,570 sec. This increased slosh activity is reasonable considering the change in vehicle attitude. Sloshing did not appreciably affect the attitude control system during powered flight.

At orbital injection, the pitch down maneuver caused slosh waves in the LOX and LH2 tanks. LH2 slosh resembled that of S-IVB-203.

During parking orbit coast, a vapor bubble existed in the bottom of the LOX tank. During restart maneuvers, LOX sensors could not indicate sloshing because capillary action caused them to read liquid all the time.

There was no significant LH2 slosh during parking orbit coast; however, a large wave arose when the attitude realignment maneuver and LH2 repressurization occurred. It is doubtful that this wave could have reached the pressurization diffuser and caused the low rate of pressurization that occurred at this time, but it could have contributed to an undesirable pressure decay that happened late in the repressurization cycle.

2.17 Hydraulic System

The S-IVB hydraulic system performance was within predicted limits and the entire system operated satisfactorily throughout flight. All redlines were met prior to liftoff. There were no orbital thermal cycles and there was no loss of system fluid due to overboard venting as a result of reservoir fluid thermal expansion. System internal leakage was 0.67 gpm which is well within the 0.4 to 0.8 gpm allowable.

2.18 Stage Structure and Environment

Strain, acceleration, pressure, and temperature data indicated that adequate structural strength existed in the stage for the conditions encountered. Body bending moments and skin differential pressures were less than the maximum predicted values due to moderate winds. Vehicle axial accelerations were close to predicted values. Axial loads are in agreement with computed loads from liftoff to approximately R0 +70 sec. Beyond this time, the axial load values computed from stringer strain gage data appear to be low apparently because of aerodynamic heating and because of a partial integration resulting from the limited number of instrumented stringers. Axial strains in the aft skirt stringers were less than the maximum predicted strains for the strain gages mounted on the sides and tops of the stringers. Flight temperatures did not exceed maximum predicted temperatures. Propellant tank pressures did not exceed designed pressures. Differential pressures on the common bulkhead were as expected. Internal common bulkhead pressure remained substantially constant at less than 1 psia as predicted.

2.19 Forward Skirt Thermoconditioning System

The thermoconditioning system operated normally during flight. All temperatures, pressures, and flow were within design limits.

Coolant inlet temperature was 59 deg F at liftoff and 58.5 deg F near the end of first burn. Coolant exit temperatures varied between 58.5 and 61 deg F from range zero to R0 +700 sec. During second burn the inlet temperature was approximately constant at 58.8 deg F and the outlet temperature was constant at 58 deg F. A system ΔP of 15.5 psid was maintained during first and second burns. The flowrate remained constant at approximately 3.15 gpm.

2.20 Acoustic and Vibration Environment

A total of 42 acoustic and vibration measurements were monitored on the S-IVB-501 stage. All provided usable data. In general, the acoustic and vibration overall composite levels were lower at launch and higher during

Section 2 Summary

mach 1/max q periods than those for the Saturn IB flights. Vibration amplitudes on the S-IVB stage were negligible during S-II powered flight. During S-IVB powered flight the J-2 engine vibration levels were similar to those measured during acceptance firing; and the levels at other measurement locations were negligible during this period.

2.21 Aero/Thermodynamics

The S-IVB-501 stage was instrumented to obtain aerodynamic pressure data, structural temperatures, propellant heating, APS component temperatures and selected component temperatures in the forward and aft skirts. All data were within design limits and all of the test objectives were satisfied.

Pressure data obtained for the forward skirt, aft skirt, and aft inter-stage show reasonable agreement with wind tunnel data. Structural temperatures were well below design maximums as would be expected from the relatively cool flight trajectory. The APS and forward and aft skirt component temperatures were slightly higher than on S-IVB-203. There were no anomalies and no anticipated impact on design as a result of the aerodynamic and thermodynamic data evaluation.

3. TEST CONFIGURATION

This section briefly describes the configuration of the S-IVB-501 flight stage and presents pertinent stage and ground support equipment modifications. Details of specific system modifications are discussed in the appropriate sections of this report.

3.1 Stage Configuration

The general configuration of the S-IVB-501 stage is described in Douglas Report No. SM-46998B, S-IVB-501 Stage Flight Test Plan, dated 2 November 1967, and additional stage information may be found in the documents listed below:

- a. Douglas Report No. SM-47377, Saturn S-IVB-501 Stage Acceptance Firing Test Plan, revised May 9, 1966.
- b. Douglas Report No. SM-37532, S-IVB-501 Stage Acceptance Firing 15-Day Report Sacramento Test Center, dated June 1966.
- c. Drawing No. 1B59261, S-IVB-501 Stage End Item Test Plan, A Change, dated 2 May 1966.
- d. Douglas Report No. SM-53184, Narrative End Item Report on Saturn S-IVB-501 (Douglas S/N 1005), dated August 1966.
- e. Douglas Report No. DAC-56356, Saturn S-IVB-501 Stage Acceptance Firing Report, dated July 1966.
- f. Drawing No. 1B43566, AT Change, Instrumentation Program and Components List, Saturn S-IVB-501, dated August 29, 1967.

The S-IVB-501 stage was launched with the propulsion system installation configuration presented in figure 3-1. Also shown is a parts list of propulsion system components with orifice sizes, nominal pressure switch settings and nominal regulator settings. Additional propulsion system orifice characteristics and pressure switch checkout data are presented in tables 3-1 and 3-2. Serial numbers and positions of the J-2 engine, the four retrorockets, the two ullage rockets, and the two auxiliary propulsion system modules are shown in figure 3-2. Facility propellant

Section 3
Test Configuration

and pneumatic loading systems are shown in figure 3-3. Serial numbers of significant S-IVB-501 stage end items are as follows:

<u>End Item</u>	<u>Part Number</u>	<u>Serial Number</u>
Engine driven hydraulic pump	1A66240-503	MX128995
Auxiliary hydraulic pump	1A66241-509	X454668
PU electronic assembly	1A59358-525	00002
Inverter/converter assembly	1A66212-507	00004
Chilldown inverters		
LOX	1A74039-515	00029
LH2	1A74039-515	00034
Tape recorder	1A66884-501	00015
Telemetry transmitter assemblies mod II		
CF1	1B58797-501	00002
CF2	1B58797-505	00001
CF3	1B58797-1	00002
CP1	1E58796-1	00002
CS1	1B58797-503	00001
Digital range safety command receivers		
No. 1	50M10697	00102
No. 2	50M10697	00049
Safe and arm device	1B33735-503	00026
Ullage rockets		
Position 428	1A81960-1	K801-1
Position 429	1A81960-1	K801-2
LOX fill and drain valve	1A48240-505	00106
LH2 fill and drain valve	1A48240-505	00105
Tank probes		
LOX	1A48430-507	E13
LH2	1A48430-501	E12

Section 3
Test Configuration

<u>End Item</u>	<u>Part Number</u>	<u>Serial Number</u>
LOX vent and relief valve	1A48257-505	00032
LH2 vent and relief valve	1A48257-511	00048
Directional vent valve	1A49988-1	00009
LOX relief valve	1A49590-515	00548
LH2 relief valve	1A49591-533	00158
LOX tank chilldown pump	1A49423-505-009A	01791
LH2 tank chilldown pump	1A49421-503	00125
LOX prevalve	1A49968-509	00021
LH2 prevalve	1A49968-507	00024
APS module		
No. 1	1A83918-1	01005-1
Engine 1-1 (I-IV)	1A39597-509	00593
Engine 1-2 (I-P)	1A39597-509	00602
Engine 1-3 (I-II)	1A39597-509	00576
Ullage engine		4073468
No. 2	1A83918-509	01005-2
Engine 2-1 (III-II)	1A39597-509	00578
Engine 2-2 (III-P)	1A39597-509	00609
Engine 2-3 (III-IV)	1A39597-509	00619
Ullage engine		4073468
Batteries		
Aft 1	1A59741-507	15-18
Aft 2	1A68317-503	00013
Fwd 1	1A59741-503	00007
Fwd 2	1A68316-501	00019
Continuous vent valve hydraulic actuators	1B67193-507	00023
Pitch	1A66248-505-001	00037
Yaw	1A66248-505-001	00035

Section 3
Test Configuration

3.2 Stage Modifications

The following significant measurement changes and stage modifications were accomplished on the S-IVB-501 stage at the Florida Test Center.

- a. The bi-level summing network module (P/N 1B44241-1) was redesigned and measurements K0012-401, Event-Engine Ready Signal, and K0013-401, Event-Cutoff Signal, were rechanneled. Redesign of the module to a 1B44241-501 configuration eliminated the possibility of an erroneous engine cutoff lock-in indication. Rechannelization of K0012-401 and K0013-401 corrected an impedance mismatch. (WRO S-IVB-2871 ECP 0547 R2).
- b. Four pressure transducers (measurements D0002-403, Pressure-Fuel Pump Inlet, D0003-403, Pressure-Oxidizer Pump Inlet, D0054-410, Pressure-Fuel Tank Inlet, D0105-403, Pressure-LOX Tank Pressure Module Helium Gas) installed on the propulsion fittings were relocated to brackets installed on the adjacent structure. Relocation was required to isolate the transducers from high turbulences in fitting areas of the propulsion lines. (WRO S-IVB-2923 ECP 0639).
- c. Four signal conditioning modules were replaced with new modules of existing design. This change was the result of the incorporation of Rocketdyne ECP J2-547 which added four temperature sensors to the J-2 engine to monitor fuel turbine manifold and crossover duct flight measurements. (WRO S-IVB-2992 ECP 0659).
- d. Twelve temperature measurements were added to the LH2 tank. This was required to define the cause of excessive heating experienced during the orbital coast phase of the S-IVB-203 flight. (WRO S-IVB-3203 ECP 2047 R2).

C2017-408 Temperature-Forward Dome Internal -3

C2018-408 Temperature-Forward Dome Internal -4

C2019-408 Temperature-Forward Dome Internal -5

C2020-408 Temperature-Forward Dome Internal -6

Section 3
Test Configuration

C2021-408 Temperature-Forward Dome Internal -7
C2022-408 Temperature-Forward Dome Internal -8
C2023-408 Temperature-Forward Dome Internal -9
C2024-408 Temperature-Forward Dome Internal -10
C2025-408 Temperature-Fuel Tank Wall Internal -17
C2026-408 Temperature-Fuel Tank Wall Internal -16
C2027-408 Temperature-Fuel Tank Wall Internal -19
C2028-408 Temperature-Fuel Tank Wall Internal -18

- e. Telemetry measurements N0058-411, Miscellaneous-Secure Range Safety Decoder 1 Output 1, and N0059-411, Miscellaneous-Secure Range Safety Decoder 2 Output 1 were deleted from the Secure Range Safety Decoders. (WRO S-IVB-3208 ECP 2071).
- f. The range for measurements C0385-401, Temperature-Engine Thrust Chamber Exit Skin Fin 2-3, and C0386-401, Temperature-Engine Thrust Chamber Exit Skin Fin 3-4 was increased from 35 to 560 deg R, to 35 to 900 deg R. Replacement of two signal conditioning modules (P/N 1A98088-1) with modules (P/N 1A98088-507) was required. This increase in range was required to cover the peak temperatures which possibly might be encountered. (WRO S-IVB-3346 R1 ECP 2157).
- g. Temperature transducer C2005-401, Temperature-Engine Main LOX Pneumatic Line Surface was relocated on the main LOX valve second stage actuator closing pneumatic line to prevent interference with Rocketdyne clamp support. (WRO S-IVB-3767 ECP 2421).
- h. The breakpoint amplifier (P/N 1B54875-1) was redesigned to provide a unit with a balancing resistor across the -20 v supply, internal to the amplifier, to make the equivalent Delta I through the signal return wire equal to zero. (WRO S-IVB-580A ECP 0505).
- i. Three gas temperature transducers (C0271-402 Temp-Gas Interstage Area 3, C0272-402 Temp-Gas Interstage Area 3, C0273-402 Temp-Gas

Section 3
Test Configuration

- Interstage Area 5) located in the aft interstage were relocated to prevent interference with the aft interstage access kit and to stop extreme vibration. (WRO S-IVB-3267 ECP 2115).
- j. Pressure transducer for measurement D0062-424, Pressure-LH2 Circulation Return Line Tank Inlet, was relocated from the port on the LH2 recirculation line to a bracket on the adjacent structure. This was done to isolate the transducer from a thermal shock condition in the LH2 circulation line. (WRO S-IVB 3024 ECP 1002).
 - k. Pressure transducers for measurements D0016-425, Pressure-Cold Helium Sphere, D0183-409, Pressure-LH2 Tank Nonpropulsive Vent -1, and D0184-409, Pressure-LH2 Tank Nonpropulsive Vent -2, were relocated from ports on the propulsion lines to brackets located on the adjacent structure. Temperature extremes necessitated relocation. (WRO S-IVB-3156 ECP 2-46).
 - l. Temperature measurement C0291-427, Temp-APS Fairing Area 2-2, was relocated and wiring to temperature measurements C0026-427, Temp-Skin Attitude Nozzle Exit 2-1, C0046-427, Temp-Aft Skirt -2, C0117-427, Temp-Aft Skirt-9, and C0290-409, Temp-APS Fairing Area 2-1 was rerouted to prevent interference with the APS fairing. (WRO S-IVB-3227 ECP 2085).
 - m. Vibration isolator mounts for the Emergency Detection Transducers (measurements D0177-410, Pressure-Fuel Tank Ullage EDS 1, D0178-410, Pressure-Fuel Tank Ullage EDS 2, D0179-424, Pressure-Oxidizer Tank Ullage EDS 1, and D0180-424, Pressure-Oxidizer Tank Ullage EDS 2) were installed. This change was necessitated by the failure of subject transducers to qualify and meet vibration requirements. (WRO S-IVB-2874 ECP 0605).
 - n. Redundant start tank and control bottle pressure instrumentation (D0241-401, Press-GH2 Start Bottle, and D0242-401, Press-Engine Control Helium Sphere) was added to prevent a countdown hold due to failure of a single transducer. (WRO S-IVB-538 ECP J2-594).

Section 3
Test Configuration

- o. A modification kit, consisting of a system of spacers and panels to the forward and aft skirt skins, was installed to prevent flutter. (WRO S-IVB-445A ECP 330).
- p. Clips were installed on the flutter kit located on the forward skirt. (WRO S-IVB-3775 ECP 2391 R1).
- q. A third ball lock at the top of the umbilical carrier was installed to prevent separation caused by ground wind initiated vehicle movement. (WRO S-IVB-3013 ECP 0688).
- r. Eddy current testing was accomplished on all helium pressure vessels which were fabricated with titanium alloys using filler wire to verify filler material was of same composition as vessel parent metal. (WRO S-IVB 3291 ECP 2130).
- s. A new configuration of the ullage rocket jettison fuse which had the confined detonating fuse overwrapped with vinyl tape was installed. (WRO S-IVB-3322 ECP 2150).
- t. Channels were installed over stringers on the aft interstage in the retrorocket plume impingement area to provide additional protection from the heat of the retrorockets exhaust gases. The aft end of the LH2 feedline fairing was modified from a tapered configuration to a blunt configuration to reduce heating. (WRO S-IVB 3834 ECP 2523).
- u. A low thermal emissivity shroud was added between the forward skirt cold plates and the stage structure. This change was required to aid in insuring that the IU sublimator did not exceed minimum operating temperatures. (WRO S-IVB-3327 ECP 2078 R1).
- v. The hazardous gas detection system was installed in the forward skirt and the aft interstage. (WRO S-IVB-485A ECP 0443).
- w. The Schjildahl X-153 aluminized mylar used to wrap the cold plates and attached components was replaced with Schjildahl

Section 3
Test Configuration

X-850 aluminized mylar. The X-153 mylar is susceptible to accumulation of electrostatic charges. (WRO S-IVB-2877 ECP 0590).

- x. A filter assembly was installed at the accumulator outlet flange to prevent contamination from entering the pneumatic system from the accumulator. (WRO S-IVB-538 ECP J2-511).
- y. The augmented spark ignitor oxidizer orifice was changed to eliminate the potential erosion of the ASI cavity by decreasing the oxidizer flow and mixture ratio. (WRO S-IVB-583 ECP J2-598).
- z. The start tank vent and relief valve was replaced. (WRO S-IVB-538 ECP J2-568).
- aa. The J-2 engine helium regulator assemblies were replaced. (WRO S-IVB-538 ECP J2-602).
- ab. The pneumatic actuation control modules were replaced with units having thermal protection in order to meet the low temperature requirements. (WRO S-IVB-2879 ECP 2049 R1).
- ac. The LH2 continuous vent module was replaced with a module containing a solenoid operated pilot override valve and a pneumatic operated orifice shutoff valve actuator. This change was to control the shutoff valve actuation time. (WRO S-IVB-2883 ECP 2019).
- ad. The LOX and LH2 tank relief valves were replaced with valves containing a new spring guide design. (WRO S-IVB-2765 ECP 0534).
- ae. The LOX and LH2 fill and drain valves were replaced with valves which had a redesigned actuator assembly to assure consistent closing operation and eliminate binding of the gear rack and pinion gear. (WRO S-IVB-2795 ECP 0565).
- af. The LH2 and LOX chilldown system cutoff valves (P/N 1A49965) were replaced to provide valves which had passed qualification tests. (WRO S-IVB-2846 ECP 0493).

Section 3
Test Configuration

- ag. The LOX and the LH2 vent and relief valves were replaced with redesigned units. Redesign consisted of a new seal seat configuration and a new seal to reduce leakage. (WRO S-IVB-2876 ECP 0689 R1).
- ah. The LOX and LH2 fill and drain disconnects were designed to rectify a leakage problem. This consisted of redesigning the seal and support flanges on the flight half of the disconnects. (WRO S-IVB-2985 R3 ECP 0597).
- ai. The LOX tank ullage transducer sense line was modified to provide for a low pressure purge system. This prevented cyclical pressure surges due to LOX boiloff trapped in the sensing line which cause erratic ullage pressure indications. (WRO S-IVB-3021 ECP 0699).
- aj. A redundant means of EDS J-2 engine cutoff was provided by adding wiring to the 28 vdc aft power distributor; modifying the sequencer by rewiring; and deleting three diodes, one relay, and the pre valve pilot valve timer; and by adding a passive insulation for the 50-amp motor-driven switch. This modification prevented a potential loss of cutoff in the event the primary mode of engine cutoff failed. (WRO S-IVB-3049 ECP 1008 R2).
- ak. The propellant utilization system was modified to allow J-2 engine restart with the PU valve in the hardover position, approximately 4.5 to 1. (WRO S-IVB-3336 ECP 2105).
- al. The PU system electronic circuitry was modified to eliminate the capillary action effect of the LH2 PU probe. This prevented the PU system from assuming an incorrect initial condition and an incorrect engine thrust profile. (WRO S-IVB-3434 ECP 2226).
- am. A bypass line and orifice in the LOX chilldown pump container purge line was installed to assure positive pressure in the LOX pump motor container in the event of solenoid failure in the chilldown pump purge module. (WRO S-IVB-3372 ECP 2175).

Section 3
Test Configuration

- an. The LOX relief valve was replaced with a redesigned valve which had a larger diameter threaded shaft in the pilot poppet. This change provided greater poppet shaft strength to assure reliability of the controller assembly. (WRO S-IVB-3519 ECP 2180 R1).
- ao. The LH2 relief valve was replaced with a redesigned valve which had a larger diameter threaded shaft in the pilot poppet. This change provided greater poppet shaft strength to assure reliability of the controller assembly. (WRO S-IVB-3518 ECP 2234 R1).
- ap. The pneumatic power control modules were replaced with new modules having new shutoff valve seats and new vent valve seats. These changes corrected the low temperature operational and leakage problems. (WRO S-IVB-3533 ECP 2244).
- aq. The continuous vent module was replaced with a redesigned module having an improved electrical solenoid and aluminum poppets with larger threaded end for the relief override solenoid and for the relief valve. The existing solenoid had repeatedly cracked at a hermetically sealed solder joint at operating temperature. (WRO S-IVB-3501 ECP 2248).
- ar. The LOX and LH2 chilldown system shutoff valves were reworked to provide a new microswitch actuator spring for the open position indication switch. This enabled the present bellows shaft to actuate the switch during critical component cycling. (WRO S-IVB-3564 ECP 2269).
- as. The continuous vent bypass actuator control module was replaced with a redesigned module having separate vent ports for opening and closing sides of the continuous vent valve bypass. This prevented the unlatching of the locked position of the actuator. (WRO S-IVB-3617 ECP 2291).
- at. The LH2 tank repressurization control module, P/N 1B56653-511, was replaced with a P/N 1B56653-513 module which incorporates a new seat design and circle-seal check valve in the top vent of the regulator. (WRO S-IVB-3642 ECP 2304).

Section 3
Test Configuration

- au. The LOX tank pressurization control module, P/N 1B42290-503, was replaced with a P/N 1B42290-505 module. (WRO S-IVB-3644 ECP 2305).
- av. An orifice was installed to replace a union in the LOX tank repressurization system to prevent rapid LOX tank repressurization. (WRO S-IVB-3663 ECP 2319).
- aw. The APS propellant system was redesigned to provide for removal of gas formed within the APS propellant tanks. (WRO S-IVB-3318 ECP 2054).
- ax. An overboard dump for the J-2 engine LOX pump primary seal cavity drain was installed in order to minimize hazardous conditions within the aft interstage during boost. (WRO S-IVB-3756 ECP 2425).
- ay. The PU system shaping network was modified to obtain increased attenuation at slosh frequencies. (WRO S-IVB-361A ECP 0302).
- az. The PU static inverter/converter box was modified to incorporate a new module with a trim potentiometer which would allow adjustment of the 5 vdc fine mass supply (WRO S-IVB-2713 ECP 0466).
- ba. The chilldown inverter/converter reset circuit was modified to eliminate a voltage spike and thereby prevent inverter failure. (WRO S-IVB-2938 ECP 0651).
- bb. The emergency detection system (EDS) was modified to separate the engine cutoff circuits at the connector, semi-conductor, and module level, so that no single electrical component failure would cause an erroneous abort. (WRO S-IVB-2960 ECP 0634).
- bc. The LOX and LH₂ depletion sensor electronic control units and necessary wiring to verify spare depletion sensor operation in both LH₂ and LOX tanks under cryogenic conditions during actual stage loading were installed. (WRO S-IVB-2989 ECP 0681 R2).

Section 3
Test Configuration

- bd. The LH2 depletion sensor time delay module, P/N 1B59020-501, was replaced with a P/N 1A74211-505 2-amp relay module. The effect of this change was to increase the residual propellant at engine cutoff. (WRO S-IVB-3001 ECP 0686 R1).
- be. The LOX and LH2 chilldown inverter assemblies were modified by incorporating new diodes which would suppress over-voltage conditions in the low frequency range. (WRO S-IVB-3179 ECP 2053).
- bf. A redundant relay and associated wiring for the 70-lbf ullage engine start was installed. The dual 70-lbf ullage engines are started through a single relay. Relay redundancy eliminates the single point failure. (WRO S-IVB-3242 ECP 0677).
- bg. The wiring in the sequencer, aft control distributor, and interconnecting cable harness assembly was modified to provide an umbilical talkback for monitoring the reset condition of both open and closed continuous vent valve switch selector relays. (WRO S-IVB-3293 ECP 2096).
- bh. APs orificed caps, 1B72194-1 and -501, were added to ports "R" and "S" respectively (figure 13-1).
- bi. The propellant bladder within the 1B03924-504 oxidizer tank on module 2 was replaced because it had been overpressurized.

3.3 Ground Support Equipment Modifications

The following significant modifications were accomplished on the DSV-4B ground support equipment at the Florida Test Center:

- a. Model DSV-4B-315 Launcher Aft Umbilical Kit
 - (1) The ground half of the propellant fill and drain disconnects was redesigned to reduce leakage.
 - (2) A check valve in the surge vent port of the anti-debris valve was added. This change prevented moisture from entering the valve actuator cavity and thereby causing a failure.

b. Model DSV-4B-432A Pneumatic Console

- (1) The 0.068 in. orifice in the ambient helium pressurization line was replaced with a union. This change reduced the pressurization time of the helium spheres.
- (2) The AN815-4C union in the helium pressure control system was replaced with an 0.013 in. orifice. This change permitted the control of pressurization and depressurization rate of the dome regulator in the cold helium system.
- (3) A relief valve downstream of the 2,000 psi preset regulator was installed to protect the system in the event of regulator failure.

c. Model DSV-4B-438A Gas Heat Exchanger

- (1) A vent line from circuit No. 1 bleed hand valve (A12251) was installed to the vent line in the gaseous hydrogen control panel assembly. This was a safety modification to prevent the venting of GH2 from the Model DSV-4B-438A onto the umbilical tower.

d. Model DSV-4B-472 APS Fuel Installation Kit and Model DSV-4B-473 APS Oxidizer Installation Kit

- (1) The APS ullage control assembly was modified to prevent the bellows from reaching the fully compressed position.
- (2) A portable container which attaches to the APS bleed line to remove and monitor gas from APS propellant tank bladder was added.

Section 3
Test Configuration

TABLE 3-1 (Sheet 1 of 2)
S-IVB-501 STAGE AND GSE FLIGHT ORIFICES

FIND NO. *	DESCRIPTION	ORIFICE SIZE OR NOMINAL FLOWRATE	COEFFICIENT OF DISCHARGE	EFFECTIVE AREA (in.²)
12	S-IVB-501 Stage LH2 chilldown valve purge	14 scfm with 3,200 psid	--	Sintered
15C	Continuous vent bypass valve actuation control module inlet	0.017 in. dia	--	--
16	Continuous vent bypass valve bellows purge	300 scfm with 3,200 psid	--	Sintered
17	Continuous vent bypass valve switch cavity purge	15 scfm with 3,200 psid	--	Sintered
19	Continuous vent No. 1	1.090 in. dia	--	0.92
20	Continuous vent No. 2	1.090 in. dia	--	0.92
21	Continuous vent purge	1 scfm with 3,200 psid	--	Sintered
23	LH2 fill and drain valve purge	15 scfm with 3,200 psid	--	Sintered
29	LOX fill and drain valve purge	15 scfm with 3,200 psid	--	Sintered
39	LOX tank pressurization module, heat exchanger primary	0.1990 in. dia	0.84	0.0261
40	LOX tank pressurization module, heat exchanger bypass	0.1660 in. dia	0.088	0.0190
44	LH2 tank pressurization module (Overcontrol - second burn)	0.2040 in. dia	0.87	0.0884
45	LH2 tank pressurization module normal (Undercontrol)	0.2960 in. dia	0.88	0.0606**

*Indicates location on figures 3-1 and 3-3.

**Discharge coefficient and effective area are calculated for overcontrol and step orifices in combination with the undercontrol orifice.

FIND NO. *	DESCRIPTION	ORIFICE SIZE OR NOMINAL FLOWRATE	COEFFICIENT OF DISCHARGE	EFFECTIVE AREA (in.²)
46	LH2 tank pressurization module control (Overcontrol - first burn)	0.2040 in. dia	0.86	0.0876**
47	LH2 tank repressurization module outlet	0.3120 in. dia	0.75	0.0573
48	LH2 tank nonpropulsive vent purge	1 scfm with 3,200 psid	--	Sintered
49	LH2 tank nonpropulsive vent No. 1	2.100 in. dia	--	--
50	LH2 tank nonpropulsive vent No. 2	2.180 in. dia	--	--
61	LOX chilldown ramp purge	37 scfm with 475 psid	--	--
61A	LOX chilldown pump purge bypass	10 scfm with 475 psid	--	Sintered
62	LOX chilldown pump purge module	0.00166 lbm/sec with 475 psig IN and 85 psig OUT	--	--
73A	LOX sensing line purge	200 scfm with 550 psia	--	Sintered
91	LOX tank vent and relief valve	65 scfm with 3,200 psid	--	Sintered
119	LOX tank ambient repressurization	0.036 in. dia	--	0.0087
120	Engine purge control module	0.00166 lbm/sec with 475 psig IN and 85 psig OUT	--	--
AL2119	Pneumatic Console 432A Stage 1 regulator dome vent	0.018 in. dia	--	--

TABLE 3-1 (Sheet 2 of 2)
S-IVB-501 STAGE AND GSE FLIGHT ORIFICES

FIND NO. *	DESCRIPTION	ORIFICE SIZE OR NOMINAL FLOWRATE	COEFFICIENT OF DISCHARGE	EFFECTIVE AREA (in. ²)	FIND NO. *	DESCRIPTION	ORIFICE SIZE OR NOMINAL FLOWRATE	COEFFICIENT OF DISCHARGE	EFFECTIVE AREA (in. ²)
A12120	Stage 1 regulator 3,100 psig dome loading	0.018 in. dia	--	--	A11886	Pneumatic Console 431A 2,000 psig cold purge valve supply	--	--	Variable
A11852	A/S helium supply and purge	0.027 in. dia	--	--	A11897	750 psig cold purge valve supply	--	--	Variable
A11841	Console 432A CH2 inerting supply	0.031 in. dia	--	--	A11937	thrust chamber jacket purge, chilldown, and supply	0.072 in. dia	--	--
A11779	Mainstage OK pressure switch checkout, fine	0.025 in. dia	--	--	A11946	Engine control helium sphere supply	0.125 in. dia	--	--
A12054	Mainstage OK pressure switch checkout, coarse (used with A11779)	0.025 in. dia	--	--	A11954	LOX tank prepressurization supply (located in model 315 aft umbilical kit)	0.0114 in. dia	--	--
A11824	LH2 system checkout supply, fine	0.016 in. dia	--	--	A11954	Cold helium sphere prepressurization supply (same orifice as above)	0.0114 in. dia	--	--
A11820	LH2 system checkout supply, coarse (used with A11824)	0.016 in. dia	--	--	A11914	LOX umbilical purge supply	0.305 in. dia	--	--
A11837	LOX system checkout supply, fine	0.016 in. dia	--	--	A11908	Umbilical purge supply vent	--	--	Variable
A11836	LOX system checkout supply, coarse (used with A11837)	0.016 in. dia	--	--	A12153	Stage 3 regulator inlet	0.018 in. dia	--	--
A11748	Console 432A stage 1 bleed	--	--	Variable	A12152	Stage 3 regulator outlet bleed	0.0022 lbm/min	--	Sintered
A11806	Pressure switch checkout, high pressure, fine	0.018 in. dia	--	--	A12106	Heat Exchanger 436A Circuit No. 1 upstream vent (primary)	0.081 in. dia	--	--
A11810	Pressure switch checkout, high pressure, coarse (used with A11806)	0.018 in. dia	--	--	A12117	Circuit No. 1 downstream vent (secondary)	0.055 in. dia	--	--
A12113	Stage 4 regulator vent	--	--	Variable	A11971	LH2 tank prepressurization supply	0.114 in. dia	--	--
A12116	Stage 5 regulator vent	--	--	Variable	A12234	CH2 regulator dome bleed	0.0003 lbm/min	--	Sintered
A11793	Pressure switch checkout, low pressure, fine	0.015 in. dia	--	--					
A11792	Pressure switch checkout, low pressure, coarse (used with A11793)	0.015 in. dia	--	--					
A12078	Stage 2 regulator vent	--	--	Variable					

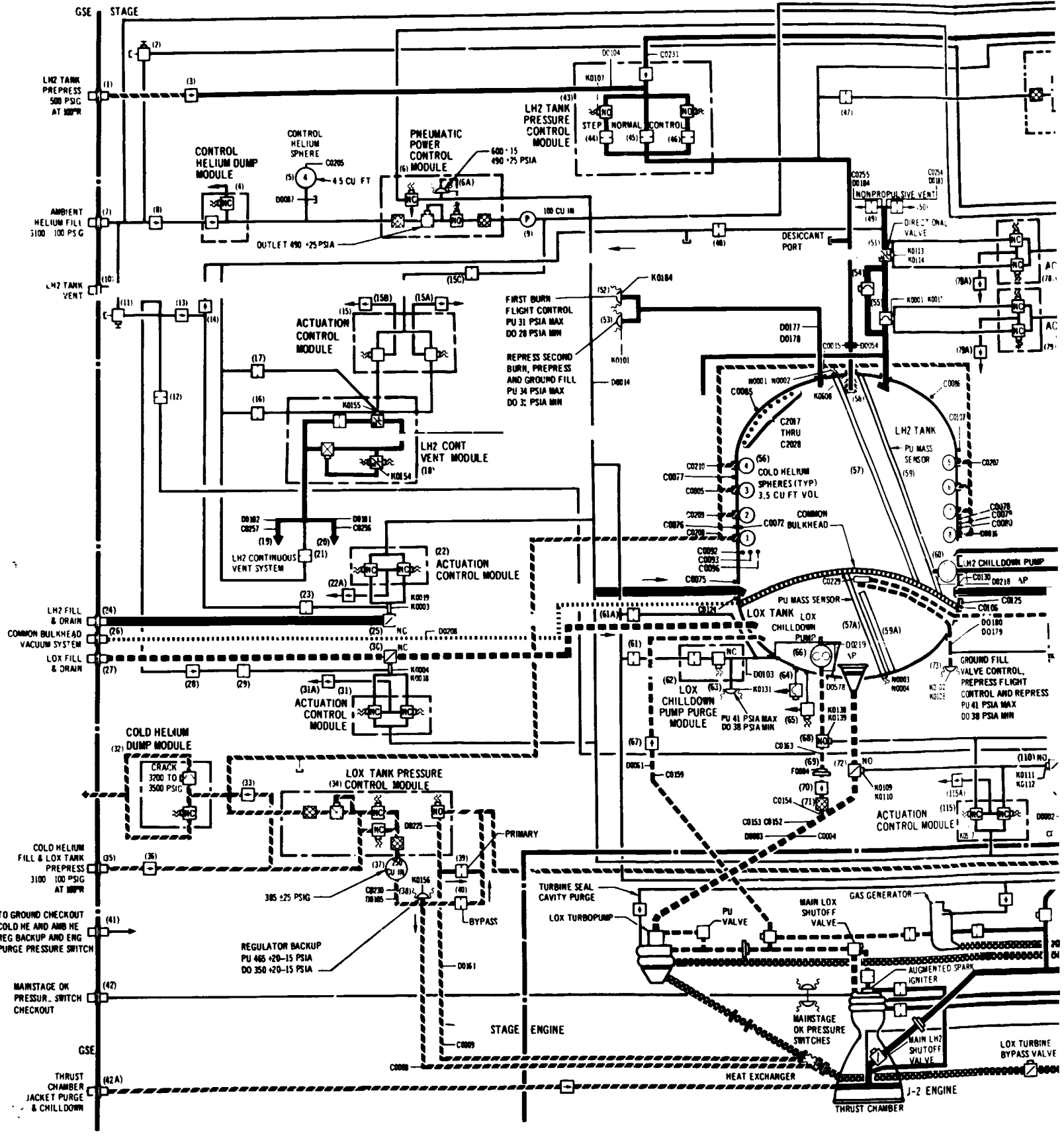
* Indicates location on figures 3-1 and 3-3.

Section 3
Test Configuration

TABLE 3-2
PRESSURE SWITCH CHECKOUT DATA

NOMENCLATURE	SPECIFICATION	PICKUP (PSIA)*		DROPOUT (PSIA)*		DEADBAND (PSI)	
		SYSTEM	CALIPS	SYSTEM	CALIPS	SYSTEM	CALIPS
LOX tank ullage P/N 1B52624-503 Serial No. 10	Pickup: 41 psia max Dropout: 38 psia min Deadband: 0.5 psi min	40.06	40.19	39.00	39.52	1.06	0.67
LOX chilldown pump purge P/N 1B52624-503 Serial No. 11	Pickup: 41 psia max Dropout: 38 psia min Deadband: 0.5 psi min	40.13	40.19	39.00	39.52	1.13	0.67
LOX tank regulator backup P/N 1B52624-509 Serial No. 10	Pickup: 450-485 psia Dropout: 335-370 psia Deadband: None	473	472	345	365	--	--
Engine pump purge P/N 1B52623-513 Serial No. 007	Pickup: 130 psia max Dropout: 105 psia min Deadband: 5 psia min	125	130	115	115	10	15
Control helium reg backup P/N 1B52624-507 Serial No. 001	Pickup: 585-615 psia Dropout: 465-515 psia Deadband: None	608	607	495	498	--	--
LH2 tank ullage-2nd burn P/N 1B52624-513 Serial No. 010	Pickup: 34 psia max Dropout: 31 psia min Deadband: 0.5 psi min	33.6	33.8	31.6	32.0	2.0	1.8
LH2 tank ullage-1st burn P/N 1B52624-1 Serial No. 015	Pickup: 31 psia max Dropout: 28 psia min Deadband: 0.5 psi min	30.5	30.4	28.0	28.1	2.5	2.3
Mainstage OK No. 1 P/N 1A57754-501 Serial No. N/A	Pickup: 500 \pm 15 psig Dropout = Pickup -75 \pm 25 psig	511		469			
Mainstage OK No. 2 P/N 1B39019-1 Serial No. N/A	Pickup: 500 \pm 15 psig Dropout = Pickup -75 \pm 25 psig	523		450			

*These values are the average of three runs.



FOLDOUT FRAME

Section 3
Test Configuration

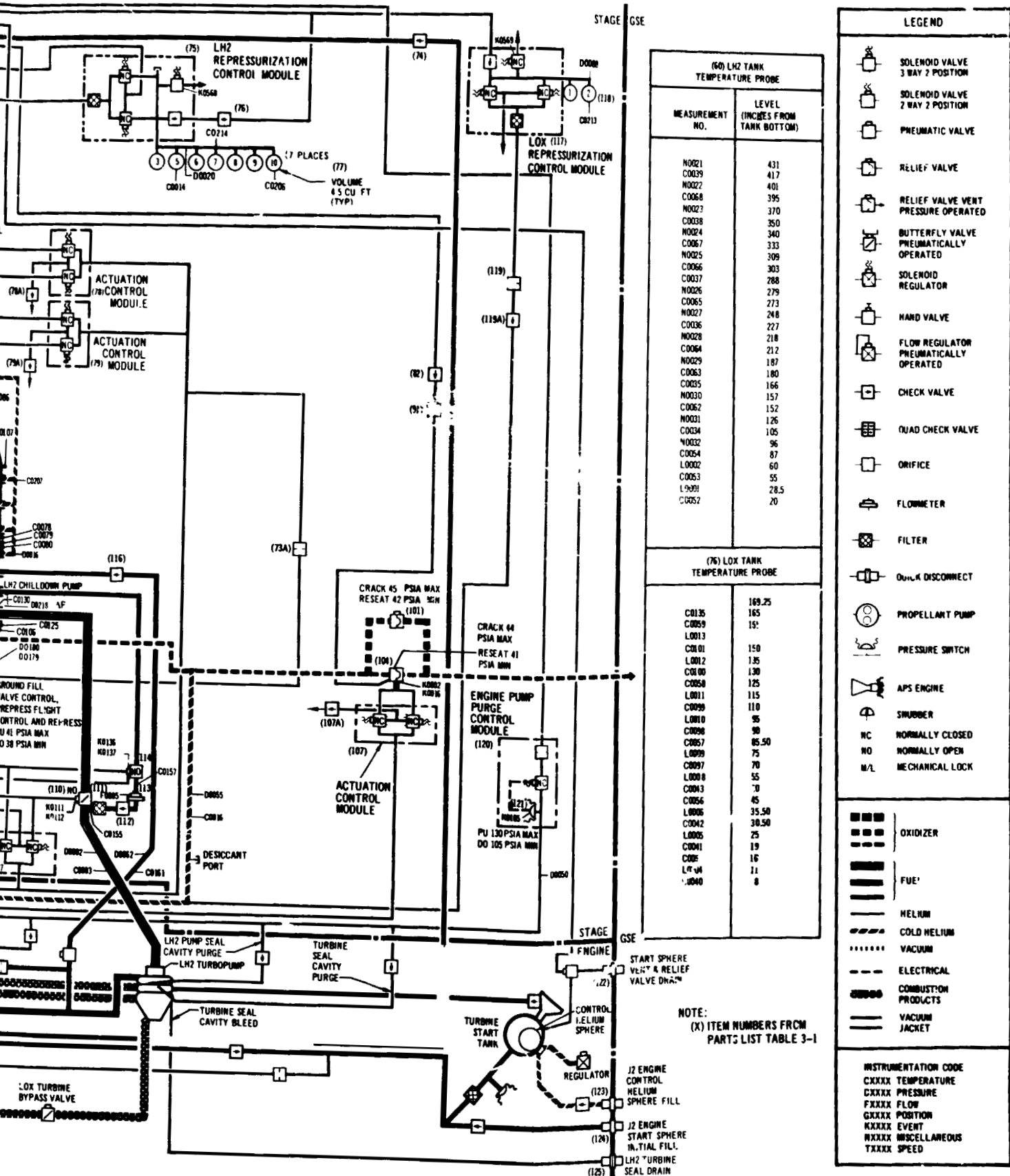


Figure 3-1. Propulsion System and Instrumentation (Sheet 1 of 2)

Section 3
Test Configuration

FIND NO.*	PART NUMBER	PART DESCRIPTION
1	7851861-1	Disconnect, LH2 tank prepressurization
2	1B53817-505	Valve hand, LOX vent and relief valve purge
3	1B65673-1	Valve, check, LH2 tank prepressurization line
4	1A57350-507	Module, control helium dump
5	1A49990-503	Sphere, control helium, 4.5 cu ft
6	1A58345-519	Module, pneumatic power control
6A	1B52624-507	Switch, control, helium regulator backup, PU 600 +15 psia, DO 490 +25 psia
7	7851823-503	Disconnect, ambient helium fill
8	1B51361-1	Valve, check, control helium fill
9	1A48857-1	Plenum, control helium, 100 cu in.
10	1A48848-505	Disconnect, LH2 ground vent
11	1B53817-505	Valve, hand, LH2 chilldown valve, vent and relief valve, continuous vent, nonpropulsive vent, and fill valves purge
12	1B40622-507	Orifice, LH2 chilldown valve purge
13	1B51361-1	Valve, check, LH2 fill and drain valve, continuous vent system and nonpropulsive vent purge
14	1B51361-1	Valve, check, continuous vent system, and nonpropulsive vent purge
15	1B66692-501	Module, actuation control, continuous vent bypass valve
15A	1B67481-1	Valve, check, continuous vent bypass valve actuation control module vent
15B	1B67481-1	Valve, check, continuous vent bypass valve actuation control module vent
15C	1B63023-1	Orifice, continuous vent bypass valve actuation control module inlet
16	1B40622-509	Orifice, continuous vent bypass valve bellows purge
17	1B40622-505	Orifice, continuous vent bypass valve switch cavity purge
18	1B67193-507	Module, continuous vent
19	1B44557-1	Orifice, continuous vent No. 1
20	1B44557-1	Orifice, continuous vent No. 2
21	1B40622-501	Orifice, continuous vent purge
22	1A49982-517	Module, actuation control, LH2 fill and drain valve
22A	1B67481-1	Valve, check, actuation control module vent, LH2 fill and drain valve
23	1B40622-505	Orifice, LH2 fill and drain valve purge
24	1B66932-501	Disconnect, LH2 fill and drain
25	1A48240-505	Valve, LH2 fill and drain
26	1B41065-1	Disconnect, common bulkhead vacuum system
27	1B66932-501	Disconnect, LOX fill and drain
28	1B51361-1	Valve, check, LOX fill and drain valve purge
29	1B40622-505	Orifice, LOX fill and drain valve purge
30	1A48240-505	Valve, LOX fill and drain
31	1A49982-517	Module, actuation control, LOX fill and drain valve
31A	1B67481-1	Valve, check, actuation control module vent, LOX fill and drain valve
32	1B57781-503	Module, cold helium dump
33	1B40824-503	Valve, check, cold helium fill
34	1B42290-505	Module, LOX tank pressurization control

FIND NO.*	PART NUMBER	PART DESCRIPTION
35	7851844-501	Disconnect, cold helium fill and relief valve
36	1B40824-503	Valve, check, cold helium fill
37	1A49991-1	Plenum, LOX tank pressurization
38	1B52624-509	Switch, pressure, cold helium regulator backup, PU 465 +20, -15 psia, DO 350 +20, -15 psia
39	1B63046-523	Orifice, LOX tank pressurization module, test primary
40	1B63047-523	Orifice, LOX tank pressurization module, test bypass
41	1A49958-517	Disconnect, ground checkout, cold helium, ambient and engine purge pressure switches
42	1A49958-517	Disconnect, mainstage OK pressure switch check
42A	1A49958-519	Disconnect, thrust chamber jacket purge and vent
43	1B64443-505	Module, control, LH2 tank pressurization
44	1B64443-505**	Orifice, LH2 tank pressurization control (vent second burn)
45	1B64443-505**	Orifice, LH2 tank pressurization control (vent first burn)
46	1B64443-505**	Orifice, LH2 tank pressurization control (vent first burn)
47	1B63437-1	Orifice, LH2 tank repressurization control vent
48	1B40622-501	Orifice, LH2 tank nonpropulsive vent purge
49	1B59265-1	Orifice, LH2 nonpropulsive vent purge
50	1B59265-1	Orifice, LH2 nonpropulsive vent purge
51	1A49988-1	Valve, directional, LH2 tank vent
52	1B52624-1	Switch, pressure, LH2 tank first burn fill
53	1B52624-513	Switch, pressure, LH2 tank prepressurization and repressurization, PU 34 psia max, DO 31 psia min
54	1A49591-533	Valve, relief, LH2 tank, crack 3 psia max, 1 psia min
55	1A48257-511	Valve, LH2 tank vent and relief, crack 17 psia max, 34 psia min
56	1A48858-1	Sphere, cold helium, 6,048 cu in.
57	1A72907-503	Probe, LH2 tank instrumentation
57A	1A48430-507	Probe, LOX mass sensor
58	1B65812-1	Diffuser, LH2 tank pressurization
59	1A48431-501	Probe, LH2 mass sensor
59A	1A69275-503	Probe, LOX instrumentation
60	1A49421-503	Pump, LH2 chilldown
61	1A48854-1	Orifice, LOX chilldown pump purge
61A	1B40622-511	Orifice, LOX chilldown pump purge bypass
62	1A58347-505	Module, LOX chilldown pump purge
63	1B52624-503	Switch, pressure, LOX chilldown pump purge, PU 41 psia max, DO 38 psia min
64	1A49423-507	Valve, relief, LOX chilldown pump purge, 65 to 85 psia (part of pump assembly)
65	1A67913-1	Valve, dump, LOX chilldown pump purge
66	1A49423-505	Pump, LOX chilldown
67	1A49964-501	Valve, check, LOX chilldown return line

*Indicates location on figures 3-1 and 3-3 **Mo

FOLDOUT FRAME

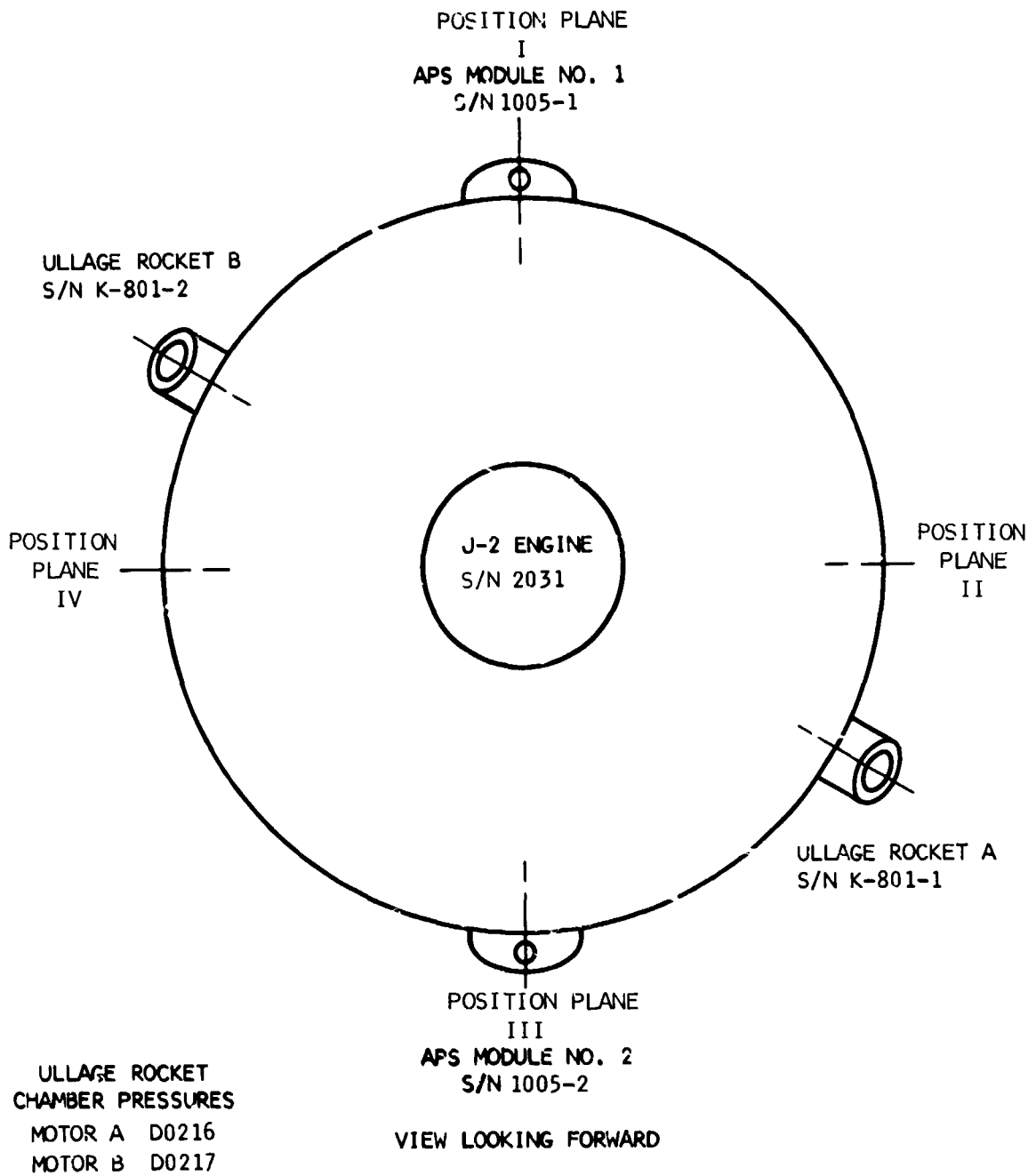
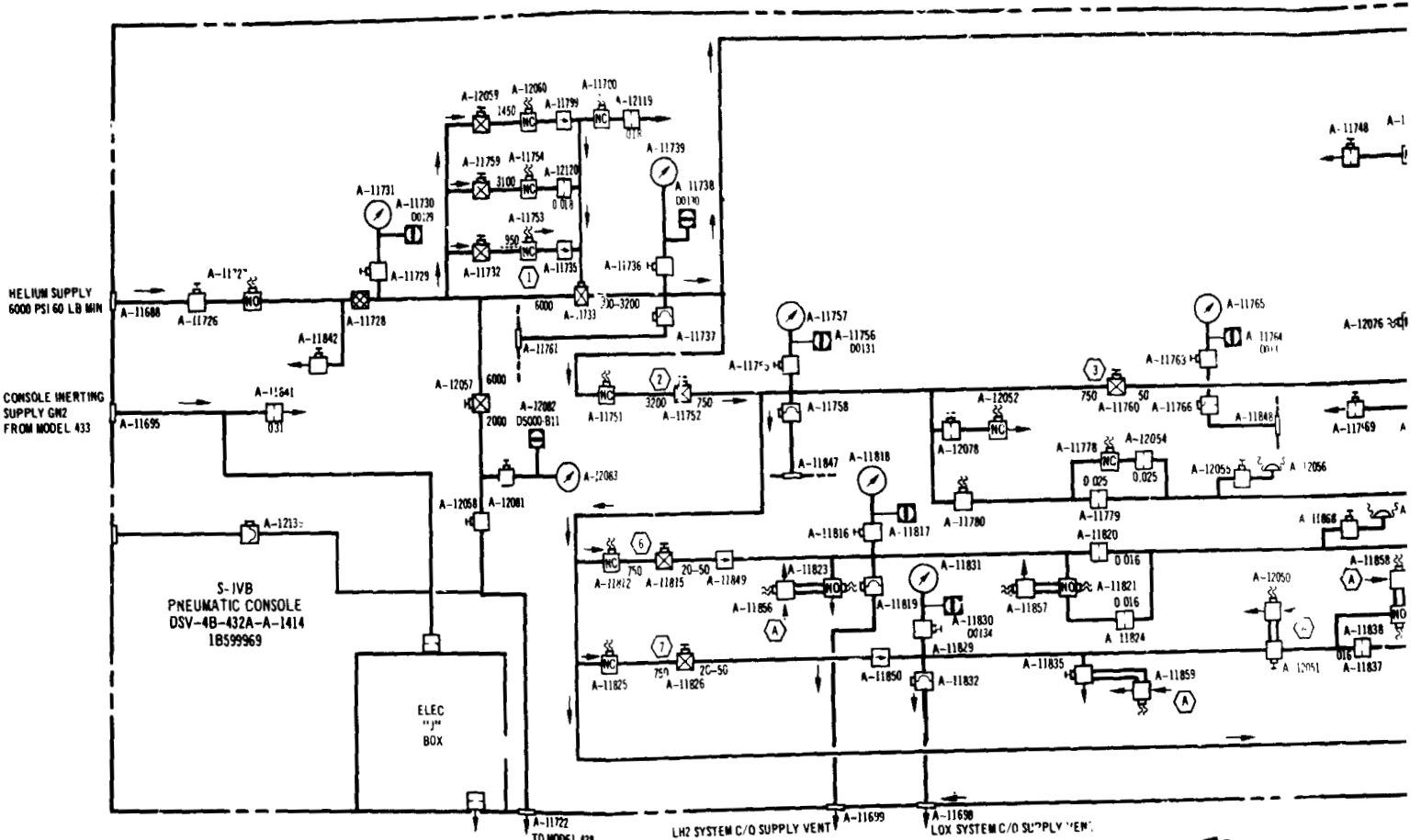


Figure 3-2. Propulsion Major Components Locations

Section 3
Test Configuration



NOTE:
SEE FIGURE 3-1 FOR
LEGEND

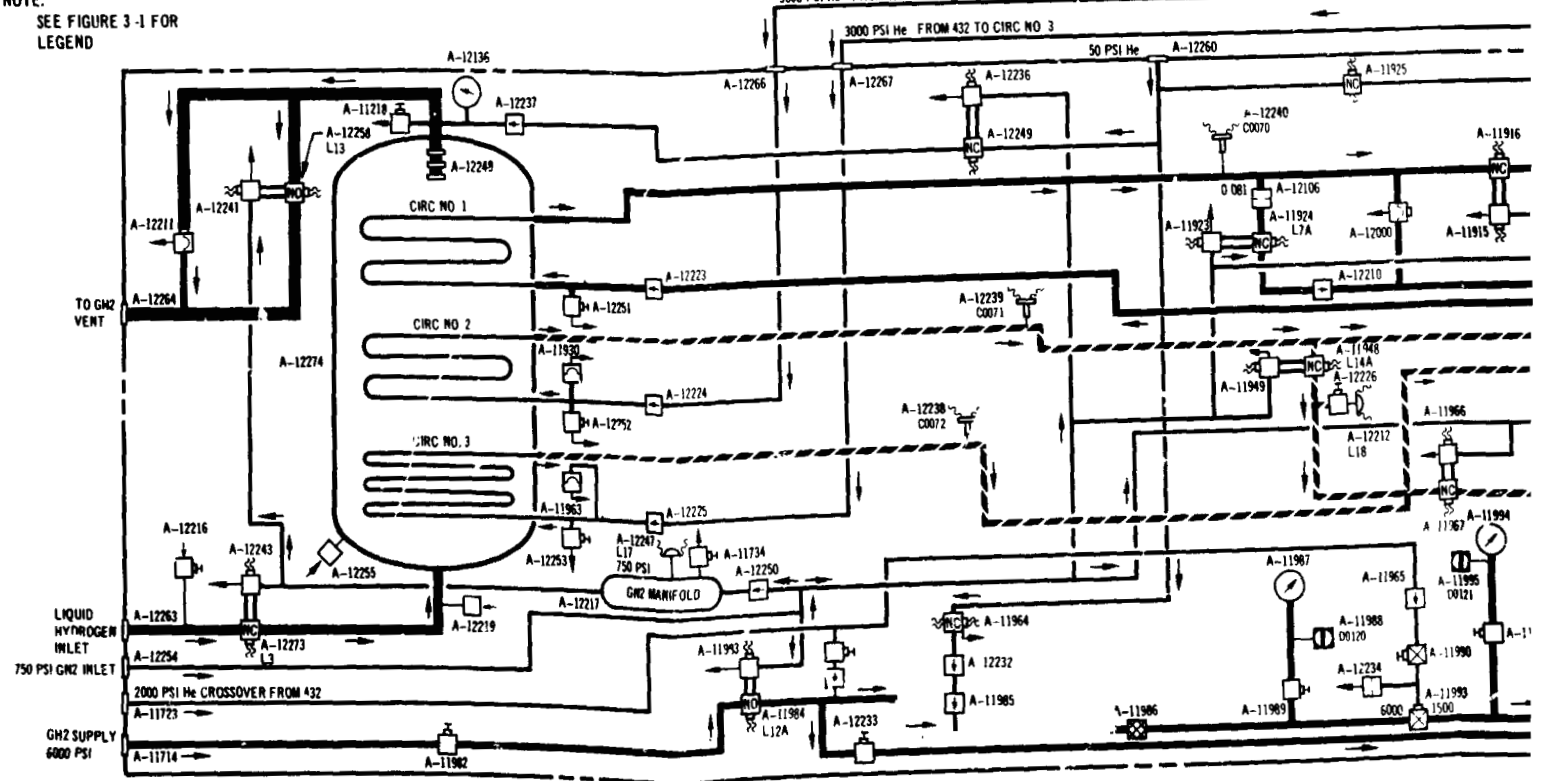
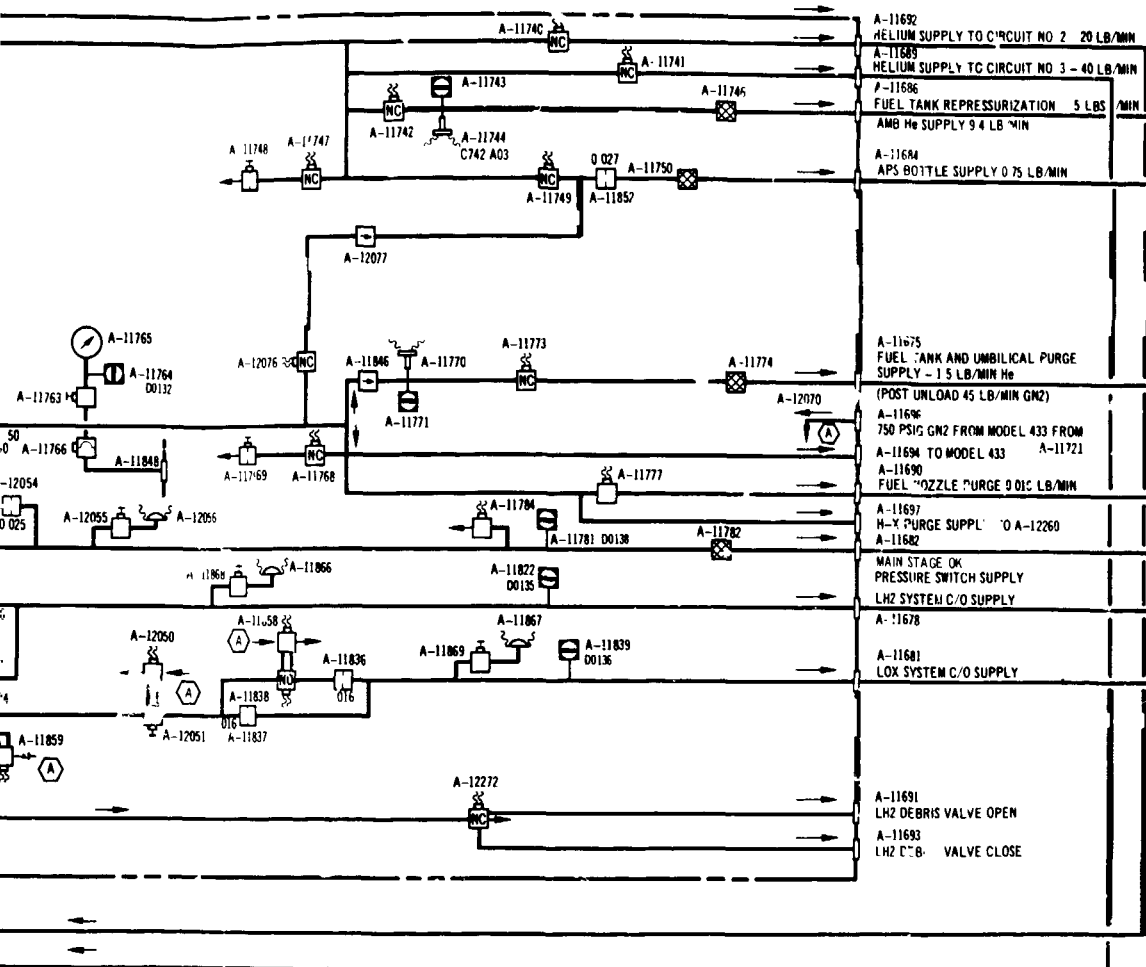
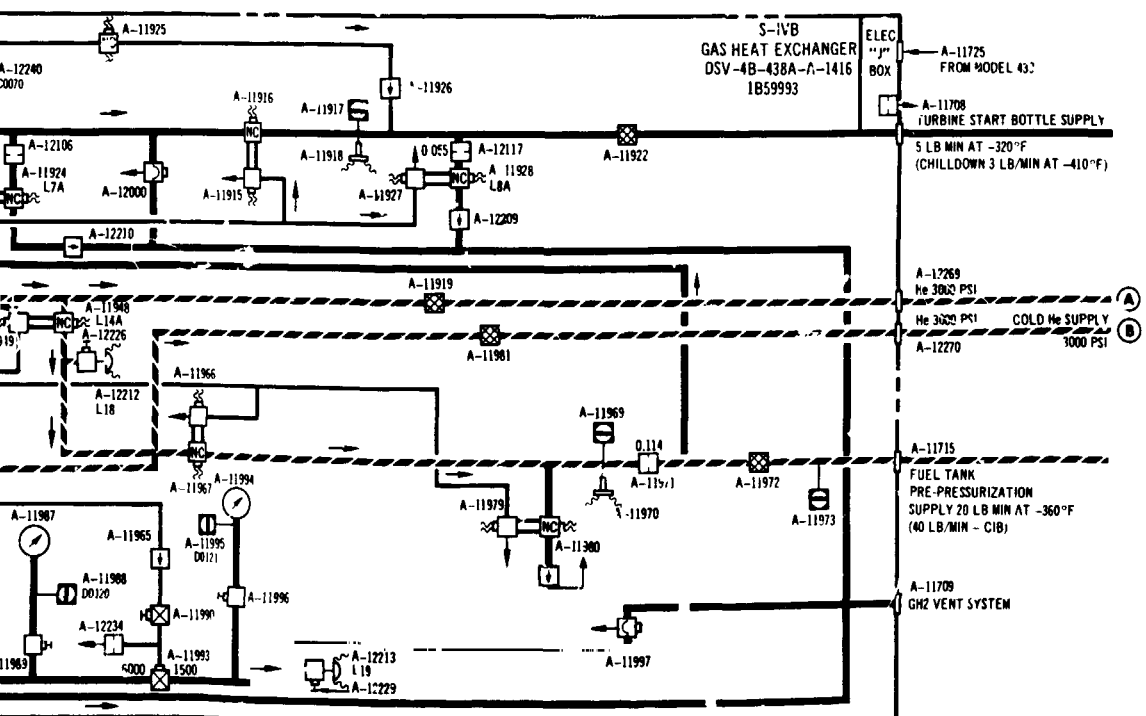


Figure 3-3. Facility Propellant and Pneumatic Loading Systems (Sheet 1 of 2)

FOLDOUT FRAME

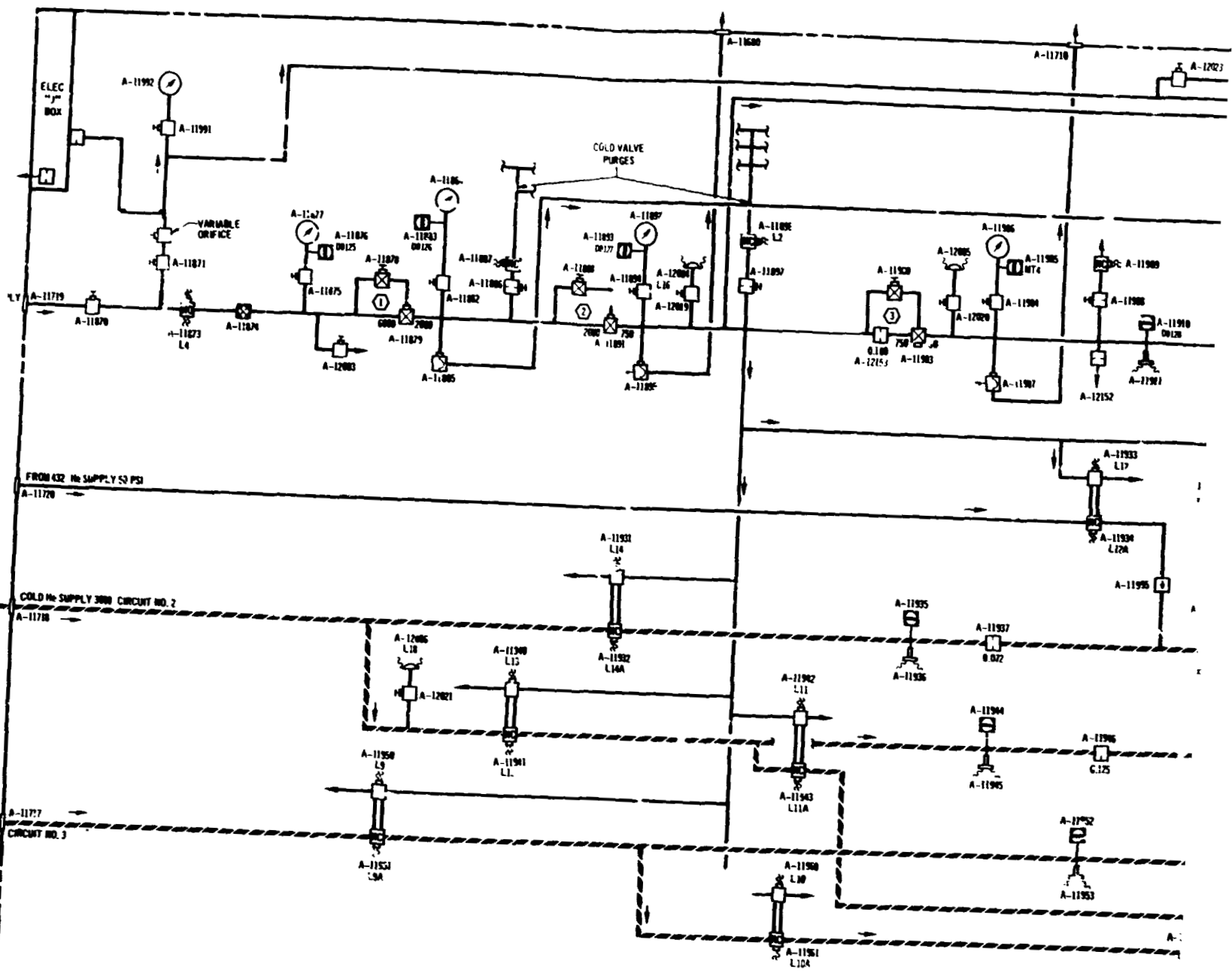


- A-11692 HELIUM SUPPLY TO CIRCUIT NO 2 20 LB/MIN
- A-11689 HELIUM SUPPLY TO CIRCUIT NO 3 40 LB/MIN
- A-11686 FUEL TANK REPRESSURIZATION 5 LBS/MIN
- A-11684 APS BOTTLE SUPPLY 0.75 LB/MIN
- A-11675 FUEL TANK AND UMBILICAL PURGE SUPPLY - 1.5 LB/MIN He (POST UNLOAD 45 LB/MIN GM2)
- A-11696 750 PSIG GM2 FROM MODEL 433 FROM A-11694 TO MODEL 433 A-11721
- A-11690 FUEL NOZZLE PURGE 0.01 LB/MIN
- A-11697 H-X PURGE SUPPLY TO A-12260
- A-11682 MAIN STAGE OK PRESSURE SWITCH SUPPLY
- A-11678 LH2 SYSTEM C/O SUPPLY
- A-11681 LOX SYSTEM C/O SUPPLY
- A-11691 LH2 DEBRIS VALVE OPEN
- A-11693 LH2 C/O VALVE CLOSE



- S-1VB GAS HEAT EXCHANGER DSV-4B-438A-A-1416 1B59993
- ELEC BOX
- A-11725 FROM MODEL 432
- A-11708 TURBINE START BOTTLE SUPPLY 5 LB/MIN AT -320°F (CHILLDOWN 3 LB/MIN AT -410°F)
- A-12269 He 3000 PSI
- A-12270 He 3000 PSI COLD He SUPPLY 3000 PSI
- A-11715 FUEL TANK PRE-PRESSURIZATION SUPPLY 20 LB/MIN AT -360°F (40 LB/MIN - C18)
- A-11709 GH2 VENT SYSTEM

FOLDOJT FRAME 2



Fig

FOLDOUT FRAME |

Section 3
Test Configuration

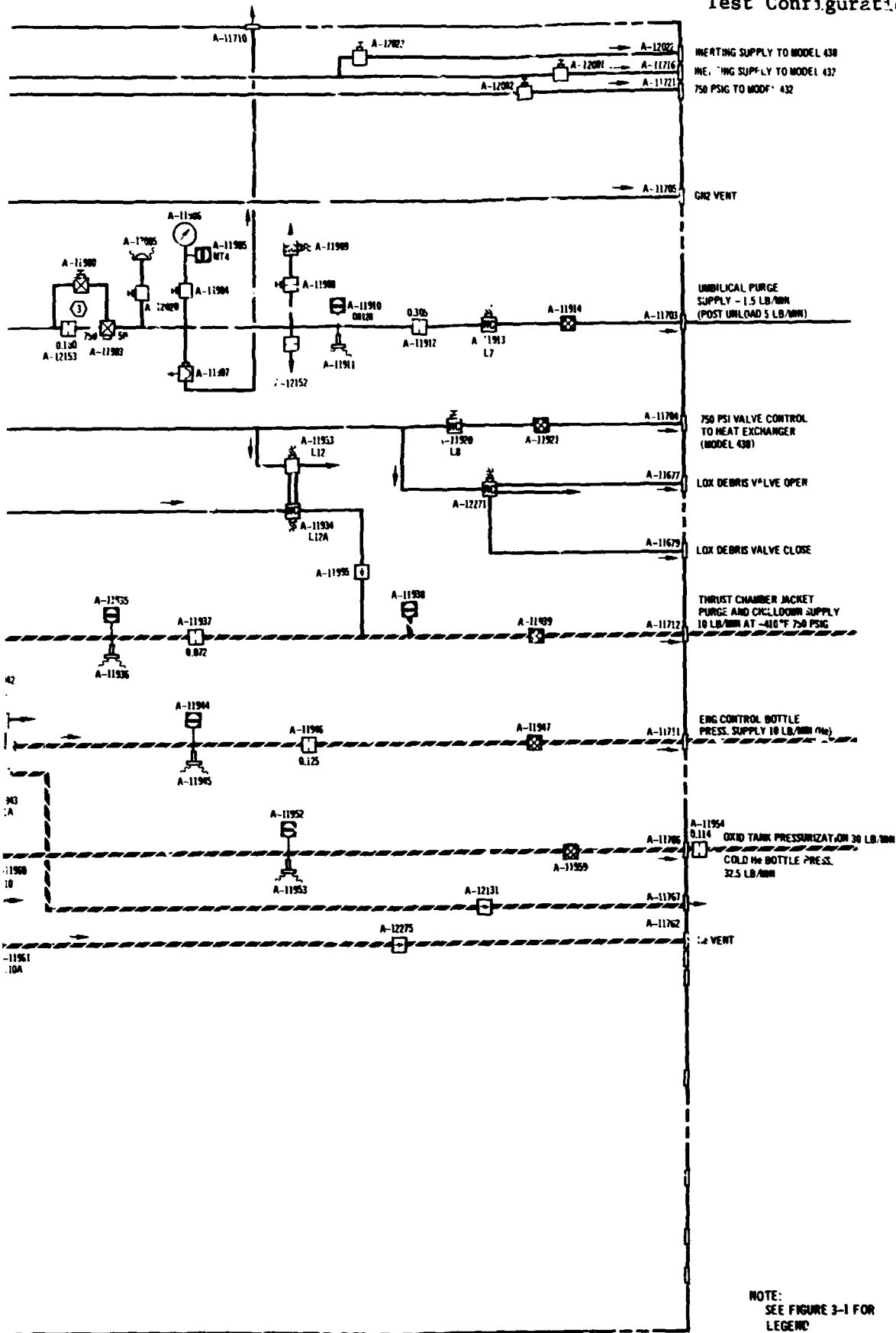


Figure 3-3. Facility Propellant and Pneumatic Loading Systems (Sheet 2 of 2)

FOLDOUT FRAME 2

4. SEQUENCE OF EVENTS

Table 4-1 presents the AS-501 flight sequence of events. Four types of items are included in the sequence.

- a. LVDC Commands - These items initiate from the Launch Vehicle Digital Computer (LVDC) in the instrument unit (IU) and direct vehicle system actions.
- b. Events - These items are monitored occurrences resulting from vehicle performance such as the time of maximum dynamic pressure.
- c. Responses - These items are responses to commands that are issued from the IU and are monitored in the S-IVB.
- d. Ground Commands - These items are manual commands issued from ground stations, which transmit signals to the LVDC to direct vehicle system actions.

In the sequence, all commands and events are preceded by an item number. Sequential series of related commands and responses are listed under the same event number with lower case letters distinguishing separate items. The overall powered flight sequence was close to predicted and proper S-IVB response was given to all commands issued from the IU

4.1 Predicted and Monitored Times

The predicted times in the sequence were obtained from Douglas Report No. SM-46998B, S-IVB-501 Stage Flight Test Plan, revised 2 November 1967.

Commands issued from the LVDC to the S-IC stage, S-II stage, S-IVB stage, and IU, were monitored at the LVDC. Times for these items were obtained from MSFC. Commands issued from the LVDC to the S-IVB stage were also monitored at the S-IVB switch selector. These times were obtained from the Contractor's data. Ground commands were monitored at the Mission Control Center and at the LVDC if received. Monitored times for S-IVB events were obtained from the Contractor's postflight analysis of parameters associated with each event.

Section 4
Sequence of Events

The time from range zero is provided for all items. Range zero, which is by definition the first even second prior to liftoff, occurred at 1200:01.0 Greenwich Mean Time.

A time from base is given for all LVDC commands which were preprogrammed. A time from base is not applicable (N/A) for items such as events and command responses which were not preprogrammed.

A dash (-) was inserted in the flight sequence table for item times which are not available. Some items such as command responses had no predicted times. Loss of flight time for some items was attributed to the following causes:

- a. Telemetry blackout - R0 +151.521 to R0 +153.719 sec.
- b. Early cutoff of S-IVB stage second burn (establishing TB7) caused loss of two TB6 commands. (Table 4-1, item No. 348 and 350.)

The accuracies listed in table 4-1 are related to the telemetry-channel sampling rates; therefore, the items occurred at the times indicated or earlier by the amount listed in the accuracy column. The accuracy of IU signals is not shown since this information is not available.

4.2 Time Bases

Seven sequential series of preprogrammed commands were issued from the LVDC. Each sequential series was initiated by the establishment of its time base in the LVDC. Listed below are the seven time bases with their respective originating events.

- a. Time base one, TB1 - IU umbilical disconnect
- b. Time base two, TB2 - S-IC inboard engine cutoff
- c. Time base three, TB3 - S-IC outboard engines cutoff
- d. Time base four, TB4 - S-II J-2 engines cutoff
- e. Time base five, TB5 - First S-IVB engine cutoff
- f. Time base six, TB6 - Begin restart preparations (LVDC solves an equation)
- g. Time base seven, TB7 - Second S-IVB engine cutoff

4.3 Ground Commands

Seven sequential series of commands to the LVDC were initiated from the ground by flight controller action. These commands were not preplanned and their purpose was that of closing the S-IVB LH2 continuous vent valves. Inflight telemetry data available to the flight controllers was interpreted by the controllers as indicating that the valves remained open after onboard commands had been sent to close the valves. The pre-programmed series of ground commanded signals issued automatically following each flight controller attempt to close the valves is listed below.

- a. LH2 Tank Repressurization Control Valve Open OFF
- b. LH2 Tank Continuous Vent Valve Close ON
- c. LH2 Tank Continuous Vent Valve Close OFF

This series of signals was sent seven times with the second, third and fourth series (issued from Corpus Christi) being received by the LVDC. The first and fifth series were sent during handover from Goldstone to Corpus Christi and from Corpus Christi to Merrit Island, Florida (MILA), respectively, with transmission, therefore, not being complete and automatically rejected by the IU. The sixth and seventh series were sent from MILA with an erroneous address and were also rejected by the IU.

4.4 Ground Sequence of Events

Table 4-2 presents the ground sequence of events from approximately R0 -15 min to liftoff. These events are related to the S-IVB-501 stage and associated ground support equipment and are derived from the digital events evaluation. No out of sequence events or other anomalies occurred.

Section 4
Sequence of Events

TABLE 4-1 (Sheet 1 of 43)
FLIGHT SEQUENCE OF EVENTS

ITEM NO.	EVENT	PREDICTED TIME *		SIGNAL MONITORED AT	MONITORED TIME *		DATA SOURCE	ACCURACY (ms)
		TIME FROM RANGE ZERO (hr:min:sec) (sec)	TIME FROM BASE (sec)		TIME FROM RANGE ZERO* (hr:min:sec) (sec)	TIME FROM BASE (sec)		
1	Guidance Reference Release	-00:00:16.7 (-16.7)	N/A	IU	-00:00:17.638 (-17.633)	N/A	MSFC	--
2	S-IC Engine Start	-00:00:06.0 (-6.0)	N/A	IU	-00:00:06.688 (-6.688)	N/A	MSFC	--
3	First Motion	00:00:00.0 (0)	N/A	GSE	-00:00:00.48 (-0.48)	N/A	MSFC	--
4	Holddown Arms Release	00:00:00.0 (0)	N/A	IU	-00:00:00.41 (-0.41)	N/A	MSFC	--
5	Range Zero	00:00:00.0 (0)	N/A	IU	00:00:00.0 (0)	N/A	MSFC	--
6	<u>Time Base 1</u> AS-501 Liftoff; IU Umbilical Disconnect	00:00:00.3 (0.3)	TB1 +0.0	IU	00:00:00.263 (0.263)	TB1 +0.0	MSFC	--
7	Yaw Maneuver Start	00:00:01.3 (1.30)	N/A	IU	00:00:00.979 (0.979)	N/A	MSFC	--
8	Signal from LVDC for: Auto - Abort Enable Relays Reset	00:00:05.3 (5.30)	TB1 +5.0	IU	00:00:05.216 (5.216)	TB1 +4.953	MSFC	--
9	Tower Clearance	--	--	--	00:00:09.85 (9.85)	N/A	MSFC	--
10	Yaw Maneuver Stop	00:00:09.3 (9.30)	N/A	IU	00:00:10.161 (10.161)	N/A	MSFC	--
11	Roll Maneuver Start	00:00:12.3 (12.30)	N/A	IU	00:00:11.063 (11.063)	N/A	MSFC	--
12	Roll Maneuver Start	00:00:12.3 (12.30)	N/A	IU	00:00:11.063 (11.063)	N/A	MSFC	--
13	Signal from LVDC for: Multiple Engine Cutoff Enable	00:00:14.3 (14.30)	TB1 +14.0	IU	00:00:14.213 (14.213)	TB1 +13.950	MSFC	--
14	Signal from LVDC for: S-IC Telemetry Calibrate On	00:00:25.3 (25.30)	TB1 +27.0	IU	00:00:25.214 (25.214)	TB1 +24.951	MSFC	--
15	Signal from LVDC for: Telemetry Calibrator Inflight Calibrate On	00:00:27.3 (27.30)	TB1 +27.0	IU	00:00:27.234 (27.234)	TB1 +26.971	MSFC	--
16	Signal from LVDC for: S-IC Telemetry Calibrate Off	00:00:30.1 (30.10)	TB1 +29.0	IU	00:00:30.037 (30.037)	TB1 +29.774	MSFC	--
17	Roll Maneuver Stop	00:00:30.3 (30.30)	N/A	IU	00:00:31.990 (31.990)	N/A	MSFC	--
18	Signal from LVDC for: Launch Vehicle Engines EDS Cutoff Enable	00:00:30.3 (30.3)	TB1 +30.0	IU	00:00:30.212 (30.212)	TB1 +29.949	MSFC	--
19	Signal from LVDC for: Telemetry Calibrator Stop Inflight Calibrate Off	00:00:32.3 (32.3)	TB1 +32.0	IU	00:00:32.223 (32.223)	TB1 +31.960	MSFC	--

*See notes at end of table

Section 4
Sequence of Events

TABLE 4-1 (Sheet 2 of 43)
FLIGHT SEQUENCE OF EVENTS

ITEM NO.	EVENT	PREDICTED TIME*		SIGNAL MONITORED AT	MONITORED TIME*		DATA SOURCE	ACCURACY* (ms)
		TIME FROM RANGE ZERO (hr:min:sec) (sec)	TIME FROM BASE (sec)		TIME FROM RANGE ZERO* (hr:min:sec) (sec)	TIME FROM BASE (sec)		
20	Signal from LVDC for: Fuel Pressurizing Valve No. 2 Open & Tape Recorder Record	00:00:49.8 (49.8)	TB1 +49.5	IU	00:00:49.721 (49.721)	TB1 +49.458	MSFC	--
21	Signal from LVDC for: Start Data Recorders	00:01:14.4 (74.4)	TB1 +74.1	IU	00:01:14.322 (74.322)	TB1 +74.059	MSFC	--
22	Maximum Dynamic Pressure	00:01:19.1 (79.1)	N/A	N/A	00:01:18.0 (78.0)	N/A	MSFC	--
23	Signal from LVDC for: Telemetry Calibrator Inflight Calibrate On	00:01:30.3 (90.3)	TB1 +90.0	IU	00:01:30.225 (90.225)	TB1 +89.962	MSFC	--
24	Signal from LVDC for: Telemetry Calibrator Inflight Calibrate Off	00:01:35.5 (95.3)	TB1 +95.0	IU	00:01:35.220 (95.220)	TB1 +94.957	MSFC	--
25	Signal from LVDC for: Fuel Pressurizing Valve No. 3 Open	00:01:35.6 (95.6)	TB1 +95.3	IU	00:01:35.518 (95.518)	TB1 +95.255	MSFC	--
26	Signal from LVDC to Flight Control Computer for: Switch Point No. 2	00:01:45.3 (105.3)	TB1 +105.0	IU	00:01:45.214 (105.214)	TB1 +104.951	MSFC	--
27	Signal from LVDC for: S-IC Telemeter Calibrate On	00:01:55.3 (115.3)	TB1 +115.0	IU	00:01:55.214 (115.214)	TB1 +114.950	MSFC	--
28a	Signal from LVDC for: Special Calibrate Relays On	00:01:59.3 (119.3)	TB1 +119.0	IU	00:01:59.236 (119.236)	TB1 +118.973	MSFC	--
28b	Signal Received in S-IVB for: Special Calibrate Relays On	--	--	S-IVB	00:01:59.225 (119.225)	N/A	DAC(FM)	13
29a	Signal from LVDC for: Regular Calibrate Relays On	00:01:59.5 (119.5)	TB1 +119.2	IU	00:01:59.413 (119.413)	TB1 +119.150	MSFC	--
29b	Signal Received in S-IVB for: Regular Calibrate Relays On	--	--	S-IVB	00:01:59.400 (119.400)	N/A	DAC(FM)	13
30	Signal from LVDC to Flight Control Computer for: Switch Point No. 2	00:02:00.3 (120.3)	TB1 +120.0	IU	00:02:00.213 (120.213)	TB1 +119.950	MSFC	--
31	Signal from LVDC for: S-IC Telemeter Calibrate Off	00:02:00.5 (120.5)	TB1 +120.2	IU	00:02:00.425 (120.425)	TB1 +120.162	MSFC	--
32a	Signal from LVDC for: Regular Calibrate Relays Off	00:02:04.0 (124.0)	TB1 +123.7	IU	00:02:04.425 (124.425)	TB1 +124.162	MSFC	--

*See notes at end of table

Section 4
Sequence of Events

TABLE 4-1 (Sheet 3 of 43)
FLIGHT SEQUENCE OF EVENTS

ITEM NO.	EVENT	PREDICTED TIME *		SIGNAL MONITORED AT	MONITORED TIME *		DATA SOURCE	ACCURACY* (ms)
		TIME FROM RANGE ZERO (hr:min:sec) (sec)	TIME FROM BASE (sec)		TIME FROM RANGE ZERO* (hr:min:sec) (sec)	TIME FROM BASE (sec)		
32b	Signal Received in S-IVB for: Regular Calibrate Relays Off	--	--	S-IVB	00:02:04.424 (124.424)	N/A	DAC(FM)	13
33a	Signal from LVDC for: Special Calibrate Relays Off	00:02:04.2 (124.2)	TB1 +123.9	IU	00:02:04.614 (124.614)	TB1 +124.351	MSFC	--
33b	Signal Received in S-IVB for: Special Calibrate Relays Off	--	--	S-IVB	00:02:04.599 (124.599)	N/A	DAC(FM)	13
34	Signal from LVDC for: Fuel Pressurizing Valve No. 4 Open	00:02:13.8 (133.8)	TB1 +133.5	IU	00:02:13.724 (133.724)	TB1 +133.461	MSFC	--
35a	Signal from LVDC for: Fast Record On	00:02:14.2 (134.2)	TB1 +133.9	IU	00:02:14.114 (134.114)	TB1 +133.851	MSFC	--
35b	Signal Received in S-IVB for: Fast Record On	--	--	S-IVB	00:02:14.099 (134.099)	N/A	DAC(FM)	13
36	Signal from LVDC for: IU Tape Recorder Record On	00:02:14.3 (134.3)	TB1 +134.0	IU	00:02:14.213 (134.213)	TB1 +133.950	MSFC	--
37	Signal from LVDC for: S-IC Two Engine Out Auto-Abort Inhibit Enable	00:02:14.5 (134.5)	TB1 +134.2	IU	00:02:14.426 (134.426)	TB1 +134.163	MSFC	--
38	Signal from LVDC for: S-IC Two Engine Out Auto-Abort Inhibit	00:02:14.7 (134.7)	TB1 +134.4	IU	00:02:14.613 (134.613)	TB1 +134.350	MSFC	--
39	Signal from LVDC for: Excessive Rate (P, Y & R) Auto-Abort Inhibit Enable	00:02:14.9 (134.9)	TB1 +134.6	IU	00:02:14.818 (134.818)	TB1 +134.555	MSFC	--
40	Signal from LVDC for: Excessive Rate (P, Y & R) Auto-Abort Inhibit	00:02:15.1 (135.1)	TB1 +134.8	IU	00:02:15.035 (135.035)	TB1 +134.772	MSFC	--
41	Signal from LVDC for: Two Adjacent Outboard Engines Out Enable	00:02:15.3 (135.3)	TB1 +135.0	IU	00:02:15.213 (135.213)	TB1 +134.950	MSFC	--
42	Time Base 2 S-IC Inboard Engine Cutoff	00:02:15.5 (135.5)	TB2 +0.0	S-IC	00:02:15.469 (135.469)	TB2 +0.0	MSFC	--
43	Signal from LVDC for: Start First PAM-FM/FM Calibration	00:02:15.9 (135.9)	TB2 +0.4	S-II	00:02:15.820 (135.820)	TB2 +0.351	MSFC	--
44	Signal from LVDC for: Stop First PAM-FM/FM Calibration	00:02:20.9 (140.9)	TB2 +5.4	S-II	00:02:20.820 (140.820)	TB2 +5.351	MSFC	--

*See notes at end of table

Section 4
Sequence of Events

TABLE 4-1 (Sheet 4 of 43)
FLIGHT SEQUENCE OF EVENTS

ITEM NO.	EVENT	PREDICTED TIME *		SIGNAL MONITORED AT	MONITORED TIME *		DATA SOURCE	ACCURACY (ms)
		TIME FROM RANGE ZERO (hr:min:sec) (sec)	TIME FROM BASE (sec)		TIME FROM RANGE ZERO (hr:min:sec) (sec)	TIME FROM BASE (sec)		
45	Signal from LVDC for: S-II Ordnance Arm	00:02:24.4 (144.4)	TB2 +8.9	IU	00:02:24.319 (144.319)	TB2 +8.250	MSFC	--
46	Signal from LVDC for: Separation and Retro EBW Firing Units Arm	00:02:24.6 (144.6)	TB2 +9.1	IU	00:02:24.530 (144.530)	TB2 +9.061	MSFC	--
47	Stop Pitch Maneuver	00:02:24.7 (144.7)	N/A	IU	00:02:24.5068 (144.5068)	N/A	MSFC	--
48	Signal from LVDC for: Q-Ball Power (5 th)	00:02:24.8 (144.8)	TB2 +9.3	IU	00:02:24.719 (144.719)	TB2 +9.250	MSFC	--
49	Signal from LVDC for: Camera Lights On	00:02:25.0 (145.0)	TB2 +9.5	IU	00:02:24.929 (144.929)	TB2 +9.460	MSFC	--
50	Signal from LVDC for: S-IC Telemetry Measurement Switch Over	00:02:25.2 (145.2)	TB2 +9.7	IU	00:02:25.120 (145.120)	TB2 +9.651	MSFC	--
51	Signal from LVDC for: Enable Outboard Engines Cutoff	00:02:25.4 (145.4)	TB2 +9.9	IU	00:02:25.325 (145.325)	TB2 +9.850	MSFC	--
52	<u>Time Base 3</u> S-IC Outboard Engines Cutoff	00:02:32.5 (152.5)	TB3 +0.0	IU	00:02:30.769 (150.769)	TB3 +0.0	MSFC	--
53	Signal from LVDC for: Camera Motor On	00:02:32.6 (152.6)	TB3 +0.1	IU	00:02:30.848 (150.848)	TB3 +0.079	MSFC	--
54	Signal from LVDC for: S-II LH2 Recirculation Pumps Off	00:02:32.7 (152.7)	TB3 +0.2	IU	00:02:30.948 (150.948)	TB3 +0.179	MSFC	--
55	Signal from LVDC for: S-II Ullage Trigger	00:02:33.0 (153.0)	TB3 +0.5	IU	00:02:31.235 (151.235)	TB3 +0.496	MSFC	--
56	Signal from LVDC for: Camera Event Mark	00:02:33.1 (153.1)	TB3 +0.6	IU	00:02:31.335 (151.335)	TB3 +0.566	MSFC	--
57	Signal from LVDC for: S-IC/S-II Separation	00:02:33.2 (153.2)	TB3 +0.7	IU	00:02:31.426 (151.426)	TB3 +0.657	MSFC	--
58	Signal from LVDC for: Switch Control to S-II Enable S-II Engine Out and S-II Second Separation Indication "A"	00:02:33.5 (153.5)	TB3 +0.8	IU	00:02:31.521 (151.521)	TB3 +0.752	MSFC	--
59	Signal from LVDC for: S-II Engines Cutoff Reset	00:02:33.4 (153.4)	TB3 +0.9	IU	00:02:31.622 (151.622)	TB3 +0.853	MSFC	--

*See notes at end of table

Section 4
Sequence of Events

TABLE 4-1 (Sheet 5 of 43)
FLIGHT SEQUENCE OF EVENTS

ITEM NO.	EVENT	PREDICTED TIME *		SIGNAL MONITORED AT	MONITORED TIME *		DATA SOURCE	ACCURACY* (ms)
		TIME FROM RANGE ZERO (hr:min:sec) (sec)	TIME FROM BASE (sec)		TIME FROM RANGE ZERO* (hr:min:sec) (sec)	TIME FROM BASE (sec)		
60	Signal from LVDC for: Engines Ready Bypass	00:02:33.5 (153.5)	TB3 +1.0	IU	--	--	--	--
61	Signal from LVDC for: Prevalves Lockout Reset	00:02:33.6 (153.6)	TB3 +1.1	IU	--	--	--	--
62	Signal from LVDC for: S-II Engine Start	00:02:33.9 (153.9)	TB3 +1.4	IU	00:02:32.210 (152.210)	TB3 +1.44'	MSFC	--
63	Signal from LVDC for: Camera Event Mark	00:02:34.0 (154.0)	TB3 +1.5	IU	--	--	--	--
64	Signal from LVDC for: Enable S-II Engine Out & S-II Second Separation Indication "B"	00:02:34.1 (154.1)	TB3 +1.6	IU	--	--	--	--
65	Signal from LVDC for: Engine Ready Bypass Reset	00:02:34.3 (154.3)	TB3 +1.8	IU	--	--	--	--
66	Signal from LVDC for: S-II Hydraulic Accumulators Unlock	00:02:35.5 (155.5)	TB3 +3.0	IU	00:02:33.719 (153.719)	TB3 +2.250	MSFC	--
67	Signal from LVDC for: Chilled Valves Close	00:02:38.9 (158.9)	TB3 +6.4	IU	00:02:37.123 (157.123)	TB3 +6.354	MSFC	--
68	Signal from LVDC for: S-II Start Phase Limiter Cutoff Arm	00:02:39.2 (159.2)	TB3 +6.7	IU	00:02:37.419 (157.419)	TB3 +6.650	MSFC	--
69	Signal from LVDC for: Activate PU System	00:02:39.4 (159.4)	TB3 +6.9	IU	00:02:37.637 (157.637)	TB3 +6.868	MSFC	--
70	Signal from LVDC for: S-II Start Phase Limiter Cutoff Arm Reset	00:02:40.2 (160.2)	TB3 +7.7	IU	00:02:38.433 (158.433)	TB3 +7.664	MSFC	--
71	Signal from LVDC for: IU Tape Recorder Record Off	00:02:43.6 (163.6)	TB3 +11.1	IU	00:02:41.821 (161.821)	TB3 +11.052	MSFC	--
72	Signal from LVDC for: Stop Data Recorders	00:02:43.8 (163.8)	TB3 +11.3	IU	00:02:42.037 (162.037)	TB3 +11.268	MSFC	--
73a	Signal from LVDC for: Fast Record Off	00:02:44.0 (164.0)	TB3 +11.5	IU	00:02:42.219 (162.219)	TB3 +11.450	MSFC	--
73b	Signal Received in S-IVB for: Fast Record Off	--	--	S-IVB	00:02:42.197 (162.197)	N/A	DAC(FM)	13
74	Signal from LVDC for: Water Coolant Valve Open	00:03:00.1 (180.1)	TB3 +27.6	IU	00:02:58.318 (178.318)	TB3 +27.549	MSFC	--

*See notes at end of table

Section 4
Sequence of Events

TABLE 4-1 (Sheet 6 of 43)
FLIGHT SEQUENCE OF EVENTS

ITEM NO.	EVENT	PREDICTED TIME *		SIGNAL MONITORED AT	MONITORED TIME		DATA SOURCE	ACCURACY* (ms)
		TIME FROM RANGE ZERO (hr:min:sec) (sec)	TIME FROM BASE (sec)		TIME FROM RANGE ZERO* (hr:min:sec) (sec)	TIME FROM BASE (sec)		
75	Signal from LVDC for: S-II Second Plane Separation	00:03:03.2 (183.2)	TB3 +30.7	IU	00:03:01.437 (181.437)	TB3 +30.668	MSFC	--
76	Signal from LVDC for: Camera Event Mark	00:03:03.3 (183.3)	TB3 +30.8	IU	00:03:01.534 (181.534)	TB3 +30.765	MSFC	--
77	Signal from LVDC for: Camera Event Mark	00:03:04.3 (184.3)	TB3 +31.8	IU	00:03:02.533 (182.533)	TB3 +31.764	MSFC	--
78	Signal from LVDC for: LET Jettison "A"	00:03:08.9 (188.9)	TB3 +36.4	IU	00:03:07.133 (187.133)	TB3 +36.364	MSFC	--
79	Signal from LVDC for: LET Jettison "B"	00:03:09.1 (189.1)	TB3 +36.6	IU	00:03:07.319 (187.319)	TB3 +36.550	MSFC	--
80	Signal from LVDC for: Camera Eject No. 1	00:03:10.5 (190.5)	TB3 +38.0	IU	00:03:08.718 (188.718)	TB3 +37.949	MSFC	--
81	Signal from LVDC for: Camera Eject No. 2	00:03:11.1 (191.1)	TB3 +38.6	IU	00:03:09.333 (189.333)	TB3 +38.564	MSFC	--
82	Signal from LVDC for: Camera Eject No. 3	00:03:11.6 (191.6)	TB3 +39.1	IU	00:03:09.848 (189.848)	TB3 +39.064	MSFC	--
83	Initiate Iterative Guidance Mode	00:03:12.4 (192.4)	N/A	IU	00:03:10.879 (190.879)	N/A	MSFC	--
84	Signal from LVDC to Flight Control Computer for: Switch Point No. 3	00:03:33.3 (213.9)	TB3 +61.4	IU	00:03:32.132 (212.132)	TB3 +61.363	MSFC	--
85	Signal from LVDC for: Start Second PAH-FM/FM Calibration	00:04:37.5 (277.5)	TB3 +125.0	IU	00:04:35.742 (275.742)	TB3 +124.973	MSFC	--
86	Signal from LVDC for: Stop Second PAH-FM/FM Calibration	00:04:42.5 (282.5)	TB3 +130.0	IU	00:04:40.719 (280.719)	TB3 +129.950	MSFC	--
87	Signal from LVDC to Flight Control Computer for: Switch Point No. 4	00:05:43.9 (343.9)	TB3 +191.4	IU	00:05:42.120 (342.120)	TB3 +191.351	MSFC	--
88	Signal from LVDC for: Telemetry Calibration Inflight Calibrate On	00:05:50.1 (350.1)	TB3 +197.6	IU	00:05:48.319 (348.319)	TB3 +197.570	MSFC	--
89	Signal from LVDC for: Telemetry Calibrator Inflight Calibrate Off	00:05:55.1 (355.1)	TB3 +202.6	IU	00:05:53.329 (353.329)	TB3 +202.560	MSFC	--

*See notes at end of table

Section 4
Sequence of Events

TABLE 4-1 (Sheet 7 of 43)
FLIGHT SEQUENCE OF EVENTS

ITEM NO.	EVENT	PREDICTED TIME*		SIGNAL MONITORED AT	MONITORED TIME*		DATA SOURCE	ACCURACY (ms)
		TIME FROM RANGE ZERO (hr:min:sec) (sec)	TIME FROM BASE (sec)		TIME FROM RANGE ZERO* (hr:min:sec) (sec)	TIME FROM BASE (sec)		
90	Signal from LVDC for: Measurement Control Switch No. 2 Activate	00:06:05.2 (365.2)	TB3 +212.7	IU	00:06:03.426 (363.426)	TB3 +212.657	MSFC	--
91	Signal from LVDC for: Start Third PAM-FM/FM Calibration	00:06:17.5 (377.5)	TB3 +225.0	IU	00:06:15.720 (375.720)	TB3 +224.951	MSFC	--
92	Signal from LVDC for: Stop Third PAM-FM/FM Calibration	00:06:22.5 (382.5)	TB3 +230.0	IU	00:06:20.720 (380.720)	TB3 +229.951	MSFC	--
93	S-II Mixture Ratio Shift Sensed Guidance	00:07:00.0 (420.0)	N/A	IU	00:07:15.692 (435.692)	N/A	MSFC	--
94	Signal from LVDC for: S-II LR2 Step Pressurization	00:07:52.5 (472.5)	TB3 +320.0	IU	00:07:50.718 (470.718)	TB3 +319.949	MSFC	--
95a	Signal from LVDC for: Special Calibrate Relays On	00:07:57.5 (477.5)	TB3 +325.0	IU	00:07:55.729 (475.729)	TB3 +324.960	MSFC	--
95b	Signal Received in S-IVB for: Special Calibrate Relays On	--	--	S-IVB	00:07:55.730 (475.730)	N/A	DAC (FM)	13
96a	Signal from LVDC for: Regular Calibrate Relays On	00:07:57.6 (477.6)	TB3 +325.2	IU	00:07:55.919 (475.919)	TB3 +325.150	MSFC	--
96b	Signal Received in S-IVB for: Regular Calibrate Relays On	--	--	S-IVB	00:07:55.900 (475.900)	N/A	DAC(FM)	13
97	Signal from LVDC for: Telemetry Calibrate Inflight Calibrate On	00:07:57.8 (477.8)	TB3 +325.4	IU	00:07:56.130 (476.130)	TB3 +325.361	MSFC	--
98a	Signal from LVDC for: Regular Calibrate Relays Off	00:08:02.5 (482.5)	TB3 +330.0	IU	00:08:00.722 (480.722)	TB3 +329.953	MSFC	--
98b	Signal Received in S-IVB for: Regular Calibrate Relays Off	--	--	S-IVB	00:08:00.725 (480.725)	N/A	DAC(FM)	13
99a	Signal from LVDC for: Special Calibrate Relays Off	00:08:02.7 (482.7)	TB3 +330.2	IU	00:08:00.936 (480.936)	TB3 +330.166	MSFC	--
99b	Signal Received in S-IVB for: Special Calibrate Relays Off	--	--	S-IVB	00:08:00.925 (480.925)	N/A	DAC(FM)	13
100	Signal from LVDC for: Telemetry Calibrator In-flight Calibrate Off	00:08:02.9 (482.9)	TB3 +330.4	IU	00:08:01.119 (481.119)	TB3 +330.350	MSFC	--

*See notes at end of table

Section 4
Sequence of Events

TABLE 4-1 (Sheet 8 of 43)
FLIGHT SEQUENCE OF EVENTS

ITEM NO.	EVENT	PREDICTED TIME*		SIGNAL MONITORED AT	MONITORED TIME*		DATA SOURCE	ACCURACY* (ms)
		TIME FROM RANGE ZERO (hr:min:sec) (sec)	TIME FROM BASE (sec)		TIME FROM RANGE ZERO* (hr:min:sec) (sec)	TIME FROM BASE (sec)		
101a	Signal from LVDC for: Rate Gyro Off	00:08:03.1 (483.1)	TB3 +330.6	IU	00:08:01.325 (481.325)	TB3 +330.556	MSFC	--
101b	Signal Received in S-IVB for: Rate Gyro Off	--	--	S-IVB	00:08:01:325 (481.325)	N/A	DAC(FM)	13
102a	Signal from LVDC for: Charge Ullage Ignition On	00:08:03.3 (483.3)	TB3 +330.8	IU	00:08:01.538 (481.538)	TB3 +330.769	MSFC	--
102b	Signal Received in S-IVB for: Charge Ullage Ignition On	--	--	S-IVB	00:08:01.575 (481.575)	N/A	DAC(FM)	13
103	Signal from LVDC for: S-II/S-IVB Ordnance Arr	00:08:03.5 (483.5)	TB3 +331.0	IU	00:08:01.720 (481.720)	TB3 +330.951	MSFC	--
104	Signal from LVDC for: IU Tape Recorder Record On	00:08:03.7 (483.7)	TB3 +331.2	IU	00:08:01.929 (481.929)	TB3 +331.160	MSFC	--
105a	Signal from LVDC for: Fast Record On	00:08:03.9 (483.9)	TB3 +331.4	IU	00:08:02.119 (482.119)	TB3 +331.350	MSFC	--
105b	Signal Received in S-IVB for: Fast Record On	--	--	S-IVB	00:08:02.100 (482.100)	N/A	DAC(FM)	13
106	Signal from LVDC for: Start Recorders	00:08:04.1 (484.1)	TB3 +331.6	IU	00:08:02.327 (482.327)	TB3 +331.558	MSFC	--
107	Signal from LVDC for: S-II LOX Depletion Sensor Cutoff Arm	00:08:04.3 (484.3)	TB3 +331.8	IU	00:08:02.518 (482.518)	TB3 +331.749	MSFC	--
108	Signal from LVDC for: S-II LH2 Depletion Sensor Cutoff Arm	00:08:04.5 (484.5)	TB3 +332.0	IU	00:08:02.725 (482.725)	TB3 +331.956	MSFC	--
109	Time Base 4 S-II J-2 Engines Cutoff	00:08:36.8 (516.8)	TB4 +0.0	IU	00:08:39.759 (519.759)	TB4 +0.0	MSFC	--
110	Signal from LVDC for: Start Recorder Timers	00:08:36.9 (516.9)	TB4 +0.1	IU	00:08:39.936 (519.936)	TB4 +0.177	MSFC	--
111a	Signal from LVDC for: Prevalves Closed Off	00:08:37.0 (517.0)	TB3 +0.2	IU	00:08:40.028 (520.028)	TB4 +0.269	MSFC	--
111b	Signal Received in S-IVB for: Prevalves Closed Off	--	--	S-IVB	00:08:40.032 (520.032)	N/A	DAC(FM)	13
112a	Signal from LVDC for: S-IVB Engine Cutoff Off	00:08:37.1 (517.1)	TB4 +0.3	IU	00:08:40.120 (520.120)	TB4 +0.361	MSFC	--
112b	Signal Received in S-IVB for: S-IVB Engine Cutoff Off	--	--	S-IVB	00:08:40.123 (520.123)	N/A	DAC(FM)	13

*See notes at end of table

Section 4
Sequence of Events

TABLE 4-1 (Sheet 9 of 43)
FLIGHT SEQUENCE OF EVENTS

ITEM NO.	EVENT	PREDICTED TIME *		SIGNAL MONITORED AT	MONITORED TIME *		DATA SOURCE	ACCURACY* (ms)
		TIME FROM RANGE ZERO (hr:min:sec) (sec)	TIME FROM BASE (sec)		TIME FROM RANGE ZERO* (hr:min:sec) (sec)	TIME FROM BASE (sec)		
113a	Signal from LVDC for: Engine Ready Bypass	00:08:37.3 (517.3)	TB4 +0.5	IU	00:08:40.212 (520.212)	TB4 +0.453	MSFC	--
113b	Signal Received in S-IVB for: Engine Ready Bypass	--	--	S-IVB	00:08:40.214 (520.214)	N/A	DAC(FM)	13
114a	Signal from LVDC for: LOX Chilldown Pump Off	00:08:37.4 (517.4)	TB4 +0.6	IU	00:08:40.309 (520.309)	TB4 +0.550	MSFC	--
114b	Signal Received in S-IVB for: LOX Chilldown Pump Off	--	--	S-IVB	00:08:40.312 (520.312)	N/A	DAC(FM)	13
115a	Signal from LVDC for: Fire Ullage Ignition On	00:08:37.5 (517.5)	TB4 +0.7	IU	00:08:40.432 (520.432)	TB4 +0.673	MSFC	--
115b	Signal Received in S-IVB for: Fire Ullage Ignition On	--	--	S-IVB	00:08:40.435 (520.435)	N/A	DAC(FM)	13
116	Signal from LVDC for: S-II/S-IVB Separation	00:08:37.6 (517.6)	TB4 +0.8	IU	00:08:40.528 (520.528)	TB4 +0.770	MSFC	--
117	Ullage Thrust Buildup to 75 percent (Average)	--	--	--	00:08:40.5 (520.5)	N/A	DAC	--
118	S-II Retrorocket Thrust Buildup to 10 percent (Average)	--	--	--	00:08:40.57 (520.57)	N/A	MSFC	--
119	First Axial Separation Motion	00:08:37.675 (517.675)	N/A	N/A	00:08:40.600 (520.600)	N/A	MSFC	--
120	S-II Retrorocket Thrust Buildup to 90 percent (Average)	--	--	--	00:08:40.59 (520.59)	N/A	MSFC	--
121a	Signal from LVDC for: S-IVB Engine Start Interlock Bypass On	00:08:37.7 (517.7)	TB4 +0.9	IU	00:08:40.620 (520.620)	TB4 +0.861	MSFC	--
121b	Signal Received in S-IVB for: S-IVB Engine Start Interlock Bypass On	--	--	S-IVB	00:08:40.623 (520.623)	N/A	DAC(FM)	13
122a	Signal from LVDC for: S-IVB Engine Start On	00:08:37.8 (517.8)	TB4 +1.0	IU	00:08:40.713 (520.713)	TB4 +0.954	MSFC	--
122b	Signal Received in S-IVB for: S-IVB Engine Start On	--	--	S-IVB	00:08:40.717 (520.717)	N/A	DAC(FM)	13

*See notes at end of table

Section 4
Sequence of Events

TABLE 4-1 (Sheet 10 of 43)
FLIGHT SEQUENCE OF EVENTS

ITEM NO.	EVENT	PREDICTED TIME *		SIGNAL MONITORED AT	MONITORED TIME *		DATA SOURCE	ACCURACY* (ms)
		TIME FROM RANGE ZERO (hr:min:sec) (sec)	TIME FROM BASE (sec)		TIME FROM RANGE ZERO* (hr:min:sec) (sec)	TIME FROM BASE (sec)		
122c	<u>J-2 Engine Start Sequence</u>							
	1. Helium Control Solenoid Energized (Pickup)	--	--	S-IVB	00:08:40.717 (520.717)	--	DAC(PCM)	10
	2. Main Fuel Valve Closed (Dropout)	--	--	S-IVB	00:08:40.761 (520.761)	--	DAC(PCM)	10
	3. Main Fuel Valve Open (Pickup)	--	--	S-IVB	00:08:40.899 (520.899)	--	DAC(PCM)	10
	4. Gas Generator Valve Closed (Dropout)	--	--	S-IVB	00:08:43.997 (523.997)	--	DAC(PCM)	10
	5. Gas Generator Valve Open (Pickup)	--	--	S-IVB	00:08:44.727 (524.727)	--	DAC(PCM)	10
	6. Main Oxidizer Valve Leaves Closed Position (Dropout)	--	--	S-IVB	00:08:44.197 (524.197)	--	DAC(PCM)	10
	7. Start Tank Discharge Valve Open (Dropout)	--	--	S-IVB	00:08:24.278 (524.278)	--	DAC(PCM)	10
	8. Oxidizer Turbine Bypass Valve Open (Dropout)	--	--	S-IVB	00:08:24.375 (524.375)	--	DAC(PCM)	10
	9. Oxidizer Turbine Bypass Valve Closed (Drop Out)	--	--	S-IVB	00:08:40.939 (520.939)	--	DAC(PCM)	10
	10. Mainstage OK Pressure Switch No. 1 (Drop Out)	--	--	S-IVB	00:08:45.480 (525.480)	--	DAC(PCM)	10
	11. Mainstage OK Pressure Switch No. 2 (Pick Up)	--	--	S-IVB	00:08:45.540 (525.540)	--	DAC(PCM)	10
	12. Main Oxidizer Valve Reaches Open Position (Pick Up)	--	--	S-IVB	00:08:46.637 (526.637)	--	DAC(PCM)	10
	13. Gas Generator Spark System On (Drop Out)	--	--	S-IVB	00:08:47.402 (527.402)	--	DAC(PCM)	10
	14. Thrust Chamber Spark System On (Drop Out)	--	--	S-IVB	00:08:47.402 (527.402)	--	DAC(PCM)	10
123	Signal from LVDC for: Flight Control Computer S-IVB Burn Mode On "A"	00:08:38.0 (518.0)	TB4 +1.2	IU	00:08:40.924 (520.924)	TB4 +1.165	MSFC	--
124	Signal from LVDC for: Flight Control Computer S-IVB Burn Mode On "B"	00:08:38.1 (518.1)	TB4 +1.3	IU	00:08:41.020 (521.020)	TB4 +1.261	MSFC	--

*See notes at end of table

Section 4
Sequence of Events

TABLE 4-1 (Sheet 11 of 43)
FLIGHT SEQUENCE OF EVENTS

ITEM NO.	EVENT	PREDICTED TIME *		SIGNAL MONITORED AT	MONITORED TIME *		DATA SOURCE	ACCURACY* (ms)
		TIME FROM RANGE ZERO (hr:min:sec) (sec)	TIME FROM BASE (sec)		TIME FROM RANGE ZERO* (hr:min:sec) (sec)	TIME FROM BASE (sec)		
125	S-II J-2 Engine Thrust Decay to 5 percent (Average)	00:08:38.2 (518.2)	TB4 +1.3	N/A	00:08:40.2 (520.2)	N/A	MSFC	100
126	Signal from LVDC for: S-IVB Engine Out Indication Enable "A" On	00:08:38.4 (518.4)	TB4 +1.6	IU	00:08:41.314 (521.314)	TB4 +1.555	MSFC	--
127	Signal from LVDC for: S-IVB Engine Out Indication Enable "B" On	00:08:38.6 (518.6)	TB4 +1.8	IU	00:08:41.530 (521.530)	TB4 +1.771	MSFC	--
128	Separation Complete (217 in. Axial Clearance)	00:08:38.66 (518.66)	N/A	N/A	00:08:41.572 (521.572)	N/A	DAC	10
129a	Signal from LVDC for: Fuel Chill-down Pump Off	00:08:39.0 (519.0)	TB4 +2.2	IU	00:08:41.914 (521.914)	TB4 +2.155	MSFC	--
129b	Signal Received in S-IVB for: Fuel Chillo-down Pump Off	--	--	S-IVB	00:08:41.917 (521.917)	N/A	DAC(FM)	13
130a	Signal from LVDC for: LOX Tank Flight Pressure System On	00:08:40.6 (520.6)	TB4 +3.8	IU	00:08:43.514 (523.514)	TB4 +3.755	MSFC	--
130b	Signal Received in S-IVB for: LOX Tank Flight Pressure System On	--	--	S-IVB	00:08:43.518 (523.518)	N/A	DAC(FM)	13
131a	Signal from LVDC for: Fuel Injection Temperature OK Bypass	00:08:40.8 (520.8)	TB4 +4.0	IU	00:08:43.731 (523.731)	TB4 +3.972	MSFC	--
131b	Signal Received in S-IVB for: Fuel Injection Temperature OK Bypass	--	--	S-IVB	00:08:43.733 (523.733)	N/A	DAC(FM)	13
132a	Signal from LVDC for: Engine Start Off	00:08:41.0 (521.0)	TB4 +4.2	IU	00:08:43.911 (523.911)	TB4 +4.152	MSFC	--
132b	Signal Received in S-IVB for: Engine Start Off	--	--	S-IVB	00:08:43.912 (523.912)	N/A	DAC(FM)	13
133	J-2 Thrust Buildup - 10 percent	--	--	N/A	00:08:44.745 (524.745)	N/A	DAC	10
134a	Signal from LVDC for: First Burn Relay On	00:08:42.6 (522.6)	TB4 +5.8	IU	00:08:45.509 (525.509)	TB4 +5.750	MSFC	--
134b	Signal Received in S-IVB for: First Burn Relay On	--	--	S-IVB	00:08:45.515 (525.515)	N/A	DAC(FM)	13

*See notes at end of table

Section ,
Sequence of Events

TABLE 4-1 (Sheet 12 of 43)
FLIGHT SEQUENCE OF EVENTS

ITEM NO.	EVENT	PREDICTED TIME*		SIGNAL MONITORED AT	MONITORED TIME*		DATA SOURCE	ACCURACY* (ms)
		TIME FROM RANGE ZERO (hr:min:sec) (sec)	TIME FROM BASE (sec)		TIME FROM RANGE ZERO* (hr:min:sec) (sec)	TIME FROM BASE (sec)		
135	Guidance Initiation	00:08:42.8 (522.8)	N/A	IU	00:08:47.654 (527.654)	--	MSFC	--
136	Start Artificial Tau Mode	00:08:42.8 (522.8)	N/A	IU	00:08:47.654 (527.654)	--	MSFC	--
137	J-2 Thrust Buildup - 90 percent	00:08:43.3 (523.3)	N/A	N/A	00:08:46.229 (526.229)	N/A	MSFC	--
138a	Signal from LVDC for: Emergency Playback Enable On	00:08:44.6 (524.6)	TB4 +7.8	IU	00:08:47.521 (527.521)	TB4 +7.762	MSFC	--
138b	Signal Received in S-IVB for: Emergency Playback Enable On	--	--	S-IVB	00:08:47.528 (527.528)	N/A	DAC(FM)	13
139a	Signal from LVDC for: Fast Record Off	00:08:44.8 (524.8)	TB4 +8.0	IU	00:08:47.708 (527.708)	TB4 +7.949	MSFC	--
139b	Signal Received in S-IVB for: Fast Record Off	--	--	S-IVB	00:08:47.712 (527.712)	N/A	DAC(FM)	13
140a	Signal from LVDC for: PU Activate On	00:08:45.8 (525.8)	TB4 +9.0	IU	00:08:48.709 (528.709)	TB4 +8.950	MSFC	--
140b	Signal Received in S-IVB for: PU Activate On	--	--	S-IVB	00:08:48.712 (528.712)	N/A	DAC(FM)	13
141a	Signal from LVDC for: Charge Ullage Jettison On	00:08:47.1 (527.1)	TB4 +10.3	IU	00:08:50.018 (530.018)	TB4 +10.259	MSFC	--
141b	Signal Received in S-IVB for: Charge Ullage Jettison On	--	--	S-IVB	00:08:50.022 (530.022)	N/A	DAC(FM)	13
142a	Signal from LVDC for: Fire Ullage Jettison On	00:08:49.6 (529.6)	TB4 +12.8	IU	00:08:52.525 (532.525)	TB4 +12.766	MSFC	--
142b	Signal Received in S-IVB for: Fire Ullage Jettison On	--	--	S-IVB	00:08:52.531 (532.531)	N/A	DAC(FM)	13
143	Stop Artificial Tau Mode	00:08:49.8 (529.8)	N/A	IU	00:08:56.054 (536.054)	N/A	MSFC	-
144a	Signal from LVDC for: Ullage Charging Reset	00:08:52.9 (532.9)	TB4 +16.1	IU	00:08:55.810 (535.810)	TB4 +16.050	MSFC	--
144b	Signal Received in S-IVB for: Ullage Charging Reset	--	--	S-IVB	00:08:55.815 (535.815)	N/A	DAC(FM)	13
145a	Signal from LVDC for: Ullage Firing Reset	00:08:53.1 (533.1)	TB4 +16.3	IU	00:08:56.024 (536.024)	TB4 +16.264	MSFC	--
145b	Signal Received in S-IVB for: Ullage Firing Reset	--	--	S-IVB	00:08:56.038 (536.038)	N/A	DAC(FM)	13

*See notes at end of table

Section 4
Sequence of Events

TABLE 4-1 (Sheet 13 of 43)
FLIGHT SEQUENCE OF EVENTS

ITEM NO.	EVENT	PREDICTED TIME*		SIGNAL MONITORED AT	MONITORED TIME*		DATA SOURCE	ACCURACY* (ms)
		TIME FROM RANGE ZERO (hr:min:sec) (sec)	TIME FROM PASE (sec)		TIME FROM RANGE ZERO* (hr:min:sec) (sec)	TIME FROM BASE (sec)		
146	S-IVB PU Valve Reaches Hardover Position	00:08:54.5 (534.5)	N/A	N/A	00:08:50.7 (530.7)	N/A	DAC	13
147	Signal from LVDC for: IU Tap Recorder Record Off	00:08:55.7 (535.7)	TB4 +18.9	IU	00:08:58.611 (538.611)	TB4 +18.859	MSFC	--
148a	Signal from LVDC for: Emergency Playback Enable Off	00:08:58.1 (538.1)	TB4 +21.3	IU	00:09:01.009 (541.009)	TB4 +21.250	MSFC	--
148b	Signal Received in S-IVB for: Emergency Playback Enable Off	--	--	S-IVB	00:09:01.012 (541.012)	N/A	DAC(FM)	13
149	S-IC Impact	00:08:58.42 (538.42)	N/A	N/A	00:08:56.95 (536.95)	N/A	MSFC	--
150	Signal from LVDC for: Telemetry Calibrator Inflight Calibrate On	00:08:59.2 (539.2)	TB4 +22.4	IU	00:09:02.111 (542.111)	TB4 +22.352	MSFC	--
151	Signal from LVDC for: Telemetry Calibrator Inflight Calibrate Off	00:09:04.2 (540.2)	TB4 +27.4	IU	00:09:07.110 (547.110)	TB4 +27.351	MSFC	--
152a	Signal from LVDC for: Regular Calibrate Relays On	00:09:08.6 (548.6)	TB4 +31.8	IU	00:09:11.509 (551.509)	TB4 +31.750	MSFC	--
152b	Signal Received in S-IVB for: Regular Calibrate Relays On	--	--	S-IVB	00:09:11.512 (551.512)	N/A	DAC(FM)	13
153a	Signal from LVDC for: Regular Calibrate Relays Off	00:09:13.6 (553.6)	TB4 +36.8	IU	00:09:16.509 (556.509)	TB4 +36.750	MSFC	--
153b	Signal Received in S-IVB for: Regular Calibrate Relays Off	--	--	S-IVB	00:09:16.512 (556.512)	N/A	DAC(FM)	13
154	Introduction of Chi Tilde Guidance Mode	00:10:21.4 (621.4)	N/A	IU	00:10:32.250 (632.250)	N/A	MSFC	--
155a	Signal from LVDC for: Chillover Shutoff Pilot Valve Closed On	00:10:22.1 (622.1)	TB4 +105.3	IU	00:10:25.011 (625.011)	TB4 +105.250	MSFC	--
155b	Signal Received in S-IVB for: Chillover Shutoff Pilot Valve	--	--	S-IVB	00:10:25.019 (625.019)	N/A	DAC(FM)	13
156	Freeze Body Attitude (Chi Freeze)	00:10:49.4 (649.4)	N/A	IU	00:10:57.911 (657.911)	N/A	MSFC	--
157a	Signal from LVDC for: Engine Pump Purge Control Valve Enable On	00:10:50.5 (650.5)	TB5 -7.0	IU	00:10:53.679 (658.679)	TB5 -7.205	MSFC	--

*See notes at end of table

Section 4
Sequence of Events

TABLE 4-1 (Sheet 14 of 13)
FLIGHT SEQUENCE OF EVENTS

ITEM NO.	EVENT	PREDICTED TIME*		SIGNAL MONITORED AT	MONITORED TIME*		DATA SOURCE	ACCURACY* (ms)
		TIME FROM RANGE ZERO (hr:min:sec) (sec)	TIME FROM BASE (sec)		TIME FROM RANGE ZERO* (hr:min:sec) (sec)	TIME FROM BASE (sec)		
157b	Signal Received in S-IVB for: Engine Pump Purge Control Valve Enable On	--	--	S-IVB	00:10:58.683 (658.683)	N/A	DAC(FM)	13
158a	Signal from LVDC for: S-IVB Engine Cutoff (Guidance Cutoff)	00:10:56.6 (656.6)	N/A	IU	00:11:05.631 (665.631)	N/A	MSFC	--
158b	Signal Received in S-IVB for: S-IVB Engine Cutoff (Guidance Cutoff)	--	--	S-IVB	00:11:05.639 (665.639)	N/A	DAC(FM)	13
158c	<u>Time Base 5</u> LVDC Initiates TB5	00:10:56.6 (656.6)	TB5 +0.0	IU	00:11:05.884 (665.884)	TB5 +0.0	MSFC	--
158d	LVDC Sends Redundant Signal for: S-IVB Engine Cutoff	--	--	IU	00:11:05.967 (665.967)	TB5 +0.083	MSFC	--
158e	Signal Received in S-IVB for: S-IVB Engine Cutoff (Redundant Signal)	--	--	S-IVB	00:11:05.974 (665.974)	N/A	DAC(FM)	13
159a	Signal from LVDC for: Point Level Sensor Disarming	00:10:56.7 (656.7)	TB5 +0.1	IU	00:11:06.060 (666.060)	TB5 +0.176	MSFC	--
159b	Signal Received in S-IVB for: Point Level Sensor Disarming	--	--	S-IVB	00:11:06.067 (666.067)	N/A	DAC(FM)	13
160	S-IVB J-2 Thrust Decay to 5 Percent (Average)	--	N/A	N/A	00:11:06.076 (666.076)	N/A	DAC	10
161a	Signal from LVDC for: S-IVB Ullage Engine No. 1 On	00:10:56.9 (656.9)	TB5 +0.3	IU	00:11:06.150 (666.150)	TB5 +0.266	MSFC	--
161b	Signal Received in S-IVB for: S-IVB Ullage Engine No. 1 On	--	--	S-IVB	00:11:06.158 (666.158)	N/A	DAC(FM)	13
162a	Signal from LVDC for: S-IVB Ullage Engine No. 2 On	00:10:57.0 (657.0)	TB5 +0.4	IU	00:11:06.271 (666.271)	TB5 +0.387	MSFC	--
162b	Signal Received in S-IVB for: S-IVB Ullage Engine No. 2 On	--	--	S-IVB	00:11:06.278 (666.278)	N/A	DAC(FM)	13
163	Signal from LVDC for: Ullage Thrust Present On	00:10:57.2 (657.2)	TB5 +0.6	IU	00:11:06.443 (666.443)	TB5 +0.559	MSFC	--
164a	Signal from LVDC for: First Burn Relay Off	00:10:57.3 (657.3)	TB5 +0.7	IU	00:11:06.568 (666.568)	TB5 +0.684	MSFC	--
164b	Signal Received in S-IVB for: First Burn Relay Off	--	--	S-IVB	00:11:06.575 (666.575)	N/A	DAC(FM)	13
165a	Signal from LVDC for: PU Activate Off	00:10:57.5 (657.5)	TB5 +0.9	IU	00:11:06.735 (666.735)	TB5 +0.851	MSFC	--
165b	Signal Received in S-IVB for: PU Activate Off	--	--	S-IVB	00:11:06.742 (666.742)	N/A	DAC(FM)	13

*See notes at end of table

Section 4
Sequence of Events

TABLE 4-1 (Sheet 15 of 43)
FLIGHT SEQUENCE OF EVENTS

ITEM NO.	EVENT	PREDICTED TIME*		SIGNAL MONITORED AT	MONITORED TIME*		DATA SOURCE	ACCURACY* (ms)
		TIME FROM RANGE ZERO (hr:min:sec) (sec)	TIME FROM BASE (sec)		TIME FROM RANGE ZERO* (hr:min:sec) (sec)	TIME FROM BASE (sec)		
166a	Signal from LVDC for: Prevalves Closed On	00:10:57.6 (657.6)	TB5 +1.0	IU	00:11:06.833 (666.833)	TB5 +0.949	MSFC	--
166b	Signal Received in S-IVB for: Prevalves Closed On	--	--	S-IVB	00:11:06.841 (666.841)	N/A	DAC(FM)	13
167a	Signal from LVDC for: LOX Tank Flight Pressure System Off	00:10:57.7 (657.7)	TB5 +1.1	IU	00:11:06.934 (666.934)	TB5 +1.050	MSFC	--
167b	Signal Received in S-IVB for: LOX Tank Flight Pressure System Off	--	--	S-IVB	00:11:06.941 (666.941)	N/A	DAC(FM)	13
168a	Signal from LVDC for: Coast Period On	00:10:57.9 (657.9)	TB5 +1.3	IU	00:11:07.141 (667.141)	TB5 +1.257	MSFC	--
168b	Signal Received in S-IVB for: Coast Period On	--	--	S-IVB	00:11:07.148 (667.148)	N/A	DAC(FM)	13
169a	Signal from LVDC for: Engine Dump Purge Control Valve Enable On	00:10:58.1 (658.1)	TB5 +1.5	IU	00:11:07.355 (667.355)	TB5 +1.471	MSFC	--
169b	Signal Received in S-IVB for: Engine Dump Purge Control Valve Enable On	--	--	S-IVB	00:11:07.361 (667.361)	N/A	DAC(FM)	13
170a	Signal from LVDC for: PU Fuel Boiloff Bias Cutoff On	00:10:58.3 (658.3)	TB5 +1.7	IU	00:11:07.535 (667.535)	TB5 +1.651	MSFC	--
170b	Signal Received in S-IVB for: PU Fuel Boiloff Bias Cutoff On	--	--	S-IVB	00:11:07.542 (667.542)	N/A	DAC(FM)	13
171	Signal from LVDC for: Flight Control Computer S-IVB Burn Mode Off "B"	00:11:59.9 (659.9)	TB5 +3.3	IU	00:11:09.134 (669.134)	TB5 +3.250	MSFC	--
172	Signal from LVDC for: Flight Control Computer S-IVB Burn Mode Off	00:11:00.1 (660.1)	TB5 +3.5	IU	00:11:09.349 (669.349)	TB5 +3.465	MSFC	--
173a	Signal from LVDC for: Aux Hydraulic Pump Coast Mode On	00:11:00.3 (660.3)	TB5 +3.7	IU	00:11:09.534 (669.534)	TB5 +3.650	MSFC	--
173b	Signal Received in S-IVB for: Aux Hydraulic Pump Coast Mode On	--	--	S-IVB	00:11:09.542 (669.542)	N/A	DAC(FM)	13
174a	Signal from LVDC for: Aux Hydraulic Pump Flight Mode Off	00:11:00.5 (660.5)	TB5 +3.9	IU	00:11:09.742 (669.742)	TB5 +3.858	MSFC	--

*See notes at end of table

Section 4
Sequence of Events

TABLE 4-1 (Sheet 16 of 43)
FLIGHT SEQUENCE OF EVENTS

ITEM NO.	EVENT	PREDICTED TIME*		SIGNAL MONITORED AT	MONITORED TIME*		DATA SOURCE	ACCURACY (ms)
		TIME FROM RANGE ZERO (hr:min:sec) (sec)	TIME FROM BASE (sec)		TIME FROM RANGE ZERO* (hr:min:sec) (sec)	TIME FROM BASE (sec)		
174b	Signal Received in S-IVB for: Aux Hydraulic Pump Flight Mode Off	--	--	S-IVB	00:11:09.749 (669.749)	N/A	DAC(FM)	13
175	Signal from LVDC for: S-IVB Engine Out Indication "A" Enable Reset	00:11:06.6 (666.6)	TB5 +10.0	IU	00:11:15.855 (675.855)	TB5 +9.971	MSFC	--
176	Signal from LVDC for: S-IVB Engine Out Indication "B" Enable Reset	00:11:06.8 (666.8)	TB5 +10.2	IU	00:11:16.036 (676.036)	TB5 +10.152	MSFC	--
177	Indicate Pitch Maneuver (end of Chi Freeze)	00:11:11.6 (671.6)	N/A	IU	00:11:21.278 (681.278)	N/A	MSFC	--
178a	Signal from LVDC for: SSB Transmitter Group Off	00:11:18.8 (678.8)	TB5 +22.2	IU	00:11:23.034 (688.34)	TB5 +22.150	MSFC	--
178b	Signal Received in S-IVB for: SSB Transmitter Group Off	--	--	S-IVB	00:11:28.042 (688.042)	N/A	DAC(FM)	13
179a	Signal from LVDC for: SSB Group Off	00:11:19.0 (679.0)	TB5 +22.4	IU	00:11:28.262 (688.262)	TB5 +22.378	MSFC	--
179b	Signal Received in S-IVB for: SSB Group Off	--	--	S-IVB	00:11:28.253 (688.253)	N/A	DAC(FM)	13
180a	Signal from LVDC for: Continuous Vent Pilot Valve Open On	00:11:55.6 (715.6)	TB5 +59.0	IU	00:12:04.833 (724.833)	TB5 +58.949	MSFC	--
180b	Signal Received in S-IVB for: Continuous Vent Pilot Valve Oper On	--	--	S-IVB	00:12:04.842 (724.842)	N/A	DAC(FM)	13
181	Signal from LVDC for: Telemetry Calibrator Inflight Calibrate On	00:11:56.2 (716.2)	TB5 +59.6	IU	00:12:05.434 (725.434)	TB5 +59.550	MSFC	--
182a	Signal from LVDC for: Prevalves Close Off	00:11:57.1 (717.1)	TB5 +60.5	IU	00:12:06.338 (726.338)	TB5 +60.454	MSFC	--
182b	Signal Received in S-IVB for: Prevalves Closed Off	--	--	S-IVB	00:12:06.345 (726.345)	N/A	DAC(FM)	13
183a	Signal from LVDC for: Chillover Shutdown Pilot Valve Close Off	00:11:57.3 (717.3)	TB5 +60.7	IU	00:12:06.555 (726.555)	TB5 +60.671	MSFC	--
183b	Signal Received in S-IVB for: Chillover Shutdown Pilot Valve Closed Off	--	--	S-IVB	00:12:06.563 (726.563)	N/A	DAC(FM)	13
184a	Signal from LVDC for: Continuous Vent Pilot Valve Open Off	00:11:57.6 (717.6)	TB5 +61.0	IU	00:12:06.852 (726.852)	TB5 +60.968	MSFC	--

*See notes at end of table

Section 4
Sequence of Events

TABLE 4-1 (Sheet 17 of 43)
FLIGHT SEQUENCE OF EVENTS

ITEM NO.	EVENT	PREDICTED TIME *		SIGNAL MONITORED AT	MONITORED TIME *		DATA SOURCE	ACCURACY* (ms)
		TIME FROM RANGE ZERO (hr:min:sec) (sec)	TIME FROM BASE (sec)		TIME FROM RANGE ZERO* (hr:min:sec) (sec)	TIME FROM BASE (sec)		
184b	Signal Received in S-IVB for: Continuous Vent Pilot Valve Open Off	--	--	S-IVB	00:12:06.861 (726.861)	N/A	DAC(FM)	13
185	Signal from LVDC for: Telemetry Calibrator Inflight Calibrate Off	00:12:01.2 (721.2)	TB5 +64.6	IU	00:12:10.435 (730.435)	TB5 +64.551	MSFC	--
186a	Signal from LVDC for: S-IVB Ullage Engine No. 1 Off	00:12:24.6 (744.6)	TB5 +88.0	IU	00:12:33.836 (753.836)	TB5 +87.952	MSFC	--
186b	Signal Received in S-IVB for: Ullage Engine No. 1 Off	--	--	S-IVB	00:12:33.844 (753.844)	N/A	DAC(FM)	13
187a	Signal from LVDC for: S-IVB Ullage Engine No. 2 Off	00:12:24.7 (744.7)	TB5 +88.1	IU	00:12:33.936 (753.936)	TB5 +88.052	MSFC	--
187b	Signal Received in S-IVB for: S-IVB Ullage Engine No. 2 Off	--	--	S-IVB	00:12:33.941 (753.941)	N/A	DAC(FM)	13
188	Signal from LVDC for: S-IVB Ullage Thrust Present Off	00:12:24.9 (744.9)	TB5 +88.3	IU	00:12:24.143 (754.143)	TB5 +88.259	MSFC	--
189a	Signal from LVDC for: Emergency Playback Enable On	00:12:34.9 (754.9)	TB5 +98.3	IU	00:12:44.140 (764.140)	TB5 +98.256	MSFC	--
189b	Signal Received in S-IVB for: Emergency Playback Enable On	--	--	S-IVB	00:12:44.156 (764.156)	N/A	DAC(FM)	13
190	Signal from LVDC for: Tape Recorder Playback Reverse On	00:12:39.1 (759.1)	TB5 +102.5	IU	00:12:47.329 (767.329)	TB5 +102.551	MSFC	--
191	Signal from LVDC for: Tape Recorder Playback Reverse Off	00:14:04.1 (844.1)	TB5 +187.5	IU	--	--	--	--
192a	Signal from LVDC for: Emergency Playback Enable Off	00:14:04.9 (844.9)	TB5 +188.3	IU	--	--	--	--
192b	Signal Received in S-IVB for: Emergency Playback Enable Off	--	--	S-IVB	00:14:14.140 (854.140)	N/A	DAC(FM)	13
193a	Signal from LVDC for: Slow Record On	00:15:44.0 (944.9)	TB5 +288.3	IU	--	--	--	--
193b	Signal Received in S-IVB for: Slow Record On	--	--	S-IVB	00:15:54.140 (954.140)	N/A	DAC(FM)	13

*See notes at end of table

Section 4
Sequence of Events

TABLE 4-1 (Sheet 18 of 43)
FLIGHT SEQUENCE OF EVENTS

ITEM NO.	EVENT	PREDICTED TIME*		SIGNAL MONITORED AT	MONITORED TIME*		DATA SOURCE	ACCURACY* (ms)
		TIME FROM RANGE ZERO (hr:min:sec) (sec)	TIME FROM BASE (sec)		TIME FROM RANGE ZERO* (hr:min:sec) (sec)	TIME FROM BASE (sec)		
194a	Signal from LVDC for: Slow Record On	00:15:47.9 (947.9)	TB5 +291.3	IU	--	--	--	--
194b	Signal Received in S-IVB for: Slow Record On	--	--	S-IVB	00:15:57.170 (957.130)	N/A	DAC(FM)	13
195	S-II Impact	00:19:14.18 (1154.18)	N/A	N/A	00:20:38.40 (1238.40)	N/A	MSFC	--
196a	Signal from LVDC for: Engine Pump Purge Control Valve Enable Off	00:20:59.2 (1259.2)	TB5 +602.6	IU	00:21:08.433 (1268.433)	TB5 +602.549	MSFC	--
196b	Signal Received in S-IVB for: Engine Pump Purge Control Valve Enable Off	--	--	S-IVB	00:21:08.440 (1268.440)	N/A	DAC(FM)	13
197a	Signal from LVDC for: Slow Record On	00:37:02.9 (2222.9)	TB5 +1566.3	IU	00:37:12.134 (2232.134)	TB5 +1566.250	MSFC	--
197b	Signal Received in S-IVB for: Slow Record On	--	--	S-IVB	00:37:12.130 (2232.130)	N/A	DAC(FM)	13
198a	Signal from LVDC for: Slow Record Off	00:37:34.9 (2254.9)	TB5 +1598.3	IU	00:37:44.134 (2264.134)	TB5 +1598.250	MSFC	--
198b	Signal Received in S-IVB for: Slow Record Off	--	--	S-IVB	00:37:44.150 (2264.150)	N/A	DAC(FM)	13
199a	Signal from LVDC for: Recorder Playback On	00:37:35.1 (2235.1)	TB5 +1593.5	IU	00:37:44.334 (2254.334)	TB5 +1593.450	MSFC	--
199b	Signal Received in S-IVB for: Recorder Playback On	--	--	S-IVB	00:37:44.350 (2264.350)	N/A	DAC(FM)	13
200a	Signal from LVDC for: Recorder Playback Off	00:40:21.1 (2420.1)	TB5 +1763.5	IU	00:40:29.334 (2429.334)	TB5 +1763.450	MSFC	--
200b	Signal Received in S-IVB for: Recorder Playback Off	--	--	S-IVB	00:40:29.350 (2429.350)	N/A	DAC(FM)	13
201a	Signal from LVDC for: Slow Record On	00:41:41.9 (2501.9)	TB5 +1845.3	IU	00:41:51.134 (2511.134)	TB5 +1845.250	MSFC	--
201b	Signal received in S-IVB for: Slow Record On	--	--	S-IVB	00:41:51.140 (2511.140)	N/A	DAC(FM)	13
202a	Signal from LVDC for: Slow Record On	00:41:44.9 (2504.9)	TB5 +1848.3	IU	00:41:54.134 (2514.134)	TB5 +1848.250	MSFC	--
202b	Signal Received in S-IVB for: Slow Record On	--	--	S-IVB	00:41:54.130 (2514.130)	N/A	DAC(FM)	13
203a	Signal from LVDC for: Telemetry Calibrator Inflight Calibrate On	00:51:46.9 (3106.9)	TB5 +2450.3	IU	00:51:56.134 (3116.134)	TB5 +2450.250	MSFC	--
204a	Signal from LVDC for: Special Calibrate Relays On	00:51:47.1 (3107.1)	TB5 +2450.5	IU	00:51:56.335 (3116.335)	TB5 +2450.451	MSFC	--

*See notes at end of table

Section 4
Sequence of Events

TABLE 4-1 (Sheet 19 of 43)
FLIGHT SEQUENCE OF EVENTS

ITEM NO.	EVENT	PREDICTED TIME*		SIGNAL MONITORED AT	MONITORED TIME*		DATA SOURCE	ACCURACY (ms)
		TIME FROM RANGE ZERO (hr:min:sec) (sec)	TIME FROM BASE (sec)		TIME FROM RANGE ZERO* (hr:min:sec) (sec)	TIME FROM BASE (sec)		
204b	Signal received in S-IVB for: Special Calibrate Relays On	--	--	S-IVB	00:51:56.350 (3116.350)	N/A	DAC(FM)	13
205a	Signal from LVDC for: Regular Calibrate Relays On	00:51:47.3 (3107.3)	TB5 +2450.7	IU	00:51:56.535 (3116.535)	TB5 +2450.651	MSFC	--
205b	Signal Received in S-IVB for: Regular Calibrate Relays On	--	--	S-IVB	00:51:56.550 (3116.550)	N/A	DAC(FM)	13
206	Signal from LVDC for: Telemetry Calibrator Inflight Calibrate Off	00:51:52.1 (3112.1)	TB5 +2455.5	IU	00:52:01.334 (3121.334)	TB5 +2455.450	MSFC	--
207a	Signal from LVDC for: Regular Calibrate Relays Off	00:51:52.3 (3112.3)	TB5 +2455.7	IU	00:52:01.534 (3121.534)	TB5 +2455.650	MSFC	--
207b	Signal Received in S-IVB for: Regular Calibrate Relays Off	--	--	S-IVB	00:52:01.540 (3121.540)	N/A	DAC(FM)	13
208a	Signal from LVDC for: Special Calibrate Relays Off	00:51:52.5 (3112.5)	TB5 +2455.9	IU	00:52:01.735 (3121.735)	TB5 +2455.851	MSFC	--
208b	Signal Received in S-IVB for: Special Calibrate Relays Off	--	--	S-IVB	00:52:01.730 (3121.730)	N/A	DAC(FM)	13
209	Signal from LVDC for: Telemetry Calibrator Inflight Calibrate On	01:27:56.1 (5270.1)	TB5 +4613.5	IU	01:27:59.334 (5279.334)	TB5 +4613.450	MSFC	--
210a	Signal from LVDC for: Slow Record On	01:27:50.3 (5270.3)	TB5 +4613.7	IU	01:27:59.534 (5279.534)	TB5 +4613.650	MSFC	--
210b	Signal Received in S-IVB for: Slow Record On	--	--	S-IVB	01:27:59.450 (5279.450)	N/A	DAC(FM)	13
211a	Signal from LVDC for: Special Calibrate Relays On	01:27:50.5 (5270.5)	TB5 +4613.9	IU	01:27:59.734 (5279.734)	TB5 +4613.850	MSFC	--
211b	Signal Received in S-IVB for: Special Calibrate Relays On	--	--	S-IVB	01:27:59.650 (5279.650)	N/A	DAC(FM)	13
212a	Signal from LVDC for: Regular Calibrate Relays On	01:27:50.7 (5270.7)	TB5 +4614.1	IU	01:27:59.934 (5279.934)	TB5 +4614.050	MSFC	--
212b	Signal Received in S-IVB for: Regular Calibrate Relays On	--	--	S-IVB	01:27:59.875 (5279.875)	N/A	DAC(FM)	13
213	Signal from LVDC for: Telemetry Calibrator Inflight Calibrate Off	01:27:55.1 (5275.1)	TB5 +4618.5	IU	01:28:04.334 (5284.334)	TB5 +4618.450	MSFC	--
214a	Signal from LVDC for: Regular Calibrate Relays Off	01:27:55.7 (5275.7)	TB5 +4619.1	IU	01:28:04.934 (5284.934)	TB5 +4619.050	MSFC	--

*See notes at end of table

Section 4
Sequence of Events

TABLE 4-1 (Sheet 20 of 43)
FLIGHT SEQUENCE OF EVENTS

ITEM NO.	EVENT	PREDICTED TIME *		SIGNAL MONITORED AT	MONITORED TIME *		DATA SOURCE	ACCURACY* (ms)
		TIME FROM RANGE ZERO (hr:min:sec) (sec)	TIME FROM BASE (sec)		TIME FROM RANGE ZERO* (hr:min:sec) (sec)	TIME FROM BASE (sec)		
214b	Signal Received in S-IVB for: Regular Calibrate Relays Off	--	--	S-IVB	01:28:04.625 (5284.625)	N/A	DAC(FM)	13
215a	Signal from LVDC for: Special Calibrate Relays Off	01:27:55.9 (5275.9)	TB5 +4619.3	IU	01:28:04.934 (5284.934)	TB5 +4619.050	MSFC	--
215b	Signal Received in S-IVB for: Special Calibrate Relays Off	--	--	S-IVB	01:28:04.875 (5284.875)	N/A	DAC(FM)	13
216a	Signal from LVDC for: Slow Record Off	01:28:22.3 (5302.3)	TB5 +4645.7	IU	01:28:31.534 (5311.534)	TB5 +4645.650	MSFC	--
216b	Signal Received in S-IVB for: Slow Record Off	--	--	S-IVB	01:28:31.550 (5311.550)	N/A	DAC(FM)	13
217a	Signal from LVDC for: Recorder Playback On	01:28:22.5 (5302.5)	TB5 +4645.9	IU	01:28:31.734 (5311.734)	TB5 +4645.850	MSFC	--
217b	Signal Received in S-IVB for: Recorder Playback On	--	--	S-IVB	01:28:31.780 (5311.780)	N/A	DAC(FM)	13
218a	Signal from LVDC for: Recorder Playback Off	01:34:12.7 (5652.7)	TB5 +4996.1	IU	01:34:21.934 (5661.934)	TB5 +4996.050	MSFC	--
218b	Signal Received in S-IVB for: Recorder Playback Off	--	--	S-IVB	01:34:21.950 (5661.950)	N/A	DAC(FM)	13
219a	Signal from LVDC for: Slow Record On	01:34:12.9 (5652.9)	TB5 +4996.3	IU	01:34:22.134 (5662.134)	TB5 +4996.250	MSFC	--
219b	Signal Received in S-IVB for: Slow Record On	--	--	S-IVB	01:34:22.150 (5662.150)	N/A	DAC(FM)	13
220a	Signal from LVDC for: Slow Record On	01:34:15.5 (5655.9)	TB5 +4999.3	IU	01:34:25.134 (5665.134)	TB5 +4999.250	MSFC	--
220b	Signal Received in S-IVB for: Slow Record On	--	--	S-IVB	01:34:25.160 (5665.160)	N/A	DAC(FM)	13
221	Signal from LVDC for: Telemetry Calibrator Inflight Calibrate On	01:44:09.7 (6309.7)	TB5 +5653.1	IU	01:45:18.951 (6318.951)	TB5 +5653.067	MSFC	--
222a	Signal from LVDC for: Special Calibrate Relays On	01:45:09.9 (6309.9)	TB5 +5653.3	IU	01:45:19.141 (6319.141)	TB5 +5653.257	MSFC	--
222b	Signal Received in S-IVB for: Special Calibrate Relays On	--	--	S-IVB	01:45:19.190 (6319.190)	N/A	DAC(FM)	13
223a	Signal from LVDC for: Regular Calibrate Relays On	01:45:10.1 (6310.1)	TB5 +5653.5	IU	01:45:19.354 (6319.354)	TB5 +5653.470	MSFC	--
223b	Signal Received in S-IVB for: Regular Calibrate Relays On	--	--	S-IVB	01:45:19.360 (6319.360)	N/A	DAC(FM)	13
224	Signal from LVDC for: Telemetry Calibrator Inflight Calibrate Off	01:45:14.7 (6314.7)	TB5 +5658.1	IU	01:45:23.934 (6323.934)	TB5 +5658.050	MSFC	--

*See notes at end of table

Section 4
Sequence of Events

TABLE 4-1 (Sheet 21 of 43)
FLIGHT SEQUENCE OF EVENTS

ITEM NO.	EVENT	PREDICTED TIME*		SIGNAL MONITORED AT	MONITORED TIME*		DATA SOURCE	ACCURACY* (ms)
		TIME FROM RANGE ZERO (hr:min:sec) (sec)	TIME FROM BASE (sec)		TIME FROM RANGE ZERO* (hr:min:sec) (sec)	TIME FROM BASE (sec)		
225a	Signal from LVDC for: Regular Calibrate Relays Off	01:45:15.1 (6315.1)	TB5 +5658.5	IU	01:45:24.334 (6324.334)	TB5 +5658.450	MSFC	--
225b	Signal Received in S-IVB for: Regular Calibrate Relays Off	--	--	S-IVB	01:45:24.380 (6324.380)	N/A	DAC(FM)	13
226a	Signal from LVDC for: Special Calibrate Relays Off	01:45:15.3 (6315.3)	TB5 +5658.7	IU	01:45:24.534 (6324.534)	TB5 +5658.650	MSFC	--
226b	Signal Received in S-IVB for: Special Calibrate Relays Off	--	--	S-IVB	01:45:24.580 (6324.580)	N/A	DAC(FM)	13
227a	Signal from LVDC for: Slow Record On	02:08:43.9 (7723.9)	TB5 +7067.3	IU	--	--	--	--
227b	Signal Received in S-IVB for: Slow Record On	--	--	S-IVB	--	--	--	--
228a	Signal from LVDC for: Slow Record Off	02:09:15.3 (7755.9)	TB5 +7099.3	IU	--	--	--	--
228b	Signal Received in S-IVB for: Slow Record Off	--	--	S-IVB	--	--	--	--
229a	Signal from LVDC for: Recorder Playback On	02:09:16.1 (7756.1)	TB5 +7099.5	IU	--	--	--	--
229b	Signal Received in S-IVB for: Recorder Playback On	--	--	S-IVB	--	--	--	--
230a	Signal from LVDC for: Recorder Playback Off	02:13:19.9 (7999.9)	TB5 +7343.3	IU	02:13:29.134 (8009.134)	TB5 +7343.250	MSFC	--
230b	Signal Received in S-IVB for: Recorder Playback Off	--	--	S-IVB	02:13:29.150 (8009.150)	N/A	DAC(FM)	13
231a	Signal from LVDC for: Slow Record On	02:13:20.1 (8000.1)	TB5 +7343.5	IU	02:13:29.334 (8009.334)	TB5 +7343.450	MSFC	--
231b	Signal Received in S-IVB for: Slow Record On	--	--	S-IVB	02:13:29.350 (8009.350)	N/A	DAC(FM)	13
232a	Signal from LVDC for: Slow Record On	02:13:23.1 (8003.1)	TB5 +7346.5	IU	02:13:32.334 (8012.334)	TB5 +7346.450	MSFC	--
232b	Signal Received in S-IVB for: Slow Record On	--	--	S-IVB	02:13:32.350 (8012.350)	N/A	DAC(FM)	13
233a	Signal from LVDC for: Special Calibrate Relays On	02:24:35.9 (8675.9)	TB5 +8019.3	IU	02:24:45.134 (8685.134)	TB5 +8019.250	MSFC	--
233b	Signal Received in S-IVB for: Special Calibrate Relays On	--	--	S-IVB	02:24:45.038 (8685.038)	N/A	DAC(FM)	13
234a	Signal from LVDC for: Regular Calibrate Relay On	02:24:36.1 (8676.1)	TB5 +8019.5	IU	02:24:45.334 (8685.334)	TB5 +8019.450	MSFC	--

*See notes at end of table

Section 4
Sequence of Events

TABLE 4-1 (Sheet 22 of 43)
FLIGHT SEQUENCE OF EVENTS

ITEM NO.	EVENT	PREDICTED TIME*		SIGNAL MONITORED AT	MONITORED TIME*		DATA SOURCE	ACCURACY* (ms)
		TIME FROM RANGE ZERO (hr:min:sec)	TIME FROM BASE (sec)		TIME FROM RANGE ZERO* (hr:min:sec)	TIME FROM BASE (sec)		
234b	Signal Received in S-IVB for: Regular Calibrate Relays On	--	--	S-IVB	02:24:45.213 (8685.213)	N/A	DAC(FM)	13
235	Signal from LVDC for: Telemetry Calibrator Inflight Calibrate On	02:24:36.3 (8676.3)	TB5 +8019.7	IU	02:24:45.534 (8685.534)	TB5 +8019.650	MSFC	--
236a	Signal from LVDC for: Regular Calibrate Relays Off	02:24:41.1 (8681.1)	TB5 +8024.5	IU	02:24:50.334 (8690.334)	TB5 +8024.450	MSFC	--
236b	Signal Received in S-IVB for: Regular Calibrate Relays Off	--	--	S-IVB	02:24:50.213 (8690.213)	N/A	DAC(FM)	13
237a	Signal from LVDC for: Special Calibrate Relays Off	02:24:41.3 (8681.3)	TB5 +8024.7	IU	02:24:50.534 (8690.534)	TB5 +8024.650	MSFC	--
237b	Signal Received in S-IVB for: Special Calibrate Relays Off	--	--	S-IVB	02:24:50.413 (8690.413)	N/A	DAC(FM)	13
238	Signal from LVDC for: Telemetry Calibrator Inflight Calibrate Off	02:24:41.5 (8681.5)	TB5 +8024.9	IU	02:24:50.734 (8690.734)	TB5 +8024.850	MSFC	--
239a	Signal from LVDC for: Slow Record On	02:50:15.9 (10,215.9)	TB5 +9559.3	IU	02:50:25.134 (10,225.134)	TB5 +9559.250	MSFC	--
239b	Signal Received in S-IVB for: Slow Record On	--	--	S-IVB	02:50:25.748 (10,225.748)	N/A	DAC(FM)	13
240a	Signal from LVDC for: Slow Record Off	02:50:47.9 (10,247.9)	TB5 +9591.3	IU	02:50:57.143 (10,257.143)	TB5 +9559.250	MSFC	--
240b	Signal Received in S-IVB for: Slow Record Off	--	--	S-IVB	02:50:57.657 (10,257.657)	N/A	DAC(FM)	13
241a	Signal from LVDC for: Recorder Playback On	02:50:48.1 (10,248.1)	TB5 +9591.5	IU	02:50:57.344 (10,257.344)	TB5 +9591.460	MSFC	--
241b	Signal Received in S-IVB for: Recorder Playback On	--	--	S-IVB	02:50:57.857 (10,257.857)	N/A	DAC(FM)	13
242a	Signal from LVDC for: Recorder Playback Off	02:55:32.1 (10,532.1)	TB5 +9875.5	IU	02:55:41.334 (10,541.334)	TB5 +9875.450	MSFC	--
242b	Signal Received in S-IVB for: Recorder Playback Off	--	--	S-IVB	02:55:41.488 (10,541.488)	N/A	DAC(FM)	13
243a	Signal from LVDC for: Slow Record On	02:55:32.3 (10,532.3)	TB5 +9875.7	IU	02:55:41.534 (10,541.534)	TB5 +9875.650	MSFC	--
243b	Signal Received in S-IVB for: Slow Record On	--	--	S-IVB	02:55:41.698 (10,541.698)	N/A	DAC(FM)	13
244a	Signal from LVDC for: Slow Record On	02:55:35.3 (10,535.3)	TB5 +9878.7	IU	02:55:44.535 (10,544.535)	TB5 +9878.651	MSFC	--
244b	Signal Received in S-IVB for: Slow Record On	--	--	S-IVB	02:55:44.647 (10,544.647)	N/A	DAC(FM)	13

*See notes at end of table

Section 4
Sequence of Events

TABLE 4-1 (Sheet 23 of 43)
FLIGHT SEQUENCE OF EVENTS

ITEM NO.	EVENT	PREDICTED TIME*		SIGNAL MONITORED AT	MONITORED TIME*		DATA SOURCE	ACCURACY* (ms)
		TIME FROM RANGE ZERO (hr:min:sec) (sec)	TIME FROM BASE (sec)		TIME FROM RANGE ZERO* (hr:min:sec) (sec)	TIME FROM BASE (sec)		
245	Signal from LVDC for: Telemetry Calibrator Inflight Calibrate On	03:00:56.7 (10,856.7)	TB5 +10,200.1	IU	--	--	--	--
246a	Signal from LVDC for: Special Calibrate Relays On	03:00:56.9 (10,856.9)	TB5 +10,200.3	IU	--	--	--	--
246b	Signal Received in S-IVB for: Special Calibrate Relays On	--	--	S-IVB	--	--	--	--
247a	Signal from LVDC for: Regular Calibrate Relays On	03:00:57.1 (10,857.1)	TB5 +10,200.5	IU	--	--	--	--
247b	Signal Received in S-IVB for: Regular Calibrate Relays On	--	--	S-IVB	--	--	--	--
248	Signal from LVDC for: Telemetry Calibrator Inflight Calibrate Off	03:01:01.7 (10,861.7)	TB5 +10,205.1	IU	--	--	--	--
249a	Signal from LVDC for: Regular Calibrate Relays Off	03:01:02.1 (10,862.1)	TB5 +10,205.5	IU	--	--	--	--
249b	Signal Received in LVDC for: Regular Calibrate Relays Off	--	--	S-IVB	--	--	--	--
250a	Signal from LVDC for: Special Calibrate Relays Off	03:01:02.3 (10,862.3)	TB5 +10,205.7	IU	--	--	--	--
250b	Signal Received in S-IVB for: Special Calibrate Relays Off	--	--	S-IVB	--	--	--	--
251a	Signal from LVDC for: Aux Hydraulic Pump Flight Mode On	03:01:44.6 (10,904.6)	TB5 +10,248.0	IU	03:01:53.950 (10,913.950)	TB5 +10,247.950	MSFC	--
251b	Signal Received in S-IVB for: Aux Hydraulic Pump Flight Mode On	--	--	S-IVB	03:01:53.870 (10,913.870)	N/A	DAC(FM)	13
252a	Signal from LVDC for: Aux Hydraulic Pump Coast Mode Off	03:01:44.8 (10,904.8)	TB5 +10,248.2	IU	03:01:54.035 (10,914.035)	TB5 +10,248.151	MSFC	--
252b	Signal Received in S-IVB for: Aux Hydraulic Pump Coast Mode Off	--	--	S-IVB	03:01:54.060 (10,914.060)	N/A	DAC(FM)	13
253a	Signal from LVDC for: Fuel Chillo-down Pump On	03:01:49.6 (10,909.6)	TB5 +10,253.0	IU	03:01:58.839 (10,918.839)	TB5 +10,252.956	MSFC	--
253b	Signal Received in S-IVB for: Fuel Chillo-down Pump On	--	--	S-IVB	03:01:58.860 (10,918.860)	N/A	DAC(FM)	13

*See notes at end of table

Section 4
Sequence of Events

TABLE 4-1 (Sheet 24 of 43)
FLIGHT SEQUENCE OF EVENTS

ITEM NO.	EVENT	PREDICTED TIME*		SIGNAL MONITORED AT	MONITORED TIME*		DATA SOURCE	ACCURACY* (ms)
		TIME FROM RANGE ZERO (hr:min:sec) (sec)	TIME FROM BASE (sec)		TIME FROM RANGE ZERO* (hr:min:sec) (sec)	TIME FROM BASE (sec)		
254a	Signal from LVDC for: LOX Chilldown Pump On	03:01:54.6 (10,914.6)	TB5 +10,258.0	IU	03:02:03.834 (10,923.834)	TB5 +10,257.950	MSFC	--
254b	Signal Received in S-IVB for LOX Chill-down Pump On	--	--	S-IVB	03:02:03.860 (10,923.860)	N/A	DAC(FM)	13
255a	Signal from LVDC for: Feed Duct Prevalves Closed On	03:02:04.6 (10,924.6)	TB5 +10,268.0	IU	03:02:13.834 (10,933.834)	TB5 +10,267.950	MSFC	--
255b	Signal Received in S-IVB for: Feed Duct Prevalves Closed On	--	--	S-IVB	03:02:13.850 (10,933.850)	N/A	DAC(FM)	13
256	<u>Time Base 6</u> Begin Restart Preparations	03:05:56.6 (11,156.6)	TB6 +0.0	IU	03:05:59.576 (11,159.576)	TB6 +0.0	MSFC	--
257a	Signal from LVDC for: S-IVB Ullage Engine No. 1 On	03:05:56.8 (11,156.8)	TB6 +0.2	IU	03:05:59.731 (11,159.731)	TB6 +0.155	MSFC	--
257b	Signal Received in S-IVB for: S-IVB Ullage Engine No. 1 On	--	--	S-IVB	03:05:59.750 (11,159.750)	N/A	DAC(FM)	13
258a	Signal from LVDC for: S-IVB Ullage Engine No. 2 On	03:05:56.9 (11,156.9)	TB6 +0.3	IU	03:05:59.828 (11,159.828)	TB6 +0.252	MSFC	--
258b	Signal Received in S-IVB for: Ullage Engine No. 2 On	--	--	S-IVB	03:05:59.860 (11,159.860)	N/A	DAC(FM)	13
259	Initiate Pitch & Yaw Maneuver for Restart Attitude Orientation	03:05:56.5 (11,156.5)	N/A	IU	03:06:00.0 (11,160.0)	N/A	DAC	1000
260	Signal from LVDC for: S-IVB Ullage Thrust Present On	03:05:57.1 (11,157.1)	TB6 +0.5	IU	03:06:00.039 (11,160.039)	TB6 +0.463	MSFC	--
261a	Signal from LVDC for: LH2 Tank Vent Valve Boost Close On	03:05:57.4 (11,157.4)	TB6 +0.8	IU	03:06:00.338 (11,160.338)	TB6 +0.762	MSFC	--
261b	Signal Received in S-IVB for: LH2 Tank Vent Valve Boost Close On	--	--	S-IVB	03:06:00.360 (11,160.360)	N/A	DAC(FM)	13
262a	Signal from LVDC for: LOX Tank Vent Valve Boost Close On	03:05:57.6 (11,157.6)	TB6 +1.0	IU	03:06:00.527 (11,160.527)	TB6 +0.951	MSFC	--
262b	Signal Received in S-IVB for: LOX Tank Vent Valve Boost Close On	--	--	S-IVB	03:06:00.550 (11,160.550)	N/A	DAC(FM)	13
263a	Signal from LVDC for: Continuous Vent Pilot Valve Close On	03:05:57.8 (11,157.8)	TB6 +1.2	IU	03:06:00.732 (11,160.732)	TB6 +1.156	MSFC	--
263b	Signal Received in S-IVB for: Continuous Vent Pilot Valve Close On	--	--	S-IVB	03:06:00.760 (11,160.760)	N/A	DAC(FM)	13

*See notes at end of table

Section 4
Sequence of Events

TABLE 4-1 (Sheet 25 of 43)
FLIGHT SEQUENCE OF EVENTS

ITEM NO.	EVENT	PREDICTED TIME *		SIGNAL MONITORED AT	MONITORED TIME *		DATA SOURCE	ACCURACY* (ms)
		TIME FROM RANGE ZERO (hr:min:sec) (sec)	TIME FROM BASE (sec)		TIME FROM RANGE ZERO* (hr:min:sec) (sec)	TIME FROM BASE (sec)		
264a	Signal from LVDC for: LH2 Repress Control Valve Open On	03:05:58.8 (11,158.8)	TB6 +2.2	IU	03:06:01.729 (11,161.729)	TB6 +2.153	MSFC	--
264b	Signal Received in S-IVB for: LH2 Re-press Control Valve Open On	--	--	S-IVB	03:06:01.770 (11,161.770)	N/A	DAC(FM)	13
265a	Signal from LVDC for: LH2 Tank Vent Valve Boost Close Off	03:05:59.4 (11,159.4)	TB6 +2.8	IU	03:06:02.326 (11,162.326)	TB6 +2.750	MSFC	--
265b	Signal Received in S-IVB for: LH2 Tank Vent Valve Boost Close Off	--	--	S-IVB	03:06:02.340 (11,162.340)	N/A	DAC(FM)	13
266a	Signal from LVDC for: LOX Tank Vent Valve Boost Close Off	03:05:59.6 (11,159.6)	TB6 +3.0	IU	03:06:02.531 (11,162.531)	TB6 +2.955	MSFC	--
266b	Signal Received in S-IVB for: LOX Tank Vent Valve Boost Close Off	--	--	S-IVB	03:06:02.570 (11,162.570)	N/A	DAC(FM)	13
267a	Signal from LVDC for: Continuous Vent Pilot Valve Close Off	03:05:59.8 (11,159.8)	TB6 +3.2	IU	03:06:02.762 (11,162.762)	TB6 +3.186	MSFC	--
267b	Signal Received in S-IVB for: Continuous Vent Pilot Valve Close Off	--	--	S-IVB	03:06:02.970 (11,162.970)	N/A	DAC(FM)	13
268a	Signal from LVDC for: Fuel Chilldown Pump On	03:06:02.6 (11,162.6)	TB6 +6.0	IU	03:06:05.542 (11,165.542)	TB6 +5.966	MSFC	--
268b	Signal Received in S-IVB for: Fuel Chilldown Pump On	--	--	S-IVB	03:06:05.580 (11,165.580)	N/A	DAC(FM)	13
269a	Signal from LVDC for: LOX Chilldown Pump On	03:06:07.6 (11,167.6)	TB6 +11.0	IU	03:06:10.426 (11,170.426)	TB6 +10.950	MSFC	--
269b	Signal Received in S-IVB for: LOX Chilldown Pump On	--	--	S-IVB	03:06:10.570 (11,170.570)	N/A	DAC(FM)	13
270a	Signal from LVDC for: Prevalves Close On	03:06:17.6 (11,177.6)	TB6 +21.0	IU	03:06:20.537 (11,180.537)	TB6 +20.961	MSFC	--
270b	Signal Received in S-IVB for: Prevalves Close On	--	--	S-IVB	03:06:20.580 (11,180.580)	N/A	DAC(FM)	13

*See notes at end of table

Section 4
Sequence of Events

TABLE 4-1 (Sheet 26 of 43)
FLIGHT SEQUENCE OF EVENTS

ITEM NO.	EVENT	PREDICTED TIME*		SIGNAL MONITORED AT	MONITORED TIME*		DATA SOURCE	ACCURACY* (ms)
		TIME FROM RANGE ZERO (hr:min:sec) (sec)	TIME FROM BASE (sec)		TIME FROM RANGE ZERO* (hr:min:sec) (sec)	TIME FROM BASE (sec)		
271	Stop Yaw Maneuver	--	--	IU	03:06:55.0 (11,215.0)	N/A	DAC	1000
	<u>First Ground Initiated Command Sequence</u>							
272	Signal from Ground to LVDC for: LH2 Tank Repressurization Control Valve Open Off (Not Received by LVDC)	--	--	Ground	03:06:49 (11,209)	N/A	MSC	1000
273	Signal from Ground to LVDC for: LH2 Tank Continuous Vent Valve Close On (Not Received by LVDC)	--	--	Ground	--	--	MSC	--
274	Signal from Ground to LVDC for: LH2 Tank Continuous Vent Valve Close Off (Not Received by LVDC)	--	--	Ground	--	--	MSC	--
	<u>Second Ground Initiated Command Sequence</u>							
275a	Signal from Ground to LVDC for: LH2 Tank Repressurization Control Valve Open Off	--	--	Ground	03:07:20.0 (11,240.0)	N/A	MSC	1000
275b	Signal from LVDC for: LH2 Tank Repressurization Control Valve Open Off	--	--	IU	03:07:21.982 (11,241.982)	N/A	MSFC	--
275c	Signal Received in S-IVB for: LH2 Tank Repressurization Control Valve Open Off	--	--	S-IVB	03:07:22.650 (11,242.050)	N/A	DAC(FM)	13
276a	Signal from Ground to LVDC for: LH2 Tank Continuous Vent Valve Close On	--	--	Ground	--	--	MSC	--
276b	Signal from LVDC for: LH2 Tank Continuous Vent Valve Close On	--	--	IU	03:07:22.851 (11,242.851)	N/A	MSFC	--
276c	Signal Received in S-IVB for: LH2 Tank Continuous Vent Valve Close On	--	--	S-IVB	03:07:22.930 (11,242.930)	N/A	DAC(FM)	13
277a	Signal from Ground to LVDC for: LH2 Tank Continuous Vent Valve Close Off	--	--	Ground	--	--	MSC	--

*See notes at end of table

Section 4
Sequence of Events

TABLE 4-1 (Sheet 27 of 43)
FLIGHT SEQUENCE OF EVENTS

ITEM NO.	EVENT	PREDICTED TIME*		SIGNAL MONITORED AT	MONITORED TIME*		DATA SOURCE	ACCURACY* (ms)
		TIME FROM RANGE ZERO (hr:min:sec) (sec)	TIME FROM BASE (sec)		TIME FROM RANGE ZERO* (hr:min:sec) (sec)	TIME FROM BASE (sec)		
277b	Signal from LVDC for: LH2 Tank Continuous Vent Valve Close Off	--	--	IU	03:07:24.612 (11,244.612)	N/A	MSFC	--
277c	Signal Received in S-IVB for: LH2 Tank Continuous Vent Valve Close Off	--	--	S-IVB	03:07:24.710 (11,244.710)	N/A	DAC(FM)	13
	<u>Third Ground Initiated Command Sequence</u>							
278a	Signal from Ground to LVDC for: LH2 Tank Repressurization Control Valve Open Off	--	--	Ground	03:08:13.0 (11,293.0)	N/A	MSC	1000
278b	Signal from LVDC for: LH2 Tank Repressurization Control Valve Open Off	--	--	IU	03:08:15.308 (11,295.308)	N/A	MSFC	--
278c	Signal Received in S-IVB for: LH2 Tank Repressurization Control Valve Open Off	--	--	S-IVB	03:08:15.390 (11,295.390)	N/A	DAC(FM)	13
279a	Signal from Ground to LVDC for: LH2 Tank Continuous Vent Valve Close On	--	--	Ground	--	--	MSC	--
279b	Signal from LVDC for: LH2 Tank Continuous Vent Valve Close On	--	--	IU	03:08:15.183 (11,296.183)	N/A	MSFC	--
279c	Signal Received in S-IVB for: LH2 Tank Continuous Vent Valve Close On	--	--	S-IVB	03:08:16.274 (11,296.274)	N/A	DAC(FM)	13
280a	Signal from Ground to LVDC for: LH2 Tank Continuous Vent Valve Close Off	--	--	Ground	--	--	MSC	--
280b	Signal from LVDC for: LH2 Tank Continuous Vent Valve Close Off	--	--	IU	03:08:17.962 (11,297.962)	N/A	MSFC	--
280c	Signal Received in S-IVB for: LH2 Tank Continuous Vent Valve Close Off	--	--	S-IVB	03:08:18.057 (11,298.057)	N/A	DAC(FM)	13
281	Stop Pitch Maneuver	--	--	IU	03:08:15.0 (11,295.0)	N/A	DAC	1000
	<u>Fourth Ground Initiated Command Sequence</u>							
282a	Signal from Ground to LVDC for: LH2 Tank Repressurization Control Valve Open Off	--	--	Ground	03:08:43.0 (11,323.0)	N/A	MSC	1000

*See notes at end of table

Section 4
Sequence of Events

TABLE 4-1 (Sheet 28 of 43)
FLIGHT SEQUENCE OF EVENTS

ITEM NO.	EVENT	PREDICTED TIME*		SIGNAL MONITORED AT	MONITORED TIME*		DATA SOURCE	ACCURACY* (ms)
		TIME FROM RANGE ZERO (hr:min:sec) (sec)	TIME FROM BASE (sec)		TIME FROM RANGE ZERO* (hr:min:sec) (sec)	TIME FROM BASE (sec)		
282b	Signal from LVDC for: LH2 Tank Repressurization Control Valve Open Off	--	--	IU	03:08:45.329 (11,325.329)	N/A	MSFC	--
282c	Signal Received in S-IVB for: LH2 Tank Repressurization Control Valve Open Off	--	--	S-IVB	03:08:45.413 (11,325.413)	N/A	DAC(FM)	13
283a	Signal from Ground to LVDC for: LH2 Tank Continuous Vent Valve Close On	--	--	Ground	--	--	MSC	--
283b	Signal from LVDC for: LH2 Tank Continuous Vent Valve Close On	--	--	IU	03:08:46.212 (11,326.212)	N/A	MSFC	--
283c	Signal Received in S-IVB for: LH2 Tank Continuous Vent Valve Close On	--	--	S-IVB	03:08:46.296 (11,326.296)	N/A	DAC(FM)	13
284a	Signal from Ground to LVDC for: LH2 Tank Continuous Vent Valve Close OFF	--	--	Ground	--	--	MSC	--
284b	Signal from LVDC for: LH2 Tank Continuous Vent Valve Close OFF	--	--	IU	03:08:48.033 (11,328.033)	N/A	MSFC	--
284c	Signal Received in S-IVB for: LH2 Continuous Vent Valve Close OFF	--	--	S-IVB	03:08:48.117 (11,328.117)	N/A	DAC(FM)	13
<u>Fifth Ground Initiated Ground Sequence</u>								
285	Signal from Ground to LVDC for: LH2 Tank Repressurization Control Valve Open Off (Not Received by LVDC)	--	--	Ground	03:09:20 (11,360)	N/A	MSC	1,000
286	Signal from Ground to LVDC for: LH2 Tank Continuous Vent Valve Close On (Not Received by LVDC)	--	--	Ground	--	--	MSC	--
287	Signal from ground to LVDC for: LH2 Tank Continuous Vent Valve Close Off (Not Received by LVDC)	--	--	Ground	--	--	MSC	--

*See notes at end of table

Section 4
Sequence of Events

TABLE 4-1 (Sheet 29 of 43)
FLIGHT SEQUENCE OF EVENTS

ITEM NO.	EVENT	PREDICTED TIME*		SIGNAL MONITORED AT	MONITORED TIME*		DATA SOURCE	ACCURACY* (ms)
		TIME FROM RANGE ZERO (hr:min:sec) (sec)	TIME FROM BASE (sec)		TIME FROM RANGE ZERO* (hr:min:sec) (sec)	TIME FROM BASE (sec)		
<u>Sixth Ground Initiated Command Sequence</u>								
288	Signal from Ground to LVDC for LH2 Tank Re-pressurization Control Valve Open Off (Not Received by LVDC)	--	--	Ground	03:09:40 (11,380)	N/A	MSC	1,000
289	Signal from Ground to LVDC for: LH2 Tank Continuous Vent Valve Close On (Not Received by LVDC)	--	--	Ground	--	--	MSC	--
290	Signal from Ground to LVDC for: LH2 Tank Continuous Vent Valve Close Off (Not Received by LVDC)	--	--	Ground	--	--	MSC	--
<u>Seventh Ground Initiated Command Sequence</u>								
291	Signal from Ground to LVDC for: LH2 Tank Re-pressurization Control Valve Open Off (Not Received by LVDC)	--	--	Ground	--	--	MSC	--
292	Signal from Ground to LVDC for: LH2 Tank Continuous Vent Valve Close On (Not Received by LVDC)	--	--	Ground	--	--	MSC	--
293	Signal from Ground to LVDC for: LH2 Tank Continuous Vent Valve Close Off (Not Received by LVDC)	--	--	Ground	--	--	MSC	--
294	Signal from LVDC for: Telemetry Calibration Inflight Calibrate On	03:09:32.1 (11,372.1)	TB6 +215.5	IU	03:09:35.026 (11,375.026)	TB6 +215.450	MSFC	--
295a	Signal from LVDC for: Special Calibrate Relays On	03:09:32.3 (11,372.3)	TB6 +215.7	IU	03:09:35.231 (11,375.231)	TB6 +215.655	MSFC	--
295b	Signal Received in S-IVB for: Special Calibrate Relays On	--	--	S-IVB	03:09:35.264 (11,375.264)	N/A	DAC(FM)	13
296a	Signal from LVDC for: Regular Calibrate Relays On	03:09:32.5 (11,372.5)	TB6 +215.9	IU	03:09:35.448 (11,375.448)	TB6 +215.872	MSFC	--
296b	Signal Received in S-IVB for: Regular Calibrate Relays On	--	--	S-IVB	03:09:35.481 (11,375.481)	N/A	DAC(FM)	13
297	Signal from LVDC for: Telemetry Calibrate Inflight Calibrate Off	03:09:37.1 (11,377.1)	TB6 +220.5	IU	03:09:40.026 (11,380.026)	TB6 +220.450	MSFC	--
298a	Signal from LVDC for: Regular Calibrate Relays Off	03:09:37.5 (11,377.5)	TB6 +220.9	IU	03:09:40.440 (11,380.440)	TB6 +220.864	MSFC	--

*See notes at end of table

Section 4
Sequence of Events

TABLE 4-1 (Sheet 30 of 43)
FLIGHT SEQUENCE OF EVENTS

ITEM NO.	EVENT	PREDICTED TIME*		SIGNAL MONITORED AT	MONITORED TIME*		DATA SOURCE	ACCURACY* (ms)
		TIME FROM RANGE ZERO (hr:min:sec) (sec)	TIME FROM BASE (sec)		TIME FROM RANGE ZERO* (hr:min:sec) (sec)	TIME FROM BASE (sec)		
298b	Signal Received in S-IVB for: Regular Calibrate Relays Off	--	--	S-IVB	03:09:40.473 (11,380.473)	N/A	DAC(FM)	13
299a	Signal from LVDC for: Special Calibrate Relays Off	03:09:37.7 (11,377.7)	TB6 +221.1	IU	03:09:40.626 (11,380.626)	TB6 +221.050	MSFC	--
299b	Signal Received by S-IVB for: Special Calibrate Relays Off	--	--	S-IVB	03:09:40.658 (11,380.658)	N/A	DAC(FM)	13
300a	Signal from LVDC for: SSB/FM Group ON	03:09:37.9 (11,377.9)	TB6 +221.3	IU	03:09:40.831 (11,380.831)	TB6 +221.255	MSFC	--
300b	Signal Received in S-IVB for: SSB/FM Group ON	--	--	S-IVB	03:09:40.863 (11,380.863)	N/A	DAC(FM)	13
301a	Signal from LVDC for: SSB/FM Transmitter ON	03:09:38.1 (11,378.1)	TB6 +221.5	IU	03:09:41.046 (11,381.046)	TB6 +221.470	MSFC	--
301b	Signal Received in S-IVB for: SSB/FM Transmitter ON	--	--	S-IVB	03:09:41.078 (11,381.078)	N/A	DAC(FM)	13
302a	Signal from LVDC for: LOX Repress Valve Open ON	03:10:13.6 (11,413.6)	TB6 +257.0	IU	03:10:16.527 (11,416.527)	TB6 +256.951	MSFC	--
302b	Signal Received in S-IVB for: LOX Repress Valve Open ON	--	--	S-IVB	03:10:16.560 (11,416.560)	N/A	DAC(FM)	13
303a	Signal from LVDC for: PU Activate ON	03:11:03.6 (11,463.6)	TB6 +307.0	IU	03:11:06.532 (11,466.532)	TB6 +306.956	MSFC	--
303b	Signal Received in S-IVB for: PU Activate ON	--	--	S-IVB	03:11:06.561 (11,466.561)	N/A	DAC(FM)	13
304a	Signal from LVDC for: PU Valve Hardover Position ON	03:11:03.8 (11,463.8)	TB6 +307.2	IU	03:11:06.747 (11,466.747)	TB6 +307.171	MSFC	--
304b	Signal Received in S-IVB for: PU Valve Hardover Position ON	--	--	S-IVB	03:11:06.775 (11,466.775)	N/A	DAC(FM)	13
305a	Signal from LVDC for: Prevalve Closed OFF	03:11:12.3 (11,472.8)	TB6 +316.2	IU	03:11:15.737 (11,475.737)	TB6 +316.161	MSFC	--
305b	Signal Received in S-IVB for: Prevalve Closed OFF	--	--	S-IVB	03:11:15.767 (11,475.767)	N/A	DAC(FM)	13

*See notes at end of table

Section 4
Sequence of Events

TABLE 4-1 (Sheet 31 of 43)
FLIGHT SEQUENCE OF EVENTS

ITEM NO.	EVENT	PREDICTED TIME *		SIGNAL MONITORED AT	MONITORED TIME *		DATA SOURCE	ACCURACY * (-)
		TIME FROM RANGE ZERO (hr:min:sec) (sec)	TIME FROM BASE (sec)		TIME FROM RANGE ZERO* (hr:min:sec) (sec)	TIME FROM BASE (sec)		
306	Signal from LVDC for: S-IVB Restart Alert	03:11:13.6 (11,473.6)	TB6 +317.0	IU	03:11:16.527 (11,476.527)	TB6 +316.951	MSFC	--
307a	Signal from LVDC for: Engine Cutoff Off	03:11:22.2 (11,482.2)	TB6 +325.6	IU	03:11:25.126 (11,485.126)	TB6 +325.550	MSFC	--
307b	Signal Received in S-IVB for: Engine Cutoff Off	--	--	S-IVB	03:11:25.158 (11,485.158)	N/A	DAC(FM)	13
308a	Signal from LVDC for: Engine Ready Bypass	03:11:22.4 (11,482.4)	TB6 +325.8	IU	03:11:25.331 (11,485.331)	TB6 +325.755	MSFC	--
308b	Signal Received in S-IVB for: Engine Ready Bypass	--	--	S-IVB	03:11:25.362 (11,485.362)	N/A	DAC(FM)	13
309a	Signal from LVDC for: LH2 Repress Control Valve Open Off	03:11:22.6 (11,482.6)	TB6 +326.0	IU	03:11:25.549 (11,485.549)	TB6 +325.973	MSFC	--
309b	Signal Received in S-IVB for: LH2 Repress Control Valve Open Off	--	--	S-IVB	03:11:25.580 (11,485.580)	N/A	DAC(FM)	13
310a	Signal from LVDC for: Fuel Chill-down Pump Off	03:11:22.8 (11,482.8)	TB6 +326.2	IU	03:11:25.720 (11,485.726)	TB6 +326.150	MSFC	--
310b	Signal Received in S-IVB for: Fuel Chill-down Pump Off	--	--	S-IVB	03:11:25.758 (11,485.758)	N/A	DAC(FM)	13
311a	Signal from LVDC for: LOX Chill-down Pump Off	03:11:23.0 (11,483.0)	TB6 +326.4	IU	03:11:25.940 (11,485.940)	TB6 +326.364	MSFC	--
311b	Signal Received in S-IVB for: LOX Chill-down Pump Off	--	--	S-IVB	03:11:25.971 (11,485.971)	N/A	DAC(FM)	13
312a	Signal from LVDC for: Repress Control Valve Open Off	03:11:23.4 (11,483.4)	TB6 +326.8	IU	03:11:26.325 (11,486.325)	TB6 +326.749	MSFC	--
312b	Signal Received in S-IVB for: Repress Control Valve Open Off	--	--	S-IVB	03:11:26.355 (11,486.355)	N/A	DAC(FM)	13
313a	Signal from LVDC for: Engine Start On	03:11:23.6 (11,483.6)	TB6 +327.0	IU	03:11:26.536 (11,486.536)	TB6 +326.960	MSFC	--
313b	Signal Received in S-IVB for: Engine Start On	--	--	S-IVB	03:11:26.567 (11,486.567)	N/A	DAC(FM)	13

*See notes at end of table

Section 4
Sequence of Events

TABLE 5-1 (Sheet 32 of 43)
FLIGHT SEQUENCE OF EVENTS

ITEM NO.	EVENT	PREDICTED TIME *		SIGNAL MONITORED AT	MONITORED TIME *		DATA SOURCE	ACCURACY (ms)
		TIME FROM RANGE ZERO (hr:min:sec) (sec)	TIME FROM BASE (sec)		TIME FROM RANGE ZERO* (hr:min:sec) (sec)	TIME FROM BASE (sec)		
313c	<u>J-2 Engine Start Sequence</u>							
	1. Helium Control Solenoid Energized	--	--	S-IVB	03:11:26.567 (11,486.567)	--	DAC	10
	2. Main Fuel Valve Closed (Dropout)	--	--	S-IVB	03:11:26.567 (11,486.567)	--	DAC	10
	3. Main Fuel Valve Open (Pickup)	--	--	S-IVB	03:11:26.649 (11,486.649)	--	DAC	10
	4. Gas Generator Valve Closed (Dropout)	--	--	S-IVB	03:11:34.917 (11,494.917)	--	DAC	10
	5. Gas Generator Valve Open (Pickup)	--	--	S-IVB	03:11:35.483 (11,495.483)	--	DAC	10
	6. Main Oxidizer Valve Leaves Closed Position (Dropout)	--	--	S-IVB	03:11:34.942 (11,494.942)	--	DAC	10
	7. Start Tank Discharge Valve Open (Dropout)	--	--	S-IVB	03:11:35.063 (11,495.063)	--	DAC	10
	8. Oxidizer Turbine Bypass Valve Open (Dropout)	--	--	S-IVB	03:11:35.520 (11,495.520)	--	DAC	10
	9. Oxidizer Turbine Bypass Valve Closed (Pickup)	--	--	S-IVB	03:11:35.575 (11,495.575)	--	DAC	10
	10. Mainstage OK Pressure Switch 1 (Dropout)	--	--	S-IVB	03:11:36.294 (11,496.294)	--	DAC	10
	11. Mainstage OK Pressure Switch 2 (Dropout)	--	--	S-IVB	03:11:36.369 (11,496.369)	--	DAC	10
	12. Main Oxidizer Valve Reaches Open Position (Pickup)	--	--	S-IVB	03:11:37.436 (11,497.436)	--	DAC	10
	13. Gas Generator Spark System On (Dropout)	--	--	S-IVB	03:11:38.266 (11,498.266)	--	DAC	10
	14. Thrust Chamber Spark System On (Dropout)	--	--	S-IVB	03:11:38.266 (11,498.266)	--	DAC	10
314	Signal from LVDC for: Out Indication "A" Enable On	03:11:24.4 (11,484.4)	TB6 +327.8	IU	03:11:27.326 (11,487.326)	TB6 +327.750	MSFC	--
315	Signal from LVDC for: Out Indication "B" Enable On	03:11:24.6 (11,484.6)	TB6 +328.0	IU	03:11:27.544 (11,487.544)	TB6 +327.968	MSFC	--

*See notes at end of table

Section 4
Sequence of Events

TABLE 4-1 (Sheet 33 of 43)
FLIGHT SEQUENCE OF EVENTS

ITEM NO.	EVENT	PREDICTED TIME*		SIGNAL MONITORED AT	MONITORED TIME*		DATA SOURCE	ACCURACY* (ms)
		TIME FROM RANGE ZERO (hr:min:sec) (sec)	TIME FROM BASE (sec)		TIME FROM RANGE ZERO* (hr:min:sec) (sec)	TIME FROM BASE (sec)		
316a	Signal from LVDC for: Ullage Engine No. 1 Off	03:11:26.6 (11,486.6)	TB6 +330.0	IU	03:11:29.527 (11,489.527)	TB6 +329.951	MSFC	--
316b	Signal Received in S-IVB for: Ullage Engine No. 1 Off	--	--	S-IVB	03:11:29.558 (11,489.558)	N/A	DAC(FM)	13
317a	Signal from LVDC for: Ullage Engine No. 2 Off	03:11:26.7 (11,486.7)	TB6 +330.1	IU	03:11:29.626 (11,489.626)	TB6 +330.050	MSFC	--
317b	Signal Received in S-IVB for: Ullage Engine No. 2 Off	--	--	S-IVB	03:11:29.658 (11,489.658)	N/A	DAC(FM)	13
318	Signal from LVDC for: Ullage Thrust Present Off	03:11:26.9 (11,486.9)	TB6 +330.3	IU	03:11:29.832 (11,489.832)	TB6 +330.256	MSFC	--
319	Signal from LVDC for: Control Computer S-IVB Burn Mode On "B"	03:11:31.2 (11,491.2)	TB6 +334.6	IU	03:11:34.144 (11,494.144)	TB6 +334.568	MSFC	--
320	Signal from LVDC for: Computer S-IVB Burn Mode On "A"	03:11:31.4 (11,491.4)	TB6 +334.8	IU	03:11:34.327 (11,494.327)	TB6 +334.751	MSFC	--
321	Signal from LVDC for: Injection Temperature OK Bypass	03:11:31.6 (11,491.6)	TB6 +335.0	IU	03:11:34.541 (11,494.541)	TB6 +334.965	MSFC	--
322	Signal Received in S-IVB for: Injection Temperature OK Bypass	--	--	S-IVB	03:11:34.572 (11,494.572)	N/A	DAC(FM)	13
323a	Signal from LVDC for: LOX Tank Flight Press System On	03:11:31.8 (11,491.8)	TB6 +335.2	IU	03:11:34.726 (11,494.726)	TB6 +335.150	MSFC	--
323b	Signal Received in S-IVB for: Tank Flight Press System On	--	--	S-IVB	03:11:34.758 (11,494.758)	N/A	DAC(FM)	13
324a	Signal from LVDC for: Coast Period Off	03:11:32.0 (11,492.0)	TB6 +335.4	IU	03:11:34.933 (11,494.933)	TB6 +335.357	MSFC	--
324b	Signal Received in S-IVB for: Coast Period Off	--	--	S-IVB	03:11:34.964 (11,494.964)	N/A	DAC(FM)	13
325a	Signal from LVDC for: Engine Start Off	03:11:32.2 (11,492.2)	TB6 +335.6	IU	03:11:35.126 (11,495.126)	TB6 +335.550	MSFC	--
325b	Signal Received in S-IVB for: Engine Start Off	--	--	S-IVB	03:11:35.157 (11,495.157)	N/A	DAC(FM)	13
326	J-2 Thrust Buildup (10%)	--	N/A	N/A	03:11:35.511 (11,495.511)	N/A	DAC	10
327	J-2 Thrust Buildup (90%)	03:11:34.0 (11,494.0)	N/A	N/A	03:11:37.061 (11,497.061)	N/A	MSFC	--

*See notes at end of table

Section 4
Sequence of Events

TABLE 4-1 (Sheet 34 of 43)
FLIGHT SEQUENCE OF EVENTS

ITEM NO.	EVENT	PREDICTED TIME*		SIGNAL MONITORED AT	MONITORED TIME*		DATA SOURCE	ACCURACY* (ms)
		TIME FROM RANGE ZERO (hr:min:sec) (sec)	TIME FROM BASE (sec)		TIME FROM RANGE ZERO* (hr:min:sec) (sec)	TIME FROM BASE (sec)		
328a	Signal from LVDC for: Second Burn Relay ON	03:11:34.2 (11,494.2)	TB6 +337.6	IU	03:11:37.145 (11,497.145)	TB6 +337.569	MSFC	--
328b	Signal Received in S-IVB for: Second Burn Relay ON	--	--	S-IVB	03:11:37.175 (11,497.175)	N/A	DAC(FM)	13
329a	Signal from LVDC for: PU Valve Hardover Position Off	03:11:36.6 (11,496.6)	TB6 +340.0	IU	03:11:39.531 (11,499.531)	TB6 +339.955	MSFC	--
329b	Signal Received in S-IVB for: PU Valve Hardover Position OFF	--	--	S-IVB	03:11:39.560 (11,499.560)	N/A	DAC(FM)	13
330	Guidance Initiation	03:11:36.5 (11,496.5)	N/A	IU	03:11:39.992 (11,499.992)	N/A	MSFC	--
331	Start Artificial Tau Mode	03:11:36.5 (11,496.5)	N/A	IU	03:11:39.992 (11,499.992)	N/A	MSFC	--
332	Stop Artificial Tau Mode	03:11:43.5 (11,503.5)	N/A	IU	03:11:41.541 (11,501.541)	N/A	MSFC	--
333	PU Valve Reaches Hardover Position	--	N/A	N/A	03:11:51.8 (11,511.8)	N/A	DAC	100
334	PU Valve Cutback	--	N/A	N/A	03:12:30.1 (11,550.1)	N/A	DAC	100
335	Start Artificial Tau Mode	03:12:26.5 (11,546.5)	N/A	IU	03:12:31.3 (11,551.3)	N/A	MSFC	--
336	Stop Artificial Tau Mode	03:12:56.5 (11,576.5)	N/A	IU	03:12:49.8 (11,569.8)	N/A	MSFC	--
337	Engine Mixture Ratio Cutback	--	N/A	N/A	03:12:51.5 (11,571.5)	N/A	DAC	100
338a	Signal from LVDC for: SSB/FM Transmitter OFF	03:15:49.1 (11,749.1)	TB6 +592.5	IU	03:15:52.035 (11,752.035)	TB6 +592.459	MSFC	--
338b	Signal Received in S-IVB for: SSB/FM Transmitter OFF	--	--	S-IVB	03:15:52.070 (11,752.070)	N/A	DAC(FM)	13
339a	Signal from LVDC for: SSB/FM Group OFF	03:15:49.3 (11,749.3)	TB6 +592.7	IU	03:15:52.227 (11,752.227)	TB6 +592.651	MSFC	--
339b	Signal Received in S-IVB for: SSB/FM Group OFF	--	--	S-IVB	03:15:52.261 (11,752.261)	N/A	DAC(FM)	13

*See notes at end of table

Section 4
Sequence of Events

TABLE 4-1 (Sheet 35 of 43)
FLIGHT SEQUENCE OF EVENTS

ITEM NO.	EVENT	PREDICTED TIME*		SIGNAL MONITORED AT	MONITORED TIME*		DATA SOURCE	ACCURACY* (ms)
		TIME FROM RANGE ZERO (hr:min:sec) (sec)	TIME FROM BASE (sec)		TIME FROM RANGE ZERO* (hr:min:sec) (sec)	TIME FROM BASE (sec)		
340	Signal from LVDC for: Flight Control Computer Switch Point No. 5	03:15:53.6 (11,753.6)	TB6 +597.0	IU	03:15:56.526 (11,756.526)	TB6 +596.950	MSFC	--
341	Signal from LVDC for: Telemetry Calibrate Inflight Calibrate ON	03:15:55.2 (11,755.2)	TB6 +598.6	IU	03:15:58.132 (11,758.132)	TB6 +598.556	MSFC	--
342a	Signal from LVDC for: Special Calibrate Relays ON	03:15:55.4 (11,755.4)	TB6 +598.8	IU	03:15:58.327 (11,758.327)	TB6 +598.751	MSFC	--
342b	Signal Received in S-IVB for: Special Calibrate Relays ON	--	--	S-IVB	03:15:58.361 (11,758.361)	N/A	DAC(FM)	13
343a	Signal from LVDC for: Regular Calibrate Relays ON	03:15:55.6 (11,755.6)	TB6 +599.0	IU	03:15:58.533 (11,758.533)	TB6 +598.957	MSFC	--
343b	Signal Received in S-IVB for: Regular Calibrate Relays ON	--	--	S-IVB	03:15:58.565 (11,758.565)	N/A	DAC(FM)	13
344	Signal from LVDC for: Telemetry Calibrate Inflight Calibrate OFF	03:16:00.2 (11,760.2)	TB6 +603.6	IU	03:16:03.134 (11,763.134)	TB6 +603.558	MSFC	--
345a	Signal from LVDC for: Regular Calibrate Relays OFF	03:16:00.6 (11,760.6)	TB6 +604.0	IU	03:16:03.526 (11,763.526)	TB6 +603.950	MSFC	--
345b	Signal Received in S-IVB for: Regular Calibrate Relays OFF	--	--	S-IVB	03:16:03.561 (11,763.561)	N/A	DAC(FM)	13
346a	Signal from LVDC for: Special Calibrate Relays OFF	03:16:00.8 (11,760.8)	TB6 +604.2	IU	03:16:03.742 (11,763.742)	TB6 +604.166	MSFC	--
346b	Signal Received in S-IVB for: Special Calibrate Relays OFF	--	--	S-IVB	03:16:03.778 (11,763.778)	N/A	DAC(FM)	13
347	Introduction of Chi Tilde Guidance Mode	03:16:12.0 (11,772.0)	N/A	IU	03:15:58.18 (11,758.18)	N/A	MSFC	--
348	Signal from LVDC for: Chilldown Shutoff Pilot Valve Closed ON	03:16:24.0 (11,784.0)	TB6 +627.4	IU	Not Issued	--	MSFC	--

*See notes at end of table

Section 4
Sequence of Events

TABLE 4-1 (Sheet 36 of 43)
FLIGHT SEQUENCE OF EVENTS

ITEM NO.	EVENT	PREDICTED TIME*		SIGNAL MONITORED AT	MONITORED TIME*		DATA SOURCE	ACCURACY (ms)
		TIME FROM RANGE ZERO (hr:min:sec) (sec)	TIME FROM BASE (sec)		TIME FROM RANGE ZERO* (hr:min:sec) (sec)	TIME FROM BASE (sec)		
349	Signal from LVDC for: Freeze Body Attitude (Chi Freeze)	03:16:34.4 (11,794.4)	N/A	IU	03:16:21.0 (11,781.0)	N/A	DAC	100
350	Signal from LVDC for: Point Level Sensor Arming	03:16:49.2 (11,809.2)	TB6 +652.6	IU	Not Issued	--	MSFC	--
351a	LVDC Sends Signal for: Cutoff S-IVB Engine (Guidance Cutoff)	03:16:40.1 (11,800.1)	N/A	IU	03:16:26.228 (11,786.228)	N/A	MSFC	--
351b	S-IVB Receives Signal for: Cutoff S-IVB Engine (Guidance Cutoff)	--	--	S-IVB	03:16:26.265 (11,786.265)	N/A	DAC(FM)	13
351c	Time Base 7 LVDC Initiates Time Base 7	03:16:40.1 (11,800.1)	TB7 +0.0	IU	03:16:26.479 (11,786.479)	TB7 +0.0	MSFC	--
351d	LVDC Sends Redundant Signal for: Cutoff S-IVB Engine	03:16:40.1 (11,800.1)	N/A	IU	03:16:26.561 (11,786.561)	TB7 +0.082	MSFC	--
351e	Signal Received in S-IVB for: Cutoff S-IVB Engine (Redundant Signal)	--	--	S-IVB	03:16:26.599 (11,786.599)	N/A	DAC(FM)	13
352a	Signal from LVDC for: LOX Tank Vent Valve Open ON	03:16:40.3 (11,800.3)	TB7 +0.2	IU	03:16:26.653 (11,786.653)	TB7 +0.174	MSFC	--
352b	Signal Received in S-IVB for: LOX Tank Vent Valve Open	--	--	S-IVB	03:16:26.691 (11,786.691)	N/A	DAC(FM)	13
353	S-IVB J-2 Thrust Decay to 5 percent (Average)	--	N/A	N/A	03:16:26.702 (11,786.702)	--	DAC	10
354a	Signal from LVDC for: Point Level Sensors Disarming	03:16:40.4 (11,800.4)	TB7 +0.3	IU	03:16:26.744 (11,786.744)	TB7 +0.265	MSFC	--

*See notes at end of table

Section 4
Sequence of Events

TABLE 4-1 (Sheet 37 of 43)
FLIGHT SEQUENCE OF EVENTS

ITEM NO.	EVENT	PREDICTED TIME*		SIGNAL MONITORED AT	MONITORED TIME*		DATA SOURCE	ACCURACY* (ms)
		TIME FROM RANGE ZERO (hr:min:sec) (sec)	TIME FROM BASE (sec)		TIME FROM RANGE ZERO* (hr:min:sec) (sec)	TIME FROM BASE (sec)		
354b	Signal Received in S-IVB for: Point Level Sensors Disarming	--	--	S-IVB	03:16:26.781 (11,786.781)	N/A	DAC(FM)	13
355a	Signal from LVDC for: LH2 Tank Vent Valve Open ON	03:16:40.5 (11,800.5)	TB7 +0.4	IU	03:16:26.841 (11,786.841)	TB7 +0.362	MSFC	--
355b	Signal Received in S-IVB for: LH2 Tank Vent Valve Open ON	--	--	S-IVB	03:16:26.880 (11,786.880)	N/A	DAC(FM)	13
356a	Signal from LVDC for: Second Burn Relay OFF	03:16:40.9 (11,800.9)	TB7 +0.8	IU	03:16:27.228 (11,787.228)	TB7 +0.749	MSFC	--
356b	Signal Received in S-IVB for: Second Burn Relay OFF	--	--	S-IVB	03:16:27.268 (11,787.268)	N/A	DAC(FM)	13
357a	Signal from LVDC for: LOX Tank Flight Press System OFF	03:16:41.1 (11,801.1)	TB7 +1.0	IU	03:16:27.433 (11,787.433)	TB7 +0.954	MSFC	--
357b	Signal Received in S-IVB for: LOX Tank Flight Press System OFF	--	--	S-IVB	03:16:27.473 (11,787.473)	N/A	DAC(FM)	13
358a	Signal from LVDC for: Prevalves Closed ON	03:16:41.2 (11,801.2)	TB7 +1.1	IU	03:16:27.532 (11,787.532)	TB7 +1.053	MSFC	--
358b	Signal Received in S-IVB for: Prevalves Closed ON	--	--	S-IVB	03:16:27.572 (11,787.572)	N/A	DAC(FM)	13
359a	Signal from LVDC for: Coast Period ON	03:16:41.3 (11,801.3)	TB7 +1.2	IU	03:16:27.629 (11,787.629)	TB7 +1.150	MSFC	--
359b	Signal Received in S-IVB for: Coast Period ON	--	--	S-IVB	03:16:27.668 (11,787.668)	N/A	DAC(FM)	13
360a	Signal from LVDC for: PU Activate OFF	03:16:41.5 (11,801.5)	TB7 +1.4	IU	03:16:27.833 (11,787.833)	TB7 +1.354	MSFC	--
360b	Signal Received in S-IVB for: PU Activate OFF	--	--	S-IVB	03:16:27.871 (11,787.871)	N/A	DAC(FM)	13

*See notes at end of table

Section 4
Sequence of Events

TABLE 4-1 (Sheet 38 of 43)
FLIGHT SEQUENCE OF EVENTS

ITEM NO.	EVENT	PREDICTED TIME*		SIGNAL MONITORED AT	MONITORED TIME*		DATA SOURCE	ACCURACY (ms)
		TIME FROM RANGE ZERO (hr:min:sec) (sec)	TIME FROM BASE (sec)		TIME FROM RANGE ZERO* (hr:min:sec) (sec)	TIME FROM BASE (sec)		
361a	Signal from LVDC for: PU Inverter and DC Power OFF	03:16:41.6 (11,801.6)	TB7 +1.5	IU	03:16:27.935 (11,787.935)	TB7 +1.456	MSFC	--
361b	Signal Received in S-IVB for: PU Inverter and DC Power OFF	--	--	S-IVB	03:16:27.975 (11,787.975)	N/A	DAC(FM)	13
362a	Signal from LVDC for: LOX Chill-down Pump Purge Control Valve Open OFF	03:16:41.7 (11,801.7)	TB7 +1.6	IU	03:16:28.029 (11,788.029)	TB7 +1.550	MSFC	--
362b	Signal Received in S-IVB for: LOX Chillo-down Pump Purge Control Valve Open OFF	--	--	S-IVB	03:16:28.070 (11,788.070)	N/A	DAC(FM)	13
363	Signal from LVDC for: Flight Control Computer S-IVB Burn Mode Off "B"	03:16:43.4 (11,803.4)	TB7 +3.3	IU	03:16:29.729 (11,789.729)	TB7 +3.250	MSFC	--
364	Signal from LVDC for: Flight Control Computer S-IVB Burn Mode Off "A"	03:16:43.6 (11,803.6)	TB7 +3.5	IU	03:16:29.935 (11,789.935)	TB7 +3.456	MSFC	--
365a	Signal from LVDC for: Auxiliary Hydraulic Pump Flight Mode OFF	03:16:43.8 (11,803.8)	TB7 +3.7	IU	03:16:30.128 (11,790.128)	TB7 +3.650	MSFC	--
365b	Signal Received in S-IVB for: Auxiliary Hydraulic Pump Flight Mode OFF	--	--	S-IVB	03:16:30.167 (11,790.167)	N/A	DAC(FM)	13
366a	Signal from LVDC for: LOX Tank Vent Valve Close	03:16:50.1 (11,810.1)	TB7 +10.0	IU	03:16:36.429 (11,796.429)	TB7 +9.950	MSFC	--
366b	Signal Received in S-IVB for: LOX Tank Vent Valve Close	--	--	S-IVB	03:16:36.467 (11,796.467)	N/A	DAC(FM)	13
367a	Signal from LVDC for: LOX Tank Vent Valve Boost Close ON	03:16:53.1 (11,813.1)	TB7 +13.0	IU	03:16:39.429 (11,799.429)	TB7 +12.950	MSFC	--
367b	Signal Received in S-IVB for: LOX Tank Vent Boost Close ON	--	--	S-IVB	03:16:39.469 (11,799.469)	N/A	DAC(FM)	13
368a	Signal from LVDC for: LOX Tank Vent Valve Boost Close OFF	03:16:55.1 (11,815.1)	TB7 +15.0	IU	03:16:41.429 (11,801.429)	TB7 +14.950	MSFC	--

*See notes at end of table

Section 4
Sequence of Events

TABLE 4-1 (Sheet 39 of 43)
FLIGHT SEQUENCE OF EVENTS

ITEM NO.	EVENT	PREDICTED TIME*		SIGNAL MONITORED AT	MONITORED TIME*		DATA SOURCE	ACCURACY* (ms)
		TIME FROM RANGE ZERO (hr:min:sec) (sec)	TIME FROM BASE (sec)		TIME FROM RANGE ZERO* (hr:min:sec) (sec)	TIME FROM BASE (sec)		
368b	Signal Received in S-IVB for: LOX Tank Vent Valve Boost Close OFF	--	--	S-IVB	03:16:41.468 (11,801.468)	N/A	DAC(FM)	13
369	Initiate Maneuver to Attain Separation Inertial Attitude (End of Chi Freeze)	03:16:50.1 (11,810.1)	N/A	IU	03:16:45.0 (11,805.0)	N/A	DAC	1,000
370	Signal from LVDC for: C-Band Transponder No. 1 and No. 2 ON	--	--	IU	03:16:49.573 (11,809.573)	N/A	MSFC	--
371	Signal from LVDC for: C-Band Transponder No. 1 OFF	--	--	IU	03:16:49.664 (11,809.664)	N/A	MSFC	--
372a	Signal from LVDC for: Prevalves Closed OFF	03:17:40.6 (11,860.6)	TB7 +60.5	IU	03:17:26.929 (11,846.929)	TB7 +60.450	MSFC	--
372b	Signal Received in S-IVB for: Prevalves Closed OFF	--	--	S-IVB	03:17:26.940 (11,846.940)	N/A	DAC(FM)	13
373a	Signal from LVDC for: Chilldown Shutoff Pilot Closed OFF	03:17:40.8 (11,860.8)	TB7 +60.7	IU	03:17:27.129 (11,847.129)	TB7 +60.650	MSFC	--
373b	Signal Received in S-IVB for: Chilldown Shutoff Pilot Valve Closed OFF	--	--	S-IVB	03:17:27.140 (11,847.140)	N/A	DAC(FM)	13
374	Stop Pitch Maneuver for CSM Separation Attitude	--	--	--	03:18:00.0 (11,880.0)	N/A	DAC	1,000
375	Signal from LVDC for: C-Band Transponder No. 1 and No. 2 ON	--	--	IU	03:18:01.479 (11,881.479)	N/A	MSFC	--
376	Signal from LVDC for: C-Band Transponder No. 2 OFF	--	--	IU	03:18:01.550 (11,881.550)	N/A	MSFC	--
377	Signal from LVDC for: C-Band Transponder No. 1 and No. 2 ON	--	--	IU	03:18:09.675 (11,889.675)	N/A	MSFC	--
378	Signal from LVDC for: C-Band Transponder No. 1 OFF	--	--	IU	03:18:09.753 (11,889.753)	N/A	MSFC	--
379	Signal from LVDC for: C-Band Transponder No. 1 and No. 2 ON	--	--	IU	03:18:17.895 (11,897.895)	N/A	MSFC	--

*See notes at end of table

Section 4
Sequence of Events

TABLE 4-1 (Sheet 40 of 43)
FLIGHT SEQUENCE OF EVENTS

ITEM NO.	EVENT	PREDICTED TIME*		SIGNAL MONITORED AT	MONITORED TIME*		DATA SOURCE	ACCURACY* (ms)
		TIME FROM RANGE ZERO (hr:min:sec) (sec)	TIME FROM BASE (sec)		TIME FROM RANGE ZERO* (hr:min:sec) (sec)	TIME FROM BASE (sec)		
380	Signal from LVDC for: C-Band Transponder No. 2 OFF	--	--	IU	03:18:17.974 (11,897.974)	N/A	MSFC	--
381a	Signal from LVDC for: LH2 Tank Vent Valve Close	03:18:40.1 (11,920.1)	TB7 +120.0	IU	03:18:26.429 (11,906.429)	TB7 +119.950	MSFC	--
381b	Signal Received in S-IVB for: LH2 Tank Vent Valve Close	--	--	S-IVB	03:18:26.450 (11,906.450)	N/A	DAC(FM)	13
382	Signal from LVDC for: C-Band Transponder No. 1 and No. 2 ON	--	--	IU	03:18:26.507 (11,906.507)	N/A	MSFC	--
383	Signal from LVDC for: C-Band Transponder No. 1 OFF	--	--	IU	03:18:26.578 (11,906.578)	N/A	MSFC	--
384a	Signal from LVDC for: LH2 Tank Vent Valve Boost Close ON	03:18:43.1 (11,923.1)	TB7 +123.0	IU	03:18:29.428 (11,909.428)	TB7 +122.949	MSFC	--
384b	Signal Received in S-IVB for: LH2 Tank Vent Valve Boost Close ON	--	--	S-IVB	03:18:29.440 (11,909.440)	N/A	DAC(FM)	13
385a	Signal from LVDC for: LH2 Tank Vent Valve Boost Close OFF	03:18:45.1 (11,925.1)	TB7 +125.0	IU	03:18:31.429 (11,911.429)	TB7 +124.950	MSFC	--
385b	Signal Received in S-IVB for: LH2 Tank Vent Valve Boost Close OFF	--	--	S-IVB	03:18:31.460 (11,911.460)	N/A	DAC(FM)	13
386	Signal from LVDC for: C-Band Transponder No. 1 and No. 2 ON	--	--	IU	03:18:49.632 (11,929.632)	N/A	MSFC	--
387	Signal from LVDC for: C-Band Transponder No. 2 OFF	--	--	IU	03:18:49.702 (11,929.702)	N/A	MSFC	--
388	Stop Roll Maneuver for CSM Separation Attitude	--	--	--	03:18:50.0 (11,930.0)	N/A	DAC	1,000
389	Signal from LVDC for: C-Band Transponder No. 1 and No. 2 ON	--	--	IU	03:22:09.825 (12,129.825)	N/A	MSFC	--
390	Signal from LVDC for: C-Band Transponder No. 1 OFF	--	--	IU	03:22:09.896 (12,129.896)	N/A	MSFC	--

*See notes at end of table

Section 4
Sequence of Events

TABLE 4-1 (Sheet 41 of 43)
FLIGHT SEQUENCE OF EVENTS

ITEM NO.	EVENT	PREDICTED TIME*		SIGNAL MONITORED AT	MONITORED TIME*		DATA SOURCE	ACCURACY* (ms)
		TIME FROM RANGE ZERO (hr:min:sec) (sec)	TIME FROM BASE (sec)		TIME FROM RANGE ZERO* (hr:min:sec) (sec)	TIME FROM BASE (sec)		
391	Signal from LVDC for: C-Band Transponder No. 1 and No. 2 ON	--	--	IU	03:25:06.222 (12,306.222)	N/A	MSFC	--
392	Signal from LVDC for: C-Band Transponder No. 2 OFF	--	--	IU	03:25:06.293 (12,306.293)	N/A	MSFC	--
393	LV/SC Separation Sequence Start	03:26:40.1 (12,400.1)	TB7 +600.0	IU	03:26:26.429 (12,386.429)	TB7 +599.950	MSFC	--
394	Initiate Maneuver to Attain Vehicle Alignment for Ascension Island Communications (Pitch, Yaw, and Roll Maneuver)	--	--	--	03:28:05.0 (12,485.0)	N/A	DAC	1,000
395	Signal from LVDC for: C-Band Transponder No. 1 and No. 2 ON	--	--	IU	03:28:50.514 (12,530.514)	N/A	MSFC	--
396	Signal from LVDC for: C-Band Transponder No. 1 OFF	--	--	IU	03:28:50.585 (12,530.585)	N/A	MSFC	--
397	Signal from LVDC for: C-Band Transponder No. 1 and No. 2 ON	--	--	IU	03:30:57.561 (12,657.561)	N/A	MSFC	--
398	Signal from LVDC for: C-Band Transponder No. 2 OFF	--	--	IU	03:30:57.632 (12,657.632)	N/A	MSFC	--
399	Stop Yaw Maneuver	--	--	--	03:29:00.0 (12,540.0)	--	DAC	1,000
400	Stop Pitch Maneuver	--	--	--	03:31:10.0 (12,670.0)	--	DAC	1,000
401	Stop Roll Maneuver	--	--	--	03:31:35.0 (12,695.0)	--	DAC	1,000
402	Nominal CSM Separation	03:26:41.8 (12,401.8)	N/A	--	--	--	--	--
403	SPS (CSM) First Ignition	03:28:20.1 (12,500.1)	N/A	--	--	--	--	--
404	Signal from LVDC for: Switch PCM to Low Gain Antenna (Fail Safe)	03:45:33.4 (13,533.4)	TB7 +1,733.3	--	03:45:19.289 (13,519.768)	TB7 +1733.289	MSFC	--
405	Signal from LVDC for: Switch CCS to Low Gain Antenna	03:45:33.6 (13,533.6)	TB7 +1,733.5	--	03:45:19.499 (13,519.969)	TB7 +1733.490	MSFC	--
406	Signal from LVDC for: Telemetry Calibrator Inflight Calibrate ON	03:55:38.2 (14,138.2)	TB7 +2,338.1	IU	03:55:24.539 (14,124.539)	TB7 +2,338.060	MSFC	--

*See notes at end of table

Section 4
Sequence of Events

TABLE 4-1 (Sheet 42 of 43)
FLIGHT SEQUENCE OF EVENTS

ITEM NO.	EVENT	PREDICTED TIME*		SIGNAL MONITORED AT	MONITORED TIME*		DATA SOURCE	ACTUATOR (ms)
		TIME FROM RANGE ZERO (hr:min:sec) (sec)	TIME FROM BASE (sec)		TIME FROM RANGE ZERO* (hr:min:sec) (sec)	TIME FROM BASE (sec)		
407a	Signal from LVDC for: Special Calibrate Relays ON	03:55:38.4 (14,138.4)	TB7 +2,338.3	IU	03:55:24.740 (14,124.740)	TB7 +2,338.261	MSFC	--
407b	Signal Received in S-IVB for: Special Calibrate Relays ON	--	--	S-IVB	03:55:24.810 (14,124.810)	N/A	DAC(FM)	13
408a	Signal from LVDC for: Regular Calibrate Relays ON	03:55:38.6 (14,138.6)	TB7 +2,338.5	IU	03:55:24.940 (14,124.940)	TB7 +2,338.401	MSFC	--
408b	Signal Received in S-IVB for: Regular Calibrate Relays ON	--	--	S-IVB	03:55:25.000 (14,125.000)	N/A	DAC(FM)	13
409	Signal from LVDC for: Telemetry Calibrator Inflight Calibrate OFF	03:55:43.2 (14,143.2)	TB7 +2,343.1	IU	03:55:29.528 (14,129.528)	TB7 +2,343.049	MSFC	--
410a	Signal from LVDC for: Regular Calibrate Relays OFF	03:55:43.6 (14,143.6)	TB7 +2,343.5	IU	03:55:29.929 (14,129.929)	TB7 +2,343.450	MSFC	--
410b	Signal Received in S-IVB for: Regular Calibrate Relays OFF	--	--	S-IVB	03:55:30.000 (14,130.000)	N/A	DAC(FM)	13
411a	Signal from LVDC for: Special Calibrate Relays OFF	03:55:43.8 (14,143.8)	TB7 +2,343.7	IU	03:55:30.130 (14,130.130)	TB7 +2,343.651	MSFC	--
411b	Signal Received in S-IVB for: Special Calibrate Relays OFF	--	--	S-IVB	03:55:30.200 (14,130.200)	N/A	DAC(FM)	13
412	Signal from LVDC for: Switch PCM to High Gain Antenna	04:28:33.4 (16,133.4)	TB7 +4,313.3	IU	04:28:19.730 (16,099.730)	TB7 +4313.250	MSFC	--
413	Signal from LVDC for: Switch CCS to High Gain Antenna (Fail Safe)	04:28:33.6 (16,133.6)	TB7 +4,313.5	IU	04:28:19.957 (16,099.957)	TB7 +4313.478	MSFC	--
414	Signal from LVDC for: Switch PCM to Low Gain Antenna (Fail Safe)	05:23:33.4 (19,413.4)	TB7 +7,613.3	IU	05:23:19.731 (19,399.731)	TB7 +7,613.252	MSFC	--
415	Signal from LVDC for: Switch CCS to Low Gain Antenna	05:23:35.4 (19,415.4)	TB7 +7,613.5	IU	05:23:19.932 (19,399.932)	TB7 +7,613.453	MSFC	--
416	Signal from LVDC for: Maneuver to Align S-IVB/CSM+X Axis with Local Horizontal	05:26:42.1 (19,602.1)	N/A	IU	--	--	--	--
417	Signal from LVDC for: CCS Transmitter Inhibit OFF	05:36:40.1 (20,200.1)	TB7 +8,400.0	IU	05:36:26.479 (20,186.479)	TB7 +8399.950	MSFC	--
418	Signal from LVDC for: Switch PCM to OMNI Antenna	07:28:33.4 (26,913.4)	TB7 +15,113.3	IU	07:28:19.729 (26,879.729)	TB7 +15113.250	MSFC	--
419	Signal from LVDC for: Switch CCS to OMNI Antenna	07:28:33.6 (26,913.6)	TB7 +15,113.5	IU	07:28:19.929 (26,899.929)	TB7 +15113.450	MSFC	--

*See notes at end of table

Section 4
Sequence of Events

TABLE 4-1 (Sheet 43 of 43)
FLIGHT SEQUENCE OF EVENTS

NOTES: Predicted Time: Blank space in column indicates that time signal was received in S- VB, cannot be predicted.

Monitored Time: Blank space in column indicates that no data was received.

Time From Range Zero: 1200:01.0 (GMT)

Accuracy: No accuracy data received from MSFC

TABLE 4-2 (Sheet 1)
GROUND SEQUENCE

TIME		INDICATION	EVENT
MIN	SEC		
-14	3.028	Off	Heat Exchanger Fill Valve Open
-14	1.452	On	Level Sensor High
-13	59.874	On	Heat Exchanger Fill Valve Close
-13	38.988	Off	Level Sensor High
-13	40.246	On	Level Sensor Low
-13	39.156	Off	Level Sensor Low
-11	45.574	On	Heat Exchanger Fill Valve Open
-11	43.842	Off	Heat Exchanger Fill Valve Open
-11	36.264	On	S-IVB Aft All Test and Vent Valve Open
-11	35.370	On	S-IVB Forward All Test and Vent Valve Open
-11	35.270	On	S-IVB Forward Hydraulic Standby Hydraulic System Check
-11	34.896	Off	S-IVB Forward Hydraulic Standby Hydraulic System Check
-11	29.628	Off	S-IVB Aft All Test and Vent Valve Open
-11	26.876	On	Status S-IVB Aft Arm Ready
-11	22.602	On	Heat Exchanger Fill Valve Open
-11	21.268	Off	Heat Exchanger Fill Valve Open
-10	38.028	On	Heat Exchanger Fill Valve Open
-10	34.976	On	Heat Exchanger Fill Valve Close
-9	6.908	On	Heat Exchanger Fill Valve Open
-9	4.344	On	Heat Exchanger Fill Valve Close
-8	3.118	On	Engine Control Power On
-7	59.464	On	S-IVB Engine Cutoff
-7	41.422	On	Auxiliary Hydraulic Pump Power On
-7	38.234	On	Auxiliary Hydraulic Pump Coast Reset
-6	44.922	On	S-IC Stage Inhibit
-6	44.410	On	S-IV Stage Inhibit
-6	43.206	On	S-II Stage Inhibit
-6	3.238	Off	LOX Vent Open
-6	3.076	On	LOX Vent Closed
-6	1.688	Off	LOX Vent Closed

FOLDOUT FRAME |

TABLE 4-2 (Sheet 1 of 2)
GROUND SEQUENCE OF EVENTS

	TIME		INDICATION	EVENT
	MIN	SEC		
	-6	1.656	On	LOX Vent Open
	-5	5.176	On	All Stages Ready Power Transfer
	-5	18.340	On	Status Safe and Arm Armed
	-5	2.836	On	LH2 Chillover Pump Inverter Power On
	-4	52.062	On	Engine Start Tank Vent Valve Open
	-4	48.306	On	Engine Control Bottle Supply Valve Closed
	-4	44.288	On	Engine Control Bottle Supply Vent Valve Open
	-4	38.854	On	LOX Chillover Pump Inverter Power On
	-4	32.614	On	LH2 Prevalve Closed
	-4	32.490	On	LOX Prevalve Closer
	-4	28.230	On	S-IVB Stage Inhibit
	-3	52.128	On	APS 1 Engine Valve Power On
	-3	52.116	On	APS 2 Engine Valve Power On
	-3	52.108	On	S-IVB Preparations Complete
	-3	33.700	On	Heat Exchanger Fill Valve Open
	-3	29.564	On	Heat Exchanger Fill Valve Close
	-3	29.462	On	Cold Helium Transfer Valve Closed
	-3	6.996	On	T -187 sec Sequencer Start
	-2	59.768	On	Heat Exchanger Fill Valve Open
	-2	57.788	On	Heat Exchanger Fill Valve Close
	-2	46.656	On	LOX Vent Closed
	-2	32.350	On	LOX Tank Pressurized Command
	-2	31.030	On	LOX Fill & Drain Valve Closed
	-2	30.226	On	GN2 LOX Umbilical Purge Supply Open
	-2	24.856	On	LOX Minimum Liftoff Press OK
	-2	24.686	On	Heat Exchanger Fill Valve Open
	-2	18.552	On	Heat Exchanger Fill Valve Close
	-2	10.570	On	LOX Minimum Liftoff Press OK
	-1	36.764	Off	LH2 Tank Vent Valve Open
	-1	36.506	On	LH2 Tank Vent Valve Closed

pen
ic
lic

FOLDOUT FRAME 2

Section 4
Sequence of Events

TABLE 4-2 (Sheet 2 of 2)
GROUND SEQUENCE OF EVENTS

TIME		INDICATION	EVENT
MIN	SEC		
-1	33.428	On	Heat Exchanger Fill Valve Open
-1	30.216	On	Heat Exchanger Fill Valve Close
-1	22.910	On	LH2 100 Percent Mass
-1	20.980	On	LH2 Fill & Drain Valve Closed
-1	17.790	On	LH2 Umbilical Purge Supply Open
-1	15.104	On	LH2 Tank Pressurized
-1	15.036	On	LH2 Tank Ground Prepressurization Shutoff Valve Closed
-1	1.354	On	Heat Exchanger Fill Valve Open
	-50.266	On	Heat Exchanger Fill Valve Close
	-49.916	On	Forward Power On Internal
	-49.914	On	Aft Bus 1 On Internal
	-49.914	On	Aft Bus 2 On Internal
	-49.914	On	Stage on External Power
	-49.910	On	Stage On Internal Power
	-49.572	On	Power Transfer Complete
	-29.976	On	
	-26.764	On	LH2 Directional Vent in Flight Position
	-26.756	On	S-IVB Ready for Launch
	-8.886	On	Start Ignition Sequence
	-8.826	On	LH2 Tank Ground Prepressurization Shutoff Valve Open
	-8.808	Off	Engine Thrust Chamber Chilledown Supply Valve Open
	-8.784	On	Cold Helium Bottle Supply Close
	-8.706	On	Cold Helium Bottle Supply Line Valve Open
	-8.536	On	3,000 psi Helium Supply Closed
	-8.470	On	LH2 Ground Control Repressurization Close
	-0.308	On	S-IVB Forward Hydraulic Standby Hydraulic System Check

FOLDOUT FRAME ↑

BLE 4-2 (Sheet 2 of 2)
 FOUND SEQUENCE OF EVENTS

TIME		INDICATION	EVENT
MIN	SEC		
	-0.232	Off	S-IVB Forward Hydraulic Standby Hydraulic System Check
	+0.352	On	S-IC Commit (T-3)
	+0.364	Off	Auxiliary Hydraulic Pump Power On
	+0.364	Off	LOX Chillover Valve Open
	+0.364	Off	LH2 Chillover Valve Open
	+0.364	Off	LOX Chillover Pump Inverter Power On
	+0.364	Off	LH2 Chillover Pump Inverter Power On
	+0.364	Off	LH2 Tank Control Vent Orifice Bypass Close
	+0.364	Off	LH2 Tank Control Vent Relief Orifice Close
	+0.364	Off	Cold Helium Backup PS Enable
	+0.364	Off	Single Side Band Group On
	+0.364	Off	Engine Control Power On
	+0.364	Off	Engine Ignition Power On
	+0.364	Off	LOX Cutoff Sensor 1 Wet
	+0.364	Off	LOX Cutoff Sensor 2 Wet
	+0.364	Off	LOX Cutoff Sensor 3 Wet
	+0.364	Off	LOX Prevalve Closed
	+0.364	Off	LH2 Prevalve Closed
	+0.368	Off	S-IVB Ready for Launch
	+0.370	Off	4D30 On
	+0.370	Off	4D20 On
	+0.370	Off	4D10 On
	+0.370	Off	4D40 On
	+0.370	Off	Ready for Launch
	+0.438	Off	LH2 Nozzle Purge Supply Open
	+0.440	On	LH2 Nozzle Purge Supply Closed
	+0.590	Off	GN2 LOX Umbilical Purge Supply Open
	+0.596	On	GN2 LOX Umbilical Purge Supply Close
	1.258	On	Liftoff Indication

FOLDOUT FRAME 2

5. COUNTDOWN OPERATIONS

The AS-501 vehicle was launched at 1200:01 GMT (0700:01 EST) from Launch Complex 39A on 9 November 1967. The overall performance of the S-IVB-501 stage was satisfactory during all phases of the countdown. No significant S-IVB stage or equipment problems occurred during the countdown activity, and Douglas ground support equipment (GSE) sustained no significant damage during liftoff. The precountdown and countdown activities are reviewed and evaluated in the following paragraphs which include discussions of the prelaunch checkouts, purges, propellant and pneumatic loading, and the terminal countdown. Significant events occurred at the following times:

<u>Event</u>	<u>Time</u>
Liftoff	1200:01.263 GMT
LOX loading initiated	0513:55 GMT
LH2 loading initiated	1013:58 GMT
Cold helium loading initiated	1039:22 GMT
Terminal countdown initiated	1130:01 GMT

5.1 Propulsion System Checkouts

Preflight checkouts of the S-IVB-501 stage were conducted in accordance with handling and checkout requirements drawings listed in Douglas Report SM-53184, Narrative End Item Report on Saturn S-IVB-501 (Douglas S/N 1005), dated August 1966.

5.2 Launch Vehicle Tests

After the S-IVB-501 stage was installed on the S-II spacer in the vehicle assembly building (VAB), it was subjected to launch vehicle tests to determine that switch selector, power transfers, etc. were functional for launch. After the S-IVB stage was mated with the S-II stage, the tests were rerun as presented in table 5-1.

Section 5
Countdown Operations

5.2.1 Countdown Demonstration Test

The AS-501 vehicle countdown demonstration test (CDDT) was initiated at 0030 GMT on 27 September 1967 with the count at R0 -83 hr 30 min. The planned cutoff at R0 -8.9 sec occurred at approximately 2043:12 GMT on 13 October 1967. The test was performed in accordance with NASA procedure V-20016-SA501, Revision 004. The Douglas preparation and securing steps were conducted in accordance with Douglas procedure 1B62289. Four runs were necessary to complete Part III (R0 -13 hr to R0 -0) of the CDDT.

Run 1 (4 October) was scrubbed at 0102 GMT while in a hold at R0 -30 min because of propellant system computer problems and launch crew fatigue. LOX and LH2 aboard the S-IVB stage were drained without incident. During cold helium sphere pressurization, the pressure drop in the 6,000-psi helium supply was higher than normal because of a restriction at the inlet to the DSV-432A console. The restriction was the result of a valve malfunction--either the 6,000-psi helium inlet solenoid valve or the 6,000 psi helium inlet hand valve. Since no instrumentation existed to permit isolation of the problem to one or the other valve, both valves were removed and replaced.

Run 2 (10 October) was scrubbed (with the count at R0 -5 hr 5 min) because of S-IC helium system facilities problems. Back pressure throughout the GH2 vent system caused an S-IVB stage LH2 tank ullage pressure of 17 psia during normal replenish operations. (It was 16.7 psia during run 1 on 4 October.) For the AS-501 launch the launch mission rules were changed to accept this excessive back pressure, and the maximum allowable pressure was changed from 16.7 psia to 17.4 psia.

Run 3 (11 October) was scrubbed (with the count at R0 -3 hr 25 min) because of S-II battery problems. LOX was loaded on this day and the subsequent drain was completed without any problems.

Run 4 (12 October) was initiated at 2400 GMT (with the count at R0 -13 hr). The first terminal count sequence was terminated at R0 -16.7 sec because S-IC failed to prepressurize the LOX tank. This S-IC problem was traced

to a partially closed valve in the launch unbilical tower. The second terminal count sequence was successfully completed at approximately 2043:12 GMT on 13 October. After LH2 drain and just prior to S-IVB LOX drain, D0016-245 (cold helium sphere pressure) was erroneous and indicating abnormally high. Although the cause of the difference between the actual and the indicated pressure was not established, the transducer was removed and replaced.

5.2.2 Flight Readiness Test

The AS-501 flight readiness test was conducted on 25 October in order to verify the compatibility between, and the proper operation of, all launch vehicle and GSE systems prior to launch. This test was conducted in accordance with procedure V20017 with no apparent abnormalities.

The APS dry fire was conducted at R0 -1 hr 30 min without difficulty, and all data stations reported good results. This test verified that the APS firing program and all data stations were ready for the APS hot firing.

Because of computer problems in the plus count of the flight readiness test, simulated repressurization of the LOX and LH2 tanks for second burn was impossible, but this simulation was not required for satisfactory completion of the test. No S-IVB stage problems occurred during this test.

5.3 APS Preparations

5.3.1 APS Loading

APS module propellant loading preparations were started on 26 October and satisfactorily completed on 2 November. The loading data are presented in table 5-2. During loading the following problems were encountered:

- a. The 3,000 psi tube assembly on module 1 was discovered to be damaged and was replaced.
- b. The propellant bladder within the oxidizer tank on module 2 was overpressurized, and the oxidizer tank was replaced.

Section 5
Countdown Operations

- c. The 750 psi facility GN2 system that supplied gas for APS checkout was discovered to be wet during module 2 purge and moisture sampling. An alternate source of GN2 was established, and module 2 was purged until the moisture content was below the required 200 ppm.
- d. During module 1 oxidizer loading, the maximum differential pressure observed on the model 1875 pressure instrumentation kit was 19 psid instead of the desired 15 psid. Since the maximum allowable delta P is 20 psid, no corrective action was required.
- e. During module 2 loading, the propellant flowrate decreased to 0 gpm. Module loading was terminated, and the controls on the propellant servicer were readjusted. Module loading was then reinitiated and completed satisfactorily.

5.3.2 APS Gas Removal

Gas removal from APS modules 1 and 2 was satisfactorily accomplished during the AS-501 launch countdown. No problems were encountered during the module 2 operation, but an excess of 110 cu in. of oxidizer was removed from module 1 because of a false level indication in the sight glass. This same problem occurred during gas removal from module 2 before the APS test firing. Since the module 1 oxidizer tank contained approximately 680 cu in. of excess propellant, no corrective action was taken.

Leakage was found at the inlet sight glass of one oxidizer and one fuel gas removal assembly. These assemblies were removed, and the operation was completed with the remaining set of assemblies.

5.3.3 APS Test Firing

The APS test firing was accomplished in accordance with NASA procedure V-25303-S-IVB1. The attitude control engines were fired in a sequence that consisted of one 250-ms clearing pulse and two 65-ms pulses with

a 750-ms delay between each pulse; the ullage engines were each fired for one pulse. The firing sequence was as follows:

- a. Minus pitch - engine 2-2
- b. Minus roll - engines 1-1 and 2-1
- c. Ullage engine No. 1 - one pulse 433 ms
- d. Plus pitch - engine 1-2
- e. Plus roll - engines 1-3 and 2-3
- f. Ullage engine No. 2 - one pulse 430 ms

Analysis of the data from these firings indicated that the systems were acceptable for flight. The only irregularities were erratic data for a period of 1 hr 46 min from measurement D0038-415, which later recovered and indicated normally, and measurement D0032-415 which responded sluggishly to pressure changes during the test. The latter measurement had responded normally during confidence firing at STC.

5.4 Launch Countdown

The 104-hr countdown began at 1700 GMT (1200 EST) on 4 November and continued without interruption (except for preplanned built-in holds of 11 hr) to vehicle launch on 9 November 1967. Major Douglas activities began on 5 and 6 November for precount tasks and continued according to schedule into 7 November for mid-count operations. The final portion of the count, including LOX and LH2 loading of the launch vehicle began 8 November and progressed in accordance with the schedule to AS-501 liftoff.

5.4.1 Prelaunch Preparations and Purges

The prelaunch preparations and purges were accomplished in accordance with Douglas procedures 1B62289, S-IVB Countdown Procedure for AS-501, and 1B61615, Pneumatic Console and Heat Exchanger Operating Instructions.

During the preparations the systems were leak checked, purges and valve actuations were verified, and the helium supply was analyzed for purity and moisture content.

Section 5 Countdown Operations

The LOX and LH2 tank purges consisted of propellant tank pressurization and vent cycles until the helium concentration in the tanks exceeded 99 percent. Maximum pressure in the LOX and LH2 tanks did not exceed 30 and 25 psia, respectively, and bulkhead differential pressure limits were not exceeded.

The LH2 feed duct and engine start sphere were purged by a continuous flow of helium for several minutes. The engine purges required by Rocketdyne were accomplished just prior to LOX loading during LOX transfer chilldown.

5.4.2 Loading Operations

5.4.2.1 LOX Loading

S-IVB stage LOX loading was conducted in accordance with procedure V-35007-SA501 and was initiated at 0514 GMT by the start of LOX replenish line chilldown. Transition from slow to fast fill was smooth with no abrupt pressure spikes. Fast fill was terminated at the 96 percent level and slow fill was initiated to the 99 percent level. LOX loading was uninterrupted and required 26 min to complete. Pressures, temperatures, and flowrates are presented in table 5-3.

5.4.2.2 LH2 Loading

S-IVB stage LH2 tank loading was started when the S-II stage achieved 100 percent LH2 mass. The loading was uninterrupted and required a total of 34 min to complete. Pressures, temperatures, and flowrates are presented in table 5-3.

5.4.2.3 Helium and GH2 Loading

Final pressurization of all S-IVB stage helium spheres, both cold and ambient, was accomplished without difficulty; pressurization of the APS helium tanks from blanket to full pressure was accomplished in one step at R0 -34 min. Pressurization of the engine control sphere from ambient to full pressure was accomplished in two steps approximately 5 min apart to limit the temperature rise.

Section 5
Countdown Operations

Start sphere chilldown was initiated at R0 -18 min instead of R0 -14 min 3 sec. This sequence will be used on all future stages. J-2 engine start sphere pressurization was initiated by closing the start sphere vent valve at R0 -5 min 30 sec after approximately 12.5 min of chilldown. The sphere pressure was 1,080 psia at the initiation of pressurization and 1,255 psia after pressurization. The start sphere pressure increased 40 psia from R0 -5 min to liftoff because of ambient heating. Sphere pressurization data are presented in table 5-4.

LOX and LH2 tank prepressurization, thrust chamber chilldown, and helium and GH2 sphere loading were all satisfactorily accomplished. Data are presented in figures 5-1 through 5-4.

5.4.3 Terminal Count

The launch terminal count was initiated at R0 -30 min and, like the rest of the countdown, was completed without any significant problem. During this period, final engine and stage conditioning were accomplished. Table 5-5 presents the sequence of terminal countdown events.

5.4.3.1 Engine Conditioning

J-2 engine conditioning was initiated at R0 -23 min with a 50-psi helium purge of the engine start sphere. At R0 -20 min, a 50-psi helium purge was initiated to the thrust chamber jacket. At R0 -18 min, the engine start sphere purge was terminated, and chilldown was initiated with cold GH2 flowing through circuit No. 1 of the heat exchanger. At R0 -15 min, the thrust chamber jacket purge was terminated, and chilldown was initiated with cold helium flowing through circuits No. 2 and 3 of the heat exchanger.

The engine start sphere pressure was 1,270 psia at the initiation of the automatic sequence (IAS) and 1,295 psia at R0 -19 sec. This was slightly higher than expected but still within limits. The thrust chamber jacket temperature was 225 deg R at IAS and 214 deg R at R0 -19 sec, thus well below the 265 deg R liftoff limit.

The engine control sphere was warmer than the GH2 start sphere with a temperature differential of 13 deg R at IAS and 8 deg R at R0 -19 sec. The maximum allowable temperature differential at these times is 30 deg R.

Section 5 Countdown Operations

5.4.3.2 Stage Conditioning

LOX turbopump chilldown was initiated manually at R0 -4 min 39 sec. The LOX flowrate was 35 gpm, unpressurized, and 37.5 gpm, pressurized, which was slightly lower than expected but well within the required 32 to 50 gpm limits. The LOX pump inlet temperature at R0 -19 sec was 164.7 deg R.

LH2 turbopump chilldown was initiated manually at R0 -5 min 3 sec and was normal in every respect. The LH2 flowrate was 118 gpm, unpressurized, and 146 gpm, pressurized; the required flowrate was 130 to 160 gpm while pressurized. The LH2 pump inlet temperature at R0 -19 sec was 38.5 deg R.

LOX tank prepressurization was initiated at R0 -2 min 47 sec and was completed in 15 sec. Two LOX tank ullage pressure makeup cycles were accomplished. The ullage pressure at liftoff was 42.4 psia.

LH2 tank prepressurization was initiated at R0 -1 min 36 sec and was completed in 21.5 sec, which was considerably less time than expected because the helium temperature at the LH2 tank inlet was higher than expected. The LH2 tank ullage pressure at liftoff was 35.9 psia.

The stage pneumatic system functioned normally during stage conditioning. Regulator discharge pressure was 540 to 550 psia during periods of low demand.

5.5 Environmental Control Systems

5.5.1 Thermoconditioning and Purge System

The aft interstage thermoconditioning and purge system functioned properly during the countdown, maintaining an APS temperature within the design limits of 87 \pm 5 deg F. At liftoff, the oxidizer temperature in APS module 1 was 92 deg F and the oxidizer temperature in APS module 2 was 87 deg F.

5.5.2 Common Bulkhead Evacuation

Common bulkhead evacuation commenced at 1618 GMT on 8 November. The vacuum supply valves (VS-15 and VS-16), which are located on the

model DSV-4-303 vacuum monitor console, failed to open on command. Simultaneously, the light indications on the bulkhead vacuum monitor panel in the Launch Control Center (LCC) went out. Investigation determined that a shorted diode, CR3, was the problem, and that it had been caused by corrosion of the washers isolating the diode from the chassis mount. The washers were replaced, and the system retested.

After the problem was corrected, the model DSV-4-303 vacuum monitor console supply valves were opened at 1920 GMT with a locked-up common bulkhead internal pressure of 2.59 psia. A gas sample was taken which indicated a satisfactory (inert) atmosphere in the bulkhead as follows:

Argon	57.9%	He	0.009%
N ₂	37.2%	CO ₂	1.7%
O ₂	3.2%	Other	0.004%
H ₂	0.011%		

The bulkhead was pumped until 0588 GMT. Following LOX and LH2 loading, the bulkhead internal pressure was 0.5 psia, which was the value at liftoff. The bulkhead internal pressure remained below 1 psia throughout the flight.

Currently the model DSV-4-303 vacuum monitor console transducer and the D0545-407 common bulkhead transducer are hardwired to the LCC firing room bulkhead vacuum monitor panel to indicate the bulkhead status. However, at the present time, no satisfactory and expeditious means exist for obtaining bulkhead samples and initiating bulkhead pumpdown should the RCA 110 computer cease to support checkout operations. A change request is being initiated to hardwire the LCC firing room bulkhead vacuum monitor panel in its entirety.

5.6 Redline Limits

The redline limits for launch vehicle parameters are presented in the Apollo/Saturn V Launch Mission Rules - Apollo 4 (AS-501), dated 12 September 1967; in Douglas Report SM 46998B, Saturn S-IVB-501 Stage Flight Test Plan, revised November 1967; and in the FTC Redline Monitoring Brief. All redlines were satisfied before the launch; however, several

Section 5 Countdown Operations

limits were changed from the values given for the CDDT. The maximum allowable LH2 tank ullage pressure prior to prepressurization and the minimum allowable LOX recirculation flowrate redline values were revised because the CDDT had demonstrated that the original limits could not necessarily be satisfied.

5.7 Countdown Problems

Although the countdown was conducted with no holds other than those that were built into the program, several problems were encountered.

5.7.1 APS Bubble Removal

During the bubble removal operation, 150 cu in. of oxidizer were removed from APS module 1. Although the maximum allowable quantity to be removed was 40 cu in., the remaining quantity was well in excess of that required for flight and was, therefore, considered acceptable for launch.

5.7.2 LOX Chillover Shutoff Valve Closed Indication

The LOX chillover shutoff valve closed indication did not pick up when the valve was commanded closed for LH2 loading. Although the anomaly was reported and verified, the hardwire talkback from the measurement in the launch control complex indicated that the valve was closed. Deletion of the measurement before launch was recommended; the measurement did not function properly during flight, (see section 17).

5.7.3 LH2 Tank Vent Quick Disconnect Leak

Vapor formed at the LH2 tank vent quick disconnect during LH2 loading and persisted through the remainder of the launch countdown. A hydrogen sensor in the area picked up one indication that a small leak may have existed at the seal between the ground and the vehicle halves of the quick disconnect. The condition was not considered to be hazardous, and the countdown was continued.

A plan to modify both the vehicle half and the ground half of the quick disconnect was not accomplished because the new parts had not completed

qualification testing in time for launch. These modifications were aimed at providing a better seal at the disconnect and will be accomplished before the next launch.

5.8 Atmospheric Conditions

The atmospheric conditions for the AS-501 launch on 9 November 1967 were as follows:

Time (GMT)	1200 (Liftoff)
Ambient temperature* (deg F)	63
Dew point* (deg F)	46
Relative humidity* (percent)	52
Total cloud cover (percent)	0.4
Wind direction** (degrees East of North)	70
Wind velocity† (knots)	20
Sea level pressure (in. of mercury)	30.31

*Ambient temperature, dew point, and relative humidity from ground level NASA industrial area

**From Launch Umbilical Tower No. 1, 60-foot level

†From Launch Umbilical Tower No. 1, 390-foot level

Section 5
 Countdown Operations

TABLE 5-1
 LAUNCH VEHICLE TESTS

TEST	NASA PROCEDURE	COMPLETION DATE
Launch Vehicle Electrical Interface Mate Test	7-LLVV-3013	24 July
Launch Vehicle Propellant Dispersion System Test	7-LLVV-3003D	28 June
Launch Vehicle Power Transfer Test	7-LLVV-3002B	13 March
Launch Vehicle Flight Sequence and EBW Functional Test	7-LLVV-3004	17 March
Launch Vehicle Sequence Malfunction Test	7-LLVV-3006S	15 December
Launch Vehicle Overall Test (Plugs In)	V-20029	13 July
Launch Vehicle Overall Test No. 1 (Plugs In)	V-20010-SA501	1 August
Launch Vehicle Overall Test No. 2 (Plugs Out)	V-20012-SA501	14 August
Launch Vehicle Swing Arm Overall Test	V-20022-SA501	10 August
Launch Vehicle Simulated Flight Test	V-10013-SA501	17 August
Space Vehicle Cutoff and Malfunction Test	V-20021-SA501	13 September
Countdown Demonstration Test (CDDT)	V-20016 Rev 004	27 September to 13 October
Flight Readiness Test	V-20017 Rev 3	25 and 26 October

TABLE 5-2
APS LOADING DATA

ITEM	VOLUME (in. ³)	TEMPERATURE (deg R)
Module 1		
Oxidizer System		
Loaded	4,102	541
Offloaded	372	536
Removed with bubble bleed during burp firing	28	547
Removed with bubble bleed during countdown	150	547
Fuel System		
Loaded	4,102	544
Offloaded	88	537
Removed during countdown	20	547
Module 2		
Oxidizer System		
Loaded	4,102	541
Offloaded	372	539
Removed with bubble bleed during burp firing	70	547
Removed with bubble bleed during countdown	20	547
Fuel System		
Loaded	4,102	544
Offloaded	88	544
Removed with bubble bleed during countdown	25	547

Section 5
 Countdown Operations

TABLE 5-3
 S-IVB STAGE PROPELLANT LOADING DATA

PARAMETER	UNITS	LOX	LH2
Chiltdown initiated	GMT	0513:55	1013:58
Slow fill			
Levels	percent	0 to 5	0 to 5
Initiation time	GMT	0549	1015
Flowrate	gpm	575	582
Maximum swing arm pressure	psia	52	47
Maximum ullage pressure	psia	22.3	22.2
Fast fill			
Levels	percent	5 to 96	5 to 98
Initiation time	GMT	0552:20	1021:48
Flowrate	gpm	900	2,600
Swing arm pressure			
Maximum	psia	45	31
Stabilized	psia	39 to 40	30.5
Maximum ullage pressure	psia	23.4	18.3
Final slow fill			
Level at initiation	percent	96	98
Initiation time	GMT	0612:55	1046:52
Flowrate	gpm	225	440
Swing arm pressure	psia	22	19
Maximum ullage pressure	psia	17	17.95
Total time required	min	26	34

TABLE 5-4
SPHERE PRESSURIZATION DATA

SPHERE	VOLUME (ft ³)	FINAL PRESSURIZATION		INITIAL PRESSURE (psia)	FINAL PRESSURE (psia)	PRESSURE AT LIFTOFF (psia)	TEMPERATURE AT LIFTOFF (deg K)	MASS AT LIFTOFF (lbm)
		INITIATION TIME	REQUIRED TIME					
Repressurization								
LOX	9.0	70% LH2*	20 min	1,530	2,970	2,950	507	17.6
LH2	31.5	70% LH2*	20 min	1,500	2,970	2,940	510	60.9
Control Helium	4.5	70% LH2*	20 min	1,495	2,980	2,920	545	8.1
Cold Helium	28.0	70% LH2*	35 min	1,120	2,960	2,910	41	332
APS Helium								
Module 1	0.540	T -34 min	3.5 min	65	2,980	3,000	547	1.0
Module 2	0.540	T -34 min	3.5 min	65	2,975	2,980	546	1.0
Engine Control	0.578	T -33 min	4 min 50 sec**	40	2,990	2,980	272	1.9
Engine GH2 Start	4.224	T -5 min 30 sec	approx 20 sec	1,080	1,255	1,295	264	3.7

*T -1 hr 20 min

**Pressurized in two steps

Section 5
 Countdown Operations

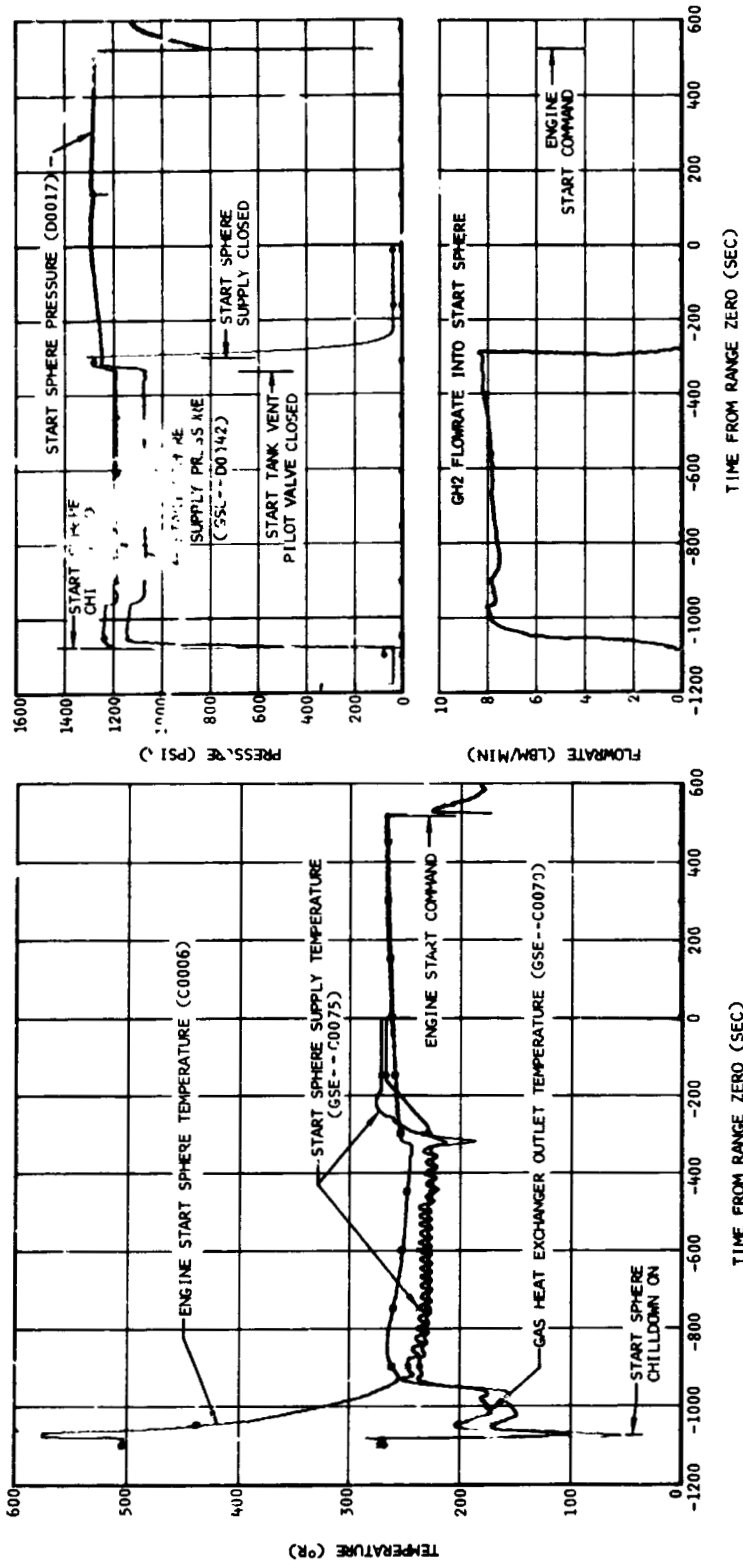


Figure 5-1. GSE Performance During Engine Start Sphere Chilldown and Loading - First Burn

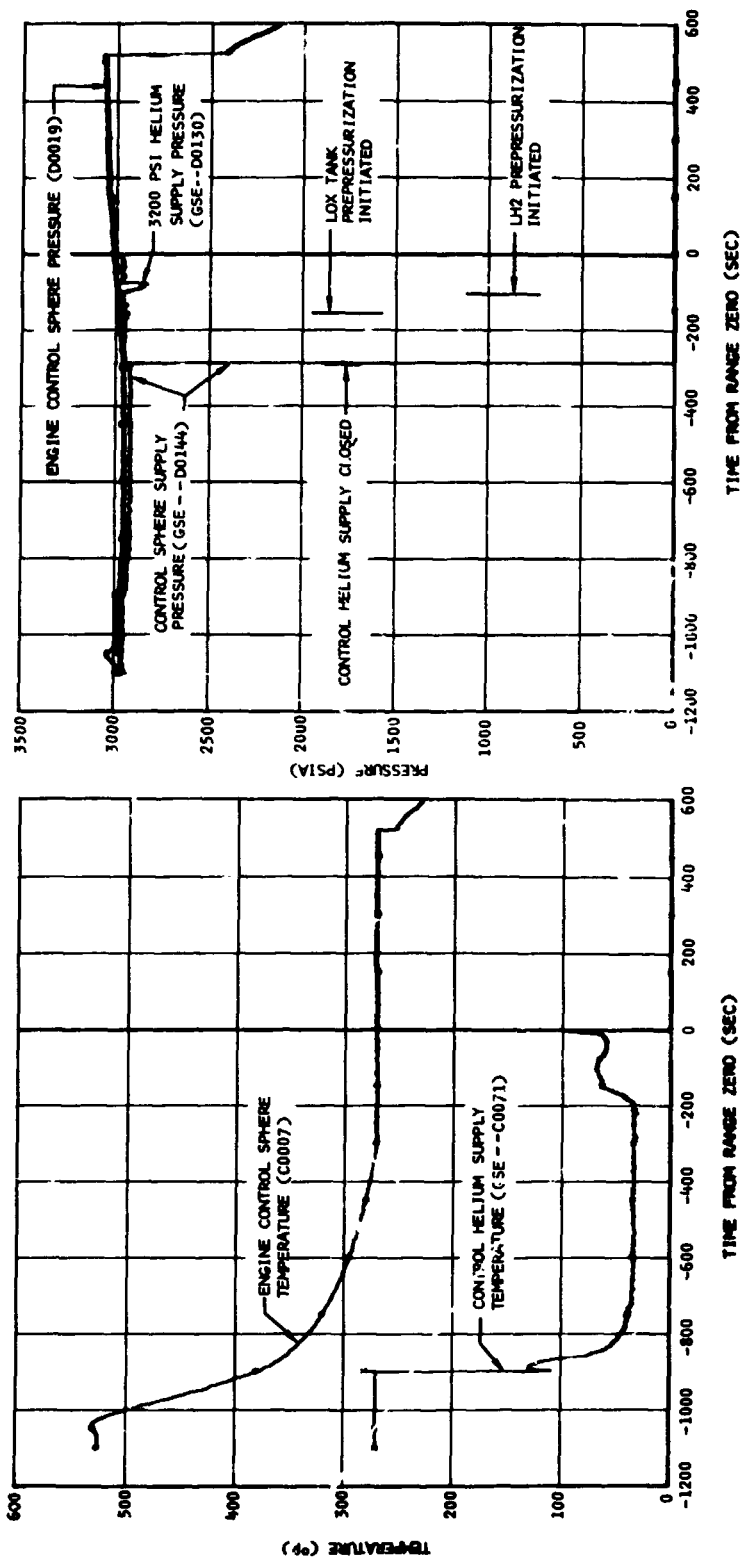


Fig. 5-2. GSE Performance During Engine Control Sphere Loading - First Burn

Section 5
 Countdown Operations

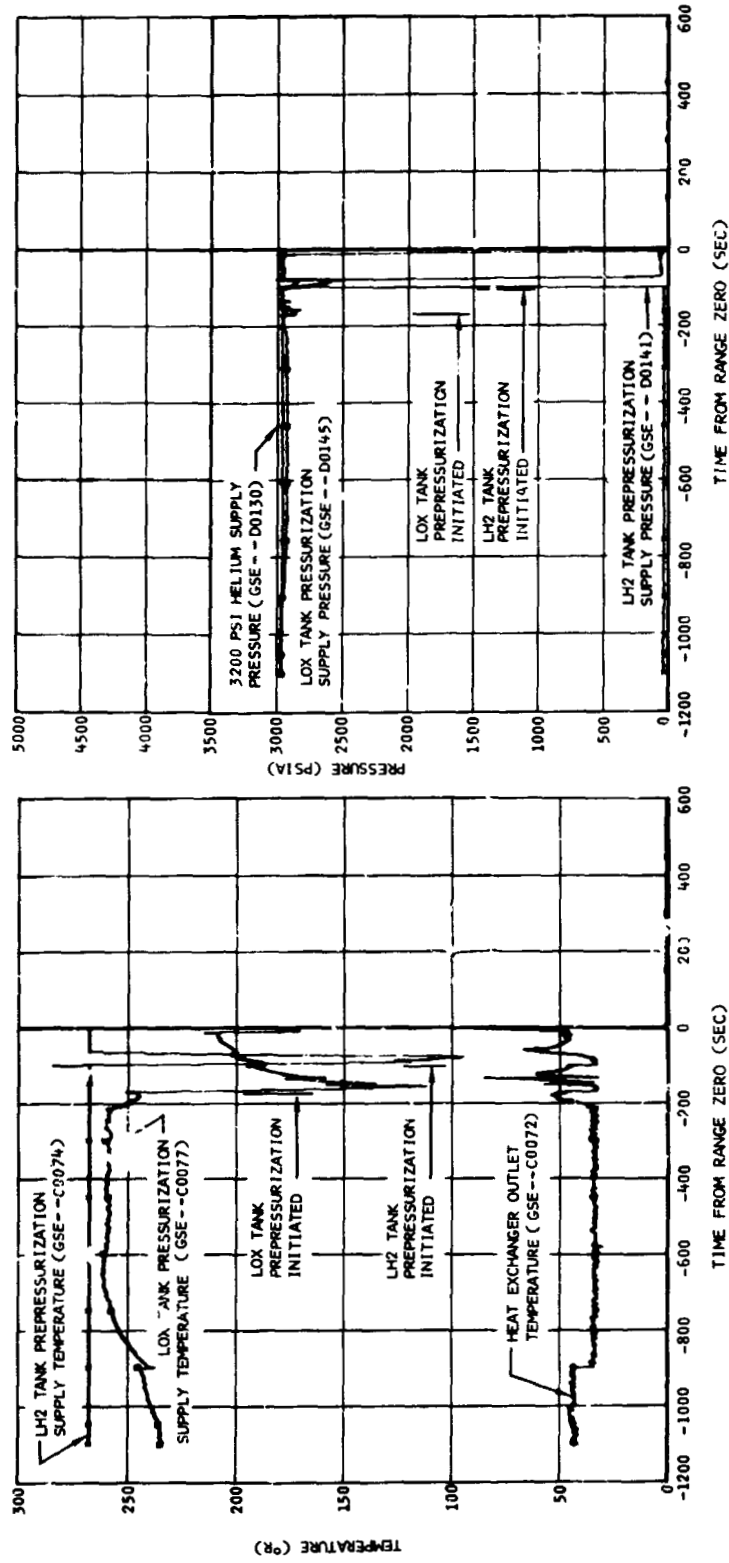


Figure 5-3. GSE Performance During LOX and LH2 Prepressurization - First Burn

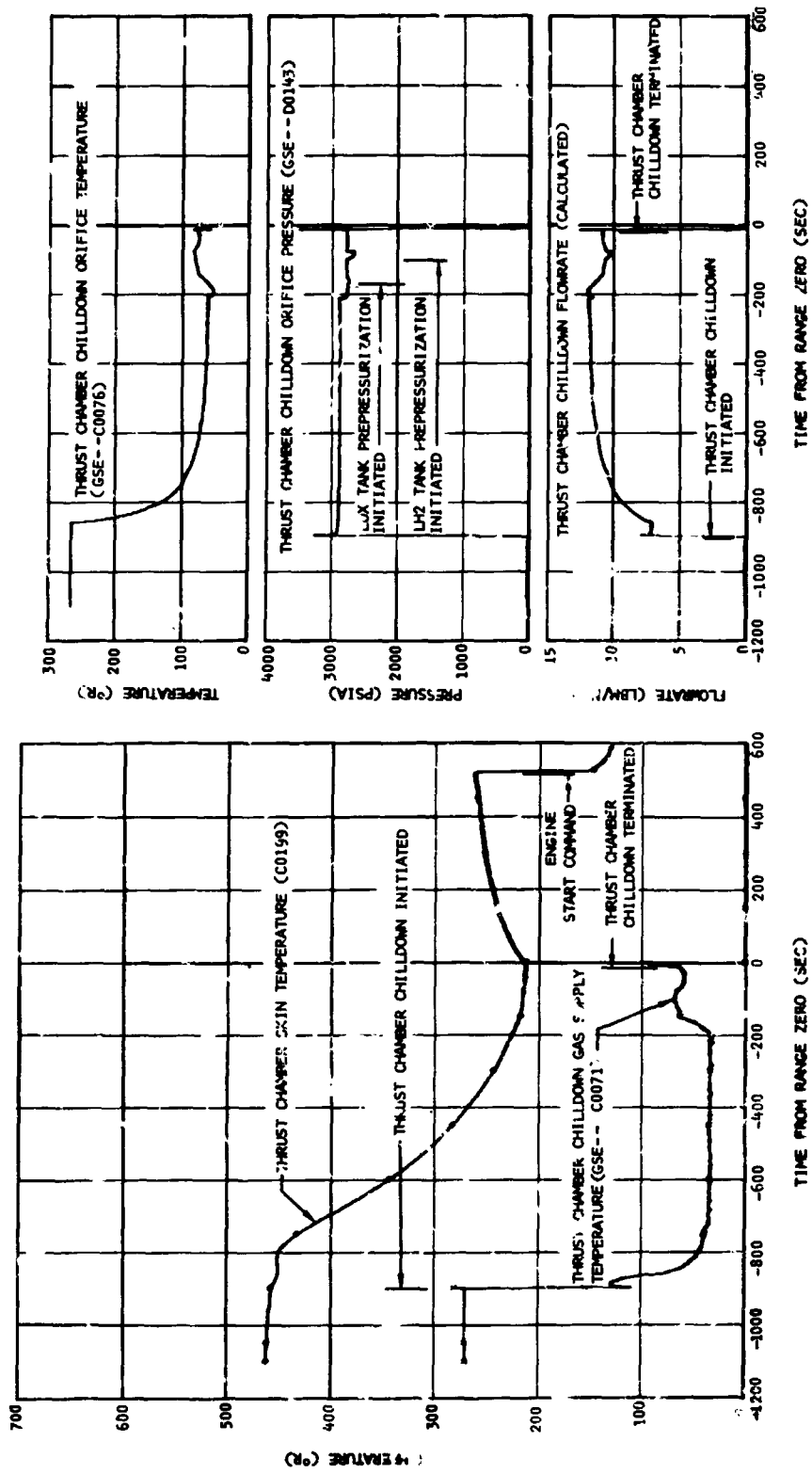


Figure 5-4. GSE Performance During Thrust Chamber Chilldown - First Burn

6. COST PLUS INCENTIVE FEE

The incentive evaluation of the S-IVB-501 flight performance includes flight mission accomplishment and telemetry performance. Performance of the S-IVB stage was within the incentive criteria presented in Douglas Report No. SM-46998B, S-IVB-501 Stage Flight Test Plan.

6.1 Flight Mission Accomplishment

Flight data evaluated to establish preconditions of flight (PCF) and end conditions of flight (ECF) were obtained from observed trajectory and attitude data transmitted by magnetic tape and printout to MDC from MSFC as requested in Douglas Report No. DAC-56334A, Douglas S-IVB Stage Data Acquisition Requirements Document for Saturn V Flights, September 1967 revision, DAC items 820, 922, 1010, and 1016. Tables 6-1 and 6-2 compare actual and allowable values of PCF and ECF, respectively.

Performance of the S-IC and S-II stages provided PCF at S-II/S-IVB Separation Command that were within allowable tolerances. Trajectory ECF at waiting orbit insertion were within tolerance; also maximum flight values of attitude errors and rates for all phases of S-IVB operation (i.e., burn phase, waiting orbit phase, and parking orbit phase) did not exceed the respective allowable tolerances. All received command signals were recognized, and all end condition command signals were given. It was concluded for purposes of incentive achievement, therefore, that all PCF and ECF were achieved.

6.2 Telemetry Performance

Evaluation of the telemetry performance indicated that the telemetry system operated at 99.1 percent efficiency during the telemetry performance evaluation period (TPEP) phase I (liftoff [LO] to first S-IVP engine cutoff plus 10 sec) and performed at 97.6 percent efficiency during the TPEP phase II (liftoff to planned LV/SC separation as defined in NASA drawing 40M37621 Interface Control Document Definition of Saturn SA-501 Flight Sequence Program).

The results of the telemetry performance analysis are shown in table 6-3.

Section 6
 Cost Plus Incentive Fee

TABLE 6-1
 MISSION ACCOMPLISHMENT - PCF

PARAMETERS	UNITS	NOMINAL	ACTUAL	ALLOWABLE DEVIATION*	ACTUAL DEVIATION
Range	km	1,476.8	1,481.9	+48.8 -36.4	+5.1
Crossrange	km	40.2	38.8	+3.4 -3.5	-1.4
Altitude	km	189.8	192.4	+4.0 -4.2	+2.6
Velocity vector magnitude	m/sec	6,857.4	6,816.5	+98.3 -97.1	-40.9
Velocity vector elevation or direction	deg	0.52	0.63	+0.36 -0.36	+0.11
Pitch attitude	deg	-96.8	-94.8	+4.5 -5.0	+2.0
Pitch rate	deg/sec	0	0	+1.5 -1.5	0
Yaw attitude	deg	0.5	-0.09	+3.6 -3.6	-0.59
Yaw rate	deg/sec	0	0.08	+1.5 -1.5	+0.08
Roll attitude	deg	0	1.2	+4.0 -4.0	+1.2
Roll rate	deg/sec	0	0.13	+1.5 -1.5	+0.13

NOTE: PCF are evaluated at the instant of Separation Command.

*Deviations consist of allowable error plus evaluation uncertainty.

TABLE 6-2
MISSION ACCOMPLISHMENT - ECF

TRAJECTORY PARAMETERS	UNITS	NOMINAL	ACTUAL	ALLOWABLE DEVIATION*	ACTUAL DEVIATION
Inclination	deg	30.275	30.302	+0.129 -0.119	+0.027
Node	deg	135.428	135.435	+0.226 -0.232	+0.007
Energy (C ₃)	mi ² /sec ²	-26,734,367	-26,672,329	+698,246 -615,953	+62,038
Eccentricity	-	0.57834	0.57888	+0.00956 -0.00854	+0.00054

ATTITUDE CONTROL PARAMETERS	UNITS	ALLOWABLE ENVELOPE*	MAXIMUM FLIGHT VALUE
S-IVB Burn phases:			
Pitch attitude error	deg	<u>+6</u>	+2.2
Yaw attitude error	deg	<u>+6</u>	-2.4
Roll attitude error	deg	<u>+6</u>	+2.5
Pitch rate	deg/sec	<u>+3</u>	+1.4, -1.4
Yaw rate	deg/sec	<u>+3</u>	+1.4
Roll rate	deg/sec	<u>+1.5</u>	-0.5
Parking Orbit:			
Pitch rate	deg/sec	<u>+1</u>	+0.40
Yaw rate	deg/sec	<u>+1</u>	-0.31
Roll rate	deg/sec	<u>+1.5</u>	-0.19
Waiting Orbit (to CSM separation)			
Pitch rate	deg/sec	<u>+1</u>	-0.55
Yaw rate	deg/sec	<u>+1</u>	+0.44
Roll rate	deg/sec	<u>+1.5</u>	-1.15

NOTE: Trajectory ECF are evaluated at waiting orbit injection (10 sec after second S-IVB Engine Cutoff Command).

*Deviations consist of allowable error plus evaluation uncertainty.

Section 6
 Cost Plus Incentive Fee

TABLE 6-3 (Sheet 1 of 3)
 FLIGHT TELEMETRY PERFORMANCE SUMMARY

ITEM	DESCRIPTION	TOTAL
1.	Total number of measurements listed in the S-IVB-501 Instrumentation Program and Components List, Douglas Drawing 1B43566, AT Change.	592
2.	<p>Measurements listed in the IP&CL which are not wholly on the S-IVB-501 Stage:</p> <p>Measurements transmitted by the S-II telemetry system:</p> <p>D0153-423 Press - Chamber Retrorocket Posit IV-I D0154-421 Press - Chamber Retrorocket Posit II-III D0155-420 Press - Chamber Retrorocket Posit I-II D0156-422 Press - Chamber Retrorocket Posit III-IV</p> <p>Measurements wholly transmitted landline to the Launch Control Center (LCC):</p> <p>D0545-407 Press - Common Bulkhead Internal - H/W D0576-408 Press - Fuel Tank Ullage Umbilical - H/W D0577-406 Press - Oxid Tank Ullage Umbilical - H/W</p>	7
3.	<p>Measurements known to be inoperative at start of automatic launch sequence, or became inoperative prior to start of automatic launch sequence:</p> <p>The function of the following measurements is to monitor the output voltage of exploding bridgewires (EBW) by means of pulse sensors during checkout. The pulse sensors are removed prior to launch, thus making the measurements inoperative during flight.</p> <p>K0141-411 Event - R/S 1 Pulse Sensor K0142-411 Event - R/S 2 Pulse Sensor K0149-404 Event - Ullage Jettison 1 P/S K0150-404 Event - Ullage Jettison 2 P/S K0169-404 Event - EBW Pulse Sensor Off Indication K0176-404 Event - Ullage Rocket Ignition P/S 1 Ind. K0177-404 Event - Ullage Rocket Ignition P/S 2 Ind.</p> <p>The following measurement was listed in the IP&CL and the capability to make the measurement existed on the stage. MSFC did not require the associated rate gyro installation, therefore, the measurement is inoperative.</p> <p>K0152-404 Event - Rate Gyro Wheel Speed OK Ind.</p> <p>The following measurement is used for checkout only. The IU flight sequencing tape is not punched to activate this measurement in flight. Therefore, it is inoperative.</p> <p>K0168-404 Event - Switch Selector Register Test</p>	10

TABLE 6-3 (Sheet 2 of 3)
FLIGHT TELEMETRY PERFORMANCE SUMMARY

ITEM	DESCRIPTION	TOTAL
	A measurement malfunctioned and became inoperative prior to the start of automatic sequence. K0139-424 Event - Oxidizer Shutoff Valve, Chill System-Closed	
4.	Measurements previously deleted from the incentive baseline by NASA direction in NASA letter I-CO-S-IVB-906, dated 16 August 1967. These forward skirt measurements were hampered to a greater or lesser degree by the inclusion of the forward skirt anti-flutter kit after the transducer installations had been made on the forward skirt area. C0081-426 Temp - Forward Skirt - 1 C0082-426 Temp - Forward Skirt - 2 C0083-426 Temp - Forward Skirt - 3 C0084-426 Temp - Forward Skirt - 4 C0108-426 Temp - Forward Skirt - 5 C0109-426 Temp - Forward Skirt - 6 C0110-426 Temp - Forward Skirt - 7 C0111-426 Temp - Forward Skirt - 8 C0112-426 Temp - Forward Skirt - 9 C0239-426 Temp - Forward Skirt - 10 C0240-426 Temp - Forward Skirt - 11 S0054-426 Strain - Axial, Fwd Skirt Loc 10A S0055-426 Strain - Axial, Fwd Skirt Loc 10B S0056-426 Strain - Axial, Fwd Skirt Loc 11A S0057-426 Strain - Axial, Fwd Skirt Loc 11B S0058-426 Strain - Axial, Fwd Skirt Loc 12A S0059-426 Strain - Axial, Fwd Skirt Loc 12B S0060-426 Strain - Axial, Fwd Skirt Loc 13A S0061-426 Strain - Axial, Fwd Skirt Loc 13B S0062-426 Strain - Axial, Fwd Skirt Loc 14A S0063-426 Strain - Axial, Fwd Skirt Loc 14B S0064-426 Strain - Axial, Fwd Skirt Loc 15A S0065-426 Strain - Axial, Fwd Skirt Loc 15B S0066-426 Strain - Axial, Fwd Skirt Loc 16A S0067-426 Strain - Axial, Fwd Skirt Loc 16B S0068-426 Strain - Axial, Fwd Skirt Loc 17A S0069-426 Strain - Axial, Fwd Skirt Loc 17B	27
5.	Measurements from which Douglas could not obtain data due to noise from unknown sources, and measurements which were degraded or prevented from being transmitted.	0
6.	The total number of measurements to be evaluated for incentive performance for both TPEP phase I and phase II is item 1 minus the sum of items 2, 3, 4, and 5.	548

Section 6
 Cost Plus Incentive Fee

TABLE 6-3 (Sheet 3 of 3)
 FLIGHT TELEMETRY PERFORMANCE SUMMARY

ITEM	DESCRIPTION	TOTAL
7.	<p>Measurements which were failures during TPEP phase I (Liftoff to first S-IVB engine cutoff plus 10 sec). Details regarding these measurement failures may be obtained in section 17 of this report.</p> <p>C0121-419 Temp - Aft Interstage - 4 C0151-401 Temp - Engine LOX Pump Surface D0195-419 Press - Ext Aft Interstage 17 D0196-419 Press - Ext Aft Interstage 18 D0210-402 Press - Interstage Internal 6</p>	5
8.	<p>Measurements which were failures during TPEP phase II (Liftoff to planned LV/SC separation as defined in NASA drawing 40M33621 Interface Control Document Definition of Saturn SA-501 Flight Sequence Program). Details regarding these measurement failures may be obtained in section 17 of this report.</p> <p>All measurements which were failures during TPEP phase I are included as phase II failures because phase II encompasses phase I. These five measurements are shown in item 7 above.</p> <p>In addition to those measurements which were failures during TPEP phase I, the following eight measurements were failures during phase II.</p> <p>C0075-409 Temp - Fuel Tank External - 1 C0077-409 Temp - Fuel Tank External - 3 C0078-409 Temp - Fuel Tank External - 4 C0079-409 Temp - Fuel Tank External - 5 C0106-409 Temp - Fuel Tank External - 7 C0217-401 Temp - Main Hydraulic Pump Flange D0181-409 Press - Fuel Tank, Continuous Vent 1 D0182-409 Press - Fuel Tank, Continuous Vent 2</p> <p>Calculation of phase I performance:</p> <p>Item 6 minus item 7, divided by item 6, multiplied by 100, and rounded off to the nearest one-tenth of one percent.</p> $\frac{548-5}{548} \times 100 = 99.1 \text{ percent}$ <p>Calculation of phase II performance:</p> <p>Item 6 minus item 8, divided by item 6, multiplied by 100, and rounded off to the nearest one-tenth of one percent.</p> $\frac{548-13}{548} \times 100 = 97.6 \text{ percent}$	13

7. TRAJECTORY

This section presents a discussion of the AS-501 trajectory. Comparisons are made between the actual observed trajectory and the preflight and postflight predicted trajectories; also, results of a simulation of the actual trajectory are presented. Observed trajectory deviations from predicted are explained in terms of S-IVB and lower stage system performance deviations, in addition to the qualitative evaluation of the accuracy of the observed mass-point trajectory.

Presented also in this section is the parking orbit continuous vent system thrust determined from trajectory analysis. A comparison of this thrust with predicted is presented.

As an area of interest, a discussion is included of the significant transient in attitude commands given by the iterative guidance mode during S-IVB second burn. Causes of this transient and its effect upon the actual trajectory are discussed.

7.1 Comparison Between Actual and Preflight Predicted Trajectories

A comparison is made between the actual trajectory (based on tracking and telemetry data) and the Douglas preflight predicted trajectory. The predicted trajectory, during S-IC and S-II stage burns, is the same as that presented in the Boeing Company document SSR 155, AS-501 Launch Vehicle Operational Trajectory Flown in Winter Winds, dated 6 October 1967. The S-IVB stage portion of the predicted trajectory is presented in Douglas Report No. SM-46998B, S-IVB-501 Stage Flight Test Plan, dated 2 November 1967. Figures 7-1 through 7-36 and table 7-1 compare the actual and predicted values of altitude, ground range, crossrange position, crossrange velocity, inertial velocity, axial acceleration, commanded and actual attitude angles, inertial flight path elevation angle, and inertial flight path azimuth angle for the S-IC/S-II burn, S-IVB first burn, parking orbit, and S-IVB second burn phases of the flight. Appendix 3 presents a detailed tabulation of the observed trajectory.

Section 7 Trajectory

The actual trajectory of the AS-501 flight was close to that predicted. The burntime of the S-IC stage was 1.73 sec less than predicted. The burntime of the S-II stage was 4.6 sec longer than predicted. At S-II/S-IVB separation, the trajectory was characterized as slow, high, long, and south of the intended path. This can be seen in table 7-1.

The slower than predicted velocity at S-II/S-IVB separation was the primary cause of the longer than predicted burntime for the S-IVB stage first burn. The first burntime was 6.1 sec longer than predicted of which 5 sec was due to low trajectory conditions at S-II/S-IVB separation. Trajectory conditions at first burn Engine Cutoff Command are presented in table 7-1. The differences in S-IVB first burn velocity and acceleration are shown in figures 7-15 and 7-16, respectively. Low S-IVB thrust contributed slightly to the longer burntime. The observed trajectory indicates that the S-IVB altitude was higher than predicted as shown in figure 7-11. The S-IVB first burn trajectory can be summarized as slow, high, and long. Figures 7-19, 7-20, and 7-21 show the pitch, yaw, and roll commanded and actual attitude angles. A summary of trajectory conditions and orbit elements at parking orbit insertion is presented in table 7-1.

The parking orbit phase of the flight was very close to that predicted. A slightly higher than predicted vent thrust did not have a significant effect on the trajectory. At S-IVB restart, the actual trajectory was slower, higher and further downrange than predicted.

The S-IVB second burn engine cutoff occurred 13.83 sec earlier than it had been predicted. This early cutoff was mainly caused by a late propellant mixture ratio shift and corresponding high S-IVB thrust early in flight which in turn caused a higher than predicted velocity and acceleration, as shown in figures 7-30 and 7-31, respectively. Altitude and ground range were quite close to their predicted values. There was a difference in crossrange velocity during second burn as shown in figure 7-29. This was caused by the yaw attitude transient shown in figure 7-35 which resulted from the thrust cutback. The two minor transients, at RO +11,520 and RO +11,680 sec, were also produced by the yaw steering command transients associated with the high stop

thrust operation. At S-IVB second burn engine cutoff conditions were fast, low, and short but nearly exactly on the desired orbit. A summary of conditions and orbit elements at waiting orbit injection is presented in table 7-1. These S-IVB stage end conditions of flight were well within the preflight determined three-sigma tolerances. The observed deviations in the waiting orbit elements are less than one-sigma deviations from predicted.

S-IVB stage impact occurred at a longitude of 161.2 deg West and a latitude of 23.4 deg North. Range time at impact was 8 hr, 3 min, 7 sec.

7.2 Postflight Predicted Trajectory Evaluation

To assist in the isolation of S-IVB performance deviations which contributed to trajectory deviations, a postflight S-IVB stage predicted trajectory was generated. This trajectory was generated using predicted S-IVB stage performance characteristics and actual S-II/S-IVB separation trajectory conditions. Trajectory deviations between the actual and the postflight predicted are due to S-IVB stage performance deviations, observed trajectory evaluation errors, and instrument unit navigation or guidance errors.

To support this evaluation, a set of parameters were selected which define the S-IVB stage trajectory. These parameters are inertial velocity, altitude, ground range, and crossrange velocity. They are presented in figures 7-37 through 7-40 for the period from S-II/S-IVB separation to waiting orbit insertion. As can be seen in these figures, the S-IVB first burn postflight predicted trajectory is nearly identical to the actual with the exception of the altitude and crossrange velocity history. Results of the trajectory simulation, which are discussed in paragraph 7.3.1, indicate that the observed trajectory first burn altitude and crossrange velocity histories are probably in error. The S-IVB first burn thrust and weight flow were slightly lower than predicted, which yielded a slower than predicted velocity history. S-IVB first burn engine performance contributed 1 sec to the 6.1 sec longer than predicted first burntime. The postflight predicted parking orbit

Section 7 Trajectory

was higher and slower than actual. Trajectory simulation results show that the altitude deviations which accumulate in the parking orbit can be explained by a 4.8 percent higher than predicted continuous vent system (CVS) thrust as discussed in paragraph 7.3.2.

At the beginning of the second burn, the postflight predicted and actual trajectory conditions were near predicted. Due to the in-tank propellant ratio at restart (excess LOX), the propellant utilization system caused a hardover high engine mixture ratio (EMR) operation (5.5/1.0 EMR), with thrust cutback to the reference mixture ratio (RMR) occurring approximately 83 sec after Engine Start Command. This thrust profile caused a higher and faster observed trajectory than was predicted and by itself would have caused an 18 sec shorter than predicted second burntime (see paragraph 7.3.1). The actual burntime was 16.8 sec shorter than predicted. The guidance system response to the thrust cutback resulted in attitude commands causing a nose down and to the right (south). This attitude excursion resulted in noticeable changes in the inertial velocity and crossrange velocity at approximately RO +11,580 sec. The nose-down pitch command reduced gravity losses considerably and produced an increase in inertial velocity from the predicted inertial velocity history. The excursion had no effect on the accomplishment of the desired end-conditions of flight. A discussion of the guidance transient is presented in paragraph 7.4.

7.2.1 Powered Flight Simulated Trajectory Evaluation

Using a five-degrees-of-freedom trajectory simulation program, propulsion system parameter histories were adjusted so that an S-IVB trajectory could be generated to closely match the observed trajectory (appendix 3, Observed Trajectory). The simulation program employed for first and second burns uses a differential correction technique which determines the necessary adjustments to thrust and weight flow from the engine analysis (section 9) and pitch and yaw engine thrust misalignment angles from the control system analysis to match the observed trajectory. These adjustments were determined for first burn by minimizing in a least-squares sense the differences in altitude, earth-fixed velocity,

Section 7
Trajectory

earth-fixed velocity azimuth angle, and longitudinal acceleration between the observed and simulated trajectories. For second burn the adjustments were determined by minimizing in a like manner differences in altitude, earth-fixed velocity, earth-fixed velocity azimuth angle, and earth-fixed downrange position.

Differences between the observed and simulated first and second burn trajectories are presented in figures 7-41 and 7-42, respectively. The average and maximum deviations between the actual and simulated trajectories are:

<u>Parameter</u>	<u>First Burn</u>	
	<u>Average Deviation</u>	<u>Maximum Deviation</u>
Altitude (ft)	6.9	10.7
Earth-fixed velocity (ft/sec)	0.844	1.890
Earth-fixed velocity azimuth angle (deg)	0.00752	0.019
Longitudinal acceleration (ft/sec ²)	0.0726	0.185
	<u>Second Burn</u>	
Altitude (ft)	79.8	180
Earth-fixed velocity (ft/sec)	0.90	1.90
Earth-fixed velocity azimuth angle (deg)	0.009	0.038
Earth-fixed downrange position (ft)	54.6	105

The maximum and average deviations are small, indicating compatibility between the shapes of the propulsion parameter histories, determined by engine analysis, and the observed trajectory. However, to obtain a match of the observed trajectory, thrust and weight flow during first burn were 0.71 percent and 0.56 percent, respectively, higher than determined by engine analysis; during second burn the simulated actual thrust and weight flow were increased by 0.81 percent and 0.67 percent, respectively, over engine analysis values. Engine analysis specific impulse was correspondingly increased by 0.14 percent during first burn and increased by 0.02 percent during second burn. Histories of the

Section 7
Trajectory

predicted and simulated thrust and weight flow are presented in figures 7-43 and 7-44 for first and second burn, respectively. The average values for these parameters are:

<u>First Burn</u>		
<u>Parameter</u>	<u>Predicted</u>	<u>Actual</u>
Average thrust (lb)	225,343	223,852
Average weight flow (lb/sec)	532.33	528.68
Average specific impulse (sec)	423.3	423.4
<u>Second Burn</u>		
Total average thrust (lb)	201,110	205,300
Total average weight flow (lb/sec)	471.3	481.5
Total average specific impulse (sec)	426.7	426.0
Average thrust at high mixture ratio (lb)	-	226,090
Average weight flow at high mixture ratio (lb/sec)	-	535.51
Average specific impulse at high mixture ratio (sec)	-	422.20
Average thrust at reference mixture ratio (lb)	201,110	197,381
Average weight flow at reference mixture ratio (lb/sec)	471.3	461.40
Average specific impulse at reference mixture ratio (sec)	426.7	427.79

These results indicate a 0.7 percent lower thrust and weight flow than predicted for first burn. During second burn the actual thrust and weight flow during the RMR operation (after mixture ratio shift) were lower than predicted by 1.8 percent and 2.1 percent, respectively, while the actual specific impulse of the RMR during operation was 0.26 percent higher than predicted.

The maximum inaccuracies in the simulated propulsion parameters due to the observed trajectory and simulation uncertainties are estimated to be 0.2 percent for thrust and weight flow and 0.3 percent for specific

impulse. An additional inaccuracy is added by the uncertainty in the ignition and cutoff weight. As a result, the total inaccuracy in thrust, weight flow, and specific impulse is 0.3 percent in each.

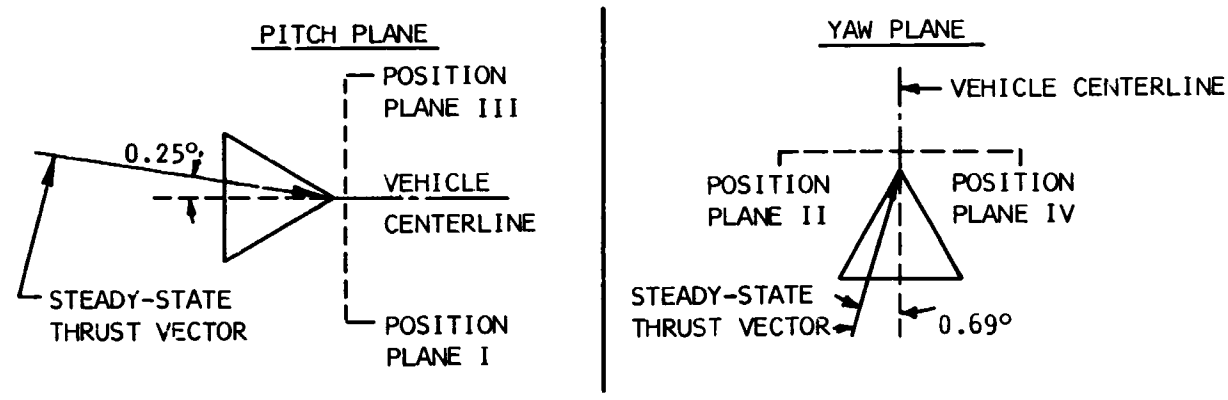
The pitch and yaw thrust misalignment angles for first burn, as determined from the flight simulation, were unrealistic and not consistent with misalignment angles indicated by control and guidance parameters. It was concluded that considerable inaccuracy exists in both altitude and crossrange data in the observed trajectory for first S-IVB burn. This was probably due to limited vehicle tracking coverage during S-IVB first burn. Only one tracking site, Bermuda, was available during most of the first burn. The pitch and yaw thrust misalignment angles for second burn, as established by control system and trajectory analysis, compare favorably. The values obtained are given below.

Second Burn

<u>Parameter</u>	<u>Control Analysis Value</u>	<u>Simulated Value</u>
Pitch thrust misalignment (deg)	0.25	0.25
Yaw thrust misalignment (deg)	0.36	0.69

A positive pitch misalignment produces a nose-above-commanded attitude, and a positive yaw misalignment produces a nose-left-of commanded attitude (looking downrange).

The steady-state thrust vector was located relative to the vehicle during second burn as shown below:



Section 7
Trajectory

The simulated S-IVB stage weights and predicted values are:

	<u>First Burn</u>		<u>Second Burn</u>	
	<u>Predicted</u>	<u>Simulated</u>	<u>Predicted</u>	<u>Simulated</u>
Engine Start Command	352,015	353,050	277,741	275,790
Engine Cutoff Command	280,408	278,581	133,282	136,070

These weights were derived from the composite best estimate ignition and cutoff weight. The weights were determined by finding the point on the trajectory reconstruction line statistically closest to the composite best estimate point. The first burn simulated masses presented above were determined using a best estimate ignition and cutoff mass established prior to the solution presented in section 8. The discrepancy introduced in mass is less than 0.1 percent. This percentage would have negligible effect on the analysis.

The flight simulation verifies the 6.1 and 16.8 sec differences between predicted and actual guidance cutoff time for first and second burn, respectively. Components of the long first burn time and short second burn time are:

<u>First Burn</u>	
<u>Contributor</u>	<u>Burntime Component (sec)</u>
Slow S-II/S-IVB separation velocity	6.1
High S-II/S-IVB separation altitude	-1.1
Low S-IVB thrust	0.4
High S-IVB initial propellant weight	<u>0.6</u>
Total	6.0

<u>Second Burn</u>	
<u>Contributor</u>	<u>Burntime Component (sec)</u>
Slow S-II/S-IVB separation velocity	-5.0
High S-II/S-IVB separation altitude	0.3
High CVS thrust	-0.3
High-stop engine operation	-18.0
Low thrust and weight flow at RMR	<u>7.0</u>
Total	-16.0

The total of these components is in close agreement with the difference observed for each S-IVB burn.

7.2.2 Orbital Simulated Trajectory Evaluation

The AS-501 mission was sensitive to parking orbit CVS thrust from two standpoints: (1) waiting orbit injection accuracy and (2) launch vehicle (LV) performance capability. Prior to the flight, it was known that higher or lower than predicted CVS thrust would produce onboard navigation errors which would directly affect LV accuracy capability. Also, it was known that lower than predicted orbital boiloff could create a performance problem by requiring low stop (4.5 EMR) operation of the J-2 engine to remove the excess hydrogen onboard at the start of second burn. For each pound of lower than predicted boiloff, 13 lbm of reserve propellant would have to be used to achieve guidance cutoff.

Using the actual parking orbit trajectory determined from guidance accelerometer and tracking data, the time history of CVS thrust was determined which produced a close fit of the observed trajectory. This actual CVS thrust history compared with the predicted CVS thrust history is presented in figure 7-45.

Figure 7-46 compares the difference between the observed altitude during parking orbit and the altitude as calculated using both actual and predicted CVS thrust.

Figure 7-45 shows that the actual CVS thrust was within tolerance except early in the first orbit and late in the second orbit. The actual CVS thrust history yields a total impulse 4.8 percent higher than predicted which indicates higher than predicted orbit boiloff.

These results are in good agreement with results obtained from the PU system and onboard temperature and pressure instrument evaluation. Since the boiloff was higher than predicted, this contributed to the PU system causing a high stop (5.5 EMR) operation early during second burn. The high boiloff actually enhanced LV performance capability since high EMR was more optimum than low or nominal EMR operation for the AS-501 mission.

Section 7 Trajectory

Since the actual CVS thrust was very close to predicted, even though it was greater than the maximum expected CVS thrust during certain regions of flight, the effect in injection errors was negligible.

7.3 Analysis of Special Areas of Concern

The transient in the commanded angles which occurred approximately 80 sec after Engine Start Command was investigated to determine the cause for the transient and whether or not it was normal response of the guidance system to the actual second burn S-IVB stage performance. To accomplish this, a five-degree-of-freedom trajectory simulation was conducted using actual S-IVB stage engine performance data and actual iterative guidance mode presettings.

The results of this simulation are shown in figure 7-47. The close agreement between actual and simulated guidance commands shows that the cause of the guidance transient was due to the thrust cutback and that guidance response to this shift was normal.

The transient in the guidance command angles resulted from the guidance system changing from calculating steering commands, based on the artificial tau mode acceleration level, to the actual inflight acceleration level at R0 +11,565 sec. The artificial tau mode acceleration level was preprogrammed for a 5.0/1.0 EMR engine operation. At the end of the artificial tau mode the actual vehicle acceleration was much higher than the preprogrammed value due to the actual high thrust engine operation. This introduced a step function of acceleration into the guidance equations and resulted in a large change in the guidance commands. Shortly after the end of the artificial tau mode the filtered acceleration, used by guidance, responded to the thrust cutback and the guidance commands began to recover to nearly the values previous to the artificial tau mode period. On AS-501, the artificial tau mode was forced to occur and end at a fixed time in flight and the selected time did not provide protection against the effects of actual thrust cutback.

TABLE 7-1 (Sheet 1 of 3)
TRAJECTORY CONDITIONS AT SIGNIFICANT EVENT TIMES

Parameter	Units	Predicted	Actual	Deviation
<u>CONDITIONS AT MAXIMUM DYNAMIC PRESSURE</u>				
Range time	(t)	79.1	78.0	-1.1
Dynamic pressure	(q)	1bf/ft ²	717.9	2.8
Altitude	(h)	43,327	43,507	180
Mach number	(M)	1.68	1.73	-0.05
Ambient pressure	(P _a)	1bf/ft ²	342.96	-2.19
Pitch angle of attack	(α)	0.0	1.4	1.4
Yaw angle of attack	(β)	0.2	1.3	1.1
<u>CONDITIONS AT S-IC/S-II SEPARATION</u>				
Range time	(t)	153.2	151.43	-1.77
Downrange distance	(X _E)	286,500	278,218	-8,282
Vertical distance	(Y _E)	208,794	209,293	499
Crossrange distance	(Z _E)	3,767	1,832	-1,935
Downrange velocity	(Ẋ _E)	7,114	7,020	-94
Vertical velocity	(Ẏ _E)	2,995	3,068	73
Crossrange velocity	(Ż _E)	69.6	17.0	-51.7
Relative velocity	(V _E)	7,720.1	7,661.2	-58.9
Inertial velocity	(V _I)	8,927.8	8,860.6	-67.2
Inertial flight path elevation angle	(γ ₁)	20.214	20.855	0.641
Inertial flight path azimuth angle	(γ ₂)	75.619	75.287	-0.332
Altitude	(h)	211,076	211,124	48
Range	(S)	294,430	275,629	-8,801
Dynamic pressure	(q)	1bf/ft ²	11.0	10.8
Pitch angle of attack	(α)	0.5	Not available	
Yaw angle of attack	(β)	0.5	Not available	
<u>CONDITIONS AT S-IC/S-II SEPARATION</u>				
Range time	(t)	517.6	520.5	2.9
Downrange distance	(X _E)	4,948,756	4,962,599	13,843
Vertical distance	(Y _E)	46,702	52,391	5,689
Crossrange distance	(Z _E)	75,847	71,263	-4,584
Downrange velocity	(Ẋ _E)	20,651	20,528	-123
Vertical velocity	(Ẏ _E)	-4,654	-4,592	62
Crossrange velocity	(Ż _E)	503.3	512.6	9.3
Relative velocity	(V _E)	21,175	21,041	-134
Inertial velocity	(V _I)	22,497	22,364	-133
Inertial flight path elevation angle	(γ ₁)	0.515	0.632	0.117
Inertial flight path azimuth angle	(γ ₂)	81.458	81.510	0.052
Altitude	(h)	622,516	631,221	8,705
Range	(S)	4,850,017	4,861,770	11,753
<u>CONDITIONS AT FIRST S-IVB ENGINE CUTOFF COMMAND</u>				
Range time	(t)	656.6	665.64	9.04
Downrange distance	(X _E)	7,940,623	8,071,253	130,630
Vertical distance	(Y _E)	-888,289	-935,762	-47,473
Crossrange distance	(Z _E)	167,476	168,151	675
Downrange velocity	(Ẋ _E)	22,522	22,461	-61
Vertical velocity	(Ẏ _E)	-8,921	-9,058	-137
Crossrange velocity	(Ż _E)	837.5	842.2	4.7
Relative velocity	(V _E)	24,238.6	24,233.5	-5.1
Inertial velocity	(V _I)	25,561.9	25,556.9	-5.0
Inertial flight path elevation angle	(γ ₁)	-0.0001	0.0151	0.0152

Deviation = Actual - Predicted

TABLE 7-1 (Sheet 2 of 3)
TRAJECTORY CONDITIONS AT SIGNIFICANT EVENT TIMES

Section 7
Trajectory

Parameter	Units	Predicted	Actual	Deviation
<u>CONDITIONS AT FIRST S-IVB ENGINE CUTOFF COMMAND (Continued)</u>				
Inertial flight path azimuth angle	(γ_{2I}) deg	86.974	87.210	0.236
Altitude	(h) ft	627,521	631,932	4,411
Range	(s) ft	7,897,479	8,032,335	134,856
<u>CONDITIONS AT PARKING ORBIT INSERTION</u>				
Range time	(t) sec	666.6	675.63	9.03
Downrange distance	(X_E) ft	8,165,391	8,295,390	129,999
Vertical distance	(Y_E) ft	-978,786	-1,028,021	-49,235
Crossrange distance	(Z_E) ft	175,939	170,665	726
Downrange velocity	(\dot{X}_E) ft/sec	22,425	22,363	-62
Vertical velocity	(\dot{Y}_E) ft/sec	-9176.2	-9313.7	-137.5
Crossrange velocity	(\dot{Z}_E) ft/sec	854.9	860.4	5.5
Relative velocity	(V_E) ft/sec	24,245.4	24,240.3	-5.1
Inertial velocity	(V_I) ft/sec	25,568.7	25,563.7	-5.0
Inertial flight path elevation angle	(γ_{1I}) deg	0.0013	0.0136	0.0123
Inertial flight path azimuth angle	(γ_{2I}) deg	87.407	87.646	0.239
Altitude	(h) ft	627,563	631,667	4,104
Range	(S) ft	8,132,851	8,267,739	134,888
<u>PARKING ORBIT ELEMENTS AT INSERTION</u>				
Apogee radius	(r_A) nmi	3,544.8	3,545.1	0.3
Perigee radius	(r_P) nmi	3,543.4	3,543.0	-0.4
Apogee velocity	(V_A) ft/sec	25,562.2	25,564.2	2.0
Perigee velocity	(V_P) ft/sec	25,572.0	25,574.4	2.4
Eccentricity	(e)	0.0002	0.0003	0.0001
Inclination	(i) deg	32.5612	32.5730	0.0118
<u>Deviation = Actual - Predicted</u>				
<u>PARKING ORBIT ELEMENTS AT INSERTION (Continued)</u>				
Period	(P) min	88.202	88.200	-0.002
Ascending node	(θ_N asc) deg	303.1737	303.2059	0.0322
Descending node	(θ_N dec) deg	123.1737	123.2059	0.0322
Energy	(C_3) ft ² /sec ²	-653,676,747	-653,688,823	-12,076
<u>CONDITIONS AT SECOND S-IVB ENGINE START COMMAND</u>				
Range time	(t) sec	11,483.60	11,486.54	2.94
Downrange distance	(X_E) ft	-84,235	-135,345	-51,110
Vertical distance	(Y_E) ft	620,273	624,182	3,909
Crossrange distance	(Z_E) ft	-1,335,678	-1,366,627	-30,949
Downrange velocity	(\dot{X}_E) ft/sec	21,617	21,613	-4
Vertical velocity	(\dot{Y}_E) ft/sec	751.2	817.2	66.0
Crossrange velocity	(\dot{Z}_E) ft/sec	10,914	10,903	-11
Relative velocity	(V_E) ft/sec	24,227.4	24,221.6	-5.8
Inertial velocity	(V_I) ft/sec	25,552.3	25,546.7	-5.6
Inertial flight path elevation angle	(γ_{1I}) deg	-0.0008	-0.0011	-0.0003
Inertial flight path azimuth angle	(γ_{2I}) deg	97.638	97.537	-0.101
Altitude	(h) ft	661,940	668,041	6,101
Range	(S) ft	1,299,774	1,333,362	33,588
<u>CONDITIONS AT SECOND S-IVB ENGINE CUTOFF COMMAND</u>				
Range time	(t) sec	11,800.1	11,786.23	-13.87
Downrange distance	(X_E) ft	7,404,794	7,037,436	-367,358
Vertical distance	(Y_E) ft	528,651	569,950	41,299
Crossrange distance	(Z_E) ft	1,990,726	1,840,494	-150,232

TABLE 7-1 (Sheet 3 of 3)
TRAJECTORY CONDITIONS AT SIGNIFICANT EVENT TIMES

Parameter	Units	Predicted	Actual	Deviation	
<u>CONDITIONS AT SECOND S-IVB ENGINE CUTOFF COMMAND (Continued)</u>					
Downrange velocity	(\dot{X}_E)	ft/sec	27,446	27,565	119
Vertical velocity	(\dot{Y}_E)	ft/sec	-1,908	-1,616	292
Crossrange velocity	(\dot{Z}_E)	ft/sec	10,393	10,398	5
Relative velocity	(V_E)	ft/sec	29,409.8	29,505.1	95.3
Inertial velocity	(V_I)	ft/sec	30,789.5	30,881.6	92.1
Inertial flight path elevation angle	(γ_I)	deg	15.1403	14.7665	-0.3738
Inertial flight path azimuth angle	(γ_{2I})	deg	102.893	102.379	-0.5141
Altitude	(h)	ft	1,856,768	1,766,536	-90,232
Range	(S)	ft	7,182,743	6,828,172	-354,571
<u>CONDITIONS AT WAITING ORBIT INJECTION</u>					
Range time	(t)	sec	11,810.1	11,796.23	-13.87
Downrange distance	(X_E)	ft	7,678,981	7,312,745	-366,236
Vertical distance	(Y_E)	ft	508,465	552,693	44,228
Crossrange distance	(Z_E)	ft	2,094,667	1,944,448	-150,219
Downrange velocity	(\dot{X}_E)	ft/sec	27,364	27,486	122
Vertical velocity	(\dot{Y}_E)	ft/sec	-2,135	-1,836	299
Crossrange velocity	(\dot{Z}_E)	ft/sec	10,389	10,394	5
Relative velocity	(V_E)	ft/sec	29,349.1	29,443.5	94.4
Inertial velocity	(V_I)	ft/sec	30,731.8	30,823.1	91.3
Inertial flight path elevation angle	(γ_I)	deg	15.3970	15.0295	-0.3675
Inertial flight path azimuth angle	(γ_{2I})	deg	103.2618	102.7568	-0.5050
<u>CONDITIONS AT WAITING ORBIT INJECTION (Continued)</u>					
Altitude	(h)	ft	1,937,645	1,845,713	-91,932
Range	(S)	ft	7,440,447	7,088,029	-352,418
<u>WAITING ORBIT ELEMENTS AT INJECTION</u>					
Apogee radius	(r_A)	nmi	12,706.7	12,740.7	34.0
Perigee radius	(r_P)	nmi	3,394.6	3,398.0	3.4
Apogee velocity	(V_A)	ft/sec	8,768.0	8,749.6	-18.4
Perigee Velocity	(V_P)	ft/sec	32,820.3	32,807.0	-13.3
Eccentricity	(e)	-	0.57834	0.57888	0.00054
Inclination	(i)	deg	30.2753	30.3022	0.0269
Period	(P)	min	302.0	303.0	1.0
Ascending Node	(θ_N asc)	deg	315.4280	315.4354	0.0074
Descending Node	(θ_N dec)	deg	135.4280	135.4354	0.0074
Energy	(C_3)	ft ² /sec ²	-287,766.053	-287,098.282	667,771

Deviation = Actual - Predicted

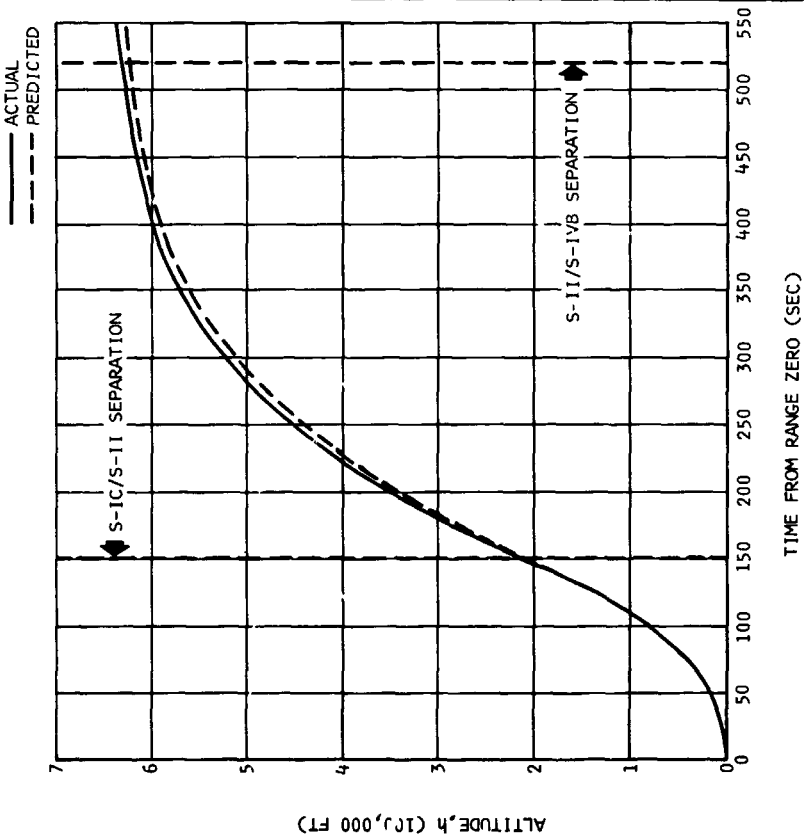
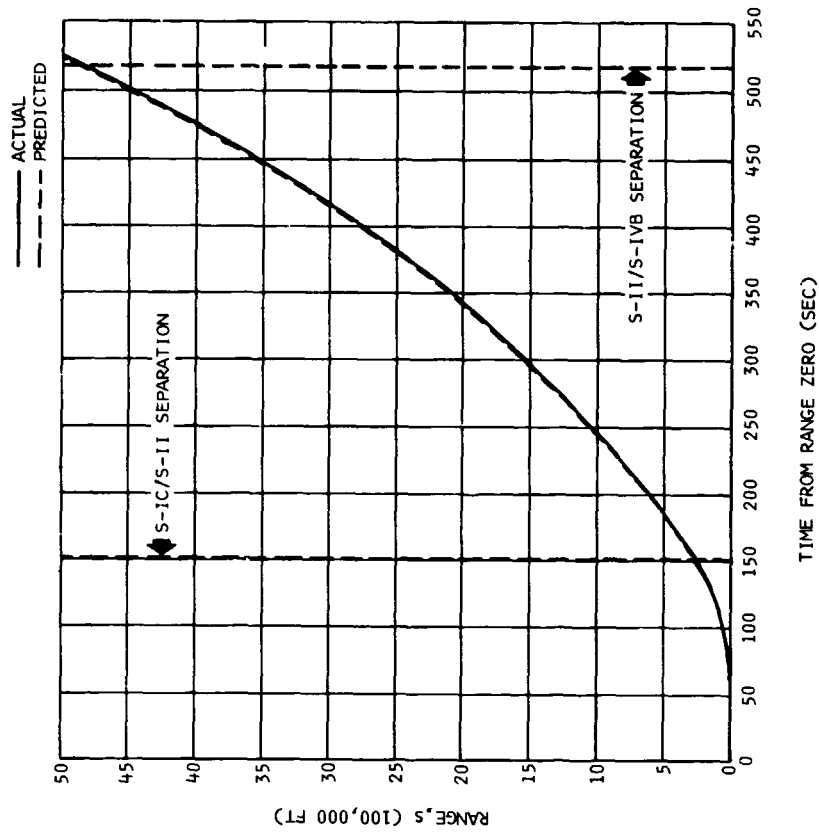


Figure 7-2. S-IC/S-II Stage Flight Range History

Figure 7-1. S-IC/S-II Stage Flight Altitude History

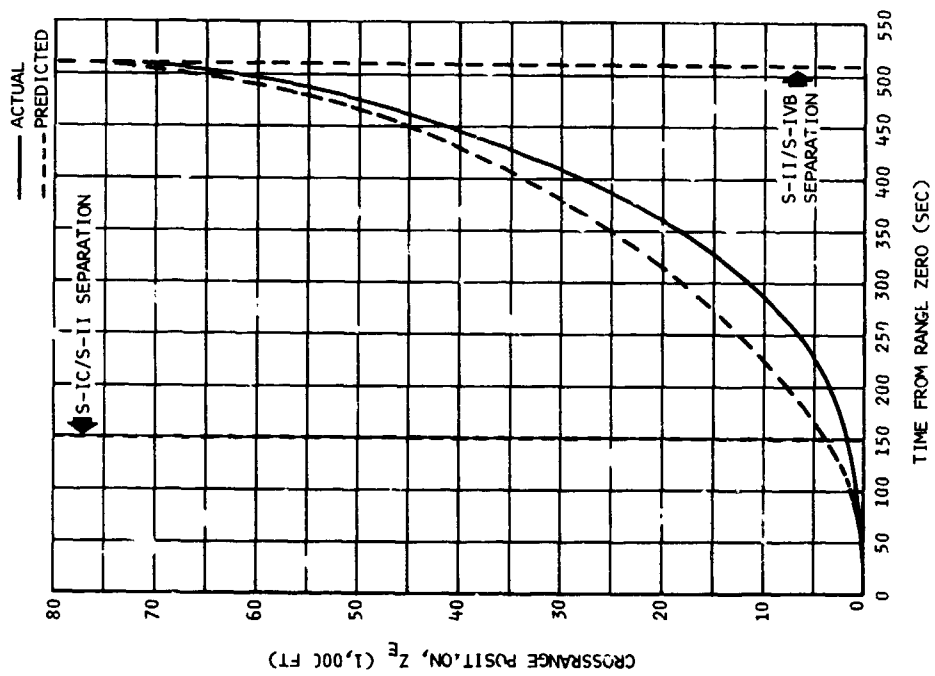


Figure 7-3. S-IC/S-II Stage Flight Crossrange Position History

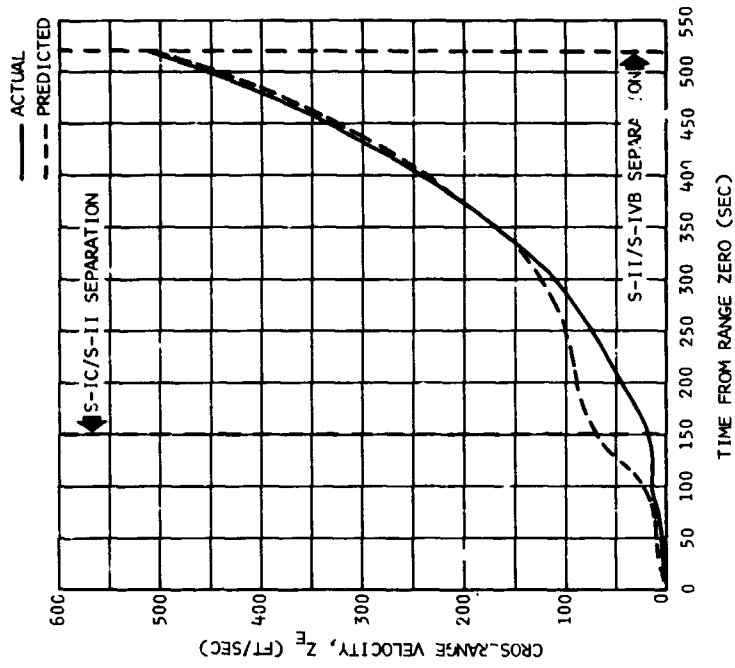


Figure 7-4. S-IC/S-II Stage Flight Crossrange Velocity History

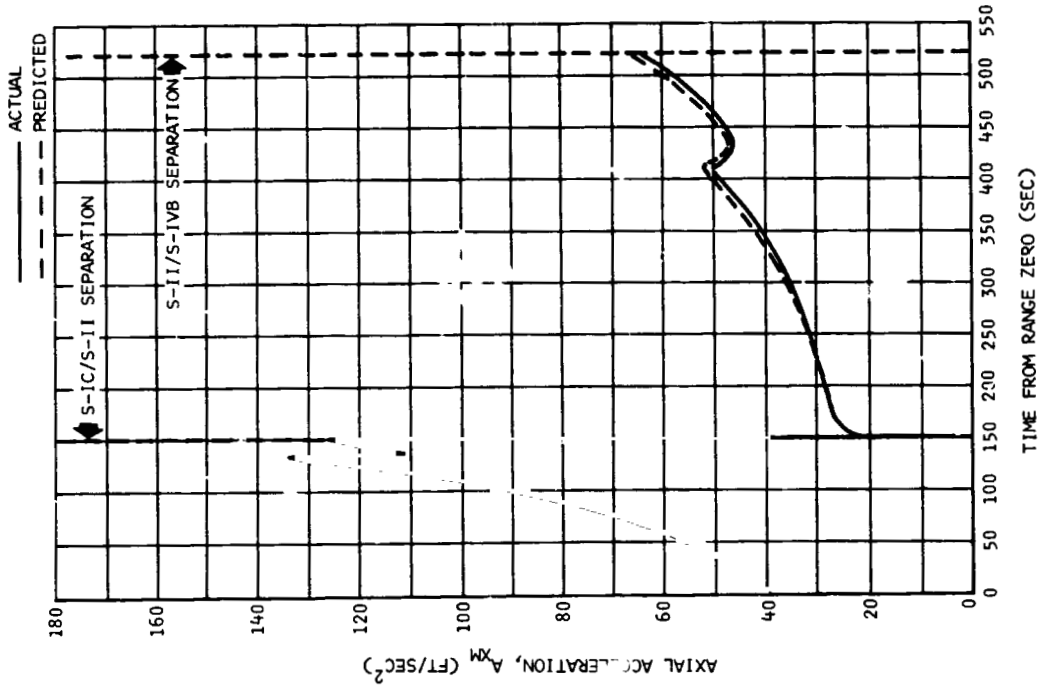


Figure 7-5. S-IC/S-II Stage Flight Inertial Velocity History

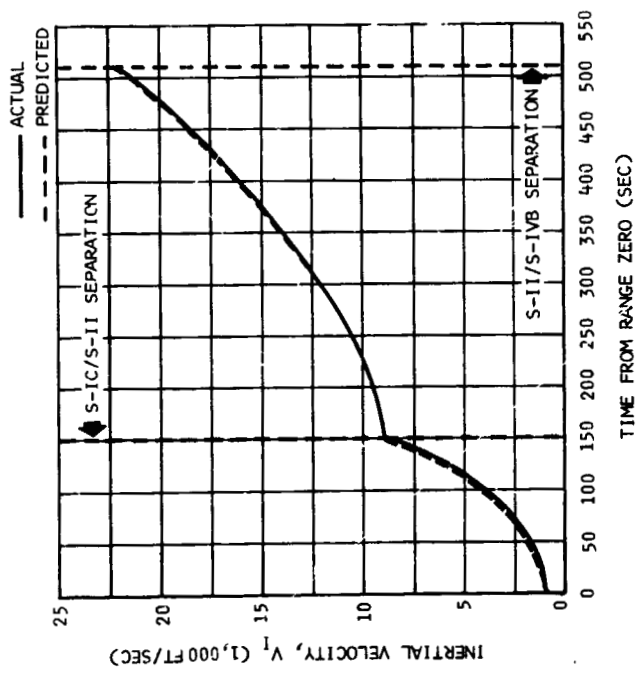


Figure 7-6. S-IC/S-II Stage Flight Axial Acceleration History

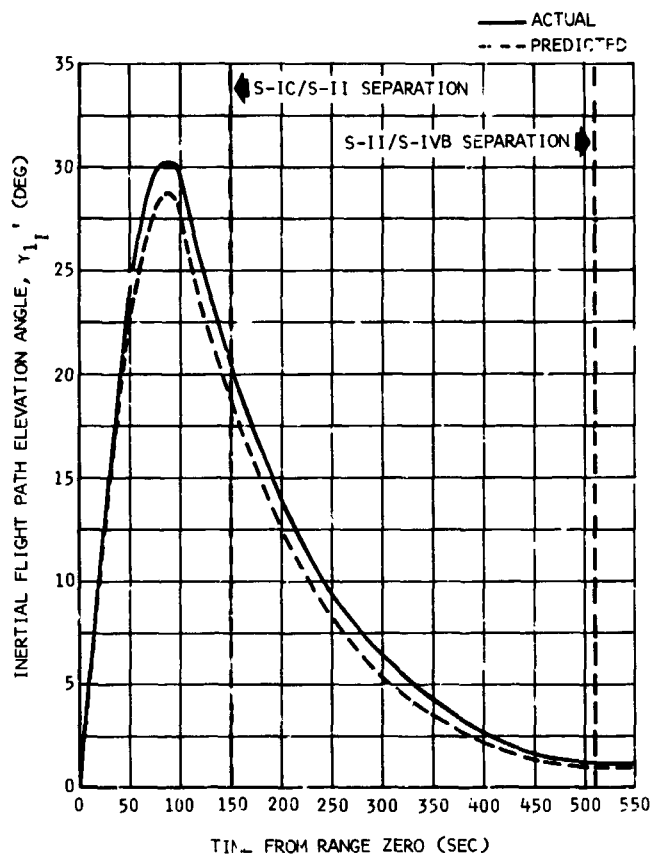


Figure 7-7. S-IC/S-II Stage Inertial Flight Path Elevation Angle History

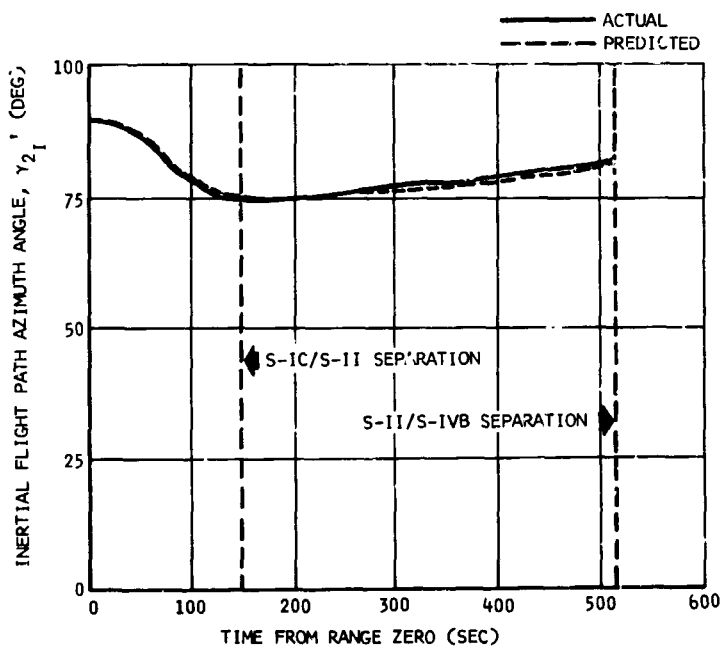


Figure 7-8. S-IC/S-II Stage Inertial Flight Path Azimuth Angle History

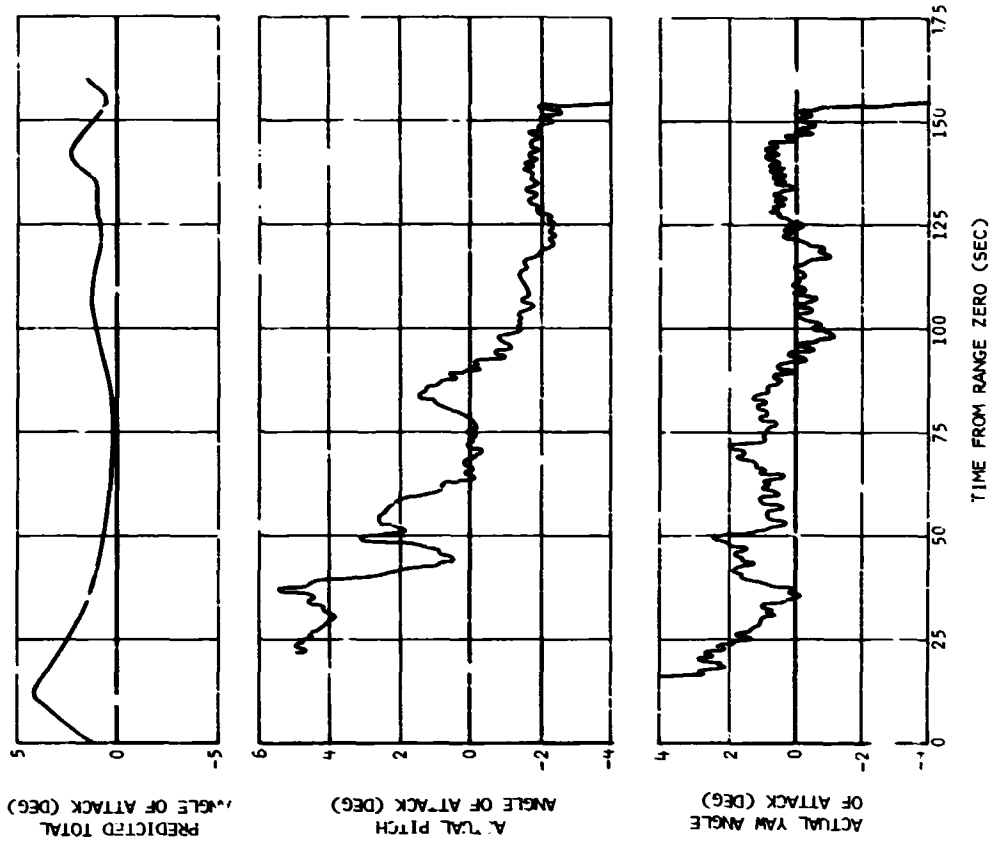


Figure 7-10. S-IC Stage Flight Angles of Attack

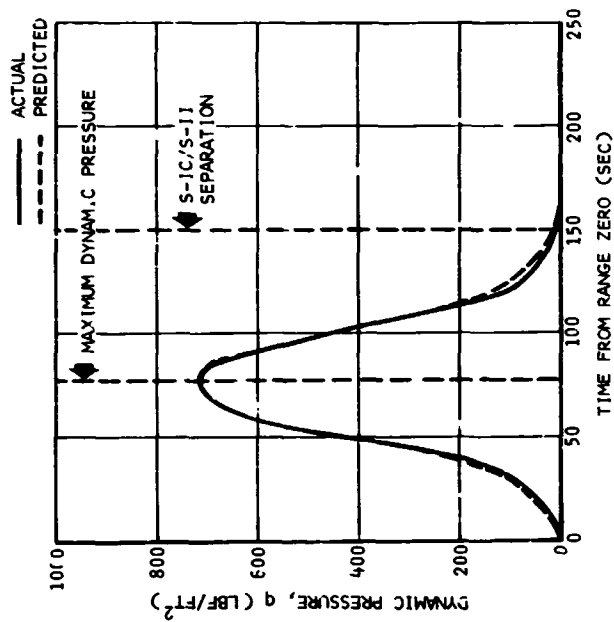


Figure 7-9. S-IC/S-II Stage Flight Dynamic Pressure History

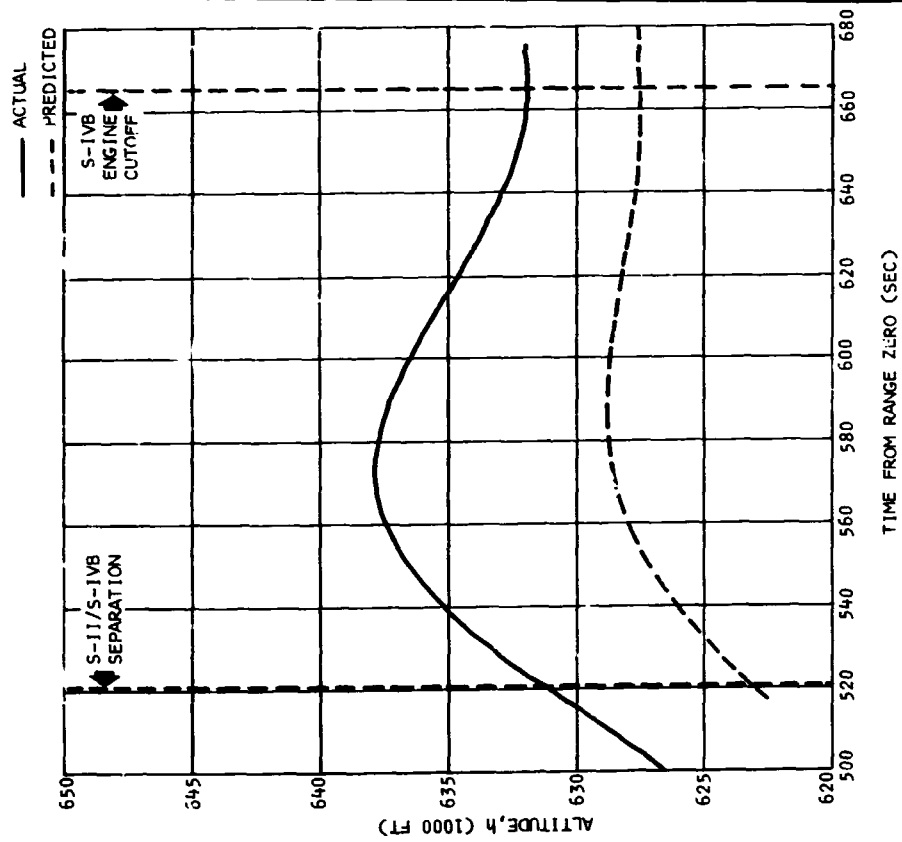
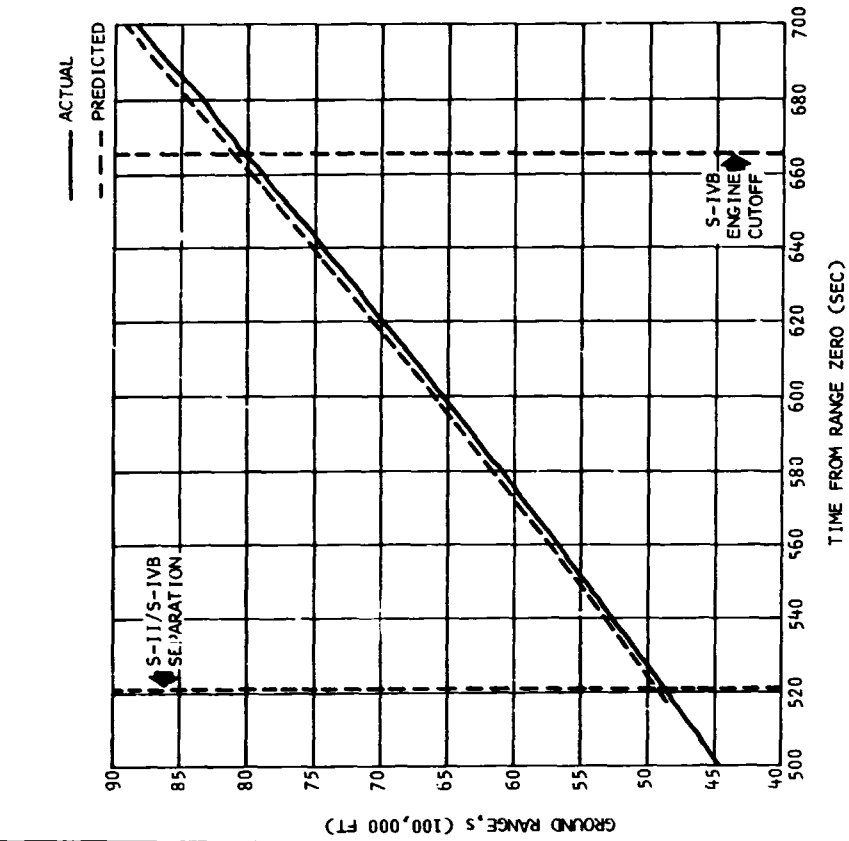


Figure 7-12. S-IVB Stage Flight Range History - First Burn

Figure 7-11. S-IVB Stage Flight Altitude History - First Burn

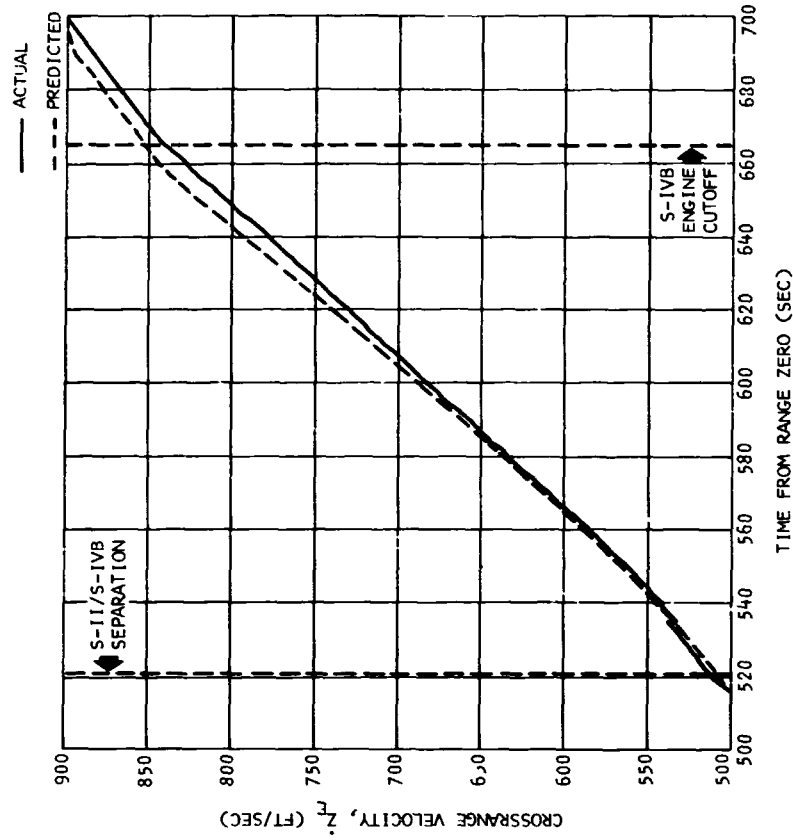


Figure 7-13. S-IVB Stage Flight Crossrange Position History - First Burn

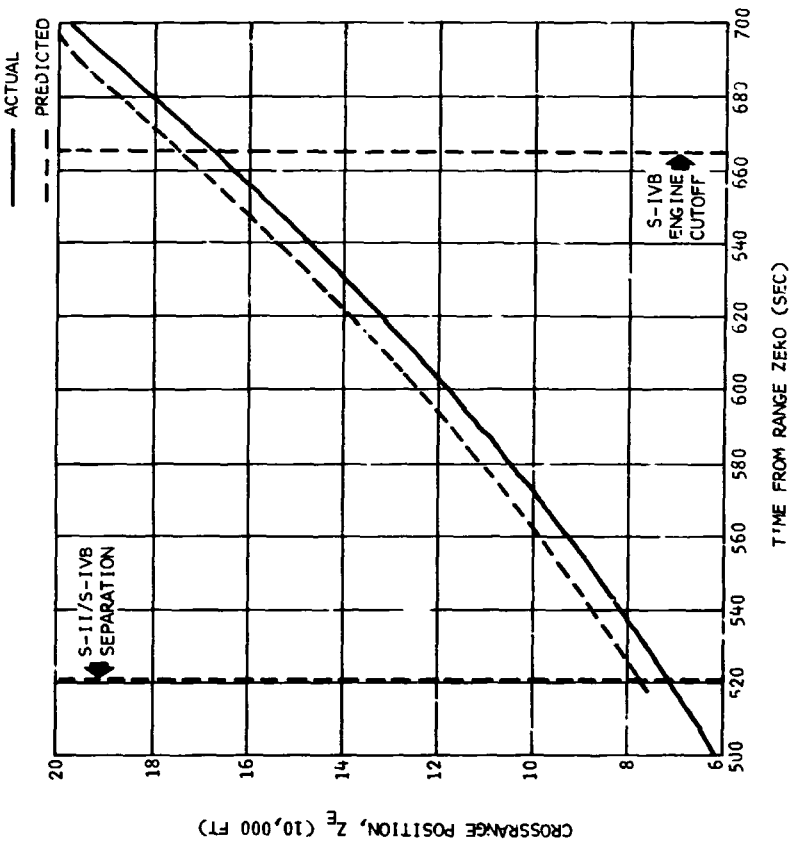


Figure 7-14. S-IVB Stage Flight Crossrange Velocity History - First Burn

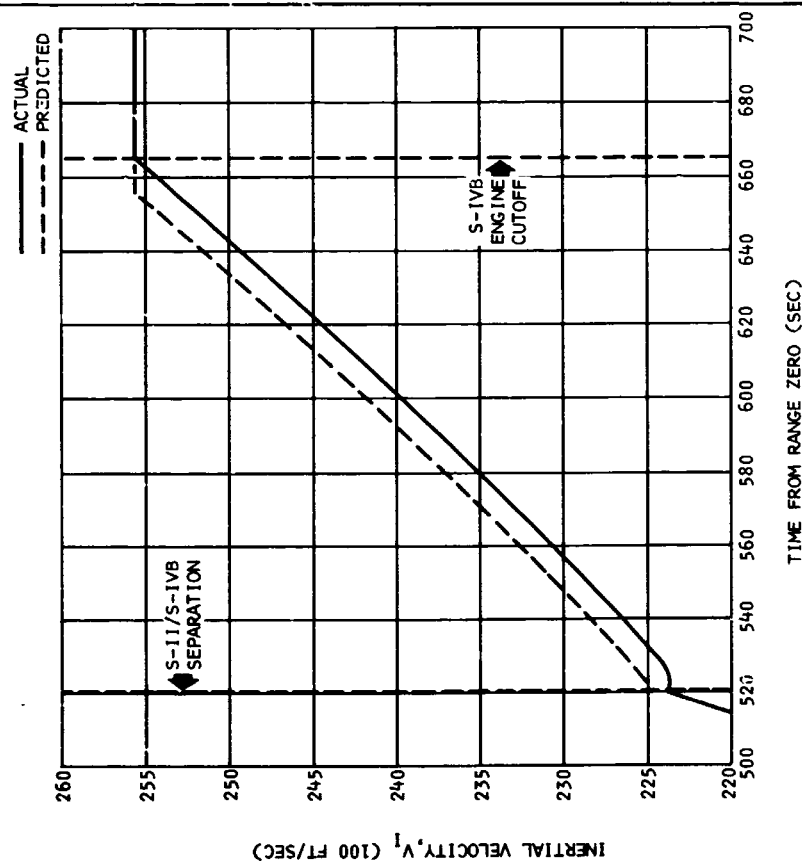
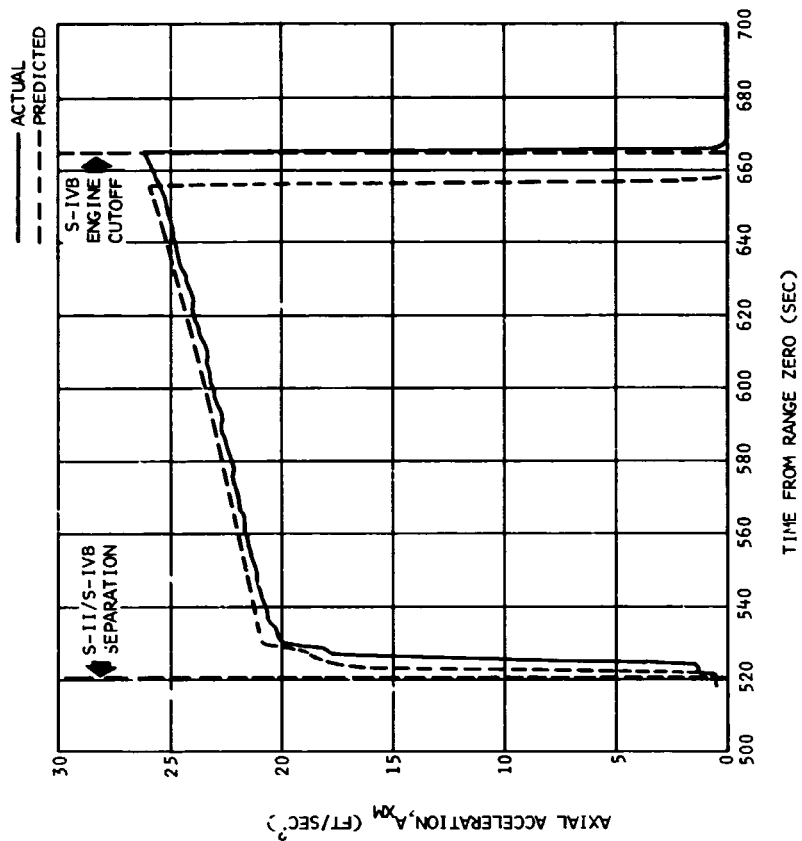


Figure 7-15. S-IVB Stage Flight Inertial Velocity History - First Burn

Figure 7-16. S-IVB Stage Flight Axial Acceleration History - First Burn

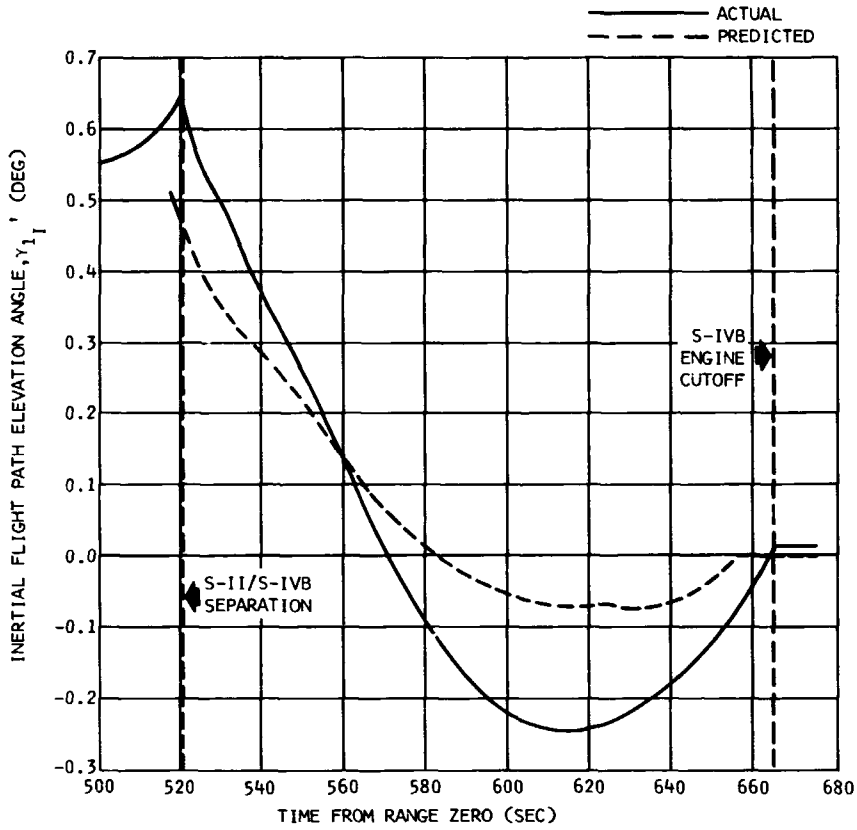


Figure 7-17. S-IVB Stage Inertial Flight Path Elevation Angle History - First Burn

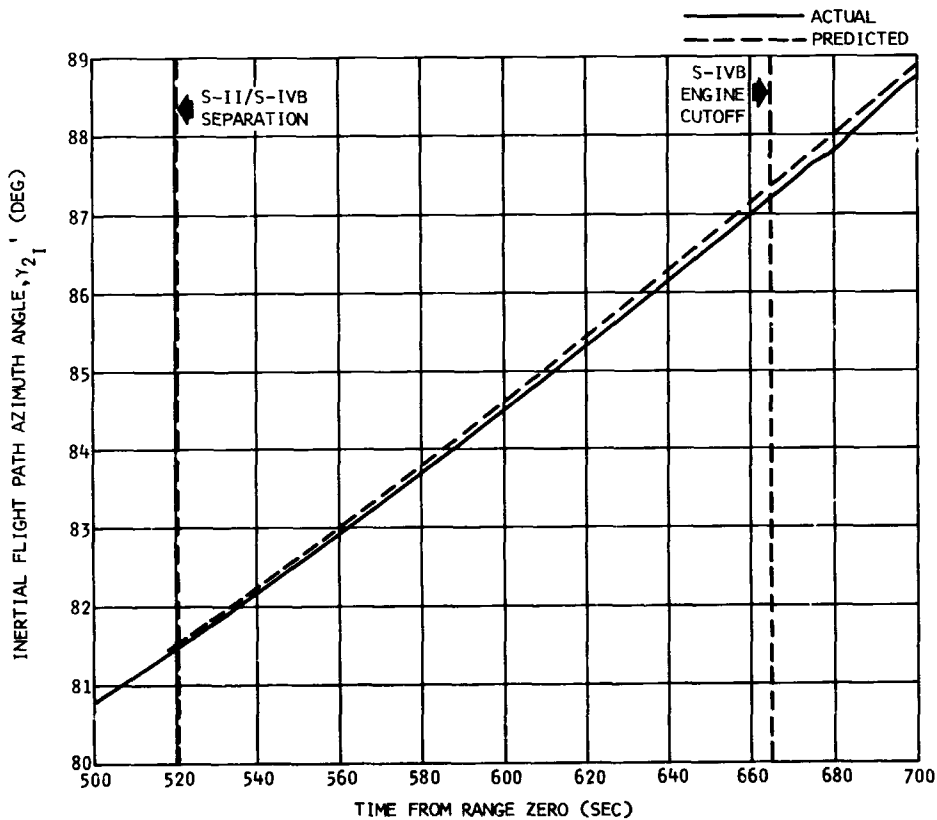


Figure 7-18. S-IVB Stage Inertial Flight Path Azimuth Angle History - First Burn

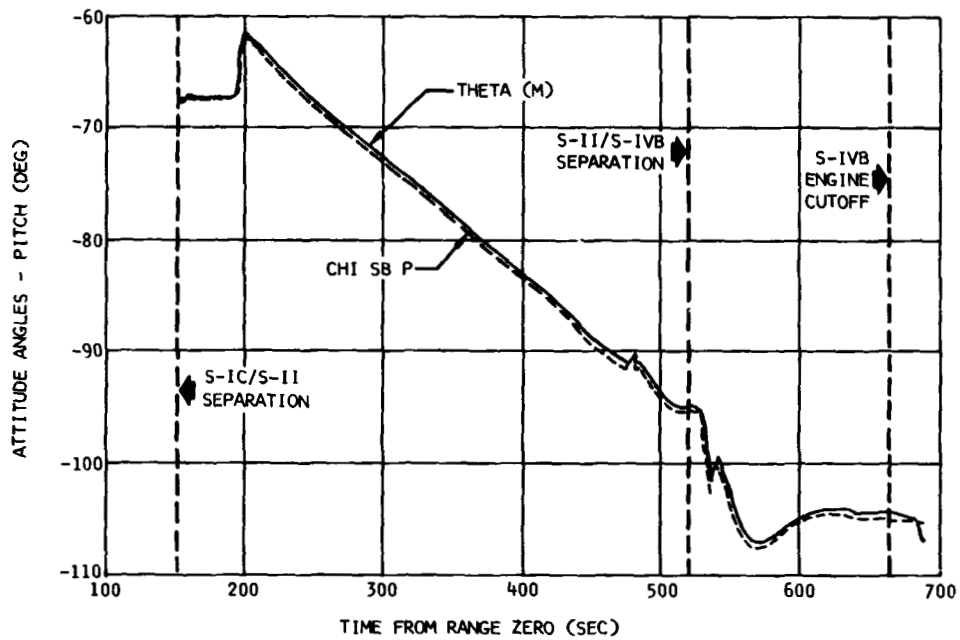


Figure 7-19. S-II/S-IVB Stage Pitch Attitude Angles - First Burn

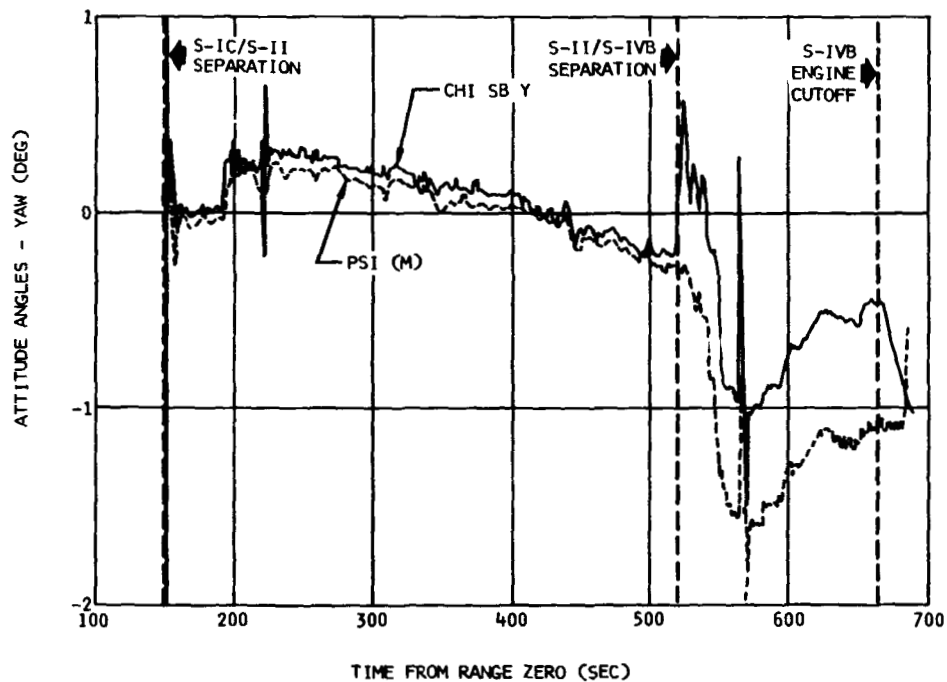


Figure 7-20. S-II/S-IVB Stage Yaw Attitude Angles - First Burn

Section 7
Trajectory

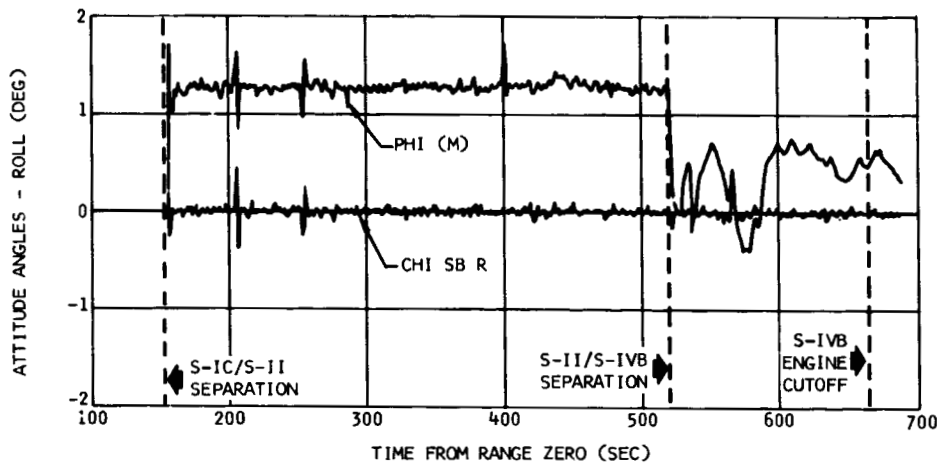


Figure 7-21. S-II/S-IVB Stage Roll Attitude Angles - First Burn

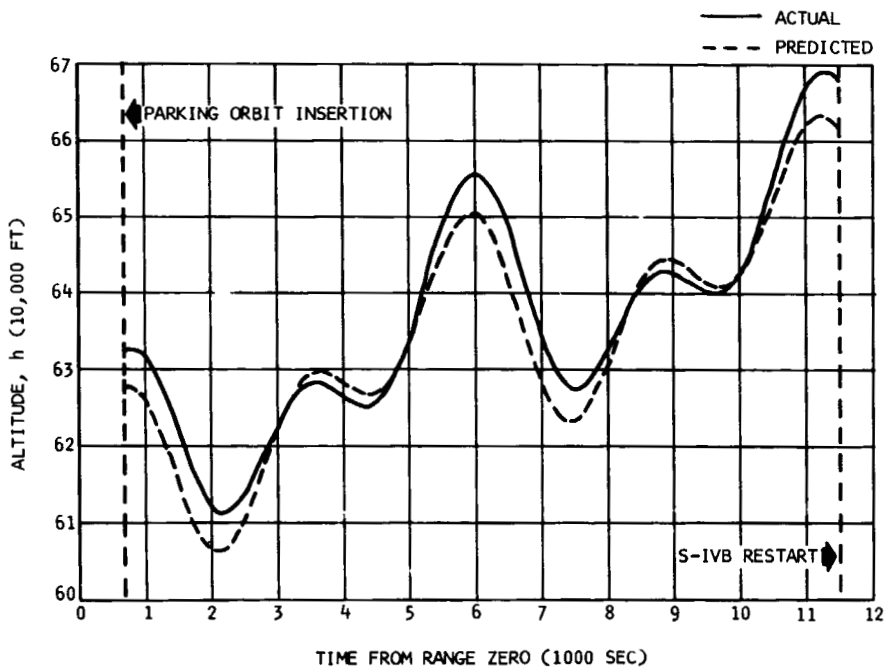


Figure 7-22. Parking Orbit Altitude History

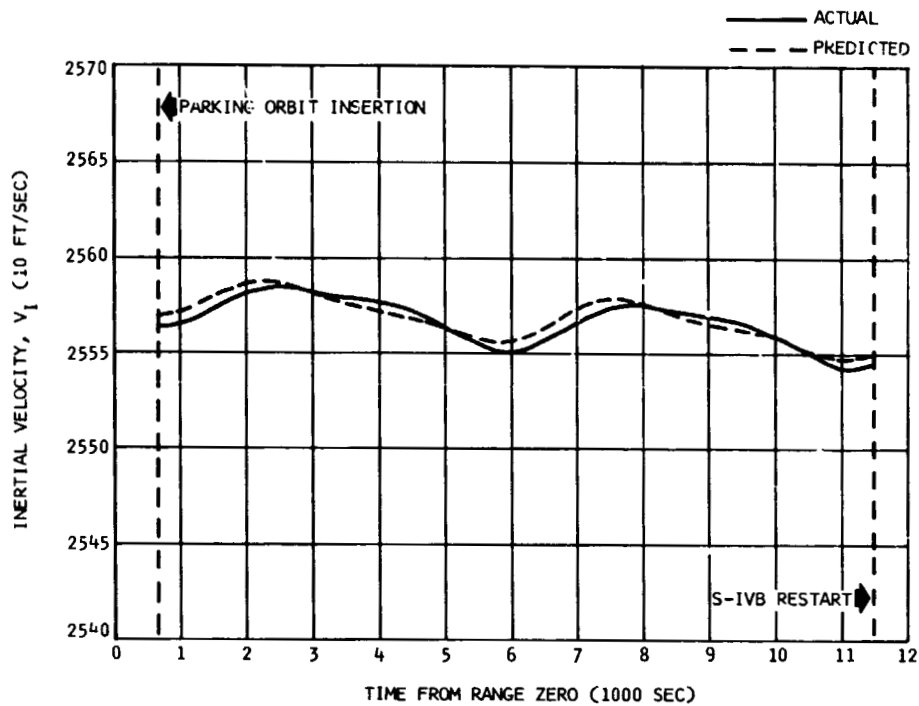


Figure 7-23. Parking Orbit Inertial Velocity History

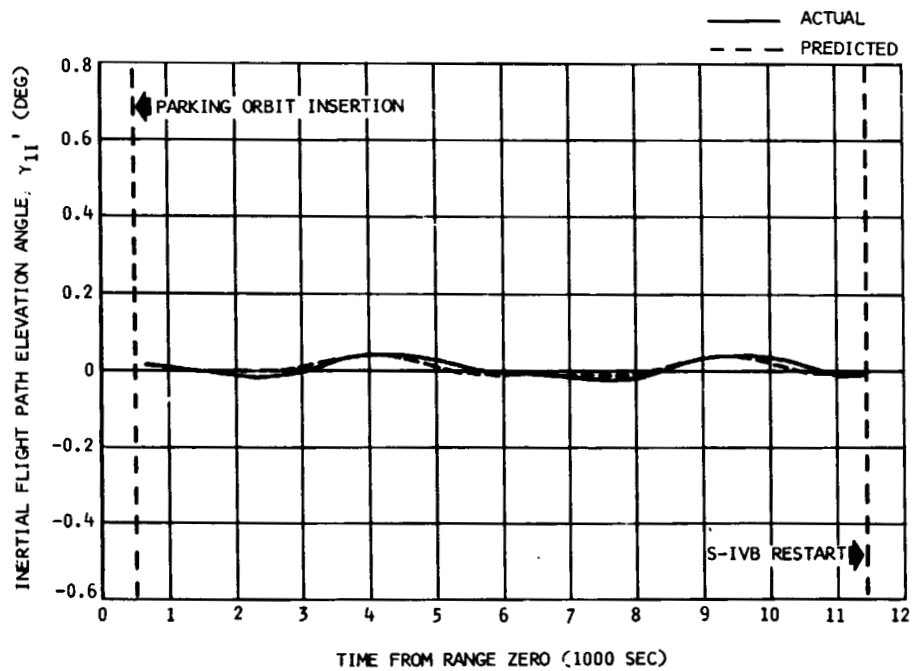


Figure 7-24. Parking Orbit Inertial Flight Path Elevation Angle History

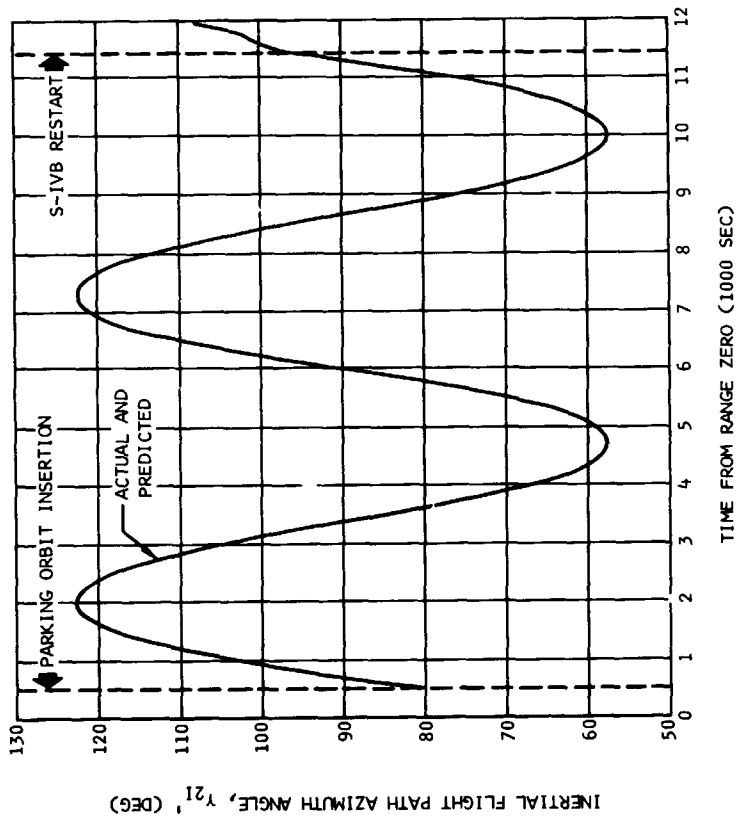
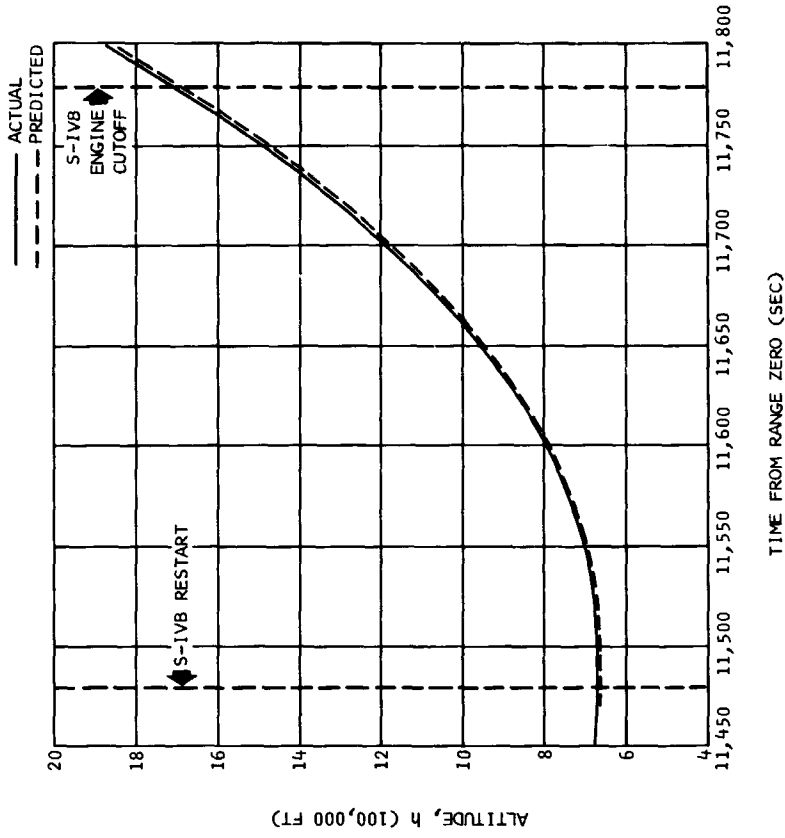


Figure 7-26. S-IVB Stage Flight Altitude History - Second Burn

Figure 7-25. Parking Orbit Inertial Flight Path Azimuth Angle History

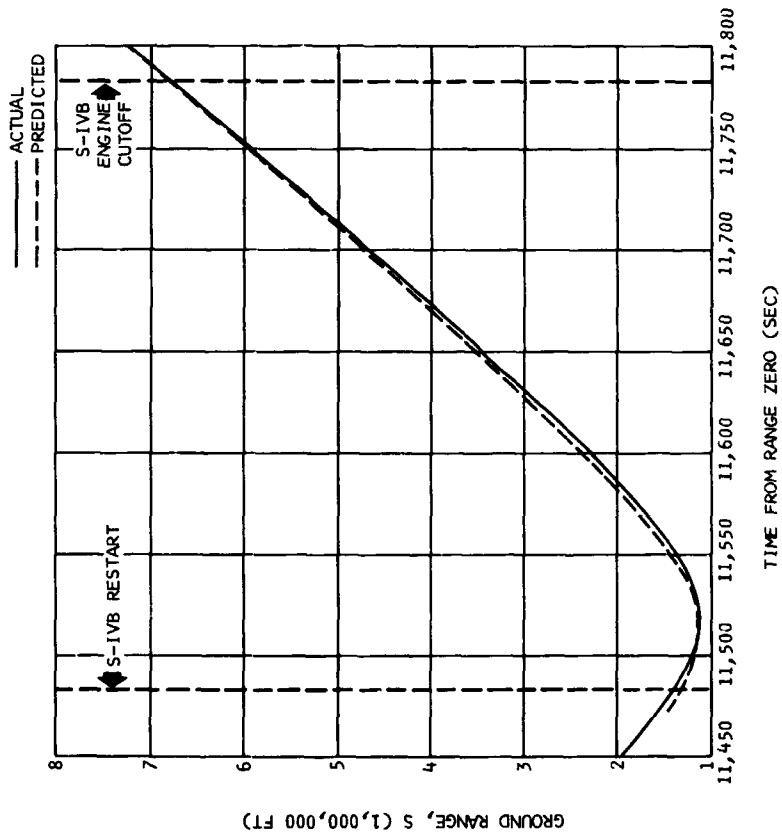
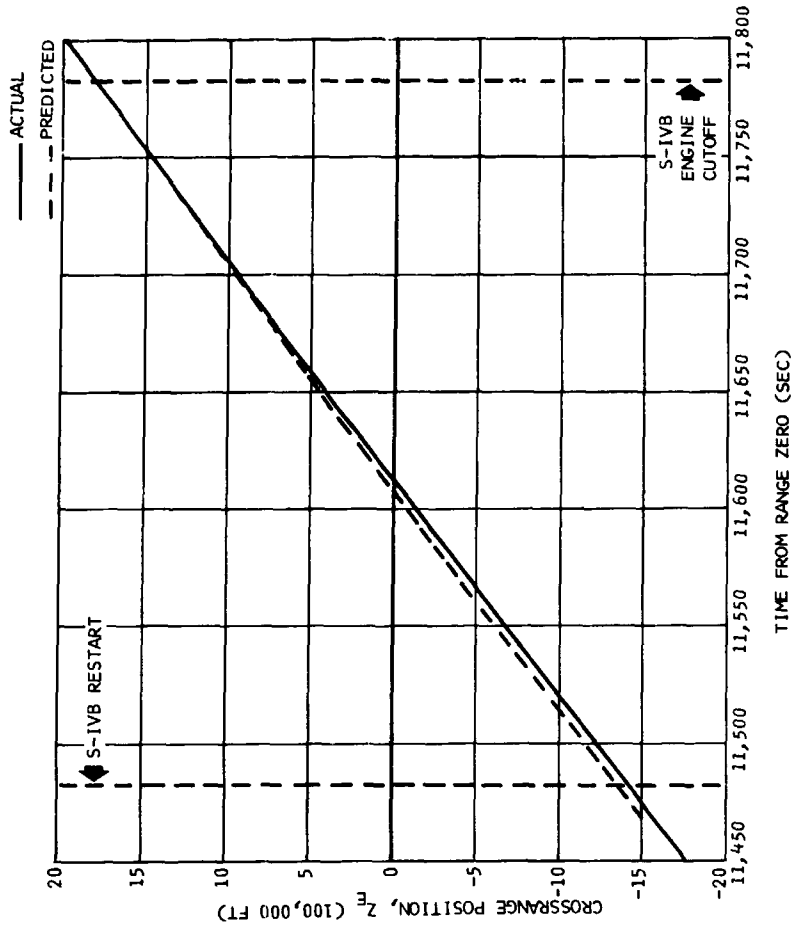


Figure 7-28. S-IVB Stage Flight Crossrange Position History - Second Burn

Figure 7-27. S-IVB Stage Flight Ground Range History - Second Burn

Section 7
Trajectory

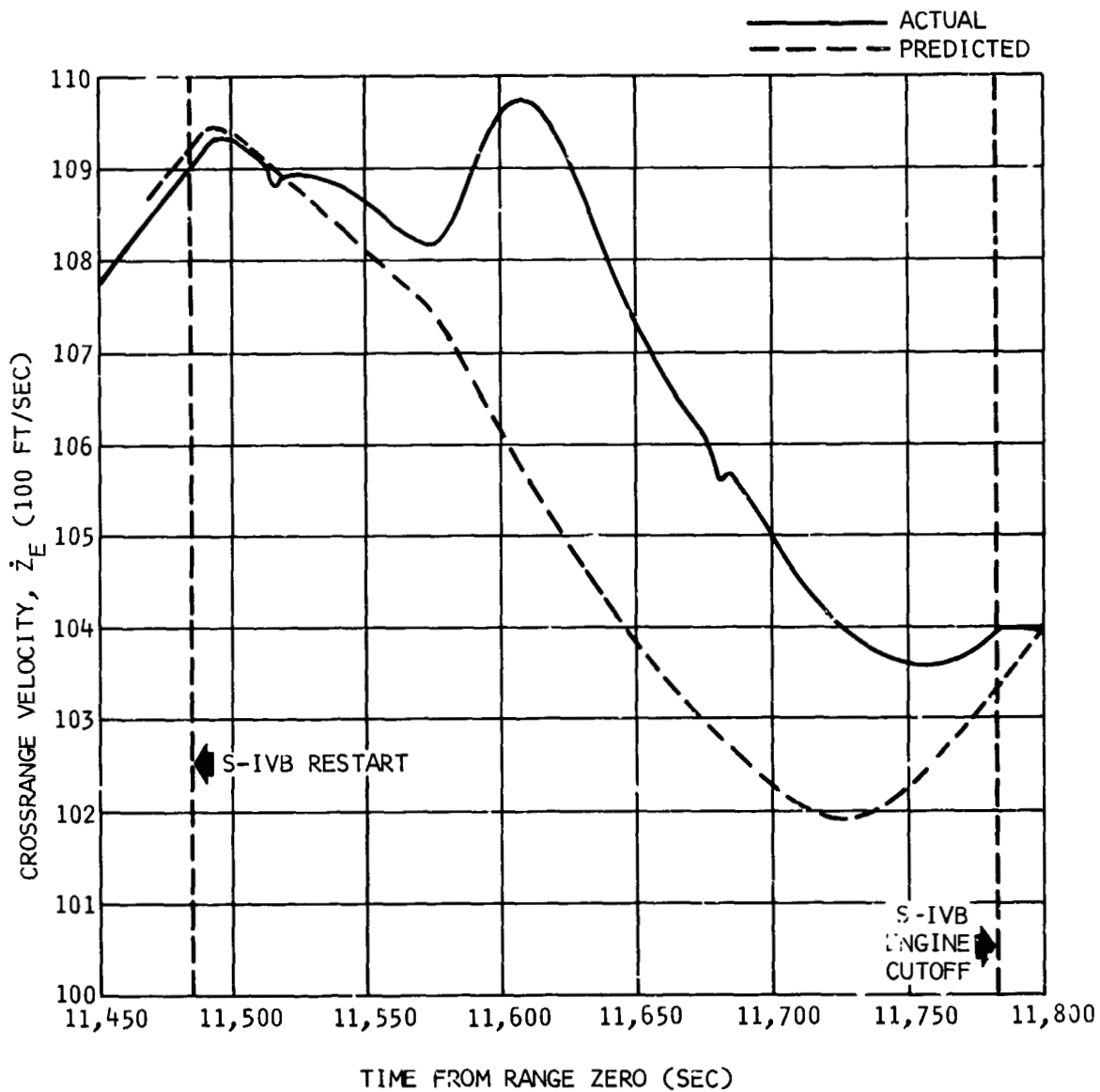


Figure 7-29. S-IVB Stage Flight Crossrange Velocity History - Second Burn

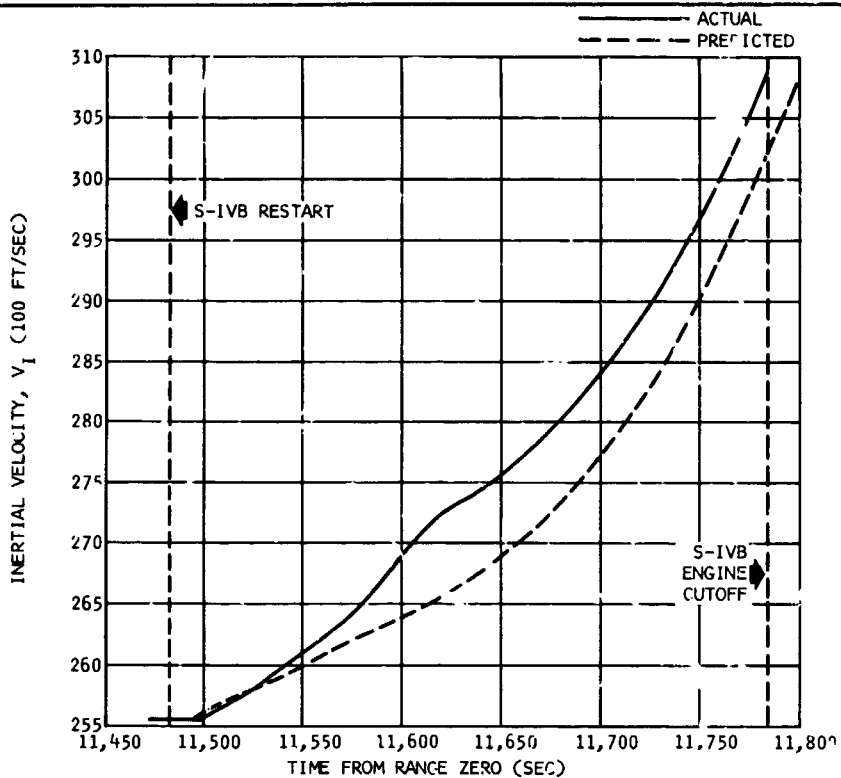


Figure 7-30. S-IVB Stage Flight Inertial Velocity History - Second Burn

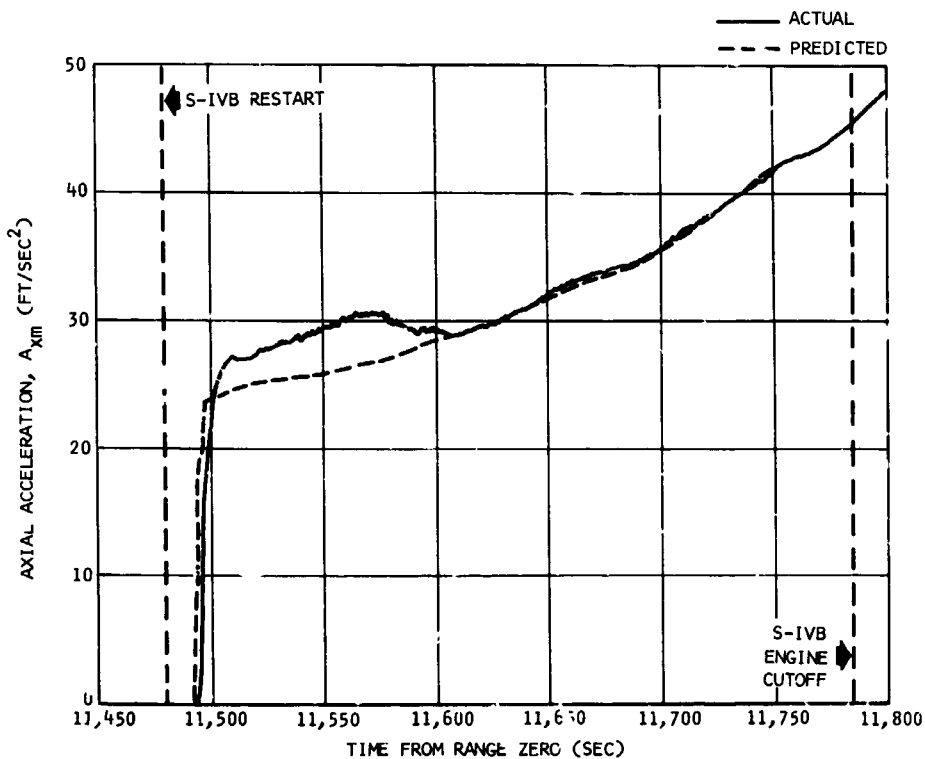


Figure 7-31. S-IVB Stage Flight Axial Acceleration History - Second Burn

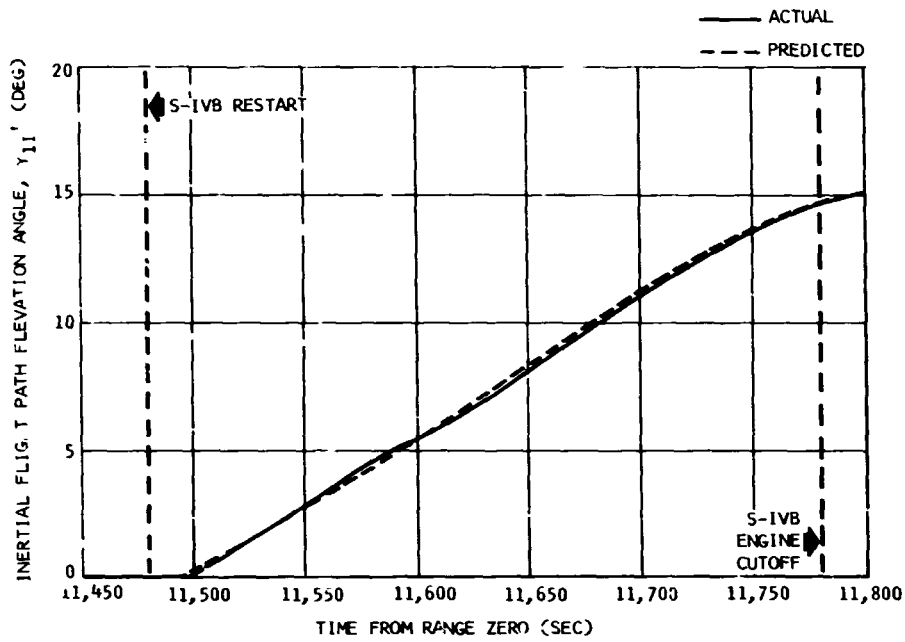


Figure 7-32. S-IVB Stage Inertial Flight Path Elevation Angle History - Second Burn

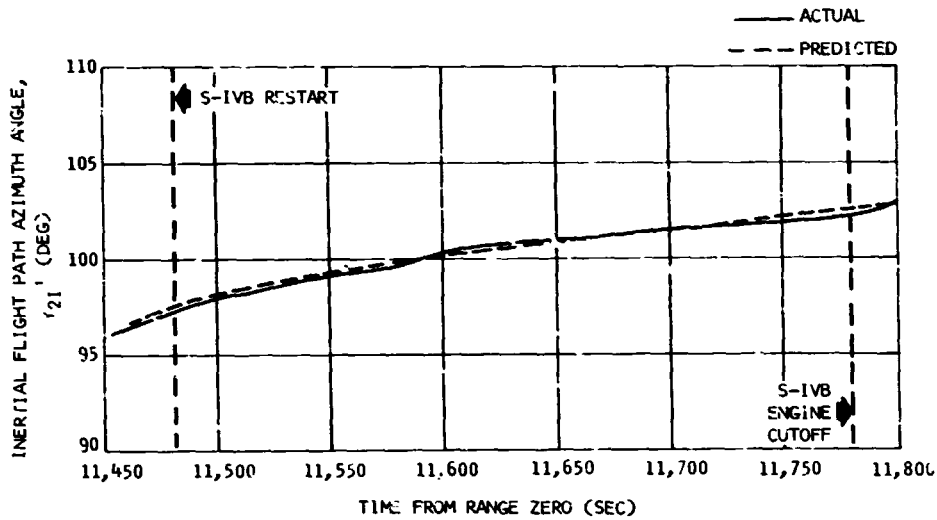


Figure 7-33. S-IVB Stage Inertial Flight Path Azimuth Angle History - Second Burn

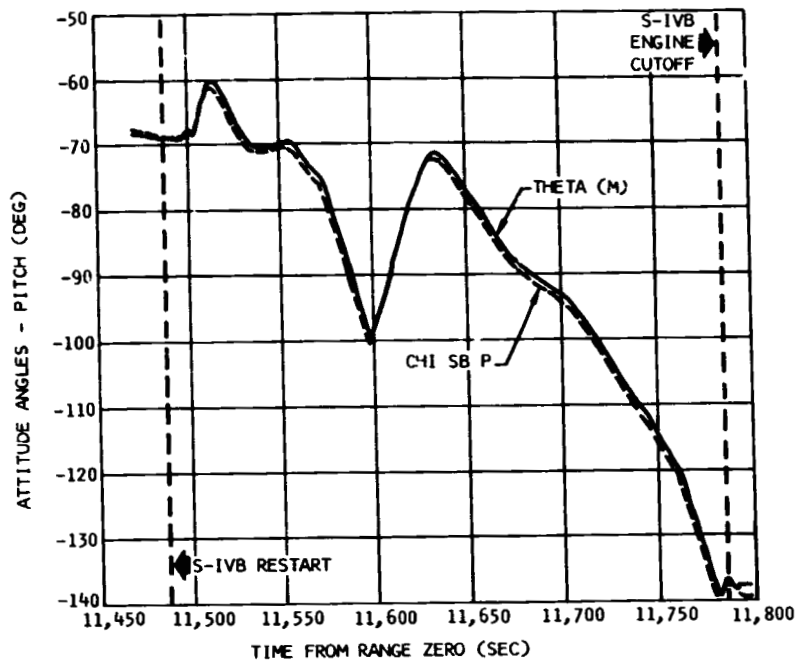


Figure 7-34. S-IVB Stage Pitch Attitude Angles - Second Burn

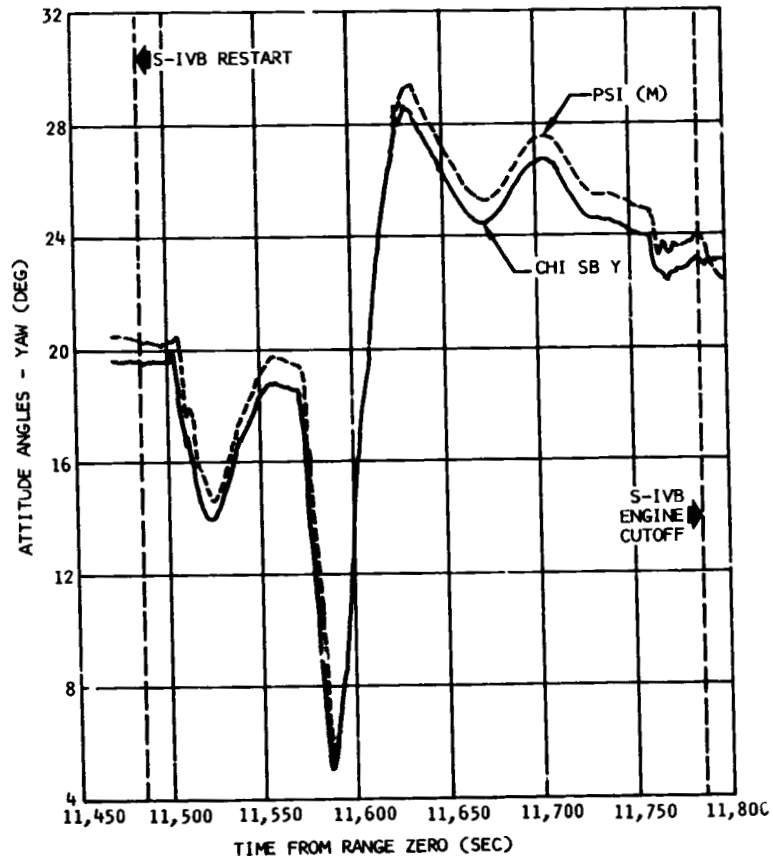


Figure 7-35. S-IVB Stage Yaw Attitude Angles - Second Burn

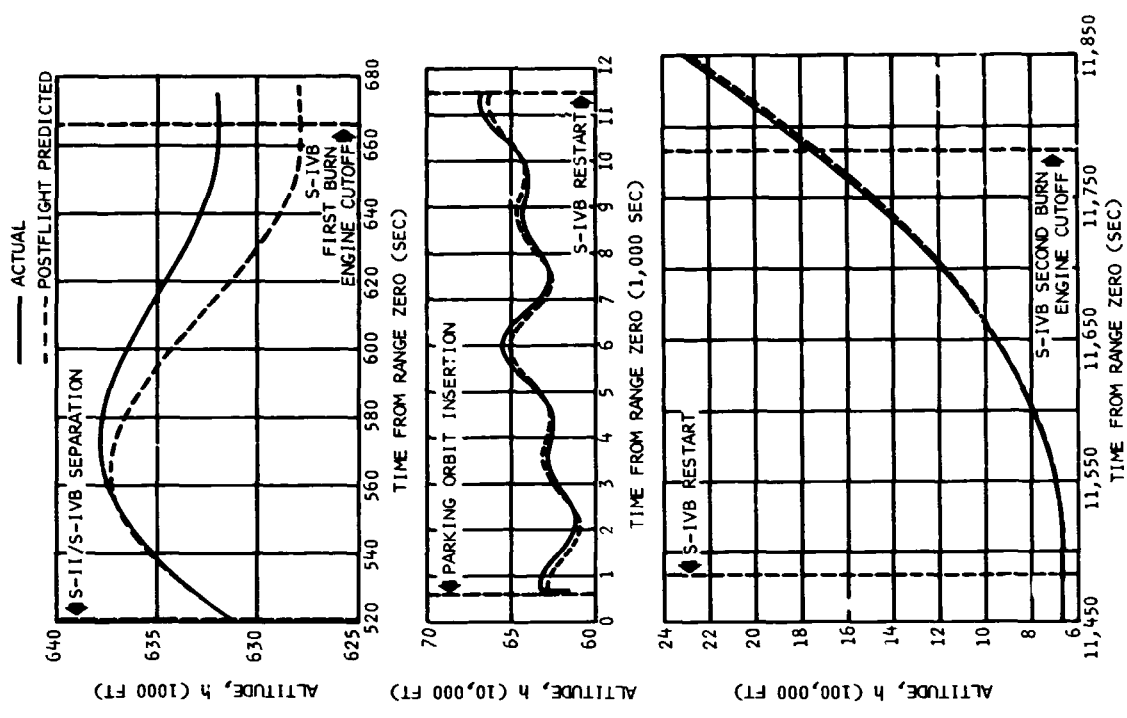


Figure 7-37. Comparison of Actual and Postflight Predicted Altitude

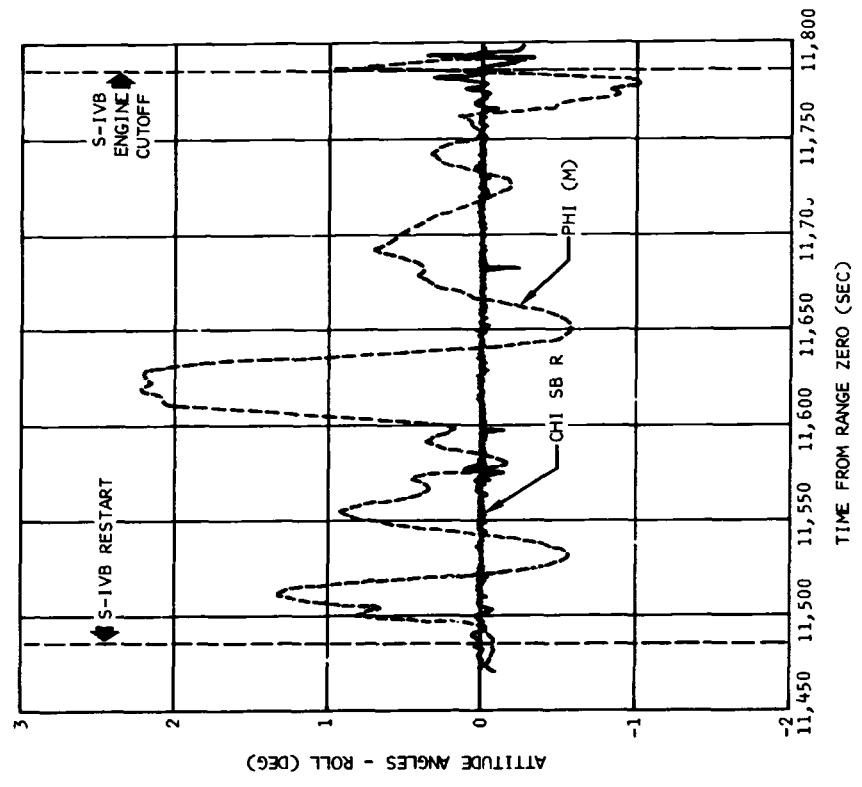


Figure 7-36. S-IVB Stage Roll Attitude Angles - Second Burn

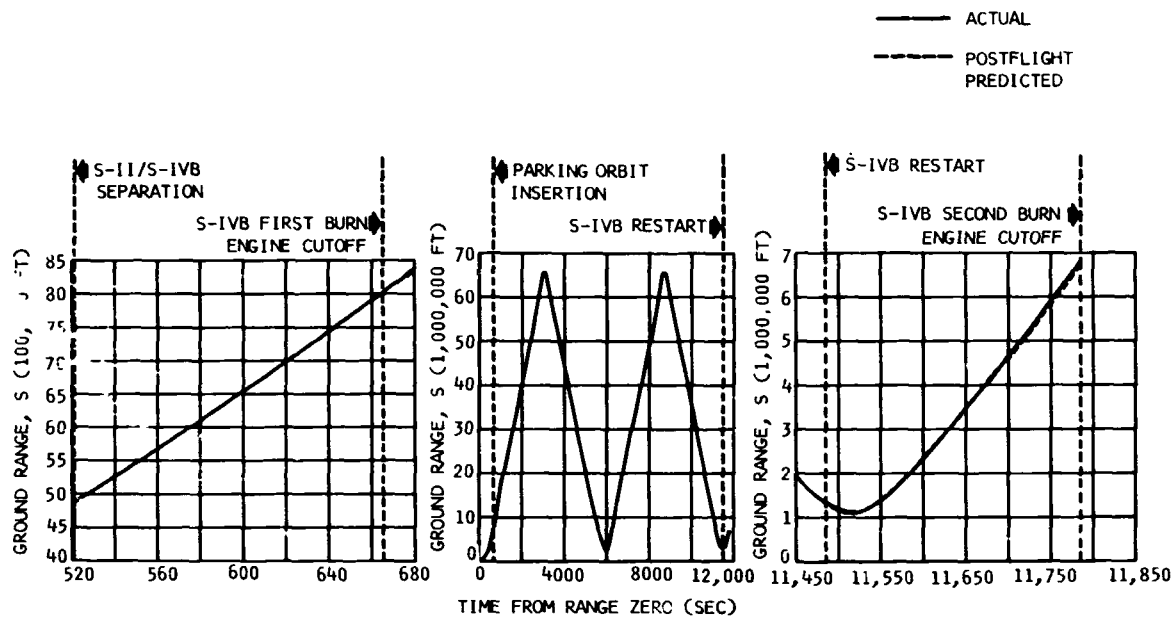


Figure 7-38. Comparison of Actual and Postflight Predicted Ground Range

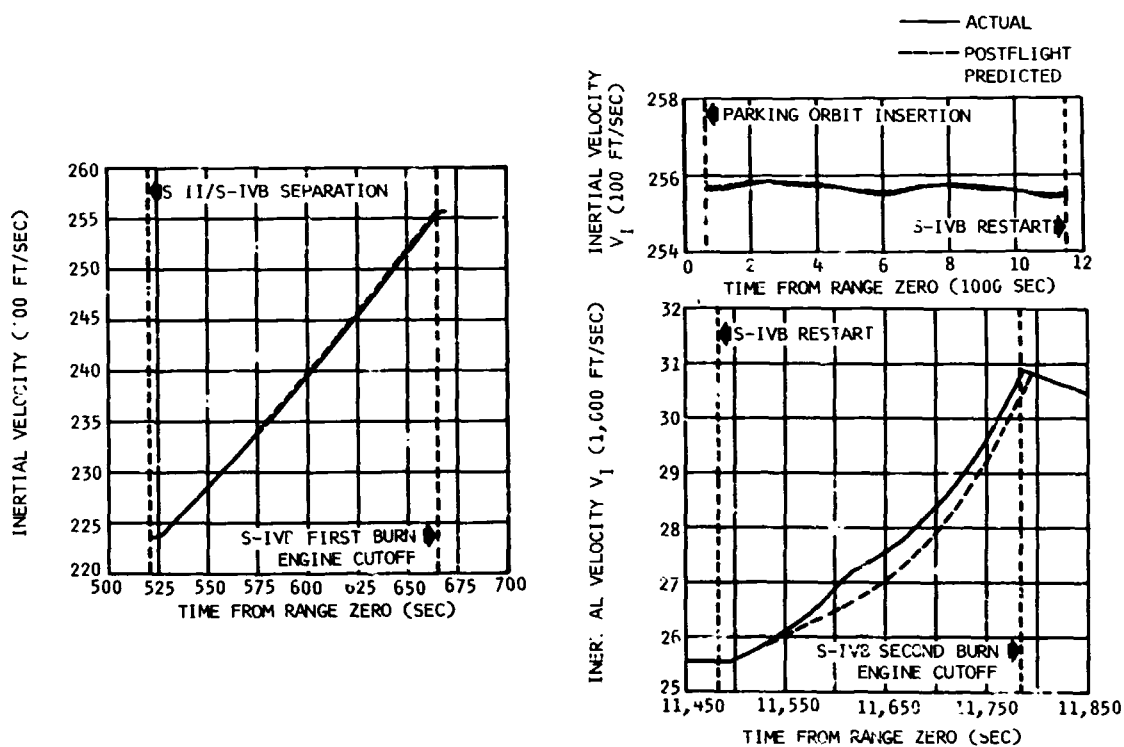


Figure 7-39. Comparison of Actual and Postflight Predicted Inertial Velocity

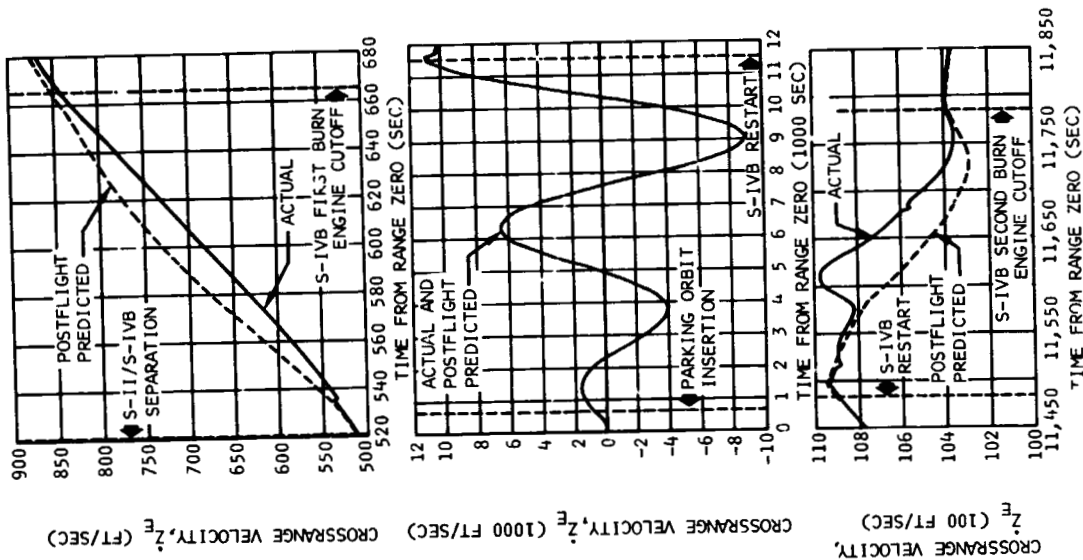
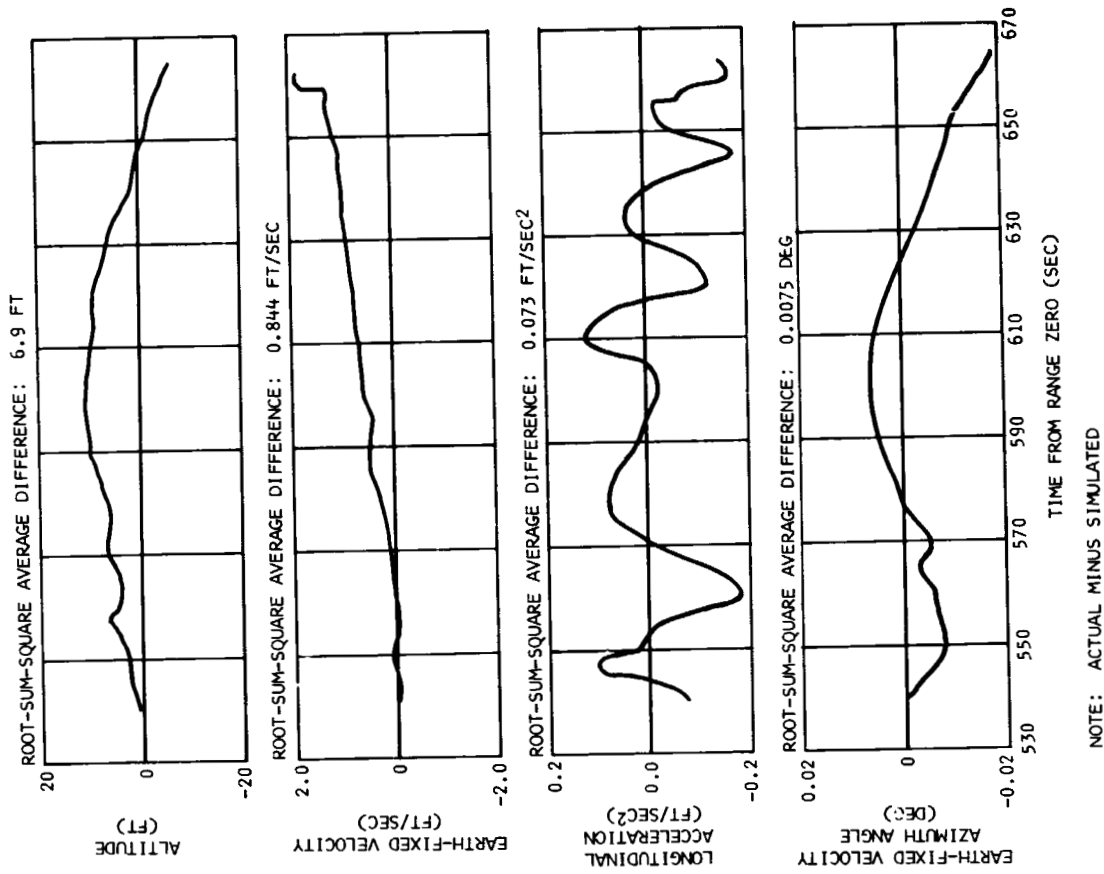


Figure 7-41. First Burn Trajectory Reconstruction Simulation Deviations from Observed Mass Point Trajectory

Figure 7-40. Comparison of Actual and Postflight Predicted Earth - Fixed Crossrange Velocity

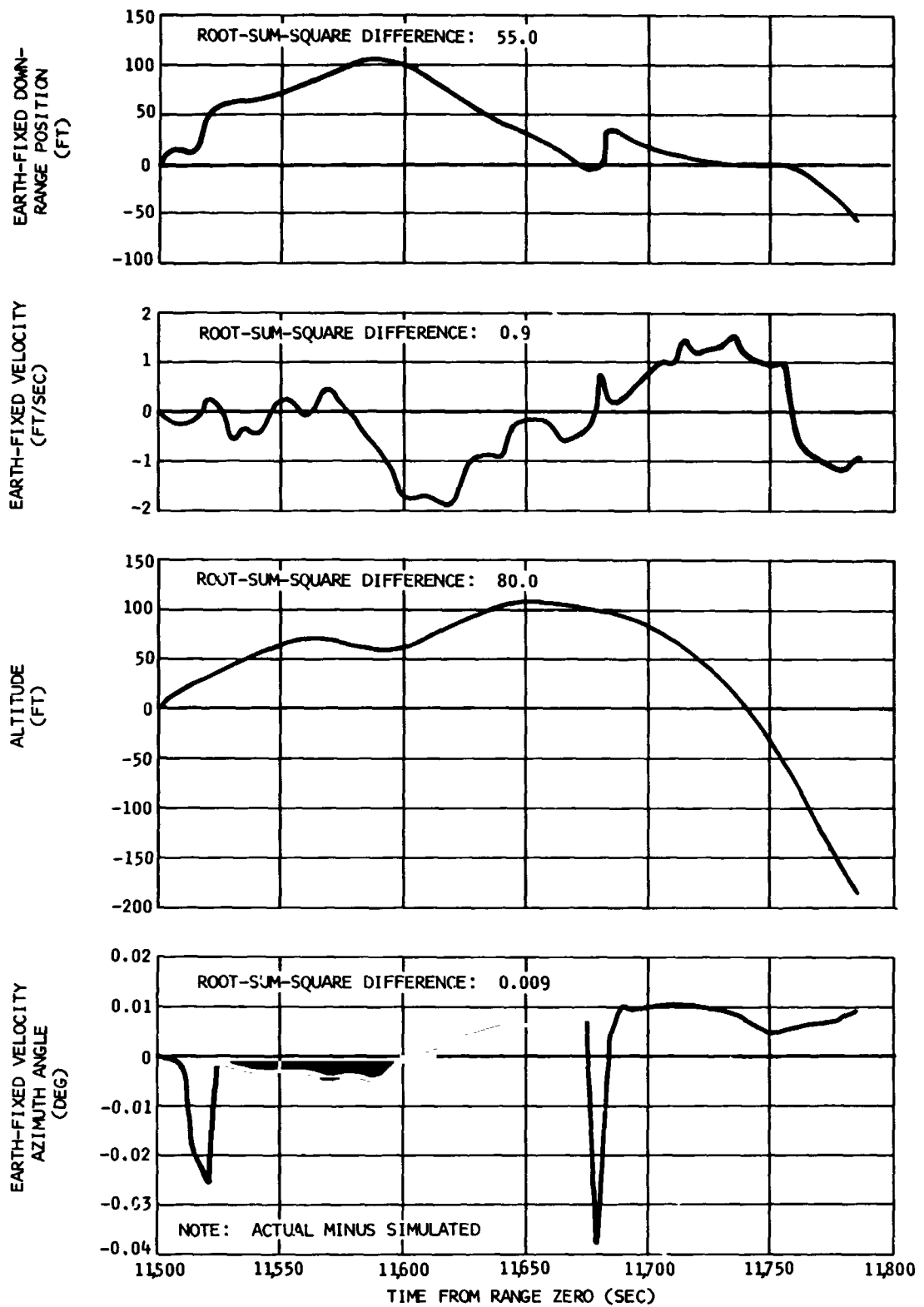


Figure 7-42. Second Burn Trajectory Reconstruction Simulation Deviations from Observed Mass Point Trajectory

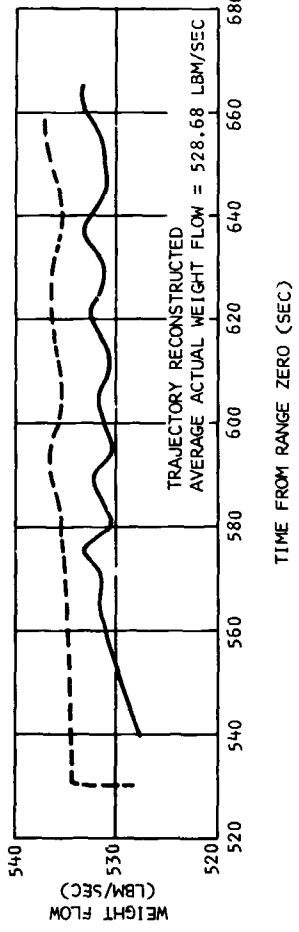
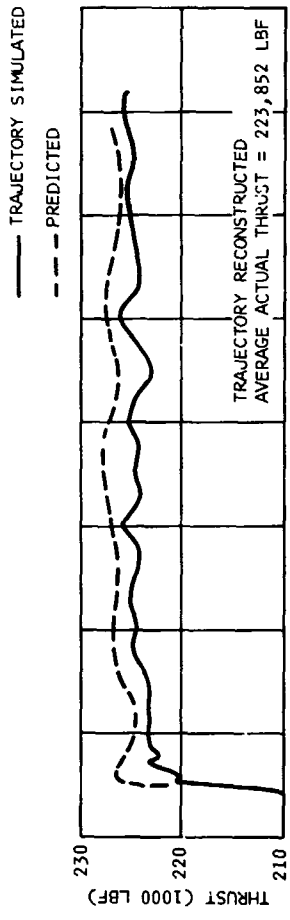
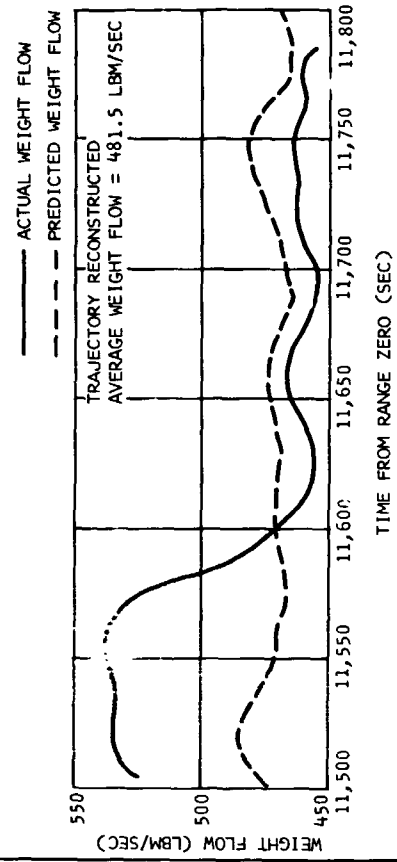
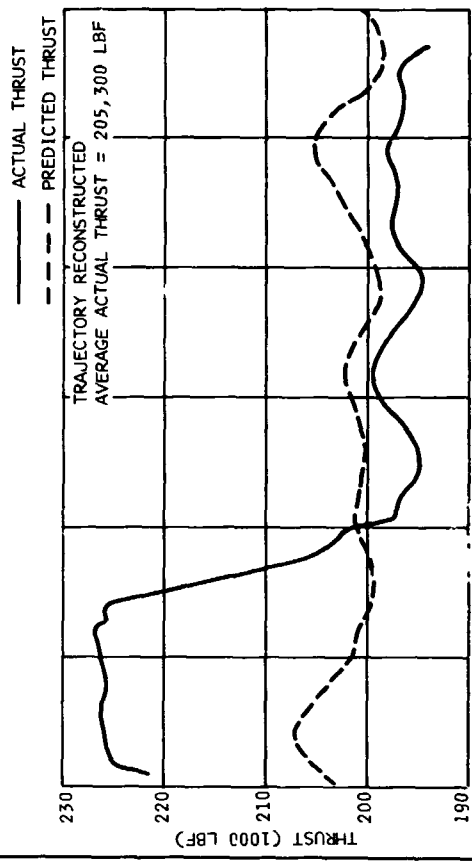


Figure 7-43. Flight Simulated First Burn Engine Steady-State Performance

Figure 7-44. Flight Simulated Second Burn Engine Steady-State Performance

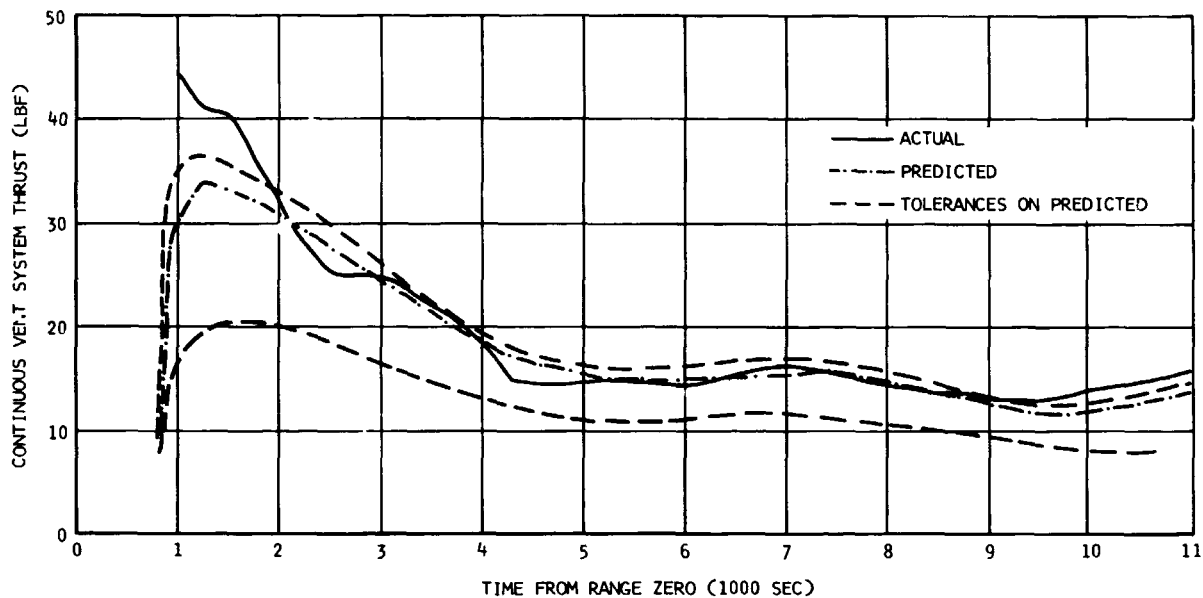


Figure 7-45. AS-501 Parking Orbit Actual and Predicted Continuous Vent System Thrust

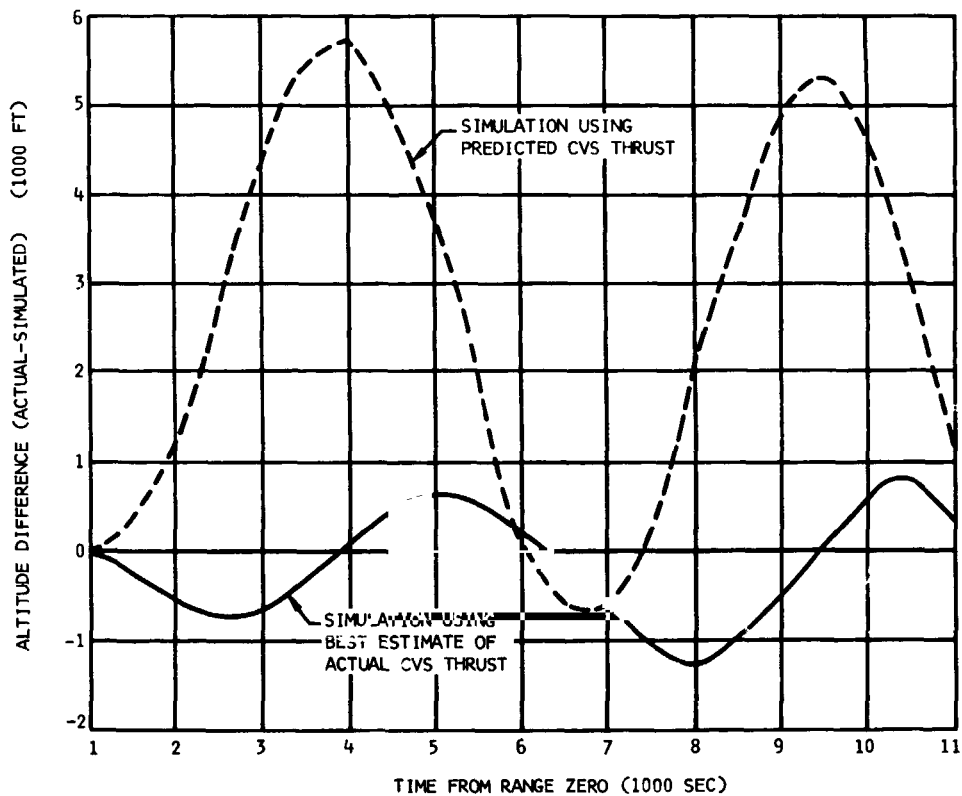


Figure 7-46. AS-501 Parking Orbit Difference Between Actual and Simulated Orbit Altitude

Section 7
Trajectory

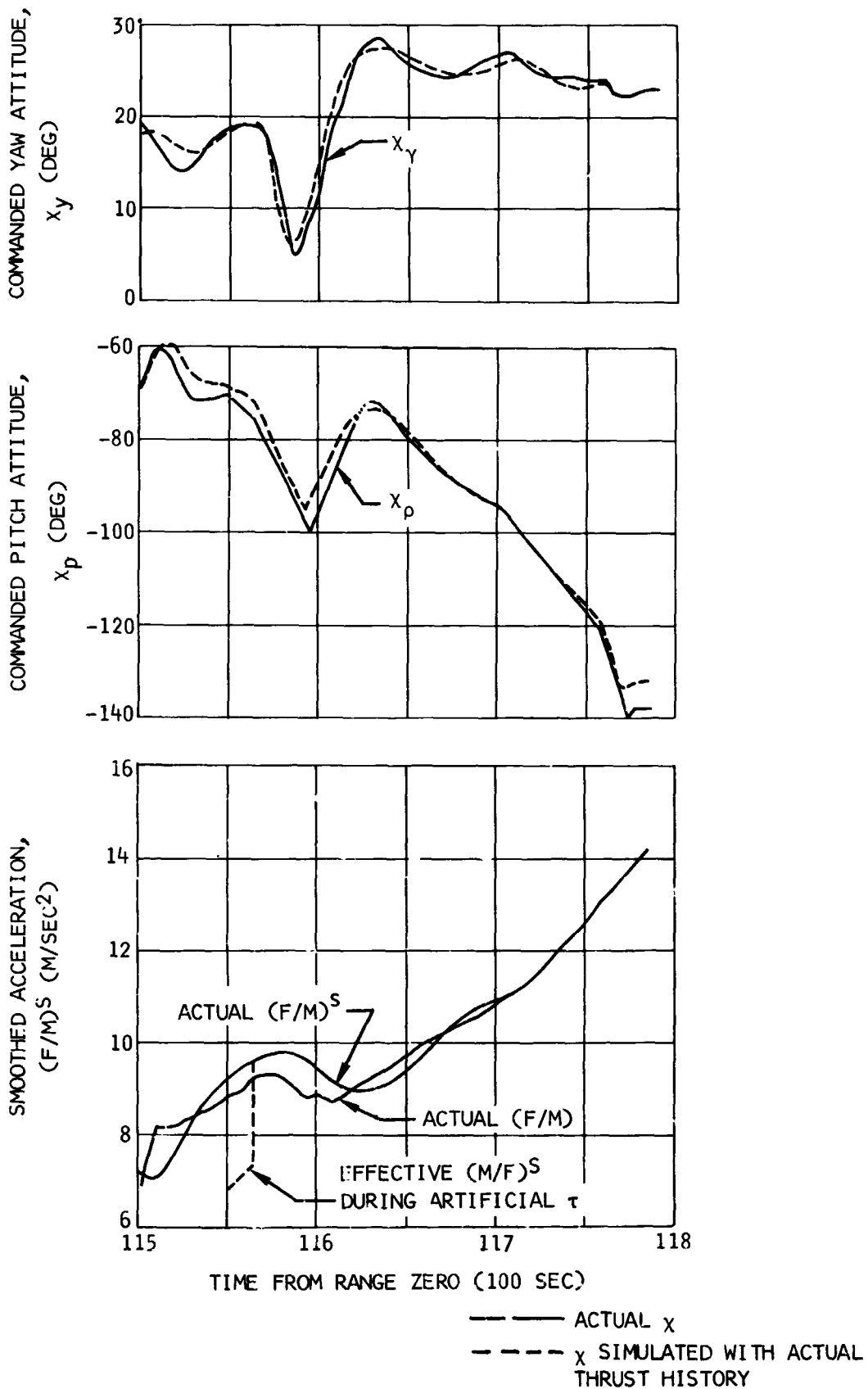


Figure 7-47. Iterative Guidance Response to Second Burn Thrust Profile

8. MASS CHARACTERISTICS

8.1 Mass Characteristics Summary

The AS-501 third flight stage (S-IVB-501, IU, and payload) mass summary presented in table 8-1, and the mass characteristics presented in appendix 1 are best estimate values.

8.2 Mass Properties Dispersion Analysis

Figures 8-1 through 8-8 present a comparison of the predicted vehicle mass characteristics and three-sigma dispersions, versus the postflight vehicle mass characteristics for the AS-501 third flight stage during S-IVB first and second burns. The figures show the postflight mass properties were within the predicted three-sigma dispersion bands.

The predicted dispersions were determined from a statistical analysis of component mass properties uncertainties and are referenced relative to time from Engine Start Command rather than event.

8.3 Third Flight Stage Best Estimate Ignition and Cutoff Masses

The best estimate method is a three dimensional statistical analysis of data from five mass measurement systems. This method develops a joint probability density function from which the most probable values and accuracies for ignition and cutoff masses are determined.

Three measurement systems provide unique values for ignition and cutoff mass while two systems provide a linear relationship between them. The best estimate method combines the unique values with the linear relationships to compute the most probable value for ignition and cutoff mass. This technique provides the optimum statistical evaluation of flight vehicle ignition and cutoff mass by constraining each measurement system to its intrinsic evaluation capability.

The five measurement systems used in determining the best estimate masses are: (1) PU volumetric, (2) PU indicated (corrected), (3) level sensors, (4) flow integral, and (5) trajectory reconstruction. A brief description of these measurement systems is as follows:

Section 8
Mass Characteristics

- a. The PU volumetric system measures propellant mass from raw PU probe output data reduced according to volumetric calibration slopes and volumetric flight nonlinearities.
- b. The PU indicated corrected system measures propellant mass from PU probe output reduced according to the preflight calibration slope and adjusted for flight flow integral nonlinearities.
- c. The level sensor system measures propellant mass at sensor activation and this mass is extrapolated to ignition or cutoff mass from flight flow integral data. This stage has level sensors located throughout the length of the propellant tanks.
- d. The trajectory reconstruction method provides the linear relationship between ignition and cutoff mass which satisfies the observed trajectory.
- e. The flow integral method provides a linear relationship between ignition and cutoff mass which represents propellant consumption derived by integrating propellant flowrates as a function of time.

Figures 8-9 and 8-10 show a graphical presentation of the best estimate analysis for first and second burns, respectively. For first burn, the third flight stage ignition mass was 353,145 \pm 460 lbm, and the cutoff mass was 279,038 \pm 404 lbm. For second burn, the third flight stage ignition mass was 275,730 \pm 438 lbm, and the cutoff mass was 136,365 \pm 279 lbm.

Figures 8-9 and 8-10 show the trajectory reconstruction and flow integral linear relationships intersect at a considerably lower ignition and cutoff mass than the best estimate values. These data indicate a bias exists between the linear relationships and the unique measurement systems. An error in total mass of payload, IU, and S-IVB dry stage affects the ignition and cutoff mass values from each unique system equally for both first and second burns. Consequently, if the actual mass value of payload, IU, and S-IVB dry stage were less than provided, the resulting best estimate would more closely agree with the linear relationships intersection.

8.3.1 Best Estimate Program Input

Table 8-2 presents a summary of the values used in determining the best estimate ignition and cutoff mass. For the unique measurement systems, the LOX, LH2, and non-propellant mass values and their predicted dispersions are shown in addition to the total mass value and dispersion used for computation. The linear relationship values are presented as utilized for best estimate analysis.

Section 8
Mass Characteristics

TABLE 8-1
MASS SUMMARY (lbm)

ITEM	S-IC LIFTOFF	S-II/S-IVB SEPARATION	S-IVB FIRST ESC	END FUEL LEAD	FIRST 90 PERCENT THRUST	S-IVB FIRST ECC	S-IVB FIRST ETD*	RESTART PREPARATIONS	
Launch Escape	8,710	0	0	0	0	0	0	0	
Frost	300	0	0	0	0	0	0	0	
Separation Pkg	52	0	0	0	0	0	0	0	
Ullage Rkt Grn	117	114	108	20	0	0	0	0	
Ullage Rkt CSE	131	131	131	131	131	0	0	0	
Command Module	11,991	11,991	11,991	11,991	11,991	11,991	11,991	11,991	
Service Module	9,596	9,596	9,596	9,596	9,596	9,596	9,596	9,596	
SM Propellants	30,075	30,075	30,075	30,075	30,075	30,075	30,075	30,075	
Adapter Ring	91	91	91	91	91	91	91	91	
Adapter (SLA)	3,790	3,790	3,790	3,790	3,790	3,790	3,790	3,790	
LEM Test Article	29,500	29,500	29,500	29,500	29,500	29,500	29,500	29,500	
Veh Inst Unit	4,756	4,756	4,756	4,756	4,756	4,756	4,756	4,756	
S-IVB-501 Dry Stg	26,326	26,326	26,326	26,326	26,326	26,326	26,326	26,326	
LOX in Tank	194,028	194,028	194,028	194,028	193,648	131,424	131,267	131,133	
LOX Ullage Gas	35	35	35	39	42	234	234	375	
LOX Below Tank	367	367	367	367	397	397	367	367	
LH2 in Tank	41,125	41,095	41,095	41,083	40,946	29,607	29,577	26,669	
LH2 Ullage Gas	78	108	108	108	109	141	142	338	
LH2 Below Tank	48	48	48	53	58	58	48	48	
Cold Helium	319	319	319	319	318	272	272	272	
APS Prop + He	622	622	622	622	622	622	620	520	
GH2 in Start Trk	5	5	5	5	1	7	7	7	
Helium Repress	78	78	78	78	78	78	78	78	
Service Items	30	30	30	30	30	30	30	30	
Env Cont fluid	43	43	43	43	43	43	43	43	
TOTAL MASS	362,214	353,149	353,143	353,053	352,549	279,038	278,810	276,015	
TIME FROM RANGE ZERO (sec)	0.263	520.5	520.7	523.7	526.2	665.6	667.3	11,159.6	

*End of thrust decay

FOLDOUT FRAME

BLE 8-1
SUMMARY (lbm)

* RESTART PREPARATIONS	S-IVB SECOND ESC	END FUEL LEAD	SECOND 90 PERCENT THRUST	PU VALVE CUTBACK	S-IVB SECOND ECC	S-IVB SECOND ETD*	CSM SEPARATION	END
0	0	0	0	0	0	0	0	0
0	0	0	0	0	0	0	0	0
0	0	0	0	0	0	0	0	0
0	0	0	0	0	0	0	0	0
0	0	0	0	0	0	0	0	0
11,991	11,991	11,991	11,991	11,991	11,991	11,991	0	0
9,596	9,596	9,596	9,596	9,596	9,596	9,596	0	0
30,075	30,075	30,075	30,075	30,075	30,075	30,075	0	0
91	91	91	91	91	91	91	0	0
3,790	3,790	3,790	3,790	3,790	3,790	3,790	3,790	3,790
29,500	29,500	29,500	29,500	29,500	29,500	29,500	29,500	29,500
4,756	4,756	4,756	4,756	4,756	4,756	4,756	4,756	4,756
26,326	26,326	26,326	26,326	26,326	26,326	26,326	26,326	26,326
131,133	131,129	131,129	130,817	107,519	14,546	14,412	14,342	14,342
375	380	383	385	410	522	522	459	459
367	367	367	397	397	397	367	367	367
26,669	26,579	26,547	26,394	22,204	3,631	3,603	2,941	2,941
338	390	392	393	411	492	493	940	940
48	48	55	58	58	58	48	48	48
272	272	269	268	251	177	177	177	177
529	335	333	333	329	310	310	289	235
7	7	7	1	7	7	7	7	7
78	26	26	26	26	26	26	26	26
30	30	30	30	30	30	30	30	30
43	43	43	43	43	43	43	43	43
276,015	275,731	275,709	275,271	247,811	136,364	136,162	84,041	83,937
11,159.6	11,486.6	11,494.5	11,497.1	11,550.1	11,786.2	11,787.7	12,386.4	25,000.0

FOLDOUT FRAME 2 ✓

TABLE 8-2
BEST ESTIMATE PROGRAM INPUT VALUES

UNIQUE MEASUREMENT SYSTEMS

EVENT	MEASUREMENT SYSTEM	LOX (lbm)		LH2 (lbm)		NON-PROPELLANT (lbm)		TOTAL (lbm)	
		VALUE	ERROR	VALUE	ERROR	VALUE	ERROR	VALUE	ERROR
ESC1	PU Volumetric	194,300	+965	40,994	+266	117,607	+231	352,901	+1,027
	Pt Level Sensor	194,770	+965	40,408	+266	117,607	+231	353,785	+1,027
	PU Indicated (corrected)	193,308	+1,380	40,107	+343	117,607	+231	352,022	+1,441
ECC1	PU Volumetric	131,700	+708	29,557	+219	117,552	+233	278,809	+777
	Pt Level Sensor	132,326	+731	29,874	+199	117,552	+233	279,752	+793
	PU Indicated (corrected)	131,353	+936	29,662	+247	117,552	+233	278,567	+996
ESC2	PU Volumetric	131,381	+709	26,657	+211	117,607	+238	275,645	+777
	Pt Level Sensor	131,461	+1,023	26,496	+167	117,607	+238	275,564	+1,064
	PU Indicated (corrected)	131,085	+936	26,771	+227	117,607	+238	275,463	+992
ECC2	PU Volumetric	15,059	+495	3,725	+132	117,733	+240	136,517	+566
	Pt Level Sensor	15,079	+609	3,595	+175	117,733	+240	136,407	+678
	PU Indicated (corrected)	15,133	+495	3,815	+132	117,733	+240	136,681	+566

LINEAR RELATIONSHIPS

EVENT	MEASUREMENT SYSTEM	SLOPE	INTERCEPT (lbm)	ERROR (lbm)
FIRST BURN	Flow Integral Trajectory Reconstruction	1.0	74,052	+456
	Flow Integral Trajectory Reconstruction	1.267315	C	+1,059
SECOND BURN	Flow Integral Trajectory Reconstruction	1.0	139,072	+852
	Flow Integral Trajectory Reconstruction	2.026824	0	+827

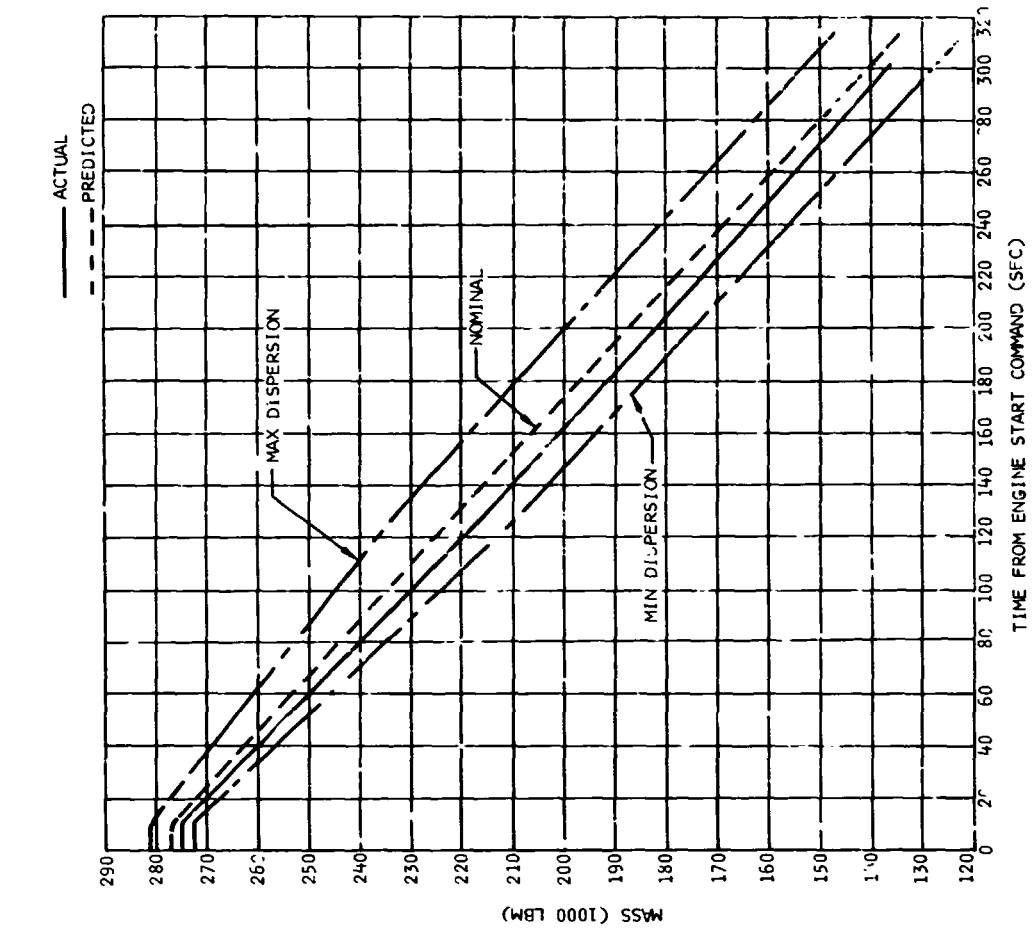


Figure 8-2. Third Flight Stage Vehicle Mass - Second Burn

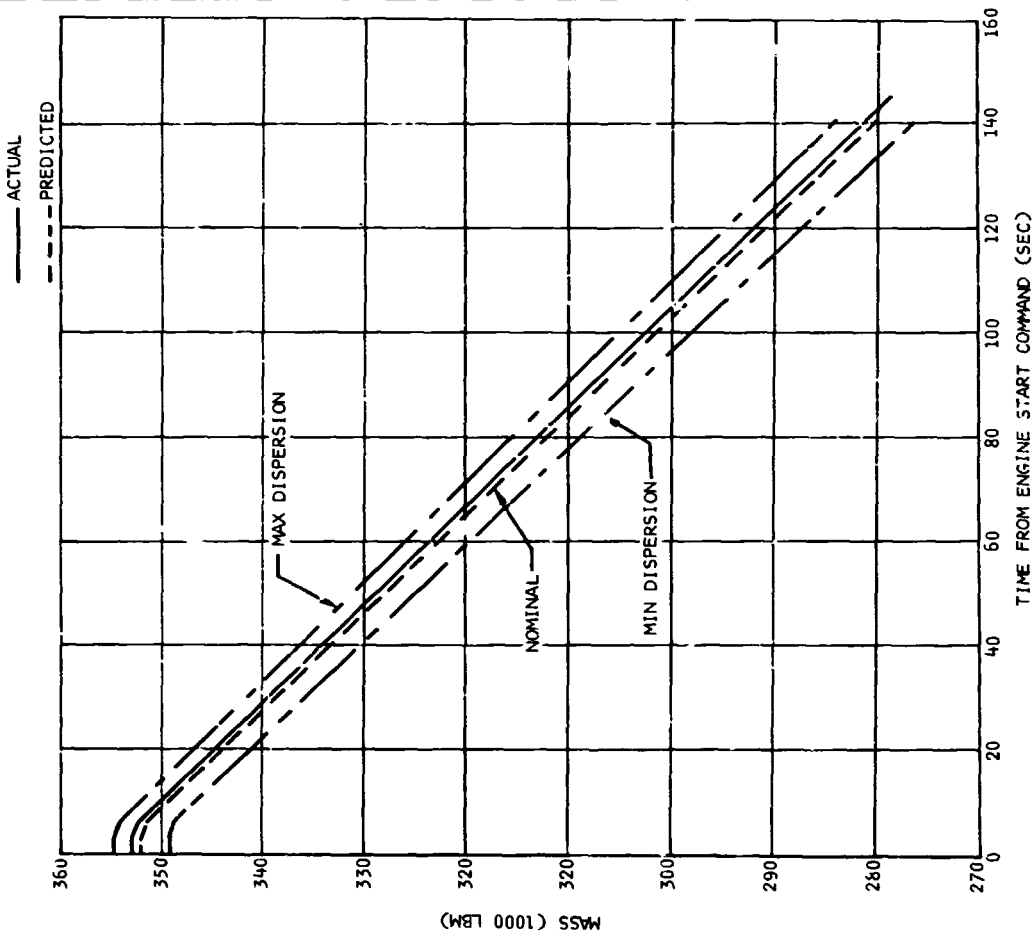


Figure 3-1. Third Flight Stage Vehicle Mass - First Burn

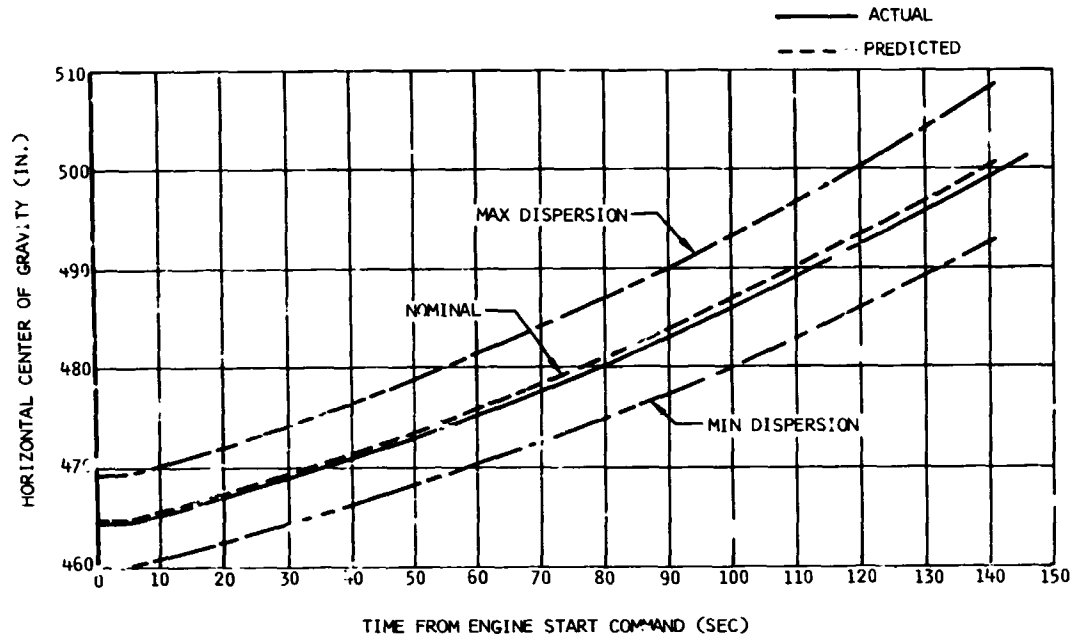


Figure 8-3. Third Flight Stage Vehicle Horizontal Center of Gravity - First Burn

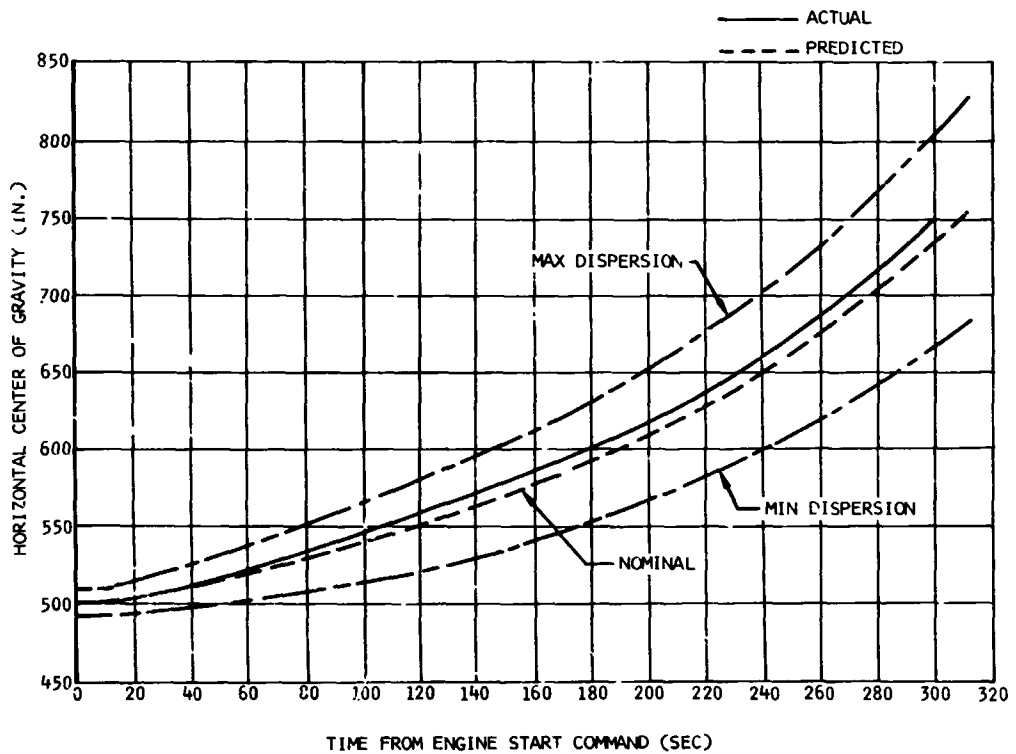


Figure 8-4. Third Flight Stage Vehicle Horizontal Center of Gravity - Second Burn

Section 8
Mass Characteristics

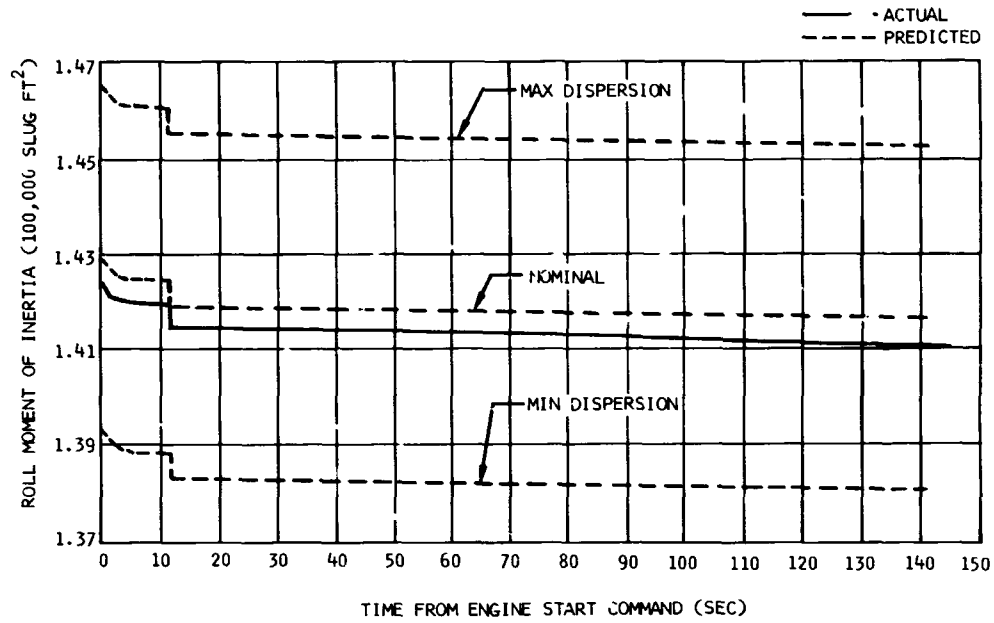


Figure 8-5. Third Flight Stage Vehicle Roll Moment of Inertia - First Burn

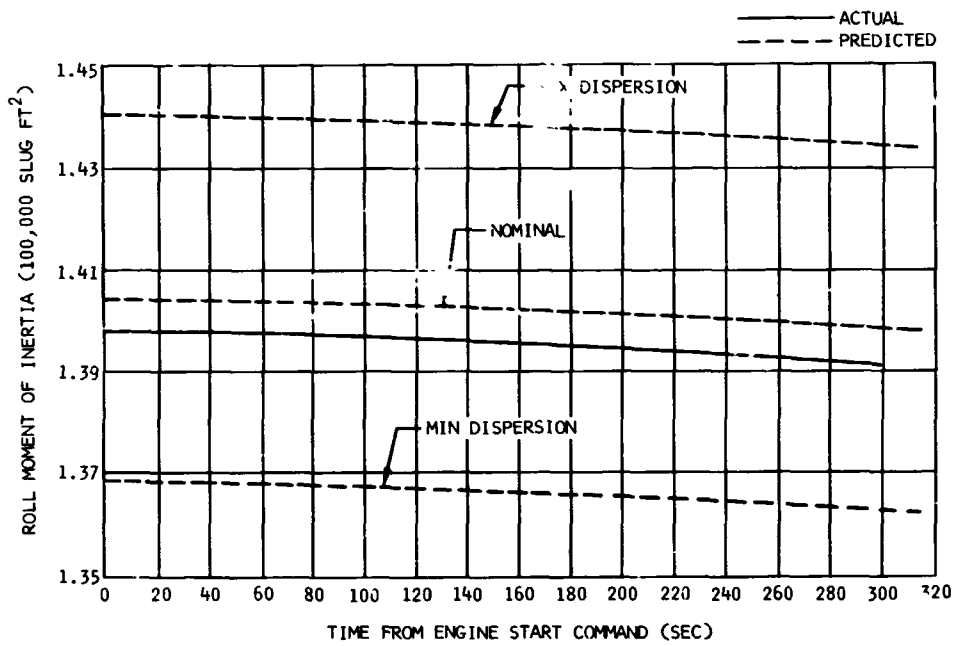


Figure 8-6. Third Flight Stage Vehicle Roll Moment of Inertia - Second Burn

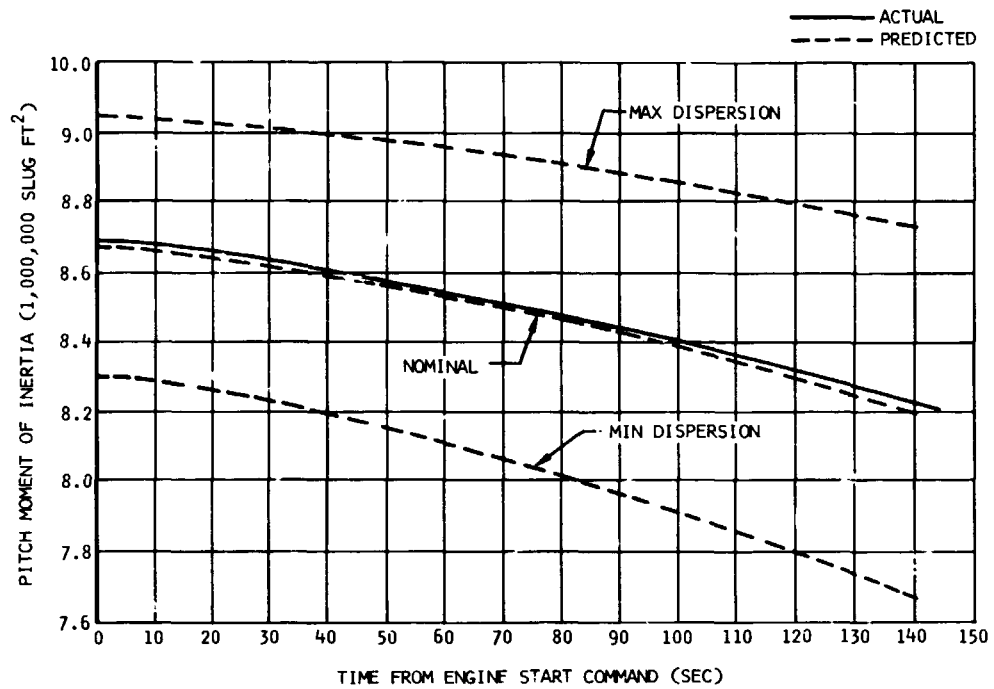


Figure 8-7. Third Flight Stage Vehicle Pitch Moment of Inertia - First Burn

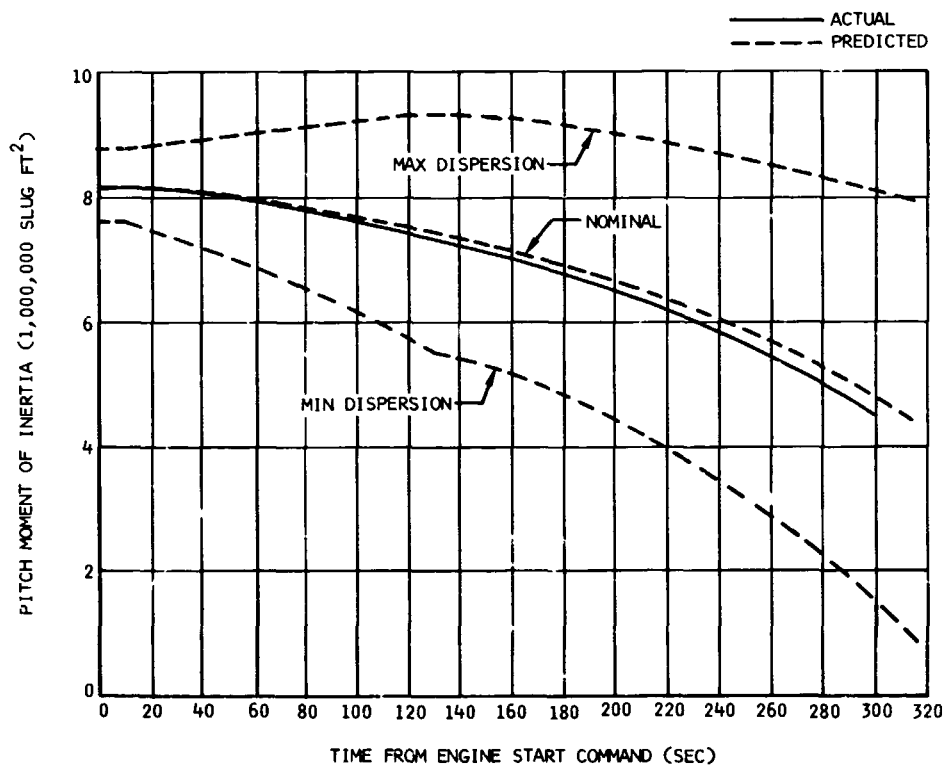


Figure 8-8. Third Flight Stage Vehicle Pitch Moment of Inertia - Second Burn

Section 8
Mass Characteristics

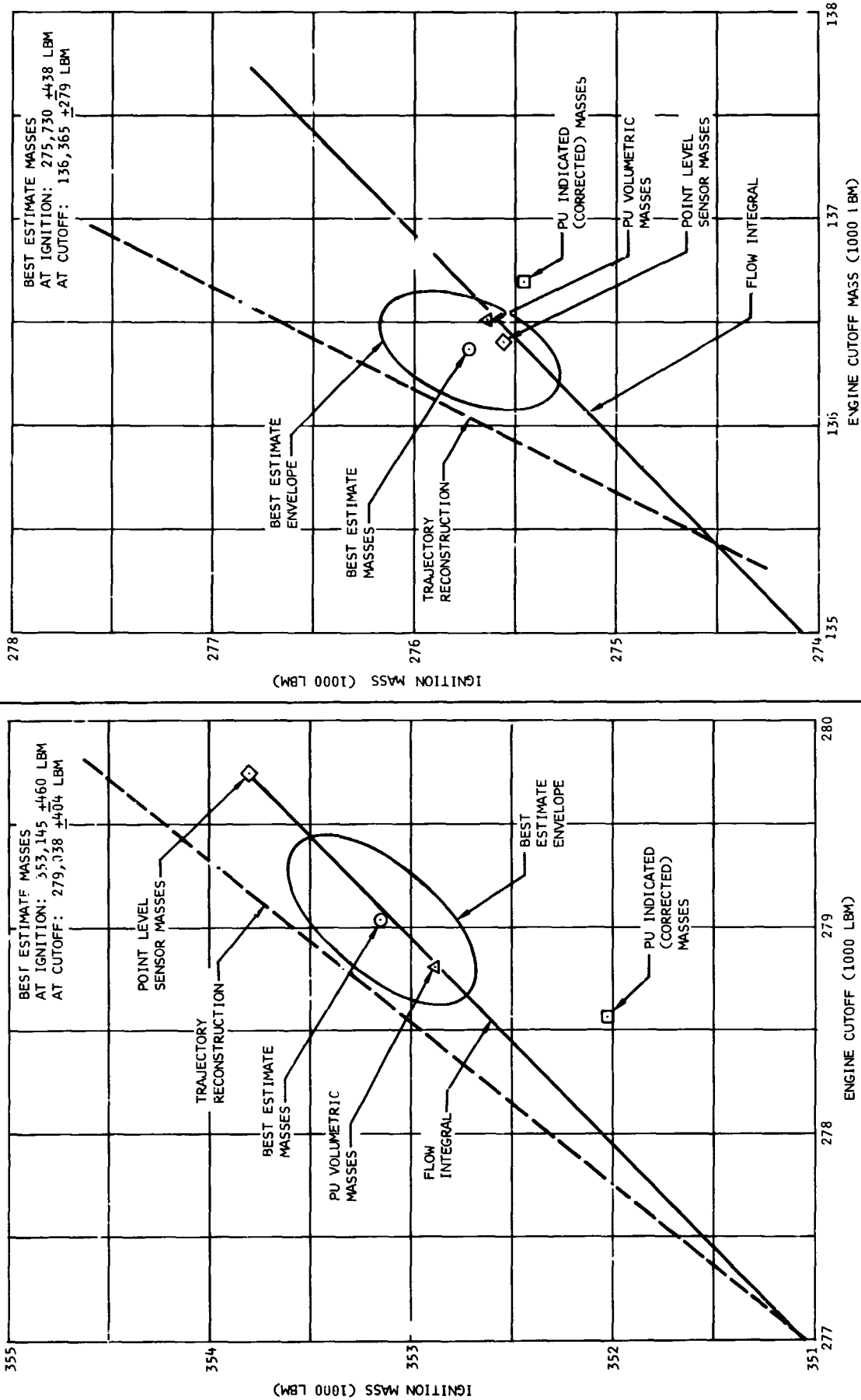


Figure 8-10. Third Flight Stage Final Best Estimate Masses - Second Burn

Figure 8-9. Third Flight Stage Final Best Estimate Masses - First Burn

9. ENGINE SYSTEM

The main propulsion system of the S-IVB stage of the AS-501 launch vehicle consisted of a Rocketdyne J-2 engine (S/N J-2031) shown schematically in figure 9-1, associated propellant ducting, and sufficient conditioning systems. The engine was rated at 225,000 lbf thrust and analysis of the engine and stage acceptance tests resulted in the establishment of the following "60 sec tag values" for the engine.

Thrust (F)	225,144 lbf
Engine mixture ratio (EMR)	5.562
Specific impulse (Isp)	423.4 sec

These tag values were established with the following engine constants:

LOX Flowmeter	5.5868 cycles/gal
LH2 Flowmeter	1.9098 cycles/gal
LOX Boot Strap Orifice	0.259 in. ²
LH2 Boot Strap Orifice	0.455 in. ²
LOX Turbine Bypass Nozzle	1.190 in. ²

The engine was equipped with a 0.640 sec start tank discharge valve (STDV) timer in the engine control circuit, however, actuation of the STDV, which determines the fuel lead duration, was controlled from the stage through the fuel injection temperature bypass circuit. With such control, the fuel leads were nominally 3 and 8 sec for the first and second burns, respectively. The engine was modified to guarantee a satisfactory start transient for the second burn. These modifications consisted of retiming the main LOX valve (MOV) opening rate, reducing the augmented spark igniter (ASI) LOX orifice and painting the crossover duct. A modification was made to the stage propellant utilization (PU) system which allowed the engine to be started with the PU valve in the fully open position for second burn start reliability. The start sphere vent and relief valve was also changed because of a leakage problem and as a result the relief setting of the sphere was reduced to 1,290 psia. This reduction also increased the second burn start reliability.

Section 9
Engine System

Significant engine events during the S-IVB powered flight phase of the AS-501 mission were as follows:

EVENT	TIME			
	RO*	ESC	PRED	DEVIATION
First Burn Engine Start Command (ESC1)	520.717	0	517.8	+2.917
First Burn Engine Cutoff Command (ECC1)	665.641	144.924	656.6	+9.041
Second Burn Engine Start Command (ESC2)	11,486.567	0	11,483.6	+2.967
Second Burn Engine Cutoff Command (ECC2)	11,786.265	299.698	11,800.1	-13.835

*RO = Range Zero

Comparisons are made to the predicted engine burntimes as published in Douglas Report No. SM-46998B, S-IVB-501 Stage Flight Test Plan, dated 2 November 1967, Revision D.

9.1 Engine Chillover and Conditioning

9.1.1 Turbopump Chillover

Chillover of the engine LOX and LH2 turbopumps was adequate to provide the conditions required for proper engine start during both burns. Figure 9-2 shows the condition of the LOX pump and figure 9-3 shows the relative condition of both pumps as they affect the restartable probe. Turbopump performance is discussed in paragraph 9.5.2. The analysis of the chillover operation is presented in paragraphs 11.3 and 12.3.

9.1.2 Thrust Chamber Chillover

9.1.2.1 First Burn

Thrust chamber chillover was initiated at RO -15 min and terminated at liftoff with a thrust chamber jacket temperature (C0199) of 214 deg R,

thus satisfying the maximum allowable redline limit of 265 deg R. At S-IVB first burn Engine Start Command the temperature was 261 deg R (figure 5-4), which is below the requirement of 330 \pm 50 deg R. The failure to meet the minimum requirement at Engine Start Command is the result of lower than predicted thrust chamber heating during boost.

The thrust chamber chilldown procedures have been re-evaluated in order to meet jacket temperature requirements on subsequent Saturn V flights. The correction will be a shorter chilldown period and a corresponding revision in the redline limits at liftoff. The lower than predicted thrust chamber chilldown temperature (figure 5-4) was a result of the reduced boost heating as discussed above. This deviation was not detrimental to the start transient. The fuel lead, which is used to condition the thrust chamber prior to mainstage was 3.008 sec for the first burn as compared to the required time of 3.0 \pm 0.050 sec (figure 9-4).

9.1.2.2 Second Burn

The second burn thrust chamber conditioning is performed totally by the fuel lead. The second burn fuel lead duration was 7.962 sec (8.0 \pm 0.050 sec required) and resulted in satisfactory chilldown of the engine thrust chamber. The thrust chamber jacket temperature decreased from 524 to 435 deg R and the LH2 injector temperature increased from 305 to 410 deg R then decreased to 162 deg R (figure 9-5). Fuel lead performance is further discussed in paragraph 9.4.1.

9.1.3 Engine Start Sphere Chilldown and Loading

Chilldown and loading of the engine GH2 start sphere met the requirements for liftoff (figure 9-6). Start sphere data from loading through first burn cutoff are presented in figure 9-7. The GH2 supply system performance, during start sphere chilldown and loading, is described in section 5. The sphere warmup rate from sphere pressurization to blowdown was 0.9 deg R/min. This low warmup rate was due to a revised chilldown sequence (paragraph 5.4.2.3).

9.1.4 Engine Control Sphere Chilldown and Loading

The engine control sphere conditioning was adequate and all objectives were accomplished. The engine start requirements (2,975 \pm 475 psia and

Section 9
Engine System

+20 deg R of start sphere temperature) were met. Control sphere data from loading through first burn cutoff are presented in figure 9-7. Significant control sphere performance data from five previous S-IVB stage firings are compared in table 9-1.

9.2 Start Sphere Performance

9.2.1 First Burn

The J-2 engine start sphere conditions at S-IVB first burn Engine Start Command during the AS-501 flight were 1,270 psia pressure and 266.2 deg R temperature with a mass of 3.62 lbm as compared to predicted values of 1,270 psia pressure, 285 deg R temperature, and 3.39 lbm mass (figure 9-8). The deviations were due to the lack of sufficient data from the revised chilldown sequence (paragraph 5.4.2.3) to update the prediction. This minor temperature deviation represented a negligible increase in the spin potential of the start sphere for the first burn. The start tank discharge valve (STDV) was commanded open at ESC1 +3.008 sec and the pressure decay initiated at ESC1 +3.19 sec. The blowdown was terminated by the STDV closure at ESC1 +3.805 sec. Approximately 2.95 lbm of GH2 were discharged during the 0.61 sec blowdown with terminal conditions as shown on figure 9-8. The start sphere began to refill with hydrogen from the fuel injection manifold and pump discharge immediately upon STDV closure. The rate of pressure increase was controlled by the orifices in the refill lines from the fuel pump discharge and injector. The start sphere pressure increased to 820 psia at ESC1 +10 sec which equalled the fuel injection pressure terminating the gas portion of the refill as shown in figure 9-9. At that time topping was initiated which involves the flow only from the fuel pump discharge to the start sphere and is characterized by increasing pressure due to mass addition and decreasing temperature due to mixing as shown in figure 9-8. The recharge capability of the start sphere, as defined by Rocketdyne, was satisfactorily demonstrated during the first burn (figure 9-10) at STDV +60 sec. The topping process was terminated at ESC1 +64.37 sec when the start sphere pressure and pump discharge pressure were in equilibrium. The pressure level was

approximately 1,100 psia at this time which can be seen on figures 9-8 and 9-9. At this time the start sphere temperature was 177 deg R (figure 9-8) with no further mass increase in the sphere. Heat input from the system caused a temperature increase and a corresponding pressure increase along a constant mass line as shown in figure 9-8. At cutoff the start sphere pressure and temperature were 1,174 psia and 186 deg R, respectively. As can be seen in figure 9-8 the cutoff conditions were not within the safe engine restart envelope but were within the expected performance conditions.

9.2.2 Orbital Coast

Figures 9-8 and 9-11 show a relatively large temperature change at Engine Cutoff Command with essentially no pressure change, which is impossible without a corresponding mass change. Leakage would be a possible explanation for such a deviation from the constant mass line, but there is no plausible explanation for the reversal of the deviation as shown by the data. A similar deviation was noted during the AS-203 orbital coast (figure 9-11) and the resultant analysis concluded that, in the zero-g environment, heat transfer becomes a very localized phenomenon because of the lack of convection effects. Therefore, the location, the installation technique, and the type of transducer, effect the acquisition of reliable start sphere bulk temperature data during orbital coast.

The anticipated temperature rise rate during orbital coast was 0.34 deg R/min with a corresponding 2 psi/min pressure rise rate. With such rates the relief setting (1,290 psia) of the vent and relief valve would be reached at ECC1 +56 min. The actual relief time was ECC1 +47.24 min resulting from a mean pressure rise rate of 2.46 psi/min, which corresponds to an isochoric temperature rise rate of 0.39 deg R/min compared to the indicated temperature rise rate of 1.08 deg R/min.

The start bottle conditions were within the required restart envelope at ECC1 +10 min at a pressure of 1,200 psia.

Section 9 Engine System

After reaching the relief setting the temperature continued to rise until second burn Engine Start Command. The relief pressure level characteristically drops with increasing environment temperature. As mentioned previously, accurate values for this temperature rise are not available in the low gravity environment. As during the S-IVB-203 analysis, an attempt was made to determine the true temperature based on the rise of the control sphere temperature and pressure. However, the control sphere was apparently leaking, thereby complicating the relationship with an unknown mass flowrate. This resulted in a constant control sphere pressure in orbit as discussed in paragraph 9.3. The first temperature data point during the second burn blowdown was considered accurate because of the forced convection induced by the blowdown flow. Extrapolations based on this data were used to determine a corrected curve shown in figure 9-11. Figure 9-11 compares the orbital coast data from the S-IVB-203 and S-IVB-501 missions. During the S-IVB-501 orbital coast (130 min) an estimated 0.85 lbm of CH₂ was vented through the relief valve to maintain the pressure as indicated in figure 9-11.

9.2.3 Second Burn

The J-2 engine start sphere conditions at S-IVB second burn Engine Start Command, were within the safe start envelope at a pressure of 1,280 psia and a temperature of 247 deg R. The mass was 3.96 lbm (figure 9-12) which represents a 9.4 percent increase in spin potential compared to the first burn. The STDV was commanded open at ESC2 +8.014 sec and the pressure decay initiated at ESC2 +8.170 sec. The blowdown was terminated by the STDV closure at ESC2 +8.886 sec. Approximately 3.29 lbm of CH₂ were discharged during the 0.716 sec blowdown with terminal conditions as shown in figure 9-13. The greater mass discharged during the second burn blowdown (as a result of the lower temperature) was calculated to have contributed approximately 3 psi of the 63 psi increase in LOX pump discharge pressure spike during the second burn start transient as compared to the first burn (figures 9-14 and 9-15). The start sphere began to refill, repeating the first burn process with the lower initial temperature resulting in a colder refill. The longer burn duration

resulted in start sphere conditions (1,190 psia pressure, 171 deg R temperature) much closer to the safe start region (figure 9-13). However, as shown in figure 9-10 the second burn refill was not within the calculated performance region. As after the first burn, the start sphere pressure increased due to the heat input and reached the relief setting at ECC2 +53.5 min. Although within the safe start envelope, further study is necessary before guaranteeing a reliable additional engine start because of the deviation from the calculated performance region. The second recharge was not a requirement for the AS-501 mission.

9.3 Engine Control Sphere Performance

9.3.1 First Burn

The results of the AS-501 flight J-2 engine control sphere analysis indicate that there was adequate helium supply on board to perform all necessary pneumatic functions.

The engine control sphere was loaded within the nominal requirement of 2,800 to 3,200 psia and within 10 deg of start sphere temperature (figure 9-7). The pressure and temperature at liftoff were 3,013 psia and 270 deg R (start sphere temperature was 262 deg R). The helium mass was 2.070 lbm. The pressure and temperature at first burn Engine Start Command were 3,075 psia and 275 deg R (start sphere temperature was 267 deg R) (figure 9-7). The indicated temperature and pressure data at liftoff and ESC1 were adjusted to eliminate the indicated mass increase during this period (tables 9-1, 9-2, and 9-3). Although the fuel lead time for the first burn start was 3.008 sec, the ignition phase control timer (0.450 \pm 0.03 sec) extended the period of high helium usage associated with the fuel lead to 3.452 sec which was normal. However, an additional extension of at least 0.348 sec was experienced due to the delay in the purge control valve closing. Rocketdyne has experienced as much as 0.7 sec delay in the closure of this valve. As a result of this extension the control sphere pressure drop associated with the fuel lead was 650 psi as compared to the predicted value of 500 psi (figure 9-16). The indicated pressure drop of 1,240 psi from ESC to ECO +1 sec was adjusted to 520 psi, when the temperature was corrected to 290 deg R,

Section 9 Engine System

and was within the required maximum ΔP of 800 psi. The performance during the first burn is shown in figure 9-17. The mass usage during first burn was 0.412 lbm leaving 1.558 lbm in the bottle at orbital insertion.

9.3.2 Orbital Coast

The measured gas temperature of 204 deg R, at the end of the post cutoff 1-sec LOX dome purge for the first burn, was below the adiabatic blowdown temperature, but above the choked flow static temperature (table 9-2). Since the transducer was located inside the sphere near the gas outlet, the localized temperature after blowdown could be approaching the static choked flow temperature. The measured temperature of 204 deg R indicates that high velocity gas flow existed across the transducer. The actual gas temperature at the start of the coast period was determined to be 224 deg R from extrapolations of orbital coast data as shown in figure 9-18. This temperature and the measured pressure were used to establish the helium mass in the control sphere following engine cutoff.

In a system where convective heat transfer is dominant, the measured temperature near the wall from a cold gas sphere in a low-g field could be higher than the actual gas temperature. In a long coast period the low convective effect could be minimized by conductivity and radiation which are independent of gravitational constant. (The low-g heat transfer investigation of the control sphere is presently being conducted by Rocketdyne.) In considering the long coast period and the small size of the control sphere, the recorded temperature at the second burn Engine Start Command was used without corrections in the present analysis.

It should be noted that the apparent recovery from 204 to 224 deg R after cutoff may have been caused by the combined effects of lack of thermal convection inside the start and control bottles combined with high radiation heat transfer from the adjacent engine turbine hardware. If this were the case more mass would be consumed as leakage in orbit; however, the total flight helium consumption would remain unchanged. The steady-state temperature and pressure prior to second burn engine start and several data points during coast were used to determine

the system leakage rate. The average system leakage rate in the 3-hr coast period was calculated to be 0.026 lbm/hr or 0.078 lbm total which is comparable to S-IVB-203 flight data.

9.3.3 Second Burn

The high helium consumption associated with the fuel lead was experienced for 8.6 sec as compared to the 8.458 sec between second burn Engine Start Command and ignition phase control timer expiration. The 0.142 deviation was due to closing time of the purge control valve. Comparing temperatures at the end of the first and second burn fuel leads (figures 9-4 and 9-5) provides an indication that the injection area was colder for the first burn. This lower temperature is a possible explanation for the difference in purge valve closing rates. A further investigation is in process as helium consumption may become critical on some future missions. The measured control sphere temperature at the end of the 8.6 sec fuel lead blowdown was 5.1 deg higher than the adiabatic temperature of 185.5 deg R. The start sphere temperature has been cooler than the control sphere following each engine start permitting some heat flow between the two spheres. The measured control sphere temperature of 190.6 deg R at the start of the second burn mainstage is 56 deg lower than the measured temperature of 246 deg R at first burn mainstage due to the longer fuel lead time. The lower blowdown temperature at the start of the second burn mainstage enabled the control sphere to recover at a higher rate than the first burn. It is illustrated as temperature rise in the first 60 sec of the second burn in figures 9-12, 9-16, and 9-17. The measured temperature at second burn engine cutoff was considered accurate because of the low helium usage in a relatively long 300-sec burn. The total helium consumption during second burn was 0.680 lbm. Considering the longer second burn fuel lead gas consumption the burn usage was close to the shorter 145-sec first burn indicating that the helium used in purging the oxidizer turbopump intermediate seal may have been low. Most of the helium usage would be attributed to the valve controls. The measured control sphere temperature at the end of the post cutoff 1-sec blowdown was again below the adiabatic temperature. The regulator outlet pressure of 408 psia and injector temperature of 200 deg R were similar to

Section 9 Engine System

the respective pressure and temperature of 404 psia and 210 deg R at the first engine cutoff. Therefore, the helium flow in the two 1-sec blow-downs is assumed to be the same. The effective gas temperature in the sphere was calculated at 183 deg R prior to further orbital heatup.

The mass in the control sphere was 0.800 lbm at a pressure of 735 psia. There were no further demands on the control helium sphere during the remainder of the mission. The total helium usage was 1.27 lbm compared to 1.46 lbm predicted. The resulting 13 percent deviation is within acceptable tolerances.

A summary of helium consumption during the mission and details of the control sphere performance are given in table 9-3.

9.4 Engine Performance

9.4.1 Fuel Lead - First and Second Burn

The results of the first and second burn fuel loads which provided inflight conditioning of the thrust chamber are presented in table 9-4. The thrust chamber bulk temperature, presented in the table, is defined as the average of three thrust chamber temperature measurements: jacket temperature C0199 and exit skin temperatures C0385 and C0386. Fuel lead flowrates presented in the table were obtained from three flight measurements: fuel injector pressure D0004, main injector fuel temperature C0200, and fuel flowmeter F0002. Flow through the injector was calculated from injector pressure and temperature measurements using theoretical flow characteristics. Weight flow through the main fuel valve (MFV) was calculated from measured flowmeter data using a constant estimated fuel density. Fuel flowrates calculated by these methods are also presented in figures 9-4 and 9-5. Some question also exists regarding flowmeter readings at the extremely low end of their operating range. The data received appears to correlate to some extent with predicted flowrates and flowrates calculated from injector temperature and pressure. The flowmeter (F0002) measures volume; therefore, the mass flowrates presented in figures 9-4 and 9-5 are also subject to any error in the density used to convert volumetric flowrates to mass

Section 9
Engine System

flowrates as well as in the calibration constants of the flowmeters. It was assumed that the flowing fluid at the flowmeter was 100 percent liquid. The greatest question in this respect occurs in the 0 to 1 sec time period. The initial surge in flow shown in figures 9-4 and 9-5 could be due to some amount of vapor flashoff as well as an initially high flowrate required to charge the system. Specific impulse during fuel lead was calculated using injector temperature (C0200) and assuming theoretical nozzle performance. Since the ASI was operating during this period, the temperature of the fluid was actually higher in the combustion chamber than in the injector. Also, since the ASI bypasses the injector, the mass flow through the thrust chamber nozzle was greater than through the injector.

During mainstage operation the total mass flow through the ASI was in the order of 1.08 lbm/sec. When converted to the pressures and temperatures existing during fuel lead, the flowrate through the ASI during fuel lead was in the order of 0.03 lbm/sec. A weight flow of this magnitude at an assumed temperature of 2,460 deg R has been analyzed through a range of injector flowrates and temperatures. This analysis determined that the net effect of the ASI on thrust and total impulse is in the order of 10 percent. This effect is not included in figures 9-4 and 9-5. Fuel lead during first start was apparently fully effective and the characteristics were in good agreement with previous flight and ground test data. The principle variance encountered in the second start fuel lead is that it was not as effective as expected. At the end of the 8 sec fuel lead period, injector fuel temperature (C0200) had dropped only to 165 deg R, and fuel flowrate had increased only to the 3 to 4 lbm/sec range. From earlier flight simulation tests a temperature of 40 deg R and a flowrate of 6 to 8 lbm/sec would be expected with the thrust chamber temperatures apparently existing at the start of the 8 sec fuel lead.

A simulated flight test has been conducted at Tullahoma with an initial thrust chamber bulk temperature of approximately 500 deg R. This is somewhat higher than the initial temperature (443 deg R) at fuel lead

Section 9 Engine System

start in the AS-501 flight second start. However, even with a somewhat warmer starting condition, the simulated flight test achieved an injector temperature of 40 deg R and a flowrate of 7 lbm/sec in 6.9 sec. This compares to 165 deg R and 3 lbm/sec at the end of 8 sec in the AS-501 operation.

Several possible influences were examined in attempting to isolate the cause of this apparent departure from predicted chilldown characteristics. The principle areas examined were: (1) the possibility of high residual asymmetrical heat, (2) low tank pressure in combination with low NPSF, (3) ullage motor exhaust plume heating, and (4) difference of thrust level between first and second burn. Figures 9-19 and 9-20 show the composite axial thrust on the S-IVB during the first and second burn start periods. It is noted that a significantly lower level of thrust is provided during the second burn period by the APS ullaging. None of the conditions investigated could be conclusively substantiated by demonstrated sensitivity factors as being the cause of the low chilldown rate. Both start transients were successfully accomplished and there were apparently no detrimental effects.

9.4.2 J-2 Engine Performance Analysis Methods and Instrumentation

Engine performance for the powered flight portion of the S-IVB-501 mission was calculated by use of computer programs AA89 and G105-1. The average of the results of the two programs, which is considered to be the best current estimate of engine performance was calculated by computer program PA49. Revised tag values based on flight data were generated by computer program G307 and used in AA89. The results of the PA49 program were used in determining the best estimate of stage propellant consumption. Computer program PA53 utilizing revised techniques and the latest Rocketdyne correlations, was used to compute start and cutoff transient performance. Computer program U123-A was used to calculate internal engine performance parameters and operating characteristics. A description of the operation and a comparison of the results of each program is presented in table 9-5. Data inputs to the computer programs with the applicable biases are shown in table 9-6.

9.4.3 Start Transients - First and Second Burn

The J-2 engine performance during both first and second burn start transients were satisfactory. The engine performance during start transients is summarized in table 9-7.

First burn thrust buildup occurred at a null PU valve position after a 3-sec fuel lead, while second burn thrust buildup occurred with the PU valve in the fully open position (maximum bypass) with an 8-sec fuel lead. During both starts the fuel lead, PU valve position, and main oxidizer valve operation were satisfactory and good starts were obtained.

Restarting the engine at PU valve full open and retiming of the main oxidizer valve (MOV) were apparently successful in overcoming the "hot crossover duct" problem and obtaining a successful restart.

Thrust buildup to the 90 percent performance level (STDV command +2.5 sec) was within the maximum and minimum thrust limits for both burns as shown in figures 9-21 and 9-22. At the end of the second burn transient, the thrust was near a minimum limit, which was expected since start occurred at a full open PU valve while the limits were established for a null PU valve position at start.

Thrust buildup was faster during flight than during the acceptance tests for both burns. This was due largely to the shorter MOV first stage plateau time during flight. As a result LOX flowrate to the thrust chamber was higher during the early phases of thrust buildup during flight. Also the second stage ramp times were slightly shorter during flight, which caused the thrust buildup to be slightly faster during the later phases of the start transient.

The thrust and total impulse at the 90 percent performance level agreed well with the log book values for first burn, but were considerably higher than the corresponding acceptance test values due to the faster opening MOV on flight. For second burn, the thrust and total impulse at the 90 percent performance level was less than the log book values due to the low EMR start (log book values are for a null PU start), but were greater than the acceptance test values due to the faster opening MOV.

Section 9
Engine System

The second burn thrust buildup was faster than first burn. This was shown by the thrust histories and by the approximately 2,000 lbf/sec greater total impulse during second burn start (from STDV command to the 90 percent performance level) even though the thrust at 90 percent performance was less due to the low EMR start. This faster buildup during second burn was also exhibited by the two acceptance test burns and could possibly be due to residual latent heat in the engine after first burn (paragraph 9.7). Figures 9-21 and 9-22 show the thrust chamber pressure, the thrust buildup, and total impulse during the start transients. Figures 9-23 and 9-24 show the measured flowrate and pump speeds for first and second burn start transients.

9.4.4 J-2 Engine Steady-State Performance

The S-IVB stage J-2 engine met all objectives during the 501 mission. Plots of selected data showing engine characteristics are presented in figures 9-25 through 9-36 for first and second burns. The engine propellant inlet conditions are discussed in sections 11 and 12.

The standard altitude engine performance level at STDV +60 sec as determined by computer program G307 (PAST - 641 deck) was as follows:

Parameter	Flight		Stage Acceptance		Engine Accept	Maximum Run-to-Run Difference	Three-Sigma Run-to-Run
	First Burn	Second Burn	First Burn	Second Burn			
Thrust (lbf)	221,861	223,795	223,578	223,529	221,826	1,969	+2,901
EMR	5.491	5.603	5.560	5.548	5.54	0.112	+0.1
Isp (sec)	422.5	421.6	422.9	423.0	423.0	1.4	+2.1

All values were within the three-sigma run-to-run deviations except for the EMR deviation between first and second burn of the flight which was caused by a gas generator (GG) performance shift as explained in paragraph 9.4.4.2.

The composite values for standard altitude steady-state performance with a comparison to the predicted are shown in figure 9-37.

Section 9
Engine System

The stage maneuvering induced some high slosh waves causing PU valve motion with resultant performance variations. There were also apparent GG performance shifts other than that mentioned above. Flow integral mass analysis indicated the following propellant consumptions by the J-2 engine during mainstage operation (the time from the 90 percent performance level, STDV +2.5 sec by definition, to Engine Cutoff Command):

	<u>LOX</u> (lbm)	<u>LH2</u> (lbm)
First Burn	62,202	11,389
Second Burn	116,007	22,797
Total	178,209	34,186

The overall engine average mainstage performance for both burns is presented in table 9-8. The variation of the "site" (data calculated at actual operating conditions) specific impulse with mixture ratio is shown in figure 9-38 while the variation of the "tag" (data corrected to standard altitude conditions) Isp and "tag" thrust with "tag" EMR is shown in figure 9-39.

Table 9-8 presents the total impulse generated during mainstage operation for first and second burn. The engine impulse provided sufficient velocity gain to complete orbital insertion, and provided the necessary velocity to place the payload in the desired trajectory during second burn. Extrapolation of the statistically weighted average of propellant residuals (15,071 lbm LOX and 3,651 lbm LH2) at cutoff indicates that an essentially simultaneous depletion would have occurred at ECC +37.6 sec. At that time an additional 7.36×10^6 lbf-sec of impulse would have been generated making the total for both burns through depletion 97.63×10^6 lbf-sec as compared to the predicted value of 97.97×10^6 lbf-sec. The 0.34 percent deviation is within the prediction accuracy of approximately 1 percent. The 2,696 sec difference between the actual and predicted depletion time is also within the prediction accuracy.

Section 9
Engine System

9.4.4.1 First Burn

Satisfactory performance of the J-2 engine was observed throughout the first burn period. Plots of selected data used as input values to the engine performance computer programs are presented in figures 9-25 through 9-30. Engine turbopump inlet conditions are presented in paragraphs 11.3 and 12.3. Computed engine performance parameters are shown in figure 9-40. The engine mixture ratio was maintained at the 5.5:1 level by the PU system from first burn Engine Start Command +10 sec until first burn Engine Cutoff Command, as discussed in paragraph 9.5.

No engine performance shifts occurred during the first burn period, however, the overall level of performance was approximately 1.5 percent lower than the predicted performance level, as shown in table 9-8. This lower performance level was observed to be a result of an approximate 1-1/2 percent lower than predicted LOX flowrate. This lower flow rate appears to have been caused by a higher than predicted gas generator LOX feedline resistance. The increased resistance thereby resulted in performance degradation similar to the performance shift observed during the S-IVB-501 acceptance test. The S-IVB-501 acceptance test performance shift was considered to be due to a shift in either PU valve or gas generator line resistance.

Table 9-9 contains the S-IVB-501 flight prediction values as originally published (revision 1) and as subsequently updated by later R/NAA revised data. These revised data were:

- a. As updated for R/NAA revised influence coefficients to reflect updated helium flowrate heat transfer effects.
- b. As further updated for engine performance versus PU valve excursion characteristics, as necessitated by revised R/NAA PU valve calibration data.

The differences between the original flight prediction values and those of item a and item b are relatively small (approximately 0.25 percent).

The thrust oscillations during the last 70 sec of first burn are shown in figure 9-41 and compared to the Contract End Item (CEI) specification in table 9-10. All parameters were within the specified limits and are tabulated in table 9-10.

9.4.4.2 Second Burn

Satisfactory performance of the J-2 engine was observed during the second burn period. Plots of selected data used as input values to the engine performance computer programs are presented in figures 9-31 through 9-36. Engine turbopump inlet conditions are presented in paragraphs 11-3 and 12-3. Computed engine performance parameters are shown in figure 9-42.

The EMR was maintained at the 5.5:1 level from ESC2 +20 sec to ESC2 +85 sec by the PU system. This high EMR period was not nominally predicted; however, the high EMR period was within the predicted performance dispersion band. It was the result of the combined effects of initial propellant loading, first burn engine performance, and propellant loss variations during orbital coast. Discussion of the PU system dispersions is contained in section 15. The data contained in table 9-8 shows that the engine performance level during this hardover EMR period was approximately 0.6 percent higher than the hardover level during the first burn period, and also was approximately 0.8 percent lower than the predicted first burn 5.5:1 performance level. This hardover performance level was observed to be at a lower gas generator LOX line resistance value, which would explain the higher gas generator and engine propellant flowrates.

It was also noted that the performance level after PU valve cutback, at the reference mixture ratio (RMR), was approximately 2.6 percent lower than the predicted value, as shown in table 9-8. This was partly due to a lower than predicted PU valve position following PU cutback (reference section 15). Table 9-9 contains second burn flight performance prediction data as originally published (revision 2) and as subsequently updated by later R/NAA revised data.

The C-1 specification limit for thrust rate of change was exceeded at two points, ESC2 +55 sec and ESC2 +296 sec. At ESC2 +55 sec a thrust slope of +850 lbf/sec was observed at which time the helium flowrate for LOX tank pressurization was increased from under to over control. It is noted that a similar helium step increase also occurred at

Section 9 Engine System

ESC2 +105 sec and at ESC2 +215 sec. However, the thrust increase slopes at these times did not exceed 300 lbf/sec. This deviation is undergoing further analysis.

Two performance perturbations were noted during second burn and are illustrated in figure 9-42. These perturbations occurred at ESC2 +105 sec and ESC2 +296 sec when significant propellant sloshing occurred because of large vehicle attitude changes (section 15).

The deviation in performance at ESC +105 sec did not exceed thrust variation limits since it occurred during performance cutback. The engine performance shift which occurred at ESC +296 sec, immediately prior to second burn cutoff, was of greater interest. The PU valve position was observed to move in response to a propellant slosh disturbance. However, the magnitude of the observed performance shift was twice as large as that which could be attributed to the PU valve position movement. Also, the direction of the performance shift reversed, while the PU valve position movement did not. Since the rate of change in performance was greater than could directly be explained by measured PU valve movement, the magnitude of the increased rate of change and the reversal in performance was attributed to a PU bypass system resistance shift. Of course it is possible that a coincident gas generator performance shift could also have occurred at this time and based on past performance of this engine, this possibility should not be discounted.

Detailed expanded data plots during the final 6 sec of second burn are presented in figures 9-43 and 9-44. It may be seen that a definite reversal in chamber pressure, flowrates and fuel turbine inlet temperature occurred. The expanded data of measured PU valve position indicates a definite lack of reversal in valve movement. At ESC2 +296 sec, when the previously described propellant slosh and engine performance shift occurred, a thrust slope of -2,400 lbf/sec was observed. The CEI specification limit during this period of -750 lbf/sec was exceeded however the specifications exclude shifts caused by internal engine performance changes. The estimated rate of change in thrust caused by the slosh is -450 lbf/sec which is within the CEI specification limits.

The thrust oscillations during second burn hardover operation are shown in figure 9-41, and are compared to the CLI specification limits in table 9-10. Thrust variations following PU valve cutback are primarily caused by the PU system effects and are discussed in section 15

9.4.5 Cutoff Transients

The J-2 engine performance during both first and second burn cutoff transients was satisfactory. The time lapse between engine cutoff, as received at the J-2 engine, and thrust decrease to 11,250 lbf (5 percent of rated thrust) was within the maximum allowable time of 800 milliseconds (ms) in both cases. Engine performance during the cutoff transients is shown in table 9-11.

The thrust decrease times during flight were greater than the log book value. This was probably due to a colder main oxidizer valve (MOV) during flight which resulted in longer valve closing times. First burn cutoff occurred with the PU valve in the closed position (high EMR), while second burn cutoff occurred with the PU valve near the null position.

The cutoff thrust and total impulse calculation method has been considerably modified since the S-IVB-001 acceptance firing. Therefore, comparisons with the acceptance firing thrust and impulse are not meaningful. However, a comparison of acceptance and flight chamber pressures during cutoff shows that during flight, the chamber pressure decayed slightly slower than during the acceptance test. This was probably due to a colder MOV and, hence, a longer closing time during flight. The flight total impulses can be compared to the log book value by adjusting the flight values to standard conditions (null PU valve position and 460 deg R MOV actuator temperature). The adjusted flight total impulses for first and second burn were in reasonably good agreement with the log book value and were in good agreement with each other.

The cutoff impulse to zero thrust from engine thrust data was 54,949 lbf/sec for first burn and 48,330 lbf/sec for second burn computed from engine thrust data. The first and second burn cutoff

Section 9
Engine System

impulse determined from inertial platform guidance acceleration data was 52,089 lbf/sec and 47,318 lbf/sec respectively (table 9-11) and is in good agreement with that determined from engine analysis.

Figures 9-45 and 9-46 present a comparison of predicted and actual impulse velocity histories based on engine and trajectory data. Data from both trajectory analysis and engine analysis indicate a higher-than-predicted cutoff impulse for both first and second burns, but deviations from predicted were within the expected three-sigma tolerance of $\pm 9,000$ lbf/sec. Figures 9-47 and 9-48 show the thrust chamber pressure, the thrust decrease, and total impulse during the cutoff transients. Figure 9-49 shows a composite of the axial thrust during first and second burn cutoffs.

9.5 Component Operation

9.5.1 Main LOX Valve

The main LOX valve opened and closed satisfactorily during both burns. The main LOX valve opening time data were as follows:

Item	Nominal	S-IVB-501 Acceptance Firing		S-IVB-501 Flight	
		1st Burn	2nd Burn	1st Burn	2nd Burn
First stage travel (ms)	50 ± 20	80	70	100*	242
First stage plateau (ms)	415 ± 99	560	570	420**	421
Second stage travel (ms)	1,600 ± 75	1,970	2,010	1,925	1,819
Total time (ms)	2,065 ± 190	2,610	2,650	2,445*	2,482

*Maximum possible value. Actual value may be slightly less.

**Minimum possible value. Actual value may be slightly greater.

These values were taken from 10 sample-per-sec data, which somewhat affected the accuracy of the reported times. However, with careful interpretation of the data, reasonably good accuracy was obtained. Retiming of the valve resulted in a shorter first stage plateau time during flight than during the acceptance test. The above table shows that the first stage plateau times were approximately 145 ms shorter during flight than during the acceptance test. Because of this change, along with the low EMR start, restart was successful (paragraph 9.4.3).

First and second stage travel times, as well as total times, were longer than the nominal values. All times were shorter during flight than during the acceptance test except for the first stage travel times. These longer than nominal first stage travel times had no detrimental effect on engine start. The total opening times during flight were approximately 165 ms less than during acceptance. Figure 9-50 compares MOV travel of S-IVB-501 flight during first burn with previous flights and the S-IVB-501 acceptance firing first burn. Figure 9-51 compares MOV travel of the S-IVB-501 flight second burn with the S-IVB-501 acceptance firing second burn and shows the effects of the retimed MOV.

The valve closing times were 319 and 261 ms for first and second burns, respectively. These long closing times were caused by the cold temperatures of the main LOX valve actuator which was 314.9 deg R and 299.3 deg R at first and second burn cutoff, respectively.

9.5.2 Pumps and Turbines

The LH2 pump performance was satisfactory during the start transients of both first and second engine start transient with no indication of stall (figure 9-52). The data indicate that the thrust chamber chill-down was adequate to prevent excessive fuel pump backpressure. Further information on the chilldown operation and GSE supply system is presented in section 5.

The performance of the LH2 and LOX pumps and turbines was satisfactory during both burns. The pump speeds and discharge pressures and temperatures responded to PU system cutback and perturbations and also to engine inlet conditions. The pressure and temperature increases

Section 9 Engine System

across the pumps were satisfactory. Temperatures and pressures for both turbines responded as expected to PU system cutback and perturbations.

The higher gas generator (GG) performance during second burn (paragraph 9.5.4) was reflected in the higher engine LOX flowrate. The increase in LOX flowrate was closely proportional to the increase in GG performance. However, the engine LH2 flowrate decreased slightly from first to second burn instead of showing the expected increase due to increased GG performance. This, along with the increased LOX flowrate, resulted in the higher engine mixture ratio observed during second burn high EMR operation. The decrease in LH2 flowrate was probably due to an observed small decrease in LH2 turbine efficiency from first to second burn. LOX pump efficiency was essentially the same during both burns. Apparently the increased energy available to the LH2 turbine due to higher GG performance during second burn was more than offset by the decrease in fuel turbine efficiency. LH2 and LOX pump and turbine data are shown in figures 9-28, 9-30, 9-34 and 9-36.

9.5.3 PU Valve

The PU valve performance was as expected during both burns with the exception of the flow resistance shift observed just prior to ECC2. The resistance shift resulted in a thrust performance shift which exceeded CEI specification limits. This type of shift, however, is specifically excluded from the specification limits. The performance shift did not adversely effect mission accomplishment. Valve performance data is shown in figures 9-26 and 9-32. The analysis of PU valve performance is provided in section 15.

9.5.4 Gas Generator

The gas generator (GG) performance was adequate during both burns, but shifted from first to second burn high EMR operation. During second burn the GG LOX flowrate was higher than during first burn due to a resistance decrease in the LOX GG supply line. This resulted in a higher GG mixture ratio and GG total flowrate during second burn which resulted in higher engine performance during second burn. The higher GG performance caused higher GG chamber pressure and higher fuel turbine inlet temperature during second burn high EMR operation. The small oscillations in GG chamber pressure and fuel turbine inlet temperature

after EMR cutback were the result of the changes in LH2 and LOX discharge pressures and flowrates due to changing engine performance. Plots of GG performance are shown in figures 9-53 and 9-54.

9.5.5 Engine Drive Hydraulic Pump

The engine-driven hydraulic pump performed satisfactorily during both burns. The average power required by the pump was 4.67 horsepower.

9.6 Engine Sequencing

The start and cutoff sequences were satisfactory in providing smooth transient operation. The exact times of certain of the events were difficult to pinpoint. The times at which closed dropout and open pickup occur for a valve may be determined either by the open and closed microswitches on the valve or by the position indicating potentiometer on the valve. It was decided to take the opening and closing times from the position potentiometer traces, as they depend less on microswitch adjustment, and are a more dependable indication of the actual operation of the valves. Because of these possible errors or differences in method of interpretation, there are some apparent inconsistencies in the sequence times.

An attempt was made to obtain accurate values for valve actuation times by choosing channels which give consistent opening and closing times. As in the acceptance tests, certain of the valve actuation times differ from the nominal bench valves because of the presence of liquids in the lines, temperature differences, etc. Figure 9-14 and 9-15 show the significant time events during the start transient. Tables 9-12 and 9-13 list all available J-2 engine events during the first and second burn.

9.7 Flight Simulation Analysis

A five-deg-of-freedom trajectory simulation analysis was conducted to adjust propulsion parameter histories so that an S-IVB trajectory could be generated to closely match the observed trajectory (appendix 5, Observed Trajectory). A detailed discussion of this analysis is presented in section 7.

Section 9
Engine System

Results of the flight simulation indicate compatibility between the shapes of the propulsion parameter histories as established by engine analysis and the observed trajectory. To match the observed trajectory, however, first burn thrust and weight flow were increased by 0.71 percent and 0.56 percent, respectively, over engine analysis values. For second burn, engine analysis values of thrust and weight flow were increased by 0.81 percent and 0.67 percent, respectively. The corresponding changes in specific impulse were an increase of 0.14 percent over the engine analysis value for first burn and an increase of 0.02 percent for second burn. Average values for these parameters are:

<u>First Burn</u>			
<u>Parameter</u>	<u>Predicted</u>	<u>Actual</u>	
Average Thrust (lbf)	225,343	223,852	
Average Weight Flow (lbm/sec)	532.33	528.68	
Average Specific Impulse (sec)	423.3	423.4	
<u>Second Burn</u>			
Total Average Thrust (lbf)	201,110	205,300	
Total Average Weight Flow (lbm/sec)	471.3	481.5	
Total Average Specific Impulse (sec)	426.7	426.0	
Average Thrust at High Mixture Ratio (lbf)	-	226,090	
Average Weight Flow at High Mixture Ratio (lbm/sec)	---	535.51	
Average Specific Impulse at High Mixture Ratio (sec)	-	422.20	
Average Thrust at Reference Mixture Ratio (lbf)	201,110	197,381	
Average Weight Flow at Reference Mixture Ratio (lbm/sec)	471.3	461.40	
Average Specific Impulse at Reference Mixture Ratio (sec)	426.7	427.79	

Figures 7-43 and 7-44 present flight simulated thrust and weight flow for first and second burns, respectively.

TABLE 9-1
CONTROL SPHERE

PARAMETER	TEMPERATURE (deg R)			PRESSURE (psia)			MASS (lbm)		
	501 FLIGHT	501 ACCEPTANCE FIRING	502 ACCEPTANCE FIRING	501 FLIGHT	501 ACCEPTANCE FIRING	502 ACCEPTANCE FIRING	501 FLIGHT	501 ACCEPTANCE FIRING	502 ACCEPTANCE FIRING
Required at liftoff	262 ±30*	271 ±30*	260 ±30*	2,800 to 3,200 psia			--	--	--
Actual at liftoff	271	287	281	3,010	3,095	3,260	2.01	1.96	2.07
Before first burn engine start	271	291	286	3,075	3,193	3,345	2.03	1.99	2.11
After first burn engine cutoff	216	249	246	1,989	2,348	2,450	1.56	1.75	1.79
Before second burn engine start	239	258	276	1,878	2,301	2,764	1.48	1.67	1.84
After second burn engine cutoff	172	221	236	735	1,680	1,925	0.80	1.41	1.52
Mass used - first burn	--	--	--	--	--	--	0.51	0.24	0.32
Mass used - second burn	--	--	--	--	--	--	0.68	0.26	0.32

*Actual requirement is start sphere temperature ±30 deg R.

TABLE 9-2
ENGINE CONTROL SPHERE TEMPERATURE DATA

TIME SLICE	MEASURED DATA (deg R)	ADIABATIC BLOWDOWN (deg R)	THEORETICAL @ M = 1.0 (deg R)	GAS TEMP USED FOR CALCULATIONS (deg R)	CONDITION
Liftoff	270	-	-	270	Steady-state
1st ESC	272	-	-	272	Steady-state
1st Burn Start (end of 3.8 sec blowdown)	252	248	204	250	Start bottle cooler, average of adiabatic and measured
1st ECC	215.2	-	-	226	Working back from leakage during coast
Start of coast (end of 1 sec blowdown)	204	215	170	224	From 1 sec blowdown usage
2nd ESC	240.3	-	-	240	Steady-state
2nd burn start (end of 8.6 sec blowdown)	190.6	185.5	180	188	Average of adiabatic and measured
2nd ECC	181.7	-	-	182	Control bottle and start bottle temperature steady out
End of 1 sec blowdown	172.1	173	137	181	From 1 sec blowdown usage

Section 9
Engine System

TABLE 9-3
ENGINE CONTROL SPHERE HELIUM MASS SUMMARY

TIME SLICE	He MASS (lbm)	Δ MASS (lbm)	$\pm \Delta \dot{W}$	PRESS (psia)	TEMP (deg R)
Liftoff	2.070			3,050	270
Engine Start Command	2.070			3,075	272
3.8 sec fuel lead		0.28	0.0736 lbm/sec		
First burn start (145 sec)	1.790			2,427	250
First burn usage		0.120			
First Engine Cutoff Command	1.670			1,991	226
1 sec blowdown		0.112			
Start of coast	1.558			1,840	224
Leakage (3 hrs)		0.078	(0.026 lb/hr)		
Second Engine Start Command	1.480			1,875	240.3
8.6 sec fuel lead		0.46	0.0535 lbm/sec		
Second burn start	1.020			976	188
Second burn usage (300 sec)		0.11			
Second Engine Cutoff Command	0.910			825	182
1 sec blowdown		0.11			
Mass remaining	0.800			735	181

TABLE 9-4
FUEL LEAD CONDITIONS

CONDITION	FIRST START	SECOND START
Estimated thrust chamber bulk temperature at fuel lead start (deg R)	242	443
Fuel lead duration (sec)	3	8
Fuel temperature at the injector at the end of fuel lead (deg R)	40	165
Fuel passing through MFV during fuel lead (lbm)	15	25
Fuel between injector and MFV at the end of fuel lead (lbm)	4	8
Fuel passing through injector during fuel lead (lbm)	11	17
Total effective impulse during fuel lead (lbf-sec)	1,400	3,200

Reference paragraph 9.4.1

TABLE 9-5
COMPARISON OF COMPUTER PROGRAM RESULTS

PROGRAM	INPUT	METHOD	FIRST BURN RESULTS AT ESC1 +60 sec	SECOND BURN RESULTS AT ESC2 +60 sec
AA89	LOX and LH2 pump inlet pressures and temperatures, PU valve position, and engine tag values	Influence equations relate nominal inlet conditions to nominal performance. Using actual inlet conditions, PU valve position and engine tag values, the actual performance is simulated	F (lbf) = 222,752.2 \dot{W}_T (lbfm/sec) = 527.69 Isp (sec) = 422.1 MR = 5.51	F (lbf) = 224,752.7 \dot{W}_T (lbfm/sec) = 533.5 Isp (sec) = 421.3 MR = 5.649
G105 Mode 3	LOX and LH2 flowmeters, pump discharge pressures and temperatures, chamber pressures, chamber thrust area	Flowrates are computed from flowmeter data and propellant densities. The C_f is determined from equation $C_f = f(P_c, MR)$ and thrust is calculated from equation $F = C_f A_c P_c$.	F (lbf) = 223,312.4 \dot{W}_T (lbfm/sec) = 527.57 Isp (sec) = 423.3 MR = 5.503	F (lbf) = 225,209.3 \dot{W}_T (lbfm/sec) = 533.1 Isp (sec) = 422.4 MR = 5.653
PA49	AA89 and G105 outputs	Average	F (lbf) = 223,022.3 \dot{W}_T (lbfm/sec) = 527.6 Isp (sec) = 422.7 MR = 5.506	F (lbf) = 224,981.0 \dot{W}_T (lbfm/sec) = 533.3 Isp (sec) = 421.9 MR = 5.65
PA53	Thrust chamber pressure, chamber throat area	The C_f is computed from equation $C_f = f(P_c)$ and thrust is computed from equation $F = C_f A_c P_c$. The impulse is determined from integrated thrust.	Refer to paragraphs 9.4.3 and 9.4.5	---
G307	Major engine data include thrust chamber pressure and LOX and LH2 flowmeter data	This program supplied by Rocketdyne through MSFC (form 641).	F (lbf) = 223,473 \dot{W}_T (lbfm/sec) = 529.36 Isp (sec) = 422.2 MR = 5.534	F (lbf) = 224,944 \dot{W}_T (lbfm/sec) = 534.21 Isp (sec) = 421.1 MR = 5.667

Section 9
Engine System

TABLE 9-6
DATA INPUTS TO COMPUTER PROGRAMS

PARAMETER	PROGRAM	SELECTION	BIAS	REASON
Chamber Pressure	G105-1	D0001 (TM/FM)	-15 psi	(Rocketdyne estimation of P _c purge effect)
	PA53	D0001 (TM/FM)	98.1 percent	Agree with -15 psi steady-state bias
LH2 Pump Disch Press	G105-1	D0008 (TM/PCM)	0	
LH2 Pump Disch Temp	G105-1	C0134 (TM/PCM)	0	
LOX Pump Disch Press	G105-1	D0009 (TM/PCM)	0	
LOX Pump Disch Temp	G105-1	C0133 (TM/PCM)	0	
LH2 Flowrate	G105-1	F0002 (TM/FM)	0	
LOX Flowrate	G105-1	F0001 (TM/FM)	0	
LH2 Pump Inlet Press	AA89	D0002 (TM/PCM)	+1.38 1st burn 1.23 2nd burn	Dynamic head adjustment
LH2 Pump Inlet Temp	AA89	C0003 (TM/PCM)		
LOX Pump Inlet Press	AA89	D0003 (TM/PCM)		
LOX Pump Inlet Temp	AA89	C0004 (TM/PCM)	+2.6 1st burn 2.1 2nd burn	Dynamic heat adjustment
PU Valve Pos	AA89	G0010 (TM/PCM)	0	

TM = Telemetry, FM = Frequency Modulated, PCM = Pulse Code Modulated

TABLE 9-7
J-2 ENGINE START TRANSIENTS

PARAMETER	J-2 ENGINE LOG BOOK		S-IVB-501 FLIGHT		S-IVB-501 ACCEPT	
	FIRST	SECOND	FIRST	SECOND	FIRST	SECOND
Time of STDV Command (sec from ESC)	1.0	1.0	3.008	7.998	0.645	0.645
Thrust at 90 percent performance level (lbf)	185,599*	185,599*	183,125	166,364	148,000	155,500
Total impulse from Engine Start Command to 90 percent performance level** (lbf-sec)	—	—	186,864	192,634	—	—
Total impulse from STDV Command to 90 percent performance level** (lbf-sec)	183,576*	183,576*	187,464	189,444	123,004	151,004

*Based on stabilized thrust at null P_c and standard altitude conditions

**Defined as STDV Command +2.5 sec

TABLE 9-8
J-2 ENGINE STEADY-STATE PERFORMANCE

PARAMETER	UNITS	CLOSED PU VALVE OPERATION			REFERENCED MIXTURE RATIO OPERATION			OVERALL PERFORMANCE		
		PREDICTED	ACTUAL	PERCENT DEVIATION	PREDICTED	ACTUAL	PERCENT DEVIATION	PREDICTED	ACTUAL	PERCENT DEVIATION
Thrust	lbf	226,367	223,093	1.4	--	--	--	225,353	222,268	1.4
First Burn		--	224,366	--	201,103	195,810	2.6	200,577	203,653	1.3
Second Burn		535.29	528.26	1.3	--	--	--	532.42	525.75	1.3
Total Flowrate	lbm/sec	--	531.60	--	470.97	458.36	2.7	469.21	478.30	1.9
LOX Flowrate	lbm/sec	454.12	447.25	1.5	--	--	--	451.39	444.87	1.4
First Burn		--	451.50	--	392.17	381.53	2.7	390.77	400.55	2.3
Second Burn		81.17	81.02	0.2	--	--	--	81.04	80.88	0.2
LH2 Flowrate	lbm/sec	--	80.10	--	78.80	76.83	3.5	78.44	77.75	0.9
First Burn		5.59	5.52	1.3	--	--	--	5.57	5.50	1.3
Second Burn		--	5.64	--	4.98	4.97	0.2	4.98	5.15	3.3
Engine Mixture Ratio		422.9	422.3	0.1	--	--	--	423.3	422.8	0.1
First Burn		--	422.1	--	427.0	427.3	0.1	427.5	425.9	0.4
Second Burn										
		FIRST BURN			SECOND BURN			TOTAL		
Impulse (Mainstage)	lbf/sec	29.91 x 10 ⁶	30.99 x 10 ⁶	3.6	61.61 x 10 ⁶	58.90 x 10 ⁶	4.1	91.52 x 10 ⁶	89.89 x 10 ⁶	1.8
Impulse To Depletion	lbf/sec	--	--	--	67.75 x 10 ⁶	65.96 x 10 ⁶	2.6	97.91 x 10 ⁶	97.63 x 10 ⁶	0.34
Burntime (Mainstage)	sec	132,761	139,424	5.01	306,493	289,198	5.55	458,957	428,622	7.35
Burntime To Depletion	sec	--	--	--	336,157	326,798	2.76	484,918	482,702	0.56

Section 9
Engine System

TABLE 9-9
ENGINE PERFORMANCE PREDICTION

PREDICTION	PARAMETER	FIRST BURN		SECOND BURN	
		ESC1 +60 sec		ESC2 +60 sec	
Original flight prediction (Revision 2)*	Thrust	226,455 lbf	200,470 lbf		
	LOX Flowrate	454.4 lbm/sec	390.3 lbm/sec		
	Fuel Flowrate	81.1 lbm/sec	78.0 lbm/sec		
	Engine Mixture Ratio	5.604	5.002		
	Gas Generator Mixture Ratio	0.974	0.895		
Original flight prediction with new gain table	Thrust	226,956 lbf	204,664 lbf		
	LOX Flowrate	454.3 lbm/sec	400.3 lbm/sec		
	Fuel Flowrate	81.2 lbm/sec	78.8 lbm/sec		
	Engine Mixture Ratio	5.595	5.080		
	Gas Generator Mixture Ratio	0.979	0.915		
Original flight prediction with new gain table and revised log book PU characteristics	Thrust	226,956 lbf	204,675 lbf		
	LOX Flowrate	454.3 lbm/sec	400.7 lbm/sec		
	Fuel Flowrate	81.2 lbm/sec	78.9 lbm/sec		
	Engine Mixture Ratio	5.592	5.077		
	Gas Generator Mixture Ratio	0.979	0.914		

*Reference Douglas letter A3-860-KCBA-4.23.9-L-1931, dated 20 June 1967.

TABLE 9-10
THRUST OSCILLATION SUMMARY

PARAMETER	CEI SPEC LIMIT	THRUST VARIATIONS	
		FIRST BURN	SECOND BURN
During PU valve hardover operation			
1. Variation in mean thrust level (lbf)	+5,000	-3,100	-3,000
2. Oscillations about mean thrust level (lbf)	+2,500	+1,000	+1,100, -500
3. Rate of change of thrust (lbf/sec)	+500	-185, +180	+850
4. Thrust acceleration (lbf/sec/sec)	+125	< +100	< +100

TABLE 9-11
J-2 ENGINE CUTOFF TRANSIENTS

PARAMETER	J-2 ENGINE LOG BOOK	ENGINE PERFORM CALC		OBSERVED TRAJECTORY	
		FIRST BURN	SECOND BURN	FIRST BURN	SECOND BURN
Time for thrust decrease to 11,250 lbf (ms)	355	444	441	--	--
Thrust at Engine Cutoff Command (lbf)	197,656	223,122	196,168	--	--
Measured total impulse					
To 5 percent thrust (lbf-sec)	--	48,101	42,115	--	--
To zero thrust (lbf-sec)	--	54,949	48,330	52,389	47,318
Main oxidizer valve actuator temperature (deg R)	460	304.9	299.3	--	--
PU valve position at Engine Cutoff Command (deg)	0	33.3	-2.7	--	--
Total impulse to 5 percent thrust adjusted to null PU and 460 deg R main oxidizer valve actuator temperature (lbf-sec)	37,780	35,211	34,634	--	--

Section 9
Engine System

TABLE 9-12 (Sheet 1 of 2)
501 FLIGHT ENGINE SEQUENCE - FIRST BURN

CONTRO' EVENTS		CONTINGENT EVENTS		NOMINAL TIME FROM SPECIFIED REFERENCE	ACTUAL TIME (ms)	
MEAS NO.	EVENT AND COMMENT	MEAS NO.	EVENT AND COMMENT		FROM ESC	FROM SPECIFIED REFERENCE
K0021 (K0021)	*Engine Start Command P/U			0	0	
		K0007	Helium Control Solenoid Eng P/U	Within 10 ms of K0021	0	0
		K0010	Thrust Chamber Spark on P/U	Within 10 ms of K0021	2	2
		K0011	Gas Generator Spark on P/U	Within 10 ms of K0021	2	2
		K0006	Ignition Phase Control Solenoid Eng P/U	Within 20 ms of K0021	2	2
		K0126	LOX Bleed Valve Closed P/U	Within 130 ms of K0007	152	152
		K0127	LH2 Bleed Valve Closed P/U	Within 130 ms of K0007	68	68
		K0020	ASI LOX Valve Open P/U	Within 20 ms of K0006	103	101
		K0119	Main Fuel Valve Closed D/O	60 \pm 30 ms from K0006	54	52
		K0148	Main Fuel Valve Open P/U	80 \pm 50 ms from K0119	182	128
K0021	**Engine Start D/O			Approx 200 ms from K0021 P/U	3,198	3,198
K0096	***Start Tank Disc Control Solenoid Eng			3,000 \pm 40 ms from K0021 P/U	3,008	3,008
		K0123 (G0009)	Start Tank Disc Valve Closed D/O	100 \pm 20 ms from K0096	3,136	128
		K0122 (G0009)	Start Tank Disc Valve Open P/U	105 \pm 20 ms from K0123	3,310	174
K0005	Mainstage Control Solenoid Eng			450 \pm 30 ms from K0096	3,452	444
		K0096	Start Tank Disc Control Solenoid Eng D/O	450 \pm 30 ms from K0096 P/U	3,452	444
		K0121	Main LOX Valve Closed D/O	50 \pm 20 ms from K0005	3,480	28
		K0116 (G0005)	Gas Generator Valve Closed D/O	140 \pm 10 ms from K0005	3,280	-117
		K0122 (G0009)	Start Tank Disc Valve Open D/O	95 \pm 20 ms from K0096 D/O	3,561	109
		K0117 (G0005)	Gas Generator Valve Open P/U	50 \pm 30 ms from K0116	4,010	730
		K0124 (G0008)	LOX Turbine Bypass Valve Open D/O		3,658	
			LOX Turbine Bypass Valve 80% Closed	400 \pm 150 \pm 50 ms from K0122	3,946	385

(K0XXX) Actual number from acceptance firing event recorder.

*Engine ready and stage separation signals (or simulation) are required before this command will be executed. This command also actuates a 640 \pm 30 ms timer which controls energizing of the start tank discharge solenoid valve (K0096).

**This signal drops out after a time sufficient to lock in the engine electrical.

***An indication of fuel injection temperature of 310 \pm 40 deg R (or simulation) is required before this command will be executed. This command also actuates a 450 \pm 30 ms timer which controls the start of mainstage.

P/U = Pickup

D/O = Dropout

TABLE 9-12 (Sheet 2 of 2)
501 FLIGHT ENGINE SEQUENCE - FIRST BURN

CONTROL EVENTS		CONTINGENT EVENTS		NOMINAL TIME FROM SPECIFIED REFERENCE	ACTUAL TIME (ms)	
MEAS NO.	EVENT AND COMMENT	MEAS NO.	EVENT AND COMMENT		FROM ESC	FROM SPECIFIED REFERENCE
		K0123 (G0009)	Start Tank Disc Valve Closed P/U	250 \pm 40 ms from K0122	3,891	330
		K0125	*LOX Turbine Bypass Valve Closed P/U		4,020	
K0158	Mainstage Press Switch #1 Depress D/O				4,763	
K0159	Mainstage Press Switch #2 Depress D/O				4,823	
		K0120 (G0003)	Main LOX Valve Open P/U	2,605 \pm 150 ms from K0005	5,920	2,468
		K0010	Thrust Chamber Spark On D/O	3,300 \pm 200 ms from K0005 P/U	6,685	3,233
		K0011	Gas Generator Spark On D/O	3,300 \pm 200 ms from K0005 P/U	6,685	3,233
K0507	PU Activate Switch P/U					
K0013 (K0522)	Engine Cutoff P/U (New time reference)			0	0	0
		K0005	Mainstage Control Solenoid Enrg D/O	Within 10 ms of K0013	4	4
		K0006	Ignition Phase Control Solenoid Enrg D/O	Within 10 ms of K0013	2	2
		K0020	ASI LOX Valve Open D/O		95	
		K0120 (G0003)	Main Oxidizer Valve Open D/O	50 \pm 15 ms from K0005	33	29
		K0117	Gas Generator Valve Open D/O	75 \pm 25 \pm 35 ms from K0006	86	84
		K0118 (G0004)	Main Fuel Valve Open D/O	90 \pm 25 ms from K0006	32	30
		K0121 (G0003)	Main Oxidizer Valve Closed P/U	120 \pm 15 ms from K0120	348	315
		K0116 (G0005)	Gas Generator Valve Closed P/U	500 ms from K0006	430	428
		K0119 (G0004)	Main Fuel Valve Closed P/U	225 \pm 25 ms from K0118	451	419
K0158	**Mainstage Press Switch A Depress P/U				211	
K0159	Mainstage Press Switch B Depress P/U				211	
K0007	Helium Control Solenoid Enrg D/O			1,000 \pm 110 ms from K0013	975	975
		K0125 (G0008)	Oxidizer Turbine Bypass Valve Closed D/O		222	
		K0124 (G0008)	Oxidizer Turbine Bypass Valve Open P/U	10,000 ms from K0005	875	871
K0126	LOX Bleed Valve Closed D/O			30,000 ms from K0005	2,468	2,464
K0127	LH2 Bleed Valve Closed D/O			30,000 ms from K0005	4,217	4,213

(K0XXX) Actual number from acceptance firing event recorder.

*Within 5,000 ms of K0005 (Normally = 500 ms)

**Signal drops out when pressure reaches 425 \pm 25 psig.

P/U = Pickup

D/O = Dropout

Section 9
Engine System

TABLE 9-13 (Sheet 1 of 2)
AS-501 FLIGHT ENGINE SEQUENCE - SECOND BURN

CONTROL EVENTS		CONTINGENT EVENTS		NOMINAL TIME FROM SPECIFIED REFERENCE	ACTUAL TIME (ms)	
MEAS NO.	EVENT AND COMMENT	MEAS NO.	EVENT AND COMMENT		FROM ESC	FROM SPECIFIED REFERENCE
K0021	† Engine Start Command P/U			0	0	0
		K0007	Helium Control Solenoid Enrg P/U	Within 10 ms of K0021	0	0
		K0010	Thrust Chamber Spark On P/U	Within 10 ms of K0021	0	0
		K0011	Gas Generator Spark On P/U	Within 10 ms of K0021	0	0
		K0006	Ignition Phase Control Solenoid Enrg P/U	Within 20 ms of K0021	0	0
		K0126	LOX Bleed Valve Closed P/U	Within 130 ms of K0007	84	84
		K0127	LH2 Bleed Valve Closed P/U	Within 130 ms of K0007	84	84
		K0020	ASI LOX Valve Open P/U	Within 20 ms of K0006	39	39
		K0119	Main Fuel Valve Closed (G0004)	60 +30 ms from K0006	0	0
		K0118	Main Fuel Valve Open P/U (G0004)	80 +50 ms from K0119	182	182
K0021	*Engine Start D/O			Approx 200 ms from K0021 P/U	8,589	8,589
K0096	**Start Tank Disc Control Solenoid Enrg			8,000 +40 ms from K0021	8,014	14
		K0123 (G0009)	Start Tank Disc Valve Closed D/O	100 +20 ms from K0096	8,081	67
		K0122 (G0009)	Start Tank Disc Valve Open P/U	105 +20 ms from K0123	8,322	241
K0005	Mainstage Control Solenoid Enrg			450 +30 ms from K0096	8,458	444
		K0096	Start Tank Disc Control Solenoid Enrg D/O	450 +30 ms from K0096	8,458	444
		K0121	Main LOX Valve Closed D/O	50 +20 ms from K0005	8,375	-83
		K0116 (G0005)	Gas Generator Valve Closed D/O	140 +10 ms from K0005	8,350	-108
		.0122 (G0009)	Start Tank Disc Valve Open D/O	95 +20 ms from K0096	8,496	38
		K0117 (G0005)	Gas Generator Valve Open P/U	50 +30 ms from K0116	8,916	566
		K0124 (G0008)	LOX Turbine Bypass Valve Open D/O		8,953	
		(G0008)	LOX Turbine Bypass Valve 80% Closed	400 +150 -50 ms from K0122	8,884	388

† Engine ready and stage separation signals (or simulation) are required before this command will be executed. This command also actuates a 640 +30 ms timer which controls energizing of the start tank discharge solenoid valve (K0096).

*This signal drops out after a time sufficient to lock in the engine electrical.

**An indication of fuel injection temperature of 310 +40 deg R (or simulation) is required before this command will be executed. This command also actuates a 450 +30 ms timer which controls the start of mainstage.

P/U = Pickup D/O = Dropout

(K00XX) Actual number from acceptance firing event recorder.

TABLE 9-13 (Sheet 2 of 2)
AS-501 FLIGHT ENGINE SEQUENCE - SECOND BURN

CONTROL EVENTS		CONTINGENT EVENTS		NOMINAL TIME FROM SPECIFIED REFERENCE	ACTUAL TIME (ms)	
MEAS NO.	EVENT AND COMMENT	MEAS NO.	EVENT AND COMMENT		FROM EC	FROM SPECIFIED REFERENCE
K0158	Mainstage Press Switch #1 Depress D/O	K0123 (G0009)	Start Tank Disc Valve Closed P/U	250 \pm 40 ms from K0122	8,886	390
		K0125 (G0008)	*LOX Turbine Bypass Valve Closed P/U		9,008	
K0159	Mainstage Press Switch #2 Depress D/O				9,727	
					9,802	
K0013	Engine Cutoff P/U (New time reference)	K0120 (G0003)	Main LOX Valve Open P/U	2,605 \pm 145 ms from K0005	10,869	2,411
		K0010	Thrust Chamber Spark On D/O	3,300 \pm 200 ms from K0005 P/U	11,699	3,241
		K0011	Gas Generator Spark On D/O	3,300 \pm 200 ms from K0005 P/U	11,699	3,241
				0	0	0
		K0005	Mainstage Control Solenoid Enrg D/O	Within 10 ms of K0013	-20	-20
		K0006 (K0535)	Ignition Phase Control Solenoid Enrg D/O	Within 10 ms of K0013	-4	-4
		K0020 (K0622)	ASI LOX Valve Open D/O		73	
		K0120 (G0003)	Main Oxidizer Valve Open D/O	50 \pm 15 ms from K0005	3	23
		K0117 (G0005)	Gas Generator Valve Open D/O	75 \pm 25 ms from K0006	-88	-84
		K0118 (G0004)	Main Fuel Valve Open D/O	90 \pm 25 ms from K0006	7	11
K0007	Helium Control Solenoid Enrg D/O	K0121 (G0003)	Main Oxidizer Valve Closed P/U	120 \pm 15 ms from K0120 P/U	307	304
		K0116 (G0005)	Gas Generator Valve Closed P/U	500 ms from K0006	390	394
		K0119 (G0004)	Main Fuel Valve Closed P/U	225 \pm 25 ms from K0118	410	403
				1,000 \pm 110 ms from K0013	78	78
		K0125 (G0008)	Oxidizer Turbine Bypass Valve Closed D/O		179	
		K0124 (G0008)	Oxidizer Turbine Bypass Valve Open P/U	10,000 ms from K0005	716	736
K0126	LOX Bleed Valve Closed D/O			30,000 ms from K0005	2,764	2,784
K0127	LH2 Bleed Valve Closed D/O			30,000 ms from K0005	4,014	4,034

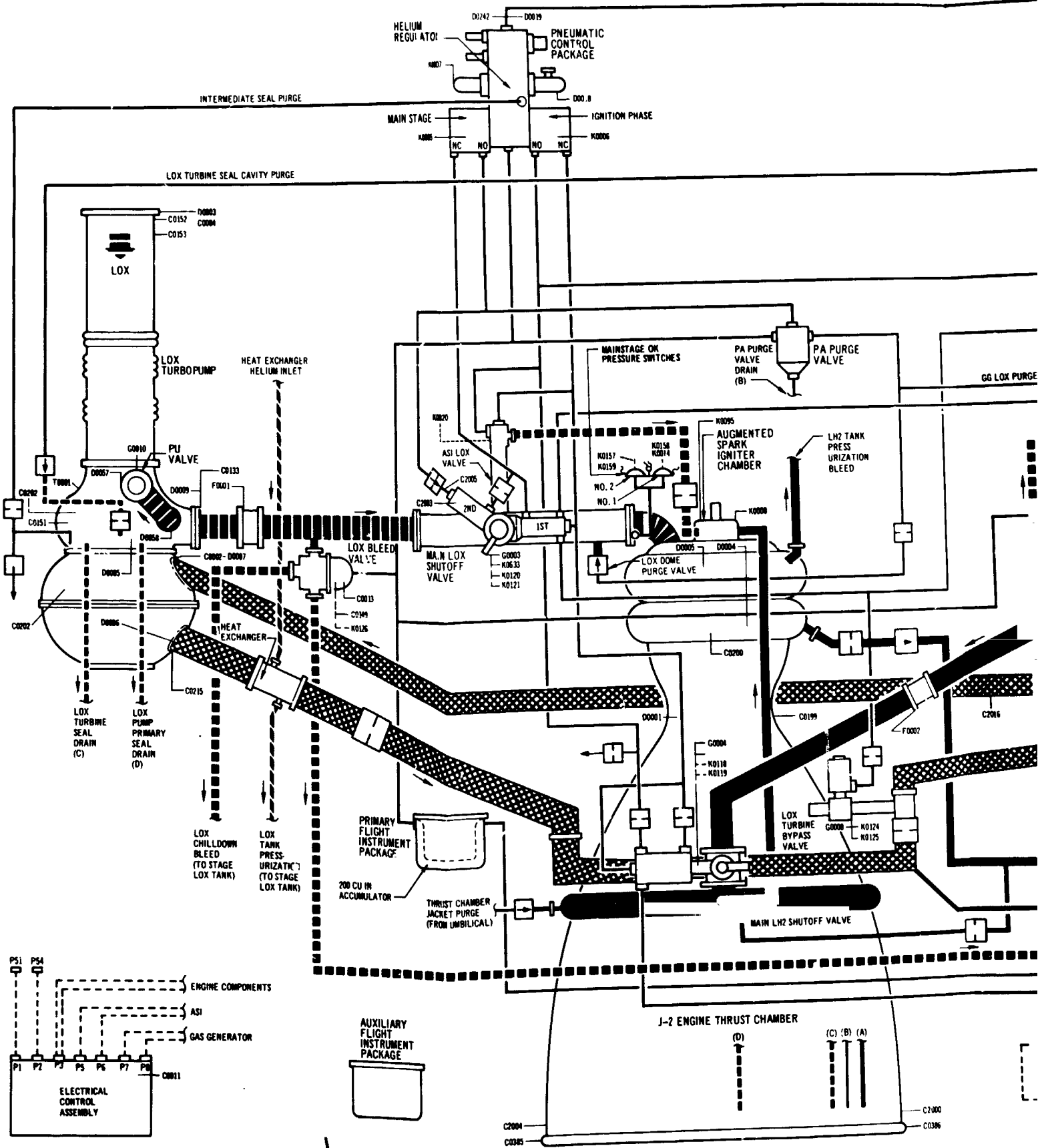
*Within 5,000 ms of K0005 (normally = 500 ms)

(K0XXX) Actual number from acceptance firing event recorder.

P/U = Pickup

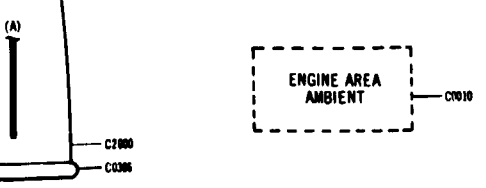
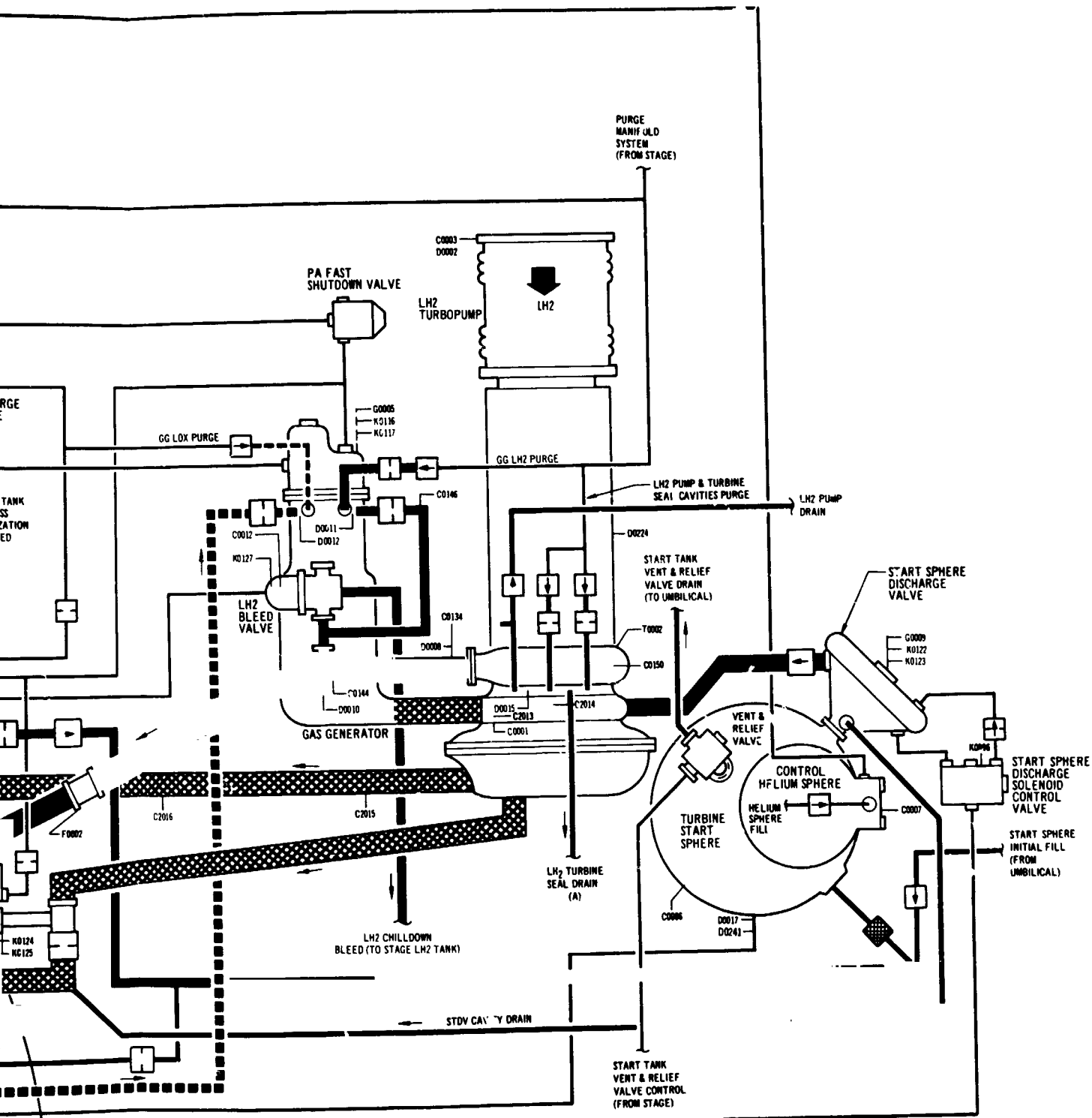
D/O = Dropout

Section 9
Engine System



FOLDOUT FRAME
FOLDOUT FRAME

Figure 9-1. J-2 Engine System



S-IVB STAGE - 501 ENGINE - J2/J31

NOTE:
SEE FIGURE 3-1 FOR
LEGEND

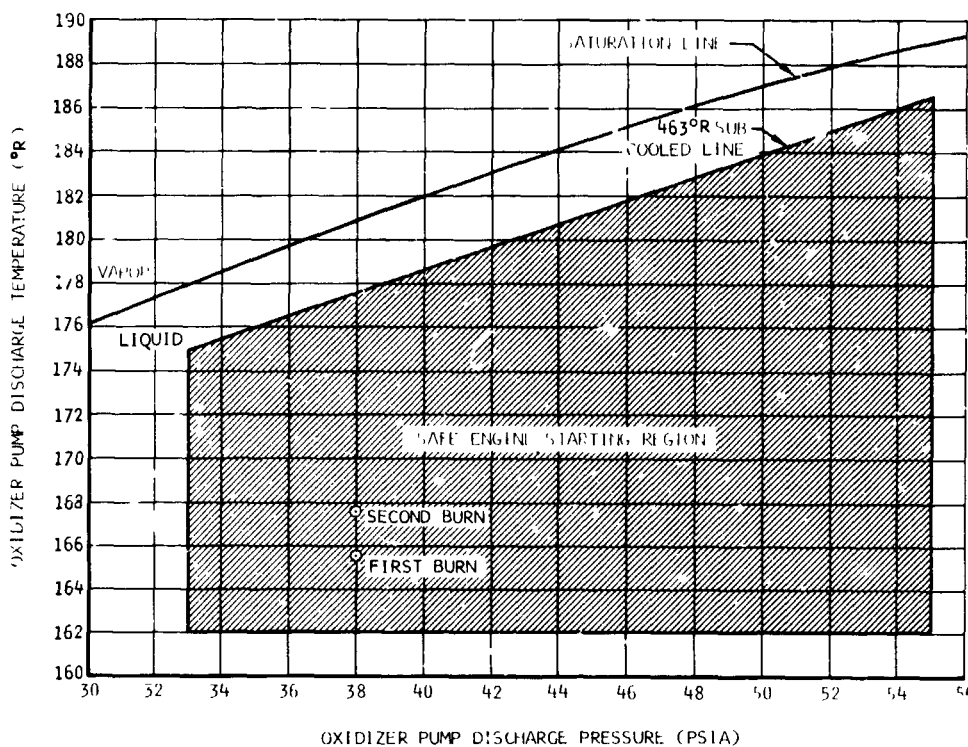


Figure 9-2. LOX Pump Discharge Pressure Versus Temperature

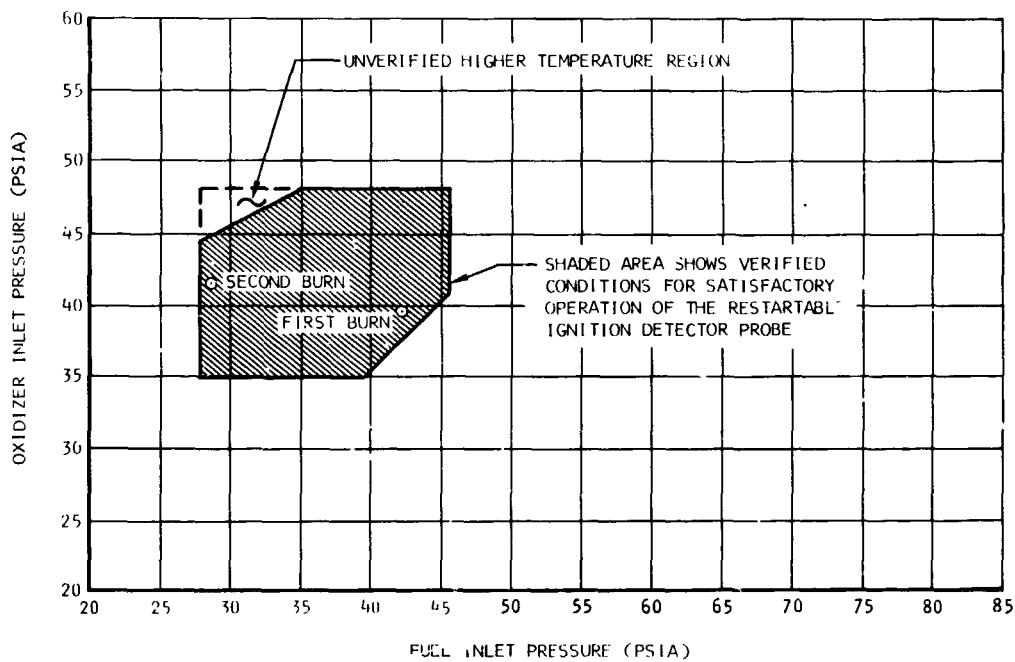


Figure 9-3. Propellant Inlet Operation Requirements for Engine Using Restartable Ignition Detector Probe

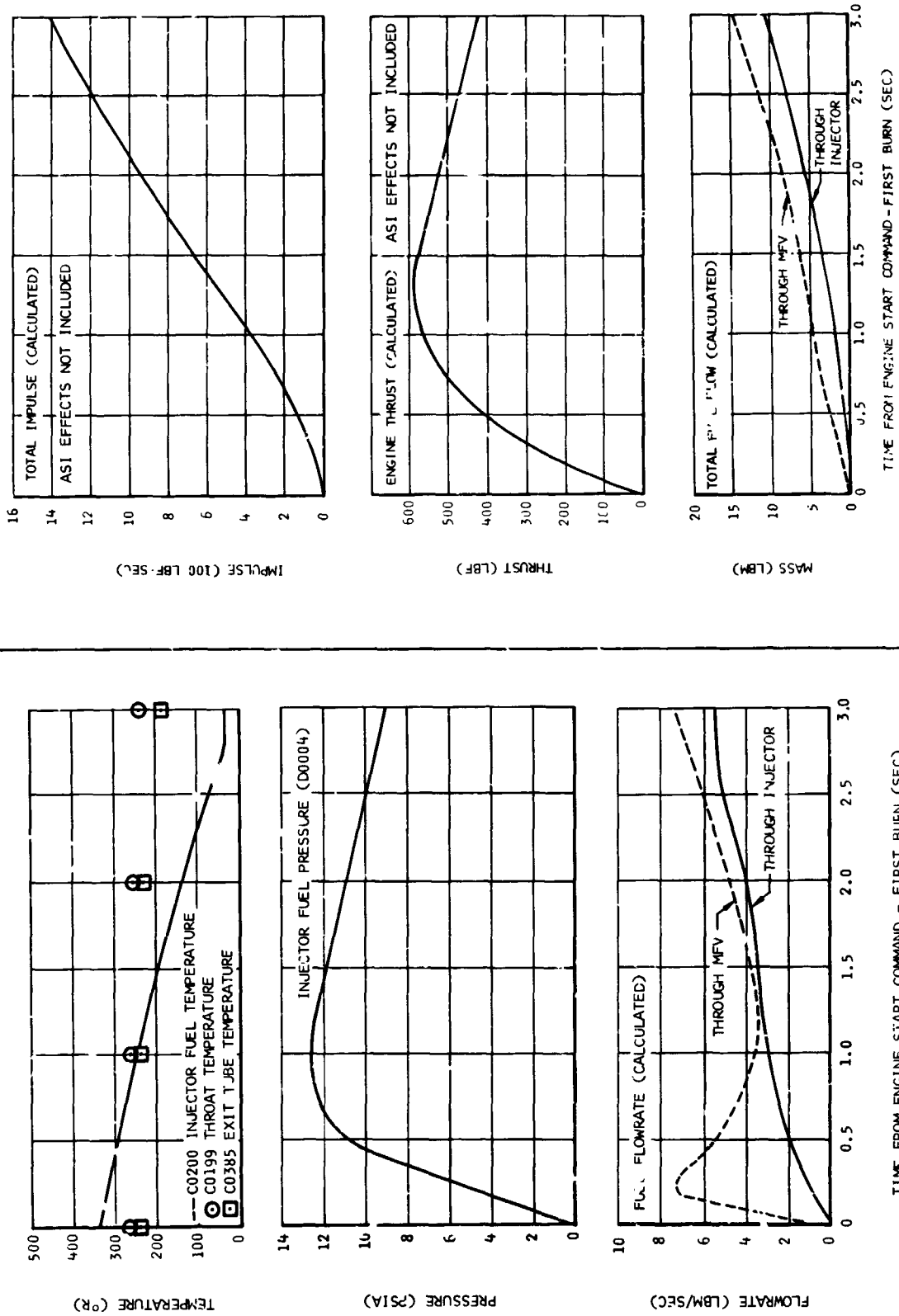


Figure 9-4. Fuel Lead - First Engine Start

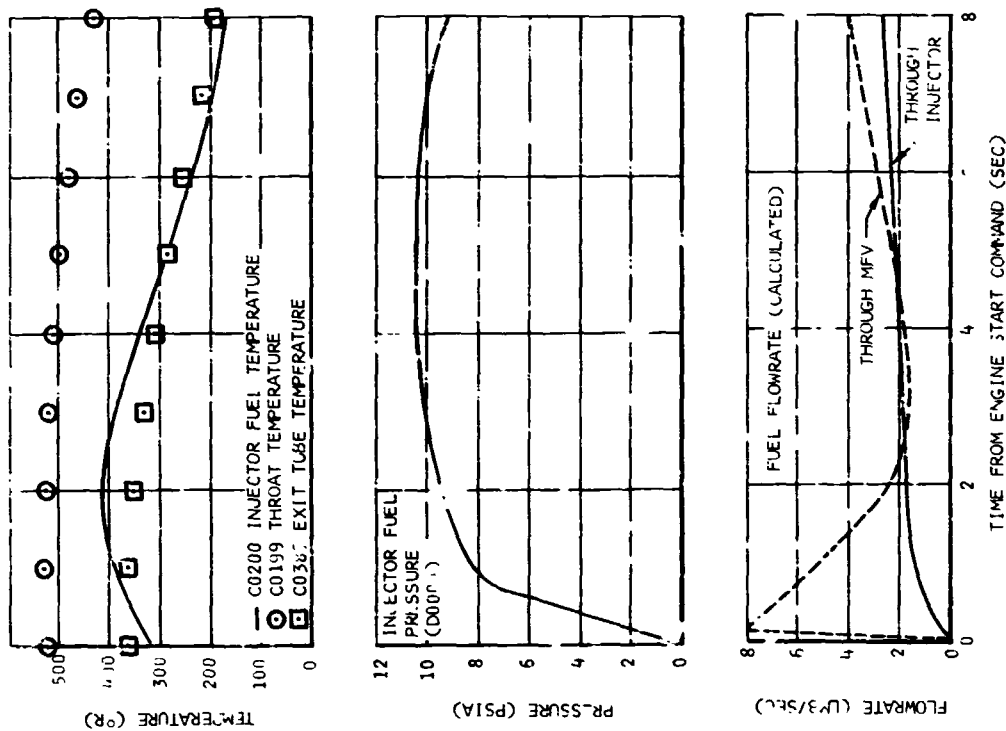
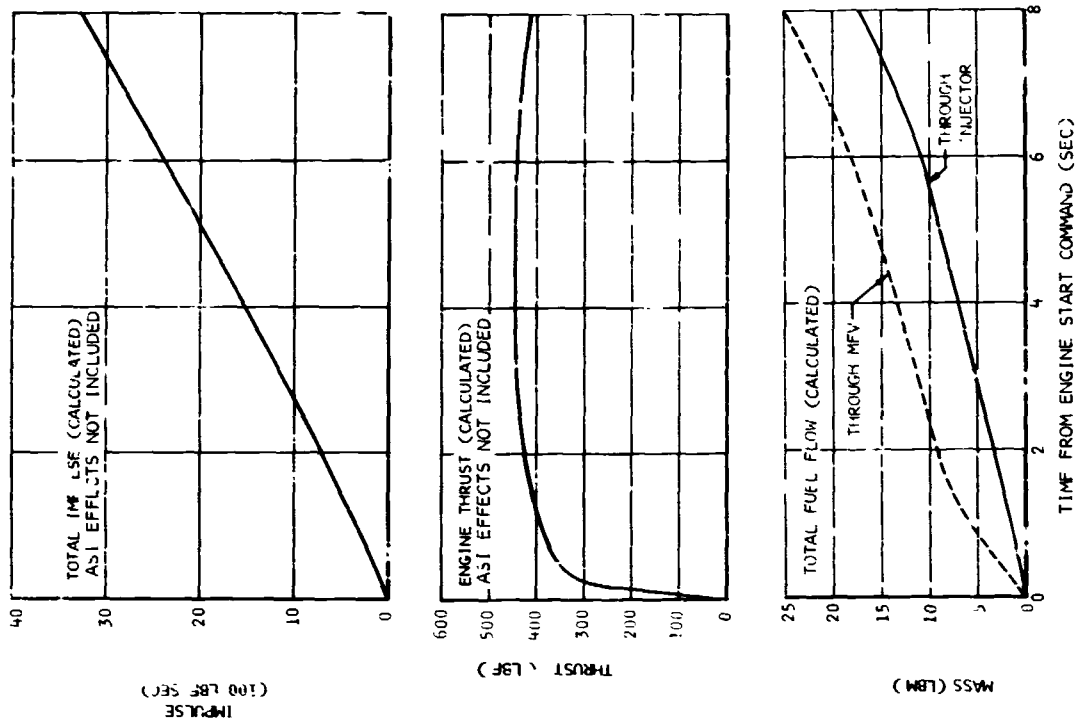


Figure 9-5. Fuel Lead - Second Engine Start

Section 9
Engine System

PARAMETER	TEMPERATURE (°R)			PRESSURE (PSIA)			MASS (LBM)		
	501 FLIGHT	501 ACCPT	502 ACCPT	501 FLIGHT	501 ACCPT	502 ACCPT	501 FLIGHT	501 ACCPT	502 ACCPT
LIFTOFF	262	271	260	1294	1245	1270	3.65	3.41	3.64
LIFTOFF REQUIREMENT	SEE LIFTOFF BOX			SEE LIFTOFF BOX			SEE LIFTOFF BOX		
FIRST ENGINE START COMMAND	266	285	272	1270	1275	1335	3.53	3.33	3.64
AFTER FIRST START SPHERE BLOWDOWN	171	196	180	100	135	150	0.49	0.57	0.66
FIRST ENGINE CUTOFF COMMAND	187	232	225	1166	1206	1255	4.74	3.89	4.18
TOTAL GH ₂ USAGE DURING FIRST START	—	—	—	—	—	—	3.04	2.76	2.98
SECOND ENGINE START COMMAND	246	248	263	1286	1294	1320	3.84	3.84	3.70
AFTER SECOND START SPHERE BLOWDOWN	170	170	178	140	200	165	0.68	0.95	0.73
SECOND ENGINE CUTOFF COMMAND	170	219	227	1185	1250	1286	5.37	4.26	4.21
TOTAL GH ₂ USAGE DURING SECOND START	—	—	—	—	—	—	3.16	2.89	2.97

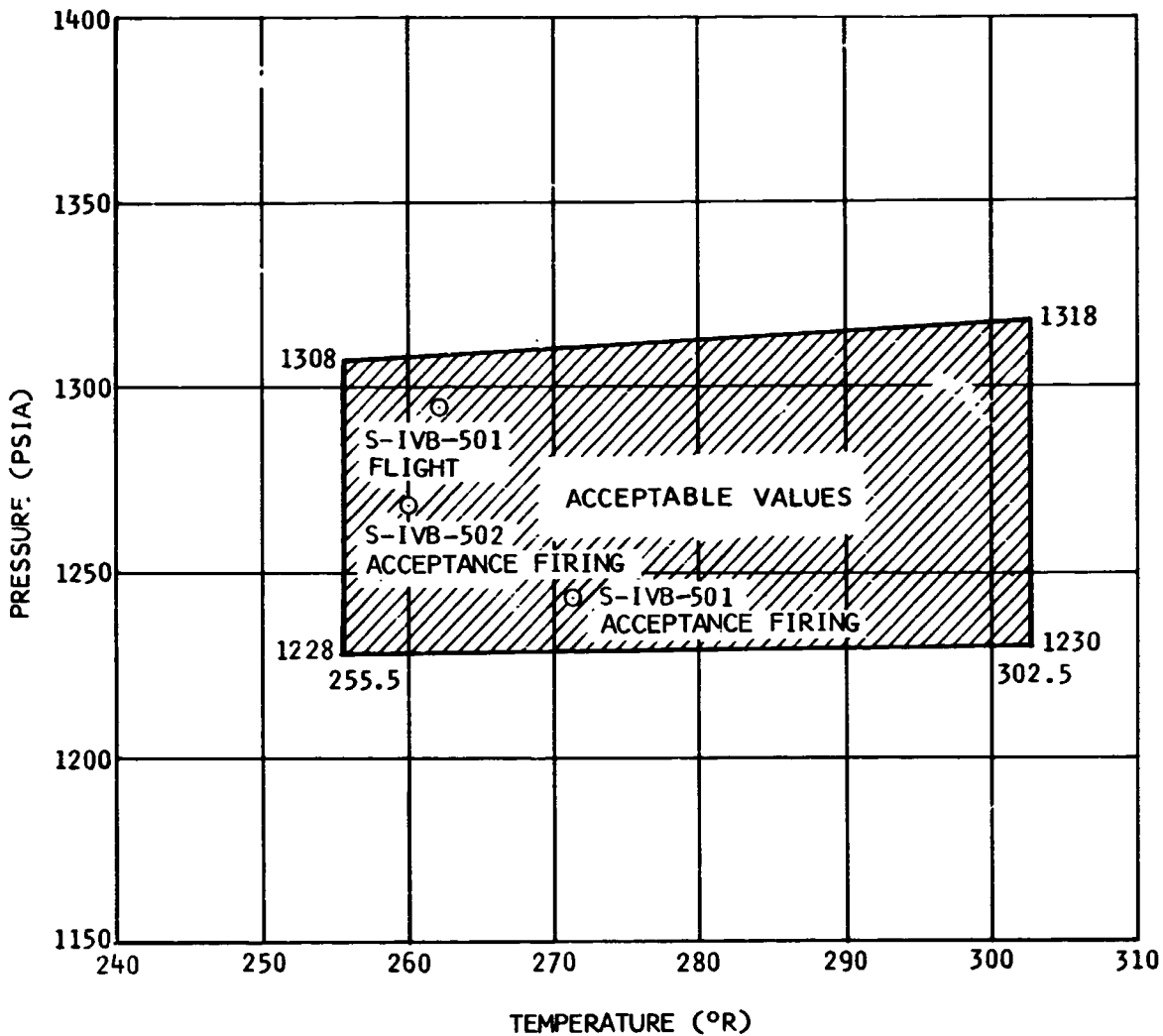


Figure 9-6. GH₂ Start Sphere Critical Limits at Liftoff

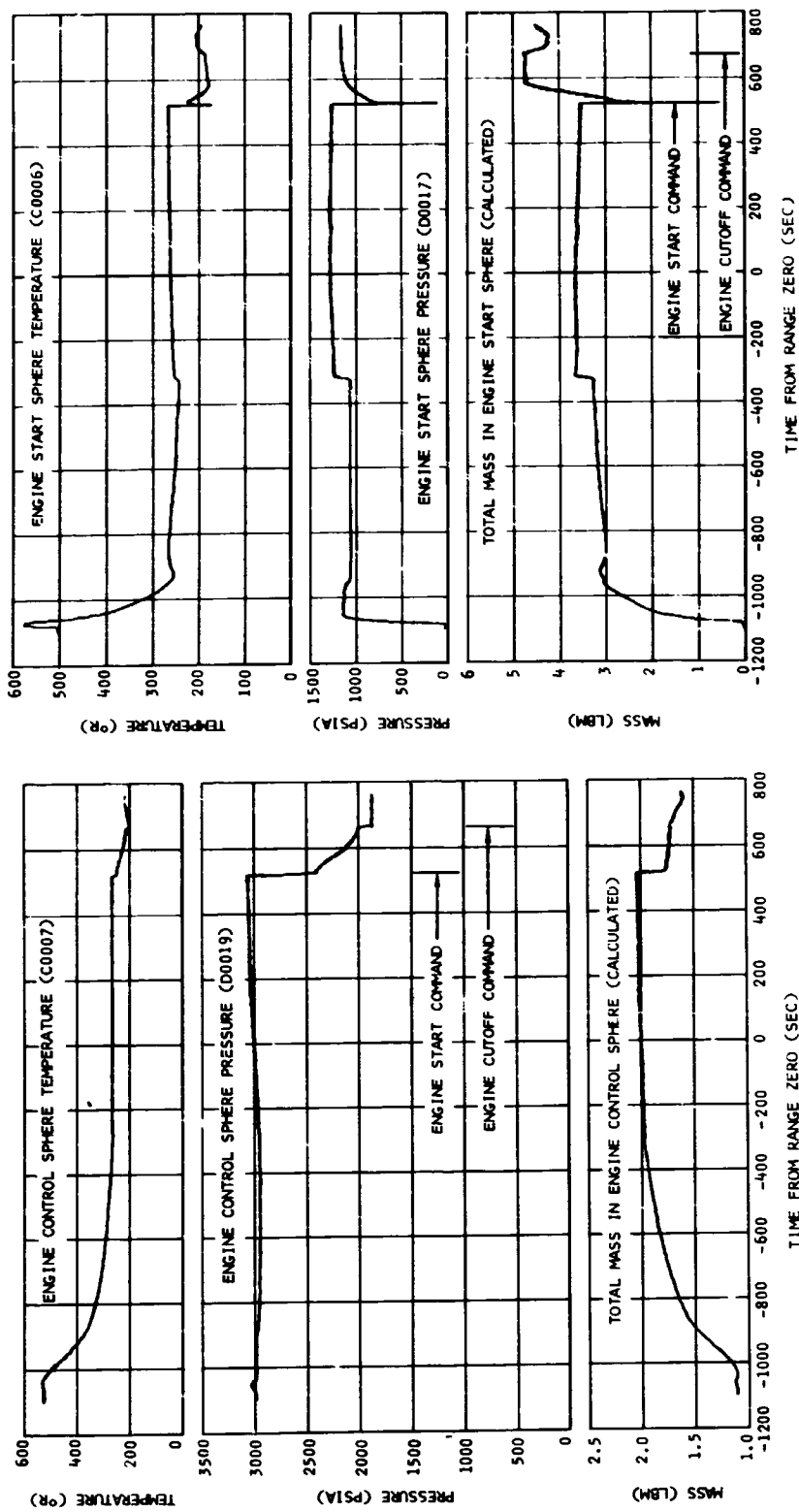


Figure 9-7. Engine Start and Control Sphere Performance - First Burn

Section 9
Engine System

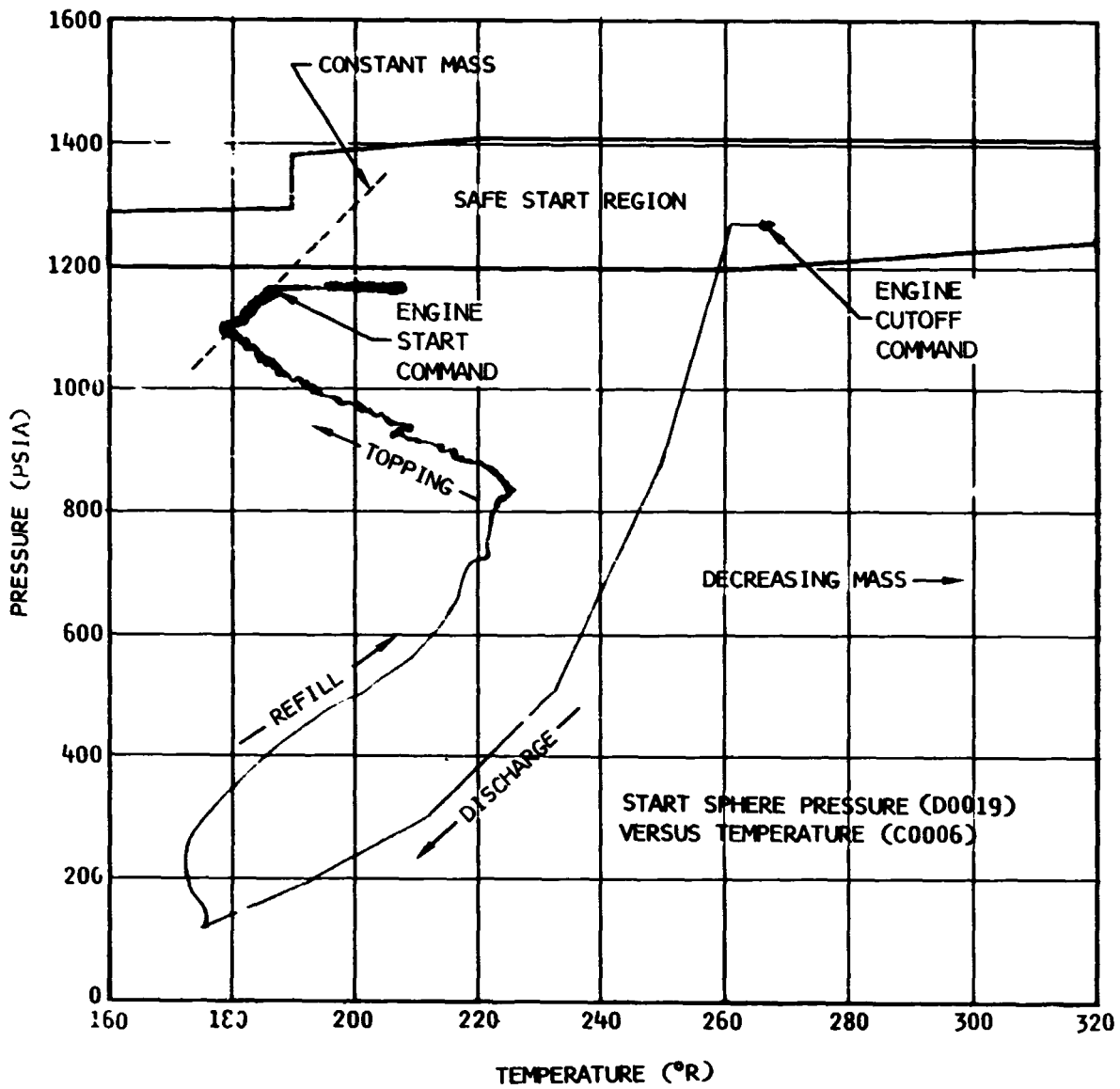


Figure 9-8. Start Sphere Refill Performance - First Burn

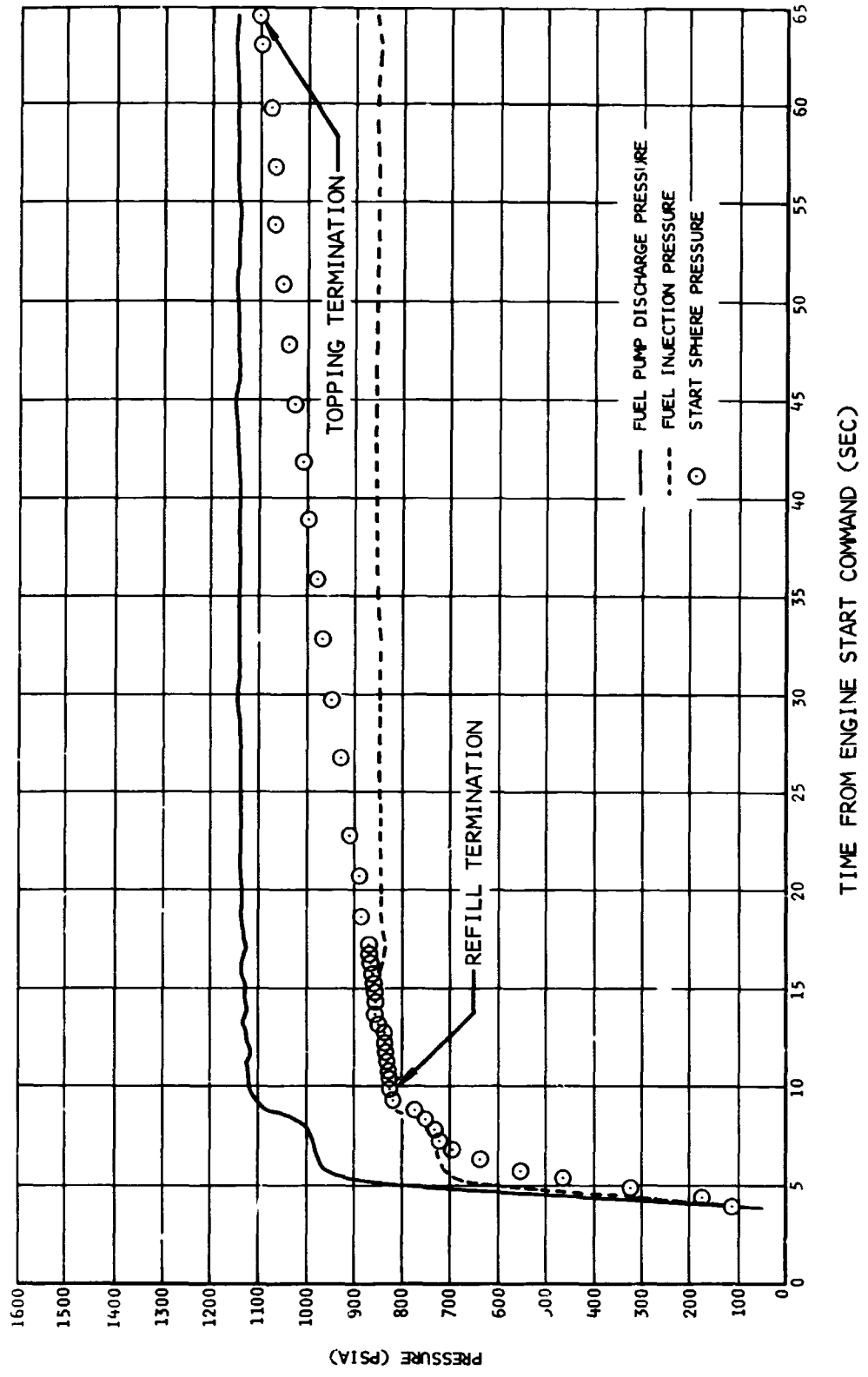
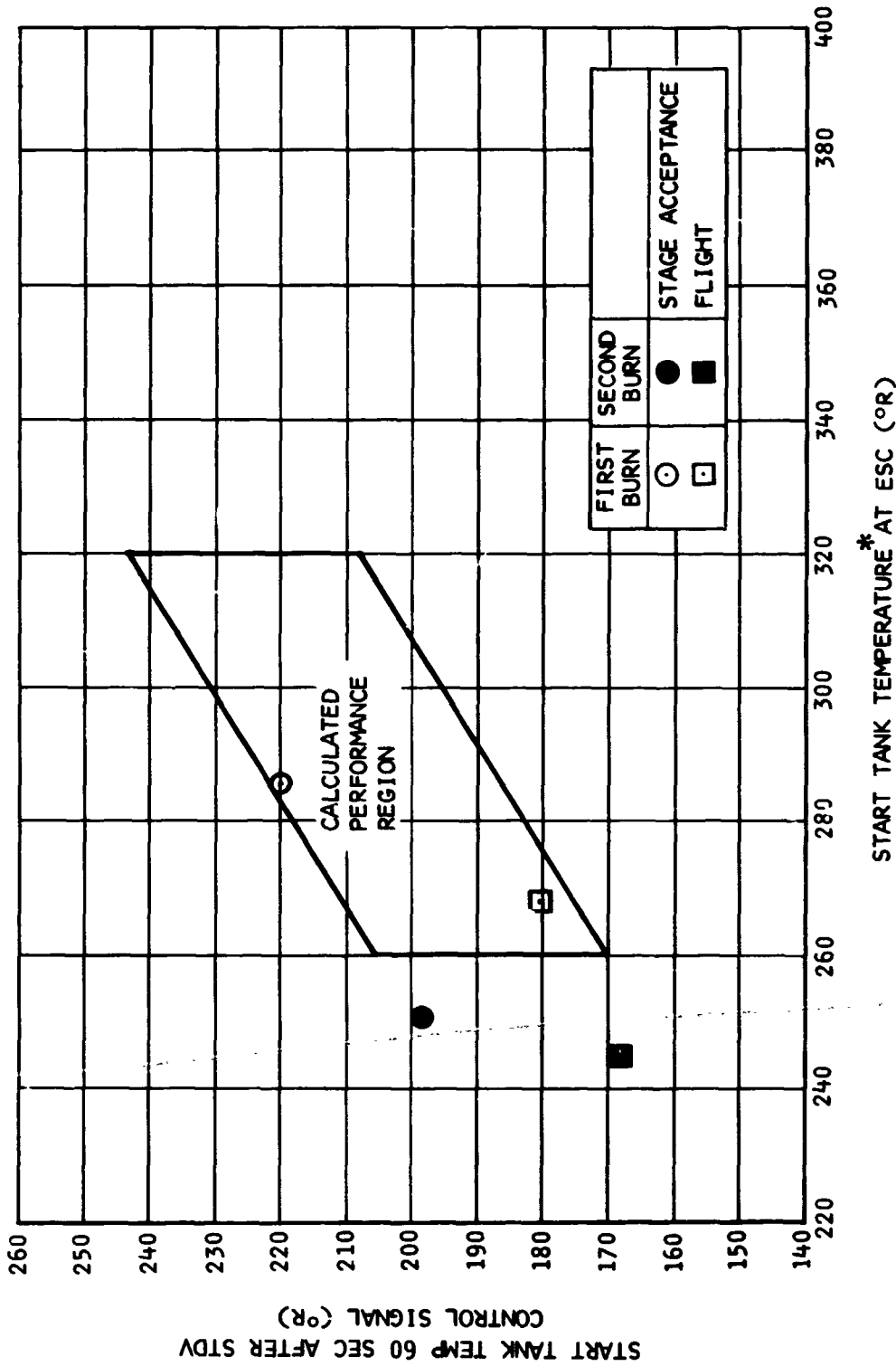


Figure 9-9. Start Sphere Refill - Second Burn

Section 9
Engine System



* DATA CORRECTED TO ZERO DIFFERENTIAL WITH RESPECT TO HELIUM TANK TEMPERATURE.
PU VALVE WAS CLOSED 5.0 SEC FROM STDV COMMAND.

Figure 9-10. Start Tank Recharge Capability

Section 9
Engine System

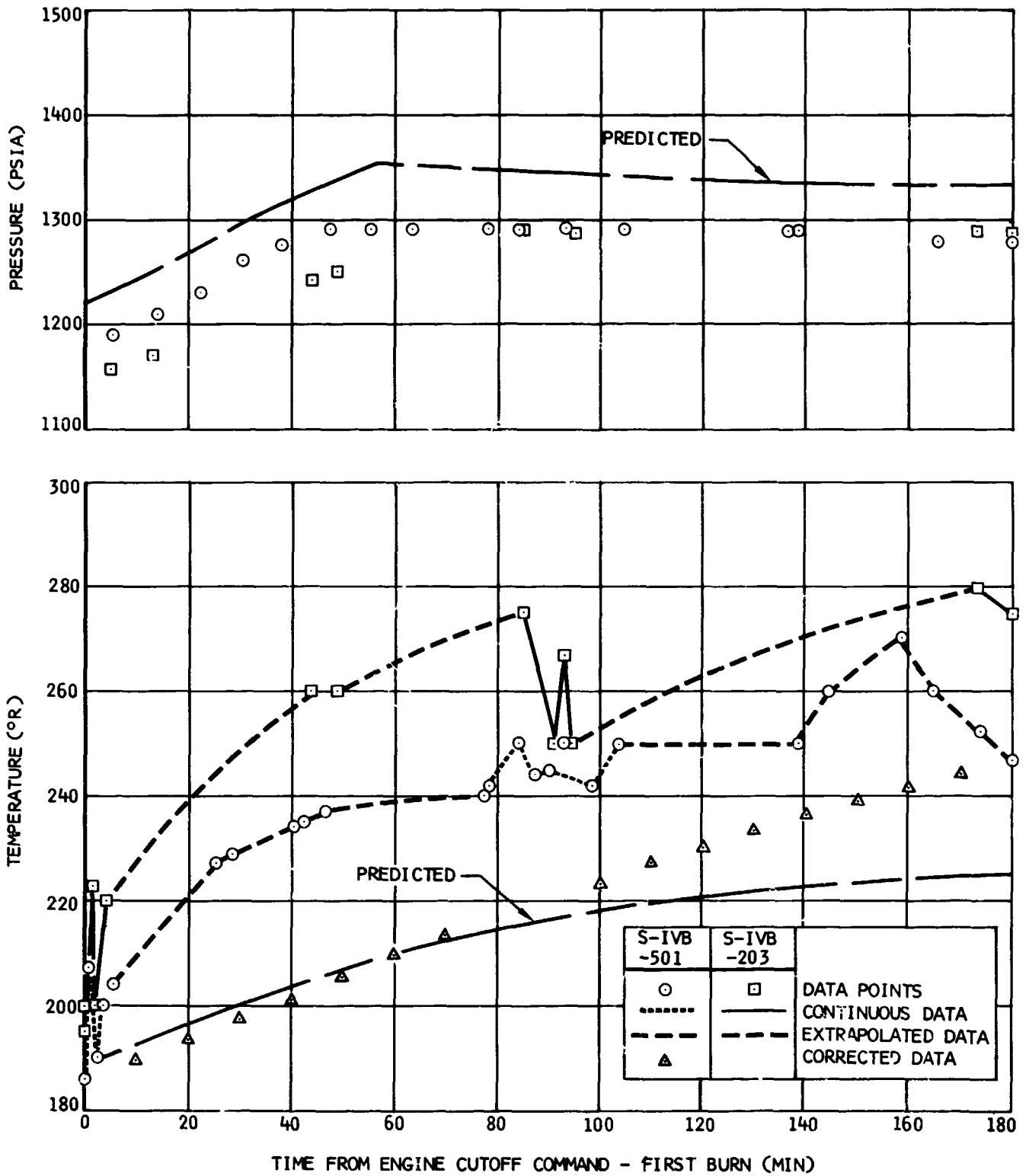


Figure 9-11. Start Sphere Orbital Conditions

Section 9
Engine System

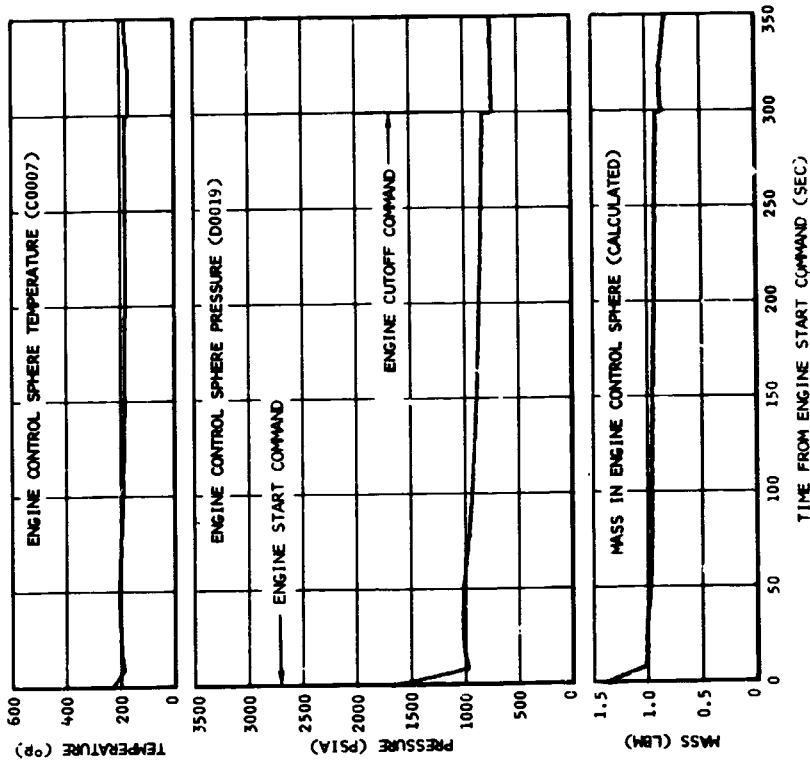
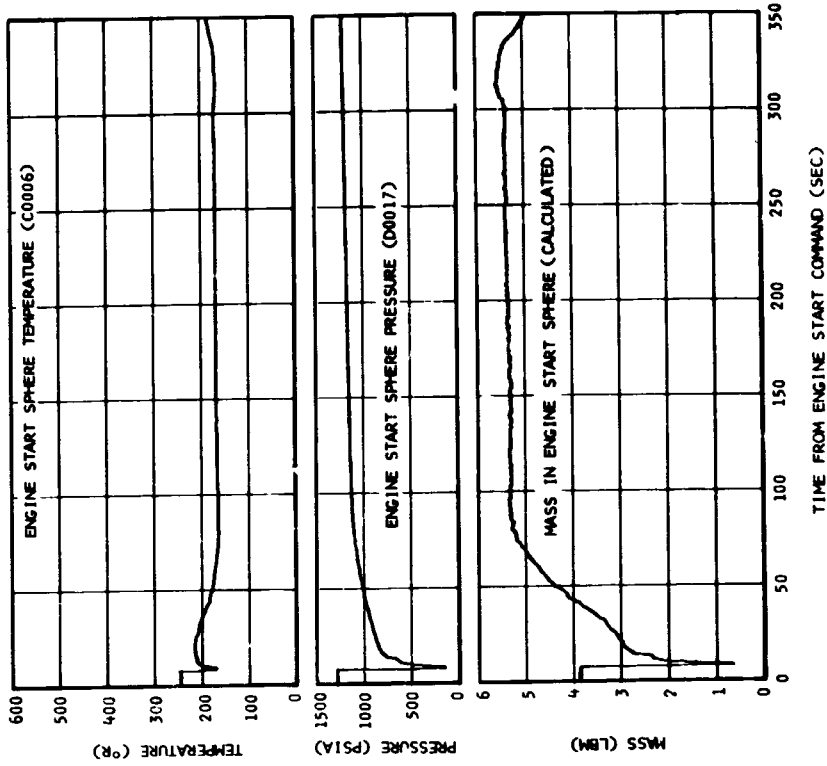


Figure 9-12. Engine Start and Control Sphere Performance During Second Burn

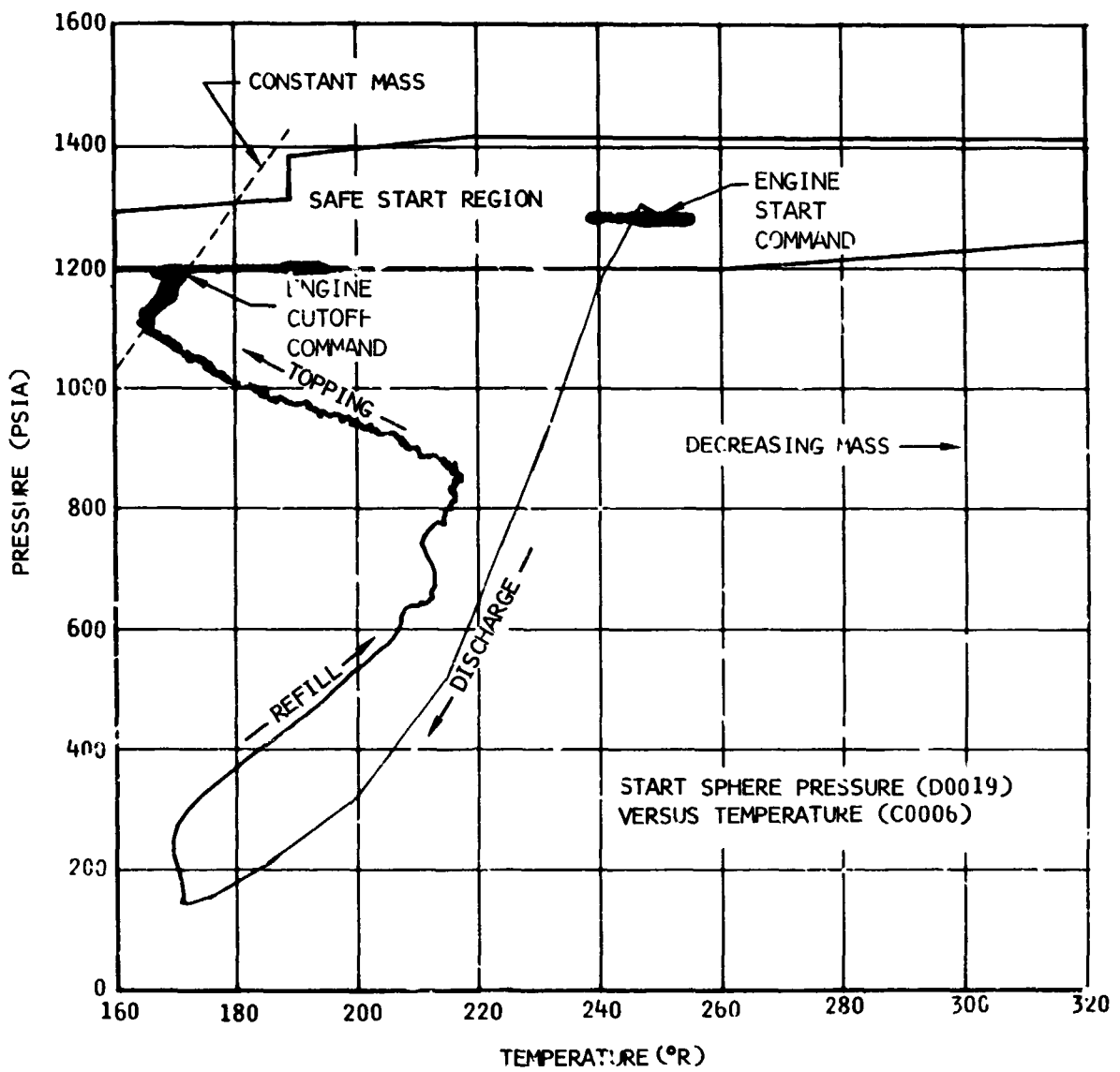


Figure 9-13. Start Sphere Refill Performance - Second Burn

Section 9
Engine System

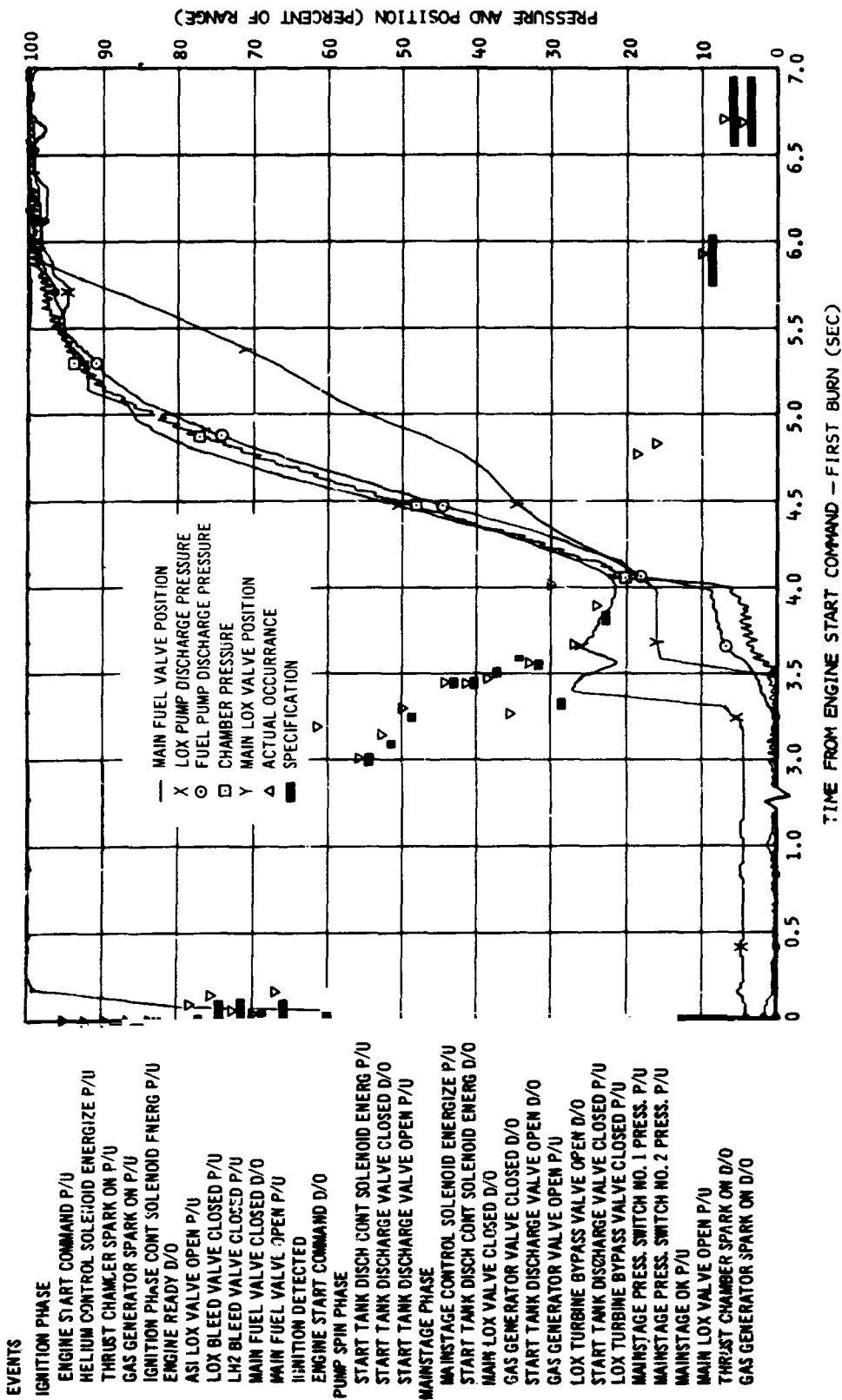


Figure 9-14. Engine Start Sequence - First Burn

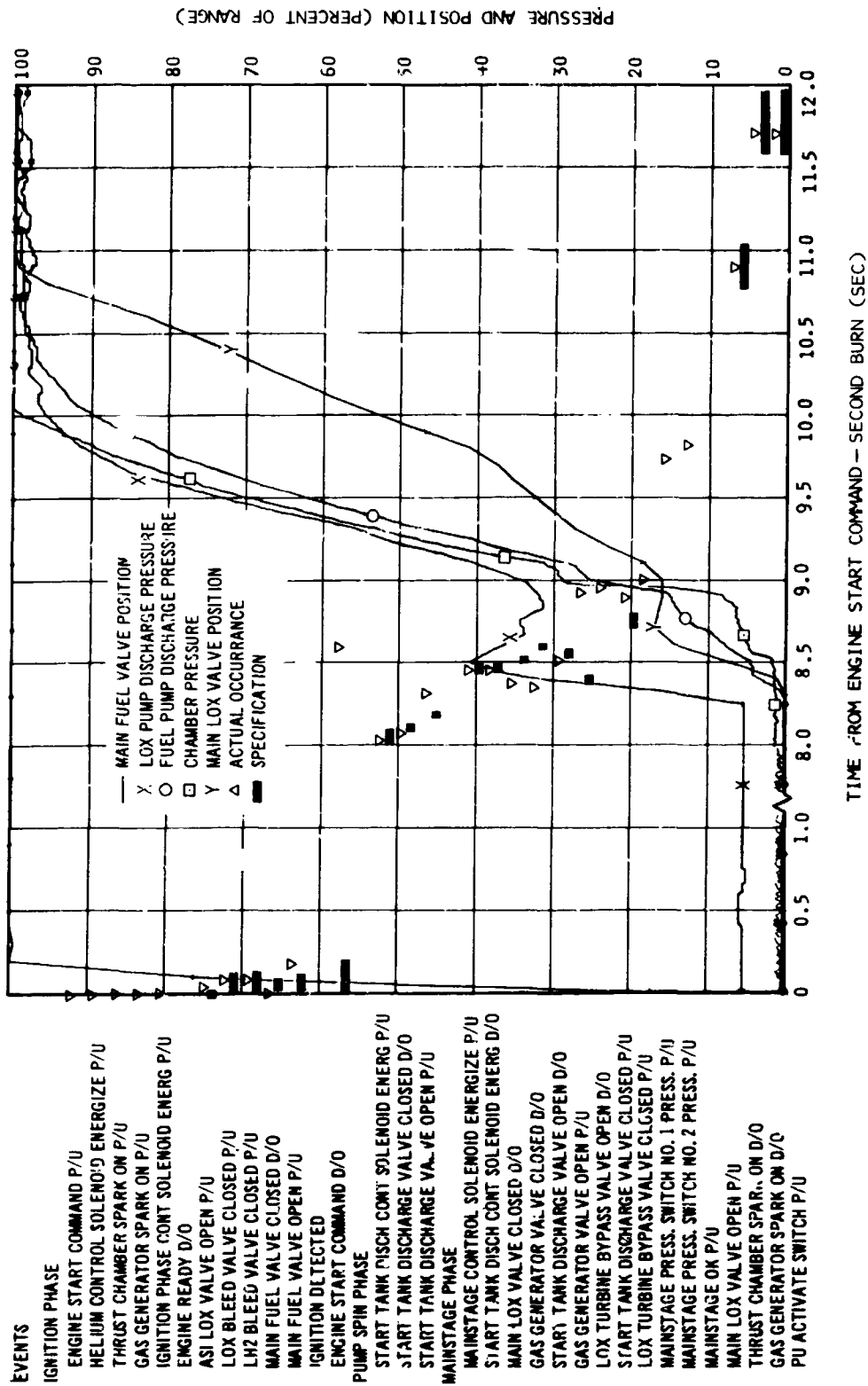


Figure 9-15. Engine Start Sequence - Second Burn

Section 9
Engine System

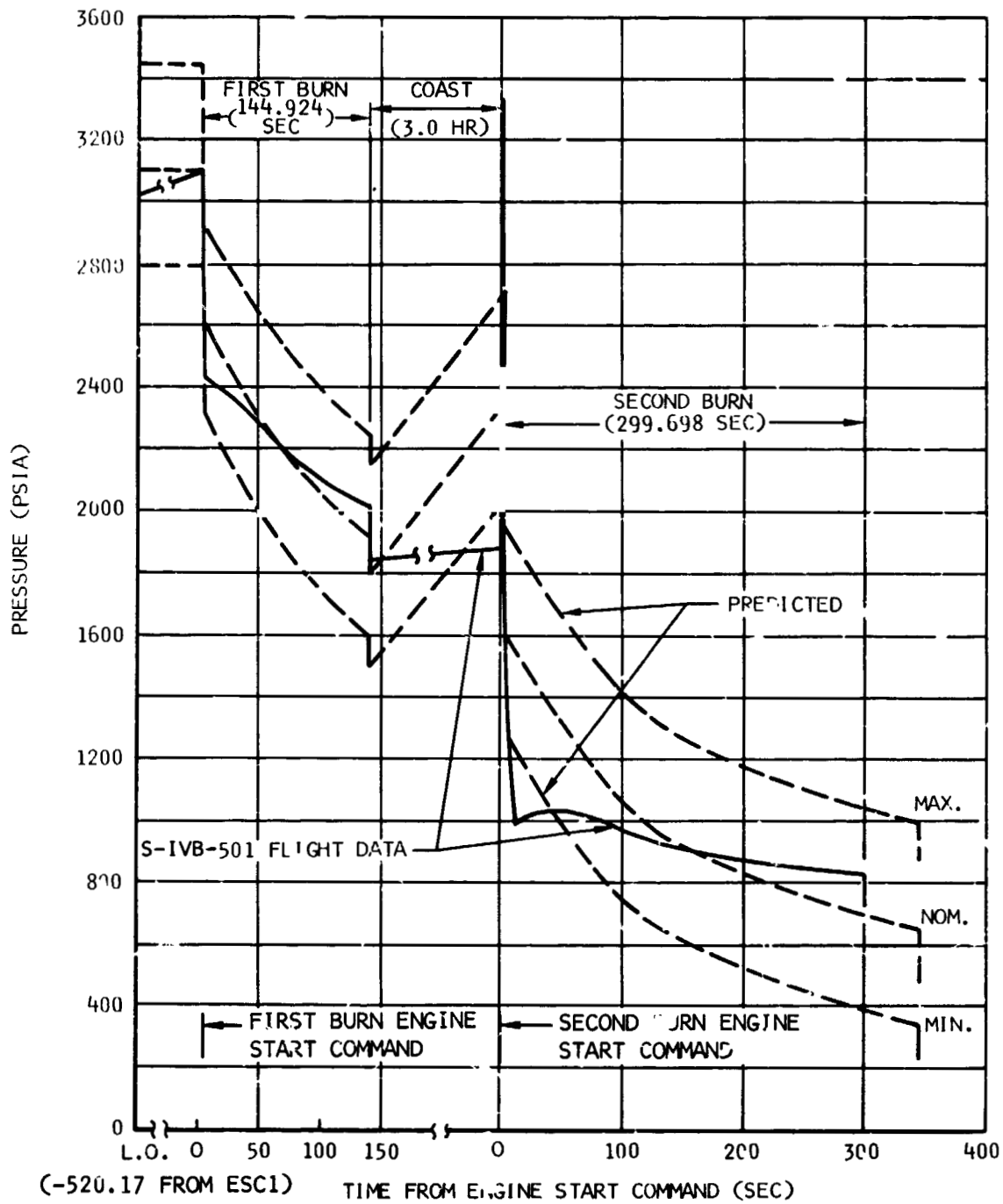


Figure 9-16. Engine Control Sphere Pressure History

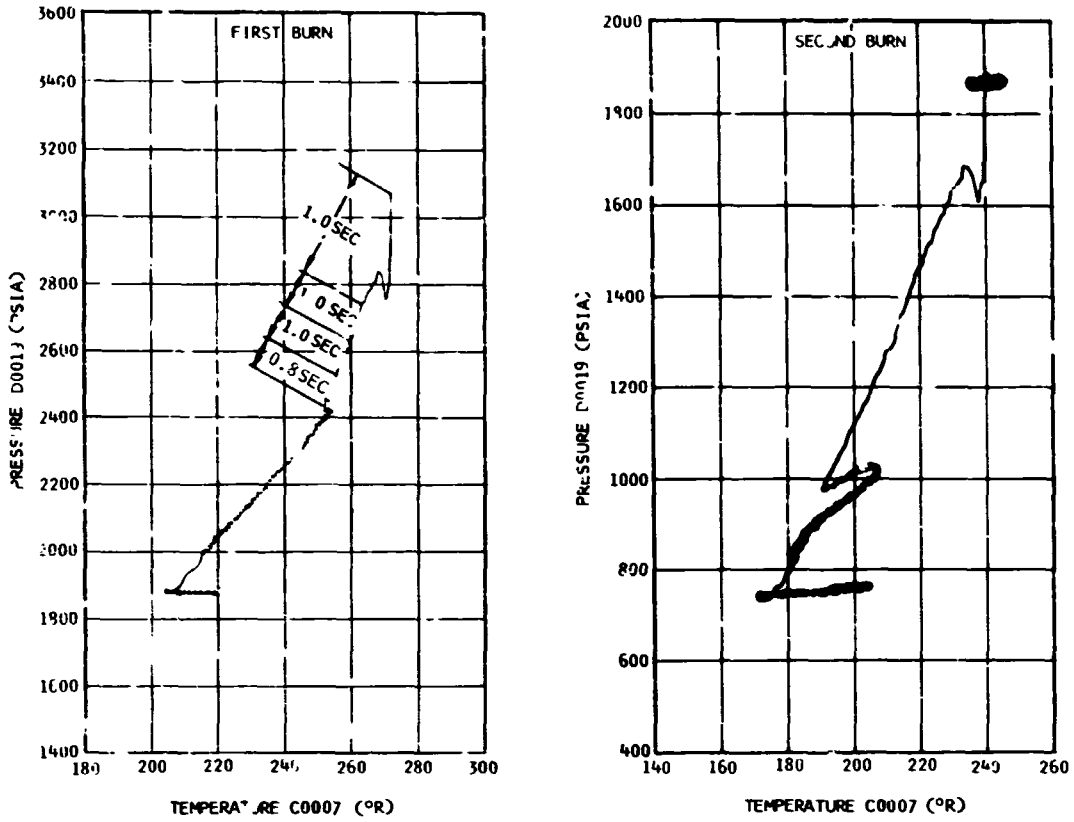


Figure 9-17. Engine Control Sphere Conditions

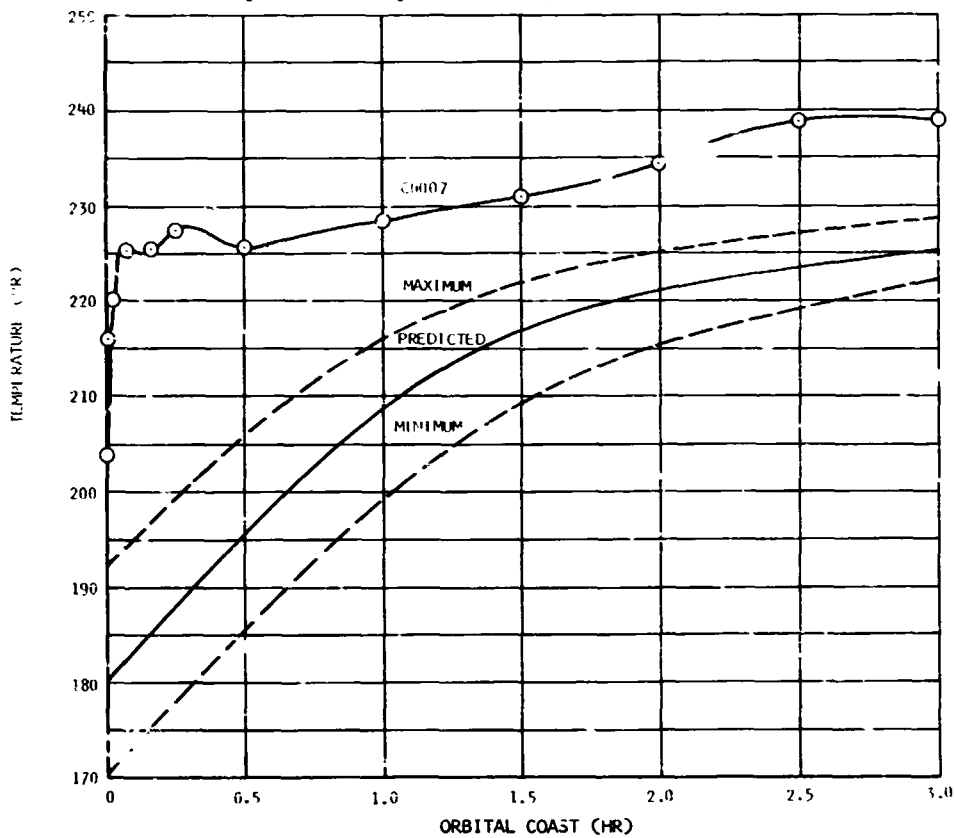


Figure 9-18. Engine Control Sphere Temperature During Orbital Coast

Section 9
Engine System

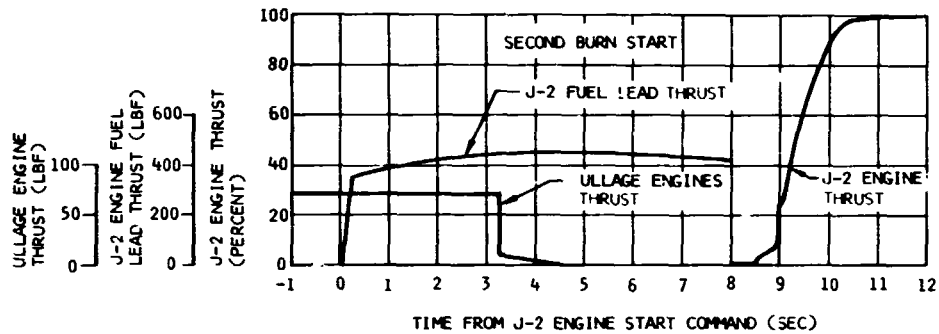
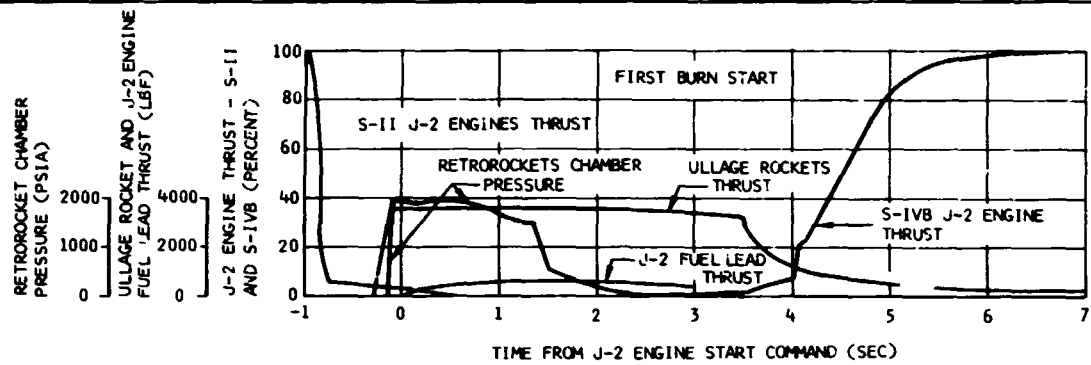


Figure 9-19. Start Transient Thrust Profiles

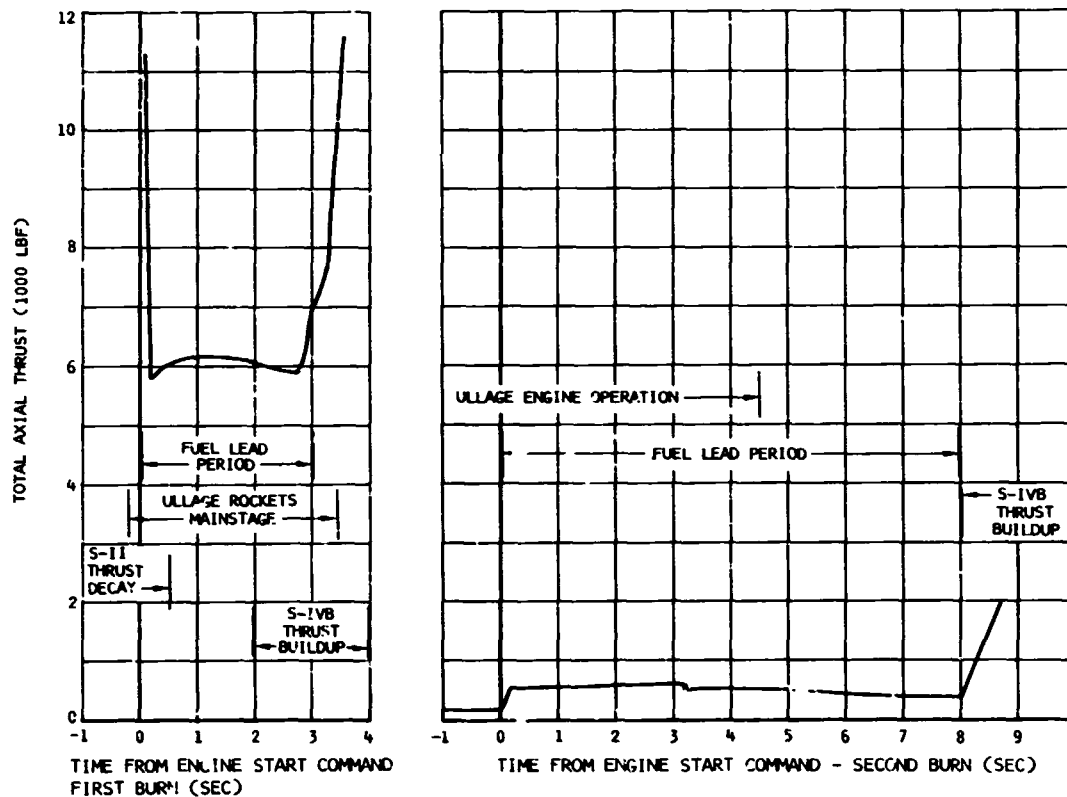


Figure 9-20. Total S-IVB Axial Thrust

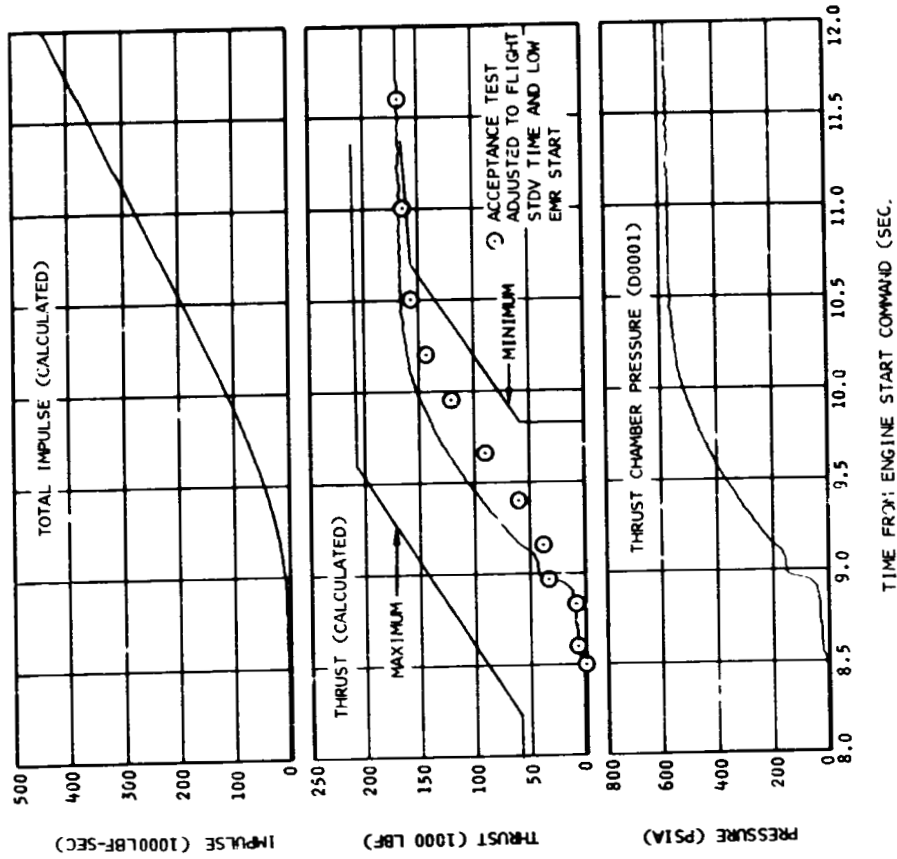


Figure 9-22. Engine Start Transient Characteristics - Second Burn

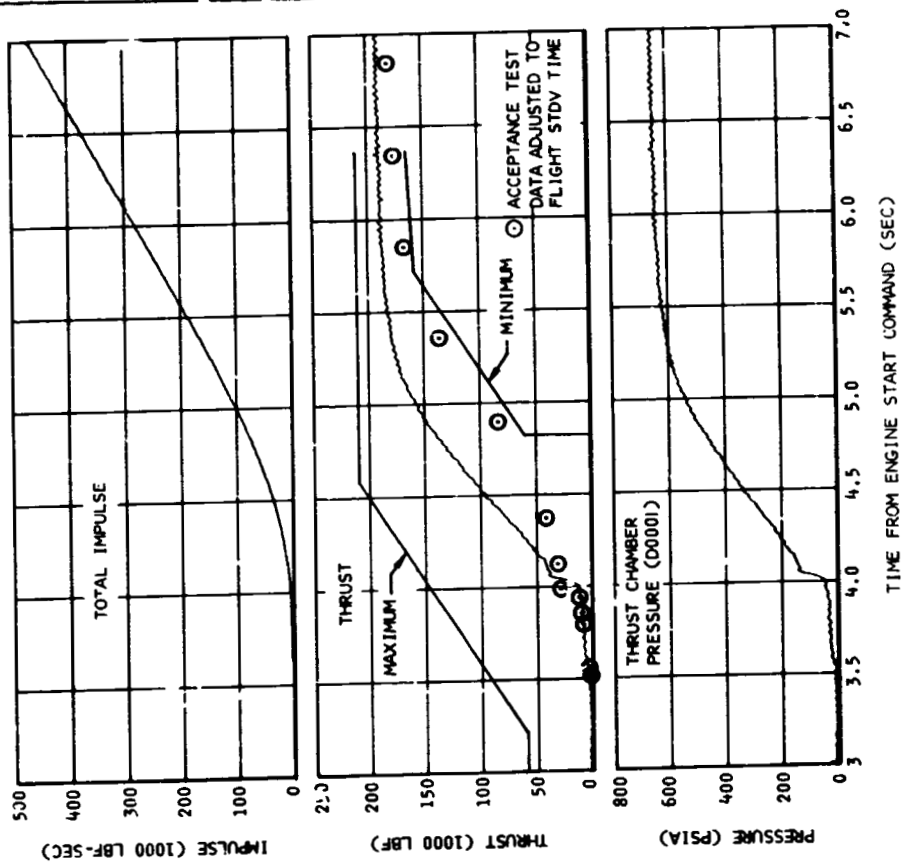


Figure 9-21. Engine Start Transient Characteristics - First Burn

Section 9
Engine System

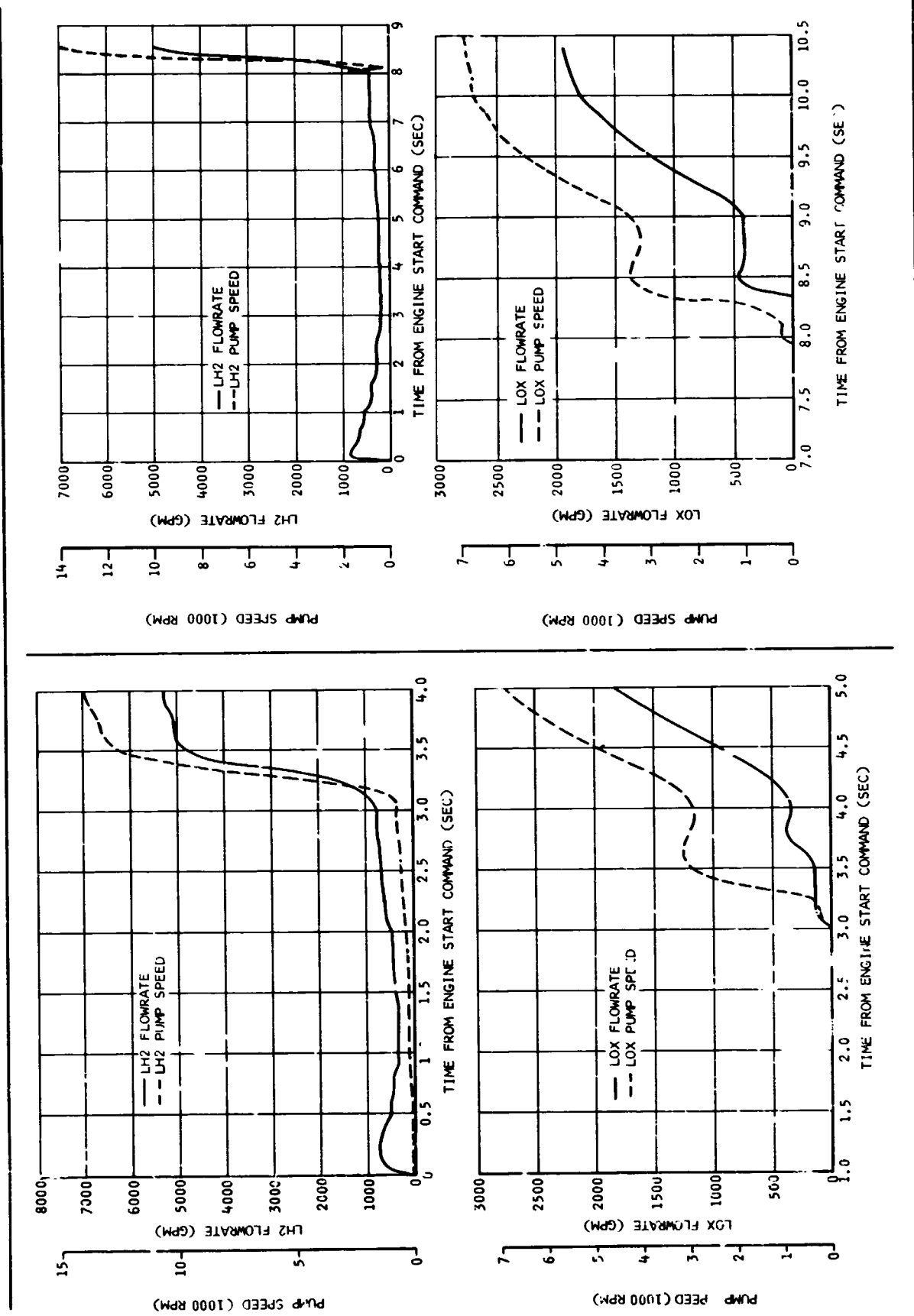


Figure 9-23. Flowrate and Pump Speed During First Burn Start Transient

Figure 9-24. Flowrate and Pump Speed During Second Burn Start Transient

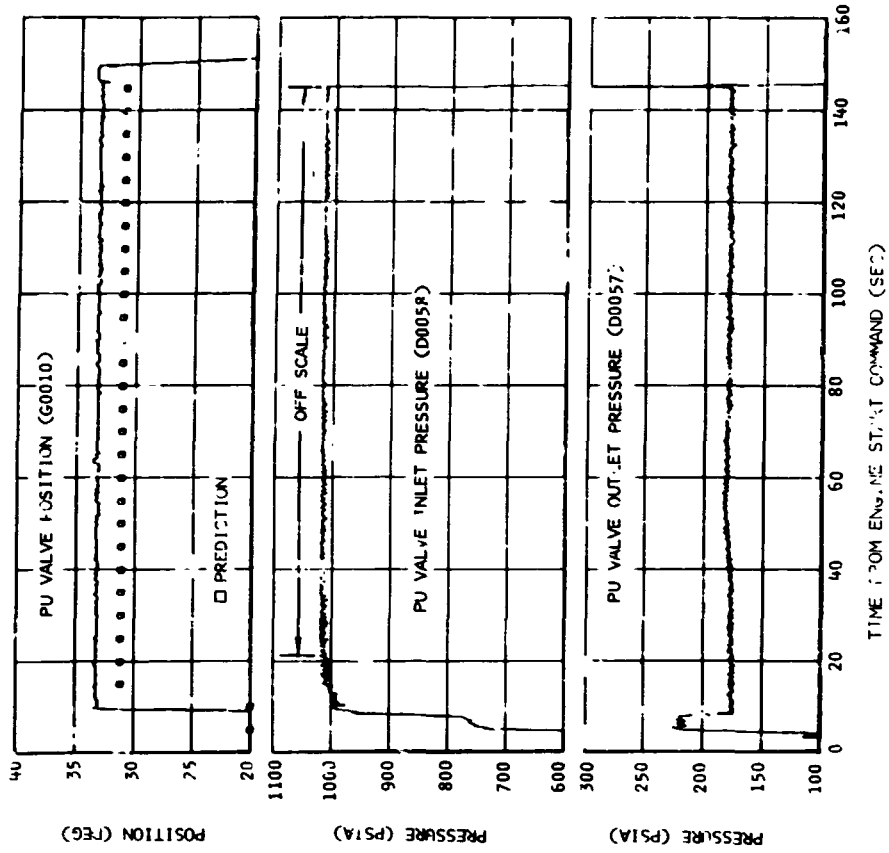


Figure 9-26. PU Valve Operation - First Burn

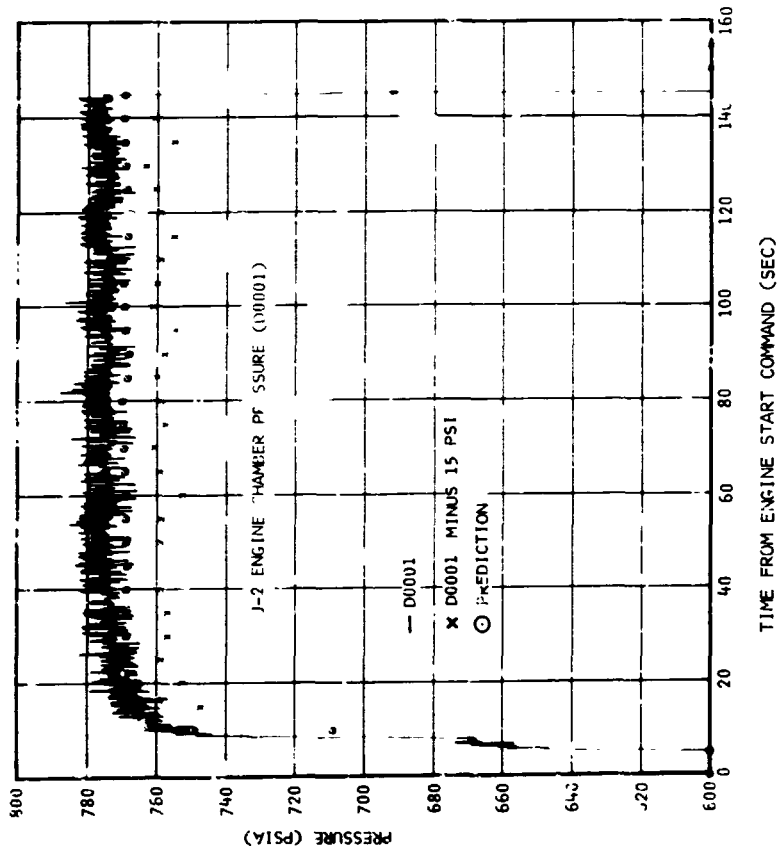


Figure 9-25. J-2 Engine Chamber Pressure - First Burn

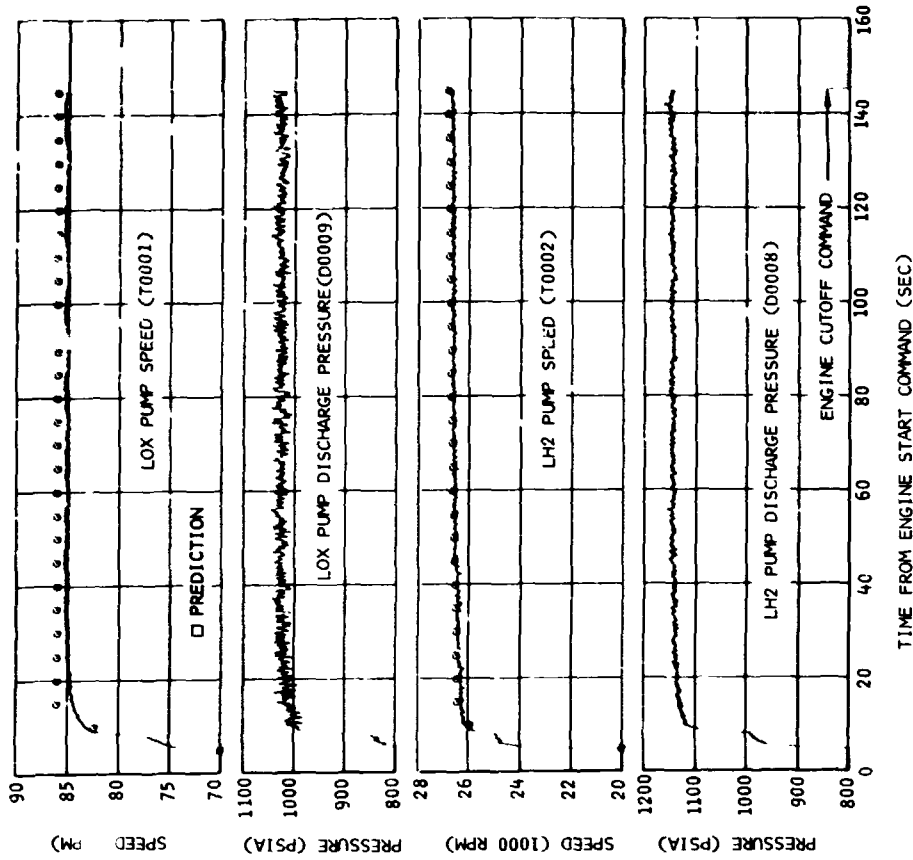


Figure 9-28. J-2 Engine Pump Operating Characteristics - First Burn

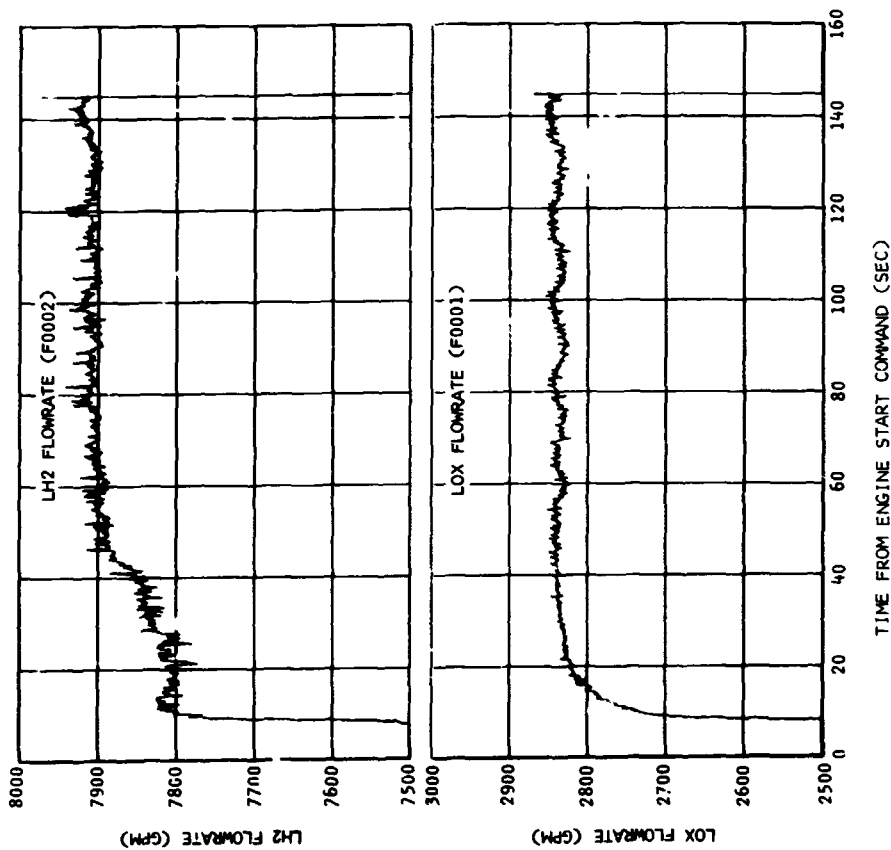


Figure 9-27. J-2 Engine Pump Flowrates - First Burn

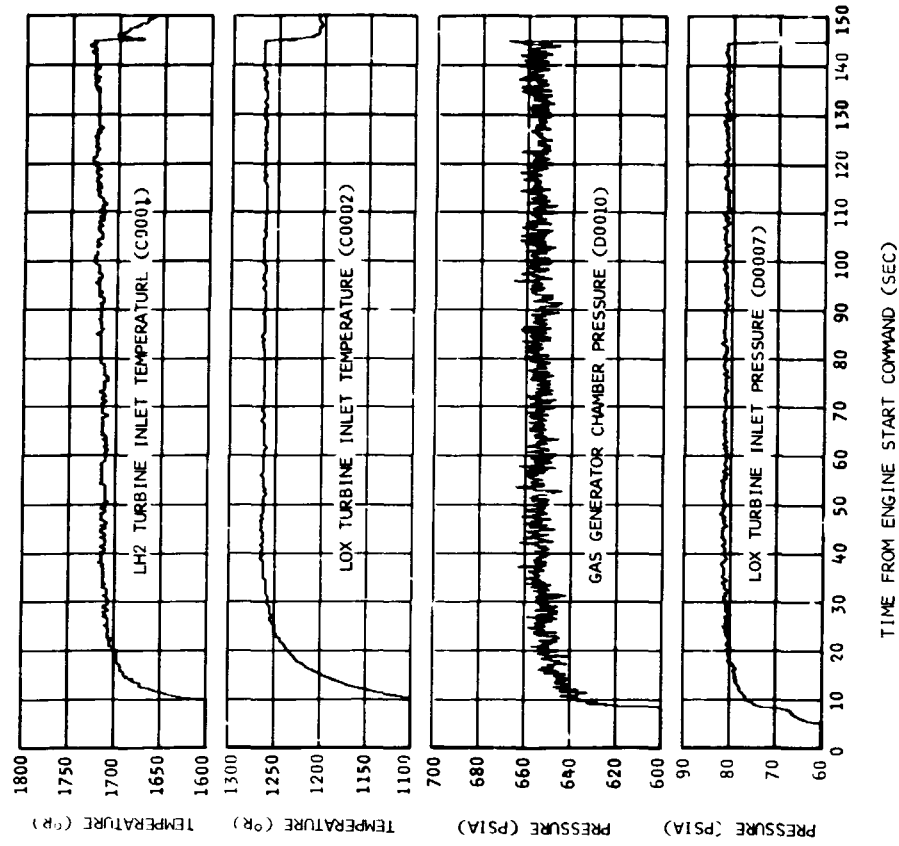


Figure 9-29. J-2 Engine Inlet Operating Conditions - First Burn

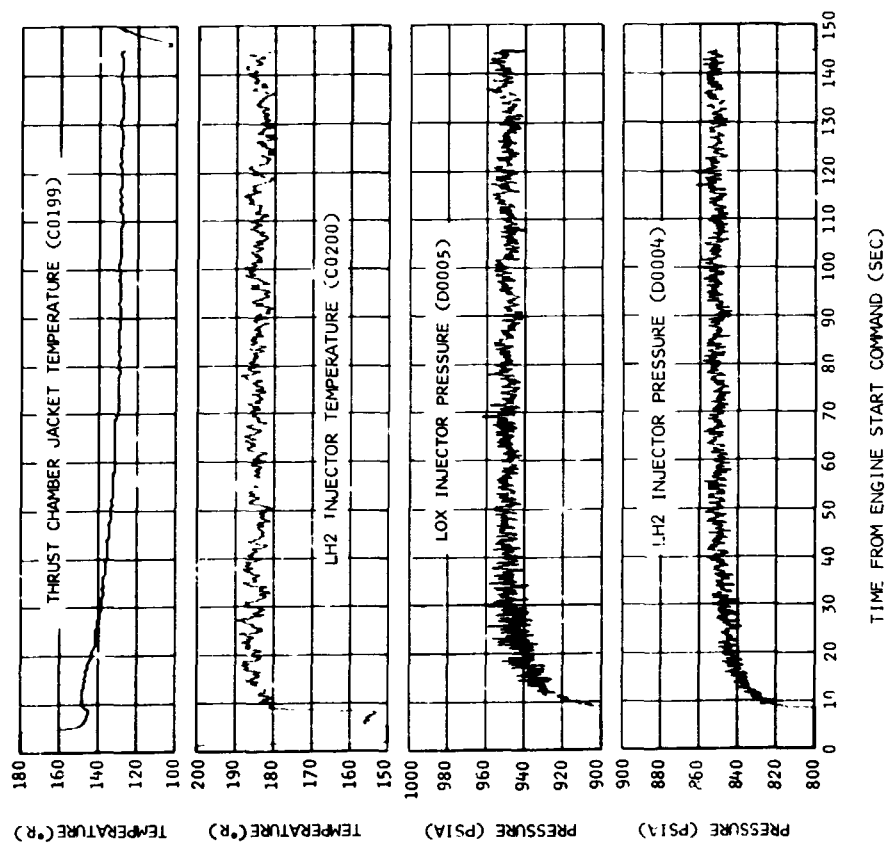


Figure 9-30. Turbine Inlet Operating Conditions - First Burn

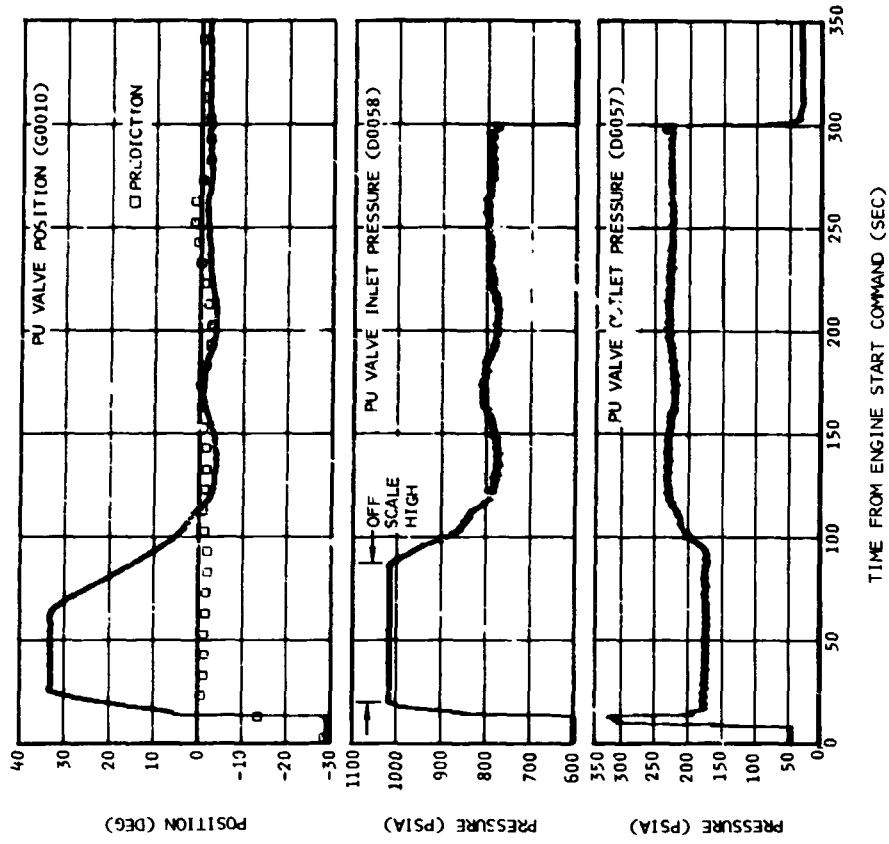


Figure 9-32. PU Valve Operation - Second Burn

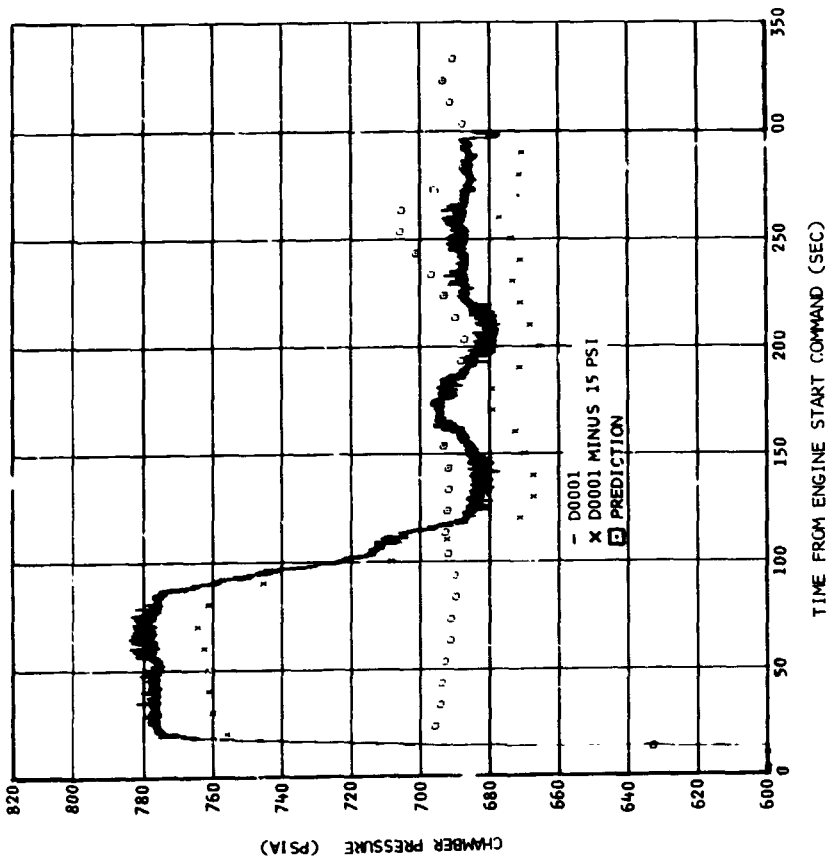


Figure 9-31. J-2 Engine Chamber Pressure - Second Burn

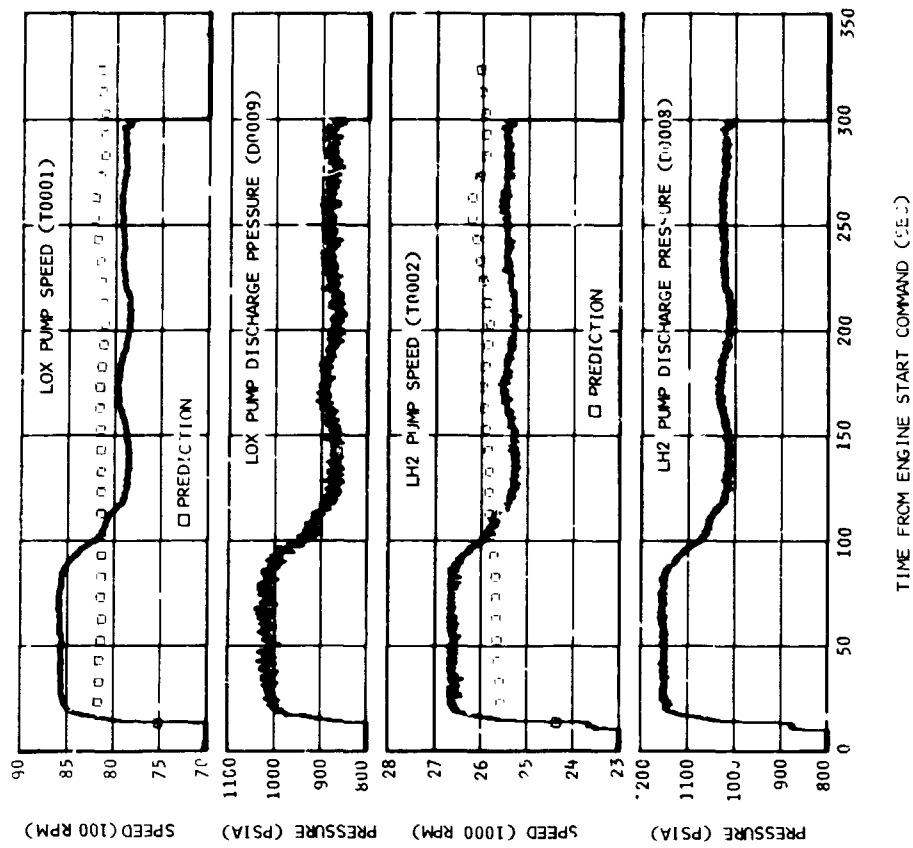


Figure 9-33. J-2 Engine Pump Flowrates - Second Burn.

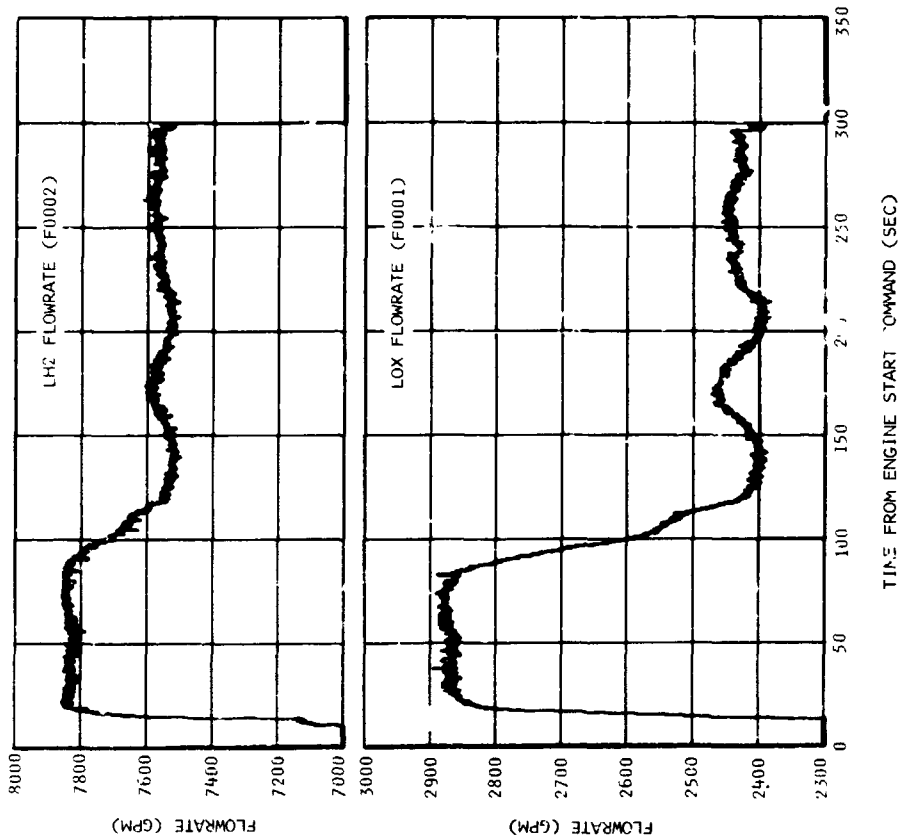


Figure 9-34. J-2 Engine Pump Operating Conditions - Second Burn

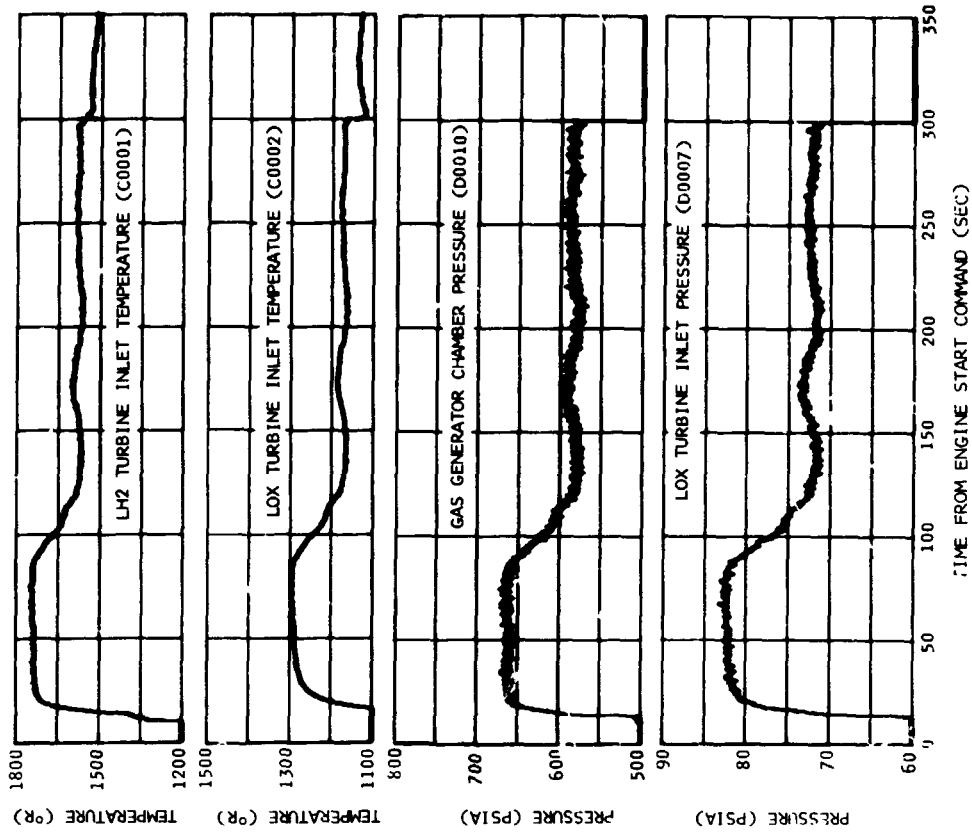


Figure 9-35. J-2 Engine Injector Supply Conditions - Second Burn

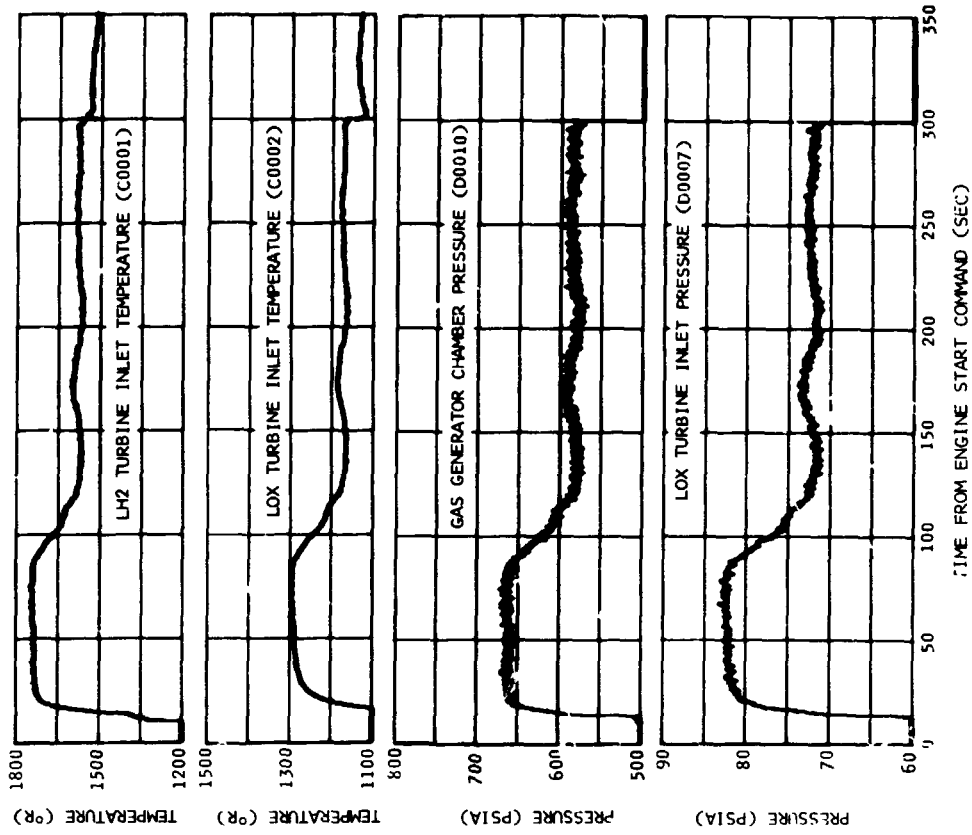


Figure 9-36. Turbine Inlet Operating Conditions - Second Burn

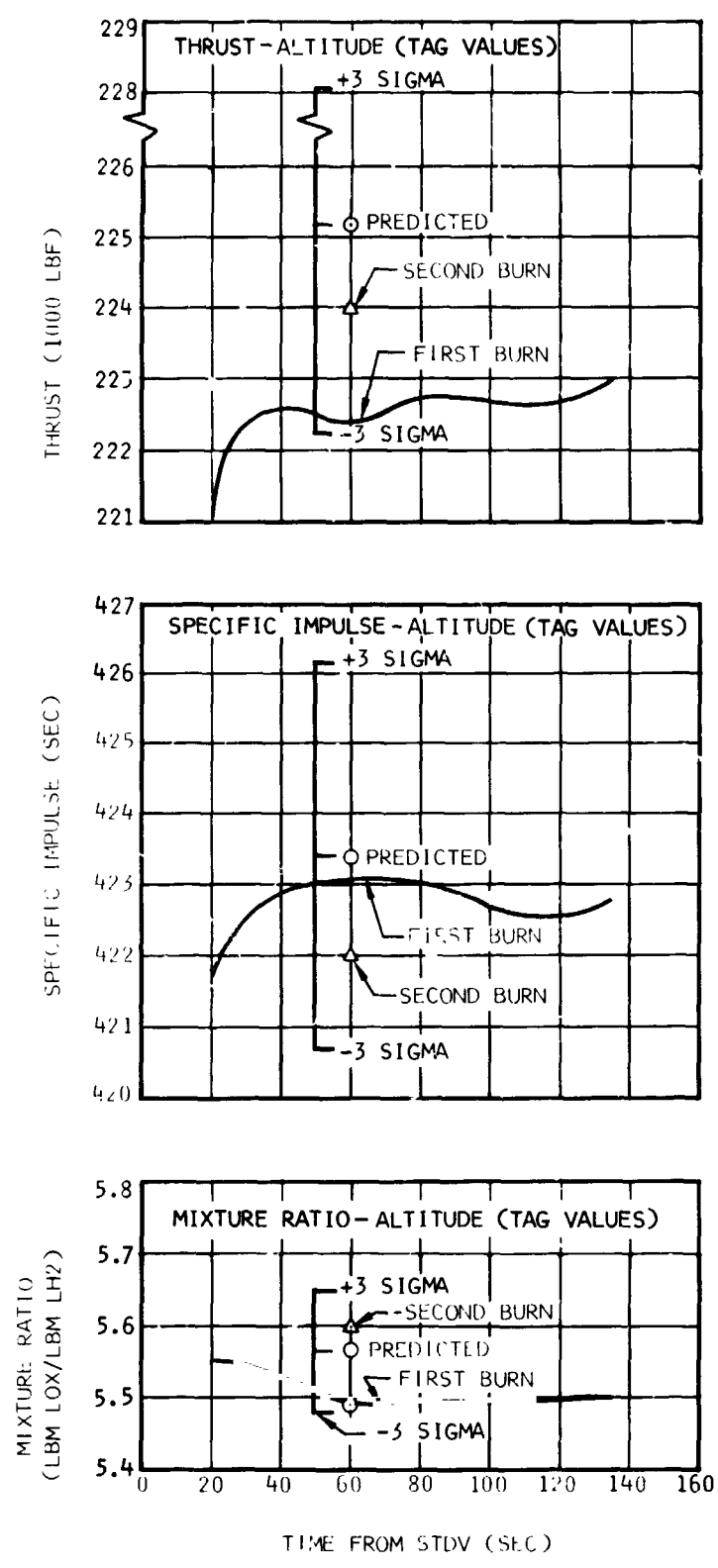


Figure 9-37. Engine Tag Values at Standard Altitude Conditions (Sheet 1 of 2)

Section 9
Engine System

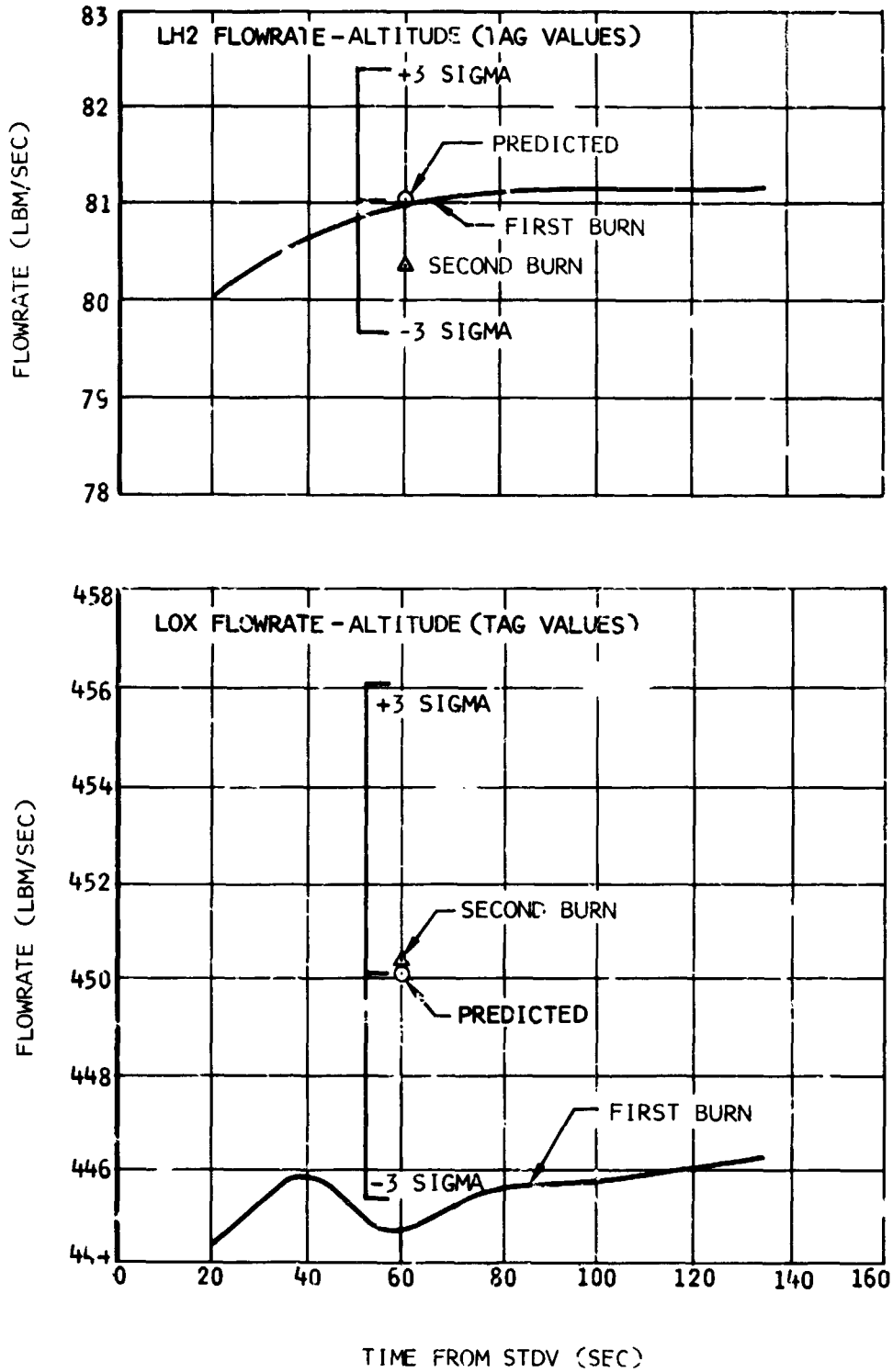


Figure 9-37. Engine Tag Values at Standard Altitude Conditions (Sheet 2 of 2)

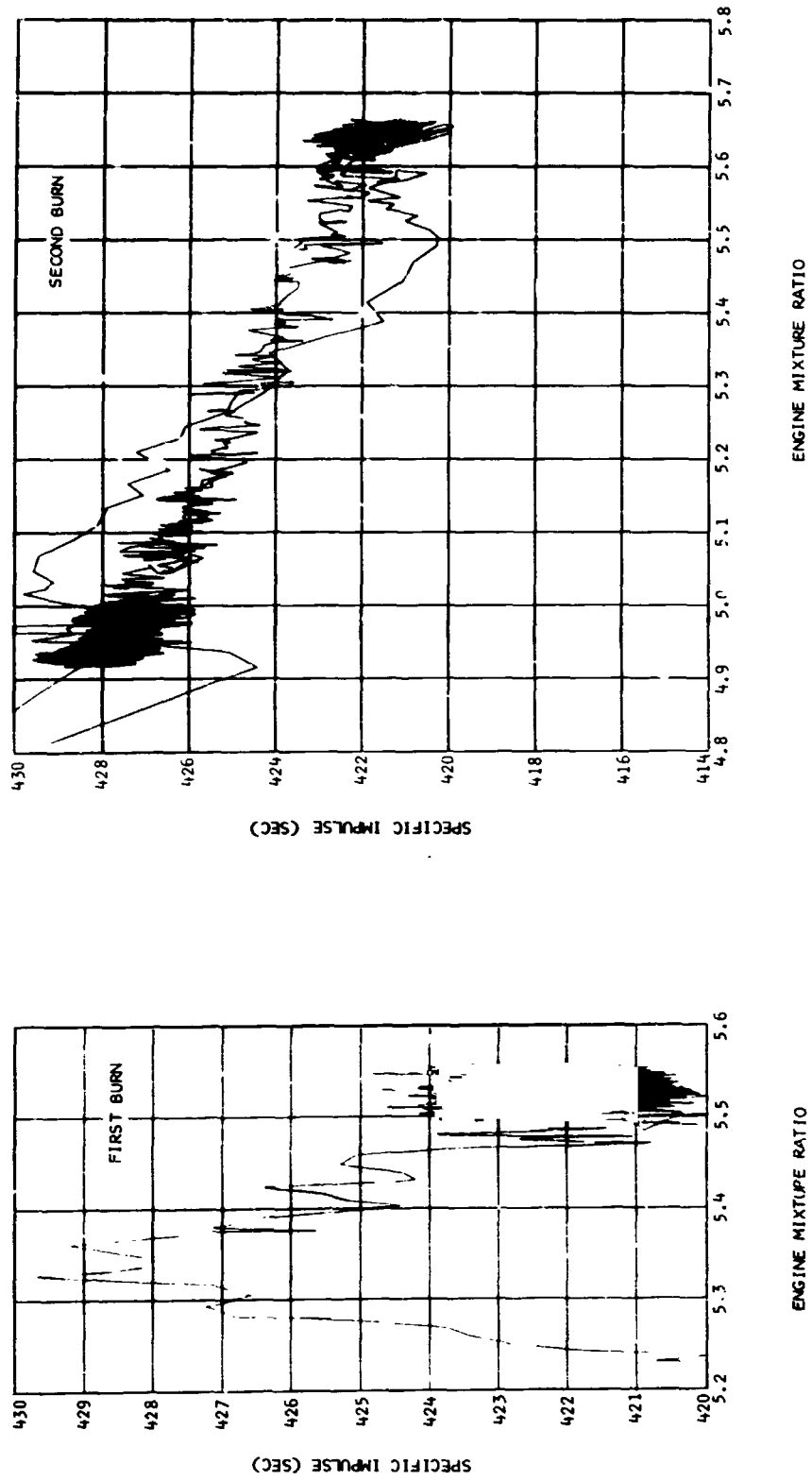


Figure 9-38. Specific Impulse Versus Engine Mixture Ratio

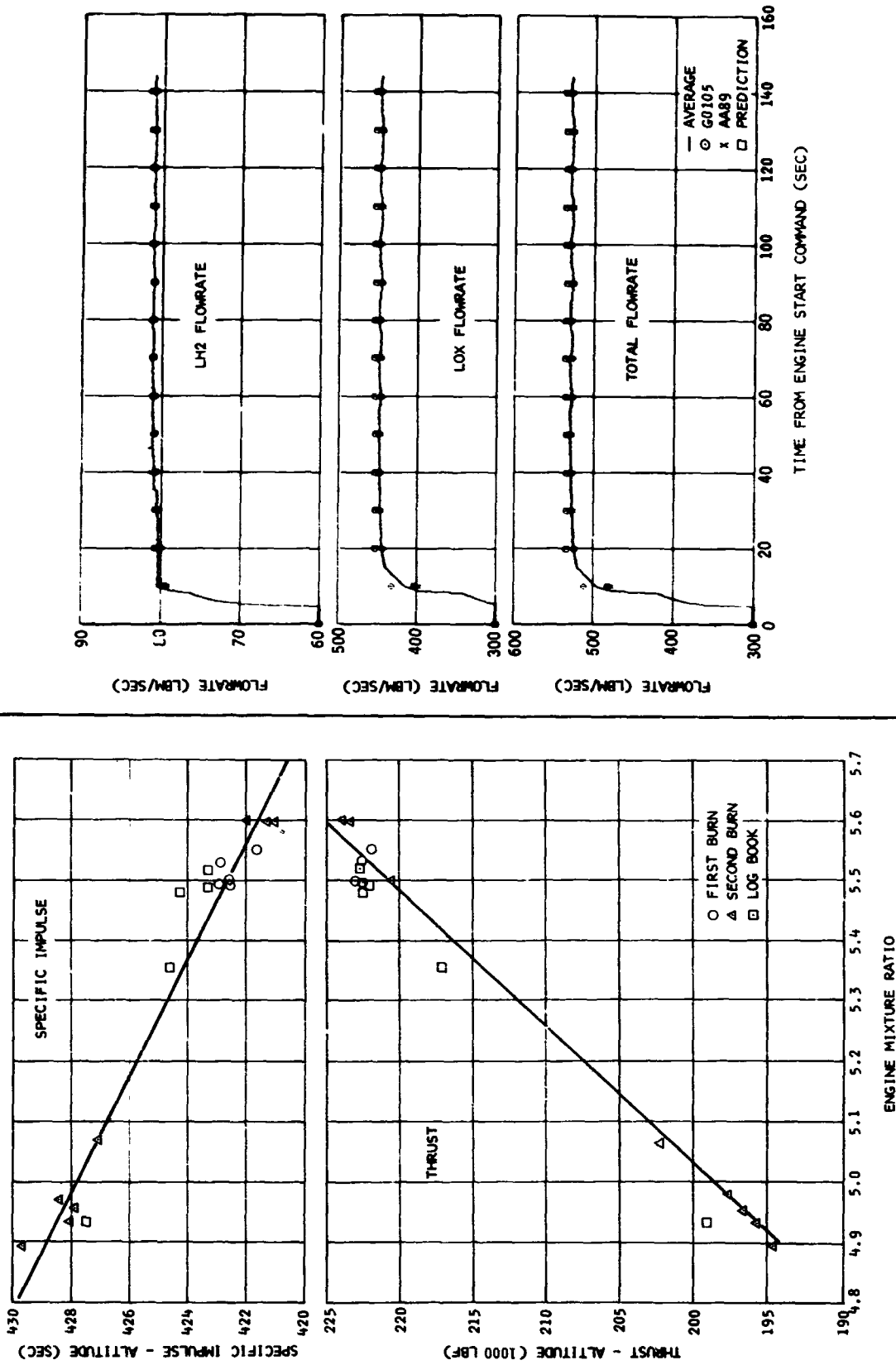


Figure 9-39. Thrust and Specific Impulse Characteristics at Standard Altitude Conditions

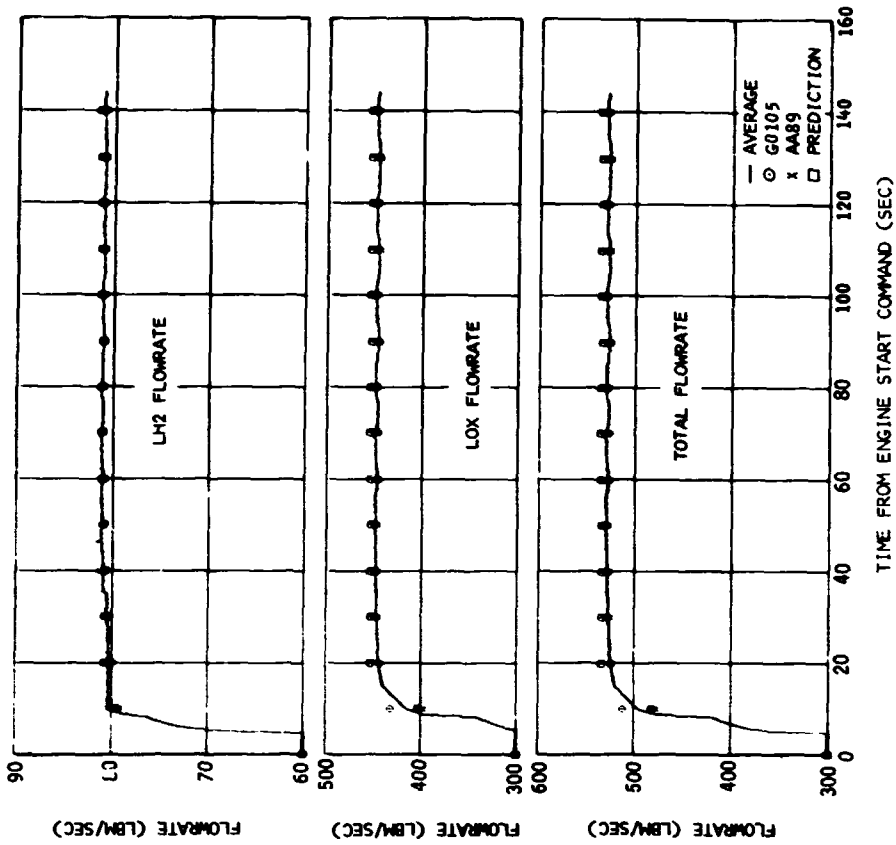


Figure 9-40. Engine Steady-State Performance - First Burn (Sheet 1 of 3)

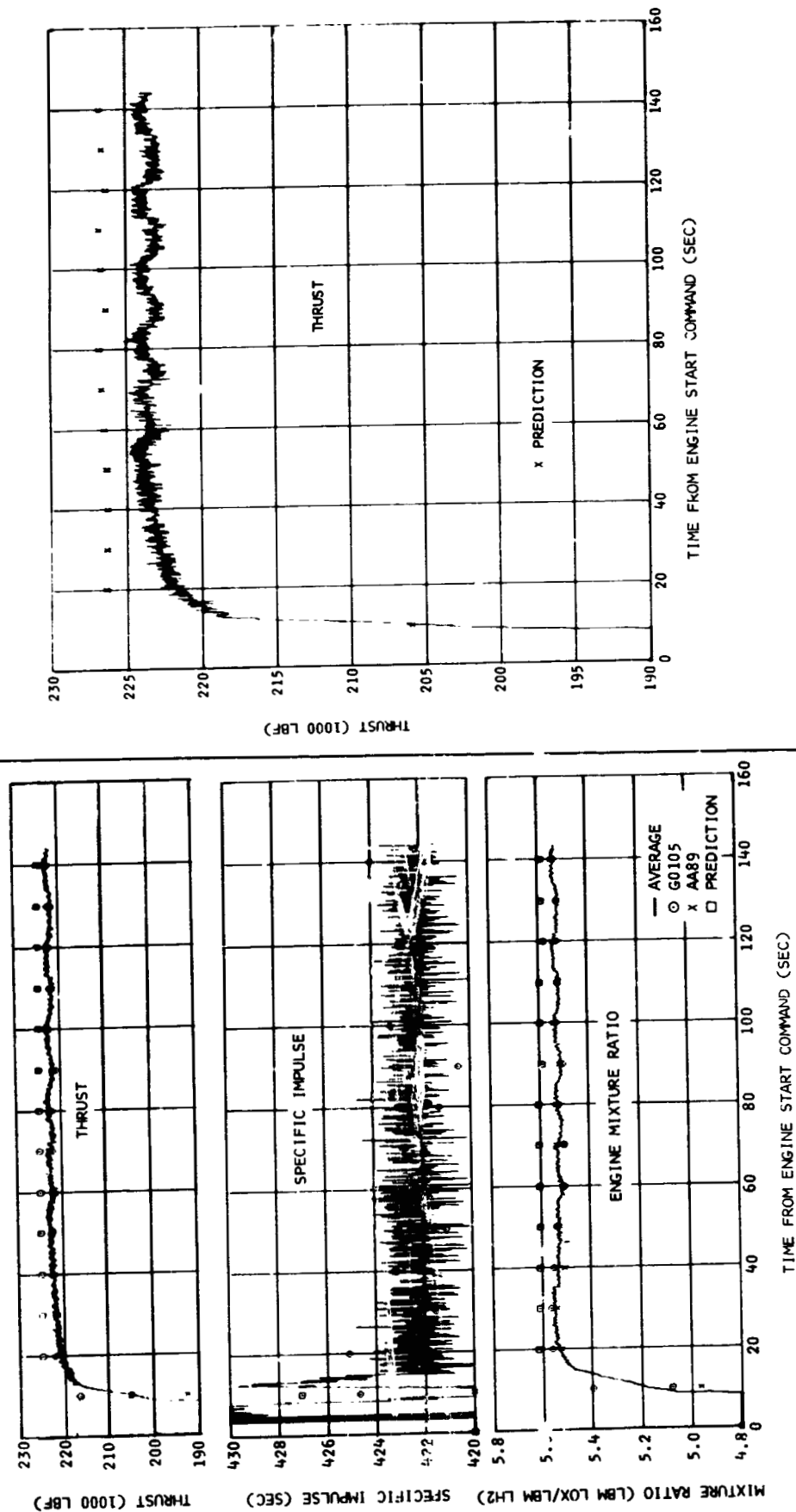


Figure 9-40. Engine Steady-State Performance - First Burn (Sheet 2 of 3)

Figure 9-40. Engine Steady-State Performance - First Burn (Sheet 3 of 3)

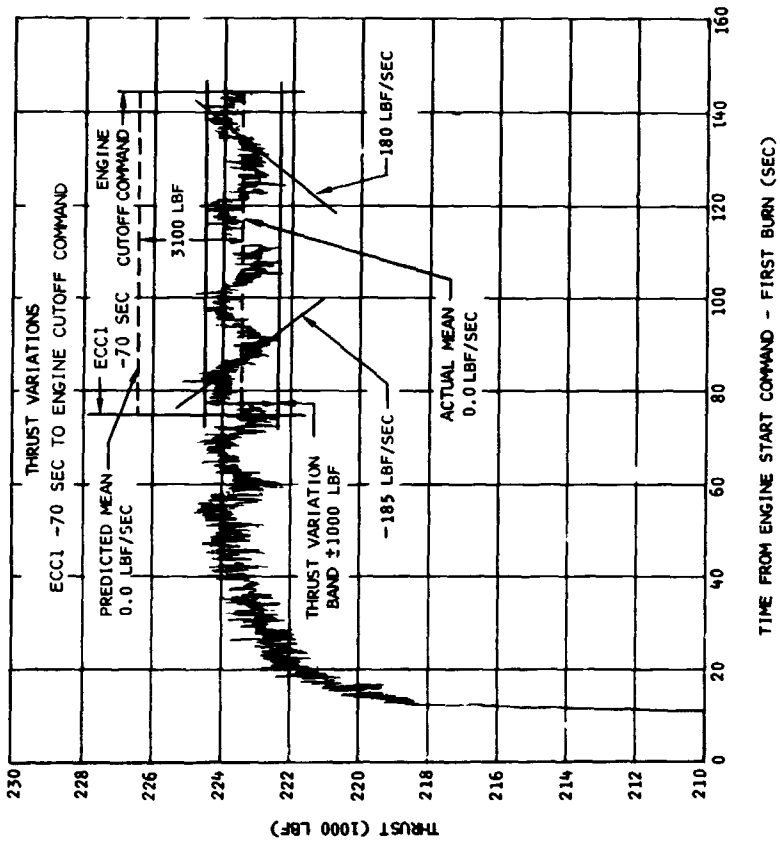
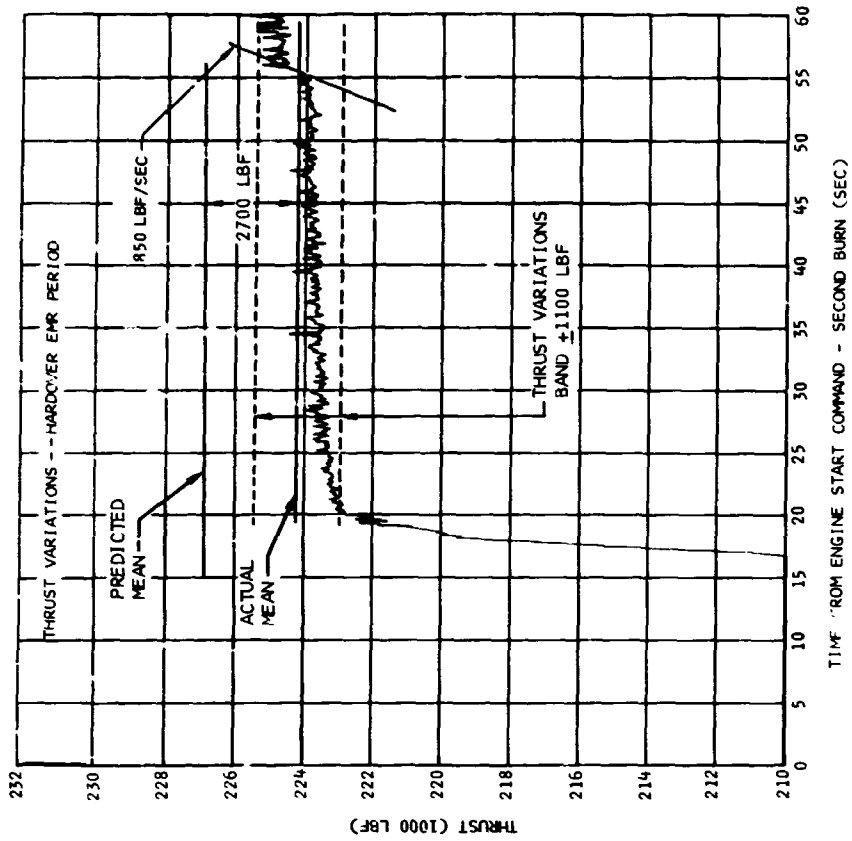


Figure 9-41. Thrust Variation

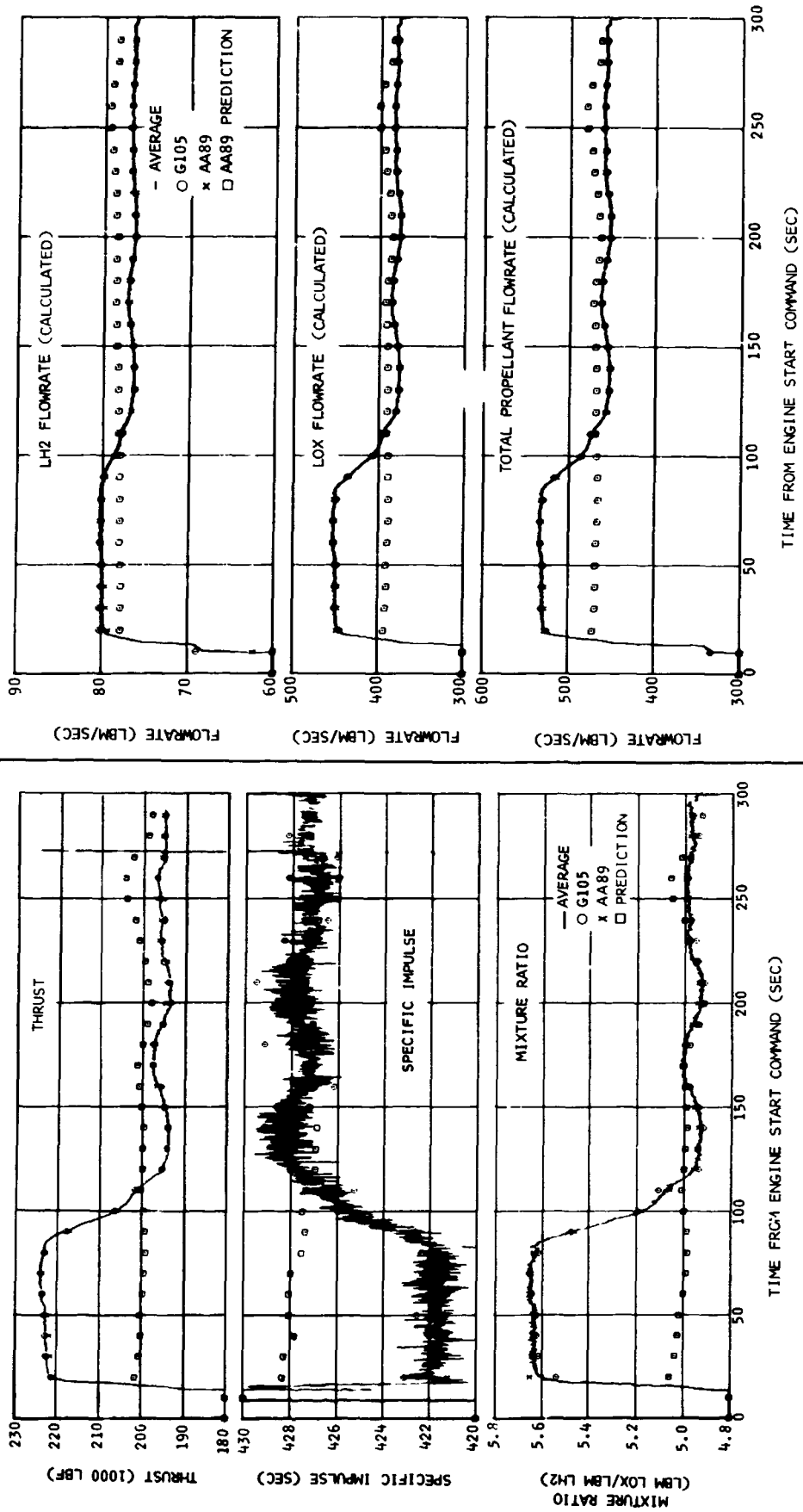


Figure 9-42. Engine Steady-State Performance - Second Burn (Sheet 1 of 2)

Section 9
Engine System

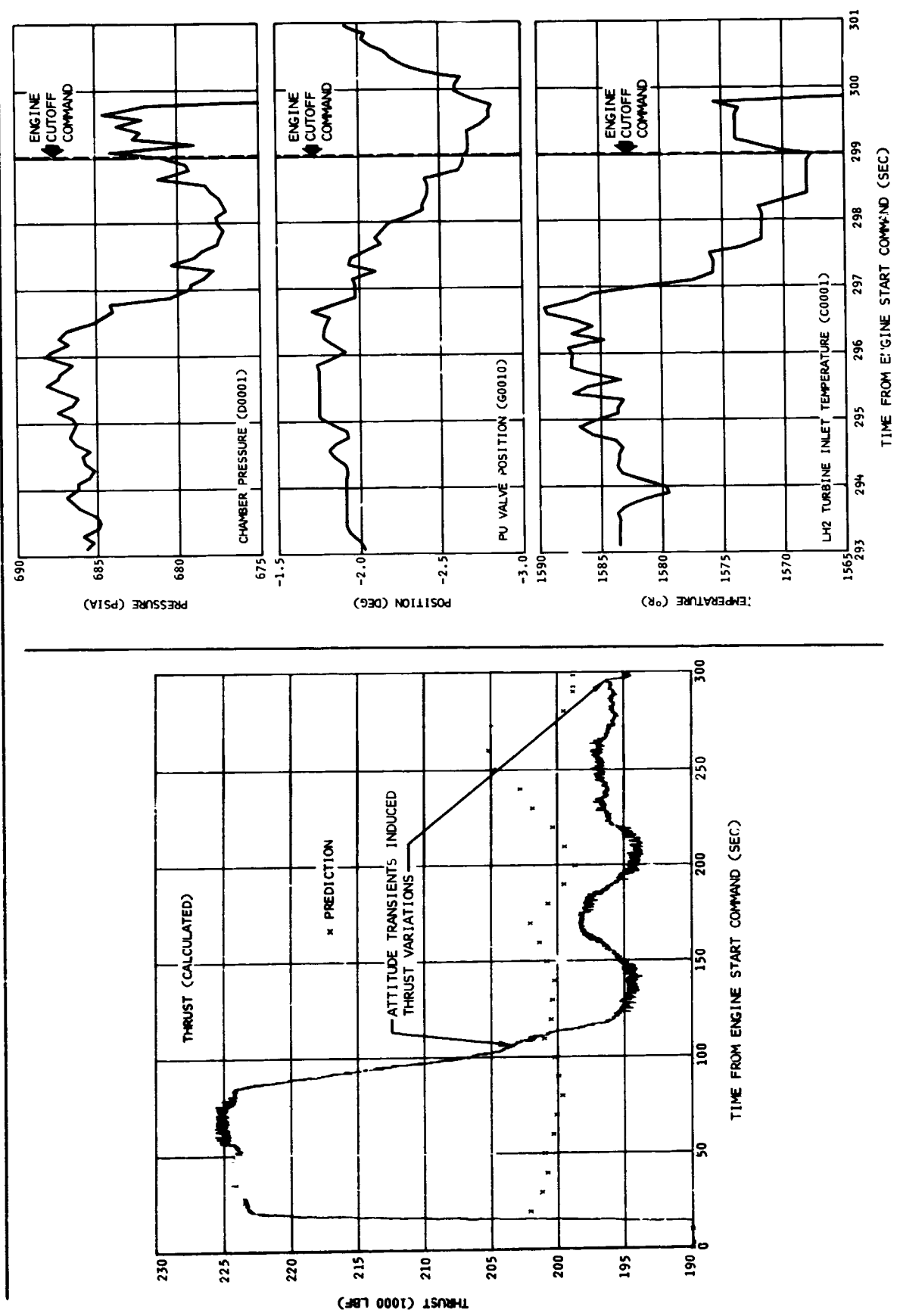


Figure 9-42. Engine Steady-State Performance - Second Burn (Sheet 2 of 2)

Figure 9-43. Expanded Pre-cutoff Data - Measured

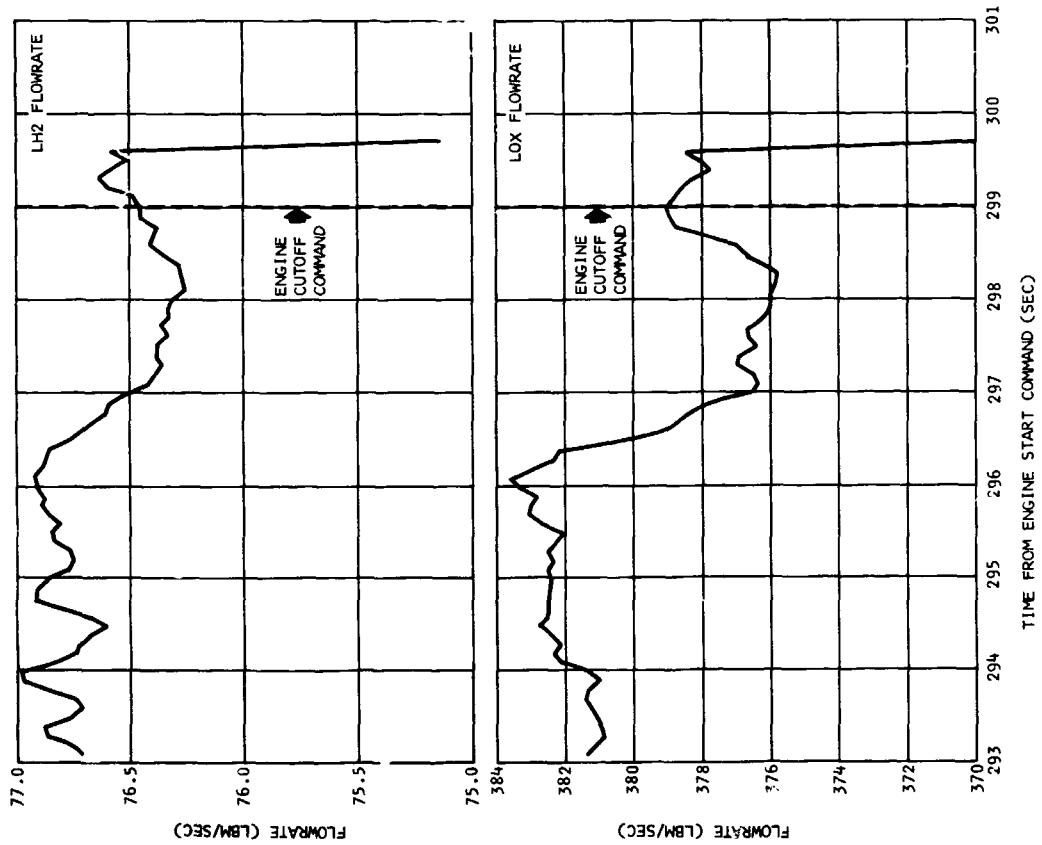


Figure 9-44. Expanded Pre-cutoff Data - Calculated

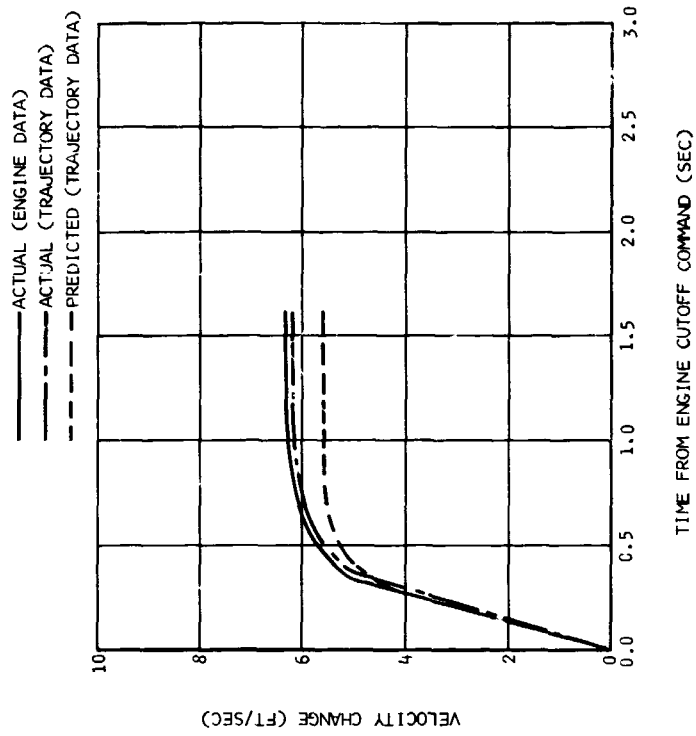


Figure 9-45. Change in Velocity due to Tailoff Impulse - First Burn

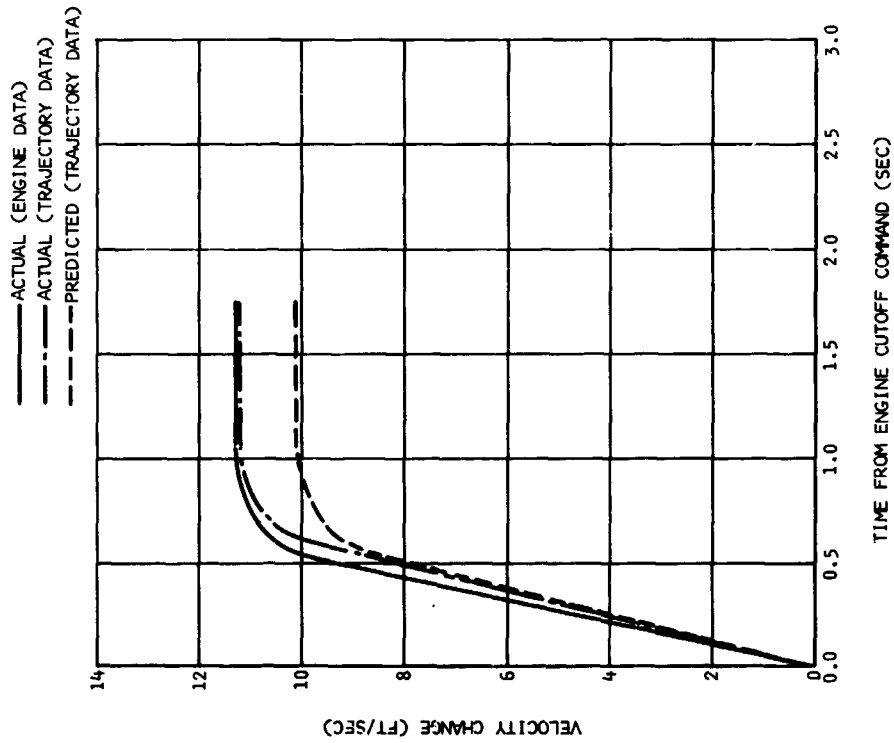
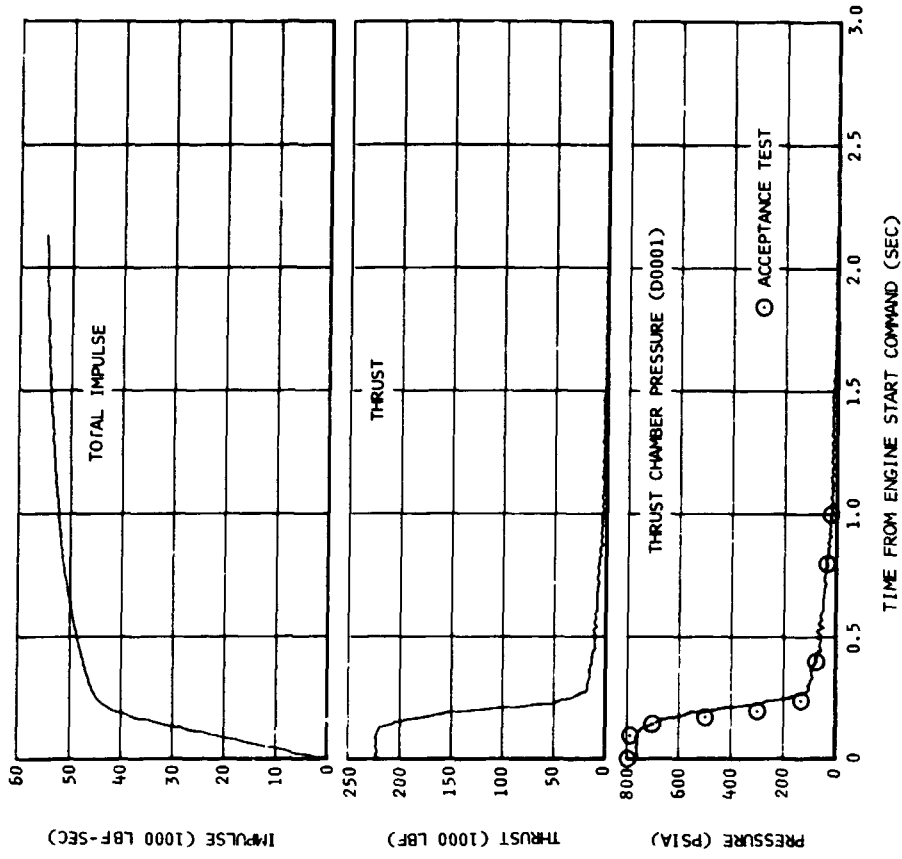


Figure 9-47. Engine Cutoff Transient Characteristics - First Burn

Figure 9-46. Change in Velocity due to Tailoff Impulse - Second Burn

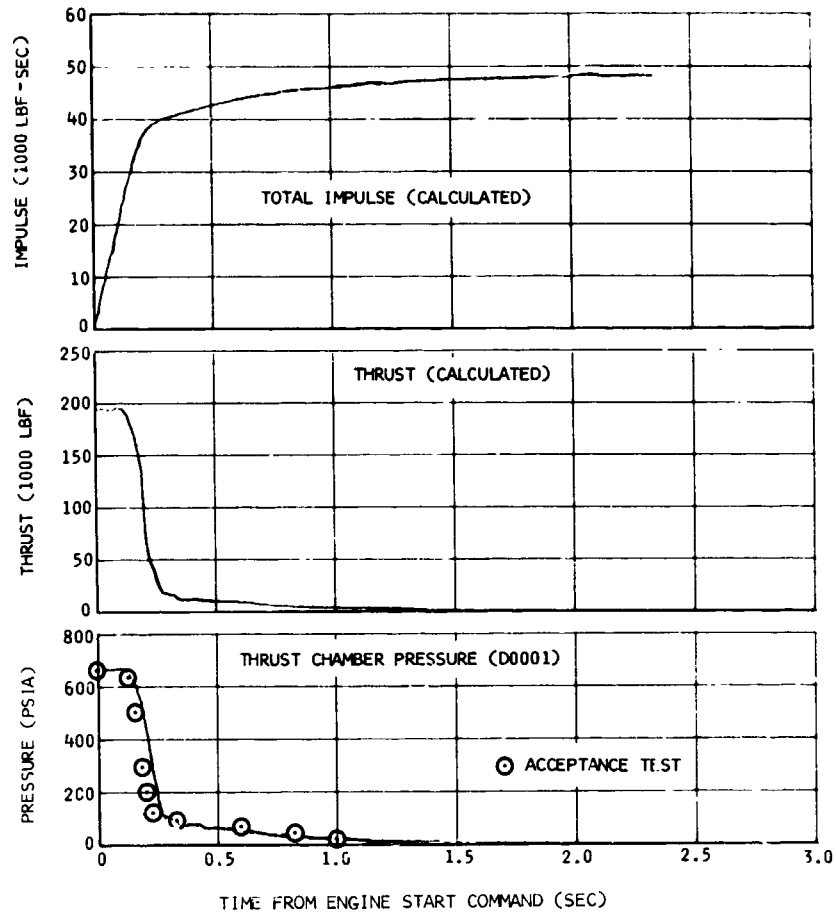


Figure 9-48. Engine Cutoff Transient Characteristics - Second Burn

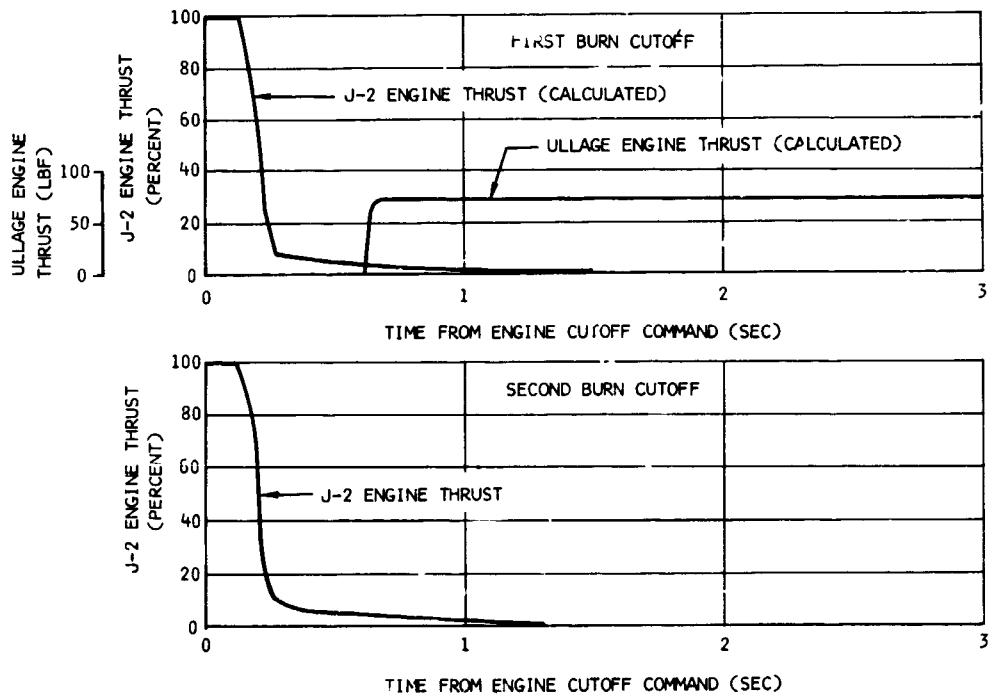


Figure 9-49. Cutoff Transient Thrust Profiles

Section 9
Engine System

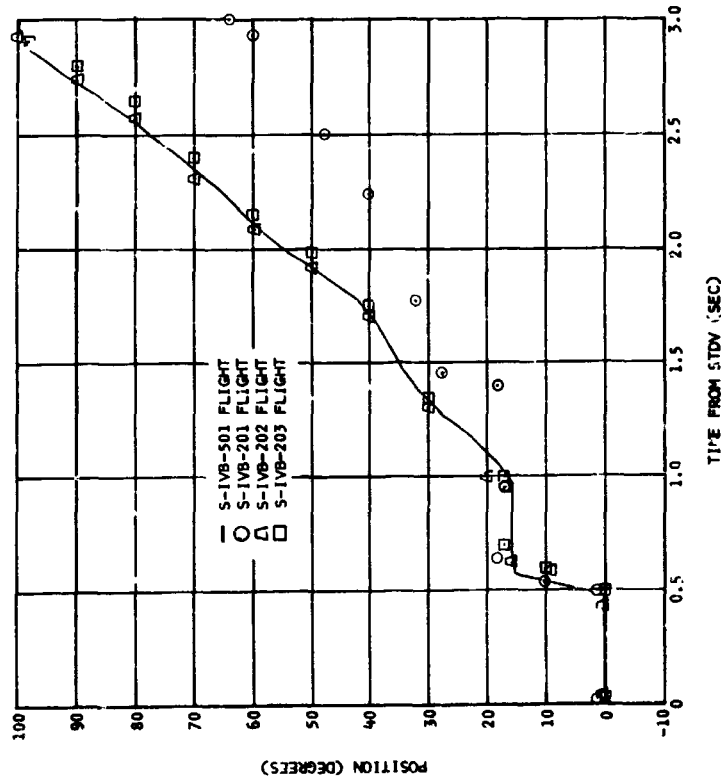
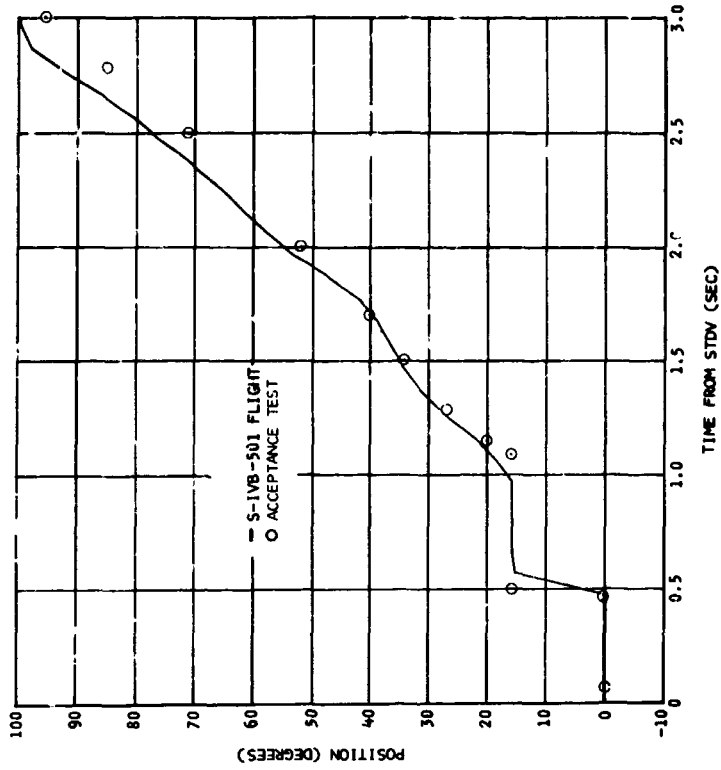


Figure 9-50. Main Oxidizer Valve Position - First Burn

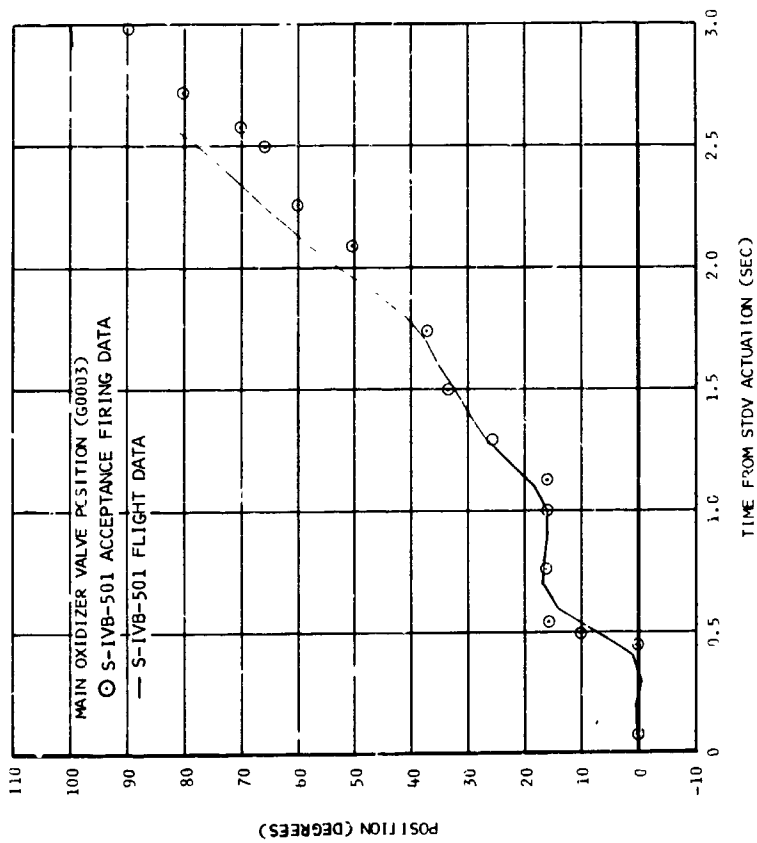
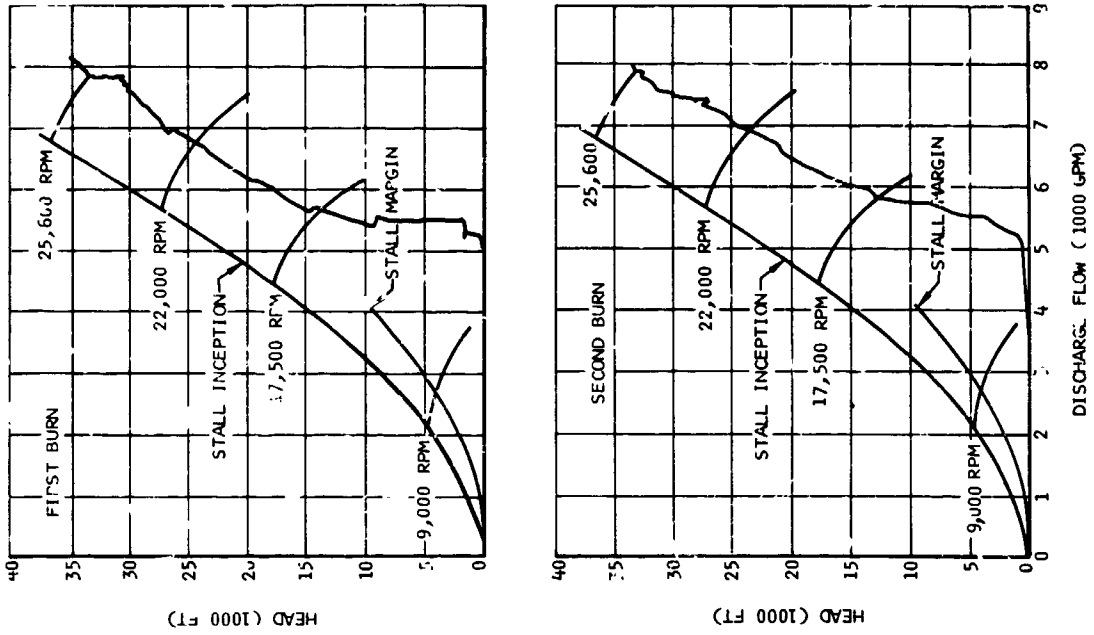


Figure 9-52. LH2 Pump Performance During Engine Start

Figure 9-51. Main Oxidizer Valve Position - Second Burn

Section 9
Engine System

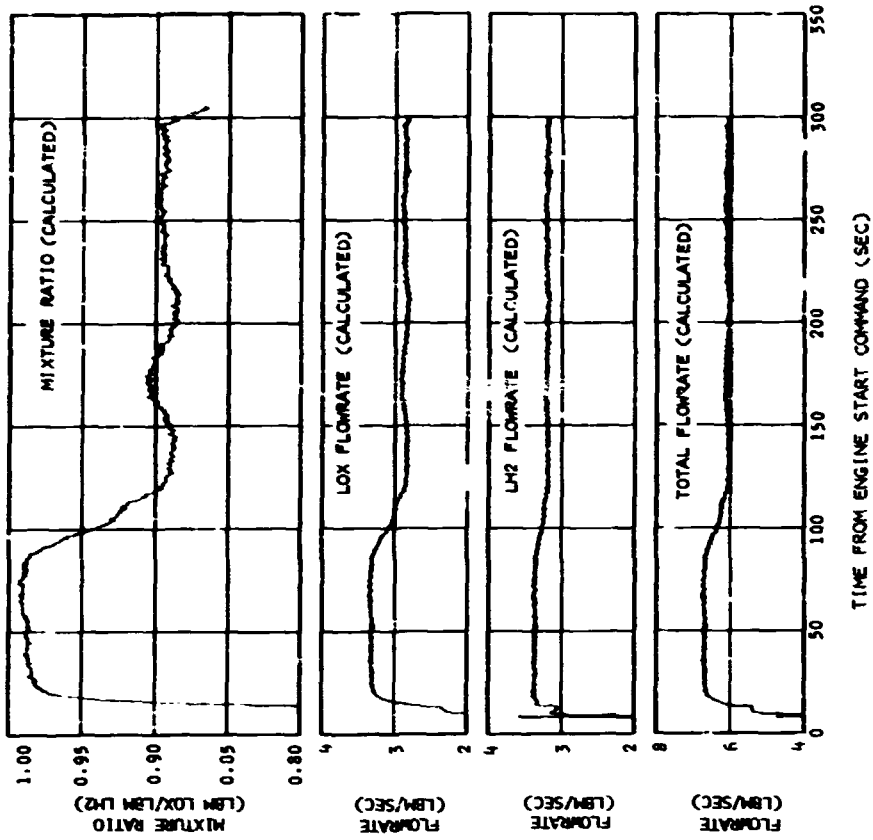


Figure 9-53. Gas Generator Performance - First Burn

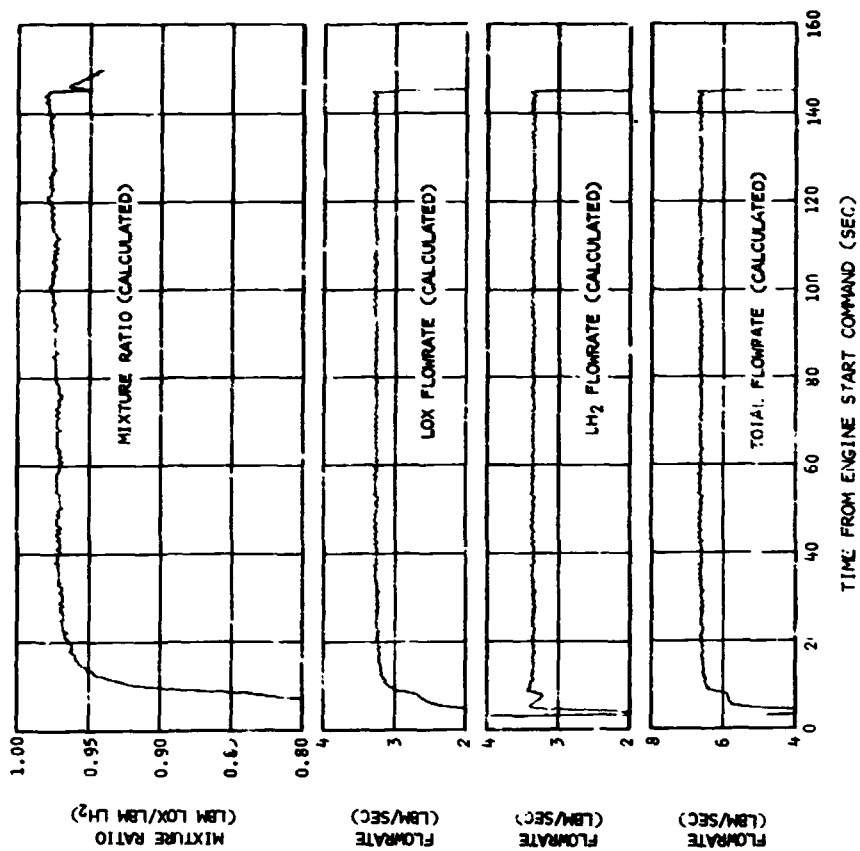


Figure 9-54. Gas Generator Performance - Second Burn

10. SOLID ROCKETS

The solid rocket motors on the S-II and S-IVB stages performed satisfactorily and accomplished their intended purpose. The S-II was separated from the S-IVB stage by the retrorockets, and the S-IVB propellants were settled prior to first burn engine ignition by the ullage rockets.

10.1 Retrorockets

The four retrorockets mounted on the S-II stage performed satisfactorily and separated the S-II and S-IVB stages. The ignition command was given at RO +520.528 and pressure buildup for all four retrorockets began within 0.02 sec of each other at RO +520.57 sec. The chamber pressure profiles for the four rockets were very similar and the maximum difference in burntimes was 0.10 sec.

Table 10-1 presents significant data for the individual rocket motors. All performance parameters were close to their nominal values. The average chamber pressure was slightly higher than nominal and the average burntime was slightly shorter. The chamber pressure, integrated over the burntime, was slightly greater than nominal. These parameters indicate slightly higher than nominal motor performance. Available information was insufficient for calculating thrust from the chamber pressure data. As a result, total impulse could not be computed. Chamber pressure profiles for the retrorockets are shown in Figure 10-1.

10.2 Ullage Rockets

Ullage rocket performance was satisfactory. The Ullage Rocket Ignition Command was given at RO +520.432 sec, with the jettison command at RO +532.525 sec. These times, relative to Engine Start Command, were very close to predicted. Table 10-2 presents the individual rocket motor performance parameters as defined in the Thiokol Chemical Co. model specification, SP-544A, dated 29 November 1965. A comparison of these data with nominal performance limits indicates that both motors performed within design specifications. Figure 10-2 presents the thrust profiles during firing.

Section 10
Solid Rockets

The solid rocket motors on the S-II and S-IVB stages performed satisfactorily and accomplished their intended purpose. The S-II was separated from the S-IVB stage by the retrorockets, and the S-IVB propellants were settled prior to first burn engine ignition by the ullage rockets

TABLE 10-1
RETROCKET PERFORMANCE

PARAMETER	MOTOR A (POS IV-I, D0153)	MOTOR B (POS II-III, D0154)	MOTOR C (POS I-II, D0155)	MOTOR C (POS III-IV, D0156)	AVERAGE	NOMINAL AT 520 DEG R
Burntime* (sec)	1,475	1,52	1,56	1,46	1,504	1,538
Average chamber pressure during burn (psia)	1,828	1,766	1,790	1,831	1,804	1,710
Chamber pressure integrated over burntime: $\int P_c dt$ (psia-sec)	2,697	2,684	2,795	2,673	2,712	2,645
Average burn rate during burn-time (in./sec)	1,047	1,016	0,990	1,058	1,028	1,005
Theoretical burntime** (sec)	1,505	1,523	1,515	1,505	1,512	1,538

*The interval between the time at which the pressure attains 10 percent of the maximum pressure during the buildup portion of the pressure curve, and the time at which the bisector of an angle (formed by the intersection of a line tangent to the pressure curve just prior to decay and a line tangent to the descending portion of the pressure curve) intersects the pressure curve.

**Theoretical burntime = $\frac{\text{Web thickness (W)}}{\text{Burn rate (r)}}$ where $W = 1.544 \pm 0.036$ in. and $r = 0.860 \left[\frac{P_c}{1000} \right]^{0.29}$ (P_c in psia).

Section 10
Solid Rockets

TABLE 10-2
ULLAGE ROCKET PERFORMANCE

PARAMETER	UNITS	MOTOR A (POS II-III, D0216)	MOTOR B (POS IV-I, D0217)	NOMINAL PERFORMANCE LIMITS	
				MAXIMUM	MINIMUM
Action time*	sec	5.93	5.93	6.08	5.01
Burntime**	sec	3.86	3.87	4.10	3.54
Maximum chamber pressure	psia	1,002	991	1,220	900
Maximum ignition chamber pressure	psia	1,010	1,008	1,470	--
Average action time chamber pressure	psia	730	725	880	680
Average burntime chamber pressure	psia	984	973	1,100	890
Maximum thrust	lbf	3,477	3,439	4,150	2,600
Maximum ignition thrust	lbf	3,505	3,498	5,100	--
Average action time thrust	lbf	2,534	2,515	3,045	2,345
Average burntime thrust	lbf	3,414	3,276	3,786	3,090
Action time total impulse	lbf-sec	15,029	14,913	15,595	14,335
Burntime total impulse	lbf-sec	13,180	13,064	13,590	12,500

*The time interval between 10 percent of maximum chamber pressure during the start transient and 10 percent of maximum chamber pressure during the cutoff transient.

**The time interval between 10 percent of maximum chamber pressure during the start transient and 75 percent of maximum chamber pressure during the cutoff transient.

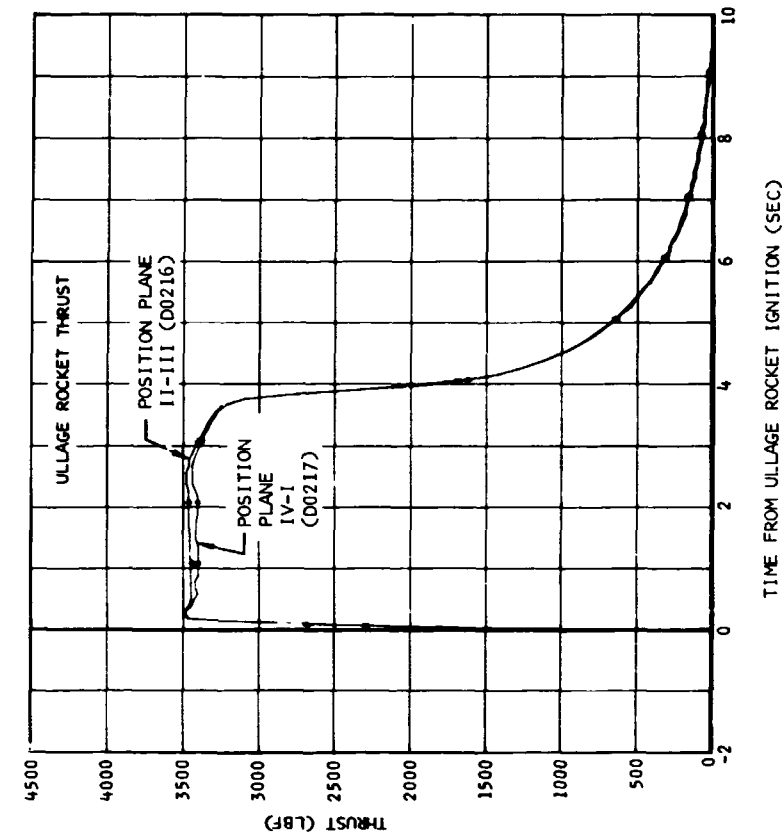


Figure 10-2. Ullage Rocket Performance

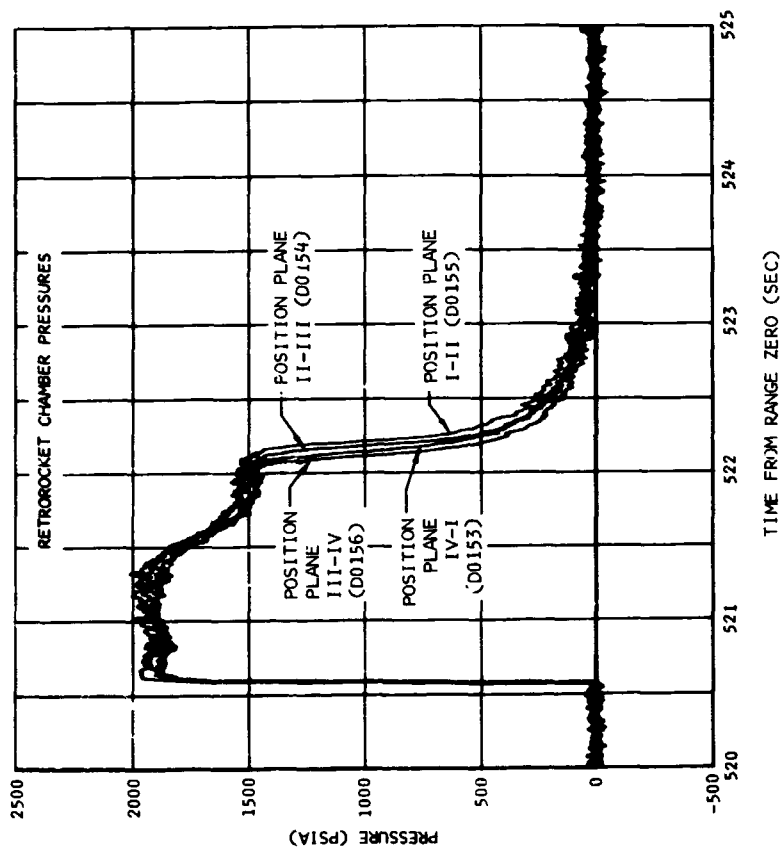


Figure 10-1. Retrorocket Performance

11. OXIDIZER SYSTEM

The oxidizer system performed satisfactorily, supplying LOX to the engine pump inlet within the specified operating limits throughout both periods of J-2 engine operation. The available net positive suction pressure (NPSP) at the LOX pump inlet exceeded the engine manufacturer's minimum requirement at all times.

11.1 Pressurization Control

The LOX tank pressurization system (figure 11-1) satisfactorily maintained pressure in the LOX tank during both periods of S-IVB powered flight. The cold helium supply was adequate; however, cold helium supply pressure decreased during the first and waiting orbit. The repressurization system was not required to repressurize the LOX tank for second burn.

11.1.1 First Burn

11.1.1.1 Prepressurization and Boost

LOX tank prepressurization started at R0 -167 sec and increased the LOX tank ullage pressure from ambient to 40.5 psia within 15 sec (figure 11-2). Two makeup cycles were required to maintain the LOX tank ullage pressure before the ullage temperature stabilized. The pressurization control pressure switch controlled the pressure between 39 and 40.5 psia. At R0 -97 sec, the ullage pressure increased from 40 to 42.6 psia because of LH2 tank prepressurization, with a minor contribution from the LOX vent valve purge and the LOX pressure sense line purge. Table 11-1 compares prepressurization data from the S-IVB-501 and 502 acceptance firings to that from S-IVB-501 flight.

During the first 10 sec of S-IC boost, the ullage pressure decreased 1.2 psia (from 42.4 to 41.2 psia). The pressure continued to decrease to a minimum of 39.9 psia after 100 sec of boost, then increased to 40.5 psia by S-IC cutoff. The pressure was relatively stable at 40 psia during S-II boost, increasing slightly to 40.2 psia by S-IVB first burn Engine Start Command (ESC1).

Section 11 Oxidizer System

The initial ullage pressure decrease after liftoff may have been caused by LOX slosh, which tends to chill the ullage. The chilling continued through S-IC boost, as shown by the ullage temperatures in figure 11-2. The pressure was relatively stable during S-II boost because the g force was lower and the ullage collapse was less than it was during S-IC boost.

11.1.1.2 Pressurization

The LOX tank ullage pressure and temperature and the pressurant flowrate are shown in figure 11-3. The ullage pressure was 40.2 psia at first burn Engine Start Command, satisfying the engine start requirements, and was sufficient throughout S-IVB powered flight to meet the minimum NPSP requirement. During the start transient, the ullage pressure decreased to a minimum of 35.8 psia before the pressurant flowrate became large enough to increase the ullage pressure. During first burn the ullage pressure cycled three more times than predicted because the ullage pressure decrease during the start transient was 1 psia more than predicted and the control band was smaller than that used for the predictions.

The ullage pressure increased slightly during the first few seconds after first burn Engine Start Command because the pressurization system was activated at first engine start and allowed the pressurant to flow during the 3-sec fuel lead.

The LOX tank pressurant flowrate varied from 0.38 to 0.42 lbm/sec during overcontrol system operation, and from 0.25 to 0.3 lbm/sec during undercontrol. This variation is normal because the heat exchanger bypass orifice inlet temperature changes as the system chills down. During S-IVB first burn, 47 lbm of helium were used; 332 lbm had been loaded. Table 11-2 compares the pressurization system data from S-IVB-501 and 502 acceptance firings to that from S-IVB-501 flight.

11.1.1.3 Cold Helium Supply

The cold helium supply was more than adequate to meet flight requirements. The cold helium supply system data are presented in table 11-3 and figure 11-4. The values quoted for mass calculations were based upon

sphere temperatures and pressures at the indicated times. The results of these mass calculations disagree with the results obtained by flow integration and are considered inferior to them because the spheres are at different temperatures and the compressibility factor cannot be exactly determined.

11.1.1.4 J-2 Engine Heat Exchanger

The J-2 engine heat exchanger performance data are presented in figure 11-5 and compared to S-IVB-501 and 502 acceptance firing data in table 11-4. The heat exchanger outlet temperature increased to 925 deg R by the end of 50 sec of engine operation. The temperature continued to increase to a maximum of 1,000 deg R at 9 sec prior to first burn Engine Cutoff Command (ECC1). The flowrate through the heater was relatively constant at the values given in the table.

11.1.2 Second Burn

11.1.2.1 Repressurization

The repressurization system was not required since the LOX tank ullage pressure at repressurization initiation was above the repressurization upper pressure limit. The LOX tank ullage conditions during the intended repressurization period are shown in figure 11-6. A discussion of the events that led to the high LOX tank ullage pressure at the initiation of repressurization is given in paragraph 11.2.1.

11.1.2.2 Pressurization

At second burn Engine Start Command (ESC2), the LOX tank ullage pressure (figure 11-7) was 42.6 psia, thus satisfying the engine start requirement. During second burn the ullage pressure cycled between 39 and 40.2 psia three times, which was one cycle less than predicted. The number of cycles was fewer than predicted and the ullage collapse was less than predicted. Throughout second burn the ullage pressure was sufficient to meet the minimum NPSP requirements.

Section 11 Oxidizer System

The pressurant flowrate varied from 0.28 to 0.33 lbm/sec during under-control system operation, and from 0.4 to 0.46 lbm/sec during overcontrol. Based on flow integration, 95 lbm of helium were used during the second period of S-IVB powered flight. The pressurization system performance during second burn is compared to that of S-IVB-501 and 502 stages during acceptance firing in table 11-2.

11.1.2.3 Cold Helium Supply

The cold helium supply during second burn was adequate. Existing data indicate that, after second burn engine cutoff, the pressure remained essentially constant at approximately 800 psia. (It slowly increased to 830 psia, then decreased to 800.) Significant data are presented in table 11-3 and figure 11-8. This system is further discussed in paragraph 11.1.1.3.

11.1.2.4 J-2 Engine Heat Exchanger

The J-2 engine heat exchanger performance data during second burn are presented in figure 11-9 and compared to S-IVB-501 and 502 acceptance firing data in table 11-4.

11.2 Pressurization System Conditions During Orbit

11.2.1 LOX Tank Conditions

The LOX ullage gas temperatures and liquid temperatures during the first and second orbits are shown in figure 11-10. During this period, the temperature probes indicated liquid temperatures, which suggests that liquid was dispersed throughout the ullage. The validity of this contention is doubtful as the acceleration provided by the continuous vent is sufficient to settle the liquid to the bottom of the tank; however, due to the J-2 engine shutdown transients and a pitchdown maneuver after first burn, a liquid spray may have been dispersed into the ullage. A few drops of the spray apparently settled on the gas temperature probes (C0029 and C0059). At the same time temperature probes C0099, C0100, and C0101 indicated that the liquid was creeping up the instrumentation probe, thereby filling the probe and temperature canisters.

Section 11
Oxidizer System

Because of the low g condition, the liquid remained in the canisters until some time after second burn Engine Start Command. This theory is supported by the data in figure 11-7, which show the 101, 100, and 80 percent liquid level probe temperatures taking their characteristic drop as though the probes were emerging from the liquid. Therefore, even though the liquid level at second burn Engine Start Command is below 80 percent, the ullage gas temperature during orbit cannot be determined.

During orbital coast, the aft end of the tank became quite warm as indicated by the position 1 and 2 probes and by the 1 percent gas probe (figure 11-10). During the same period, the ullage became very cold as indicated by the diffuser temperature and the 101 and 100 percent gas probes. The actual temperature of the ullage was not determined for the reasons previously stated.

The LOX tank ullage pressure (figure 11-11) decreased from 40.5 to 39.15 psia by the end of the first orbit. The pressure increased during the second orbit and was 39.9 psia when a yaw and pitch maneuver took place in preparation for second burn. At this time the ullage pressure increased sharply to 42.6 psia where it stabilized until second burn Engine Start Command.

At one time during orbital coast, the level and the relative stability of the tank pressure support the cold helium leak theory discussed in paragraph 11.2.2. That is, the leakage indicated by the mass calculations passed the LOX pressurization control module shutoff valves and entered the tank. Analysis showed that a helium leakage rate of 0.0028 lbm/sec into an ullage at 200 deg R could in fact cause the pressure stability. This approach, however, was discredited; analysis indicated that, with a stable ullage pressure, the energy loss from the ullage would have to be approximately three times the predicted. This would indicate a loss of vacuum in the common bulkhead, which did not occur. In addition, the shutoff valves would have to fail in such a way as to allow a leakage of 0.0028 lbm/sec. A review of the development

Section 11 Oxidizer System

and testing of the module reveals that leakage past the shutoff valves has never been observed. Also, the cold helium dump module which is equipped with an identical poppet arrangement has never been observed to leak. It is, therefore, highly improbable that a leak past the cold helium shutoff valves did occur.

With the leakage theory uncorroborated, the tank conditions during orbit were examined to formulate a more feasible theory for the ullage pressure stability and increase prior to repressurization.

As indicated by the tank temperatures shown in figure 11-10, a warm layer of liquid and gas formed in the aft end of the tank during orbit. This theory is supported by the liquid position 1 temperature, which went off-scale-high at 173 deg R, and the 1 percent gas probe, which indicated temperatures in excess of 170 deg R. The LOX above the warm layer and gas pocket must have been pushed into the ullage as the pocket enlarged during orbit. This would tend to stabilize the ullage pressure and even cause the pressure to increase when the vehicle was in the sun or decrease when the vehicle was in the earth shadow.

This theory was applied to the tank orbital pressure analysis and the results agreed favorably with the flight data. It was found that a LOX boiloff rate of 0.014 lbm/sec, causing GOX bubbles to form in the bottom of the tank, gives an ullage pressure profile very similar to the flight data. When the mass of GOX in the bubble was added to the gases in the tank ullage during restart operations, the analysis indicated the ullage pressure would increase 2.8 psi and the mean ullage temperature would increase approximately 5 deg. This pressure rise agrees favorably with the 2.7 psi ullage pressure increase observed when the vehicle was maneuvering prior to second burn.

11.2.2 LOX Tank Venting During Third Orbit

After S-IVB second burn Engine Cutoff Command, the ullage pressure (figure 11-12) remained momentarily at 39.2 psia. Then a 10 sec programmed LOX vent at RO +11,786 sec decreased the ullage pressure to 29.2 psia. By RO +12,000 sec, the pressure had increased to 33 psia due to vaporization of the LOX residual and ullage heating. Between

RO +12,386 sec and RO +12,550 sec, the tank pressure increased from 34.0 to 35.7 psia. The sudden increase in pressure was probably due to a substantial increase in boiloff and ullage gas heating caused by the agitation to the residuals created during spacecraft separation.

After LV/SC separation, the ullage pressure continued to increase to 41.9 psia at RO +19,120 sec. At this time an oscillation developed in the ullage pressure indication, of approximately 1 cps frequency and building to an amplitude of 4.5 psi peak-to-peak (p-p) by RO +19,240 sec. The null point of the oscillations at this time was 42.4 psia. At RO +19,660 sec, the pressure responded to a tank vent dropping to a null value of 42.0 psia with 3.6 psi p-p amplitude.

The oscillation then gradually decayed to 2.5 psi p-p amplitude about a 41.9 psia null by RO +20,500 sec when a compound oscillation developed with an irregular 0.067 cps superimposed on a steady 1 cps. A maximum amplitude of 6.5 psi p-p was noted before the secondary oscillation became erratic and began to break down at approximately RO +20,670 sec. The oscillation then decayed steadily to 0.5 psi p-p about the null point of 42.1 psia at 0.8 cps frequency by RO +21,300 sec when data was temporarily lost. Although data thereafter is sketchy, the oscillations appear to have built up to 2.6 psi p-p at 1.0 cps about a null of 42.3 psia by RO +22,400 sec and to have then decreased to 1.8 psi p-p at 1.1 cps about 42.8 psia by loss of data at RO +25,000 sec.

The data first available indicated that the oscillations were due to a cycling of the vent and relief valve which cracks and reseats at approximately the upper and lower levels of the oscillation. The tank pressure, however, was 41.9 psia when the oscillations started, and the vent valve should not have opened. Absence of LOX relief operation is not supported by tank ullage temperature data, (figure 11-13), which indicated no temperature change that would be characteristic of venting, or by the APS system, which indicated no response to venting. At first glance, the oscillations appear to have the same characteristics as those which have been noted on some previous stages during several

Section 11 Oxidizer System

tests, both at STC and KSC. However, an evaluation reveals that the mechanism known to exist in these previous occurrences is dependent upon some acceleration level for continuous oscillation, and therefore, should not exist in orbit. Further investigation of both the data and the stage configuration revealed the following information and yielded the mechanism of oscillation presented below.

When oscillations were noted on the S-IVB-501 stage during the CDDT at a time when the ground supplied sense line purge was turned off, steps were taken to prevent a recurrence during the boost and burn period of flight. The sense line purge supply was moved from ground supplied helium to the stage ambient helium system through a 200 scim sintered orifice. This new supply line was not provided with a check valve. When the stage ambient helium system developed a leak in orbit, and the helium pressure decayed below the level of the LOX ullage pressure (helium regulator discharge pressure dropped below 42 psia at RO +17,000 sec), the sense line purge not only ceased, but a reverse flow, from the tank ullage, through the sense line and purge line and out the leak, was initiated. This reverse flow carried entrained LOX through the sense line and outside the confines of the LOX tank, where it flashed off. This evaporation generated gas faster than the leakage rate could carry it off and a high pressure developed. This pressure forced the LOX back up the sense line to a point where the line was surrounded by LOX, and the evaporation ceased. The continuing leakage now reduced the pressure, and the resulting delta pressure along the length of the sense line once again drove the LOX in the line outside of the tank, causing evaporation. This cycle would continue as long as there was sufficient LOX in the ullage gas to generate gas by evaporating faster than the leakage rate. The magnitude and frequency of the oscillation are dependent upon the mass of LOX in the sense line and the heat source outside of the LOX tank.

The compound oscillation noted at RO +20,500 sec may be explained by the interaction of the previously described phenomenon operating on not one, but two masses of condensed LOX in the sense line, separated by

a gas column of some length. The entrained LOX in the sense line could quite easily have coalesced into two separate masses due to the vibratory motion of the gases.

It is obvious from the preceding discussions that the oscillations are caused by the problem in the stage pneumatic system in conjunction with the particular sense line purge configuration. Since this purge configuration is not effective on later stages, this particular oscillation mechanism should not be seen again.

11.2.3 Cold Helium Supply During Orbit

During first and second orbit, the cold helium supply pressure (figure 11-14) decreased from 1,570 to 1,430 psia - a 140-psi drop in 10,820 sec of orbital coast. Such a decrease was not indicated during the waiting orbit.

Whether the pressure decrease was a helium leak or bad data is questionable, but a search into the pressure transducer background revealed nothing that would indicate a discrepancy in the data. The sensor was tested to 140 deg R. From past calculations, the lowest temperature the transducer is expected to experience during any Saturn flight is 180 deg R after 4 1/2 hr in flight. The inside tunnel wall and the LH2 tank external wall temperatures recorded on S-IVB-501 indicate the transducer was well above 180 deg R. No discrepancies were found on this transducer. Some total supply mass calculations using maximum and minimum individual sphere temperatures were compared to the mass using average temperatures. A wide range of second burn masses can be calculated, depending on the temperature used, as shown in the following table:

<u>Time</u>	<u>Maximum Individual Sphere Temperature</u>	<u>Average Temperature</u>	<u>Minimum Individual Sphere Temperature</u>
Liftoff	332 lbm	332 lbm	332 lbm
ESC1	332 lbm	332 lbm	332 lbm
ECC1	294 lbm	294 lbm	294 lbm
ESC2	234 lbm	252 lbm	257 lbm
ECC2	168 lbm	190 lbm	203 lbm

Section 11 Oxidizer System

11.3 LOX Pump Chillover

11.3.1 First Burn

The LOX pump chillover system performed adequately. At Engine Start Command, the pump inlet conditions of 40.2 psia and 164.5 deg R were sufficient to produce an NPSP of 23.8 psi, satisfying the requirement of 12.8 psi minimum (table 11-5).

Recirculation chillover was started at R0 -278.9 sec and continued until R0 +520.9 sec when the pre valve started to open with the chillover pump still running. The pre valve-full-open signal was received at R0 +522.5 sec. The chillover pump was cut off and the shutoff valve closed approximately 0.4 sec before first burn Engine Start Command.

During chillover the pump inlet and return line pressures increased and decreased with acceleration until the pre valve was opened and the chillover pump developed head was lost. The pump inlet pressure then decreased to equal the ullage pressure. The chillover system fluid temperatures decreased during the first minute of chillover, then remained relatively constant until prepressurization (figures 11-15 and 11-16). The engine pump inlet pressure was constructed for the periods from R0 +30 to R0 +150 sec and from R0 +440 to R0 +519.8 sec because D0003 was off-scale high.

During pressurized chillover, the LOX was subcooled throughout the recirculation system. The chillover flowrate was 33.5 gpm prior to prepressurization and 35 gpm after, with a frictional pressure drop of 11.0 psi through the system. The flow coefficient, a measure of the flow resistance, was calculated from this flowrate and pressure drop data. During pressurized chillover, it was found to be $25 \text{ sec}^2/\text{in.}^2 \text{ ft}^3$.

The NPSP at the engine pump inlet was nominal at 23.6 psi at first burn Engine Start Command.

The heat input rates from the tank of the turbopump inlet (section 1), from the pump inlet to the bleed valve (section 2), and from the bleed valve to the tank inlet (section 3) decreased rapidly during the first minute of chillover. Prepressurization caused another decrease, and S-I acceleration buildup caused still another. The heat input rates remained relatively constant during the subsequent chillover process.

11.3.2 Second Burn

The LOX pump chilldown for second burn was different from that for first burn in that it started with a dry chilldown system. A special unpressurized LOX pump chilldown test was initiated 4 min prior to the initiation of restart preparations with the pre valve closed. The purpose of this test was to determine chilldown effectiveness at a lower g level than normal with the ullage engines on.

The LOX pump recirculation chilldown system performed satisfactorily (figures 11-17 and 11-18). At second burn Engine Start Command, the pump inlet pressure of 42.6 psia and temperature of 165.75 deg R were within the engine start requirements. The NPSP at second burn engine start was 25 psi, satisfying the minimum acceptable limit of 12.8 psi. Significant data are presented in table 11-5.

After approximately 40 sec of chilldown, the chilldown pump differential pressure, flowrate, and engine LOX pump pressure and temperature reached steady conditions. The chilldown system temperatures were subcooled after 60 sec and remained subcooled until the end of chilldown. After that time (ESC2 -503 sec), subcooled LOX was flowing through the entire chilldown system. The LOX tank ullage pressure was constant at 40 psia from some time before chilldown initiation until restart preparations (end of chilldown test) at ESC2 -326.0 sec. During this period, the chilldown pump differential pressure was 10.5 psid, the flowrate was approximately 36 gpm, and the engine pump inlet pressure and temperature were 48.5 psia and 165.9 deg R. However, chilldown was not complete because the bleed valve and chilldown return line temperatures and the heat input rate of section 2 were still decreasing. The LOX pump NPSP was 30.5 psi.

At ESC2 -282 sec, a 20-sec perturbation occurred in the LOX chilldown system--the chilldown pump differential pressure and flowrate dropped from nominal to near zero and recovered three times (figure 11-19) because GOX bubbles had formed on the bottom of the tank. The GOX bubble formation is attributed to heat leaks through the aft LOX dome

Section 11 Oxidizer System

during coast. APS ullage acceleration forces, beginning at ESC2 -327.8 sec, resulted in displacement of the formation from the tank bottom to the liquid surface. As a result of the APS ullage pitch and yaw maneuvers at ESC2 -326 sec, the formation slowly rose from the bottom of the tank and passed the chilldown pump inlet. During this displacement, some of the bubbles entered the LOX chilldown system. Since the chilldown pump recovered to its previous level of performance, this two-phase flow disruption did not degrade the chilldown.

The LOX tank ullage pressure started an increase of 2.5 psia at restart initiation (paragraph 11.2), thus causing a small shift in data. When the prevalve was opened at ESC2 -9.8 sec, the engine LOX pump inlet pressure dropped from 52.0 to 43.0 psia (the same value as the ullage pressure), and the pump inlet temperature was constant at 165.6 deg R. The heat input of section 2 remained constant at 4,000 Btu/hr until second burn Engine Start Command. The LOX system chilldown was complete because all parameters had stabilized long before second burn Engine Start Command.

11.4 Engine LOX Supply

The engine LOX supply system (figure 11-20) delivered the necessary quantity of LOX to the engine pump inlet throughout both firings.

11.4.1 First Burn

The NPSP at the engine interface (figure 11-21) was calculated to be 23.8 psi at first burn Engine Start Command. The NPSP decreased after first engine start and reached a minimum of 22.5 psi after 20 sec of powered flight, which was 1.9 psi above the 20.6 psi required at that time. During the remainder of the burn, the NPSP remained between 27.4 and 24.8 psi as it followed the ullage pressure. At the end of first burn, the NPSP was 26 psi which was 6.35 psi above the required.

The interface static pressure and temperature are shown in figure 11-21. The interface pressure was 40.2 psia at first burn Engine Start Command and reached a minimum of 36.5 psia after 20 sec of engine operation.

The pressure increased to 41 psia then cycled between 39 and 40 psia as it followed the ullage pressure. The interface pressure at Engine Cutoff Command was 40 psia; the temperature was 164.5 deg R at first burn Engine Start Command and at first burn Engine Cutoff Command.

When the LOX pump interface pressure and temperature were plotted in the engine LOX pump operating region (figure 11-22), they indicated that the engine LOX pump interface conditions were met satisfactorily throughout the first period of powered flight. The pump interface temperature, as plotted against the mass remaining in the LOX tank during engine operation is shown in figure 11-23. Table 11-6 compares the LOX supply parameters to those of S-IVB-501 and 502 acceptance firings.

11.4.2 Second Burn

The NPSP at the engine interface, shown in figure 11-24, was calculated to be 25 psi at second burn Engine Start Command. At the end of fuel lead the LOX pump NPSP increased rapidly to 28 psi then decreased to 24.2 psi and cycled from this value to 26 psi. At second burn Engine Cutoff Command, the NPSP was 24.2 psi which was 10.75 psi above the required.

The LOX pump static interface pressure (figure 11-24) followed the cyclic trends of the LOX tank ullage pressure. At second burn Engine Start Command and at the end of fuel lead, the interface pressure was 42.6 psia. During engine operation, the pressure cycled from 38.5 to 40 psia; it was 39 psia at second burn Engine Cutoff Command.

The interface temperature at second burn Engine Start Command and at the end of fuel lead was 165.75 deg R. It decreased to 165.5 deg R by 5 sec after start tank discharge then increased to 165.75 deg R by second burn engine cutoff.

When the LOX pump interface pressure and temperature were plotted in the engine LOX pump operating region (figure 11-25), they indicated that the engine LOX pump interface conditions were met satisfactorily throughout

Section 11
Oxidizer System

the second period of powered flight. The pump interface temperature was plotted against the mass remaining in the LOX tank during engine operation and is shown in figure 11-23. The flight data are compared to the S-IVB-501 and 502 acceptance firing data in table 11-6.

Section 11
Oxidizer System

TABLE 11-1
LOX TANK PREPRESSURIZATION DATA

PARAMETER	UNIT	S-IVB-501 FLIGHT	S-IVB-501 ACCEPTANCE FIRING	S-IVB-502 ACCEPTANCE FIRING
Prepressurization duration	sec	15	9	19
Number of makeup cycles		2	1	1
Prepressurization helium				
Flowrate	lbm/sec	0.26	0.8	0.321
Mass added to LOX tank during prepressurization	lbm	3.7	7.52	6.1
Mass added to LOX tank during makeup cycles	lbm	0.39	0.98	0.57
Ullage pressure				
At prepressurization initiation	psia	15.1	14.7	14.7
At prepressurization termination	psia	40.5	40.8	40.3
At liftoff*	psia	42.4		
At Engine Start Command	psia	40.2		36.8
Events (sec from liftoff*)				
Prepressurization initiation		-167	-158.5	-163
Prepressurization termination		-152	-149.5	-144
Engine Start Command		520.7	512.5	511.0

*Liftoff is simulated during acceptance firing.

Section 11
Oxidizer System

TABLE 11-2
1. . . TANK PRESSURIZATION DATA

PARAMETER	UNIT	S-IVB-501 FLIGHT		S-IVB-501 ACCEPTANCE FIRING		S-IVB-502 ACCEPTANCE FIRING	
		FIRST BURN	SECOND BURN	FIRST BURN	SECOND BURN	FIRST BURN	SECOND BURN
Number of secondary flow intervals		6	3	4	11	3	3
Pressure control band							
Minimum	psia	39.0	38.9	38.0	38.0	38.0	38.0
Maximum	psia	40.0	40.0	39.5	39.5	39.7	39.8
Ullage pressure							
At Engine Start Command	psia	40.2	42.6	38.0	38.0	38.0	35.0
Minimum during start transient	psia	35.8	38.8	34.7	37.1	33.8	34.6
At Engine Cutoff Command	psia	40.0	39.0	39.2	38.9	35.6	39.5
Pressurant total flowrate							
During undercontrol	lbm/sec	0.25 to 0.30	0.28 to 0.33	0.25 to 0.30	0.25 to 0.29	0.26 to 0.28	0.28
During overcontrol	lbm/sec	0.38 to 0.42	0.40 to 0.46	0.38 to 0.43	0.37 to 0.42	0.38 to 0.40	0.40 to 0.41
Maximum LOX tank vent inlet temperature	deg R	495	420	542	415	550	460

TABLE 11-3
COLD HELIUM SUPPLY DATA

PARAMETER	UNIT	S-IVB-501 FLIGHT		S-IVB-501 ACCEPTANCE FIRING		S-IVB-502 ACCEPTANCE FIRING	
		FIRST BURN	SECOND BURN	FIRST BURN	SECOND BURN	FIRST BURN	SECOND BURN
Pressure							
At Liftoff	psia	2,910	--	3,155	--	3,280	--
At Engine Start Command	psia	2,910	1,430	3,035	1,910	3,200	2,425
At Engine Cutoff Command	psia	1,570	800	1,525	860	1,670	1,090
Average temperature							
At Liftoff	deg R	41.0	--	40.0	--	41.0	--
At Engine Start Command	deg R	40.0	38.5	40.0	57.0	40.0	56.0
At Engine Cutoff Command	deg R	32.5	35.0	31.0	52.0	31.5	44.0
Helium mass							
At Engine Start Command	lbm	332	252	340	220	345	282
At Engine Cutoff Command	lbm	294	190	265	138	295.2	192
Usage calculated from sphere Conditions	lbm	38	62	75	92	50	90
Usage calculated by integration of flowrate	lbm	47	95	50.4*	93.9*	50.2	105.5

*Cold helium leak in spheres 1 and 7 as well as in the cold helium fill module check valve (no evidence of leakage during second burn according to mass).

Section 11
Oxidizer System

TABLE 11-4
J-2 HEAT EXCHANGER PERFORMANCE DATA

PARAMETER	UNIT	S-IVB-501 FLIGHT		S-IVB-501 ACCEPTANCE FIRING		S-IVB-502 ACCEPTANCE FIRING	
		FIRST BURN	SECOND BURN	FIRST BURN	SECOND BURN	FIRST BURN	SECOND BURN
Flowrate through heat exchanger							
During overcontrol	lbm/sec	0.2	0.22	0.20	0.20	0.20	0.21
During undercontrol	lbm/sec	0.073	0.074	0.075	0.075	0.075	0.075
Heat exchanger inlet temperature							
During overcontrol	deg R	50	50	70	70	75	70
During undercontrol	deg R	60	63	85	89	100	100
Minimum	deg R	45	39	65	70	70	75
Heat exchanger outlet temperature							
At end of 50-sec transient	deg R	925	940	965	935	960	940
During overcontrol	deg R	*	930	985	860	985	915
During undercontrol	deg R	*	985	1,000	890	1,000	940
At Engine Cutoff Command	deg R	990	985	992	890	995	950
Heat exchanger outlet pressure							
During overcontrol	psia	350	340	370	350	360	350
During undercontrol	psia	410	418	425	415	420	420
Average LOX vent inlet pressure							
During overcontrol	psia	67	65	67	65	64	64
During undercontrol	psia	52	50	48	46	47	47
Maximum LOX vent inlet temperature	deg R	495	420	542	555	550	540

*Temperature did not stabilize,

Section 11
Oxidizer System

**TABLE 11-5
LOX CHILLDOWN SYSTEM PERFORMANCE DATA**

PARAMETER	UNIT	S-IVB-501 FLIGHT		S-IVB-501 ACCEPTANCE FIRING		S-IVB-502 ACCEPTANCE FIRING	
		FIRST BURN	SECOND BURN	FIRST BURN	SECOND BURN	FIRST BURN	SECOND BURN
NPS?							
At Engine Start Command	psi	23.8	25	26.8	25.1	27.6	22.8
Minimum required at engine start	psi	12.8	12.8	12.8	12.8	12.8	12.8
At opening of prevalve	psi	45.5	34.0	35.3	--	36.0	31.5
Pump inlet conditions							
Pressure at Engine Start Command	psia	40.2	42.6	44.3	42.8	44.8	40.2
Temperature at Engine Start Command	deg F	164.5	165.75	165.6	165.8	165.4	165.4
Average flow coefficient	sec ² /in. ² ft ³	25.0	25.0	13.6	--	14.4	13.27
Heat absorption rate							
Section 1 (tank to pump inlet)	Btu/hr	500	500	5,500	--	2,900	4,110
Section 2 (pump inlet to bleed valve)	Btu/hr	3,500	4,000	19,000	--	13,600	24,570
Section 3 (bleed valve to tank inlet)	Btu/hr	3,500	2,000	1,500	--	4,400	6,120
Total	Btu/hr	7,500	6,500	26,000	--	20,900	34,800
Chilldown flowrate							
Unpressurized	gpm	33.5	--	38.5	19 - 35	38.7	38.6
Pressurized	gpm	35.0	37.0	42	42	40.9	40.9
Chilldown system pressure drop							
Unpressurized	psi	9.2	--	7.4	--	6.6	6.6
Pressurized	psi	11.0	10.5	8.5	--	8.3	7.7
Events**							
Chilldown initiation	sec	-278.9	-562.7	-202.9	-715.4	-203.8	-719.7
Prevalve closed	sec	-272.5	-552.0	--	--	--	--
Repressurization initiation	sec	-166.7	-326.0	-158.5	-472.3	-159.5	-700.4
Prevalve open command	sec	520.0	-10.8	509.4	-3.1	509.37	-3.14
Prevalve closed signal dropout	sec	520.9	-9.8	510.1	-2.3	510.31	-2.12
Prevalve open signal pickup	sec	522.5	-7.9	511.4	-0.9	511.59	-0.91
Delay between prevalve open command and pickup of open signal	sec	2.503	2.894	2.0	2.2	2.22	2.23
Chilldown shutoff valve closed	sec	625.298†	Not sent	512.0	-0.4	511.1	-1.7
Engine Start Command	sec	520.7	0	512.5	0	511.9	0

*During acceptance firing, liftoff is simulated.

**All first burn data are referenced to liftoff (or simulated liftoff); all second burn data are referenced to second Engine Start Command.

†LOX chilldown valve closed switch (K0139) failed before liftoff (open dropout used).

Section 11
Oxidizer System

TABLE 11-6
LOX PUMP INLET CONDITION DATA

PARAMETER	UNIT	S-IVB-501 FLIGHT		S-IVB-501 ACCEPTANCE FIRING		S-IVB-502 ACCEPTANCE FIRING	
		FIRST BURN	SECOND BURN	FIRST BURN	SECOND BURN	FIRST BURN	SECOND BURN
Pump inlet conditions							
Static pressure at engine start	psia	40.2	42.6	44.3	42.8	44.8	40.2
Temperature at engine start	deg R	164.5	165.75	165.6	165.8	165.4	165.4
Temperature at engine cutoff	deg R	164.5	165.75	165.0	169.7	165.0	169.2
NPSP requirements							
Minimum at Engine Start Command	psi	12.8	12.8	12.8	12.8	12.8	12.8
At high EMR	psi	20.8	20.8	20.8	20.8	20.8	20.8
After EMR cutback	psi	N/A	14.95	14.95	14.95	14.95	14.95
NPSP available							
At Engine Start Command	psi	23.8	25.0	26.8	25.1	27.6	22.8
At start tank discharge valve open command	psi	23.6	25.0	28.0	25.5	29.0	23.5
Maximum during firing	psi	27.5	28	28	26	29	25
Time of maximum (sec from ESC)		15	8.5	3	3	4	118
Minimum during firing	psi	22.5	24.2	25.1	18.9	20.2	17.5
Time of minimum (sec from ESC)		20	ECC	ECC	ECC	ECC	ECC
At Engine Cutoff Command	psi	26	24.2	25.1	18.9	20.2	17.5
LOX feed duct							
At high EMR							
Pressure drop	psi	1.9	1.8	2.5	2.8	2.6	2.3
Flowrate	lbm/sec	448	453	459	455	462	462
After EMR cutback							
Pressure drop	psi	N/A	1.8	N/A	0.9-1.9	N/A	1.6
Flowrate	lbm/sec	N/A	381	N/A	363	N/A	400

N/A = Not applicable

Section 11
Oxidizer System

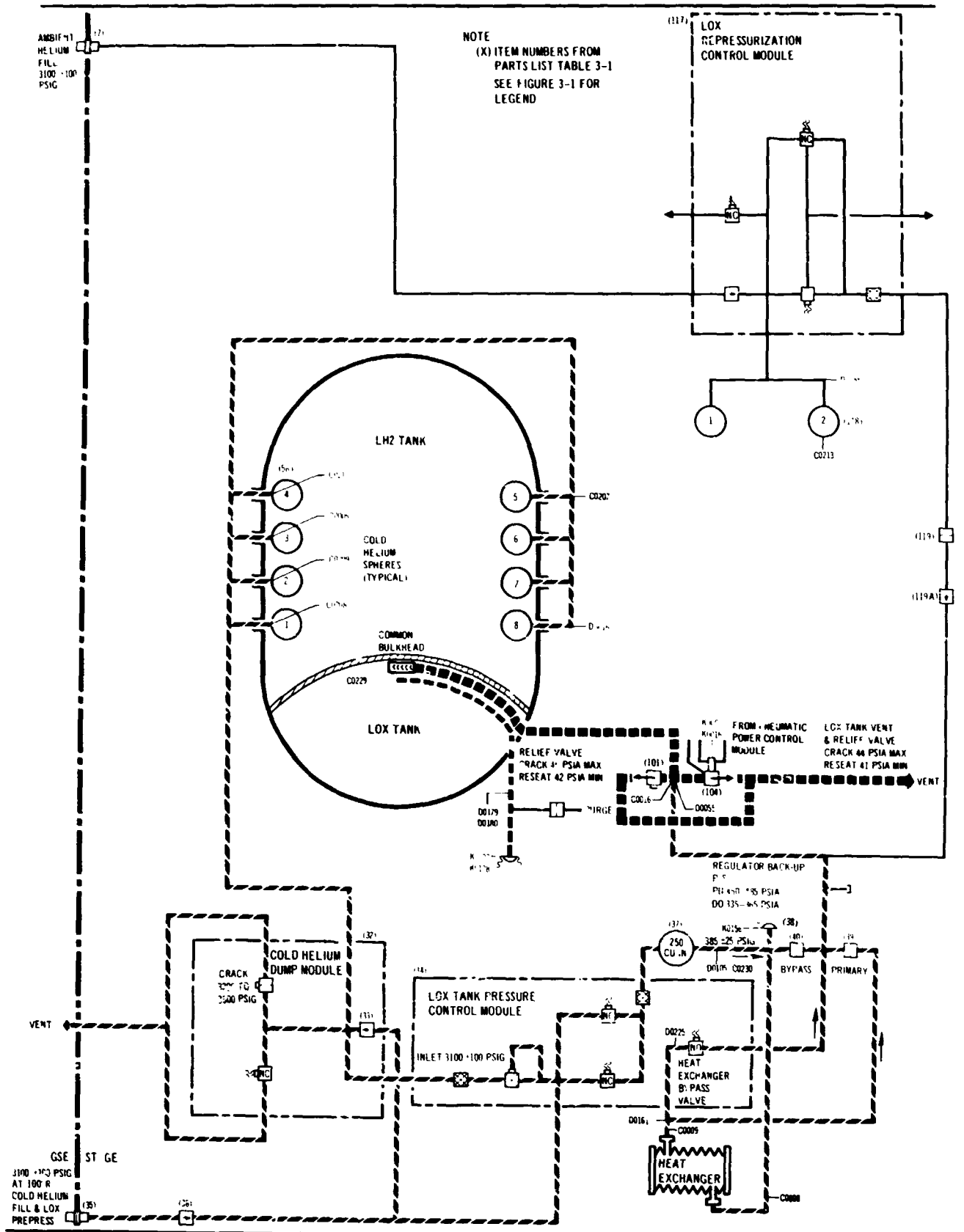


Figure 11-1. LOX Tank Pressurization System

Section 11
Oxidizer System

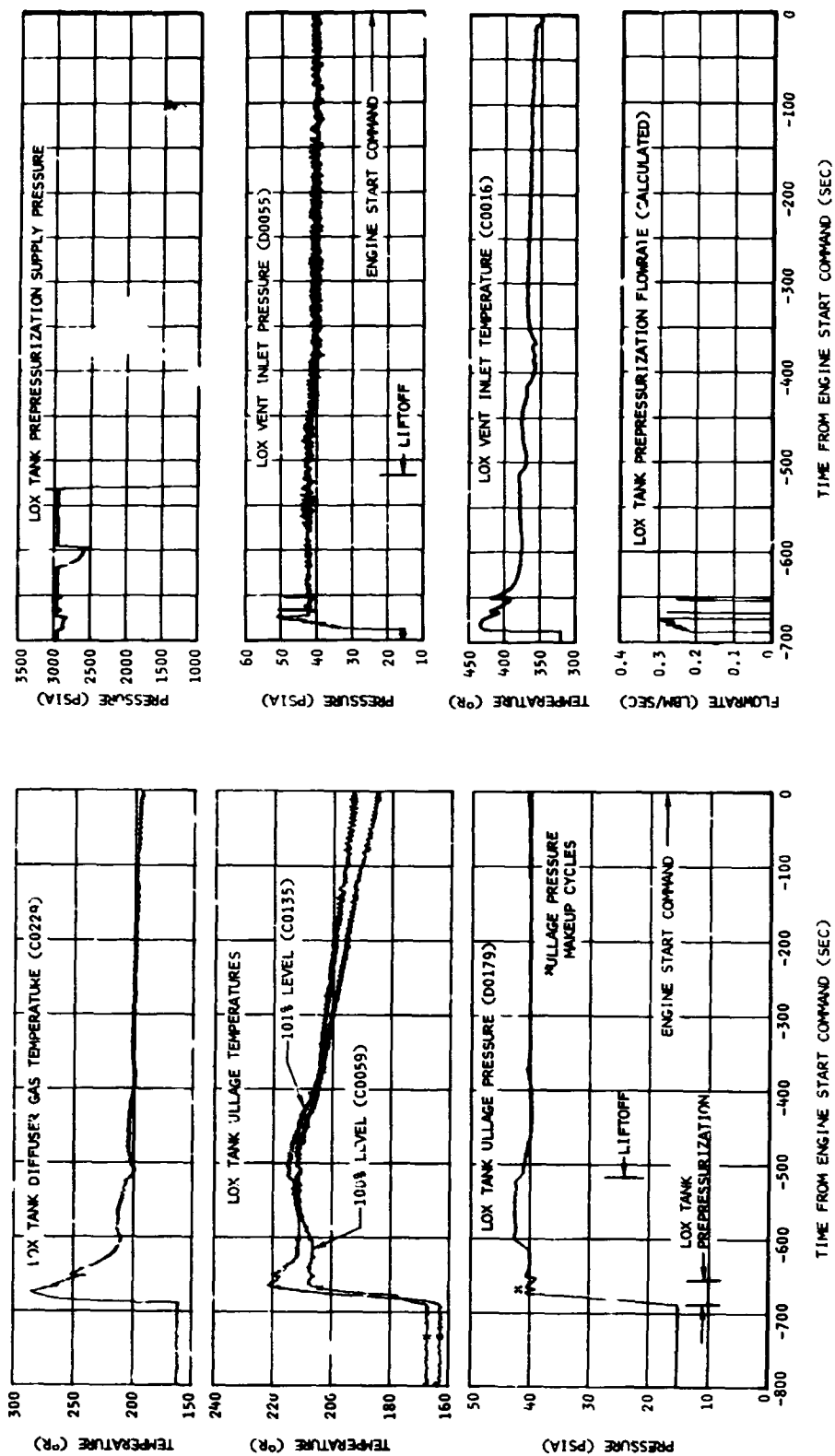


Figure 11-2. LOX Tank Conditions During Prepressurization and Boost - First Burn

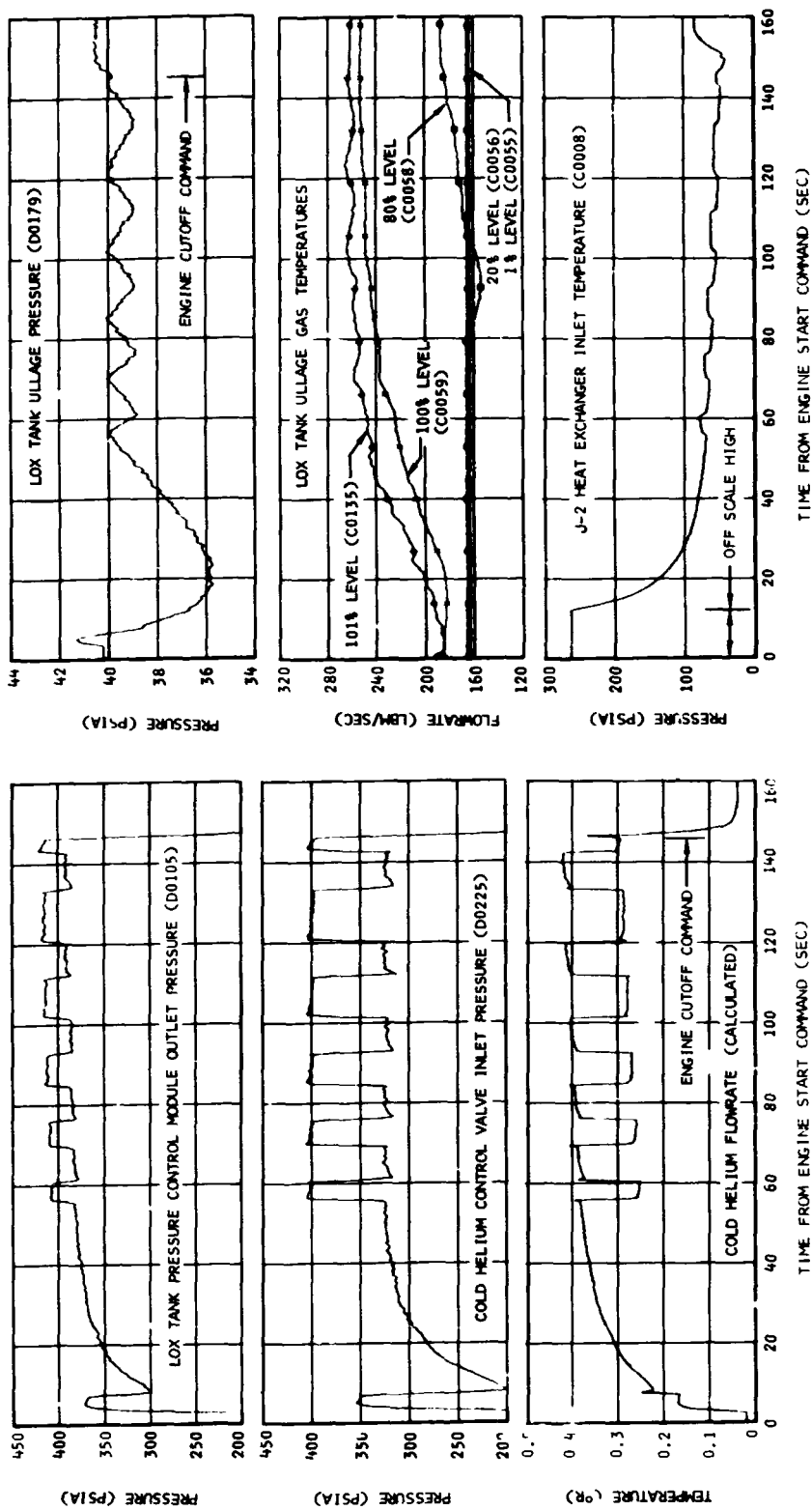


Figure 11-3. LOX Tank Pressurization System Performance - First Burn

Section 11
Oxidizer System

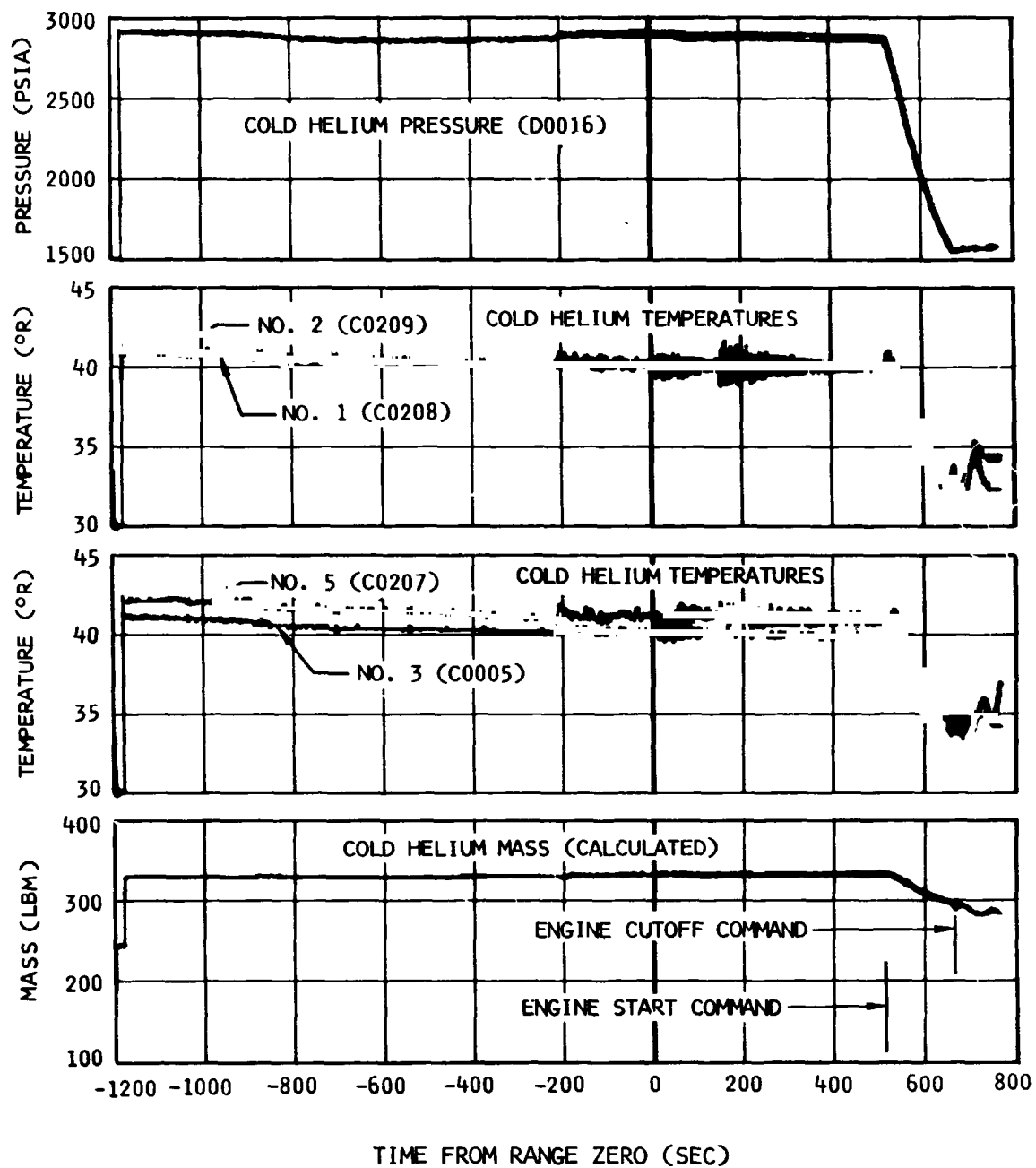


Figure 11-4. Cold Helium Supply - First Burn

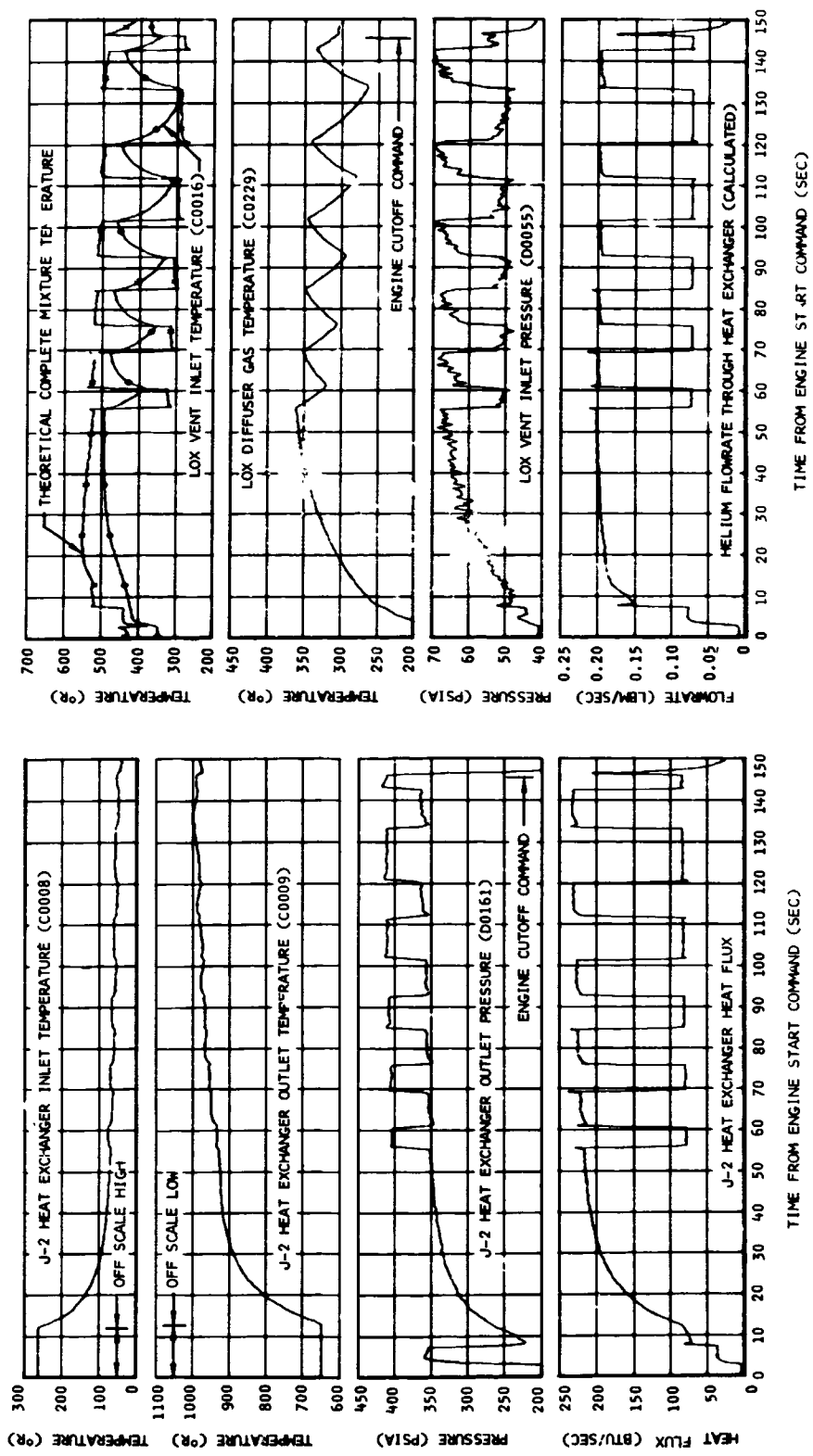


Figure 11-5. J-2 Heat Exchanger Performance - First Burn

Section 11
Oxidizer System

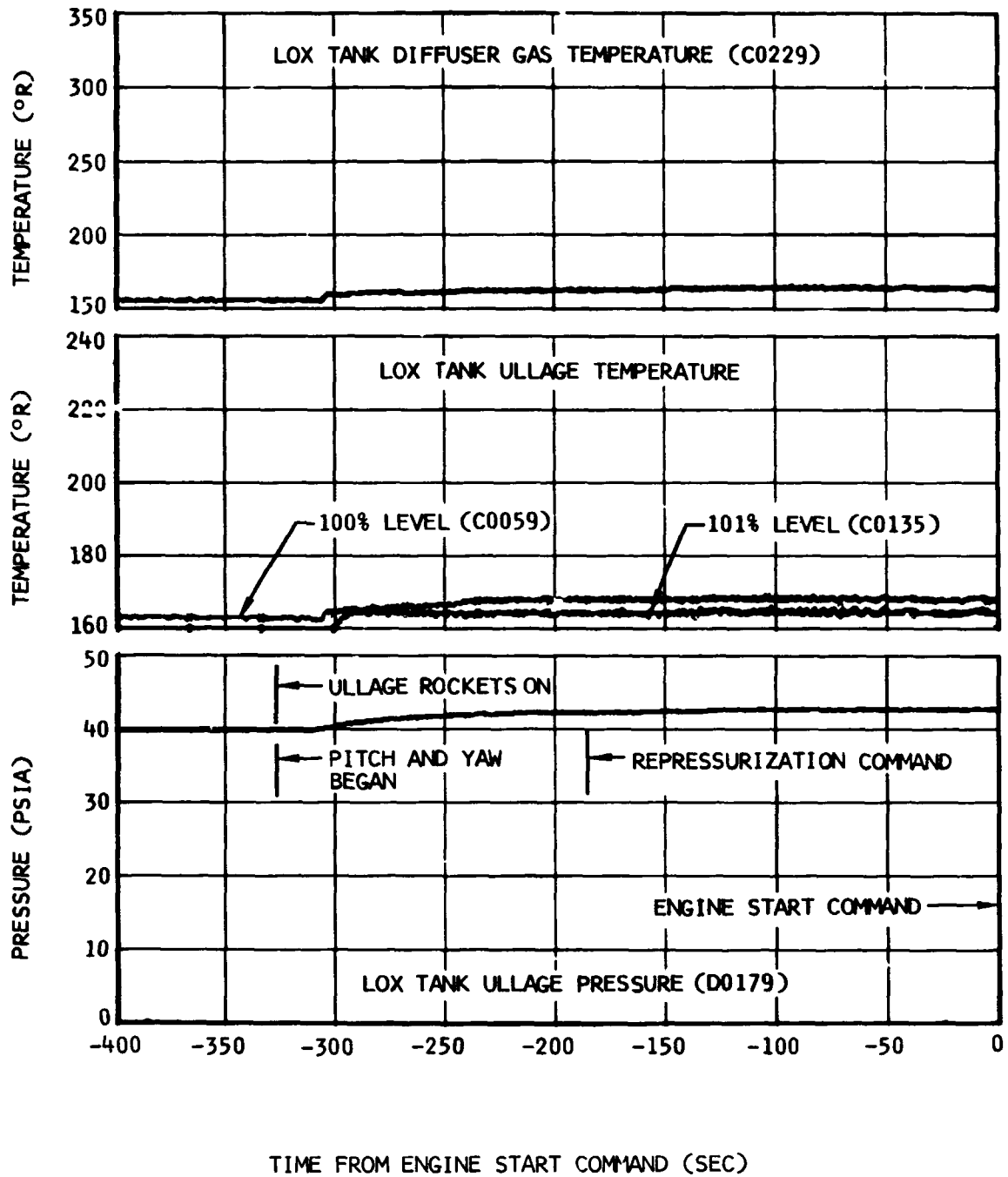


Figure 11-6. LOX Tank Conditions During Repressurization Period - Second Burn

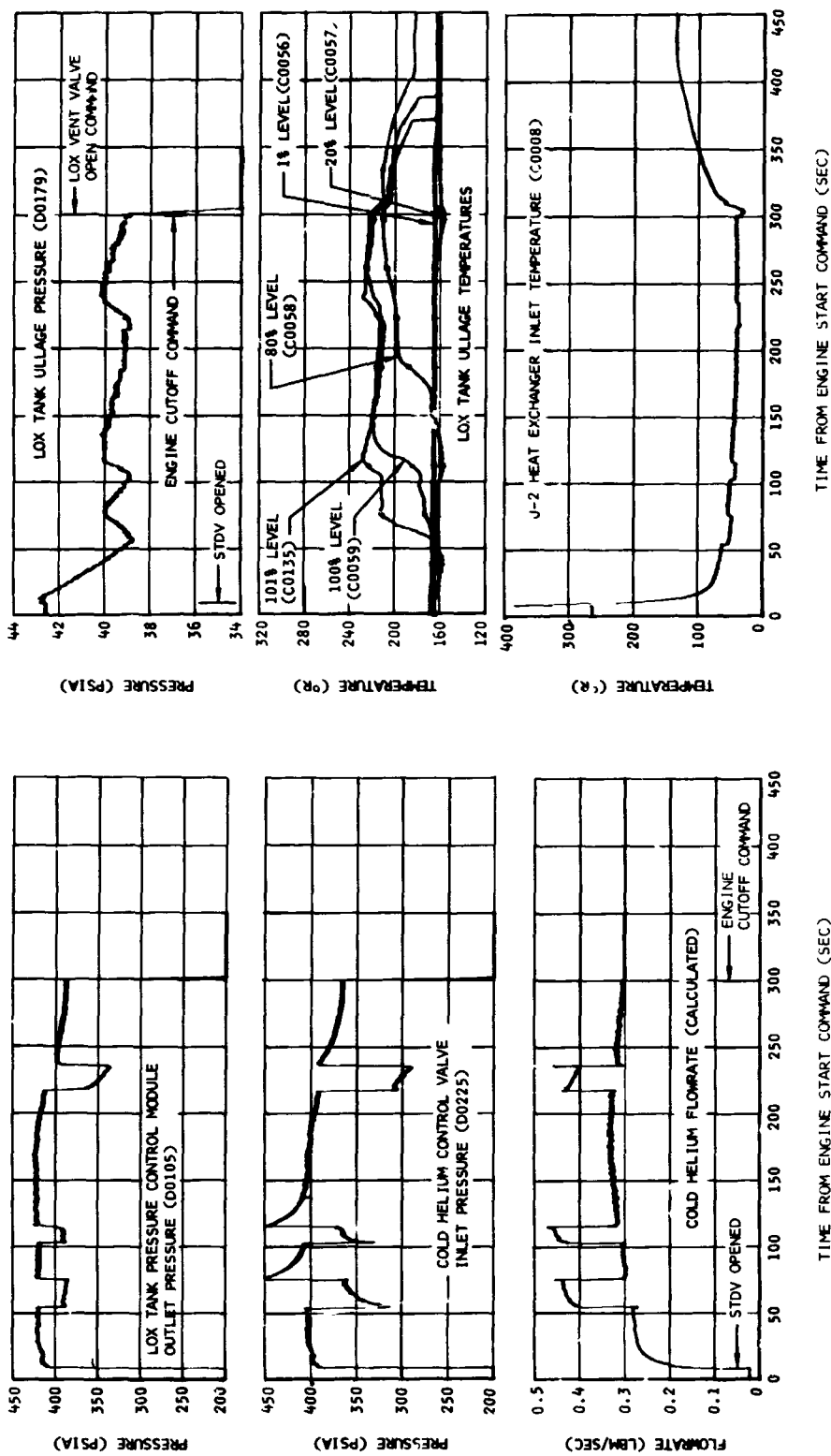


Figure 11-7. LOX Tank Pressurization System Performance - Second Burn

Section 11
Oxidizer System

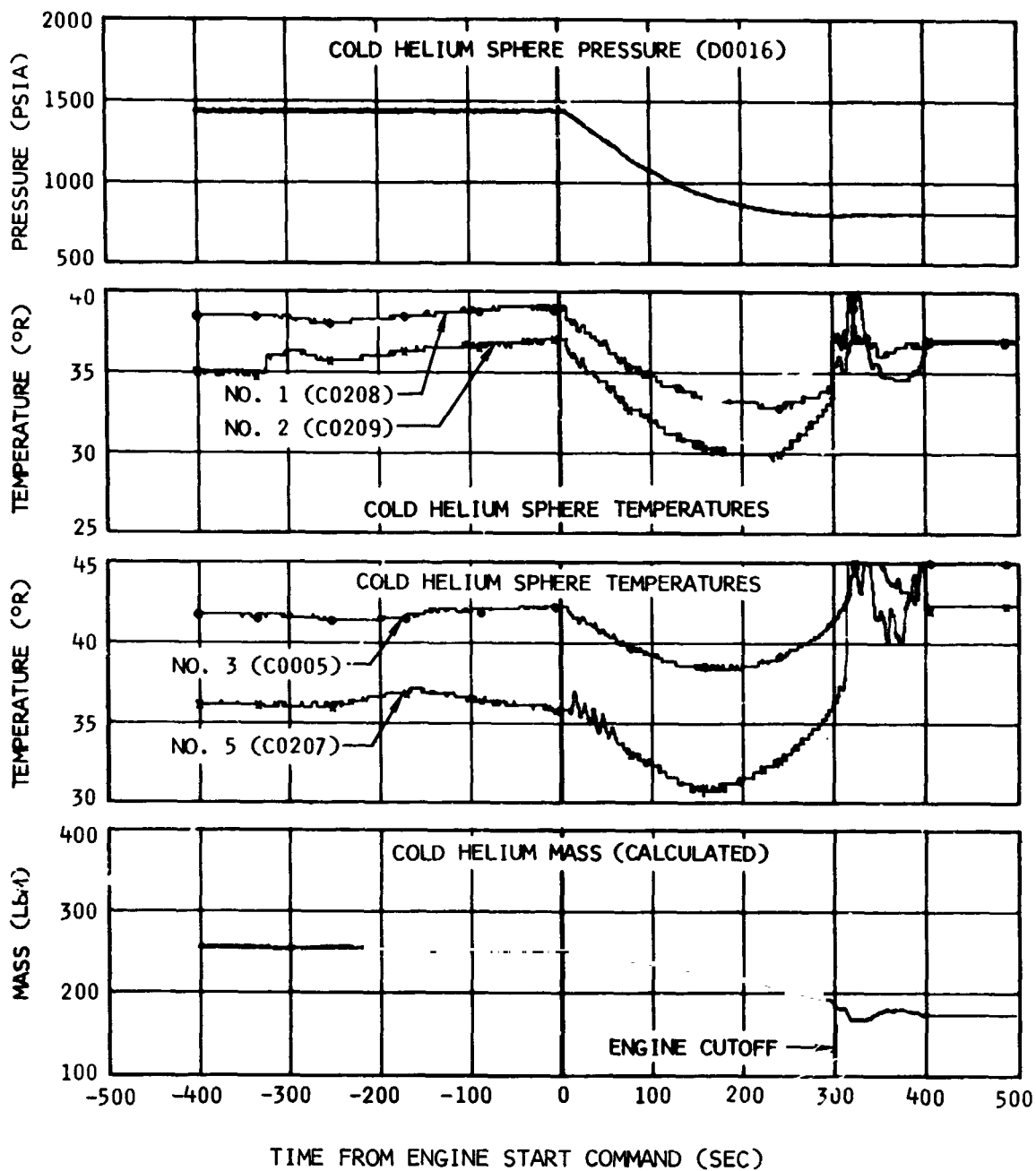


Figure 11-8. Cold Helium Supply - Second Burn

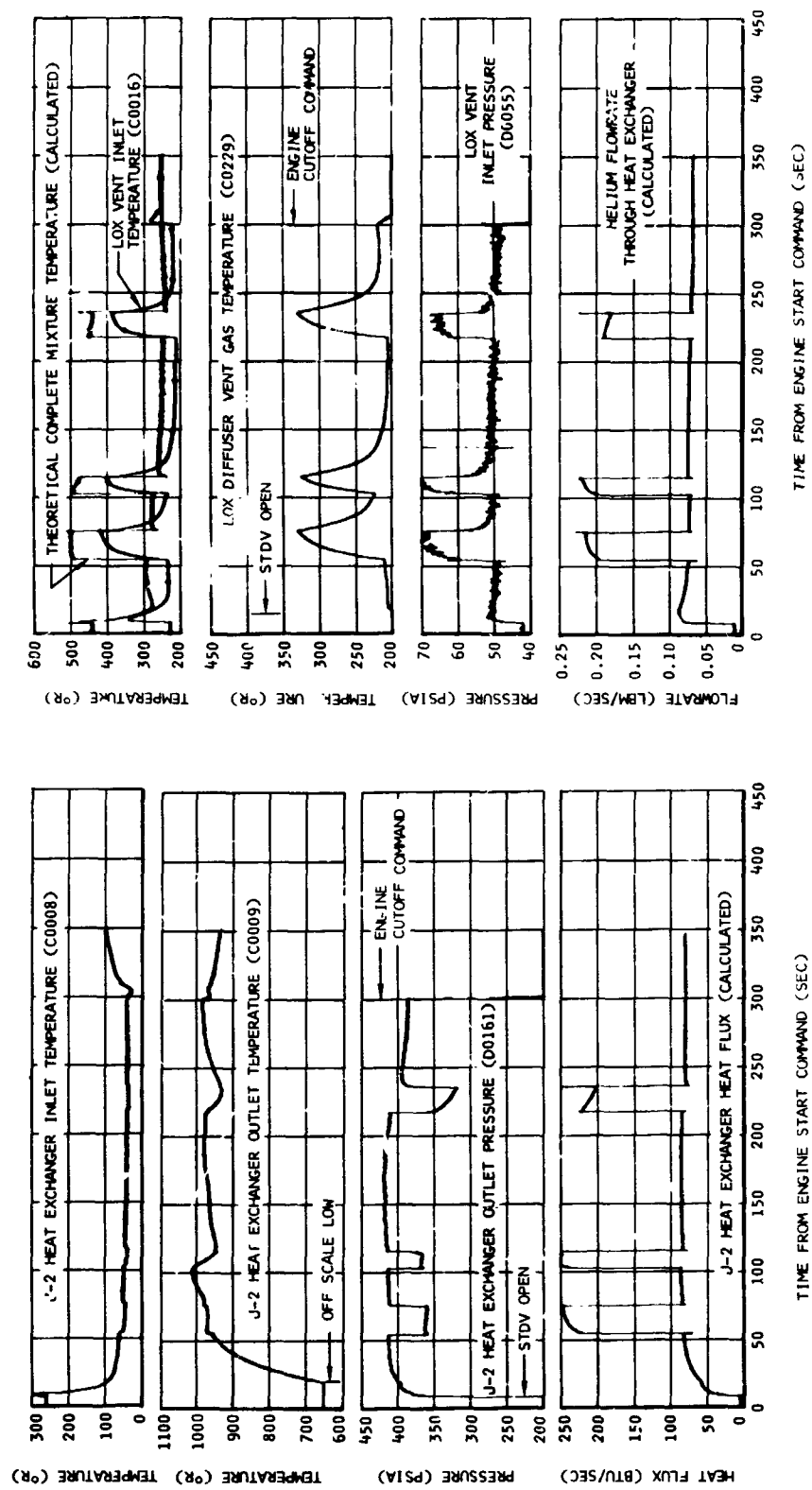


Figure 11-9. J-2 Heat Exchanger Performance - Second Burn

Section 11
Oxidizer System

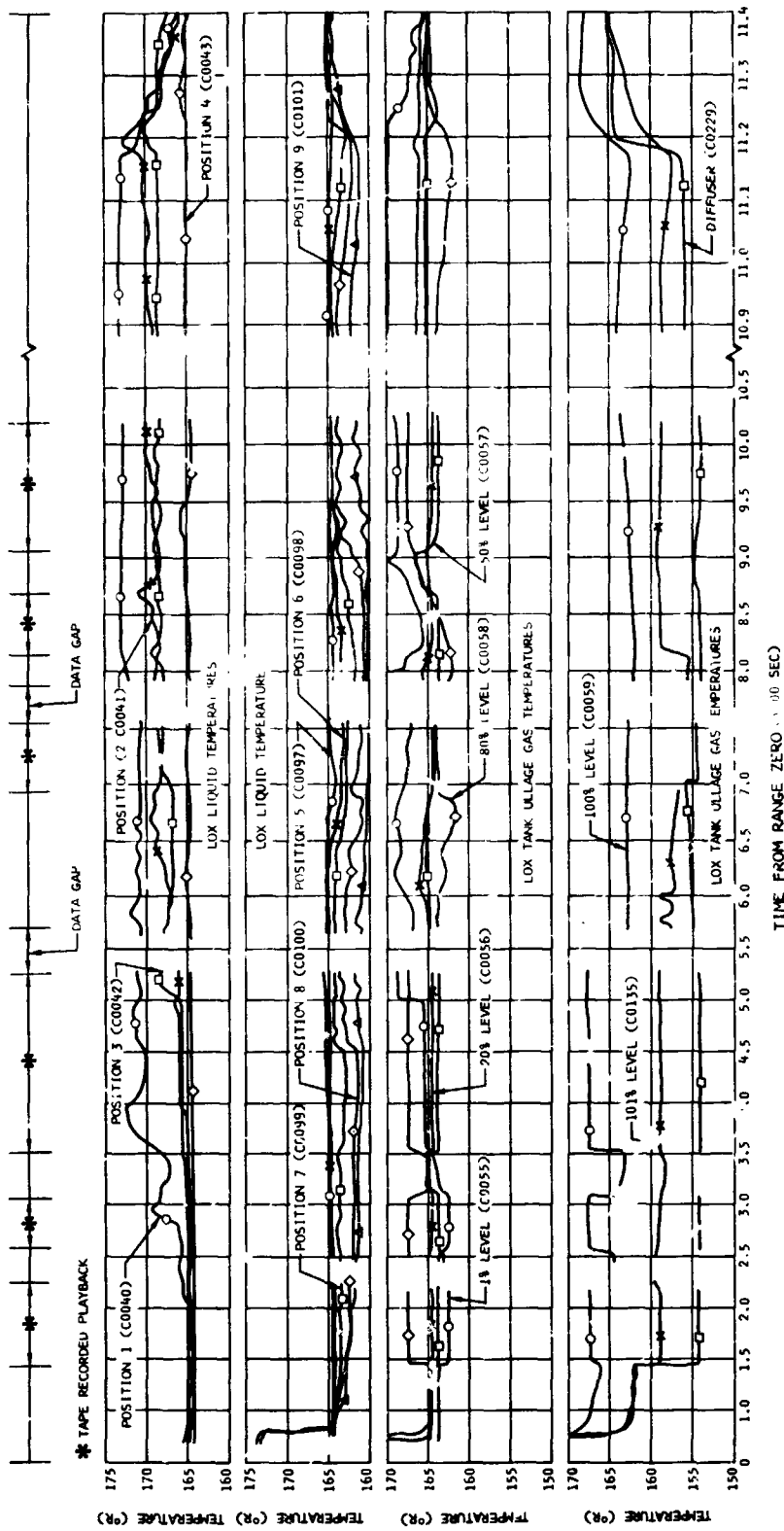


Figure 11-10. LOX Tank Temperatures During First and Second Orbits

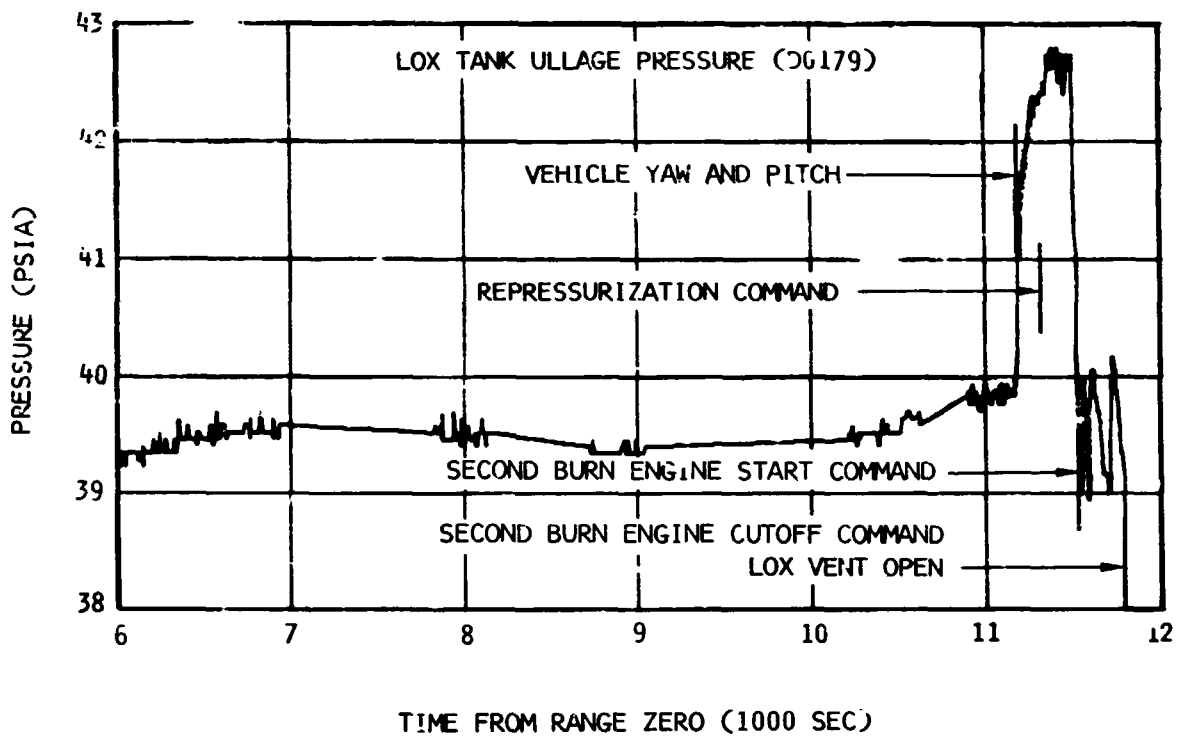
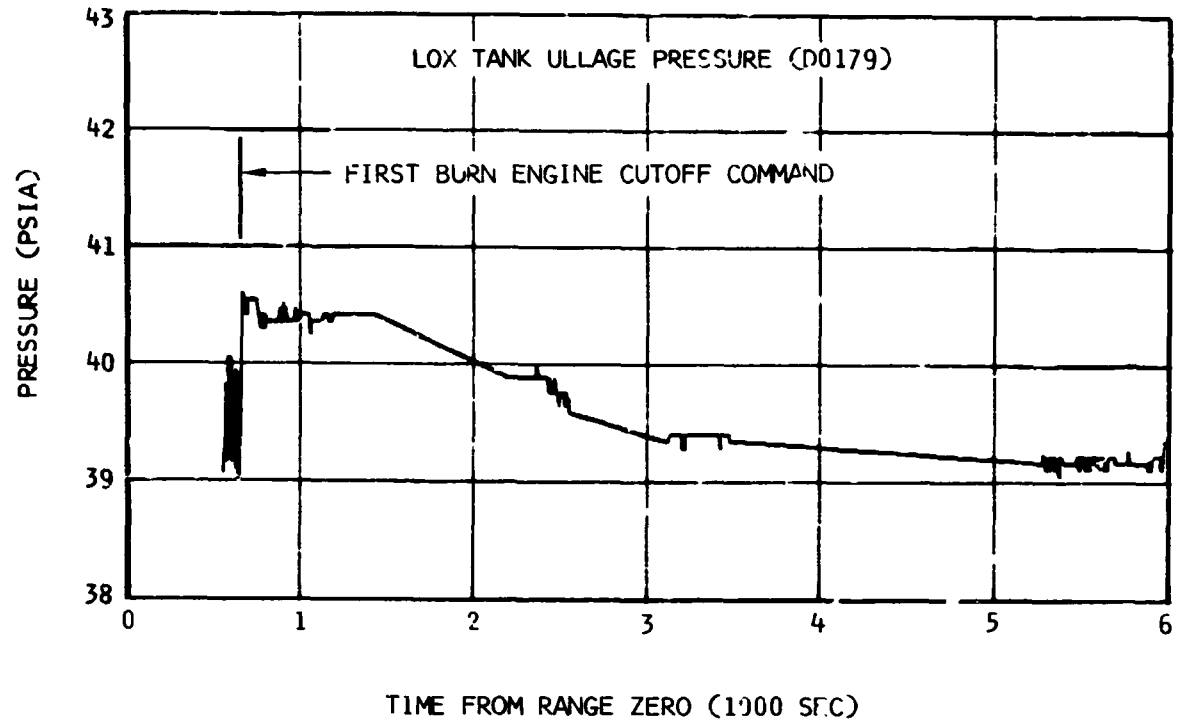


Figure 11-11. LOX Tank Ullage Pressure During First and Second Orbits

Section 11
Oxidizer System

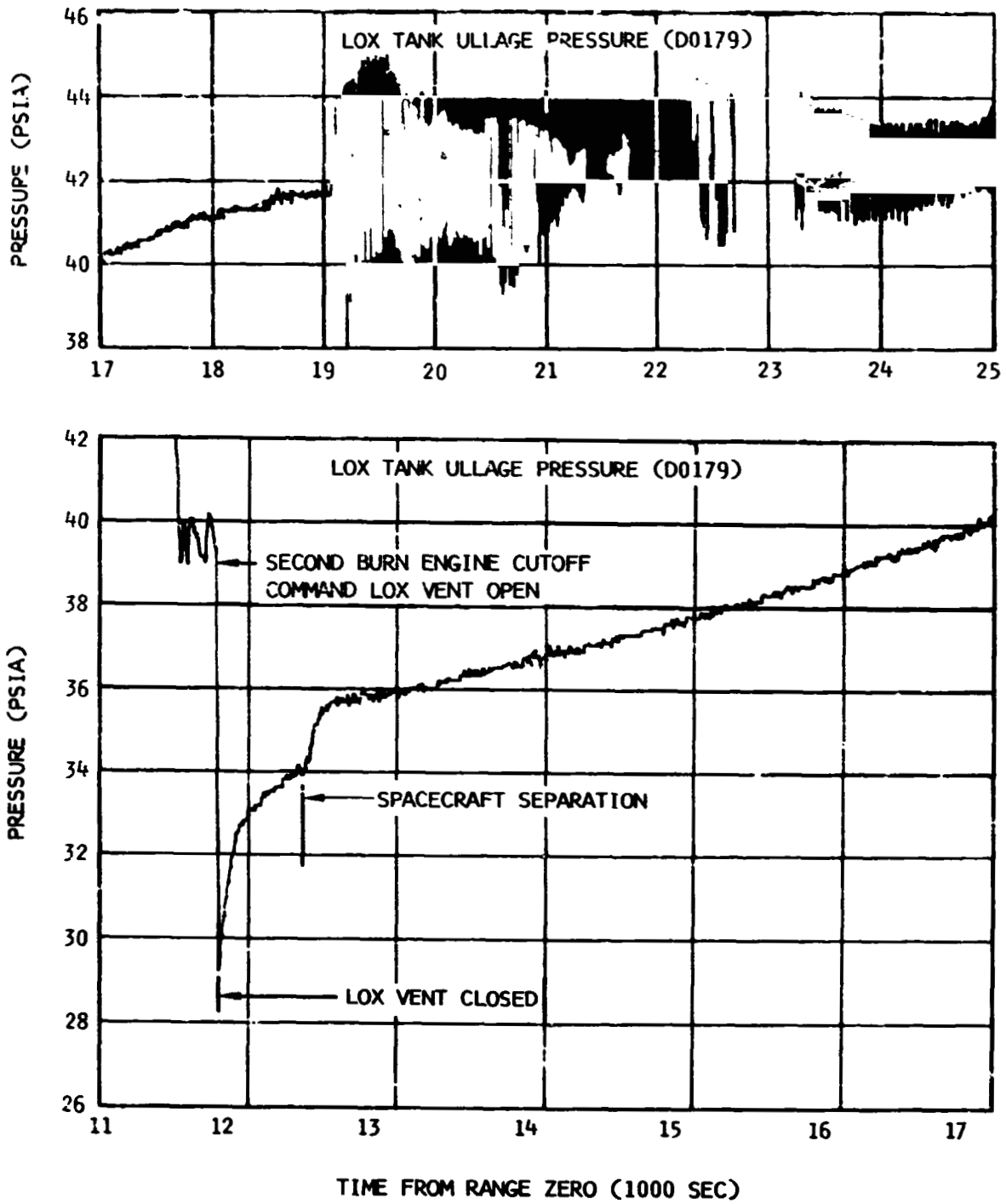


Figure 11-12. LOX Tank Ullage Pressure During Third Orbit

Section 11
Oxidizer System

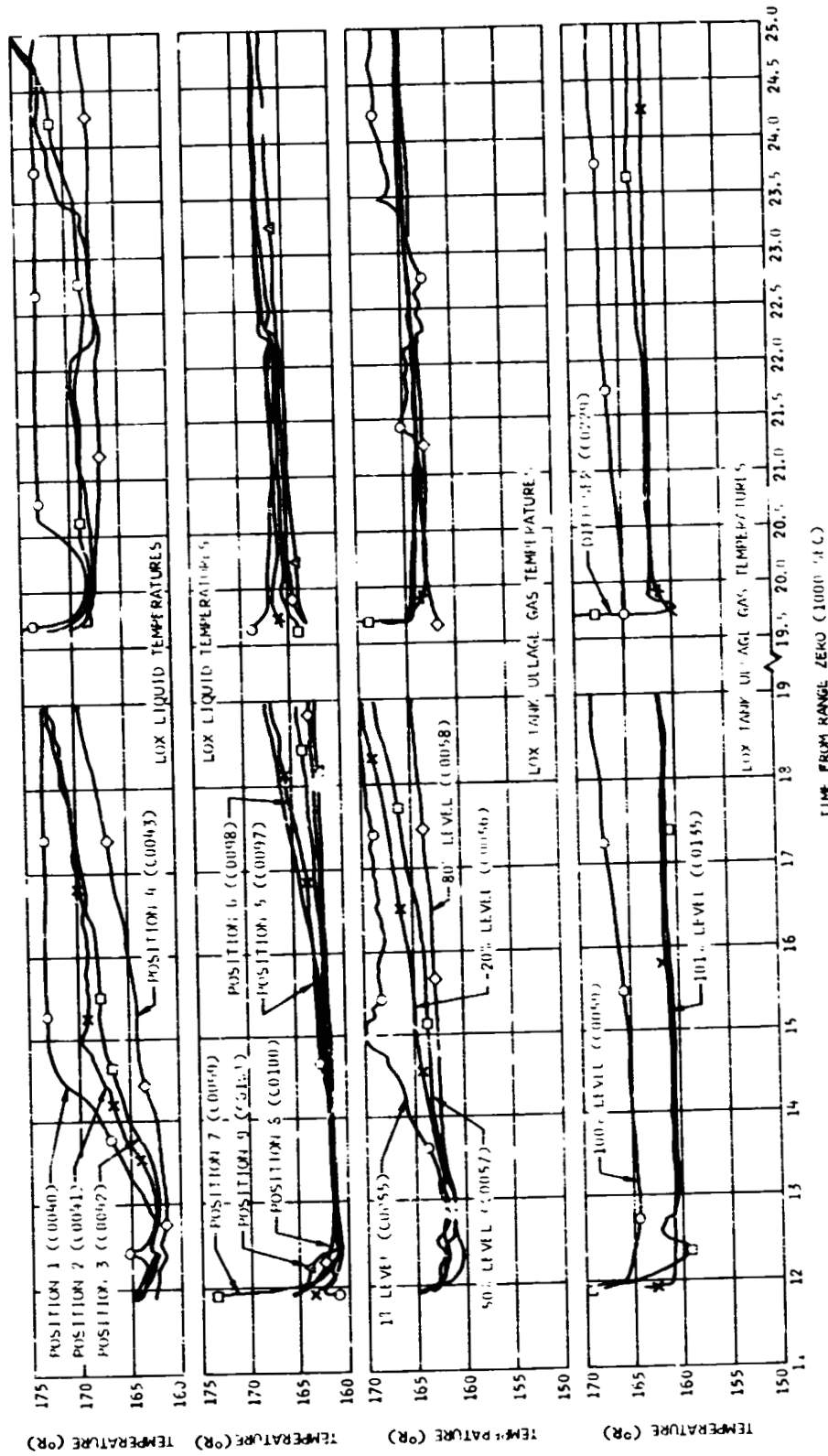


Figure 11-13. LOX Tank Temperatures During Third Orbit

Section 11
Oxidizer System

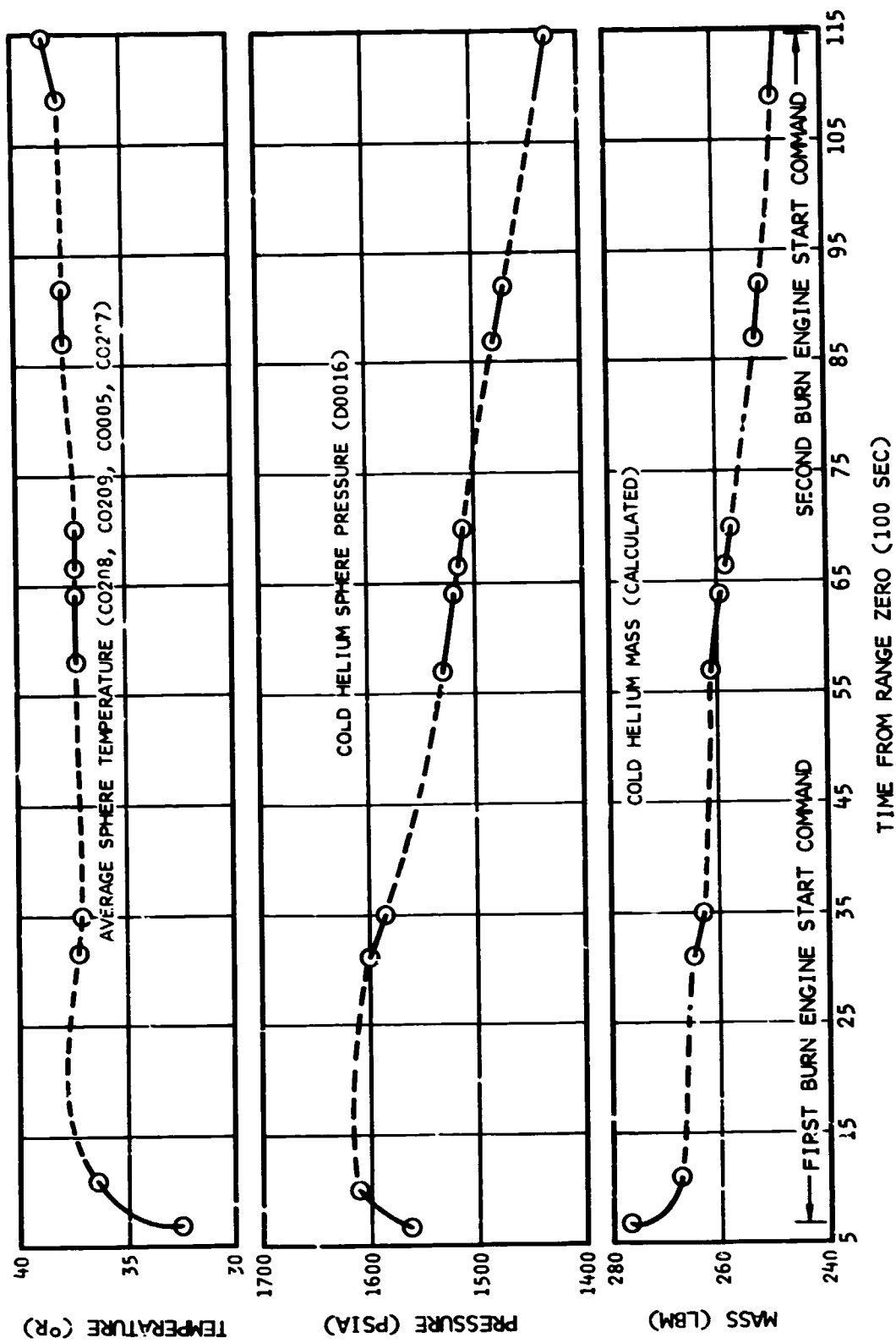


Figure 11-14. Cold Helium Sphere Conditions During Orbit

Section 11
Oxidizer System

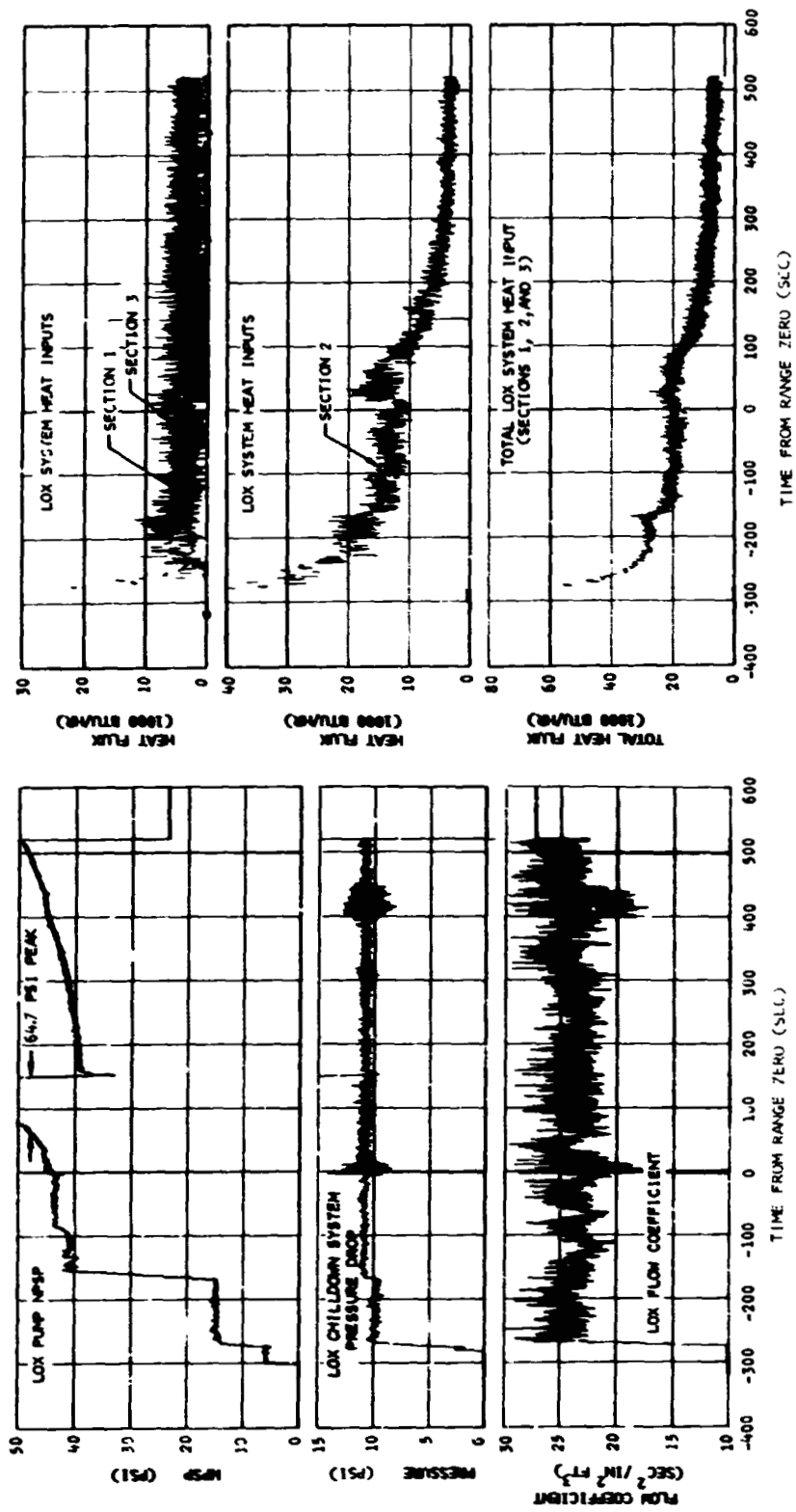


Figure 11-15. LOX Pump Chilldown System Performance - First Burn

Section 11
Oxidizer System

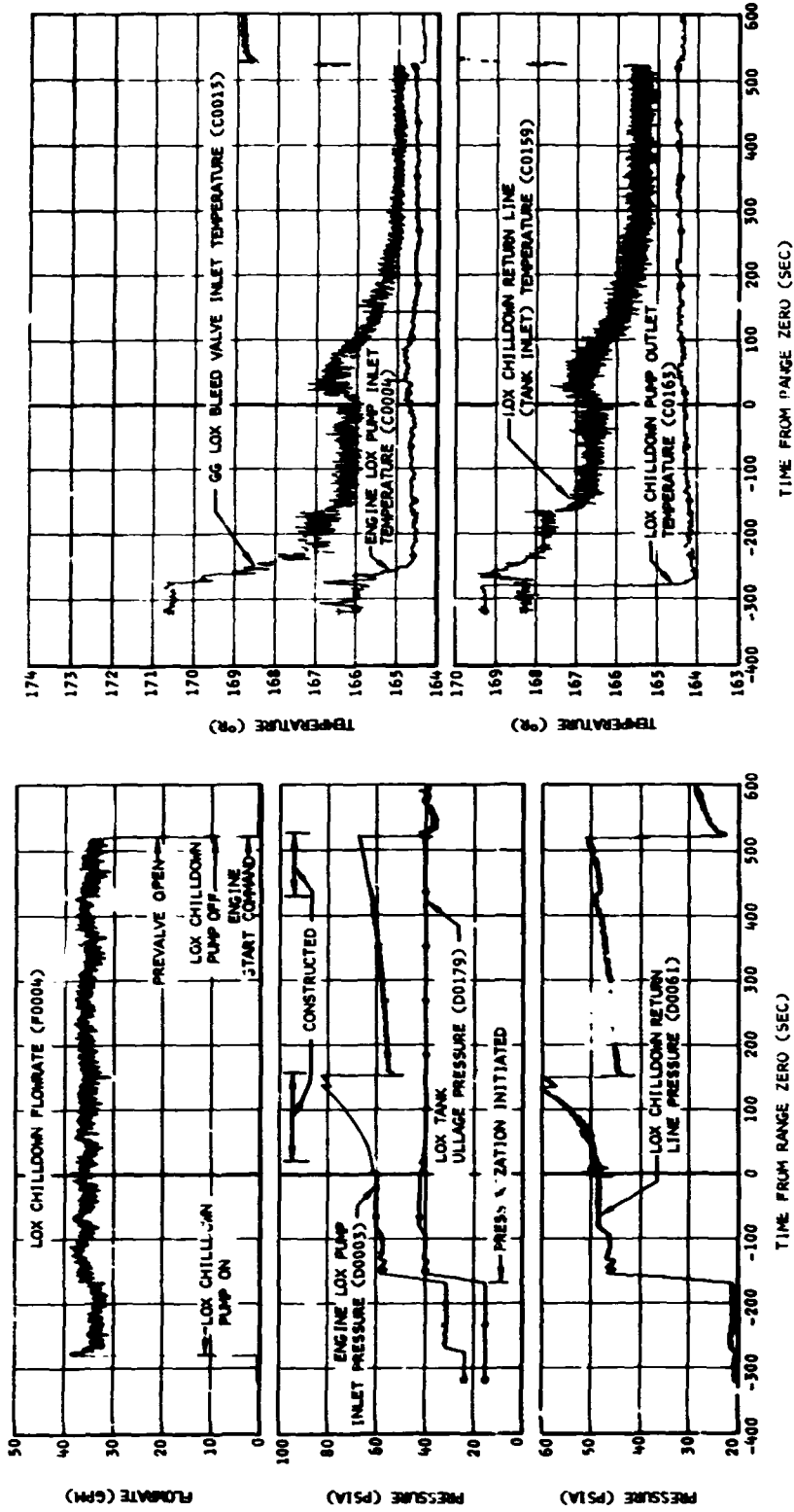


Figure 11-16. LOX Pump Chilldown System Operation - First Burn

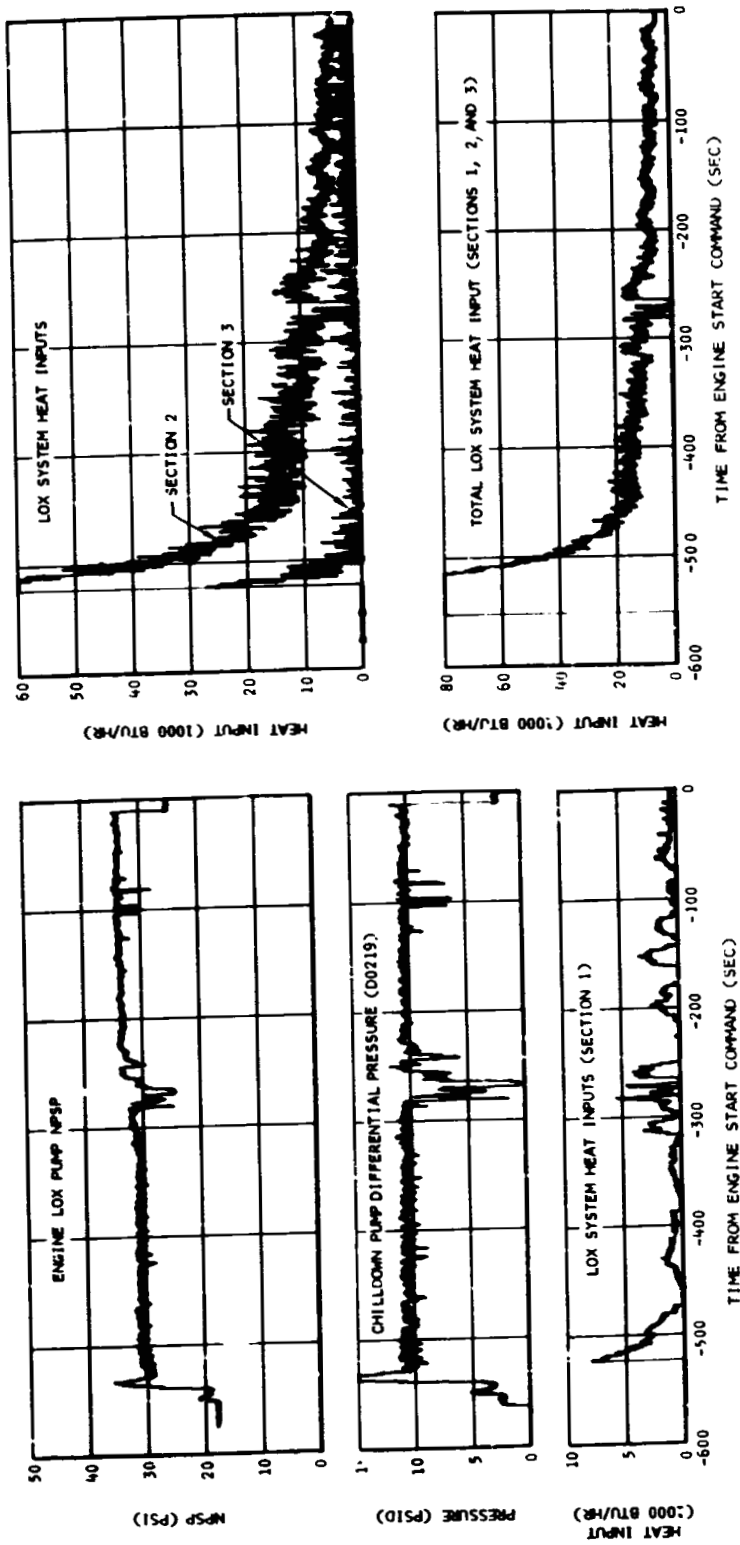


Figure 11-17. LOX Pump Chilldown System Performance - Second Burn

Section 11
Oxidizer System

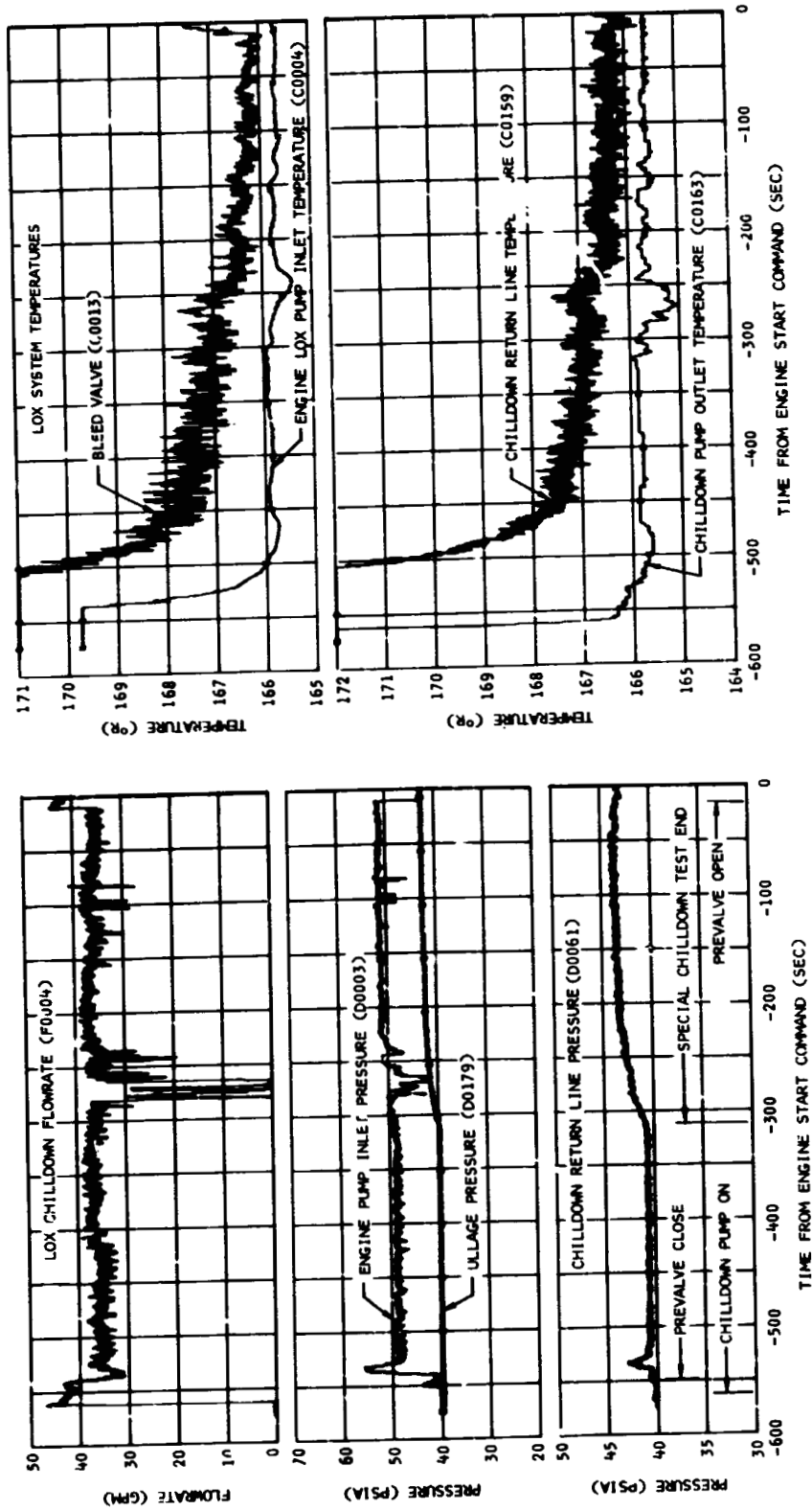


Figure 11-18. LOX Pump Chilldown System Operation - Second Burn

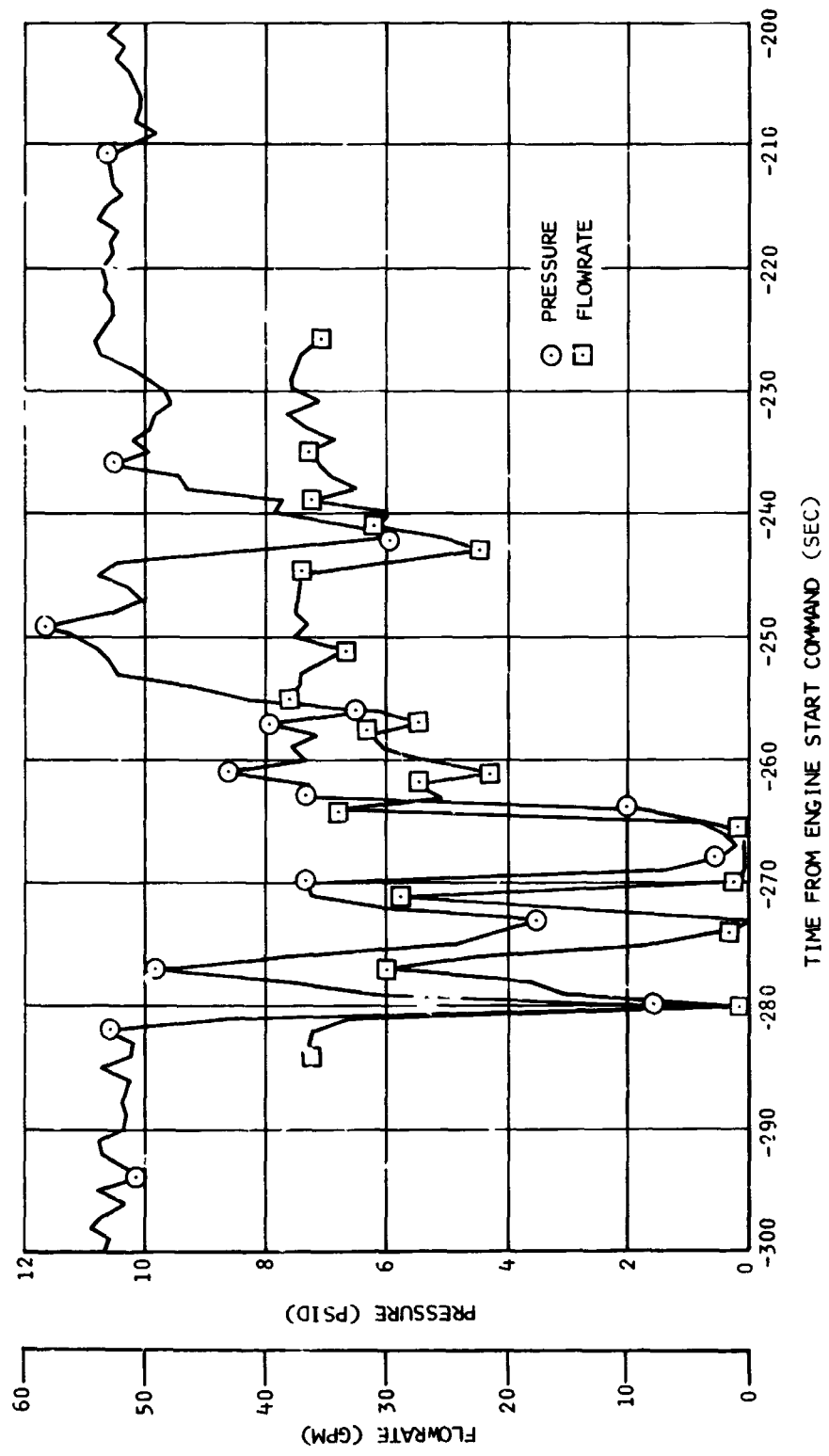


Figure 11-19. LOX Chilldown Pump Differential Pressure and Flowrate - Second Burn

Section 11
Oxidizer System

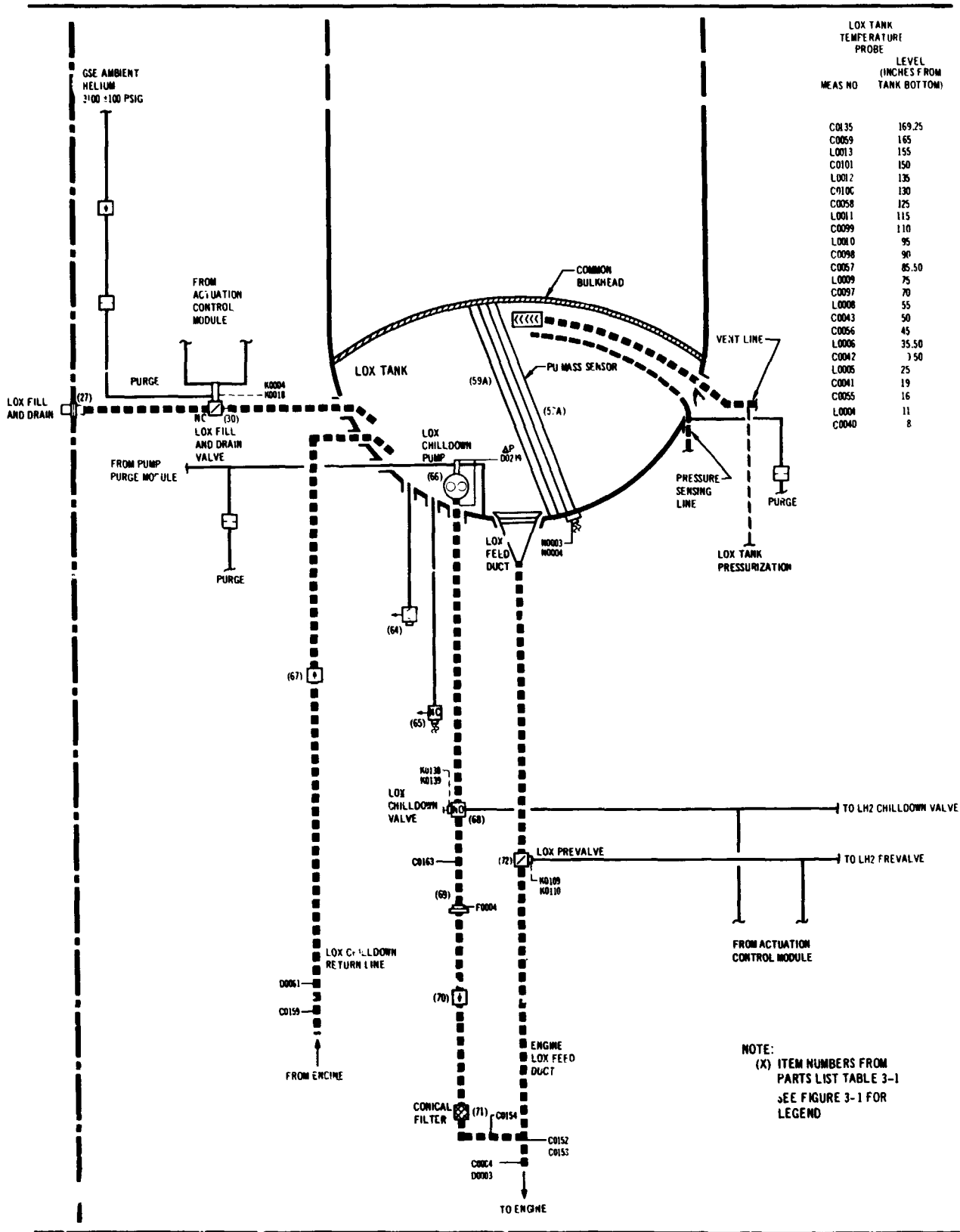


Figure 11-20. LOX System Schematic

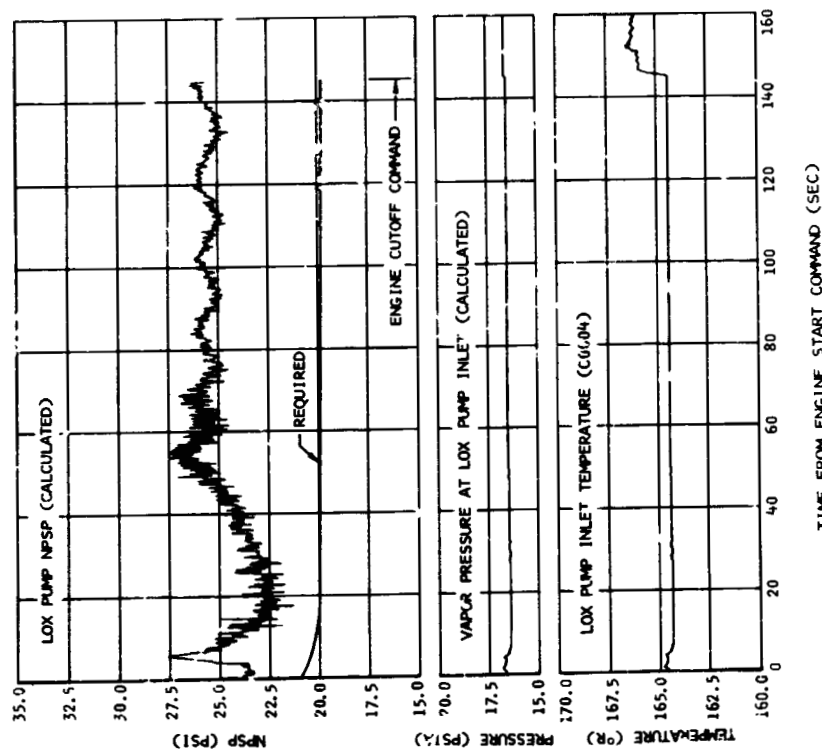
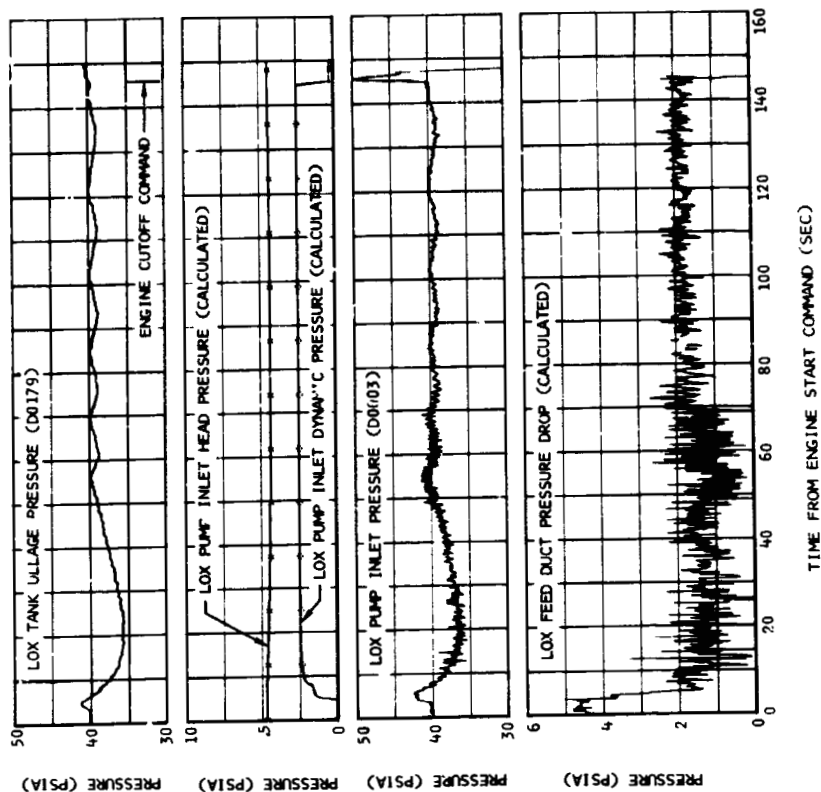


Figure 11-21. LOX Pump Inlet Conditions During Firing - First Burn

Section 11
Oxidizer System

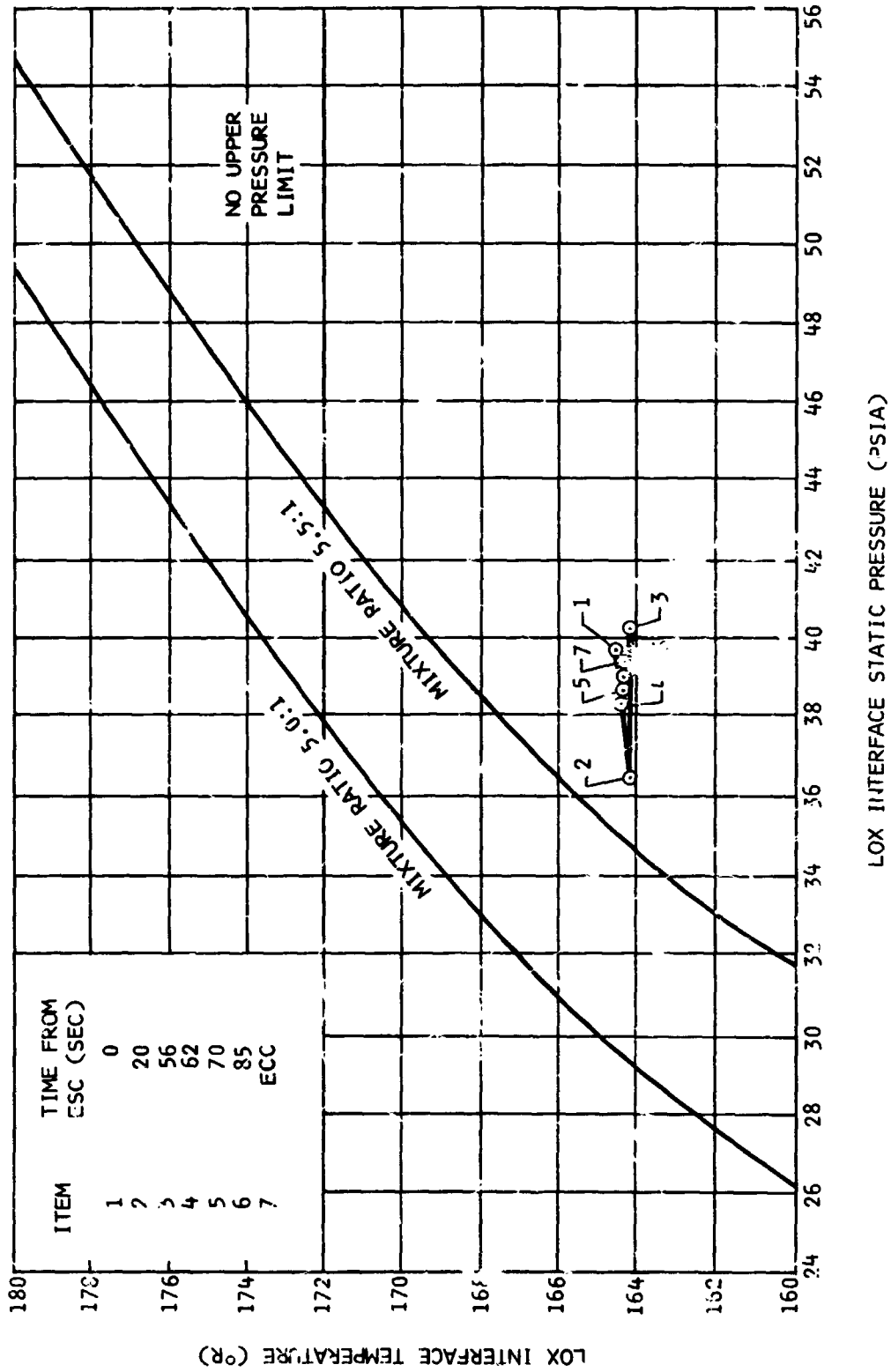


Figure 11-22. LOX Pump Interface Conditions During Firing - First Burn

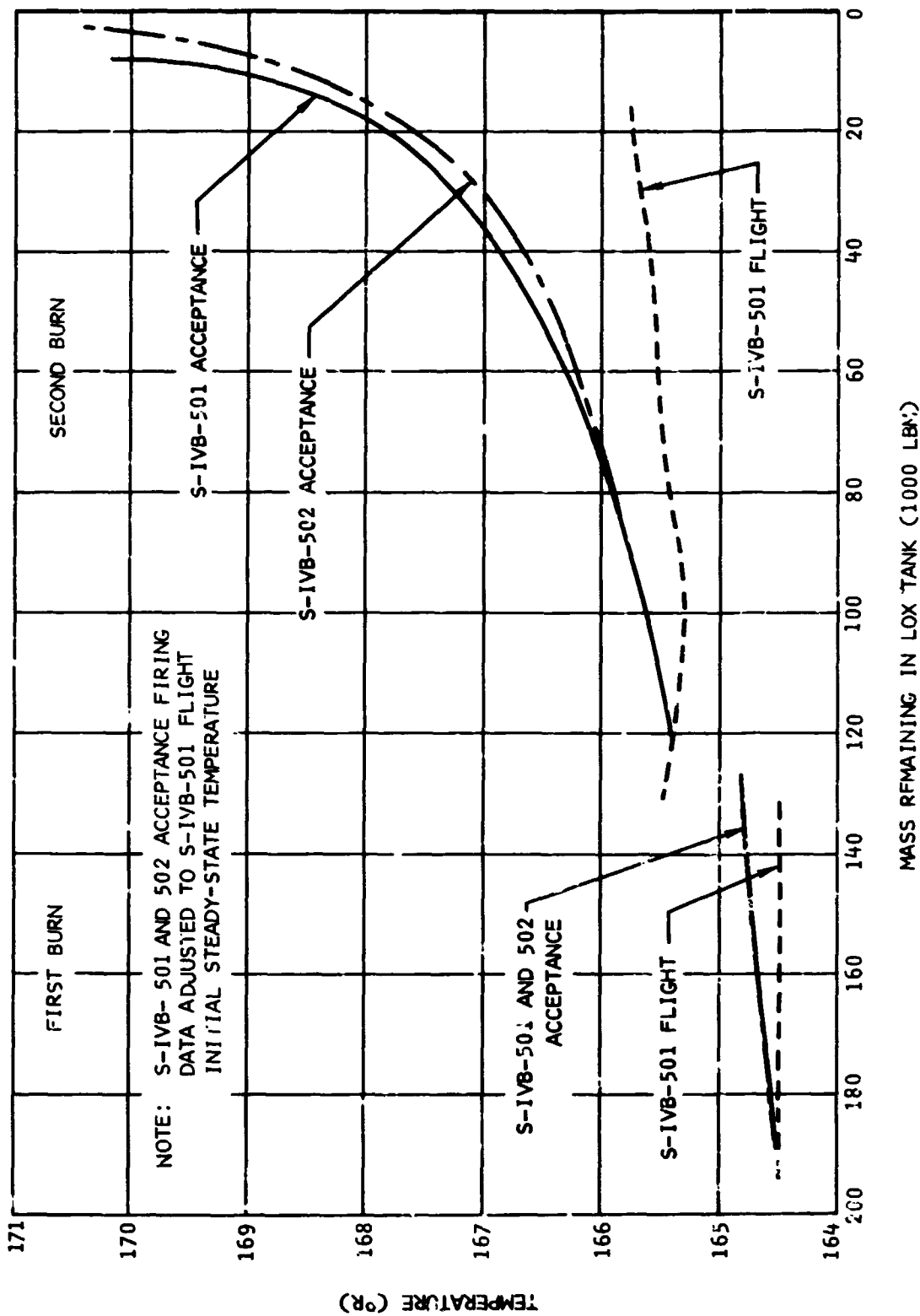


Figure 11-23. Effect of LOX Mass Level on LCX Pump Inlet Temperature

Section 11
Oxidizer System

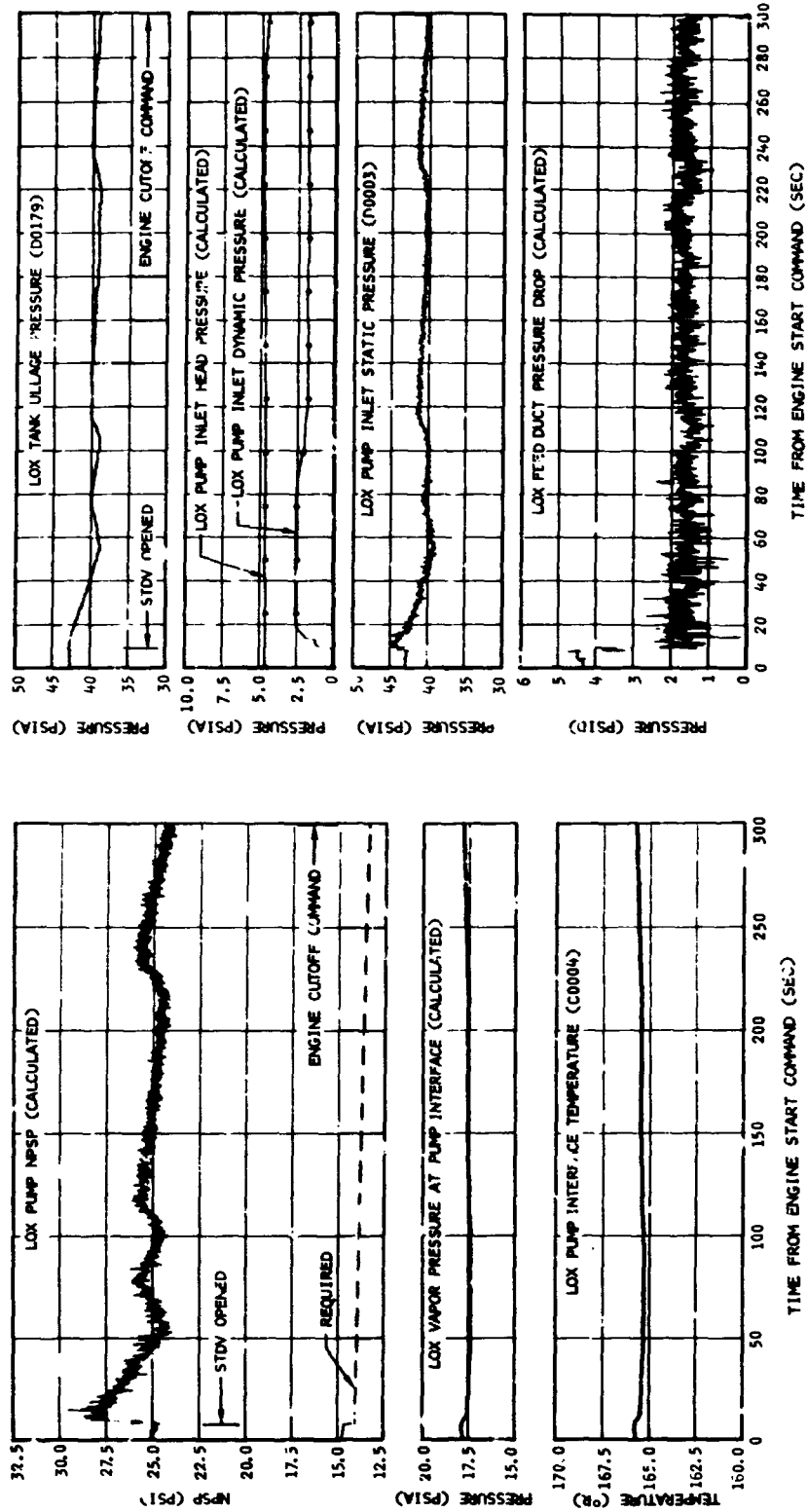


Figure 11-24. LOX Pump Inlet Conditions During Firing - Second Burn

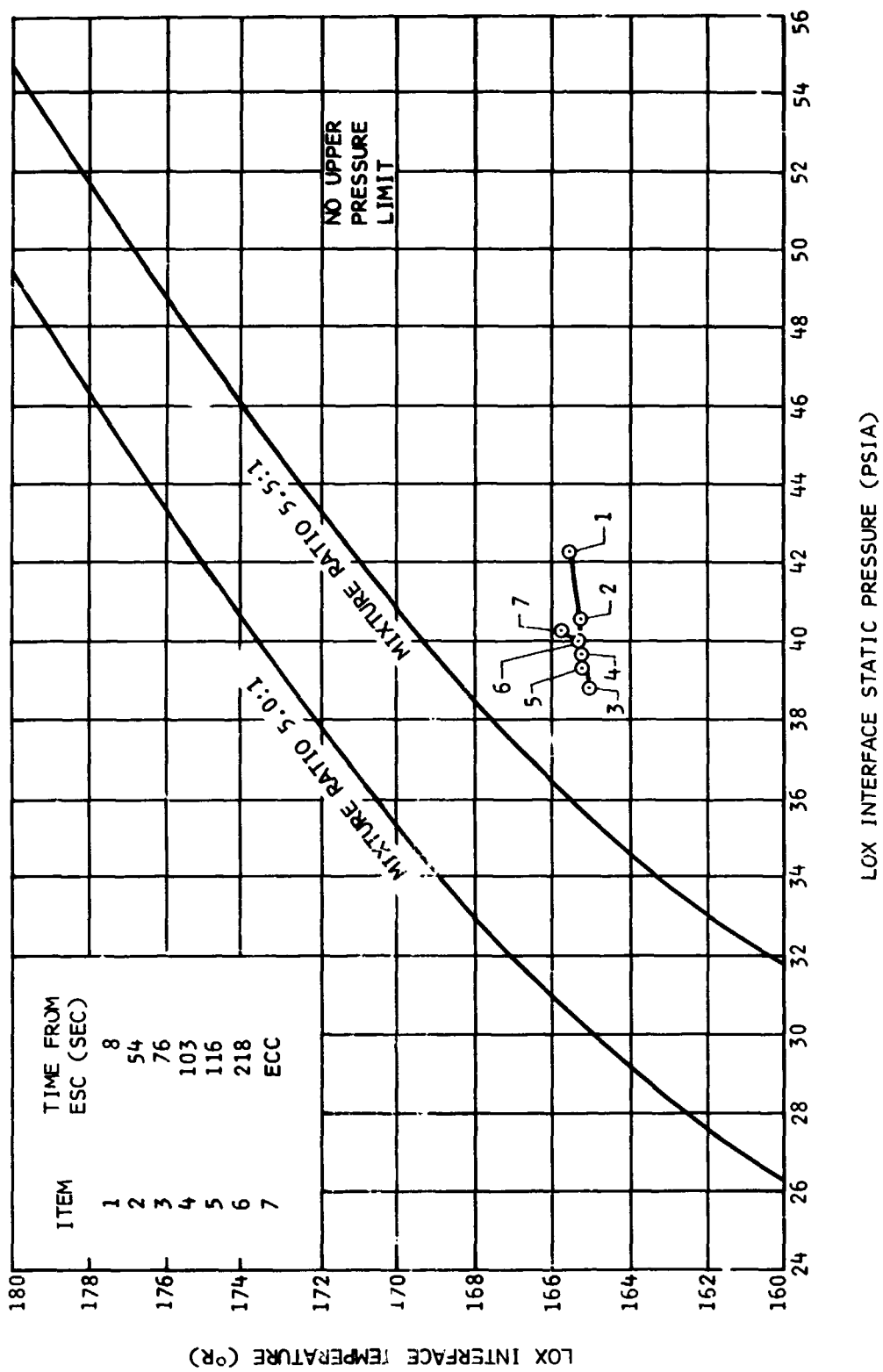


Figure 11-25. LOX Pump Interface Conditions During Firing - Second Burn

12. FUEL SYSTEM

The fuel system supplied LH2 to the engine, as designed, with the available net positive suction pressure (NPSP) exceeding the engine manufacturer's requirements through both burns, except at second burn Engine Start Command.

12.1 Pressurization Control

The LH2 tank pressurization system (figure 12-1) satisfactorily accomplished prepressurization and first burn GH2 pressurization. The LH2 tank pressures during repressurization and second burn GH2 pressurization were below the expected values. The system performance, however, was adequate during second burn mainstage.

12.1.1 First Burn

12.1.1.1 Prepressurization

The LH2 tank conditions prior to prepressurization were 37.6 deg R and 17.5 psia, and the LH2 bulk was saturated. The LH2 Prepressurization Command was received at T -96.5 sec, and the LH2 tank pressurized signal was received 21.5 sec later when the LH2 tank ullage pressure reached 33.8 psia. The ullage pressure continued to increase as the ullage warmed, reaching the relief setting of 35.9 psia by liftoff. The ullage pressure remained at this level during boost.

Approximately 8.8 lbm of helium were added during prepressurization. The comparatively small mass of helium required for pressurization was the result of the high temperature (the tank inlet temperature, C0015, did not drop below its upper range limit of 300 deg R) and the correspondingly high energy of the pressurant gas. The high pressurant gas temperature was produced by environmental heating in the helium supply line. Conditions from prepressurization to first burn Engine Start Command are summarized in figure 12-2 and compared with S-IVB-501 and 502 acceptance firing data in table 12-1.

12.1.1.2 Pressurization

At first burn Engine Start Command (ESC1), the LH2 tank ullage pressure was 35.9 psia. Between first burn engine start (which occurred at

Section 12 Fuel System

R0 +520.7 sec) and approximately ESC1 +4.8 sec, the primary, control, and step pressurization orifices were open to provide a high GH2 pressurant flowrate to the LH2 tank during engine start. From ESC1 +4.8 sec until first burn Engine Cutoff Command (ECC1) at ESC1 +144.9 sec, the control and step pressurization orifices were closed, thus limiting the pressurization flow to the primary orifice. The ullage pressure decreased normally and reached 29.0 psia at first burn Engine Cutoff Command. The actual pressure profile, although slightly lower than predicted, was satisfactory. LH2 venting did not occur during first burn.

The GH2 pressurization flowrate was approximately 0.50 lbm/sec, providing a first burn total flow of 70.1 lbm. The first burn collapse factor was similar to that during S-IVB-501 acceptance firing first burn. Conditions during first burn LH2 tank pressurization are summarized in figure 12-3 and compared with S-IVB-501 and 502 acceptance firing data in table 12-2.

12.1.2 Second Burn

12.1.2.1 Repressurization

The LH2 tank was repressurized with ambient helium from seven repressurization spheres (4.5 cu ft each). Repressurization was initiated at second burn Engine Start Command (ESC2) -325 sec (approximately R0 +11,162 sec) and was terminated prematurely from the ground approximately 80 sec later. The LH2 tank was pressurized from 19.7 psia to 32.0 psia. The ullage pressure subsequently decreased to 27.8 psia by second burn Engine Start Command. Approximately 47 lbm of ambient helium were used in the repressurization operation; approximately 14 lbm remained in the spheres. The residual helium would have provided less than 1 psi of additional pressure. Conditions during repressurization are summarized in figure 12-4 and compared with S-IVB-501 and 502 acceptance firing data in table 12-3.

The ullage pressure of 27.6 psia was lower than the minimum predicted value of 31 psia. The lower-than-predicted pressure can be attributed to the premature termination of the ambient repressurization operation, to a cooler-than-expected blowdown of the repressurization spheres (lower

heating of the pressurant gas by heat transfer from the spheres during blowdown resulted in a lower energy input into the ullage), and to an energy loss of approximately 12,000 Btu from the ullage gas resulting probably from a combination of boiloff at the liquid-gas interface and condensation of GH2 bubbles in the liquid bulk. Boiloff may have resulted from slosh induced by the attitude change maneuver at the initiation of restart preparations (ESC2 -327 sec). The presence of slosh was substantiated by liquid and temperature measurements. The condensation of GH2 bubbles in the liquid bulk would have resulted in an increase in the main ullage volume and a corresponding drop in ullage pressure. The presence of bubbles was substantiated by the apparent drop in liquid surface level of approximately 4 ft during the period between initiation of repressurization and second burn Engine Start Command.

The causes of the low repressurization system performance will be reduced on the S-IVB-502 stage flight by delaying the initiation of ambient repressurization command to ESC2 -127 sec. This delay will provide an additional 200 sec of APS ullaging for bubble removal prior to repressurization and shorten the period of possible ullage pressure decay following repressurization. In addition, the repressurization flowrate will be decreased by changing the size of the repressurization orifice, thus reducing mixing in the ullage.

12.1.2.2 Pressurization

At second burn Engine Start Command (ESC2), the LH2 tank ullage pressure was 27.8 psia, which is lower than the minimum predicted pressure of 31 psia. Between second burn Engine Start Command and ESC2 +10.6 sec, the primary, control, and step pressurization orifices were open. The control orifice was subsequently closed and the primary and step valves remained open (second burn overcontrol mode) until second burn Engine Cutoff Command (ECC2) at ESC +299.70 sec. LH2 tank ullage pressure and pressure rise rate were both lower than anticipated. Preflight predictions indicated cyclic operation within the 31 to 34 psia control band. The maximum pressure, which occurred at ECC2, was 31.9 psia.

The low pressurization performance during second burn can be attributed to an energy loss from the pressurization system and/or the ullage. Since

Section 12 Fuel System

the data show no tank leakage from active tank penetrations (such as vent systems) and indicate normal pressurant flow conditions at the tank inlet, the most likely cause of the lower-than-predicted performance is pure ullage collapse (heat transfer from the ullage). Most of the energy loss from the ullage (approximately 5,000 Btu) can be explained by heat transfer to the tank walls, which had been chilled by sloshing to liquid temperature prior to second burn Engine Start Command. The amount of boiloff (or condensation) during second burn appears to be minor. The pressurization performance will be improved on the S-IVB-502 flight by the utilization of a larger primary orifice (0.07300 in.² on S-IVB-502 flight versus 0.0606 in.² on S-IVB-501 flight). This will provide a higher pressurization rate during both burns.

The GH2 pressurization flowrate during second burn ranged from 0.70 to 0.75 lbm/sec, providing a total flow of 206 lbm of GH2. Conditions during second burn LH2 tank pressurization are summarized in figure 12-5 and compared with S-IVB-501 and 502 acceptance firing data in table 12-2.

12.2 Pressurization System Conditions During Orbit

12.2.1 LH2 Tank Nonpropulsive Vent and Relief Valve Operation

The nonpropulsive vent (NPV) and relief valve operated satisfactorily, maintaining the ullage pressure below the maximum limit. After LH2 tank prepressurization, the ullage pressure increased to 35.9 psia; the vent and relief valve cracked and then feathered until engine start (figure 12-2). After second burn cutoff the valve was opened for 120 sec, dropping the ullage pressure from 31.7 psia to 19.0 psia (figure 12-6). The LH2 tank then self-pressurized until the valve cracked at 36.2 psia. Relieving at this pressure continued until loss of telemetry coverage.

12.2.2 LH2 Tank Continuous Vent System Performance

The continuous vent system (CVS) performed satisfactorily, maintaining the LH2 tank ullage pressure at an average level of 19.5 psia and providing an average acceleration of 5×10^{-5} g for propellant settling

during coast. The only problem arose when the continuous vent nozzle pressure data erroneously indicated positive pressures (and, hence, flow) during restart repressurization (paragraph 12.2.3).

Continuous venting was initiated at RO +723 sec, as evidenced by the almost instantaneous increase in nozzle pressures, the decrease in nozzle temperatures, and the rapid decay of ullage pressure (figure 12-7). Shortly afterward, the nozzle pressure data began to diverge; by RO +3,000 sec this discrepancy was a constant 2 to 3 psi, with nozzle 1 (D0181) data higher than nozzle 2 (D0182) data. D0181 was assumed to be indicating the correct pressure level, based on flowrate calculations and the observed pressure levels. At approximately RO +4,510 sec the main poppet of the continuous vent regulator reseated, as shown by the decrease in nozzle 1 pressure to the normal level for bypass orifice flow only. From this time until the termination of continuous venting at RO +11,161 sec the main poppet periodically cracked and reseated. This periodic opening and closing of the main poppet of the CVS regulator resulted in irregular thrust and acceleration levels (figure 12-8), which may have affected propellant conditions during coast (paragraph 12.2.4).

The calculated values shown in figure 12-8 are only approximate; exact calculations could not be performed because of the possible error in the CVS nozzle 1 pressure.

12.2.3 Continuous Vent System Anomalies

Following termination of continuous venting prior to second burn, the continuous vent nozzle pressure transducers displayed abnormal (positive) pressure levels (figure 12-6). These data were mistakenly interpreted as indicative of flow through the CVS, and corrective measures were taken. Further investigation has revealed the following:

- a. LH2 tank ullage pressure data from the termination of ambient repressurization to second burn engine cutoff indicated either a flow out of the tank or thermal collapse of the incoming pressurant gases. Analyses indicated that the latter agrees more closely with the data (paragraph 12.1.2.1).

Section 12
Fuel System

- b. It was discovered that the CVS nozzle pressure transducers (D0181 and D0182) were mounted directly on the vent line and, hence, were subjected to the extremely cold (40 deg R) GH2 temperature; they had been qualified only as low as 140 deg R. Analyses to reveal what effect this temperature would have on these transducers have been inconclusive.
- c. The closed talkbacks from both the relief override valve and the bypass orifice shutoff valve were received at the proper time.
- d. At the moment of CVS termination both nozzle temperatures (C0256 and C0257) began sharp upward trends indicative of normal warm-up and a no-flow condition (figure 12-6).
- e. During second burn, no inflections of either nozzle pressure or temperature were seen, indicating no flow.

The conclusion of this investigation is that the continuous vent regulator closed as planned prior to restart.

During the coast period of S-IVB-501 flight, the main poppet was reseated for periods up to 450 sec. On S-IVB-203 the main poppet never completely reseated during periods of similar operation. Apparently the continuous vent regulator used on S-IVB-501 was somewhat less sensitive; also, the GH2 vented on S-IVB-501 was 20 to 30 deg R colder, resulting in a greater mass flowrate at the same ullage pressure.

12.2.4 LH2 Tank Conditions During Orbital Coast

LH2 tank conditions during orbital coast are shown in figure 12-7. The ullage temperatures were much colder than anticipated. Except for the 101 percent probe (C0039), the temperature probes indicated an environment which could have been either gaseous or liquid during most of the coast period. The total boiloff during orbit was not calculated because (1) the ullage volume at continuous venting termination could not be determined, and (2) the total mass vented calculation was only approximate. However, boiloff was determined from PU data (section 15), which is presently the most valid data available for this consideration.

12.3 LH2 Pump Chillo-down

12.3.1 First Burn

The LH2 pump chillo-down system performed adequately. The LH2 chillo-down was initiated at RO -302.8 sec and was continuous until RO +520.9 sec when the pre-valve opened. The chillo-down pump was turned off at RO +521.9 sec. The engine pump inlet pressure and temperature were 43.89 psia and 38.9 deg R at first burn Engine Start Command, resulting in an NPSP of 21.5 psi, which was above the 6.3 psi required. Table 12-4 compares significant LH2 chillo-down system performance data with S-IVB-501 and 502 acceptance firing data.

Chillo-down system pressures, temperatures, flowrates, and calculated performance are presented in figures 12-9 and 12-10.

The chillo-down flowrate stabilized at 115 gpm after start transients and pre-valve closing. After pressurization the flowrate was 143 gpm until first burn engine start. The heat input rate into section 1 (tank to pump inlet) during the unpressurized portion was lower than during the acceptance firing. All heat inputs during pressurized chillo-down were lower in flight than during acceptance firing. The total rate was constant at 13,600 Btu/hr for 250 sec before first burn engine start as compared to 50,000 Btu/hr during acceptance firing. The lower heat input rates during flight did not degrade chillo-down. The data fluctuations at about 132 and 150 sec were caused by S-I shutdown transients.

During unpressurized chillo-down, the LH2 pump inlet was slightly sub-cooled; immediately following pressurization, the temperature reased to 38.8 deg R as the flowrate increased. The temperature then slowly increased as the LH2 bulk warmed and, by first burn Engine Start Command, was 38.7 deg R. All chillo-down system temperatures reflected the LH2 bulk warming.

Section 12 Fuel System

The bleed valve and return line temperatures increased sharply at the initiation of prepressurization because all of the heat input went into heating the pressurized fluid and no vaporization occurred. The LH₂ entered the system sufficiently subcooled to absorb all the heat input to the system without reaching saturation temperature. After pressurization, the ullage pressure was constant but the pump inlet pressure increased and decreased with acceleration until the pre valve was opened and allowed essentially all of the flow to return to the LH₂ tank through the pre valve with no flow through the chilldown system. The pump inlet pressure then decreased (because of loss of chilldown pump heat) to 34.2 psia. The pre valve was sequenced as follows:

<u>Event</u>	<u>Time</u>
Open command received	ESC1 -0.690 sec
Valve left closed position	ESC1 +0.164 sec
Valve reached open position	ESC1 +2.063 sec

The NPSP at the pump inlet followed the ullage pressure during pressurization and reached a maximum of 27.3 psi when maximum acceleration was reached at S-I cutoff. The NPSP dropped at S-I cutoff and increased with S-II acceleration, then decreased to 14.6 psi when the pre valve was opened because of the loss of pump pressure.

The flow coefficient was calculated from flowrate and chilldown system pressure drop data to be $16.5 \text{ sec}^2/\text{in.}^2\text{ft}^3$, which was within the range calculated for previous S-IVB stages. The coefficient was used to compute average fluid quality during the unpressurized phase of the chilldown.

Prior to prepressurization, two-phase flow existed in section 2 (pump inlet to bleed valve) and in section 3 (bleed valve to tank); and the average fuel quality was 0.021 lb gas/lb mixture. This quality decreased to zero during prepressurization when the fluid in the system became subcooled.

The LH₂ chilldown system pressure drop was relatively steady at 8.8 and 7.4 psi, respectively, during the unpressurized and pressurized portions of the LH₂ chilldown operation.

12.3.2 Second Burn

The LH2 pump chilldown for second burn differed from that for first burn in that it started with a dry chilldown system. A special unpressurized LH2 pump chilldown test was initiated 4 min prior to initiation of restart preparations with the prevalve closed. The purpose of this test was to determine chilldown effectiveness at a lower g level than normal chilldown with the ullage engines on.

The recirculation chilldown system performed satisfactorily. At second burn engine start, the pump inlet pressure and temperature of 28.0 psia and 40.7 deg R were within the engine start requirements. The pump inlet NPSP at second burn engine start was 0.17 psi, which is below the minimum acceptable limit of 6.3 psi (figures 12-11 and 12-12).

The LH2 chilldown pump was started at ESC2 -567.7 sec with the LH2 tank unpressurized; the tank was pressurized at ESC2 -326.2 sec. The Prevalve Open Command was issued at ESC2 -10.803 sec with the valve starting to open at ESC2 -9.823 sec. The full open position was attained at ESC2 -7.159 sec.

Before tank pressurization, chilldown was marked by small pressure and flow fluctuations caused by the rapid vaporization of LH2 as it entered the system and came in contact with the warm hardware. This cycling is reflected throughout the system in the pressure and temperature data. The magnitude of the cycling decreased with time during the unpressurized chilldown period as the system hardware was cooled. After the LH2 tank was pressurized, the cyclic action of the system flowrate, pressures, and temperatures stopped; and the system gradually approached steady-state as engine start was approached. Just before the prevalve was opened, the chilldown flowrate was steady at 143 gpm. The pump inlet temperature and chilldown system pressure drop were also steady indicating that steady-state conditions had been obtained and chilldown was complete before it was stopped at prevalve opening.

During the 9.823 sec between the start of prevalve opening and second burn engine start, the pump inlet temperature increased from 39.7 to 40.7 deg R. This corresponds to a heatup rate of 6.1 deg/min, which

Section 12 Fuel System

falls within the range of data obtained during acceptance testing (10 deg/min) and indicates that the fuel pump was adequately chilled.

At the end of the special 4-min LH2 chilldown test, the engine pump inlet temperature was still at saturation temperature, indicating chilldown was not complete. The gas generator inlet wall and the LH2 pump outlet wall were chilled to steady-state temperatures early in the unpressurized chilldown test. This is not indicative of all hardware temperatures because these walls are thin compared to the LH2 pump body.

Normally chilldown would be started only a few seconds before repressurization; therefore, at repressurization during this flight, considerable chilldown was already accomplished. During pressurization, the LH2 pump inlet temperature dropped rapidly from 40.5 to 39.3 deg R. The LH2 pump outlet temperature also dropped and was almost stable during the remainder of chilldown. The system pressure drop and chilldown flowrate also increased and stabilized after pressurization. The pump NPSP reached a high of 16.5 psi during pressurization.

After pressurization, the LH2 tank ullage pressure decreased continuously until second burn Engine Start Command. Engine pump inlet pressure also decreased from a maximum of 39.0 to 34.5 psia at prevalve opening, while NPSP decreased from 16.5 to 9.8 psi. The chilldown return line temperature showed a decreasing profile that was similar to the ullage pressure profile. The bleed valve temperature led the ullage pressure decrease profile, indicating subcooled liquid. The engine pump inlet temperature slowly increased from 39.3 to 39.7 deg R during the ullage pressure decrease.

The LH2 pump inlet and outlet temperatures were subcooled within 30 sec after start of pressurization, but heat was still being removed from the engine and return hardware because the heat input rate into sections 2 and 3 was still decreasing rapidly. Section 1 was chilled prior to pressurization because the heat input rate was almost constant at 3,500 Btu/hr. The heat input rate to the LH2 stabilized at ESC2 -135 sec, indicating that the hardware temperature was about as low as it would get. The total heat input rate stabilized at approximately 17,000 Btu/hr.

Section 12
Fuel System

Chiltdown was terminated at ESC2 -9.823 sec when the prevalve started to open. The engine pump inlet temperature increased 1 deg R, but pump outlet temperature remained constant indicating little or no heatup of the engine LH2 pump during the 9.9 sec before fuel lead flow started. The chiltdown system pressure drop decreased from 7.7 to 3.2 psi, pump inlet pressure dropped to equal the ullage pressure (from 34.5 to 28.0 psia). As a result, NPSP dropped from 10 to 1.5 psi. When the chiltdown pump was turned off at ESC2 -0.8 sec, flowrate and system pressure drop decreased to zero, and NPSP dropped to 0.17 psi with an ullage pressure of 28.0 psia. The low LH2 tank ullage pressure is discussed in paragraph 12.1.2.2.

Figures 12-13, -14, and -15 compare S-IVB-501 second start chiltdown with S-IVB-203 first and second orbital LH2 chiltdown tests. The S-IVB-501 LH2 unpressurized chiltdown and S-IVB-203 second orbit unpressurized chiltdown are similar. The S-IVB-501 unpressurized chiltdown test data were superimposed on S-IVB-203 second orbit unpressurized chiltdown data because the g level was 4×10^{-5} which was almost the same as the 3.6×10^{-5} g during the S-IVB-501 special 4-min chiltdown test; the time between chiltdown pump on and prevalve closed was the same.

Figure 12-13 shows S-IVB-203 second orbit data superimposed on S-IVB-501 data starting when the chiltdown pumps were turned on. This comparison ends at ESC2 -327 sec, just before S-IVB-501 LH2 prepressurization. The system hardware temperatures decreased at approximately the same rate on S-IVB-501 as on S-IVB-203. The S-IVB-501 temperatures and flowrates followed those of S-IVB-203 quite closely. Heat input rate comparisons are not available during orbital unpressurized chiltdown for either S-IVB-203 or 501. (For S-IVB-502, unpressurized chiltdown is scheduled to be 495 sec.)

The S-IVB-501 pressurized chiltdown data were superimposed on S-IVB-203 first orbit pressurized chiltdown data because S-IVB-203 first orbit g level was approximately 4×10^{-4} which compared to the g level of 5.2×10^{-4} during S-IVB-501 pressurized chiltdown.

The pressurized chiltdown parameters start at ESC2 -327 sec with LH2 prepressurization (figure 12-13). The S-IVB-501 system temperatures were already cold because of unpressurized chiltdown; however, the values at

Section 12 Fuel System

prevalve opening indicate approximately the same conditions for the two flights. The temperatures during the initial transient of S-IVB-203 first orbital chilldown were about the same as during S-IVB-203 second orbit and S-IVB-501 chilldown initiation. The heat input rates were almost constant during the last 135 sec of S-IVB-501 pressurized chilldown. The S-IVB-203 first orbital chilldown heat input rates were almost constant during the last 80 sec of chilldown (figure 12-14). The average S-IVB/V heat input rate for section 2 during acceptance firing second burn chilldown was 17,500 Btu/hr (ranging from 10,000 to 25,000 Btu/hr). Using the average of 17,500 Btu/hr, section 2 chilldown on S-IVB-501 was accomplished 104 sec after the start of pressurized chilldown. The heat input rates to sections 1 and 3 stabilized before those of section 2. The S-IVB-203 first orbit heat input rates are also shown for comparison.

The mass of LH2 entering the chilldown system with respect to time, referenced to the start of chilldown, is shown in figure 12-15. Since 4 min of unpressurized chilldown and 135 sec of pressurized chilldown were required for the S-IVB-501 section 2 heat input rate to reach 17,500 Btu/hr, approximately 300 lbm of LH2 were required to pass through the system to properly chill the LH2 pump. This 300 lbm compares closely with the 325 lbm of LH2 required during the 285 sec of pressurized chilldown on the S-IVB-203 first orbit. For S-IVB-502 second burn, 127 sec of pressurized chilldown are scheduled in addition to 495 sec of unpressurized chilldown. The S-IVB-203 orbital chilldown test and the S-IVB-501 second burn chilldown indicate that these times will be sufficient to meet engine start requirements.

12.4 Engine LH2 Supply

12.4.1 First Burn

The LH2 supply system (figure 12-16) delivered the necessary quantity of LH2 to the engine pump inlet throughout first burn and maintained the pressure and temperature within a range that provided an LH2 pump NPSP that was at least 1.1 psi above the minimum requirement. The data and calculated performance are presented in figure 12-17. Table 12-5 compares the S-IVB-501 stage flight data with that from previous stages.

The LH2 pump inlet temperature and pressure, at selected times during engine operation, were plotted in the engine operating region (figure 12-18) and showed that conditions were met satisfactorily throughout first burn.

Figure 12-19 is a plot of the pump inlet temperature as a function of the propellant mass remaining within the LH2 tank and includes previous stage data for comparison. As the figure shows, the data from the three tests agree closely.

12.4.2 Second Burn

The NPSP, LH2 pump interface total pressure, and LH2 pump interface temperature during second burn are shown in figure 12-20. The NPSP at second burn Engine Start Command was 6.13 psi below the minimum required and, when the start tank discharge valve opened, it was 0.5 psi below the required. After the start tank discharge valve opened, the NPSP increased rapidly and was above the minimum required level during engine operation.

The fuel pump inlet pressure and temperature were plotted in the engine operating region (figure 12-21) and indicated that the engine fuel pump inlet conditions were satisfactorily met. The pump inlet temperature plotted against the mass remaining in the LH2 tank during second burn is shown in figure 12-19. Table 12-5 compares the LH2 supply data with that from S-IVB-501 and 502 acceptance firing data.

Section 12
Fuel System

TABLE 12-1
LH2 TANK PREPRESSURIZATION DATA

PARAMETER	UNITS	S-IVB-501 FLIGHT	S-IVB-501 ACCEPTANCE FIRING	S-IVB-502 ACCEPTANCE FIRING
Prepressurization duration	sec	21.5	34.5	41.0
Helium mass added	lbm	8.8	21.7	17.4
Ullage pressure				
At prepressurization initiation	psia	17.5	15.0	15.3
At prepressurization termination	psia	33.8	33.2	33.6
At liftoff*	psia	35.9	34.0	35.0
At Engine Start Command	psia	35.9	35.0	36.0
Rate of increase after prepressurization	psi/min	1.0	0.9	1.3
Events (sec from liftoff*)				
Prepressurization initiation		-96.5	-110.1	-114.0
Prepressurization termination		-75.0	-75.6	-73.0
Engine Start Command		520.7	512.5	511

*During acceptance firing, liftoff is simulated.

TABLE 12-2
LH2 TANK PRESSURIZATION DATA

PARAMETER	UNIT	S-IVB-501 FLIGHT		S-IVB-501 ACCEPTANCE FIRING		S-IVB-502 ACCEPTANCE FIRING	
		FIRST BURN	SECOND BURN	FIRST BURN	SECOND BURN	FIRST BURN	SECOND BURN
<u>Pressure Switch Setting</u>							
Lower	psia	28.0	31.6	28.7	31.2	29.2	30.1
Upper	psia	30.5	33.6	30.7	33.7	31.5	34.3
<u>Ullage Pressure</u>							
At Engine Start Command	psia	35.9	27.8	35.0	34.9	36	33.5
At Engine Cutoff Command	psia	29.0	31.9	28.8	32.4	28.7	32.8
<u>GH2 Pressurant Flowrate</u>							
Undercontrol - high EMR	lbm/sec	0.50	--	0.49	0.48	0.50	0.50
Undercontrol - low EMR	lbm/sec	--	--	--	0.42	--	0.47
Overcontrol - high EMR	lbm/sec	--	0.75	--	--	--	--
Overcontrol - low EMR	lbm/sec	--	0.70	--	0.59	--	0.72
Total GH2 Added	lbm	70.1	206	75	161	76	161.8

Section 12
Fuel System

TABLE 12-3
LH2 TANK REPRESSURIZATION DATA

PARAMETER	UNITS	S-IVB-501 FLIGHT	S-IVB-501 ACCEPTANCE FIRING	S-IVB-502* ACCEPTANCE FIRING
Repressurization duration	sec	80	94	279
Helium usage from repressurization spheres during repressurization	lbm	47	53	40.5
Ullage				
Volume	cu ft	4,260	4,782	4,780
Pressure at repressurization initiation	psia	19.7	15.8	15.5
Pressure at repressurization termination	psia	32.0	33.0	32.9
Events (sec from second burn Engine Start Command)				
Repressurization initiation		-325	-325	-322
Repressurization termination		-245	-231	-43

*The repressurization system was supplemented by the auxiliary pressurization system. This is not accounted for in mass calculations.

TABLE 12-4
LH2 CHILLDOWN SYSTEM PERFORMANCE DATA

PARAMETER	UNIT	S-IVB-501 FLIGHT		S-IVB-501 [†] ACCEPTANCE FIRING		S-IVB-502 [†] ACCEPTANCE FIRING	
		FIRST BURN	SECOND BURN	FIRST BURN	SECOND BURN	FIRST BURN	SECOND BURN
NPSP							
At Engine Start Command	psi	21.5*	0.17	14.4	10.6	14.3	10.5
Minimum required at engine start	psi	6.3	6.3	6.3	6.3	6.3	6.3
Maximum during chilldown	psi	27.3	16.5	22.5	--	25.6	18.6
<u>Average Flow Coefficient</u>	sec ² / in. ² ft ³	16.5	16.5	14.6	--	18.8	18.8
<u>Fuel Quality in Sections** 2 and 3</u>							
Maximum during unpressurized chilldown	lb gas/ lb mixture	0.023	--	0.052	--	0.049	0.29
At prepressurization		0.020	--	0.044	--	0.042	0.065
<u>Fuel Pump Inlet Conditions</u>							
Static pressure at Engine Start Command	psi	43.89*	28.0	36.3	35.7	38.2	35.1
Temperature at Engine Start Command	deg R	38.9	40.7	39.2	40.0	39.6	39.8
Amount of subcooling at engine start	deg R	3.6	3.0	3.5	2.6	3.7	2.7
<u>Heat Absorption Rate During Unpressurized Chilldown</u>							
Section 1**	Btu/hr	8,200	--	18,000	--	19,000	21,000
Sections 2 and 3**	Btu/hr	27,500	--	30,000	--	25,000	35,000
Total	Btu/hr	35,700	--	48,000	--	44,000	56,000
<u>Heat Absorption Rate During Pressurized Chilldown</u>							
Section 1**	Btu/hr	100	3,500	13,000	--	13,500	19,000
Section 2**	Btu/hr	12,000	11,500	27,500	--	18,000	21,000
Section 3**	Btu/hr	1,500		13,500	--	24,500	15,000
Total	Btu/hr	13,600	15,000	50,000	--	56,000	55,000
<u>Chilldown Flowrate</u>							
Unpressurized	gpm	115	32-95	100	Varied	91	82
Pressurized	gpm	143	143	147	132	135	133
<u>Chilldown Pump Pressure Differential</u>							
Unpressurized	psi	8.7	2-16.5	9.2	9.6	8.8	9.1
Pressurized	psi	7.4	7.8	6.9	8.3	7.5	7.3
<u>Events</u>							
Chilldown initiation	sec ^{††}	-302.8	-567.7	-199.8	-699.6	-200.7	-716.9
Prevalve closed		-272.8	-551.9	-196.1	-970.7	-197.0	-744.5
Prepressurization		-96.5	-326.2	-112.7	-323.2	-111.5	-323.3
Prevalve opened		520.9	-9.8	511.7	-0.7	511.3	-0.8
Chilldown pump off		521.9	-0.8	511.5	-0.9	510.9	-0.9
Chilldown shutoff valve closed		625.5	Not Sent	512.0	-0.4	511.5	-0.5
Engine Start Command		520.7	0	512.5	0	511.9	0

*The NPSP and pump inlet pressure are high at this time as the prevalves were slow in opening. The pump inlet pressure and NPSP with the prevalves open would have been 35.8 psia and 13.41 psi.

**Section 1 is tank to pump inlet; section 2 is pump inlet to bleed valve; section 3 is bleed valve to tank.

[†]During acceptance firing, liftoff is simulated.

^{††}All first burn data are referenced to liftoff (or simulated liftoff); all second burn data are referenced to second burn Engine Start Command.

Section 12
Fuel System

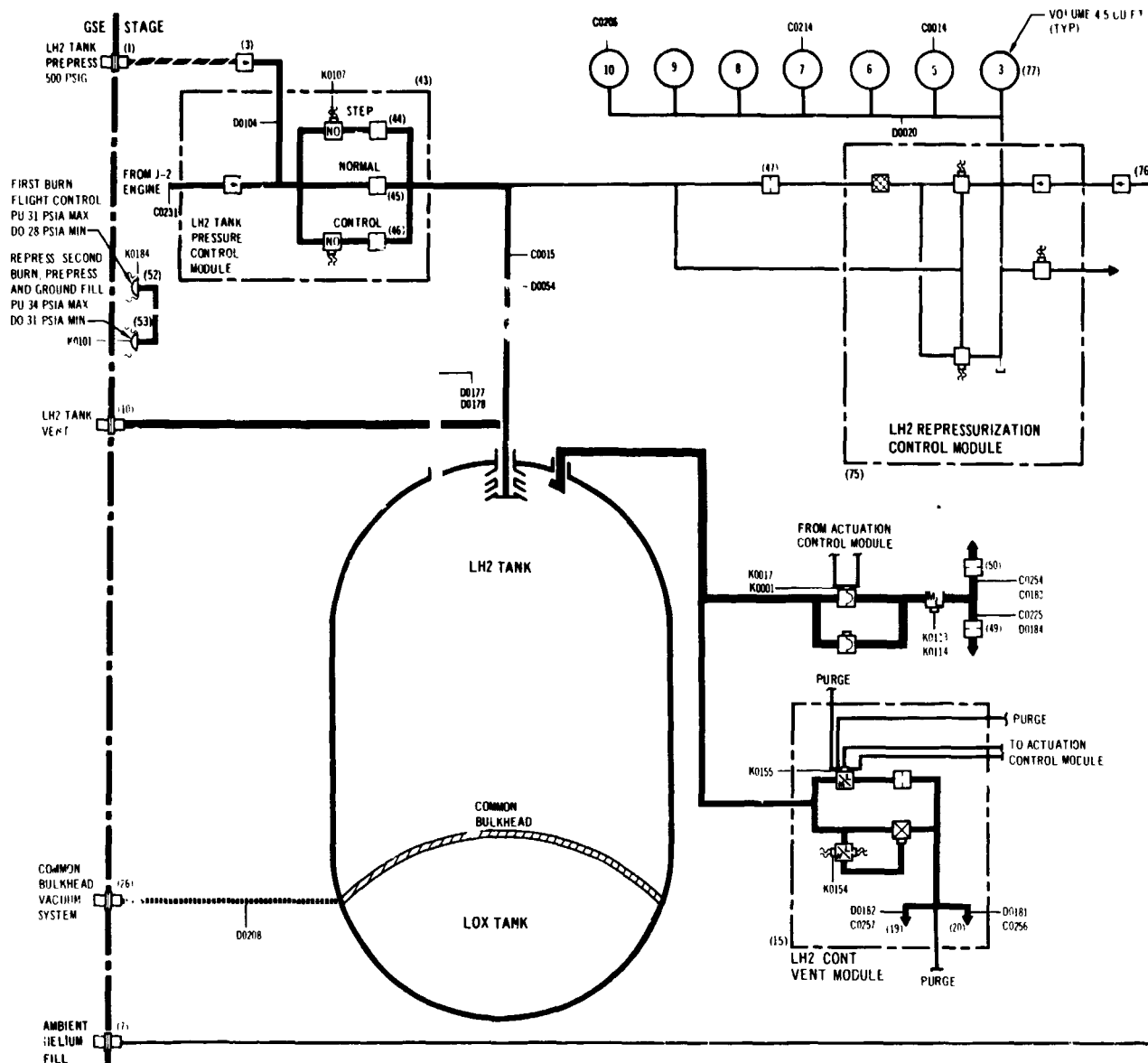
TABLE 12-5
LH2 PUMP INLET CONDITION DATA

PARAMETER	UNIT	S-IVB-501 FLIGHT		S-IVB-501 ACCEPTANCE FIRING		S-IVB-502 ACCEPTANCE FIRING	
		FIRST BURN	SECOND BURN	FIRST BURN	SECOND BURN	FIRST BURN	SECOND BURN
<u>Pump Inlet Conditions</u>							
Static pressure at engine start	psia	43.89*	28.0	36.3	35.7	38.2	25.1
Static pressure at engine cutoff	psia	27.5	31.0	26.7	30.5	27.0	30.8
Temperature at engine start	deg R	38.9	40.7	39.2	40.0	39.6	39.8
Temperature at engine cutoff	deg R	38.8	39.45	37.8	38.9	38.0	39.0
<u>NPSP Requirements</u>							
Minimum at Engine Start Command	psi	6.3	6.3	6.3	6.3	6.3	6.3
At high EMR	psi	6.3	6.3	6.3	-	6.3	-
After EMR cutback	psi	N/A	5.8	5.8	5.8	5.8	5.8
<u>NPSP Available</u>							
At Engine Start Command	psi	21.5*	0.17	14.5	10.6	15.0	10.5
At Start Tank Discharge Valve Open Command	psi	15.1	5.8	17.5	16.9	17.2	16.0
Maximum	psi	16.0	11.0	17.8	17.1	17.8	16.0
Minimum	psi	7.5	6.0	10	10.5	9.5	5.6
At Engine Cutoff Command	psi	7.5	8.75	10	4	9.5	10.0
<u>LH2 Feed Duct</u>							
<u>At High EMR</u>							
Pressure drop	psi	1.0	0.5	1.25	1.25	1.0	1.8
Flowrate	lbm/sec	81	80	82.7	81	79.5	78.5
<u>After EMR Cutback</u>							
Pressure drop	psi	N/A	0.5	--	1.0	--	1.7
Flowrate	lbm/sec	N/A	77	--	77	--	76

*The NPSP and pump inlet pressure are high at this time because the prevalues were slow in opening. The pressure and NPSP with the prevalues open would have been 35.8 psia and 13.41 psia.

N/A - Not applicable

Section 12
Fuel System



NOTE:
(X) ITEM NUMBERS FROM
PARTS LIST
SEE FIGURE 3-1 FOR
LEGEND

Figure 12-1. LH2 Tank Pressurization System

Section 12
Fuel System

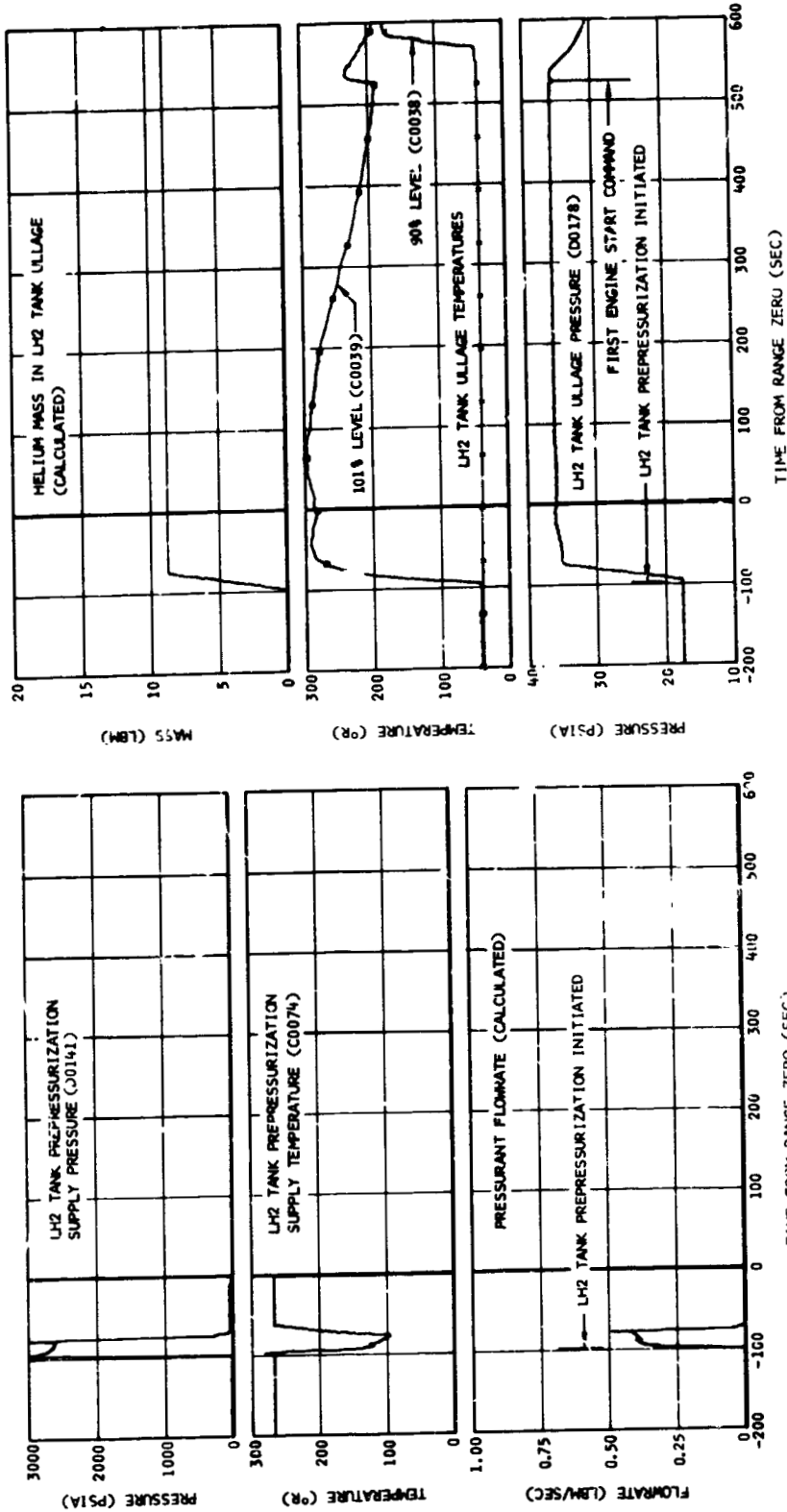


Figure 12-2. LH2 Tank Prepressurization System Performance

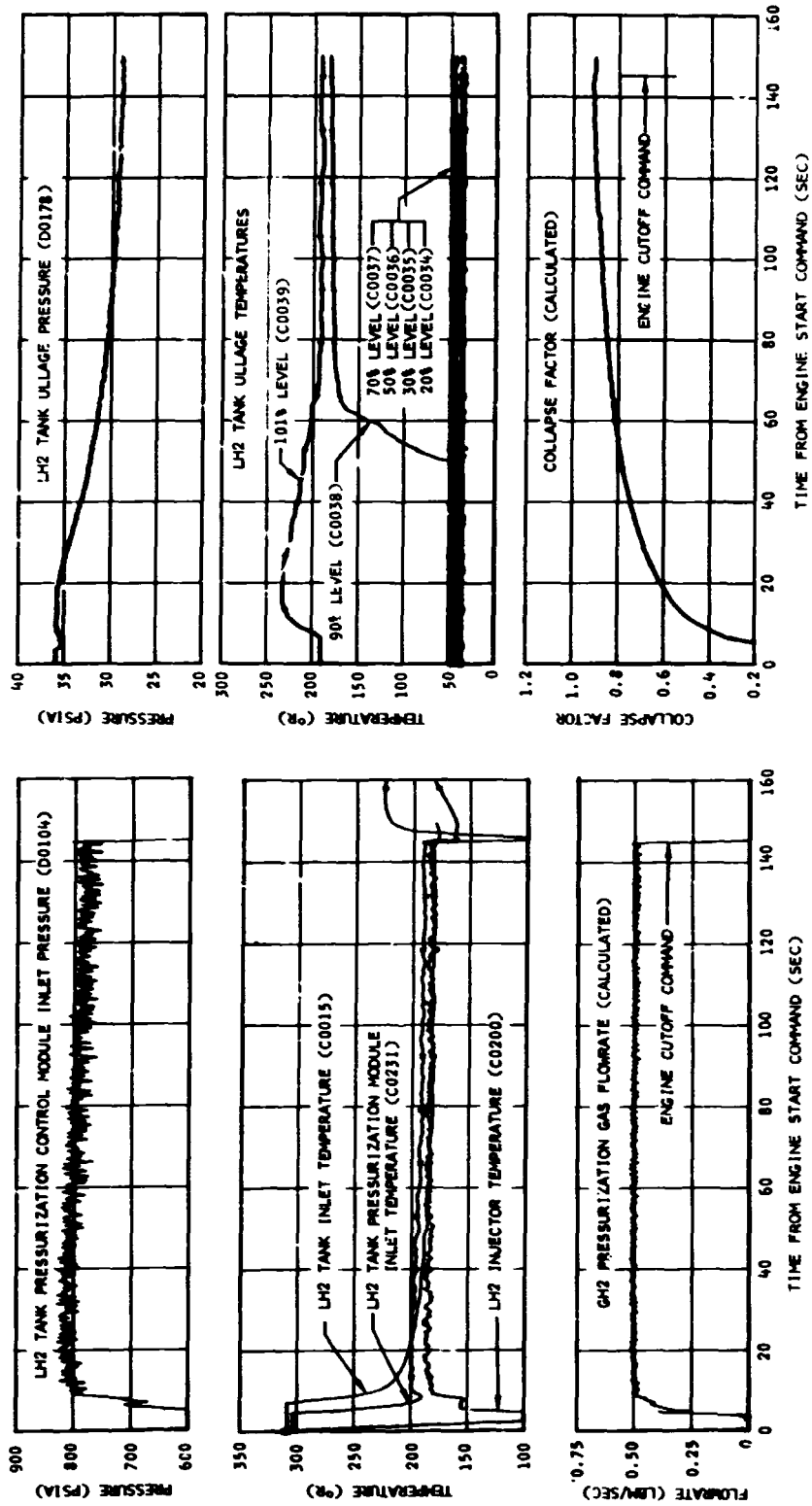


Figure 12-3. LH2 Tank Pressurization System Performance - First Burn

Section 12
Fuel System

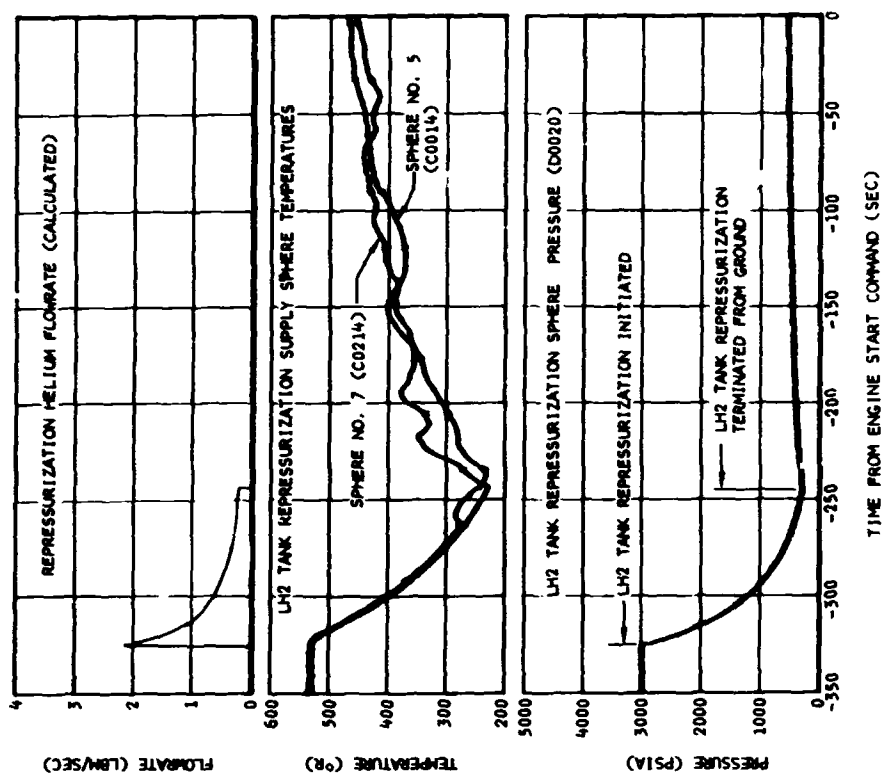
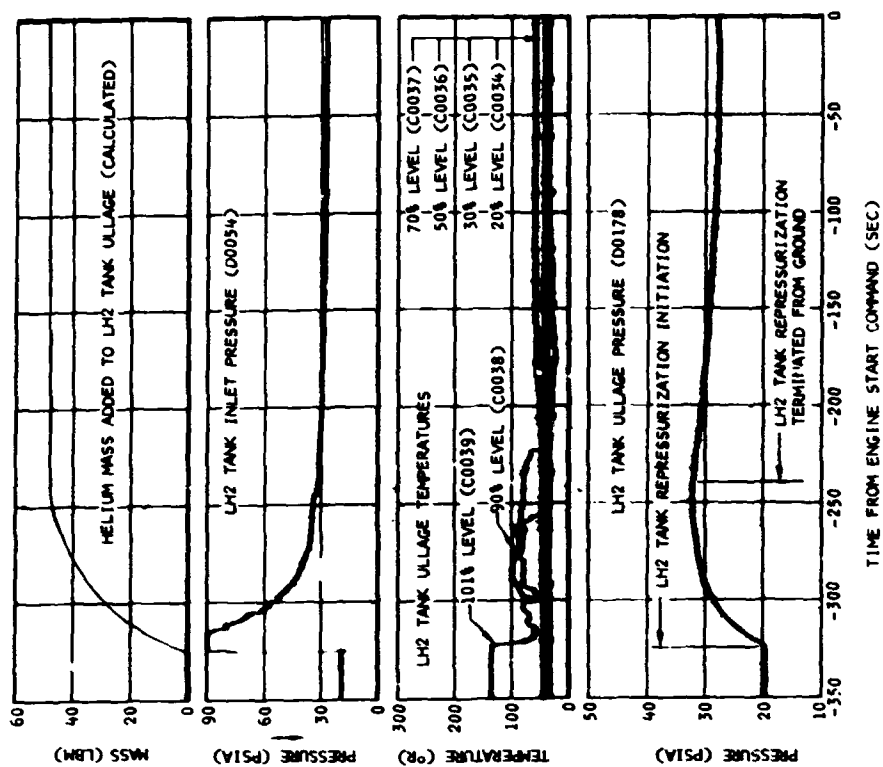


Figure 12-4. LH2 Tank Repressurization System Performance - Second Burn

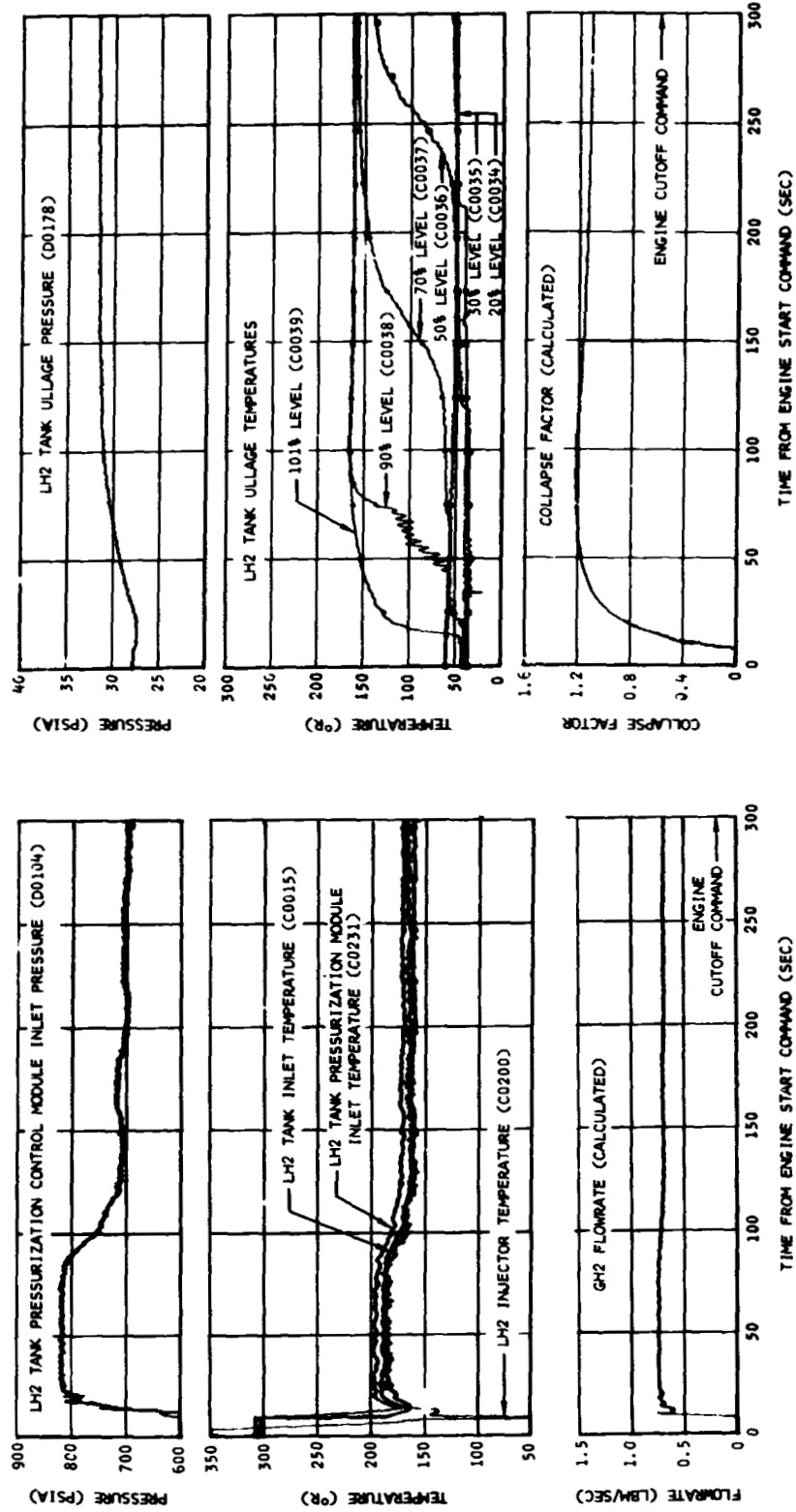


Figure 12-5. LH2 Tank Pressurization System Performance - Second Burn

Section 12
Fuel System

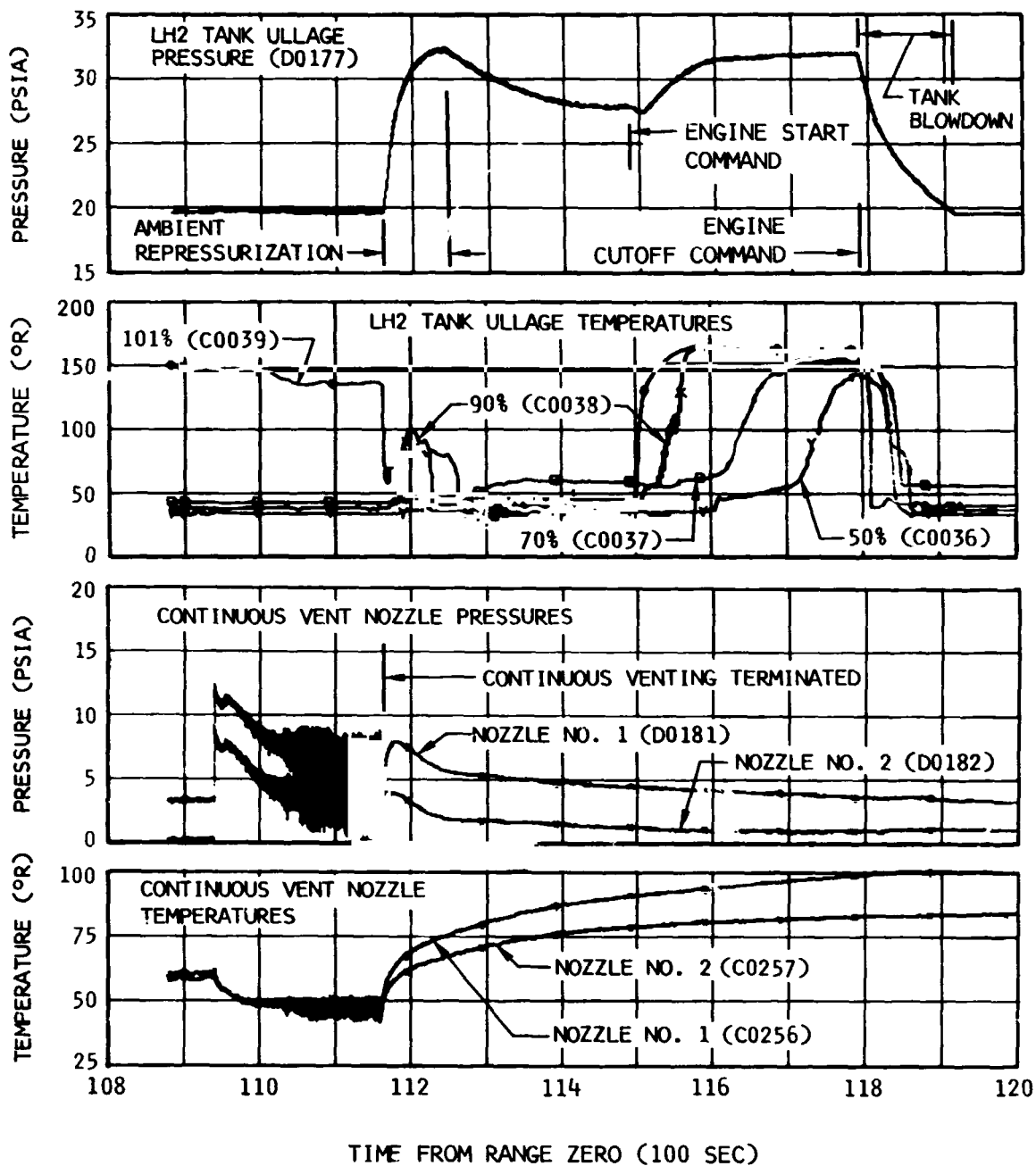


Figure 12-6. LH2 Tank Continuous Vent System Operation During Restart and Second Burn.

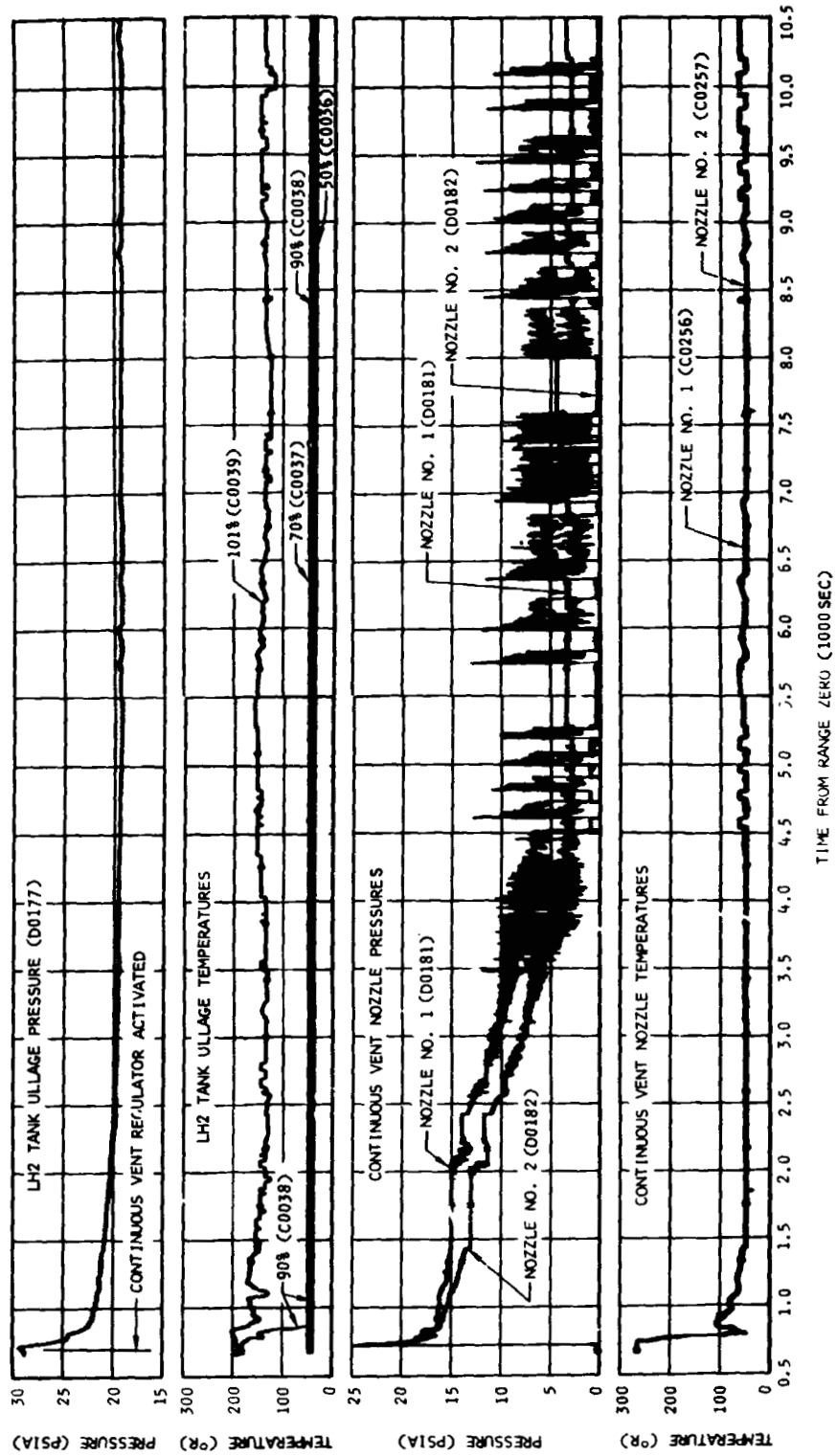


Figure 12-7. LH2 Tank Continuous Vent System Operation During Orbital Coast

Section 12
Fuel System

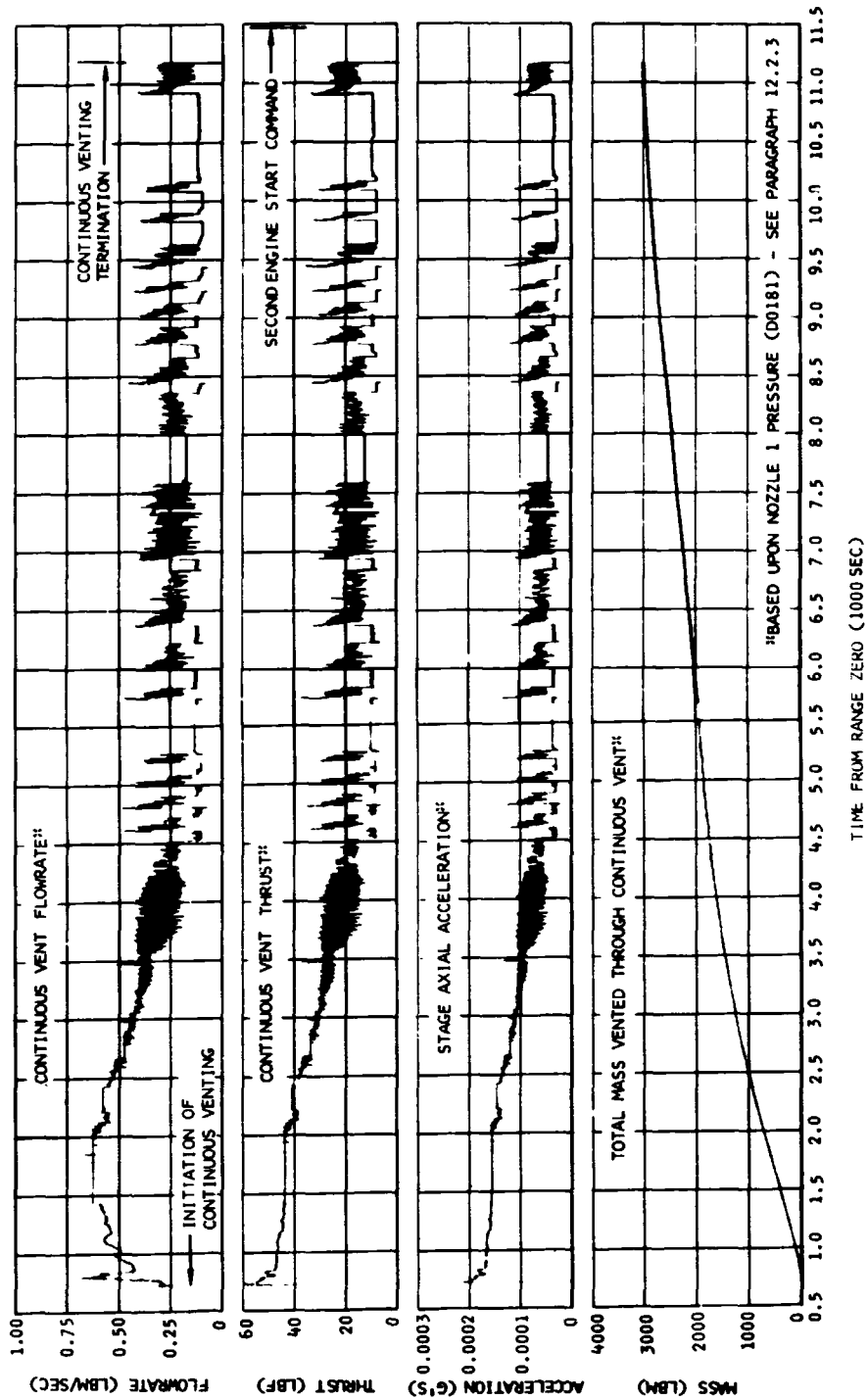


Figure 12-8. LH2 Tank Continuous Vent System Performance During Orbital Coast

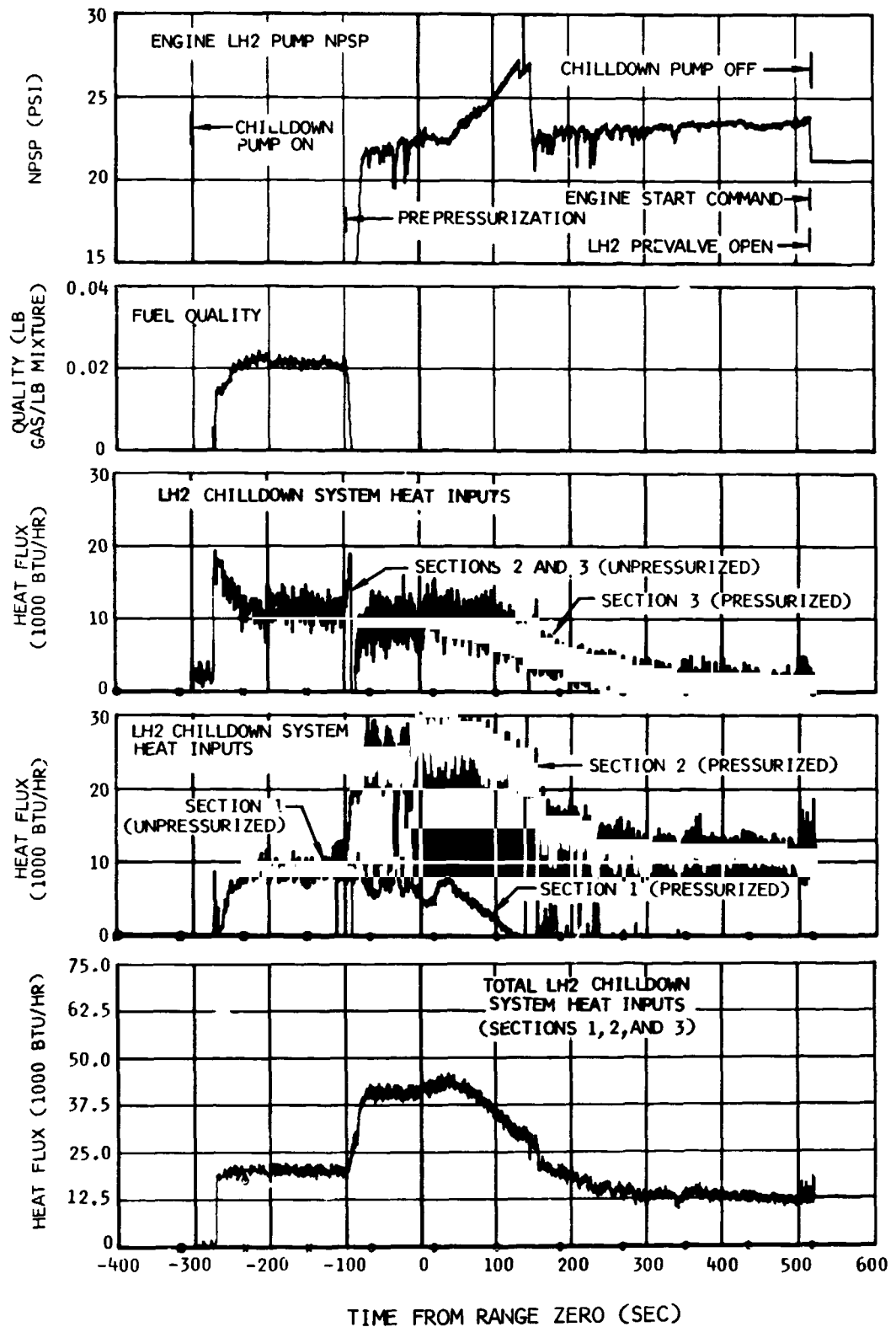


Figure 12-9. LH2 Pump Chilldown Characteristics - First Burn

Section 12
Fuel System

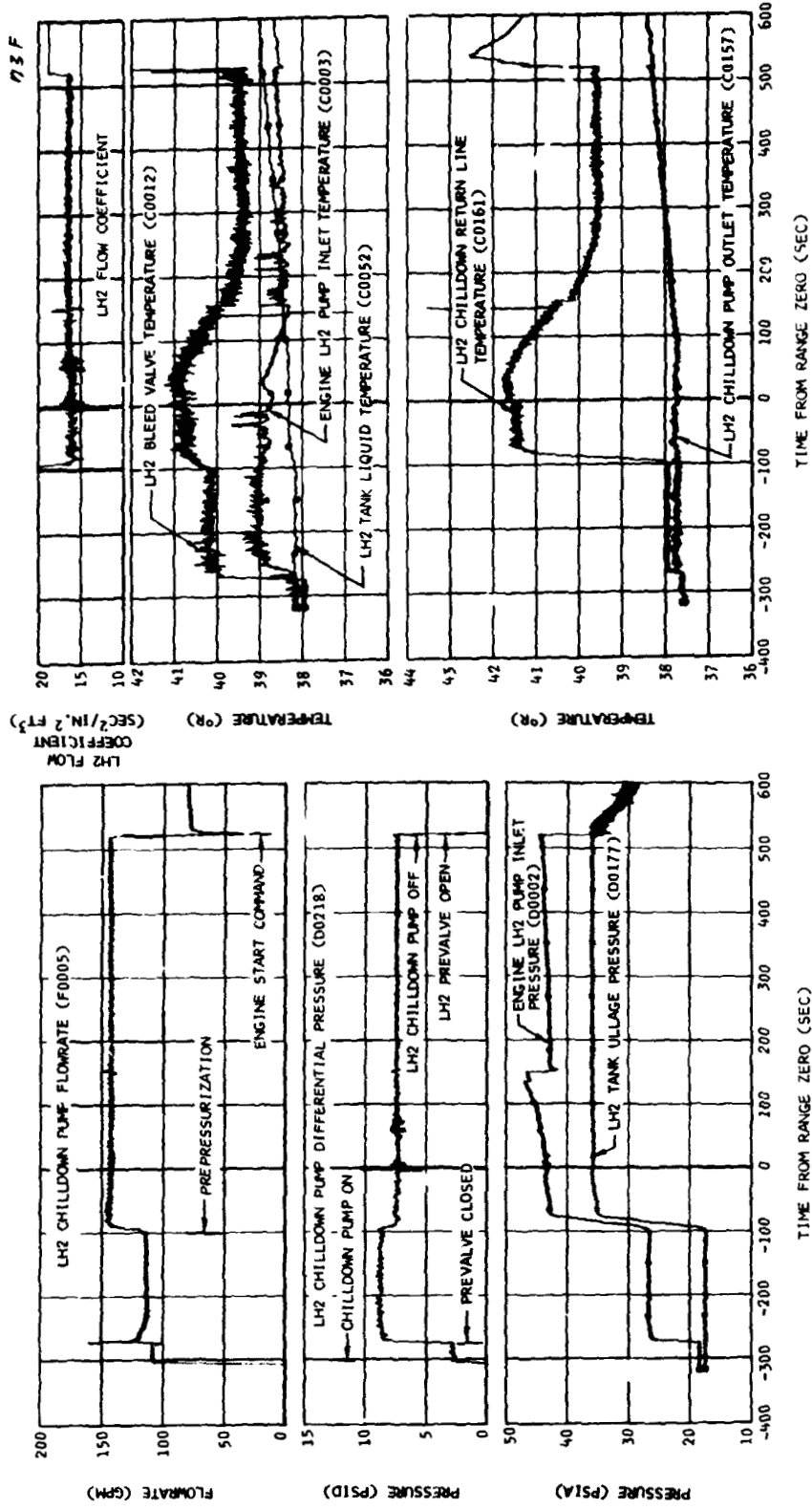


Figure 12-10. LH2 Pump Chilldown - First Burn

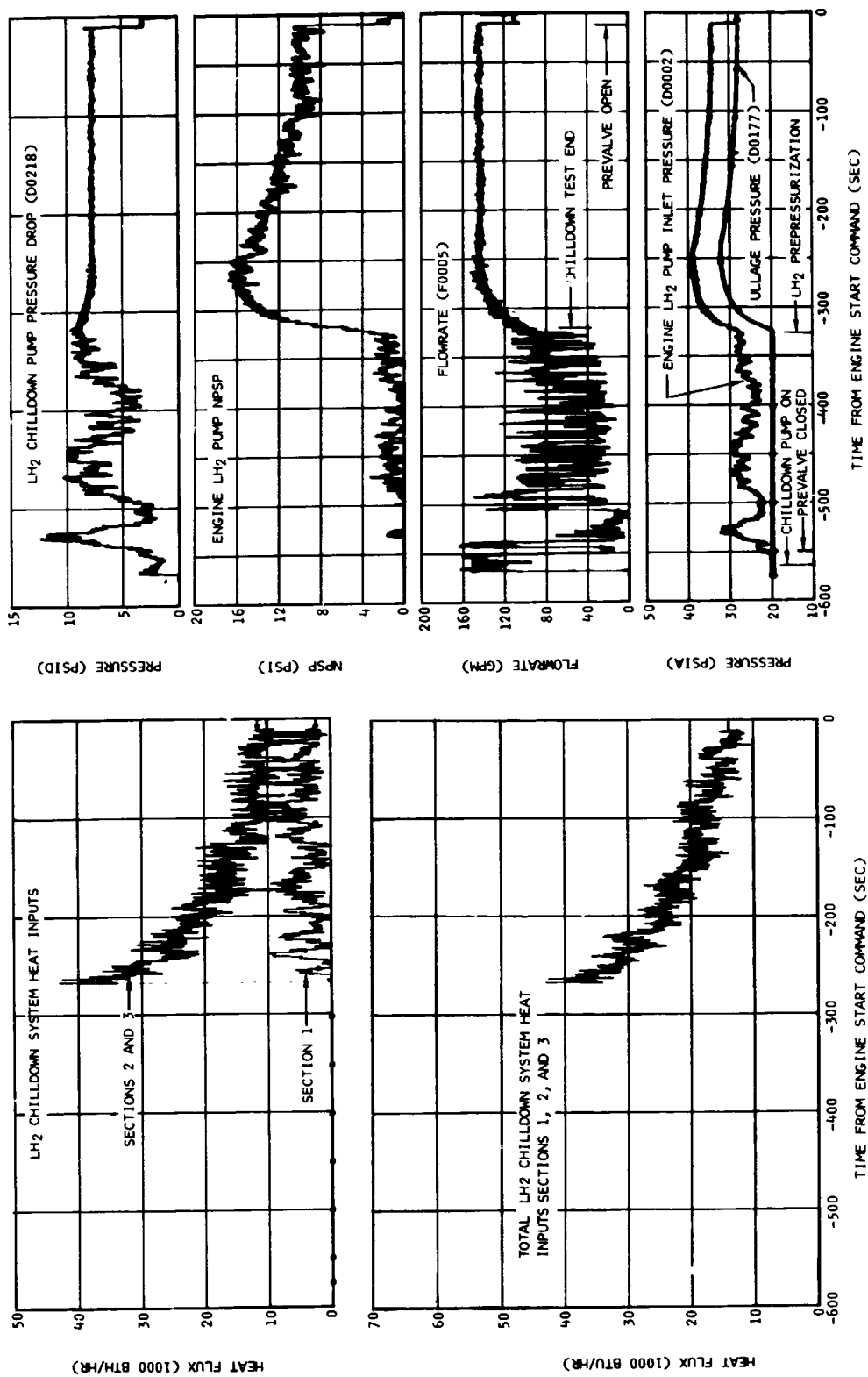


Figure 12-11. LH2 Pump Chilldown Characteristics - Second Burn

Section 12
Fuel System

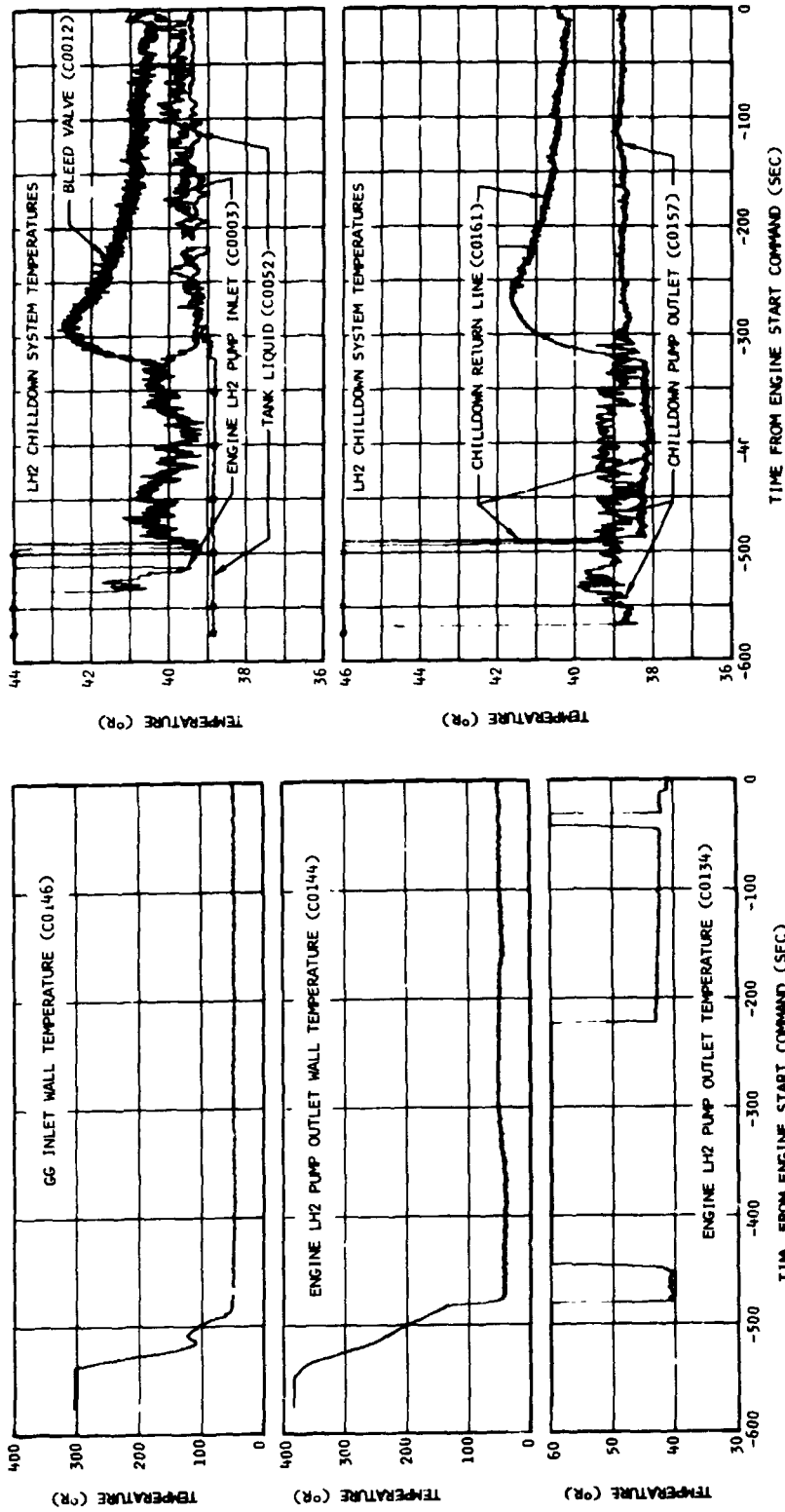


Figure 12-12. LH2 Pump Chilldown - Second Burn

Section 12
Fuel System

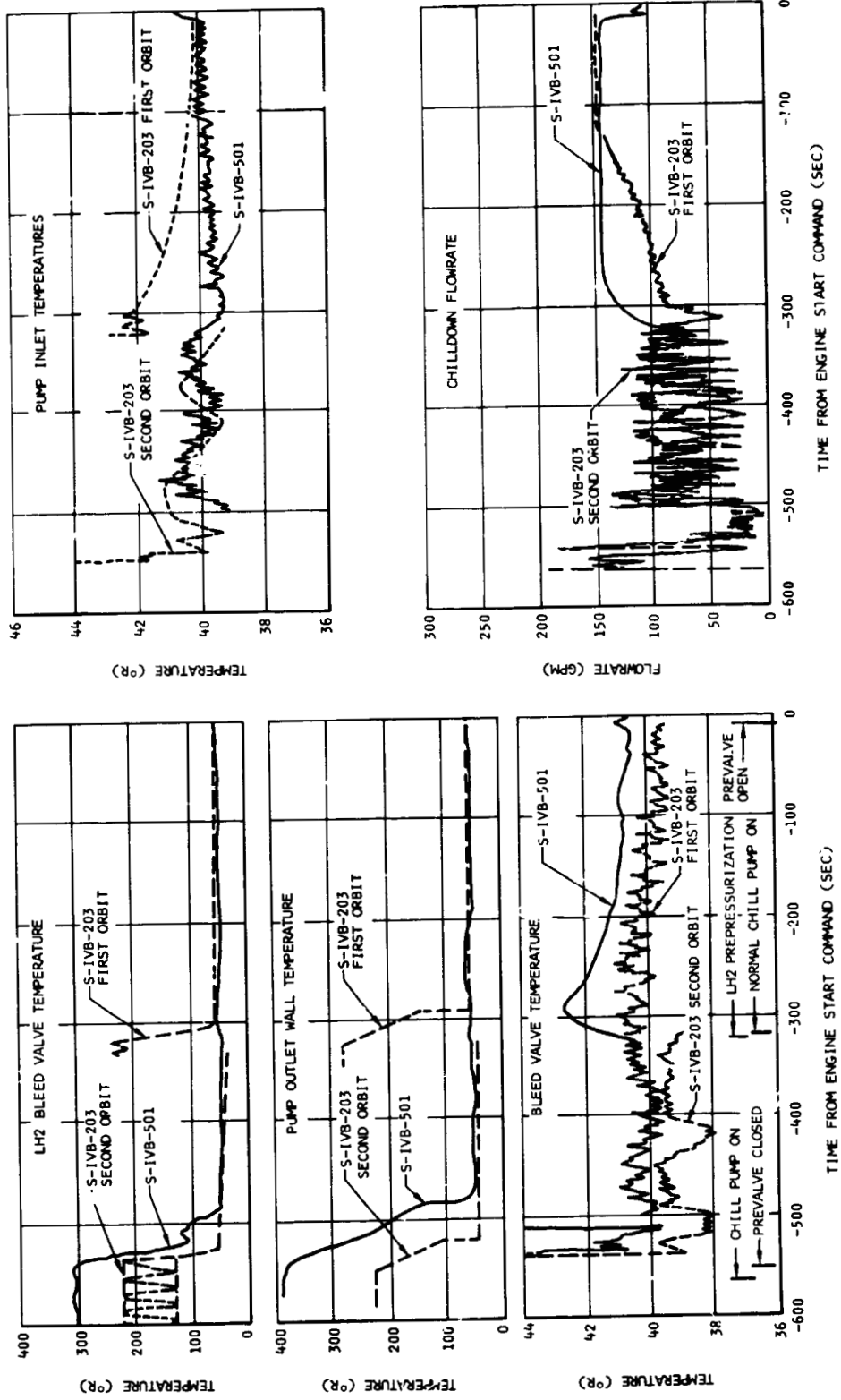


Figure 12-13. S-IVB-501/203 LH2 Orbital Chilldown Comparison - Second Burn

Section 12
Fuel System

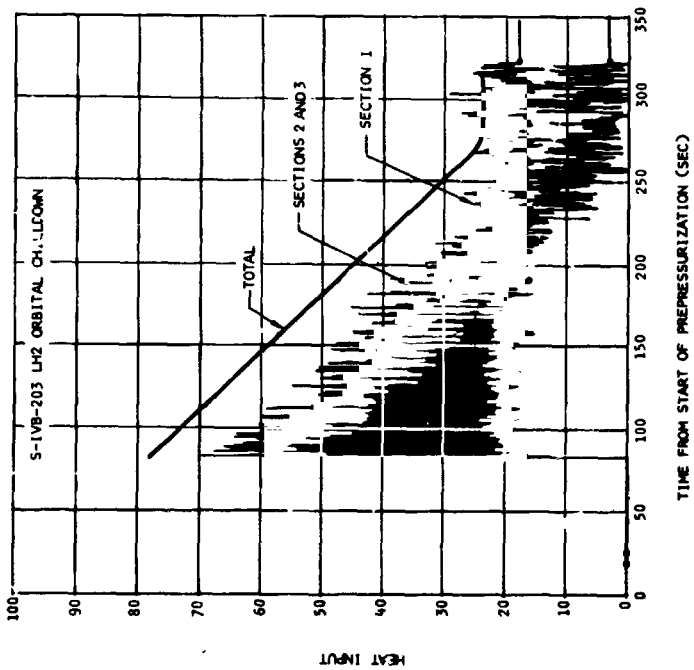
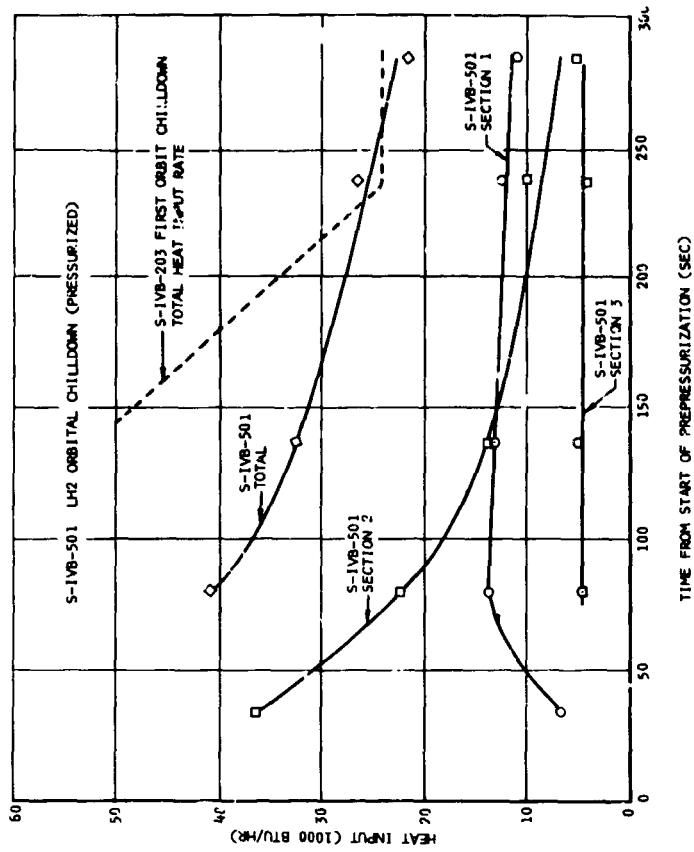


Figure 12-14. S-IVB-501/203 Heat Input Rate

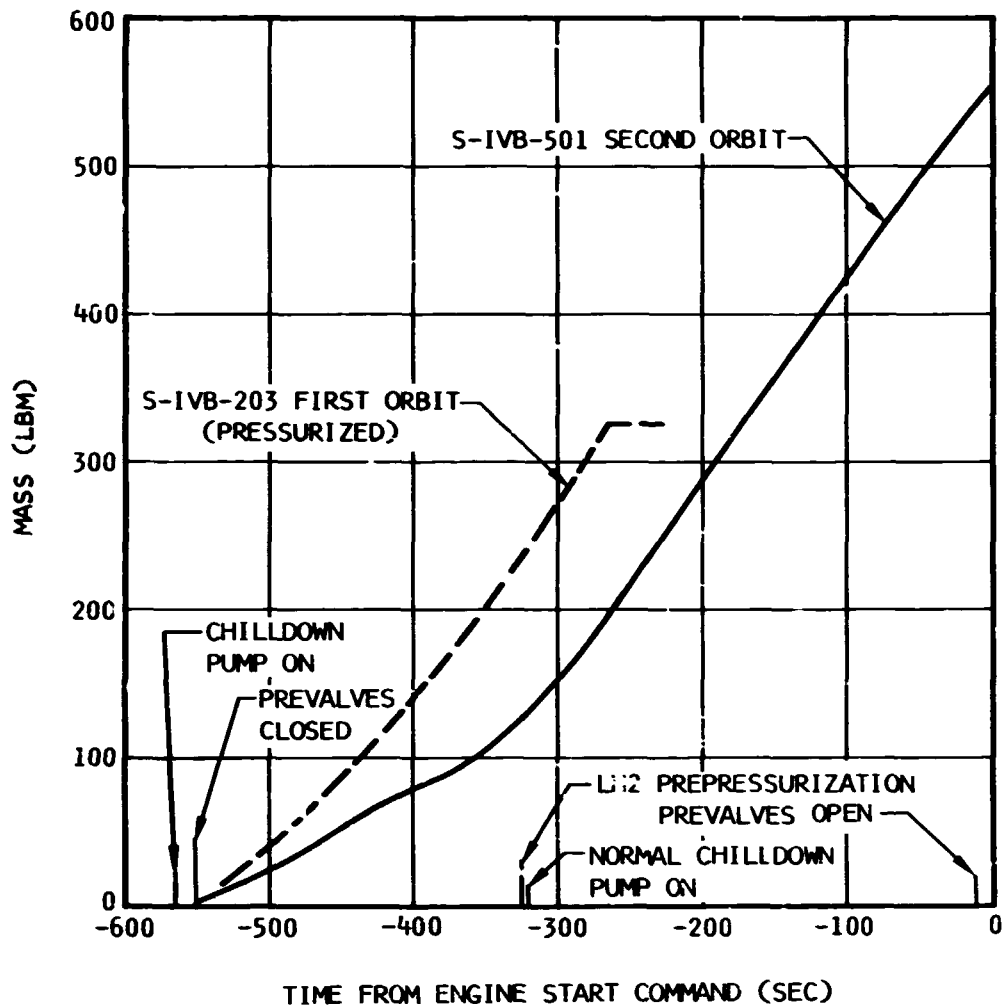


Figure 12-15. S-IVB-501/203 Mass of LH2 Entering Chilldown System

Section 12 Fuel System

NOTE:
(X) ITEM NUMBERS FROM
PARTS LIST
SEE FIGURE 3-1 FOR
LEGEND

LH2 TANK TEMPERATURE PROBE	
MEAS NO	LEVEL (INCHES FROM TANK BOTTOM)
NO021	4"
CO039	11
NO022	401
CO066	395
NO023	370
CO038	350
NO024	340
CO067	333
NO025	309
CO066	303
CO097	288
NO026	279
CO065	273
NO027	248
CO036	227
NO028	218
CO064	212
NO029	187
CO062	180
CO025	166
NO020	157
CO062	152
NO031	126
CO034	105
NO032	96
CO054	87
LO001	60
CO093	55
LO090	24.5
CO067	20

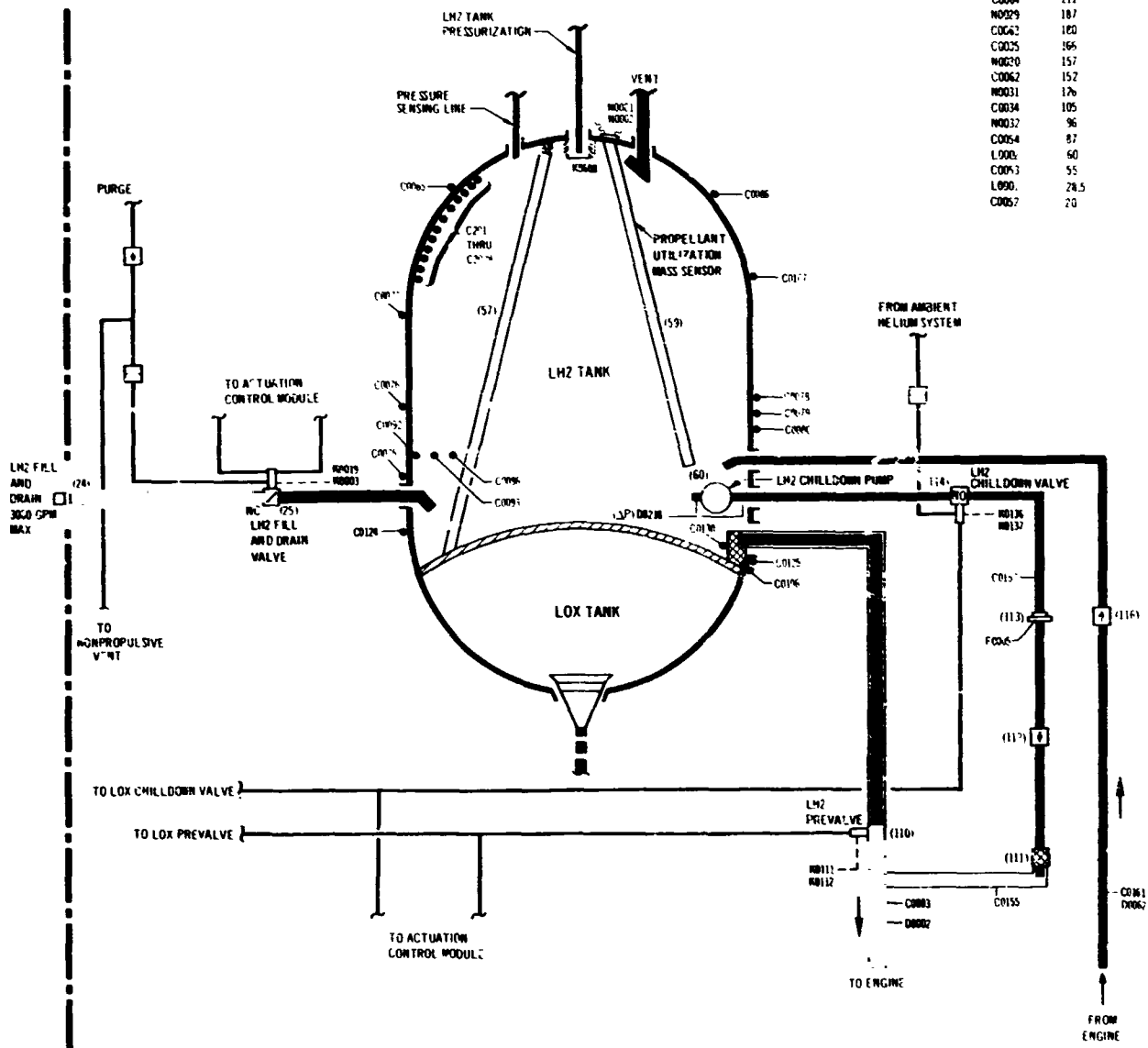


Figure 12-16. LH2 Supply System

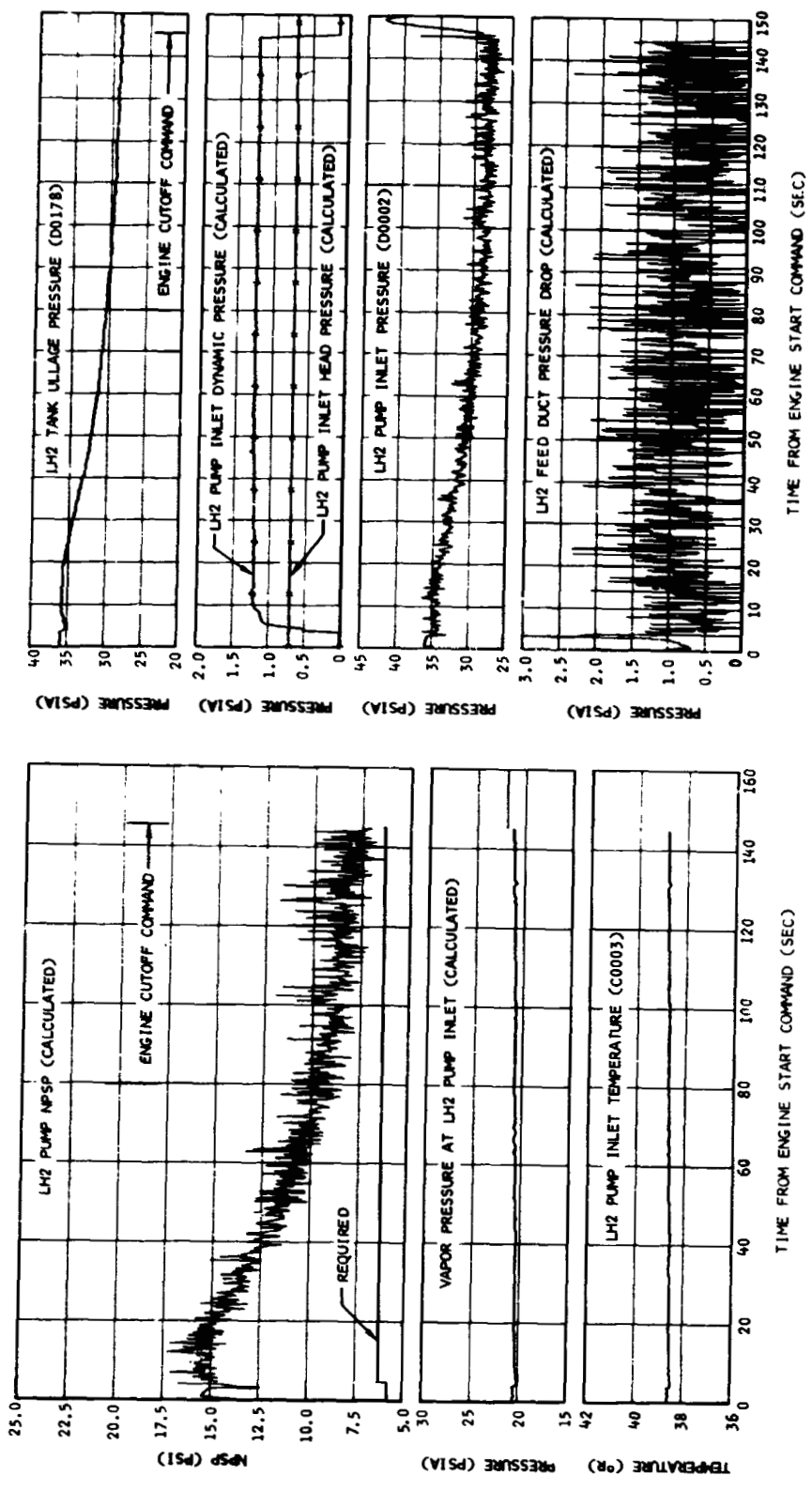


Figure 12-17. LH2 Pump Inlet Conditions - First Burn

Section 12
Fuel System

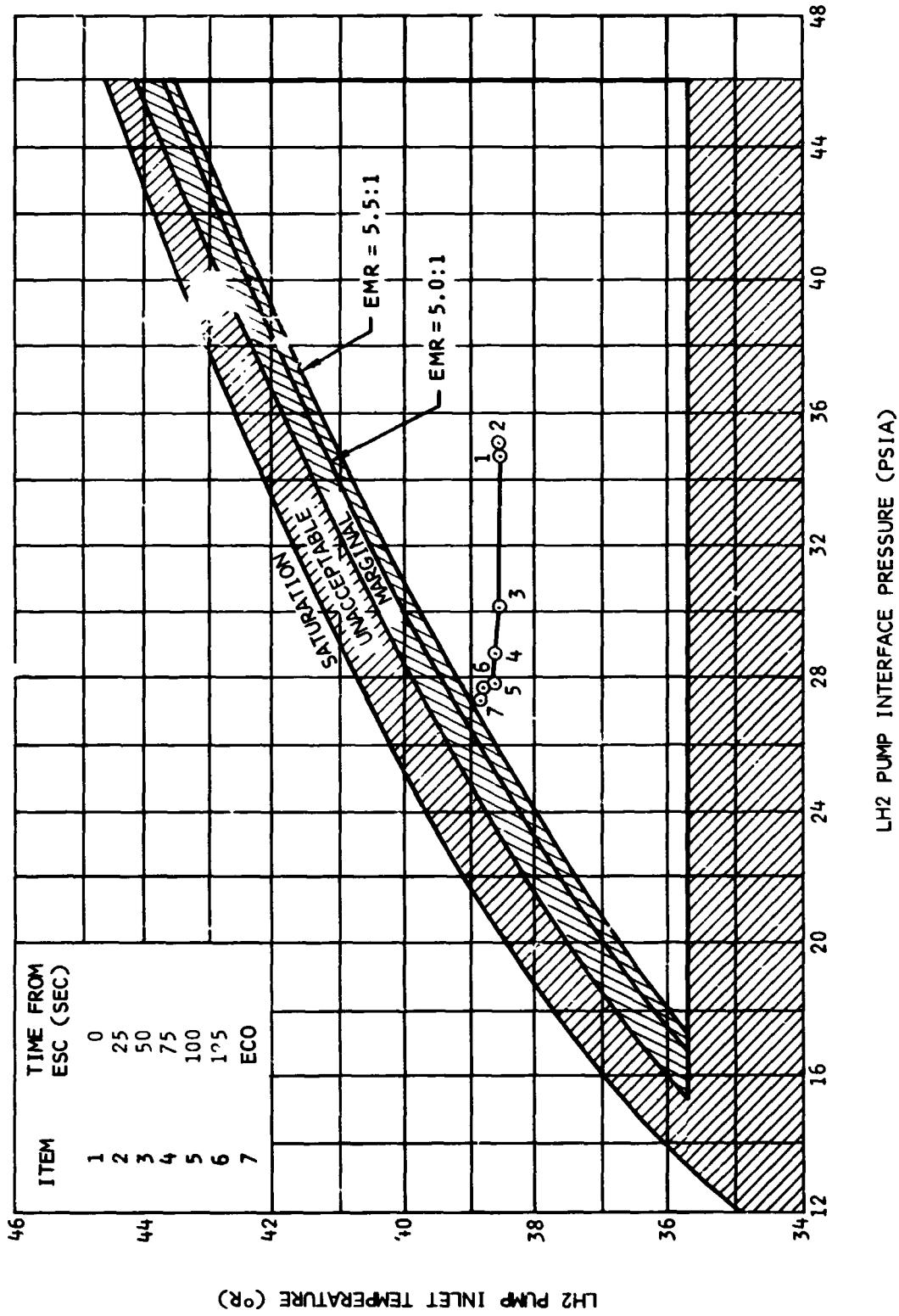


Figure 12-18. LH2 Pump Inlet Conditions During Firing - First Burn

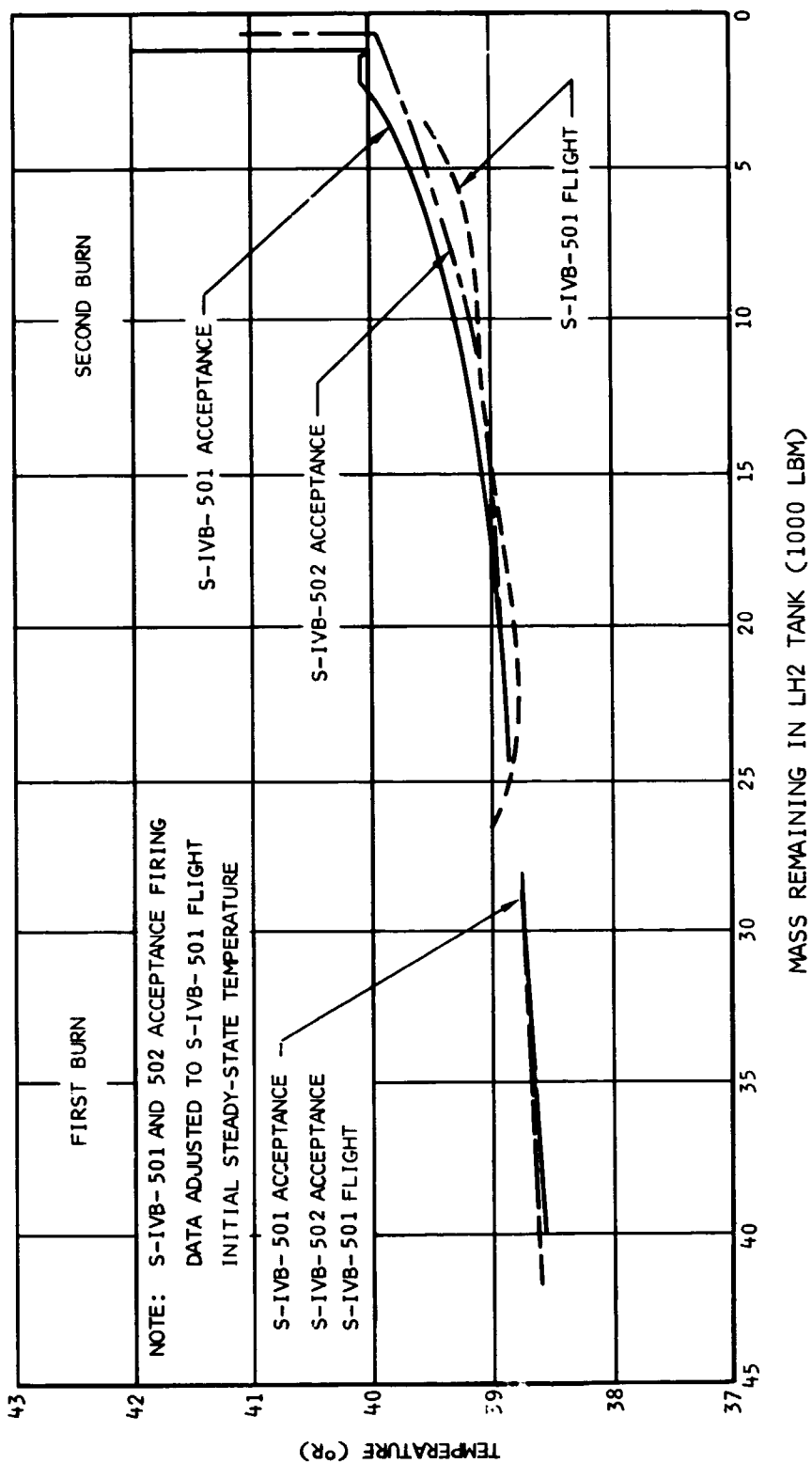


Figure 12-19. Effect of LH2 Mass Level on LH2 Pump Inlet Temperature

Section 12
Fuel System

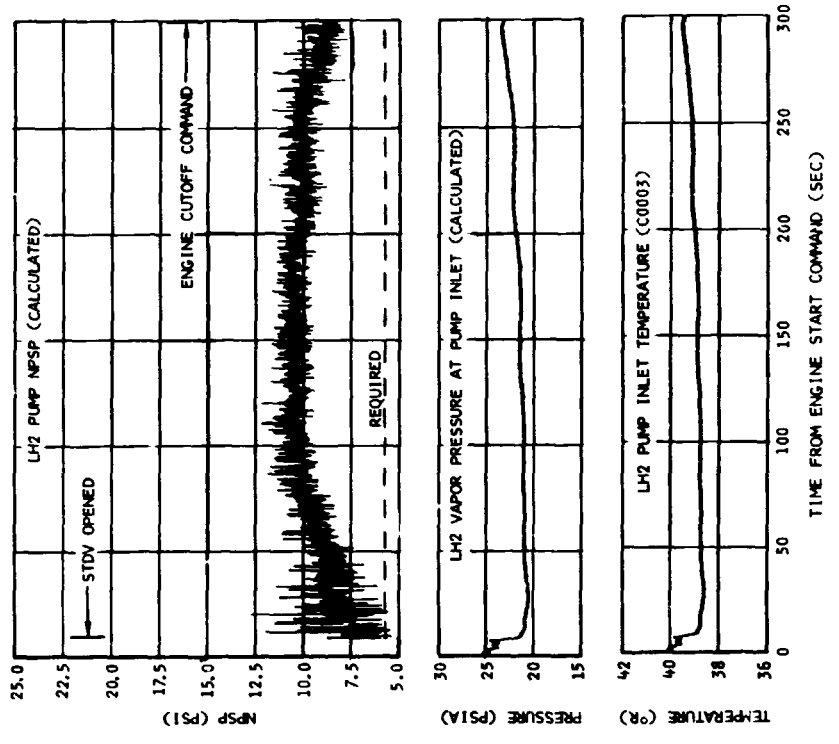
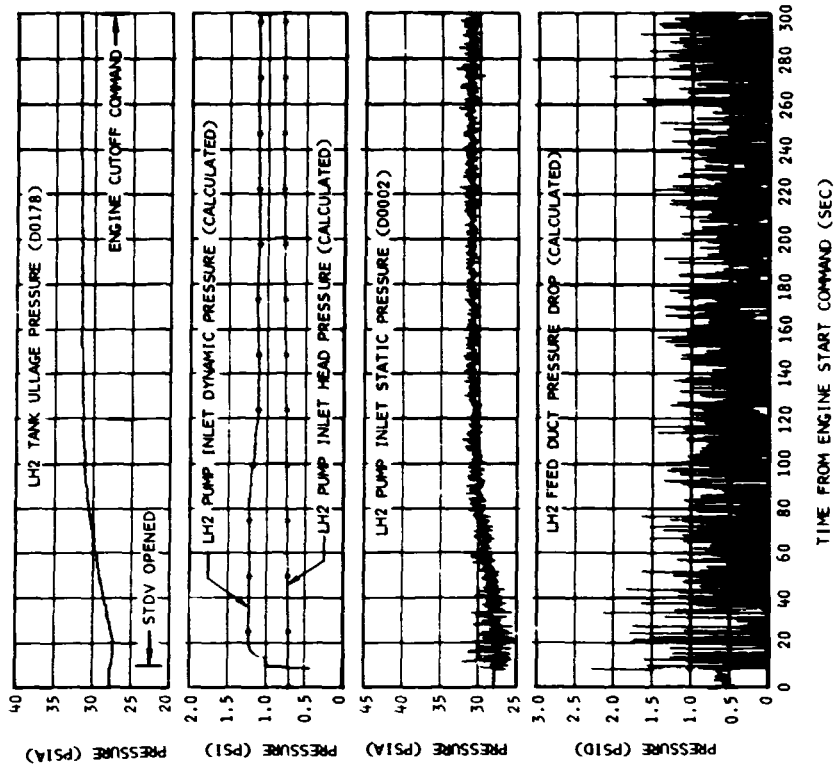


Figure 12-20. LH2 Pump Inlet Conditions - Second Burn

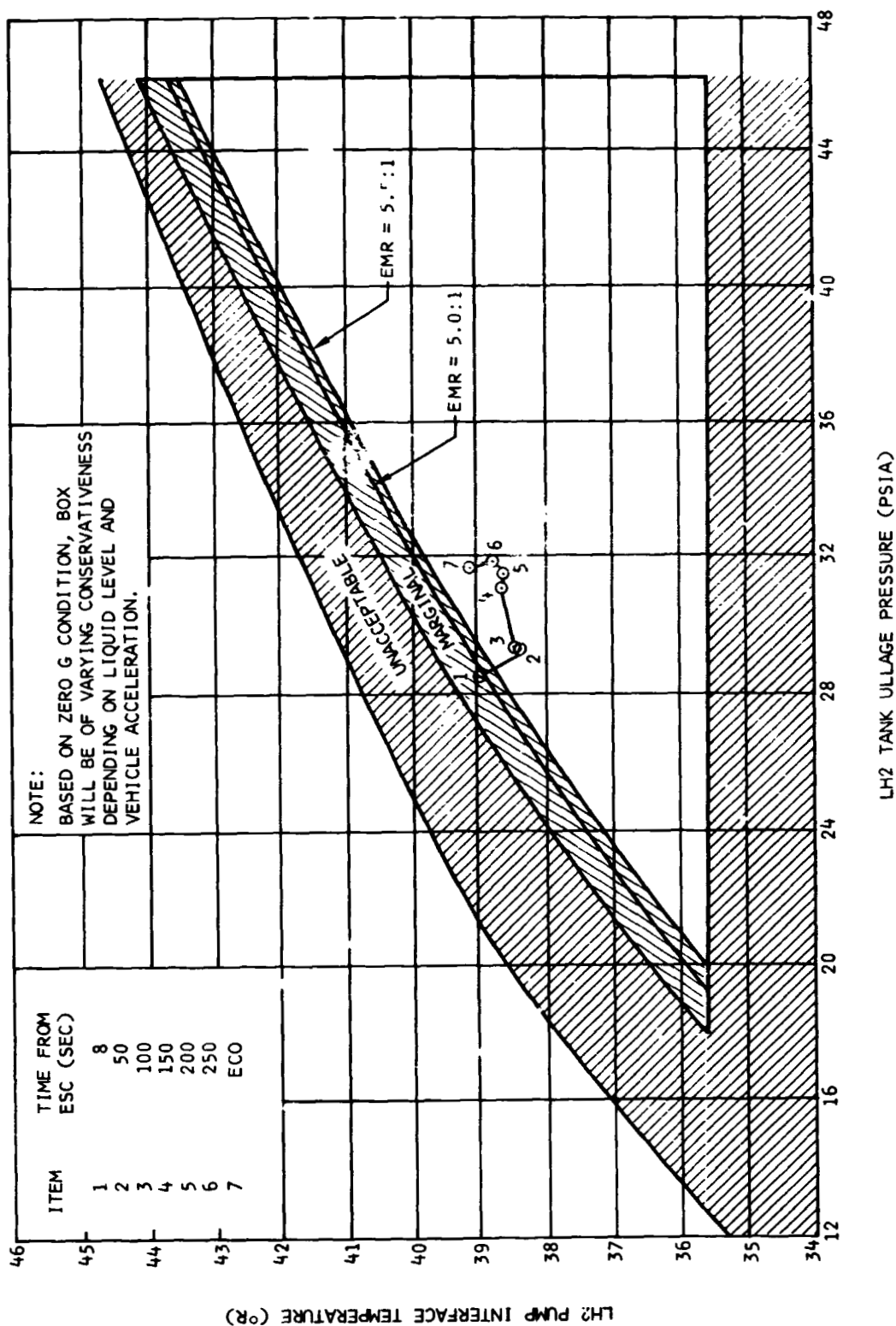


Figure 12-21. LH2 Pump Inlet Conditions During Firing - Second Burn

13. AUXILIARY PROPULSION SYSTEM

The attitude of the S-IVB stage is controlled by two auxiliary propulsion system (APS) modules (figure 13-1) mounted 180 deg apart on the aft skirt of the stage. Each module is a self contained unit composed of four basic systems: (1) The oxidizer system; (2) the fuel system; (3) the helium pressurization system; and (4) the engines. The instrumentation unit, mounted above the S-IVB stage, provides signals for operation of the APS modules.

Each module contains two 150 lbf thrust engines which provide roll control during S-IVB powered flight, and yaw and roll control during the coast periods. A third 150 lbf thrust engine in each module provides pitch control during the coast periods. Each module also contains a 72 lbf thrust engine to provide thrust for LOX and LH2 tank ullage control after first burn and during restart preparations.

13.1 APS Flight Operation

Examination of the APS flight data indicates that the operation of the two APS modules was adequate to fulfill the attitude control, maneuvering, and ullaging requirements of the mission. With the exception of the roll/yaw engines of module 1, the APS performance was as expected. The anomalies of the module 1 engines are discussed in paragraph 13-4.

13.1.1 APS Flight Objectives

All objectives of the S-IVB-501 flight with respect to the APS modules were accomplished. These were as follows:

- a. To evaluate APS operation under actual flight conditions
- b. To better substantiate APS requirements
- c. To evaluate the ability of the APS to respond to the attitude control, firing command, and ullage commands.

Section 13
Auxiliary Propulsion System

13.1.2 APS Flight Description

Approximately 1 sec after S-II engine cutoff, the APS was activated to provide roll control during S-IVB J-2 first burn.

Following S-IVB J-2 engine cutoff, APS pitch and yaw control was activated to maintain the vehicle in the desired attitude. The APS ullage engines fired for 88 sec following J-2 engine first burn to provide slosh control and propellant settling.

Approximately 330 sec prior to restart the APS ullage engines were again ignited to provide ullage control during restart preparations. The ullage engines were shut off 3 sec after second burn J-2 Engine Start Command.

After second burn J-2 engine start, the APS pitch and yaw control was deactivated, and the APS provided only roll control during J-2 engine burn. After the second J-2 engine cutoff, the APS pitch and yaw control was reactivated and the APS provided pitch, yaw, and roll control to maintain the stage in the desired attitude for the remainder of the mission.

13.2 APS Module No. 1

The operation of the helium pressurization system of module No. 1 was as expected. The propellant supply system pressure levels were as expected; however, the recorded propellant temperatures were higher than anticipated during the third orbit. The performance of engine 1-2 was near nominal throughout the mission. Engines 1-1 and 1-3 were approximately 15 percent low in performance at the start of the mission, and engine 1-3 was approximately 45 percent low at the end of the flight.

13.2.1 Helium Pressurization System (Module No. 1)

The module No. 1 helium pressurization system operation was normal with no problems encountered throughout the flight. Prior to APS activation, the helium bottle pressure was 2,960 psia and the temperature was 550 deg R yielding an initial mass in the bottle of 0.984 lbm.

Figure 13-2 shows the helium temperature, pressure, and mass as a function of mission time. The nominal and three-sigma predictions are included for comparison. The mass of helium remaining in the bottle 25,000 sec after liftoff was 0.658 lbm. This corresponds to a helium temperature of 578 deg R and a pressure of 2,010 psia. Figure 13-2 shows that the helium usage was near the nominal for all portions of the mission except the period from restart preparations through spacecraft separation, when propellant consumption was less than predicted. The regulator outlet pressure was steady at 196 psia throughout APS operation. The propellant tank ullage pressures were 188 to 192 psia. These values are within the expected range of 188 to 203 psia.

13.2.2 APS Oxidizer System (Module 1)

The oxidizer manifold supply pressure of module No. 1 was as expected during the flight. The pressure was approximately 190 psia during APS operation. The oxidizer temperature (measured at the propellant control module) was higher than expected, exceeding the transducer range of 591.7 deg R during the waiting orbit (figure 13-3). Evaluation of the data indicates that the oxidizer bulk temperature (in the tank) remained near the liftoff value of 550 deg R; therefore, this value was used for propellant consumption determination.

The oxidizer remaining in the APS as a function of mission time is shown in figure 13-3. The nominal and three-sigma predictions are included for comparison. The initial oxidizer load of module No. 1 was 182 lbm. This was less than the nominal 188 lbm due to the excess removed during gas bubble removal. The oxidizer consumption during the first two orbits was near the three-sigma maximum; however, during the restart preparations and through spacecraft separation, the consumption was less than predicted. After spacecraft separation, the consumption was near the predicted value. Table 13-1 shows the propellant consumption during significant periods of the flight. There were 70 lbm of oxidizer remaining in module No. 1 at 25,000 sec after liftoff. Therefore, 112 lbm or 62 percent of the oxidizer in module No. 1 was consumed during the flight.

Section 13 Auxiliary Propulsion System

13.2.3 APS Fuel System (Module No. 1)

The fuel system of module No. 1 performed as expected during the flight. The fuel manifold supply pressure remained at approximately 190 psia. The fuel temperature measured at the propellant control module remained between 548 and 564 deg R. Again, the data indicates that the fuel bulk temperature remained near the liftoff value of 550 deg R (figure 13-3). Therefore, this value was used to determine propellant consumption.

The fuel remaining in module No. 1 during the mission is shown in figure 13-3. The liftoff value was nominal at 125 lbm. As with the oxidizer, the consumption during the first two orbits was greater than the nominal prediction, but within the three-sigma prediction. The usage during the period from restart preparations to spacecraft separation was less than predicted. After spacecraft separation, the fuel consumption was near the predicted value. At RO +25,000 sec, 46 lbm of fuel remained in module No. 1. Thus the fuel consumption during the mission was 79 lbm or 63 percent. The fuel consumption during significant portions of the flight is shown in table 13-1.

13.3 APS Module No. 2

All systems of APS module No. 2 performed as expected. The engine 2-3 chamber pressure problem encountered during burp firing remained during the flight but became less pronounced near the end of the mission.

13.3.1 Helium Pressurization System (Module No. 2)

The module No. 2 helium pressurization system operation was normal with no problems encountered throughout the flight. Prior to APS activation, the helium bottle pressure was 2,980 psia and the temperature was 547 deg R. The mass of helium in the bottle was 0.994 lbm. Figure 13-1 shows the helium temperature, pressure, and mass as a function of mission time. The nominal and three-sigma predictions are included for comparison.

Figure 13-2 shows that the APS module No. 2 helium usage was near the nominal predicted values except during the period from restart preparations through spacecraft separation when the propellant consumption was less than predicted. The mass of helium in the bottle at RO +25,000 sec was 0.662 lbm. This corresponds to a helium temperature of 513 deg R and a pressure of 1,800 psia.

The regulator outlet pressure remained steady at 196 psia throughout APS operation. The propellant tank ullage pressures were 188 to 192 psia. Their values are within the expected range of 188 to 203 psia.

13.3.2 APS Oxidizer System (Module No. 2)

The oxidizer system of module No. 2 performed as expected during the flight. The manifold supply pressure was approximately 190 psia. The oxidizer temperature (measured at the propellant control module) ranged from 538 to 556 deg R. As with module No. 1, the data indicate that the oxidizer bulk temperature (in the tank) remained nearer 550 deg R. Therefore this value was utilized for propellant consumption calculations.

Figure 13-3 shows the oxidizer remaining in the APS as a function of mission time. The nominal and three-sigma predictions are included for comparison. The initial oxidizer load for module No. 2 was 187 lbm. The difference between this and the nominal load of 188 lbm is due to the excess oxidizer removed during gas bubble removal operations. The oxidizer consumption during the mission was near the predicted nominal except during the period from restart preparations to spacecraft separation. During this period, the consumption was less than expected. Table 13-1 shows the propellant consumption during significant portions of the flight. At RO +25,000 sec, 72 lbm of oxidizer remained in the APS; therefore 115 lbm or 62 percent of the oxidizer in module No. 2 was consumed during the flight.

13.3.3 APS Fuel System (Module No. 2)

The fuel system of module No. 2 performed as expected during the flight. The fuel manifold supply pressure was approximately 190 psia throughout

Section 13 Auxiliary Propulsion System

the flight. The fuel temperature measured at the propellant control module ranged from 546 deg R at liftoff to 586 deg R near apogee of the waiting orbit. The data indicate that the bulk temperature remained near 550 deg R throughout the flight. Therefore, this value was used to calculate propellant consumption.

The fuel remaining in module No. 2 during the mission is shown in figure 13-3. The liftoff load was nominal at 125 lbm. Fuel consumption during the mission was near nominal except during the period from restart preparations to spacecraft separation. During this period, the consumption was less than predicted. At $t_0 + 25,000$ sec, 44 lbm of fuel remained in module No. 2. Thus, 81 lbm or 65 percent of the fuel was consumed during the mission. Fuel consumption is shown in table 3-7 for significant periods of the mission.

13.4 Engine Performance

Although the APS operated adequately to fulfill the mission requirements, the performance of the roll/yaw engines of module No. 1 was low. Engine 1-1 chamber pressure oscillated abnormally for a period, and engine 1-3 chamber pressure indicated significant loss of performance near the end of the mission. The module No. 1 ullage engine chamber pressure decay was excessively long at termination of ullage engine firing. Module No. 2 performed as expected.

Since the minimum impulse bit duration of the APS engines is 0.065 sec, data used in the evaluation of engine performance must be recorded continuously. The only APS engine data from the S-IVB-501 flight meeting this requirement were the engine chamber pressures. By integrating the chamber pressure and multiplying the integral by the thrust coefficient (C_F) and the throat area (A_t), the total impulse for each pulse was determined. By dividing the total impulse by the pulse duration, the average thrust during each pulse was calculated. Due to the inaccuracies associated with the propellant consumption calculations, the specific impulse of the engines was not determined.

13.4.1 Engine Anomalies

The following anomalies were noted from the APS engine chamber pressure traces:

- a. Low chamber pressure (85 psia) exhibited by engines 1-1 and 1-3 from the start of the mission
- b. Approximately 400 cps oscillations (55 to 95 psia) in engine 1-1 chamber pressure from RO +17,000 to RO +23,000 sec
- c. Engine 1-3 chamber pressure decreased to 55 psia near the end of the mission
- d. Excessive "tail-off" of the chamber pressure of module No. 1 ullage engine.

The chamber pressure levels of the module No. 1 engines are shown in figure 13-4. The propellant temperatures (measured at the propellant control modules) and the engine injector temperatures are included for comparison of trends. The oscillations of engine 1-1 chamber pressure and the greatest decline of engine 1-3 chamber pressure occurred at the period of high oxidizer temperature. The dip in propellant and injector temperatures at approximately RO +19,600 sec is due to multiple firings of the engines which bring cooler propellant from the tank past the temperature probe. The APS engine thrust levels calculated from the chamber pressures are shown in figure 13-5 which shows that the module No. 1 engine thrusts follow the chamber pressure curves of figure 13-4 very well. The thrust levels of the module No. 2 engines improved slightly as the mission progressed.

Figure 13-6 shows typical pulses of engines 1-1, 1-3, 2-3, and the start and cutoff transients of the ullage engines.

Figure 13-7 shows the total impulse versus pulse width for pulses less than 0.300 sec. The TRW two-sigma limits are shown for comparison. The flight data agreed well with the TRW data except for the low performance of engine 1-3.

Section 13
Auxiliary Propulsion System

The following are considered possible causes of the APS chamber pressure anomalies.

- a. Valve failures
- b. Loss of throat
- c. Nitrogen tetroxide (NTO) freezing
- d. NTO vaporization
- e. Helium liberation
- f. Contamination
- g. NTO flow decay
- h. Injector tube rupture
- i. Teflon valve seat swelling
- j. Instrumentation

13.4.1.1 Valve Failures

The results of Douglas and TRW testing show that a single oxidizer valve failure decreases the chamber pressure by approximately 6 percent. A single fuel valve failure has little effect on chamber pressure. TRW testing indicated that multiple valve failures could result in as much as 40 percent decrease in total impulse obtained from a minimum impulse bit. This decrease resulted when two downstream oxidizer valves were failed open and one upstream oxidizer valve was failed closed. In light of the multiple failures required to decrease the chamber pressure to the level noted on engine 1-3, valve failures are not considered a likely cause for the S-IVB-501 anomalies.

13.4.1.2 Throat Loss

The failure mode for loss of the engine throat is the heating and erosion of the silicon-tungsten coating of the throat insert followed by erosion of the molybdenum insert itself. Since the duty cycle during the S-IVB-501 flight was much less severe than ground test duty cycles, loss of the engine throat is not considered a cause for the chamber pressure

anomalies. Also, if the throat was enlarged or lost, the engine thrust level would increase. Attitude data have confirmed a decrease in thrust level.

13.4.1.3 NTO Freezing

Evaluation of the APS modules temperatures indicate that they were well above the freezing point of NTO. In fact, the oxidizer temperature of module No. 1, measured at the propellant control module, exceeded the transducer range maximum of 592 deg R. The injector wall temperatures were around 600 deg R.

13.4.1.4 NTO Vaporization

The temperatures noted in the APS are conducive to vaporization of the oxidizer in the injectors. The vapor pressure of NTO at 590 deg R is 60 psia; at 610 deg R it is 90 psia. Since the recorded chamber pressure of engines 1-1 and 1-3 were 85 psia during the early part of the mission with engine 1-3 decreasing to 55 psia during the latter portion of the mission, it is possible that the oxidizer vaporized in the injectors. TRW testing indicated a performance loss of 15 percent with the oxidizer at 575 to 590 deg R and the fuel at 555 to 565 deg R. However, the injector wall temperature of engine 1-2 was 620 deg R during this period and this engine performed very well. Also, the vaporization of NTO in the injectors would tend to yield erratic and intermittent loss of performance, whereas the performance degradations noted during S-IVB-501 flight were consistent and repeatable. Therefore, although the propellant temperatures may have contributed to the performance degradation, the NTO vaporization affect is of a secondary nature and not the primary cause of the chamber pressure degradation. The NTO vaporization could be the cause of the chamber pressure oscillations noted on engine 1-1.

13.4.1.5 Helium Liberation

The liberation of helium from the propellants due to temperature and pressure transients would affect the engine performance in essentially the same manner as NTO vaporization. Again, this is not considered the primary cause of the performance degradation; however, helium liberation could have contributed to the oscillations noted on engine 1-1.

Section 13
Auxiliary Propulsion System

13.4.1.6 Contamination

The susceptibility of the injector valves and injector tubes to contamination is evident by an examination of the passage sizes. The injector valves stroke is 0.040 in., and the clearance between the solenoid plunger and the case is 0.0025 \pm 0.0010 in. The injector tubes are 0.0349 to 0.0358 in. for oxidizer and 0.0279 to 0.0287 in. for fuel. The inlet to the valves is protected by a 140 micron filter.

When this module was confidence fired at STC, the engine performance was nominal. Subsequent to the firing, excessive contamination of the system occurred. This contamination was a result of cleaning methods. All engines of module No. 1 were replaced. The manifolding was cleaned, but not replaced. Therefore, contamination could have existed in the system before loading for flight. It should be noted that during pre-launch burp firings, engine performance was nominal. Another source of contamination could have been the KSC GSE. After the S-IVB-501 flight, the GSE contained greenish deposits that were similar to those found at STC during Gamma site reactivation. The deposits at Gamma were caused by propellants attacking the nickel in the VOI-SHAN seals. Since module No. 1 was loaded first at KSC, the possibility of contamination was greater than for module No. 2.

Since the roll engines 1-1 and 1-3 were fired during the J-2 engine first burn and the pitch engine did not fire until after J-2 engine burn, any contamination present in the system at liftoff would tend to go to the roll engines. Also, the orientation of the propellant lines to engines 1-1 and 1-3 is such that if contamination existed during ground hold or powered flight, it would most likely settle in these lines. It should be noted that the volume of propellants used during burp firing was very small (approximately 2 in.³ per engine) and would not necessarily move such contamination to the engines.

Either of the aforementioned types of contamination could have existed in solution with the propellants. The temperature transients during the mission and especially at approximately R0 +19,000 sec could have forced this contamination out of solution, thus causing the thrust decay.

13.4.1.7 NTO Flow Decay

The NTO flow decay phenomenon is the result of the solution of iron in the NTO with subsequent dissolution of an iron nitrate compound in areas of high pressure drop. The dissolution is enhanced by the NTO undergoing a temperature drop and by NTO vaporization.

Although this phenomenon does not correlate with the initial performance loss, the conditions existing at the time of the greater loss of engine 1-3 performance were conducive to its occurrence. That is, the temperature drop across the module was on the order of 40 to 50 deg R and the injector pressure drop was approximately 100 psid during firings. Although these conditions do not exactly match those of the Rocketdyne tests in which the iron nitrates were formed, they are similar.

13.4.1.8 Injector Tube Rupture

If one or more of the injector tubes between the injector valves and the injector head were to rupture, the propellant flow to the engine would be reduced. Such a rupture occurred during TRW testing. This failure occurred when fuel was left in the thrust chamber as a result of an attempt to fire the engine with the oxidizer line frozen. After thawing the oxidizer line, a subsequent attempt to fire the engine resulted in rupturing of the oxidizer tubes. During the S-IVB-501 flight, the oxidizer temperatures were well above the freezing point. Also, the chamber pressure data did not indicate any excessive pressures. To cause a pressure decay of the magnitude noted on engine 1-3, either the fuel tube or several of the oxidizer tubes would have to rupture; therefore, this is not considered a likely cause for the S-IVB-501 anomalies.

13.4.1.9 Teflon Valve Seat Swelling

The stroke of the injector valve poppets is 0.040 in. It is possible that the teflon mating surface of the poppet could swell if exposed to high temperatures and/or NTO. However, test data indicate that such swelling occurs at temperatures greater than 735 deg R. The S-IVB-501 flight data show that the injector head temperatures of engines 1-1 and 1-3 did not exceed 610 deg R. The injector temperature of engine 1-2 reached 700 deg R; however, the performance of this engine was good.

Section 13
Auxiliary Propulsion System

Also, the duty cycle of the engines was very light. Therefore, solenoid heating should have been slight. For these reasons, and because of past experience, teflon swelling is not considered a likely cause of the S-IVB-501 anomalies.

13.4.1.10 Instrumentation

Instrumentation has been eliminated as a possible cause of the low chamber pressure values recorded on engines 1-1 and 1-3. This followed an investigation which correlated the engine thrust with vehicle roll rates. The results of this analysis are presented in table 13-2 which shows good correlation between thrust values obtained from the chamber pressure and those obtained from the vehicle roll rates. The thrust values of engine 1-3 calculated from the vehicle roll rate demonstrate the same thrust degradation as the thrust obtained from the chamber pressure.

13.4.1.11 APS Ullage Engines

The excessive "tail-off" noted on the module No. 1 ullage engine chamber pressure has received only cursory examination. The most likely cause of this anomaly is particulate contamination of the teflon valve seat. When the valve closed, the particle was forced into the teflon slowly, thus allowing a "tail-off" flow. When the valve was again opened, the teflon could have forced the particle to protrude again, so that the second closing would be similar to the first.

The preceding comments are a result of a preliminary investigation of the problem. Several avenues of investigation are still being pursued. Among them are a review of previous flight and test data, an industry survey of such problems, and perhaps some future testing.

TABLE 13-1
APS PROPELLANT USAGE DURING FLIGHT

EVENTS	MODULE 1				MODULE 2			
	OXIDIZER USAGE		FUEL USAGE		OXIDIZER USAGE		FUEL USAGE	
	(lbm)	(percent)	(lbm)	(percent)	(lbm)	(percent)	(lbm)	(percent)
First J-2 burn roll control	*	*	*	*	*	*	*	*
First ullage burn	17	9.3	13	10.4	18	9.3	14	11.2
Limit cycle operation	15	8.2	10	8.0	3	1.6	2	1.6
Second ullage burn	56	30.8	41	32.8	57	30.5	42	33.6
Second J-2 burn roll control	7	3.9	4	3.2	8	4.3	5	4.0
LOX vent disturbances and maneuver to separation attitude	5	2.8	4	3.2	7	3.7	5	4.0
Limit cycle and maneuvers after separation	12	6.6	7	5.6	22	11.8	13	10.4
Totals	112	62	79	63	115	62	81	65

*Propellant usage is not detectable with the propellant measurement method used.

Section 13
Auxiliary Propulsion System

TABLE 13-2
AS-501/S-IVB AUXILIARY PROPULSION SYSTEM (YAW/ROLL)
ENGINE THRUST CHARACTERISTICS

TIME FROM RANGE ZERO (sec)	ENGINE	IMPULSE FROM CHAMBER PRESS DATA (lb-sec) PULSE WIDTH FROM CHAMBER PRESS DATA (sec)	Δ RATE USING CHAMBER PRESSURE DATA (deg/sec)	Δ RATE FROM ROLL GIMBAL ANGLE RATES (deg/sec)	THRUST (lbf) FROM CHAMBER PRESS DATA	THRUST (lbf) FROM ROLL GIMBAL ANGLE RATES
14,507	1-3	6.35 0.059	0.03277	0.0325	107.56	106.8
14,786	1-3	6.52 0.059	0.03365	0.0345	110.59	113.32
15,014	1-3	6.68 0.059	0.03447	0.03603	113.17	118.34
22,995	1-1	6.12 0.055	0.0316	0.0285	111	100
23,049	1-3	4.65 0.059	0.024	-0.0258	79	85
23,109	1-3	4.83 0.067	0.025	-0.0212	72	61
23,118	2-2	7.2 0.055	0.0372	+0.0385	131	136
23,210	1-3	4.8 0.063	0.0248	-0.0270	76	83
23,276	1-1	5.95 0.051	0.0308	+0.0360	117	136
23,325	2-3	7.62 0.059	0.0394	-0.0427	129	140
23,376	2-1	7.59 0.059	0.0392	+0.0426	129	140
23,423	1-3	4.22 0.059	0.0217	+0.0255	72	84
23,746	1-3	4.72 0.059	0.0242	+0.0245	30	80.7
23,827	1-1	6.09 0.055	0.0314	-0.0355	111	126

Section 13
Auxiliary Propulsion System

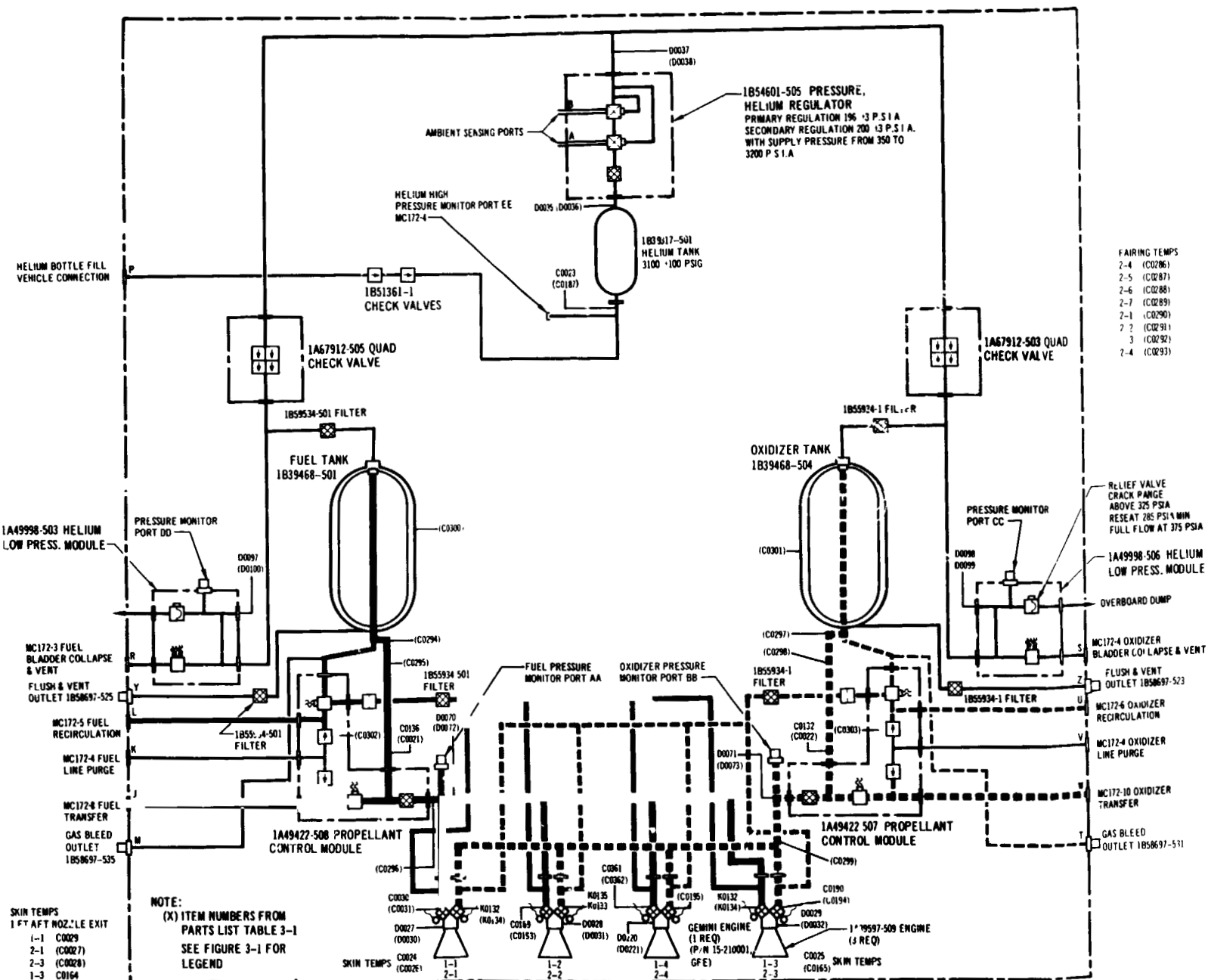


Figure 13-1. Auxiliary Propulsion System and Instrumentation

Section 13
 Auxiliary Propulsion System

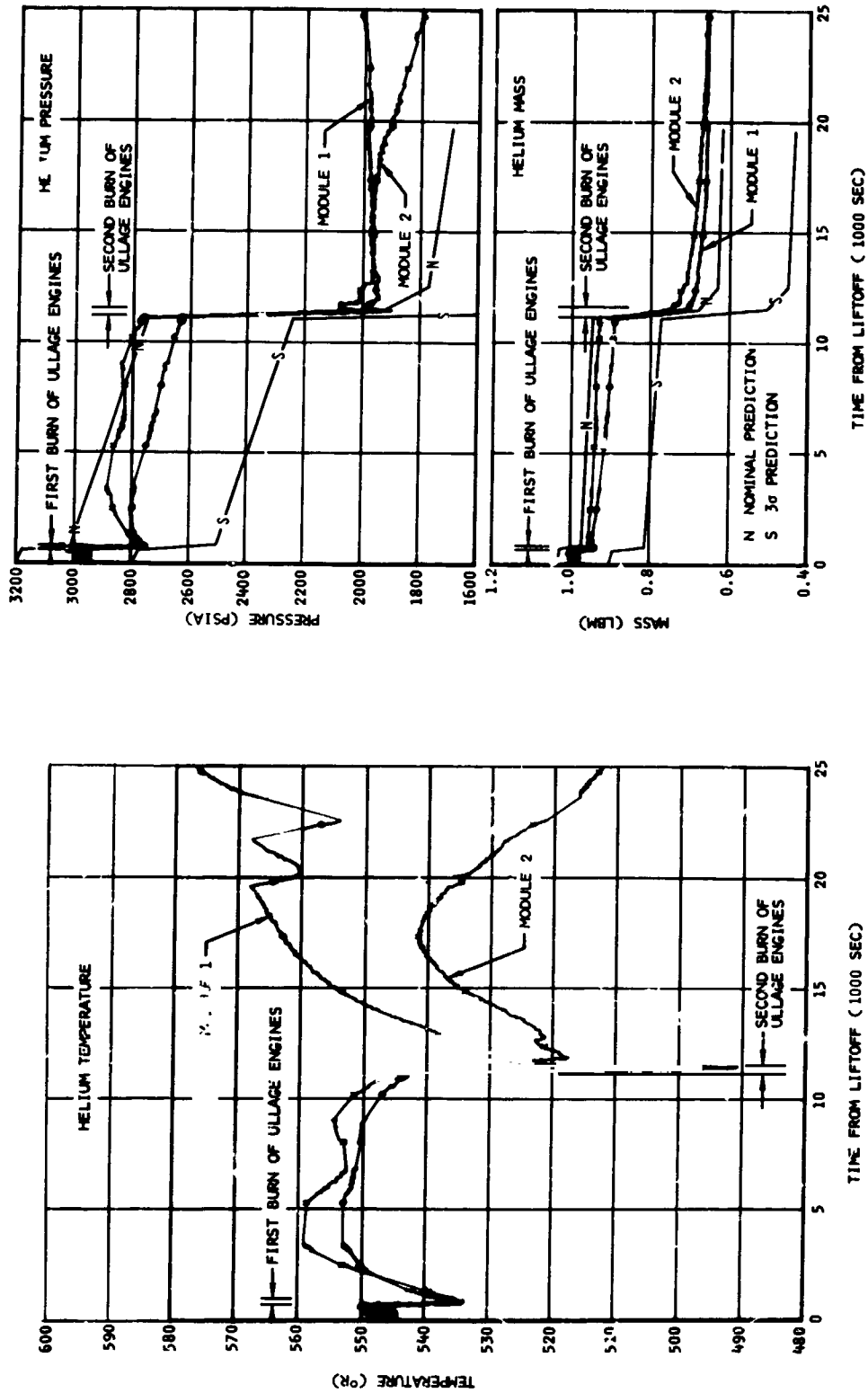


Figure 13-2. Helium Bottle Conditions

Section 13
Auxiliary Propulsion System

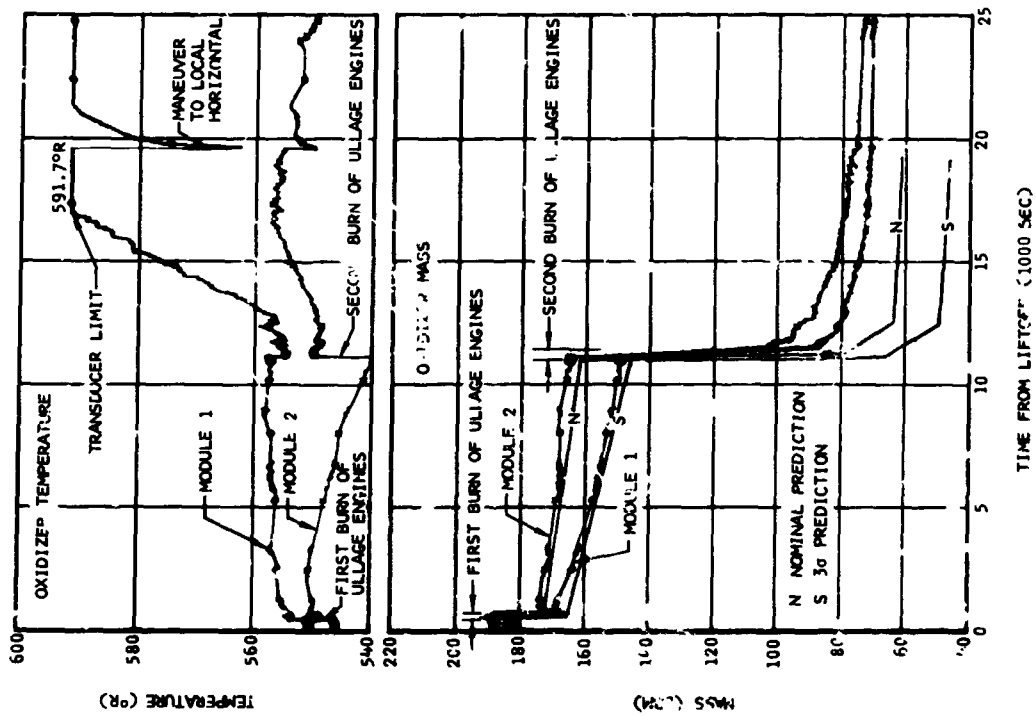
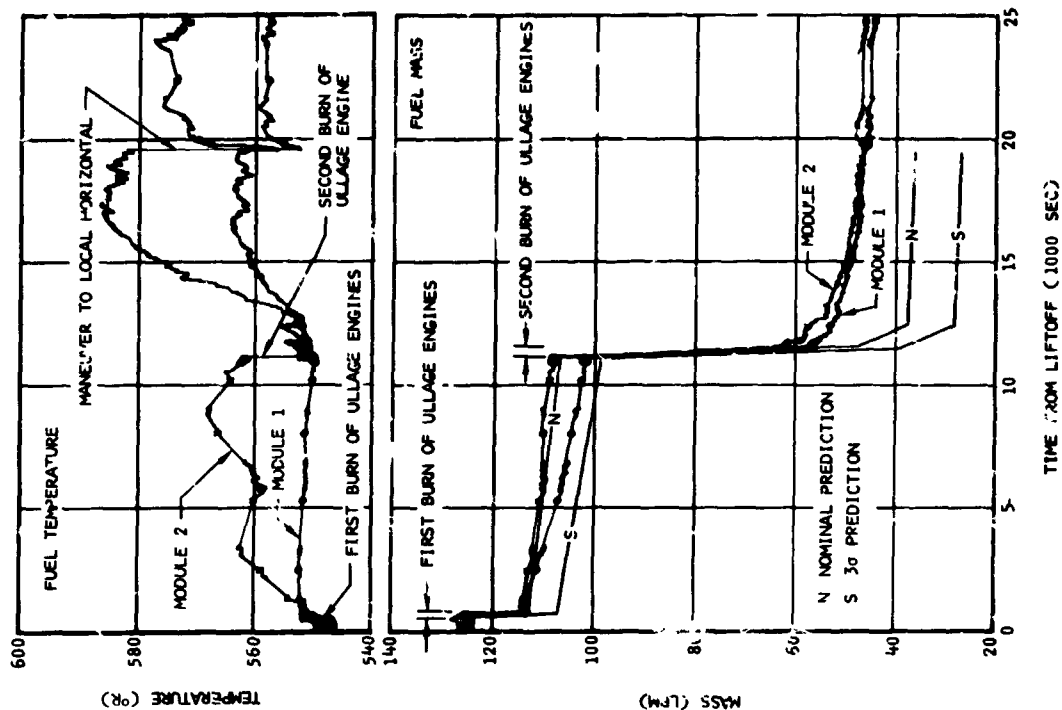


Figure 13-3. APS Propellant Conditions

Section 13
 Auxiliary Propulsion System

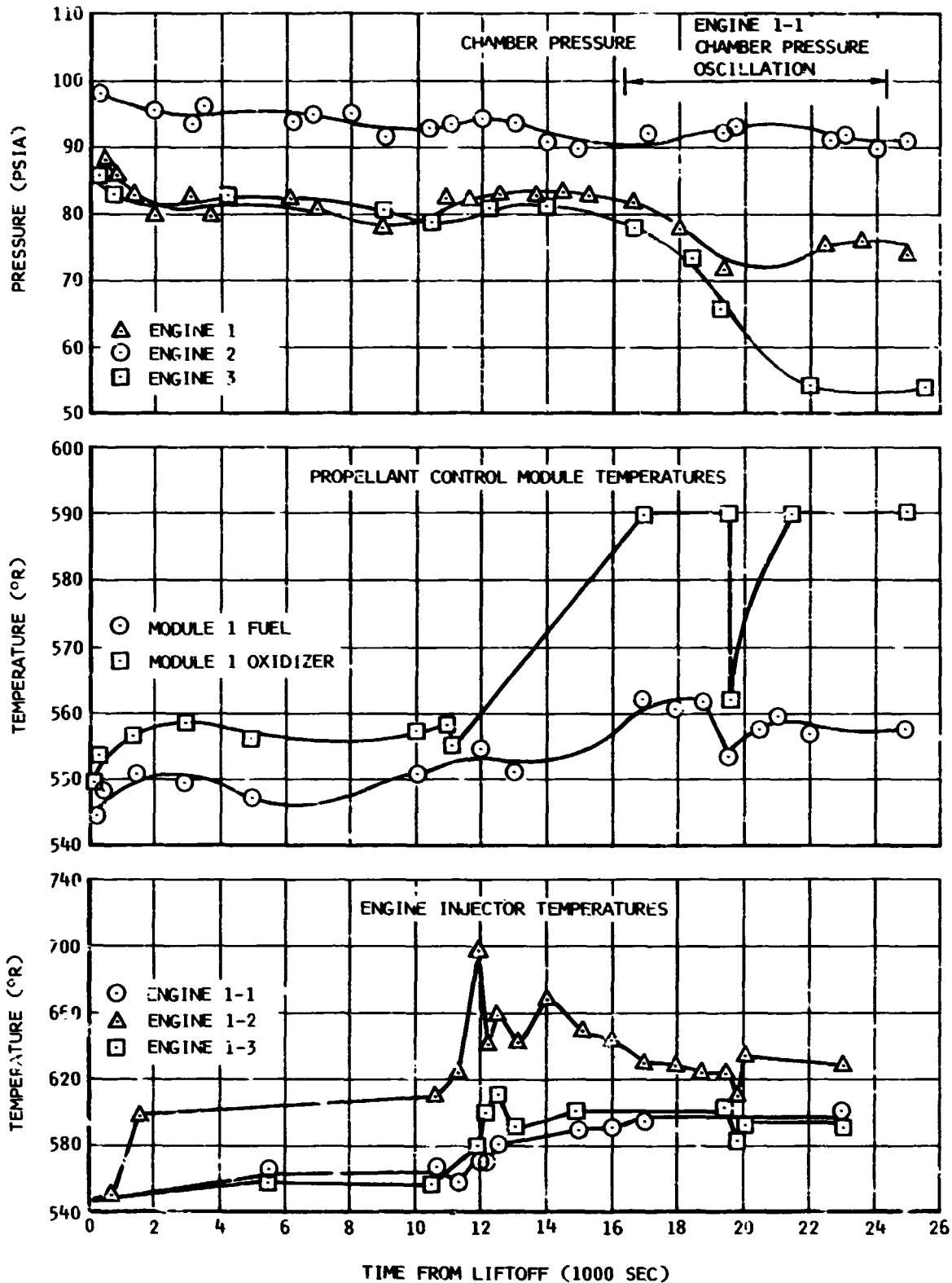


Figure 13-4. Module 1 Engine Anomaly Correlation

Section 13
 Auxiliary Propulsion System

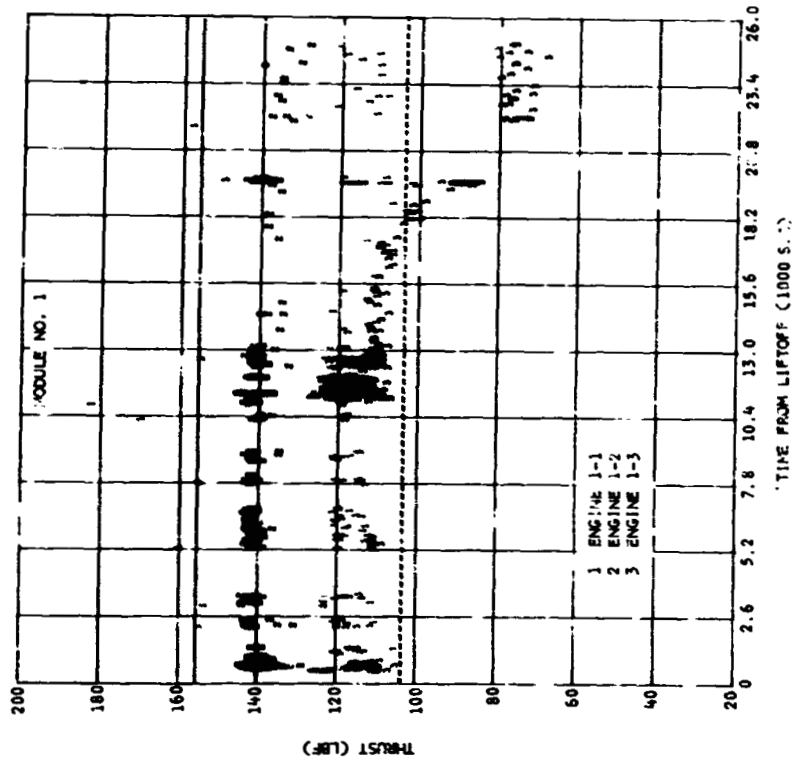
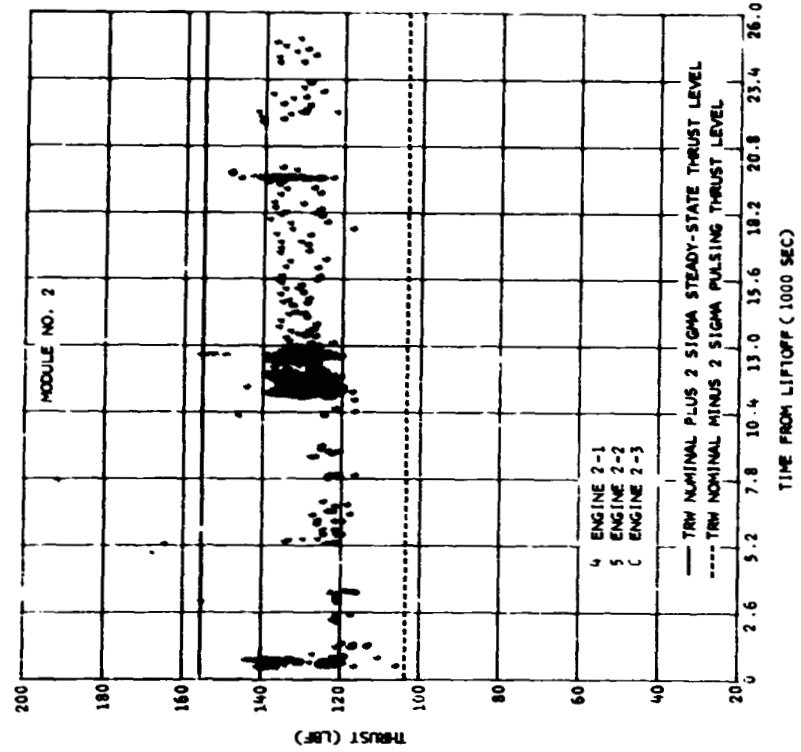
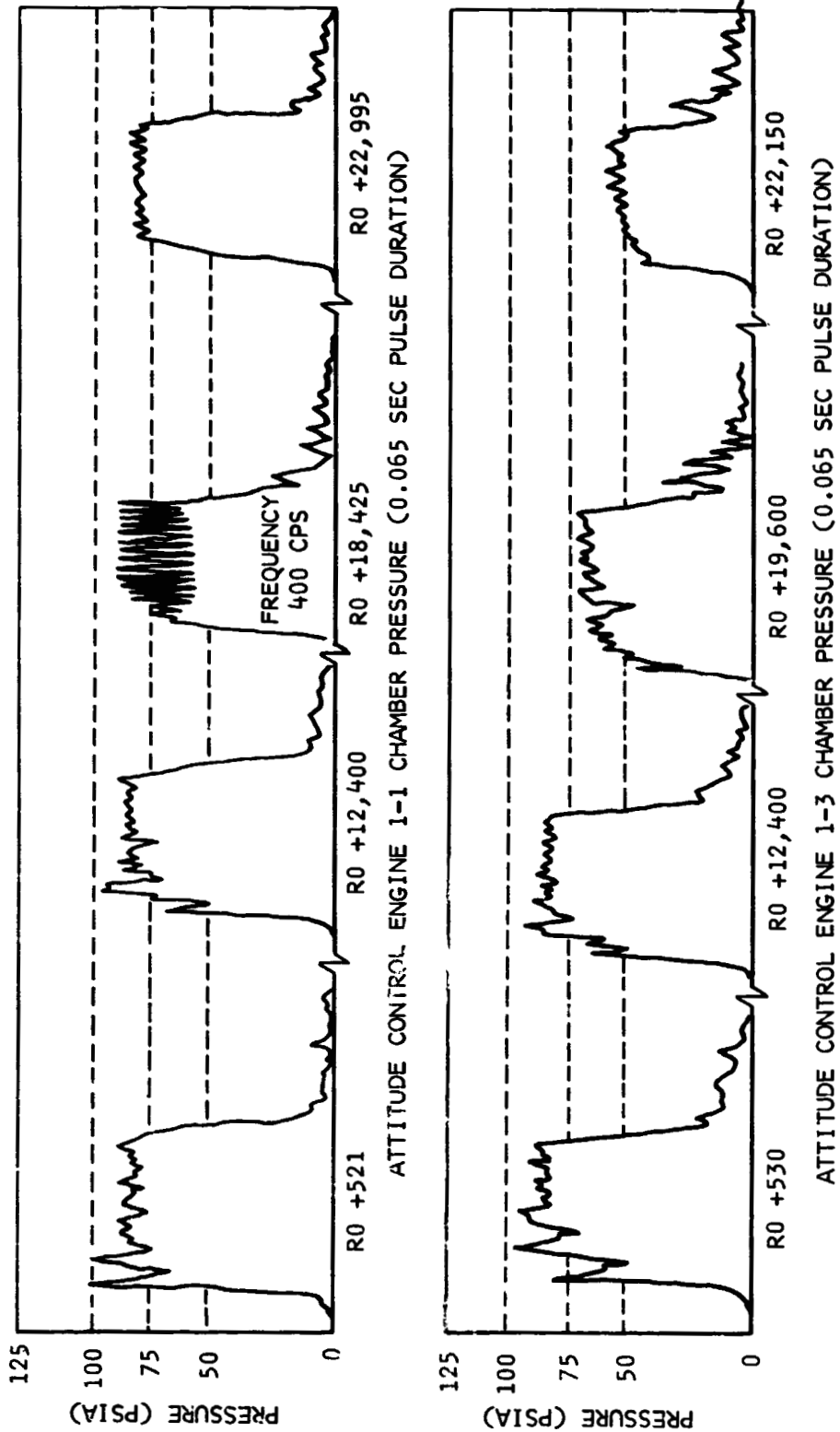


Figure 13-5. APS Thrust

Section 13
Auxiliary Propulsion System



NOTE: ALL INDICATED TIMES ARE IN SECONDS

Figure 13-6. Chamber Pressure Anomalies (Sheet 1 of 2)

Section 13
Auxiliary Propulsion System

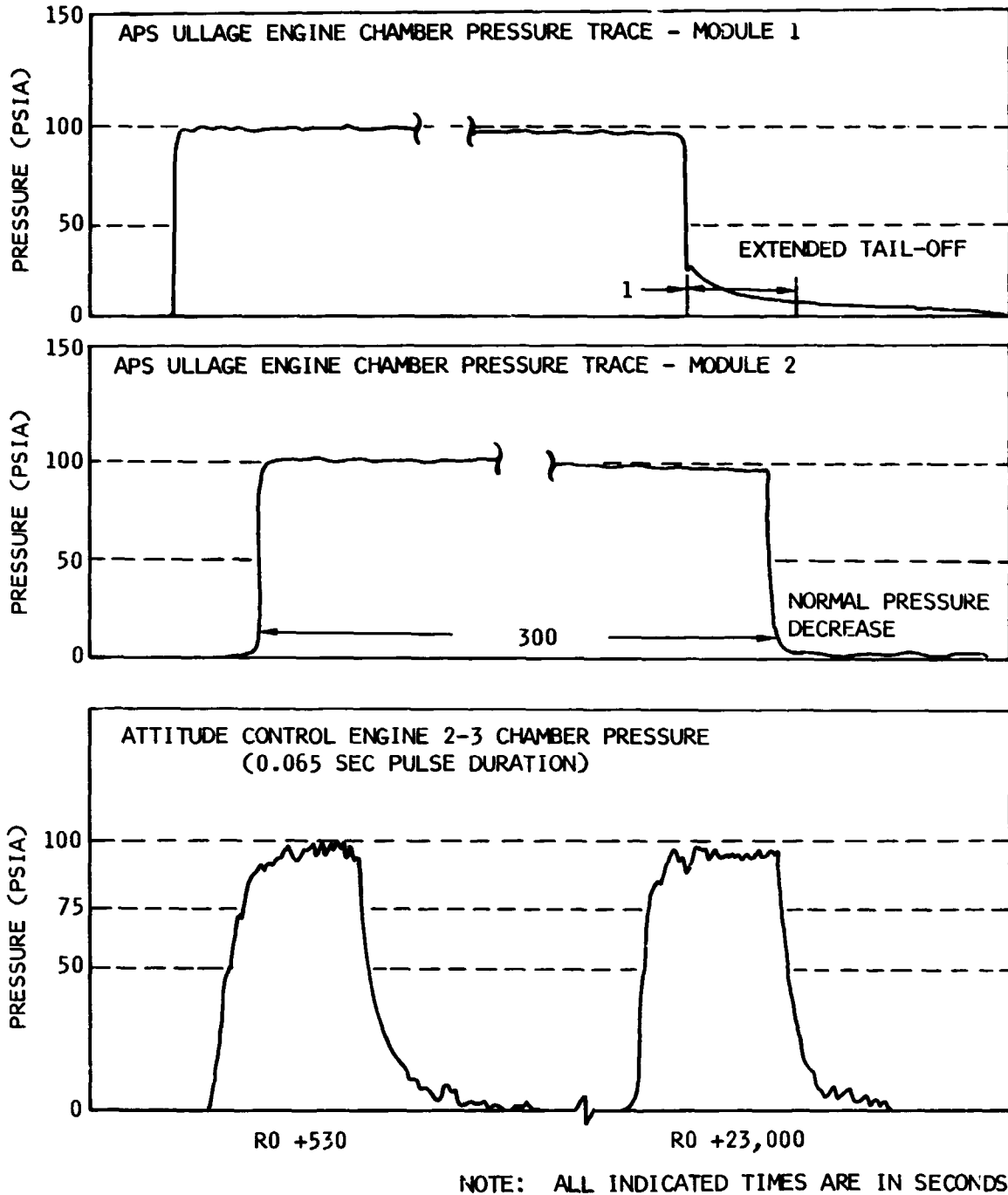


Figure 13-6. Chamber Pressure Anomalies (Sheet 2 of 2)

Section 13
Auxiliary Propulsion System

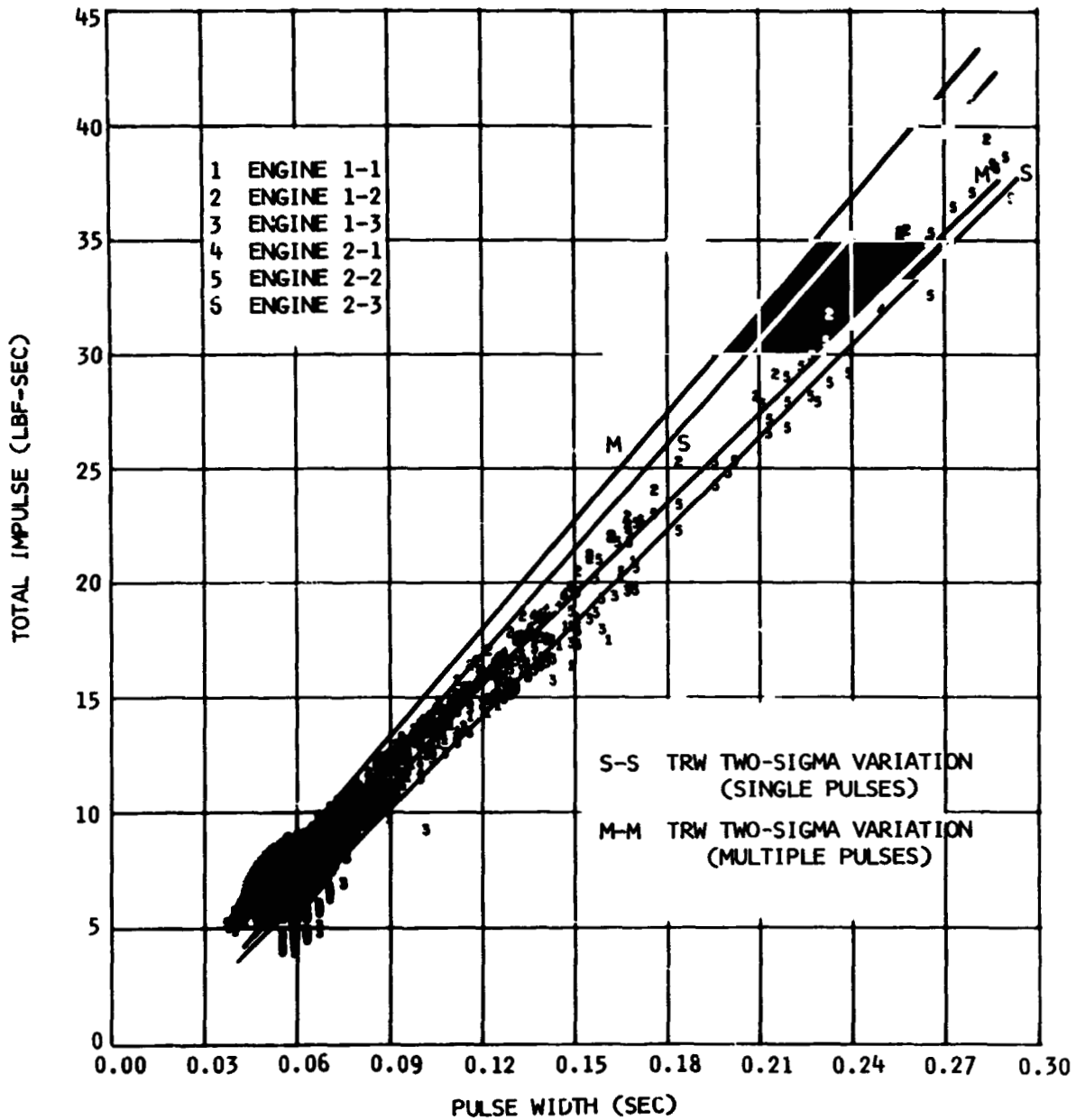


Figure 13-7. APS Total Impulse Per Pulse

14. PNEUMATIC CONTROL AND PURGE SYSTEM

The pneumatic control and purge system (figure 14-1) performed satisfactorily throughout the flight. The helium supply was adequate to complete all mission requirements and to accomplish all purges. During orbital coast, however, a system leak developed which eventually resulted in the depletion of pneumatic supply during the waiting orbit. Since all pneumatic operations were completed well before this time, the mission was not affected. Pneumatic control and purge system data is presented in table 14-1.

14.1 Ambient Helium Supply

The pneumatic supply was adequate, and system operation was normal during boost and first burn. Significant valve actuations and their respective demands on the system are shown in figure 14-2. The first indication of unusual system demand occurred during the period of prevalve closure immediately after first burn (RO +667 sec). During this period the mass loss rate (excluding that which is attributable to J-2 engine pump purge) was 12.7 scfm; the predicted loss rate was 400 scim (0.23 scfm). After prevalve opening at RO +726 sec, the average mass loss rate was 7.2 scfm, which agrees closely with the rate predicted for the J-2 engine pump purge.

Following termination of the J-2 engine pump purge, the mass loss rate was insignificant until approximately RO +8,000 sec (figure 14-3). From this time until restart preparations, the mass loss rate was essentially constant at 3.3 scfm.

During the period of prevalve closure for restart chilldown operations, the rate was established as 10.4 scfm, approximating the loss rate after first burn cutoff, which was attributed to prevalve actuation.

Pneumatic system performance during second burn operations is shown in figure 14-4. Mass usage during this period could not be accurately determined because the rapidly changing sphere conditions overshadowed the relatively small mass usage. After second burn, the pneumatic system leakage continued (figure 14-5), this time at an average rate of 4.3 scfm.

Section 14
Pneumatic Control and Purge System

14.2 Pneumatic System Leakage

As previously noted, a significant leakage problem arose at approximately RO +8,000 sec. A review of the control helium regulator discharge pressure data (D0014) indicates the leakage was downstream of the pneumatic power control module. This conclusion is based on two observations. First, D0014 indicated a level below the lockup pressure level observed during boost (figure 14-5). This difference in level indicates a flowrate commensurate with the observed leakage rate (based on tests of a similar regulator). Secondly, as the sphere was depleted below the 500 psia level, D0014 did not precisely follow the control sphere pressure D0087 (figure 14-5); instead, it showed a pressure drop, which is indicative of flow through the regulator.

Based upon this review, the flight data, and past experience, three possible leakage paths have been considered:

a. Pneumatic Power Control Module Calips Pressure Switch

Two pneumatic power control module calips pressure switches (on stages S-IVB-502 and 503) have cracked in the convoluted area of the calips side diaphragm. Failure evaluation of the S-IVB-502 switch yielded a leakage rate of approximately 100 scim (0.058 scfm), with 500 psia applied to the system side of the switch. While this is significantly less than the leakage observed on S-IVB-501, the switch is capable, based upon port sizes, of flowing a maximum of approximately 23 scfm. Since the leakage on S-IVB-501 began during a period of no pneumatic demand (and hence no force variations on the calips diaphragm), a diaphragm failure would probably have been thermally induced, rather than pressure-induced.

On future stages, the calips port on the pneumatic power control module will be capped to preclude this potential leak path until a permanent remedy is incorporated.

b. LOX and LH2 Prevalve Actuation Control Modules

Analysis of S-IVB-501 data revealed two distinctly different control helium regulator discharge pressure (D0014) response

Section 14
Pneumatic Control and Purge System

profiles during opening of the prevalues (figure 14-6). The deviation noted on the lower profile was also found to be characteristic of the closure of the LOX tank vent valve; however, the prevalue deviation was of greater amplitude and duration.

During normal operation, prevalue opening results in the termination of a constant flow demand. The regulator, however, does not sense this flow cessation immediately, so it momentarily continues to flow, causing an increase in the regulator discharge pressure (D0014), as shown in the upper trace on figure 14-6. The occurrence of an abnormal trace such as that on the lower half of figure 14-6 indicates a momentary leak for the duration of the drop in the regulator discharge pressure. The duration of this pressure drop (1.1 sec) and the net flow from the system (0.1 scfm) is suggestive of a slow-moving poppet in the actuation control module (figure 14-7). The mechanical operation of this module is such that momentary loss of pneumatic pressure can occur during slow poppet travel.

The abnormal trace is associated only with longer periods (5 to 10 min) of pneumatic power application; for shorter periods of application (1 to 2 min), the trace is normal. This indicates two possible conditions: thermally induced mechanical interference or seal creepage. Although both of these seem improbable, no other contributing factors have been found. The failure of the lower seal of this actuator control module does fulfill a set of conditions posed prior to second burn. During the period from RO +8,000 sec to prevalue closure at the beginning of restart preparations, the average leakage rate was 3.3 scfm; whereas during the prevalue closure period, the leakage rate was 10.4 scfm. The failure of the lower static seal would result in a flow area change between the prevalue "open" and "closed" state. However, failure of the lower seal during development testing and operational use has been virtually nonexistent.

Section 14

Pneumatic Control and Purge System

c. LOX and LH2 Prevalves

The high leakage rate during post-first-burn preclude closure and pre-second-burn preclude closure could be attributed to seal leakage within the preclude valves. If this were the cause of the leakage during preclude actuation, a separate leakage path must have opened to produce the leakage rate observed between RO +8,000 sec and the loss of stage pneumatics.

TABLE 14-1 (Sheet 1 of 2)
PNEUMATIC CONTROL AND PURGE SYSTEM DATA

PARAMETER	S-IVB-501 FLIGHT		S-IVB-501 ACCEPT		S-IVB-502 ACCEPT	
	FIRST	SECOND	FIRST	SECOND	FIRST	SECOND
Sphere volume (cu ft)	4.5	4.5	4.5	4.5	4.5	4.5
Sphere pressure						
At liftoff (psia)	2,921	--	3,120	--	3,205	--
At Engine Start Command (psia)	2,892	1,474	3,050	2,680	3,220	2,640
At Engine Cutoff Command (psia)	2,932	1,515*	3,050	2,620	3,110	2,640
Sphere temperature						
At liftoff (deg R)	547	--	580	--	555	--
At Engine Start Command (deg R)	543	461	577	577	549	545
At Engine Cutoff Command (deg R)	552	473*	577	577	549	546
Helium mass						
At liftoff (lbm)	8.19	--	8.25	--	9.75	--
At Engine Start Command (lbm)	8.17	5.08	8.07	7.09	8.98	7.39
At Engine Cutoff Command (lbm)	8.14	5.08*	8.07	6.94	8.76	7.36
Usage during engine operation (lbm)	0.03	0*	0	0.15	0.22	0.03
Usage during 10-min ring engine pump purge	0.62	--	0.74	--	0.84	--

*Exact value could not be determined. See paragraph 14.1.1.

Section 14
Pneumatic Control and Purge System

TABLE 14-1 (Sheet 2 of 2)
PNEUMATIC CONTROL AND PURGE SYSTEM DATA

PARAMETER	S-IVB-501 FLIGHT		S-IVB-501 ACCEPT		S-IVB-502 ACCEPT	
	FIRST	SECOND	FIRST	SECOND	FIRST	SECOND
Regulator outlet pressure						
Maintained pressure band (psia)	520 to 555	520 to 540	535 to 540	535 to 540	515 to 545	515 to 545
Minimum system pressure during start and cutoff transient	420	415	440	440	425	425
Average LOX chilldown motor container purge pressure (psia)	65	59	40	40	41	41

Section 14
Pneumatic Control and Purge System

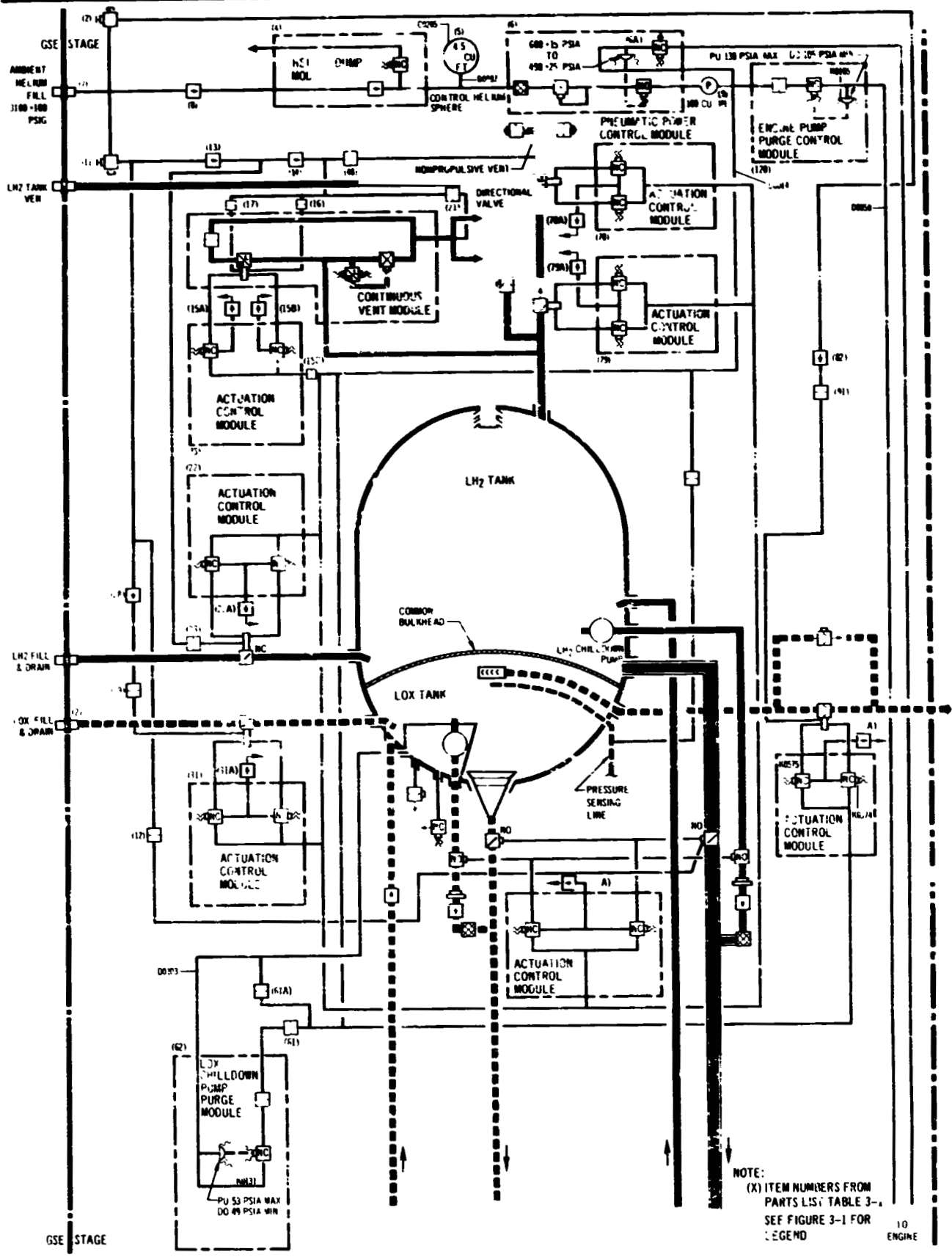


Figure 14-1. Pneumatic Control and Purge System

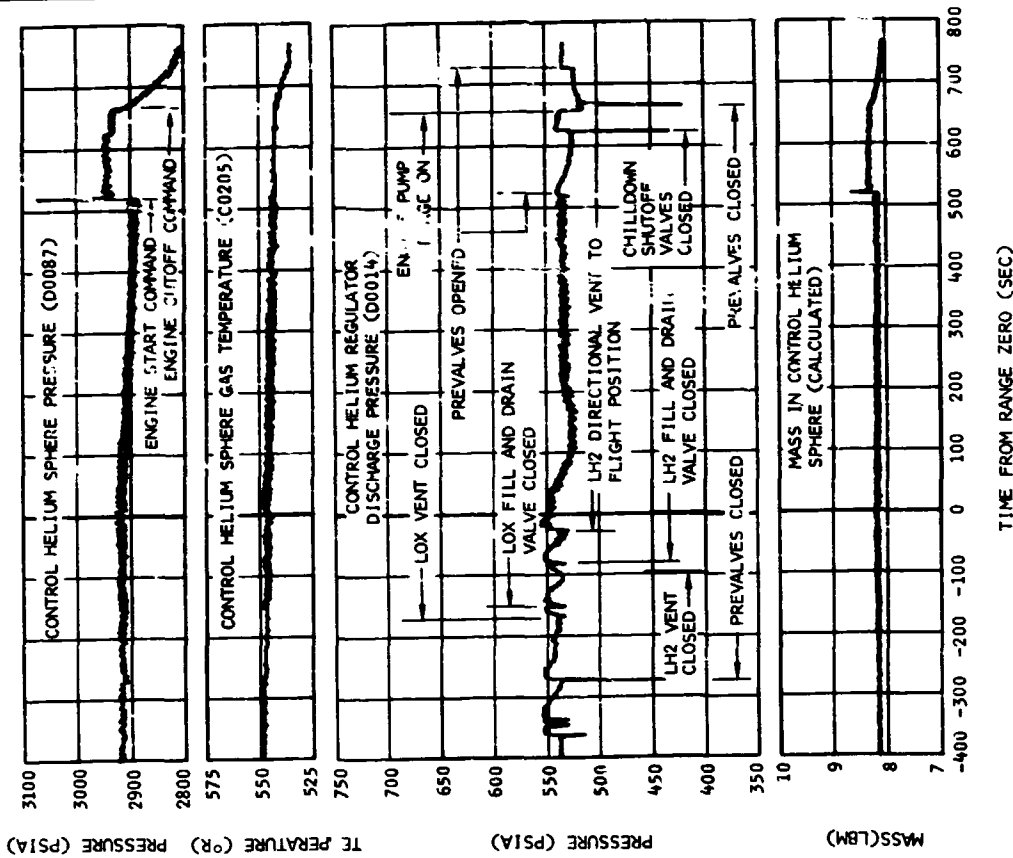


Figure 14-2. Pneumatic Control and Purge System Performance During Boost and First Turn

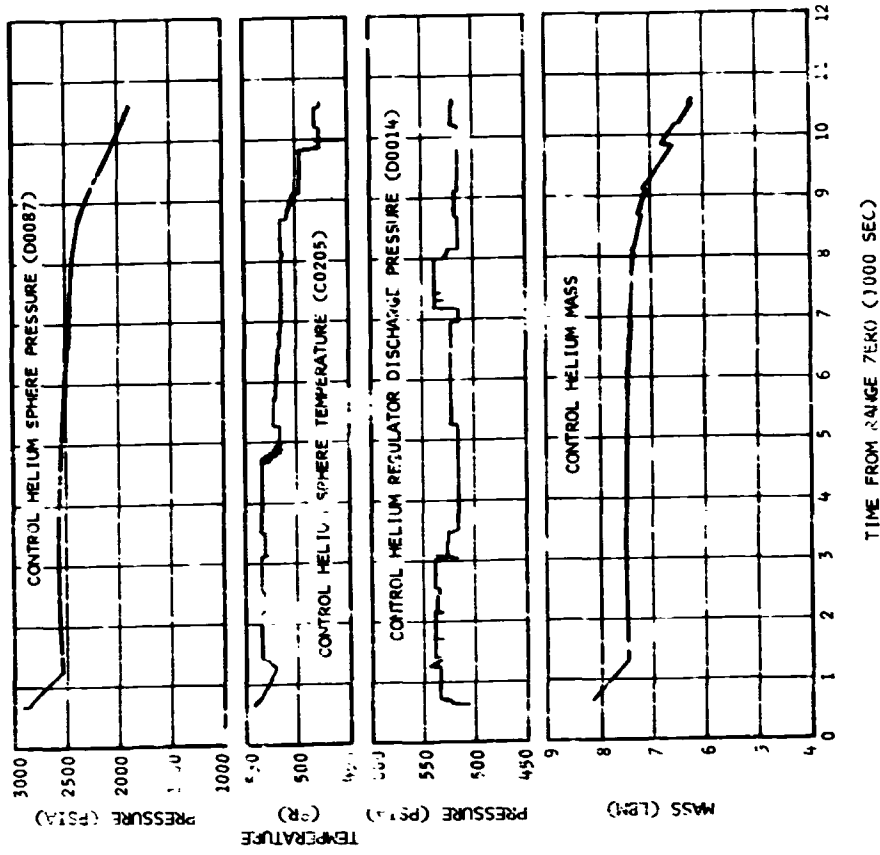


Figure 14-3. Pneumatic Control System Conditions During Orbital Coast

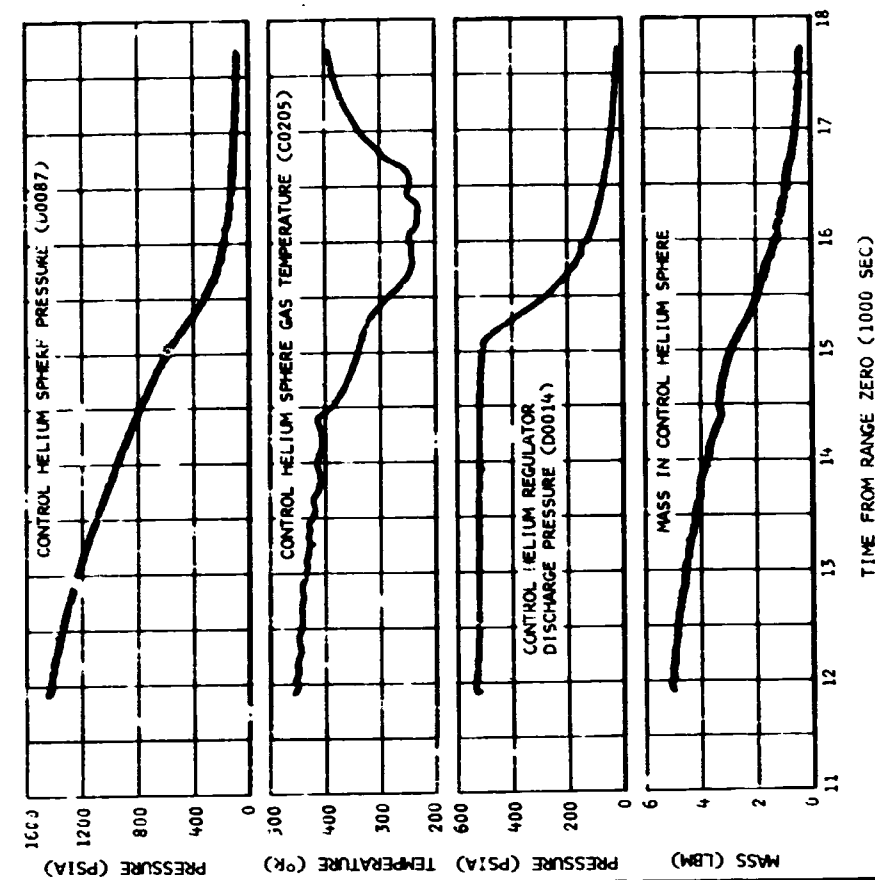


Figure 14-4. Pneumatic Control and Purge System Performance - Second Burn

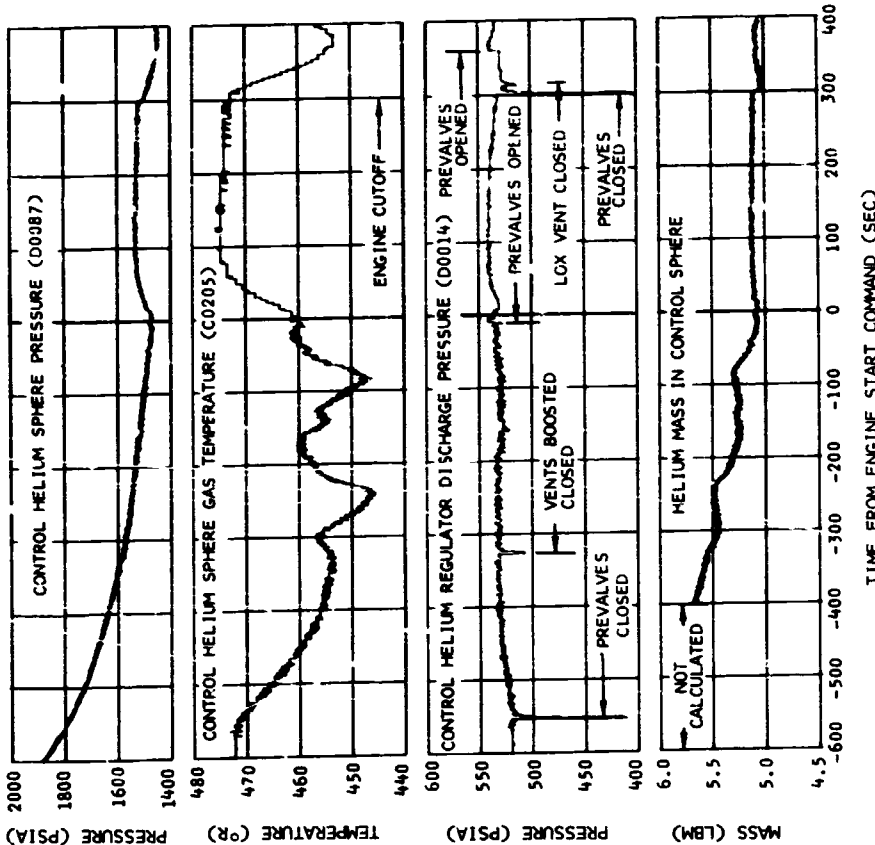


Figure 14-5. Pneumatic Control and Purge System Performance During Third Orbit

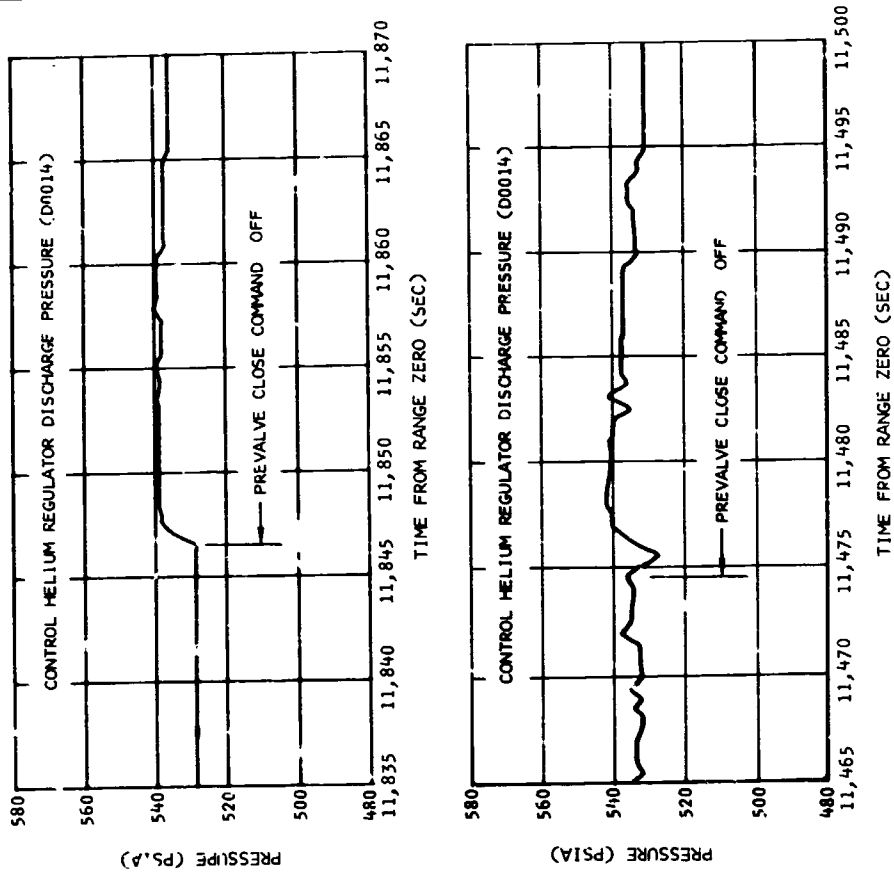
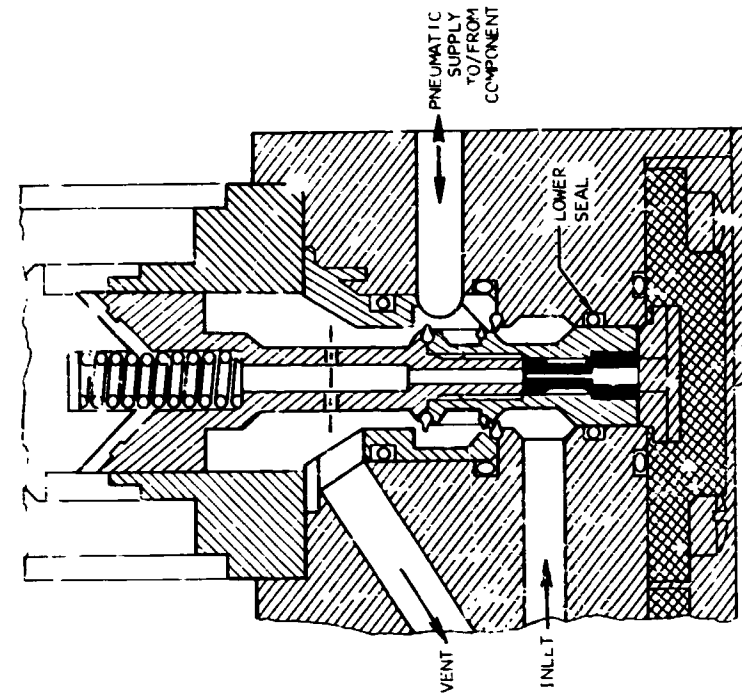


Figure 14-7. Clary Actuation Control Module

Figure 14-6. Control Helium Pressure Transient Response Characteristics

15. PROPELLANT UTILIZATION

The propellant utilization system successfully accomplished the requirements associated with propellant loading and management during burn. Loading computer indicated full load propellant values at liftoff were 99.96 and 99.85 percent of the desired indicated values for LOX and LH2, respectively. The actual best estimate propellant mass values at liftoff were 194,395 lbm LOX and 41,173 lbm LH2 as compared to desired mass values of 193,273 lbm LOX and 41,222 lbm LH2. These values were well within required loading accuracies.

Extrapolation of propellant residuals to depletion indicated that a simultaneous depletion would have occurred approximately 37.6 sec after second burn velocity cutoff. This yields a PU efficiency of 100 percent. Had second burn actually gone to depletion cutoff, PU system nonlinearities would have resulted in an approximately 20 lbm increase in LH2 residual and a LOX depletion cutoff.

The PU valve operated at the LOX rich position after activation as planned during all of first burn. PU operation at the 4.5:1.0 hardover position for engine restart was satisfactorily accomplished. System dispersions at the start of second burn then caused the PU valve to move to the 5.5:1.0 hardover position and remain there until cutback at second burn Engine Start Command (ESC2) +63.5 sec. The largest single dispersion causing this hardover operation was a larger than expected LH2 boiloff during coast. Orbital boiloff, as determined from LH2 PU mass sensor data, was 2,871 lbm as compared to the nominal predicted value of 2,613 lbm. The difference was primarily caused by flashoff during the blowdown phase following first burn. The greater than nominal LH2 boiloff plus the fact that all other system dispersions were in the LOX rich direction, caused the PU valve hardover operation during second burn.

The rise of the propellants within the sensors due to capillary action during the low acceleration coast period was present as expected. This capillary action was not removed until ESC2 +15 sec and caused an erroneous signal to be fed into the PU system. This signal did not

Section 15 Propellant Utilization

significantly affect the PU operation during second burn due to the high system dispersions; however, it would have caused a valve excursion of +9 deg if the other dispersions were not present.

Two large propellant slosh waves were caused by vehicle attitude transients during second burn. Both slosh waves induced a response in PU system performance which was reflected in engine thrust performance. The first slosh wave occurred during PU cutback and had no adverse effects. The second slosh wave occurred just prior to second burn cutoff when the chi freeze guidance mode was applied. This propellant disturbance initiated a thrust variation which exceeded the limits established in the Contract End Item (CEI) Specification. The observed thrust variation was the result of an engine performance shift coupled with the slosh induced PU valve motion. The effect of the PU system alone did not cause a sufficient thrust variation to exceed the established limits. Since engine performance shifts are excluded from CEI specification limits, all specification requirements were met.

As a result of the S-IVB-501 flight several PU changes will be made for future flights. The PU simulation model will be revised to provide a more accurate presentation of PU valve response. LH2 boiloff predictions will be revised to reflect a higher facility vent backpressure. Tank deflection nonlinearity predictions will be revised to reflect new LH2 tank skin temperatures.

15.1 PU System Calibration

The preflight propellant masses at the full calibration points were determined from the S-IVB-501 acceptance firing full load by the flow integral analysis method. The capacitance corresponding to the acceptance firing full load masses were measured values. Due to a change in engine tag values, the preflight calibration was revised September 1967 to be consistent with engine flight performance predictions. For this reason the full point calibration mass values for flight were greater than those reported in the acceptance firing evaluation report by 1,481 lbm LOX and 379 lbm LH2.

Section 15
Propellant Utilization

The propellant masses at the lower calibration point were computed from unique tank volume and predicted propellant density data. The corresponding capacitance was determined by adding the mean deviation between vendor air capacitance and measured empty capacitance to the S-IVB-501 stage vendor air capacitance. The LOX and LH2 mass sensor calibrations are listed in the following table:

PU MASS SENSOR	MASS (lbm)	CAPACITANCE	LOCATION
LOX	188,915	410.03	Full point
	1,271	282.26	Empty point
LH2	40,696	1,170.93	Full point
	204	973.28	Empty point

15.2 Propellant Mass History

The propellant mass history was determined from a best estimate stage mass analysis as described in section 8.

The best estimate propellant masses were derived as a part of the best estimate solution for S-IVB-501 third flight stage ignition and cutoff masses. Best estimate propellant masses were obtained by subtracting the total third flight stage nonpropellant mass from the total best estimate mass at ignition and cutoff. The remaining total propellant mass was then divided into LOX and LH2 according to the prevailing flow integral mixture ratio at the specific flight event time.

The five measurement systems used in determining the best estimate masses are: (a) PU volumetric, (b) level sensors, (c) flow integral, (d) PU indicated (corrected) and (e) trajectory reconstruction. A brief description of these measurement systems is as follows:

- a. The PU volumetric masses were derived from raw PU probe output data computed according to volumetric calibration slopes and volumetric flight nonlinearities. The calibration slopes (pounds per picofarad [lbm/pf]) were computed from the capacitance-propellant mass relationships at the upper and lower probe active element extremities. The propellant mass

Section 15
Propellant Utilization

at these extremities was calculated from unique tank volume determined from tank measurements and propellant density. The capacitance at the upper active element extremity was computed from vendor probe calibration data and probe full immersion tests conducted during stage acceptance firings. The capacitance at the lower active element was obtained from empty capacitance measurements made during the fast propellant drain sequence immediately after acceptance firing cutoff.

- b. The level sensor system measures propellant mass at sensor activation and this mass is extrapolated to ignition or cutoff mass from flight flow integral data. This stage has level sensors located throughout the length of the propellant tanks.
- c. The flow integral method consists of determining the mass flow-rates of LOX and LH2 and integrating as a function of time to obtain total consumed mass during firing. Flow integral mass values were based on the analysis of engine flowmeter data, thrust chamber pressure, engine influence equations, and engine tag values. The initial full load mass, using the flow integral method, is determined by adding the statistically weighted average propellant residuals at engine cutoff, the fuel pressurant added to the ullage, and the propellant lost to boiloff, to the total mass consumed.
- d. The PU indicated (corrected) system measures propellant mass from raw PU probe output reduced according to the preflight flow integral calibration slope and adjusted for flight flow integral nonlinearities.
- e. The trajectory reconstruction method provide the unique relationship between stage ignition and cutoff mass which satisfies the observed trajectory (section 7).

Mass sensor data was used for both PU volumetric and PU indicated values. The difference between the results is due primarily to the calibration deviations and not to the treatment of data.

Section 15
Propellant Utilization

At ESC2, the propellant levels within the LOX and LH2 probes were not stabilized. Consequently, the PU masses for both methods at second burn Engine Start Command were determined by extrapolation from a stable propellant level condition.

The volumetric LOX mass at second burn Engine Start Command was determined by subtracting the first burn engine thrust decay consumption and orbital boiloff usage from the indicated mass at first burn Engine Cutoff Command. The LOX consumption between ECC1 and ESC2, including engine chilldown and the thrust decay consumption, was 319 lbm. Since no LOX tank venting occurred during orbit, and since the total LOX adjustment to the first burn Engine Cutoff Command mass is only 319 lbm, this procedure provided the most accurate determination of volumetric mass at second burn Engine Start Command.

The PU indicated (corrected) LOX mass at second burn Engine Start Command was determined by adding the flow integral LOX consumption between ESC2 and ESC2 +33.5 sec to the indicated mass at ESC2 +33.5 sec.

Both PU volumetric and PU indicated (corrected) LH2 masses at second burn Engine Start Command were determined by adding the flow integral LH2 consumption between ESC2 and ESC2 +33.5 sec to the indicated values at ESC2 +33.5 sec.

The propellant masses obtained from the various measurement systems at significant flight events are presented in table 15-1.

During first burn, the best estimate total propellant consumption was 2,613 lbm greater than predicted. The flight flow integral PU volumetric, and level sensor total propellant consumption values compared favorably with the best estimate. The maximum deviation in consumption between these methods was 114 lbm. The PU indicated corrected total propellant consumption was 692 lbm less than the best estimate, while the trajectory reconstruction was 322 lbm greater.

During second burn, the best estimate total propellant consumption was 4,993 lbm less than predicted. The maximum deviation in total consumption between the flight flow integral, PU volumetric, and level sensor was 85 lbm. The three techniques deviated from the best estimate total

Section 15 Propellant Utilization

consumption by an average of -300 lbm. The PU indicated corrected total propellant consumption was 623 lbm less than the best estimate and the trajectory reconstruction was 315 lbm greater.

15.2.1 Propellant Loading

Propellant loading was accomplished automatically by the loading computer. Table 15-2 is a tabulation of the desired, indicated, and actual full propellant loads as derived from various analysis methods, and their deviations at liftoff.

The loading computer values for pressurized full load prior to liftoff were 99.96 percent of desired load for LOX and 99.85 percent for LH2. This compares closely with PU indicated corrected full load values of 99.95 percent and 99.77 percent of desired for LOX and LH2, respectively.

The best estimate total liftoff mass was greater than desired total mass by 1,073 lbm; LOX mass was 1,122 lbm greater than desired and LH2 mass was 49 lbm less than desired. The LOX overload was due primarily to a calibration error but was well within the guaranteed loading accuracy of ± 1.39 percent.

PU indicated mass at liftoff is determined from the preflight flow integral PU calibration. The PU indicated corrected masses include adjustments for the effects of total PU system flight nonlinearities.

15.2.2 Orbital Boiloff

LOX usage between first burn Engine Cutoff Command and second burn Engine Start Command was 319 lbm including first burn engine thrust decay consumption, orbital boiloff and second burn engine chilldown.

The LH2 boiloff between first burn Engine Cutoff Command and second burn Engine Start Command, as determined by the LH2 PU mass sensor, was 2,871 lbm. This boiloff value was obtained by subtracting 29 lbm for first burn engine cutoff transient from the total difference of 2,900 lbm between first burn Engine Cutoff Command and second burn Engine Start Command. The orbital boiloff is 258 lbm greater than the

predicted value of 2,613 lbm. This deviation resulted from (1) a higher than predicted facility vent system backpressure, (2) a lower than predicted CVS regulator control pressure, and (3) a slightly higher bulk heating rate than was used in the prediction (section 12).

15.2.3 PU Mass Sensor Corrections

The total volumetric inflight mass sensor corrections for LOX and LH2 indicated masses are presented in figure 15-1. The total correction is the sum of the actual measured volumetric tank-to-sensor mismatch, cg offset, and inflight tank deflection correction. Maximum LOX mass sensor error was 1,375 lbm at 85,000 total LOX load or approximately 0.70 percent error at the 45 percent level of the tank. The maximum LH2 mass sensor error was 330 lbm at 8,000 lbm total LH2 load or approximately 0.75 percent error at the 20 percent level of the tank. The LOX total correction computed from postflight data agrees very closely with the preflight prediction. The actual LH2 total correction deviated from the preflight prediction primarily due to the inflight tank deflection.

The PU system mass corrections due to tank deflections are caused by differences in tank skin temperature and differential tank pressures from those experienced during acceptance firing. Figure 15-2 presents a comparison of predicted and actual flight corrections for tank deflection for the LOX and LH2 mass sensors. The predicted LOX correction agrees very well with the postflight analysis. The irregular correction from the flight analysis after second engine start was caused by deviations in tank ullage pressure from predicted.

The actual LH2 mass sensor correction was considerably different from the preflight prediction. The major cause for this difference was the LH2 tank skin temperature history. The LH2 tank skin temperature cooled at a much faster rate than predicted during S-II stage burn resulting in a net colder actual skin temperature than predicted during first burn. The actual correction is approximately 100 lbm less than predicted during this phase. At second burn ignition, the average skin temperature was warmer than predicted, resulting in 46 lbm less correction than predicted.

Section 15 Propellant Utilization

Only two LH2 tank skin temperature measurements were available during second burn; one on the shaded side, and one on the partially shaded side. The partially shaded sensor was used for the average skin temperature during second burn.

The cg offset corrections to the PU mass sensor and level sensor propellant masses are caused by tilting of the propellant level due to the engine thrust vector passing through the third flight stage cg when the cg is displaced from the longitudinal centerline. Figure 15-3 shows the predicted and actual flight correction for the LOX and LH2 mass sensors. Good agreement was obtained between the predicted and actual cg offset corrections for both mass sensors.

15.2.4 Comparison of Level Sensor and Volumetric PU Mass at Level Sensor Activation

Table 15-3 presents the level sensor mass and volumetric PU mass at each level sensor activation during flight. The level sensor masses were computed from propellant volume at the level sensor height location and the computed propellant density at the level sensor activation time. The propellant temperature and density data used for the level sensor mass analysis are presented in figures 15-4 and 15-5.

Figure 15-6 shows the deviations between level sensor and volumetric PU mass at level sensor activation times for acceptance firing, countdown demonstration tests (CDDT) and flight. In order to compare the level sensor data to the PU data for the three tests mentioned, the PU masses for the acceptance firing were recomputed based upon the lbm/pf flight calibration slope. This procedure normalizes the volume data so that the differences between level sensor and PU mass for the three tests (acceptance firing, CDDT, and flight) are a measure of system repeatability.

Investigation and coordination with the field stations indicate the LOX and LH2 level sensor locations have not changed since S-IVB-501 acceptance firing.

The LOX data comparison shows good agreement between the CDDT and flight with the exception of the first level sensor that activated during second burn. The unusual behavior at this sensor can be attributed to an uncertainty in the level sensor activation time due to large propellant slosh during the early part of second burn. If a straight line skewed bias is drawn through the mean of the CDDT and flight data, the deviations from this line exhibit a trend similar to the deviations of the acceptance firing data about the horizontal.

The magnitude of the skewed bias at first ignition is approximately 620 lbm relative to the lowest level sensor. The cause of this apparent shift has not been definitely resolved.

The LH2 comparison shows that the deviations during flight first burn agree with those during the CDDT but, contrary to the LOX analysis, the deviations during the second burn agree with those of the acceptance firing. The flight deviations during first burn are greater than the maximum probable deviations between the two systems. At this time there is insufficient data to explain these deviations. The data available from the S-IVB-502 flight will be utilized for comparison analysis, since the level sensor configuration is the same as for S-IVB-501.

15.2.5 Propellant Residuals

Propellant residuals were computed for both engine burns using point level sensors and the PU mass sensors. Two level sensors in each tank were used for computation of first burn residuals, level sensors L0012 and L0011 in the LOX tank and N0024 and N0025 in the LH2 tank. Three level sensors in each tank were used for computation of second burn residuals, level sensors L0009, L0008, and L0006 in the LOX tank and N0029, N0030, and N0031 in the LH2 tank.

The point level sensor residuals were generated using engine consumption data to extrapolate from the level sensor activation to Engine Cutoff Command. A weighted average residual was then computed for the level sensors in each propellant tank. The final propellant residual masses at each engine cutoff are a statistically weighted average of the level

Section 15 Propellant Utilization

sensor and PU mass sensor residuals. This method provides a more accurate residual value for second burn than the stage best estimate procedure because propellant mass is measured directly without the error contributed by a higher ratio of nonpropellant mass.

Table 15-4 summarizes the propellant residual data determined by the PU mass sensor and the point level sensors.

Total masses at second burn Engine Cutoff Command (ECC2) were 15,071 lbm LOX and 3,651 lbm LH2. These total masses include unusable masses of 530 lbm LOX and 760 lbm LH2. The usable masses at ECC2 were 14,541 lbm LOX and 2,891 lbm LH2.

15.2.6 PU Efficiency

The closed-loop PU efficiency is determined by expressing the usable residual propellant at depletion cutoff as a percentage of the total propellant load. Total stage steady-state propellant consumption rates prior to the second burn velocity cutoff were 386.5 lbm/sec LOX and 76.9 lbm/sec LH2. Extrapolation of these flowrates to the theoretical depletion cutoff results in a simultaneous propellant depletion at 37.6 sec after velocity cutoff and a PU efficiency of 100 percent.

It should be noted that the above extrapolation is based on constant propellant flowrates for 37.6 sec. Had the stage actually gone to depletion cutoff, the PU system would have varied the propellant flowrates for the final period. PU system nonlinearities during the 37.6 sec to depletion would have driven the PU valve to an average -1 deg level thereby increasing the LH2 residual by approximately 20 lbm and causing a LOX depletion cutoff.

15.3 PU System Response

The PU valve was positioned at null for first burn start and remained at the null position until PU activate at ESC1 +8 sec. The PU valve was commanded to the fully closed stop at activation and remained there throughout first burn. The first burn PU valve position history is illustrated in figure 15-7. The PU valve reached the stop at

Section 15
Propellant Utilization

ESC1 +10 sec as compared to the predicted time of ESC1 +13.8 sec. This deviation between the predicted and actual valve position slope following first burn activation was due to a difference between the method used to activate the PU system in the simulation model and the actual implementation of PU activation in flight. This difference was removed in the reconstruction by activating the PU system 3 sec earlier in the simulation model. The difference between the predicted and actual valve positions on the fully closed stop is due to an error in the prediction and does not represent a performance deviation.

The PU valve reconstruction for second burn is also presented with the predicted and actual PU valve histories in figure 15-7. The PU valve was successfully commanded to the fully opened 4.5:1 EMR position at ESC2 -20 sec to satisfy engine restart requirements. The PU valve remained there until ESC2 +13 sec when the hardover command was removed. The PU valve then traveled through the null position to +5 deg by ESC2 +14 sec. The valve travel past the null position to +5 deg was caused by system overshoot.

Due to system dispersions the PU valve then traveled to the LOX rich stop. The PU valve reached the LOX rich stop at ESC2 +25.2 sec and remained there until PU valve cutback at ESC2 +63.5 sec. After cutback the average PU valve position was -2.5 deg until second burn engine cutoff at ESC2 +299.692 sec.

The PU system deviations between predicted and actual performance, which caused the PU valve LOX rich operation during second burn, are listed in the following table.

DEVIATION DESCRIPTION	DEVIATION IN EQUIVALENT LOX (lbm)
1) Loading computer	366
2) LH2 boiloff	1,277
3) LOX boiloff	98
4) Engine performance	552
5) PU system nonlinearities	200
6) Calibration	285
7) Bridge gain ratio	850
	TOTAL 3,628

Section 15
 Propellant Utilization

Equivalent LOX listed in the previous table is either the actual LOX deviation, if the deviation is in LOX, or the LOX deviation required to cause the same deviation in the case of LH2 deviations. Equivalent LOX for LH2 deviations is derived by multiplying the actual LH2 deviation by the actual PU system bridge gain ratio.

A PU valve history reconstruction reflecting the above system deviations is presented with the predicted and actual PU valve histories in figure 15-7. The individual PU valve excursions caused by each independent deviation is illustrated in figure 15-8.

The major cause of the high engine mixture ratio (EMR) operation during second burn was the higher than predicted LH2 boiloff during orbital coast. Each of the system deviations listed above are discussed in the following sections. The PU indicated and corrected propellant masses used for system deviation analysis are tabulated as follows:

EVENT	UNADJUSTED PU FINE MASS		PU FINE MASS CORRECTED FOR FLOW INTEGRAL FLIGHT NONLINEARITIES	
	LOX	LH2	LOX	LH2
Liftoff	193,179	41,129	193,299	41,144
ESC1	193,048	41,043	193,308	41,107
ECC1	131,953	29,697	131,353	29,662
ESC2	131,965	26,886	131,085	26,771
ECC2	15,803	3,998	15,133	3,815

15.3.1 Indicated Loading Computer Deviations

Indicated loading computer deviations are the difference between the desired load and the loading computer indicated load at liftoff. The indicated loading deviations were -94 lbm LOX and -93 lbm LH2. The combined effect of these two deviations is an equivalent LOX overload of 366 lbm. If this deviation had not been present in the system dispersions the PU valve would have cutback 7.5 sec earlier. Curve 1 of figure 15-8 shows the singular effect of the loading deviations on the PU valve.

15.3.2 LH2 Boiloff Deviation

The LH2 boiloff during orbit was determined from PU indicated masses corrected for PU system nonlinearities. Due to capillary action PU mass data was not valid until ESC2 +15 sec. The PU masses at second burn Engine Start Command were calculated by taking a valid PU mass and extrapolating back to ESC using engine flowmeter data. The LH2 orbital boiloff was 258 lbm higher than predicted. The majority of this deviation was caused by flashoff following first burn Engine Cutoff Command. This flashoff resulted from a higher than predicted facility LH2 vent backpressure before liftoff and a lower than predicted CVS regulator control pressure in orbit. The LH2 boiloff deviation is equivalent to 1,277 lbm of LOX equivalent error. Curve 2 of figure 15-8 shows the singular effect of this deviation. It should be noted that the LH2 boiloff deviation is the largest single contributor of the LOX rich operation. The PU valve would not have reached the LOX rich stop without this deviation.

15.3.3 LOX Boiloff Deviation

The predicted LOX mass boiloff during coast including engine chilldown was 240 lbm. The PU corrected masses indicated a LOX boiloff of 108 lbm leaving a boiloff deviation of 132 lbm. Curve 3 of figure 15-8 shows the singular effect of the LOX boiloff error. If this deviation had not been present in the system dispersions the PU valve would have cutback 2.7 sec earlier. An analysis of the LOX ullage gas conditions indicated a total LOX boiloff during coast slightly higher than the PU indicated LOX boiloff. The two methods were in satisfactory agreement and the difference does not significantly affect the total system dispersions.

15.3.4 Engine Performance Deviation

The LOX and LH2 flowrates during first burn were lower than predicted. This lower consumption resulted in an equivalent LOX error of 552 lbm at second burn Engine Start Command. The singular effect of this deviation is shown in curve 4 of figure 15-8. If this deviation had not been present in the system dispersions, the PU valve would have cutback approximately 11 sec earlier.

Section 15 Propellant Utilization

15.3.5 PU System Nonlinearity Deviations

The PU system total nonlinearities used in PU system response analysis are based on engine flowmeter analysis normalized to liftoff and second burn cutoff masses. These nonlinearities are presented in figure 15-9. Sensor capillary action at the start of second burn and two slosh waves caused by vehicle attitude transients, during second burn, caused large variations in the indicated mass data used to determine these nonlinearities. The actual PU system LOX tank-to-sensor nonlinearities with the sloshing and capillary effects removed compared favorably with the predicted. The actual LH2 tank-to-sensor nonlinearities also compared favorably with the predicted values adjusted for the actual inflight tank geometry variations. The LOX equivalent error, due to the combined differences between actual and predicted mismatch, was 200 lbm. Curve 5 of figure 15-8 shows the singular effect of this deviation. If this deviation had not been present in the system dispersions, the PU valve would have cutback 4 sec earlier.

The predicted and actual total inflight tank-to-sensor nonlinearities as determined by the volumetric method for the LOX and LH2 probes are presented in figure 15-10. These corrections were normalized to the flight first burn ignition and second burn cutoff masses for comparison with the flowmeter analysis. Satisfactory agreement was obtained between the flowmeter and volumetric nonlinearities for both the LOX and LH2 mass sensors.

15.3.6 Calibration Deviation

Calibration deviations at first burn Engine Start Command were +0.56 percent LOX and +0.09 percent LH2, thus causing the initial LOX mass to be overloaded 1,087 lbm and the initial LH2 mass to be overloaded 36 lbm. This calibration deviation was determined by comparing best estimate total masses with corrected PU indicated masses. The calibration deviation seen by the PU system at second burn Engine Start Command was 285 lbm LOX equivalent error. Curve 6 of figure 15-8 shows the singular effect of the calibration deviation. If this deviation had not been present in the system dispersions, the PU valve would have cutback approximately 7 sec earlier.

15.3.7 Bridge Gain Ratio Deviation

The desired reference mixture ratio (RMR) for the S-IVB-501 flight was 5.0:1.0. The bridge gain ratio (BGR) was electrically adjusted at 5.0:1.0 to obtain the desired RMR. The RMR obtained from flight data which includes the effects of the sensor calibration deviations, was 4.96:1.0. This indicates that the BGR was actually set at 4.95:1.0 instead of 5.0:1.0 after the sensor calibration deviations were removed. The ratio of the propellant masses at PU valve cutback time also indicated a BGR of 4.95:1.0. Curve 7 of figure 15-8 shows the singular effect of changing the BGR. As may be seen from curve 7, the valve position leveled out approximately 3 deg lower than the loading deviation curves. If this deviation had not been present in the system dispersions, the PU valve would have cutback approximately 15 sec earlier and the mean valve position would have leveled out approximately 3 deg higher.

15.3.8 Capillary Action

The rise of propellants within the mass sensors due to capillary action during the low acceleration coast period was present as expected. This capillary action experienced before and after ullaging is compared to the flight data from S-IVB-203 in figure 15-11. In both cases the sensor readings indicated that the propellants did not rise to the top of the sensors as was expected while in the low acceleration environment before ullaging. This implies that there were bubbles or vapor within the sensors which lowered the capacitance signal and corresponding mass reading and resulted in an indicated mass level within the sensors that was lower than the actual level. The indicated mass level decreased during ullaging as expected. Vehicle maneuvers during ullaging on S-IVB-501 caused propellant sloshing disturbances which are the most probable cause for the variations in the mass indications during this period. There were no maneuvers applied to S-IVB-203 during this period and, as shown by figure 15-11, there were also no variations in the mass indications, except for the expected level drop due to ullaging acceleration.

Section 15 Propellant Utilization

During fuel lead after second engine start the LH2 mass level continued to drop; however, the indicated LOX mass level within the sensors increased by approximately 7,000 lbm. This increase was probably caused by removing bubbles from the LOX sensor while in the higher acceleration environment. This resulted in a higher sensor capacitance reading. The indicated LOX propellant increase and the removal of the remaining capillary effects during mainstage, is illustrated in figure 15-12. This figure also compares the indicated mass readings with the mass in tank obtained by extrapolating engine flowmeter consumption during the first part of burn. Since the propellants were not settled until ESC2 +15 sec, the capillary action affected the PU system by charging the forward shaping network from PU hardover command off (ESC2 +13 sec) until ESC2 +15 sec. The singular effect of the capillary action on the PU valve is shown in figure 15-13. The error signal resulting from this capillary action was approximately +4 v. This deviation by itself would cause a peak PU valve excursion of approximately +9 deg. This erroneous error signal discharged to a negligible value at approximately ESC2 +50 sec. The effect of the capillary action on the error signal can be determined by comparing the actual error signal with an error signal derived from engine flowmeter data between ESC2 +13 and ESC2 +15 sec.

Figure 15-14 compares the actual telemetered PU summing point error signal, the actual error signal with the telemetry bias and high frequency noise removed, and the PU error signal obtained by using engine flowmeter derived consumption. A telemetry bias of -0.3 v was present on the actual error signal. This bias was also present on the acceptance firing data and was confirmed by flight data during restart when the summing potentiometers were deactivated by applying the 4.5:1.0 hardover command.

As can be seen from the smoothed telemetry error signal, the capillary action at the start of second burn caused an erroneous error signal until the effects of the capillary action were removed.

15.3.9 Sloshing

The redesigned forward shaping network (slosh filter) successfully removed the effects of propellant sloshing on the PU valve. Propellant sloshing within a 0.2 to 0.6 Hz range was present on the mass signals and the PU summing point error signal. However, the added filter attenuation removed the slosh effects on the signal fed to the PU valve servo.

Vehicle attitude transients resulted in two large low frequency propellant slosh waves. The slosh waves can be seen in the LOX and LH2 mismatch curves of figure 15-9. The first slosh wave appeared between ESC2 +100 and ESC2 +120 sec. This slosh wave was set off by a vehicle attitude transient following the artificial tau mode during PU cutback. The PU valve position was increased approximately 1 deg by this disturbance and resulted in a corresponding shift in engine performance parameters. The second low frequency slosh wave occurred approximately 5 sec before second burn Engine Cutoff Command. This wave was also caused by a vehicle attitude transient and occurred at the time the chi freeze guidance mode was applied. This disturbance resulted in a 1 deg valve tailoff and corresponding thrust variation which is discussed further in paragraph 15.4. The effect of these slosh waves on the PU valve position history may be seen in figure 15-7.

15.3.10 Postflight Reconstruction

The combined effects of all the previously mentioned PU system deviations on the PU valve position are illustrated by the second burn PU valve position reconstruction shown in figure 15-7. The reconstruction agrees favorably with the actual data and, therefore, verifies satisfactory PU system operations. The postfiring reconstruction deviates from the actual PU valve history at ESC2 +200 sec and at ESC2 +260 sec. These deviations are due to inaccuracies involved in deriving the LOX and LH2 mismatch.

15.4 PU System Induced Thrust Variations

Thrust variations following PU cutback are induced primarily by the PU system. Figure 15-15 presents thrust variation histories for second burn

Section 15 Propellant Utilization

following PU cutback. Table 15-5 compares the actual thrust variations observed with thrust variation limits established in the Contract End Item (CEI) Specification. Thrust variations during hardover PU valve operation are induced by engine and stage systems variations and are presented in section 9.

Between ESC2 +140 sec and ESC2 +210 sec a 3 deg PU valve excursion induced a 4,450 lbf peak-to-peak thrust oscillation. This oscillation was caused by the LOX PU sensor manufacturing nonlinearity. Manufacturing nonlinearities also resulted in other smaller variations during the remainder of the burn.

Thrust variations were within specification limits in the period following PU cutback until ESC2 +296 sec when the thrust rate and acceleration limits were exceeded. This variation was initiated by a vehicle attitude transient which occurred following the initiation of the chi freeze guidance mode. The attitude transient created a low frequency slosh wave which resulted in a 1 deg PU valve tailoff. This tailoff, however, was not sufficient to cause the observed thrust variation. The total variation was the result of an engine performance shift coupled with the PU valve tailoff. The engine performance shift was attributed to a PU valve flow resistance shift and is discussed further in paragraph 9.4.4.2.

To separate the effects of the engine performance shift from the PU system performance variation caused by the vehicle attitude transient, a flow integral simulation was run utilizing the actual PU valve position data as the primary input. The engine performance shift effects were not present on the PU valve position data. The resulting engine thrust response is given in figure 15-16. Thrust variation values were taken from this curve and are compared to the actual variations and the CEI limits in table 15-5. Thrust variations, excluding the effects of the thrust transient caused by the attitude transient and engine performance shift are also given in table 15-5. The actual rate of change of thrust observed was -2,400 lbf/sec. The reconstructed rate of change based on

Section 15
Propellant Utilization

PU valve motion was -450 lbf/sec. It may be seen that the thrust variations caused by the PU system were within the CEI specification limits and those caused by the engine performance shift exceeded the specification limits. Since engine performance shifts are specifically excluded from CEI specification limits, all thrust variation requirements for the period following PU cutback were met.

Section 15
Propellant Utilization

TABLE 15-1
PROPELLANT MASS HISTORY

EVENT	PREDICTED MASS (lbm)			PU INDICATED CORRECTED MASS (lbm)			FLIGHT FLOW INTEGRAL MASS (lbm)			PU VOLUMETRI MASS (lbm)		
	LOX	LH2	TOTAL	LOX	LH2	TOTAL	LOX	LH2	TOTAL	LOX	LH2	
LIFTOFF RO +0.26	193,273*	41,222*	234,495*	193,299	41,144	234,443	194,103	40,963	235,066	194,289	41,049	2
ENGINE START COMMAND (1st) RO +520.7	193,273	41,222	234,495	193,308	41,107	234,415	194,103	40,963	235,066	194,300	40,994	2
ENGINE CUTOFF COMMAND (1st) RO +665.6	129,844	29,703	163,016	131,353	29,662	161,015	131,603	29,476	161,079	131,700	29,557	1
PROPELLANT CONSUMED (ESC1 TO ECC1)	63,429	11,510	71,479	61,955	11,445	73,400	62,500	11,487	73,987	62,600	11,437	
ENGINE START COMMAND (2nd) RO +11,486.6	129,445	27,055	159,884	131,085	26,771	157,856	131,335	26,585	157,920	131,381	26,657	
PU VALVE CUTBACK TIME RO +11,550.1	--	--	--	107,874	22,401	130,275	107,735	22,163	129,898	108,103	22,208	
ENGINE CUTOFF COMMAND (2nd) RO +11,786.3	12,087	3,273	15,360	15,133	3,815	18,948	15,071	3,651	18,722	15,059	3,725	
PROPELLANT CONSUMED (ESC2 TO ECC2)	117,358	23,782	144,524	115,952	22,956	138,908	116,264	22,934	139,198	116,281	22,932	

*Desired

FOLDOUT FRAME

5-1
MASS HISTORY

PU VOLUMETRIC MASS (lbm)			LEVEL SENSOR MASS (lbm)			TRAJECTORY RECONSTRUCTION (lbm)	BEST ESTIMATE MASS (lbm)		
LOX	LH2	TOTAL	LOX	LH2	TOTAL	TOTAL	LOX	LH2	TOTAL
194,289	41,049	235,338	194,770	41,408	236,178	235,379	194,395	41,173	235,568
194,300	40,924	235,294	194,770	41,408	236,178	235,443	194,395	41,143	235,538
131,700	29,557	162,257	132,326	29,874	162,200	161,029	131,791	29,655	161,446
62,600	11,437	74,037	62,444	11,534	73,978	74,414	62,604	11,488	74,092
131,381	26,657	158,038	131,461	26,496	157,957	158,183	131,496	26,627	158,123
108,103	22,208	130,311	107,831	22,116	129,947	--	107,886	22,252	129,865
15,059	3,725	18,784	15,079	3,595	18,674	18,337	14,913	3,679	18,592
116,281	22,932	139,213	116,382	22,901	139,283	139,846	116,583	22,948	139,531

FOLDOUT FRAME 2

Section 15
Propellant Utilization

TABLE 15-2
PROPELLANT LOADING SUMMARY

ITEM	LOX (lbm)	LH2 (lbm)	TOTAL (lbm)
Propellant Load at Liftoff			
Desired	193,273	41,222	234,495
PU indicated	193,179	41,129	234,408
PU indicated corrected	193,299	41,144	234,443
Flight flow integral	194,103	40,963	235,066
Volumetric analysis	194,289	41,049	235,338
Level sensor analysis	194,770	41,408	236,178
Trajectory reconstruction	---	---	235,379
Best estimate	194,395	41,173	235,568
Deviation from Desired			
PU indicated	-94 (-0.05%)	-93 (-0.23%)	-187 (-0.08%)
Best estimate	1122 (0.58%)	-49 (-0.12%)	1073 (0.46%)
Deviation from Indicated			
Best estimate	1216 (0.63%)	44 (0.11%)	1260 (0.54%)
Deviation from Best Estimate			
PU indicated corrected	-1096 (-0.56%)	-29 (-0.07%)	-1125 (-0.48%)
Flight flow integral	-292 (-0.15%)	-210 (-0.51%)	-502 (-0.21%)
Volumetric analysis	-106 (-0.05%)	-124 (-0.30%)	-230 (-0.10%)
Level sensor analysis	375 (0.19%)	235 (0.57%)	610 (0.26%)
Trajectory reconstruction	---	---	-189 (-0.08%)

Section 15
Propellant Utilization

TABLE 15-3
LEVEL SENSOR AND VOLUMETRIC PU MASS

LEVEL SENSOR	ACTIVATION TIME FROM RO (sec)	LEVEL SENSOR MASS (lbm)	VOLUMETRIC PU MASS (lbm)	DEVIATION LEVEL SENSOR - PU (lbm)
(LOX)				
L0013	529.7	193,429	192,654	775
L0012	570.4	174,936	174,491	445
L0011	632.6	147,408	146,621	787
L0010	11,540.1	112,702	112,731	-29
L0009	11,628.6	75,305	74,998	307
L0008	11,713.0	43,100	42,955	145
L0006	11,775.8	19,104	18,815	289
(LP2)				
N0023	527.6	41,249	40,830	419
N0024	570.0	37,750	37,344	406
N0025	618.8	33,682	33,352	330
N0027	11,505.2	25,740	25,772	-32
N0028	11,553.9	21,979	21,820	59
N0029	11,603.2	17,855	17,934	-79
N0030	11,653.2	13,924	14,073	-149
N0031	11,705.7	9,903	9,915	-12
N0032	11,753.4	5,986	6,180	-194

Section 15
Propellant Utilization

TABLE 15-4
PROPELLANT RESIDUALS SUMMARY

LEVEL SENSOR	ACTIVATION TIME (sec)	LOX (lbm)			LH2 (lbm)		
		PU MASS SENSOR	LEVEL SENSOR	LEVEL SENSOR RESIDUAL (EXTRAPOLATED TO ECC)	PU MASS SENSOR	LEVEL SENSOR	LEVEL SENSOR RESIDUAL (EXTRAPOLATED TO ECC)
L0012	ESC1 +39.7	174,491	174,936	132,132			
L0011	ESC1 +111.9	146,621	147,408	132,551			
N0024	ESC1 +39.3				37,344	37,750	29,911
N0025	ESC1 +98.1				33,352	33,682	29,844
	ESC1 +144.926 (First Engine Cutoff)	131,700		132,326* (+731)	29,557		29,874* (+199)
L0009	ESC2 +142.1	74,998	75,305	15,031			
L0008	ESC2 +226.5	42,955	43,100	15,037			
L0006	ESC2 +289.3	18,815	19,104	15,109			
N0029	ESC2 +116.7				17,934	17,855	3,592
N0030	ESC2 +166.7				14,073	13,924	3,554
N0031	ESC2 +219.2				9,915	9,903	3,624
	ESC2 +299.692 (Second Engine Cutoff)	15,059		15,079* (+609)	3,725		3,595* (+175)
Best Estimate** Residuals-First Burn		132,051		+860	29,776		+234
Best Estimate** Residuals-Second Burn		15,071		+577	3,651		+160

*Statistical average of level sensor residuals.
 **Statistical weighted average of level sensor and PU mass sensor residuals.

Section 15
Propellant Utilization

TABLE 15-5
THRUST VARIATIONS

PARAMETER	THRUST VARIATIONS AFTER CUTBACK (cutback +75 sec to ECC -70 sec)	
	CEI 501 LIMITS	ACTUAL (COMPUTER PROGRAM PA49)
(1) Variation in mean thrust level (lbf)	+7,000 -6,000	-4,500
(2) Oscillations about mean thrust level (lbf)	+7,500	+2,225
(3) a. Rate of change of thrust; all frequencies (lbf/sec)	+510 -560	+295 -225
b. Rate of change of thrust; 0-0.1 cps (lbf/sec)	+500	+295 -225
(4) a. Thrust acceleration; all frequencies (lbf/sec/sec)	+500	<+100
b. Thrust acceleration; 0-0.1 cps (lbf/sec)	+125	<+100

PARAMETER	THRUST VARIATIONS (final 70 sec of S-IVB second burn)				
	CEI 501 LIMITS	ACTUAL (COMPUTER PROGRAM PA49)		SIMULATION (COMPUTER PROGRAM CA27)	
		INCLUDING THRUST TAILOFF	EXCLUDING THRUST TAILOFF	INCLUDING THRUST TAILOFF	EXCLUDING THRUST TAILOFF
(1) 2 cps thrust variation band (lbf)	+2,500	+1,000	+650	+700	+700
(2) Thrust band slope (lbf/sec)	+44 -80	-31	-20	-22	-18
(3) Variation of thrust band slope about nominal	+58 -50	-31	-20	-22	-18
(4) Thrust band centerline variation at 70 sec before velocity cutoff (lbf)	+6,500	-4,600	-4,700	-4,700	-4,800
(5) a. Rate of change of thrust; all frequencies (lbf/sec)	+650 -750	+400 -2,400	+400 -440	+175 -450	+175 -150
b. Rate of change of thrust; 0-0.1 cps (lbf/sec)	+354 -440	+200	+200	+150	+150
(6) a. Thrust acceleration; all frequencies (lbf/sec/sec)	+500	+485 -1,000	+310 -300	+100 -200	+100
b. Thrust acceleration, 0-0.1 cps (lbf/sec/sec)	+125	+100	+100	+100	+100

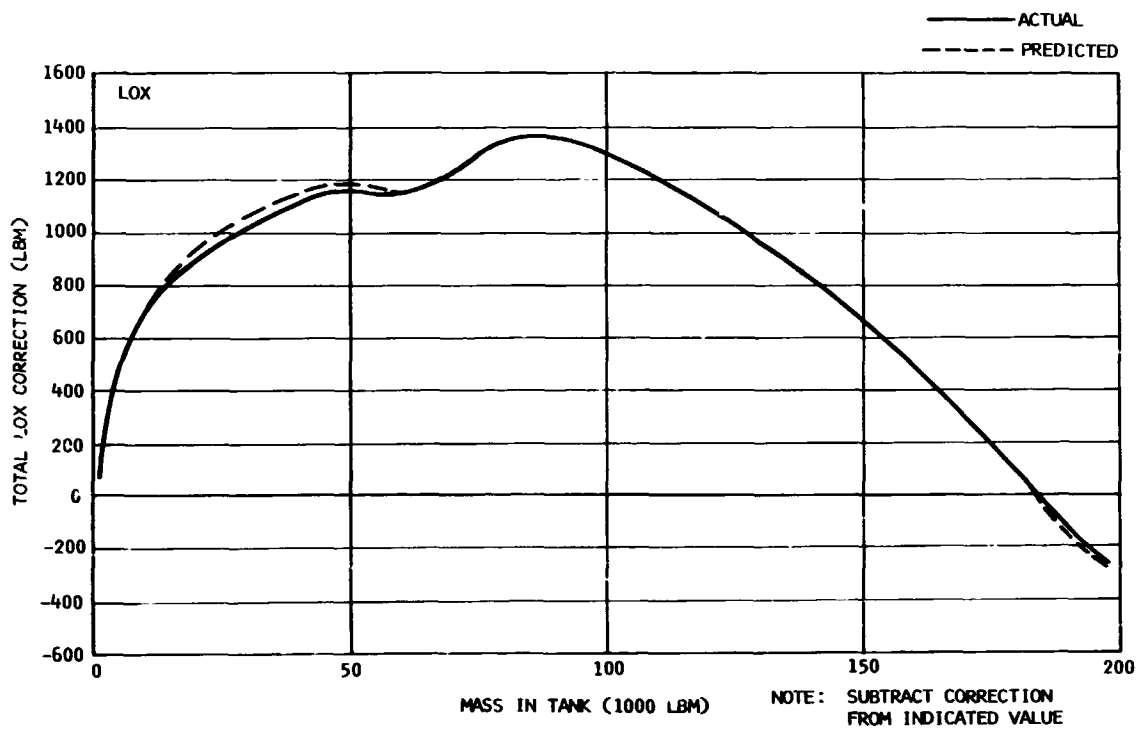
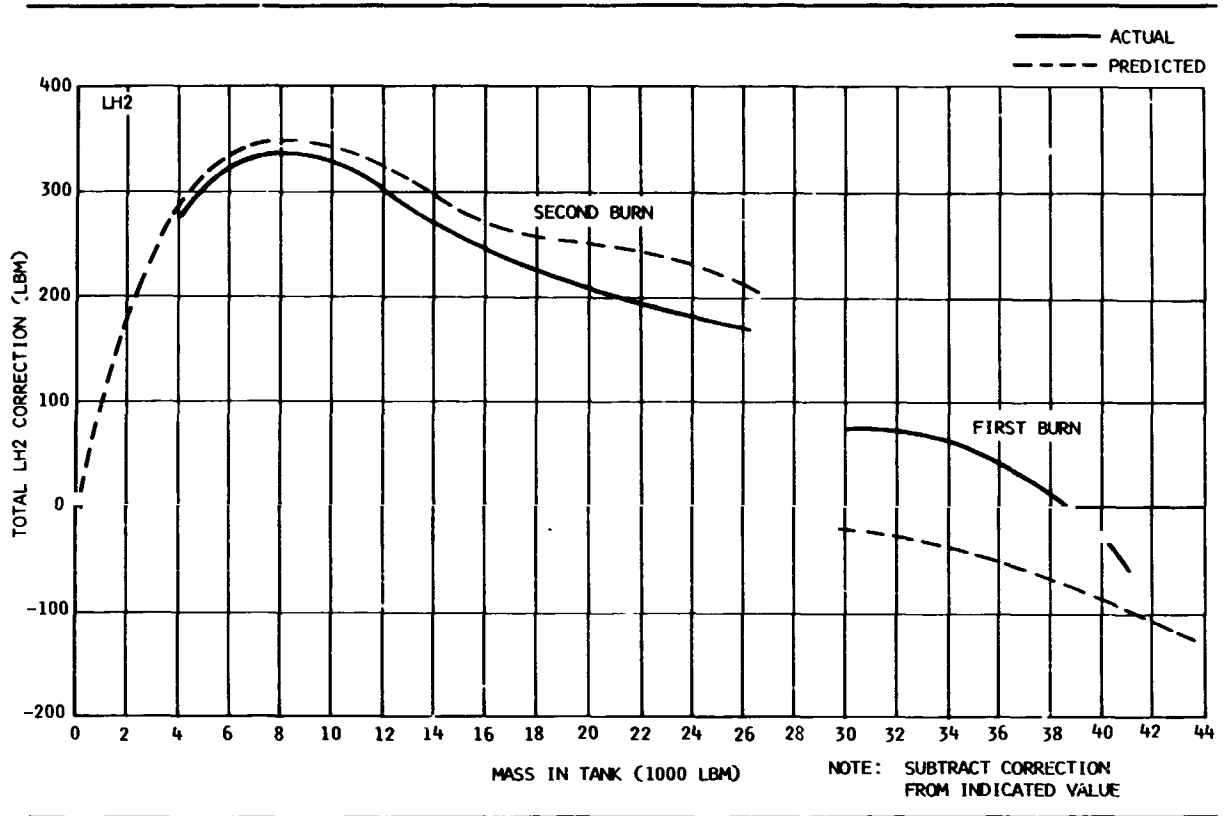


Figure 15-1. Total Tank-to-Sensor Correction for Indicated Flight Mass

Section 15
Propellant Utilization

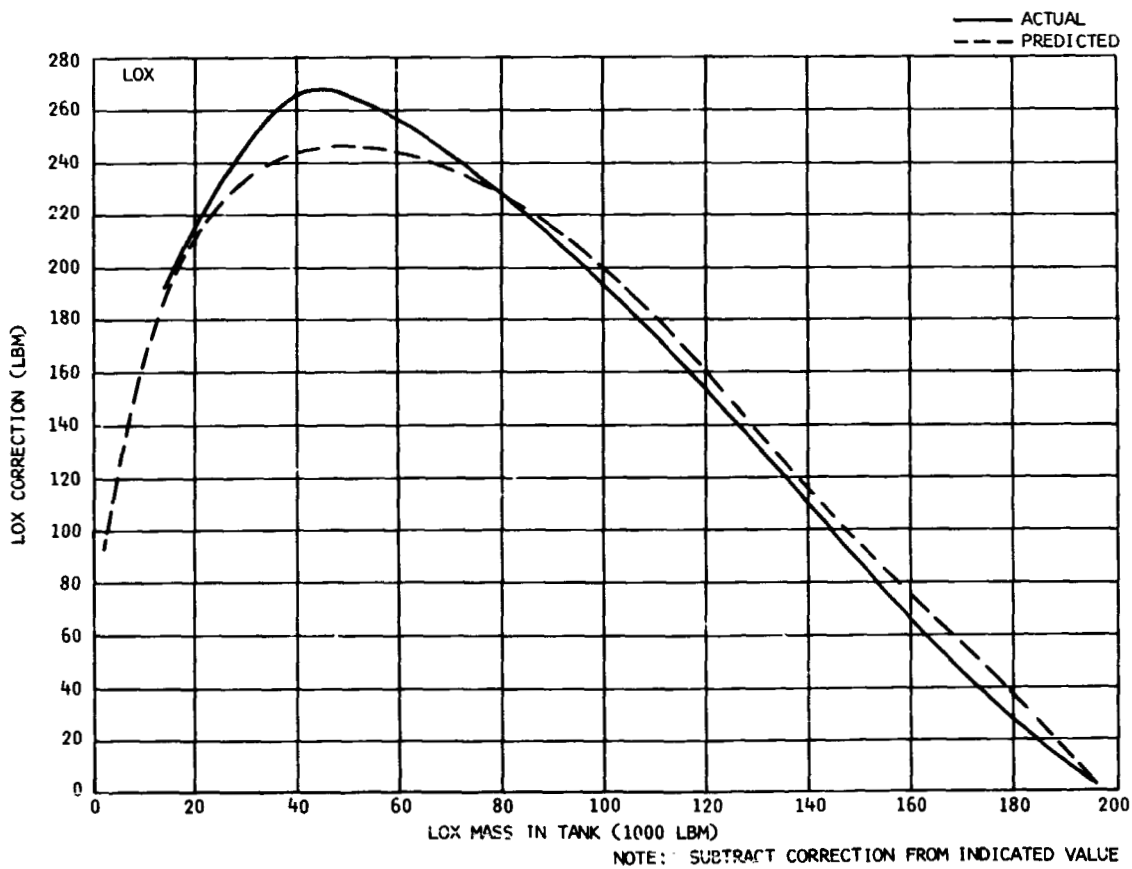
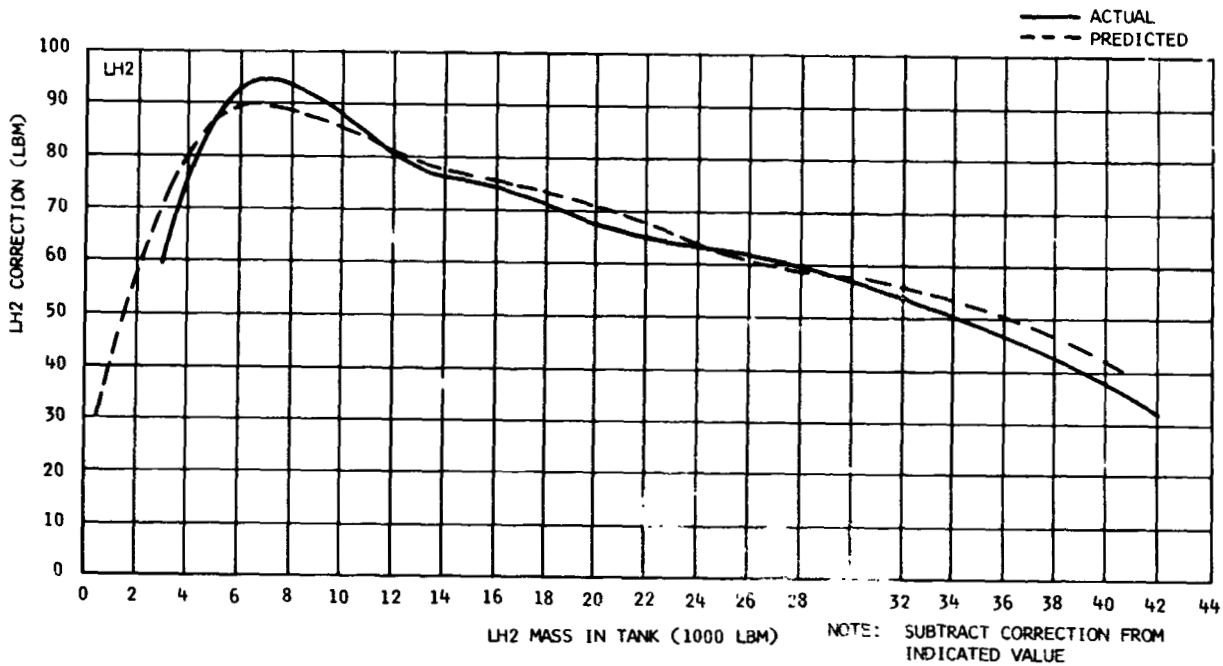


Figure 15-2. PU Mass Sensor Corrections Due to Center-of-Gravity Offset

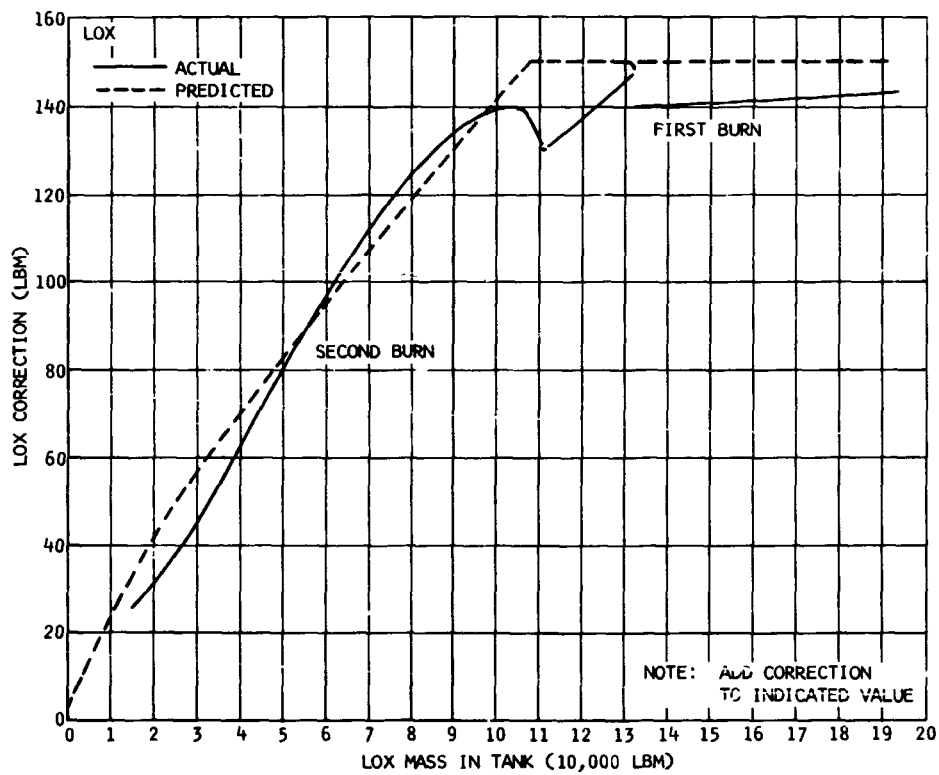
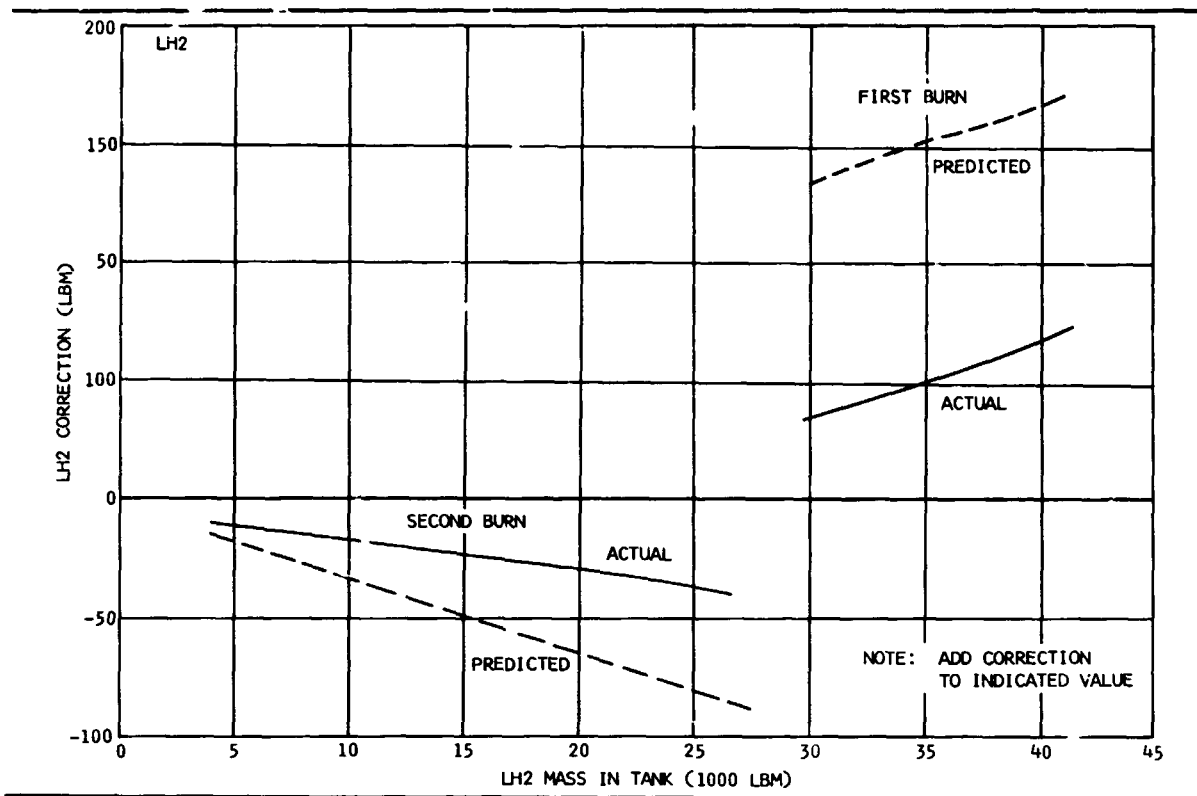


Figure 15-3. PU Mass Sensor Correction Due to Tank Deflection

Section 15
Propellant Utilization

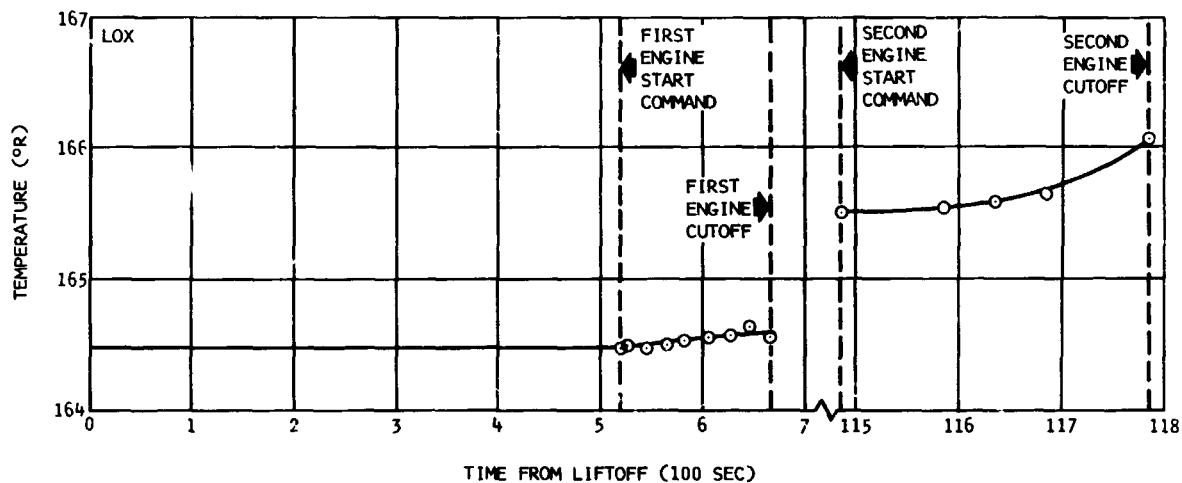
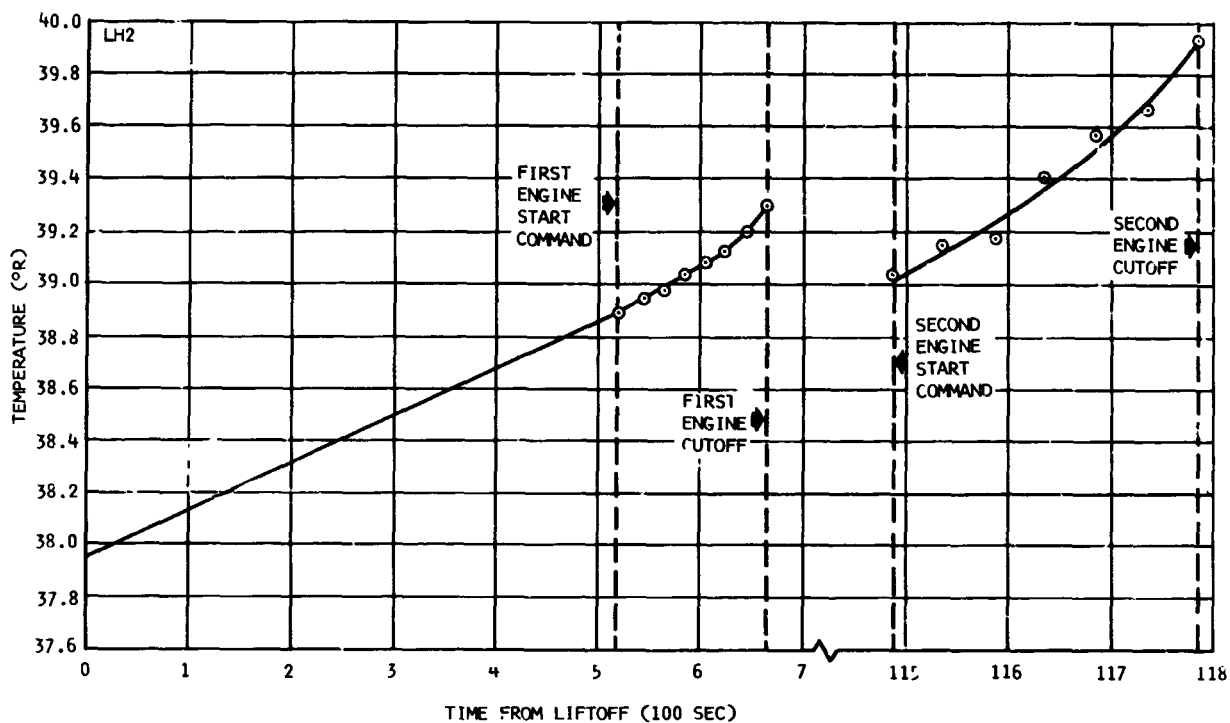


Figure 15-4. Propellant Intank Bulk Temperature Histories

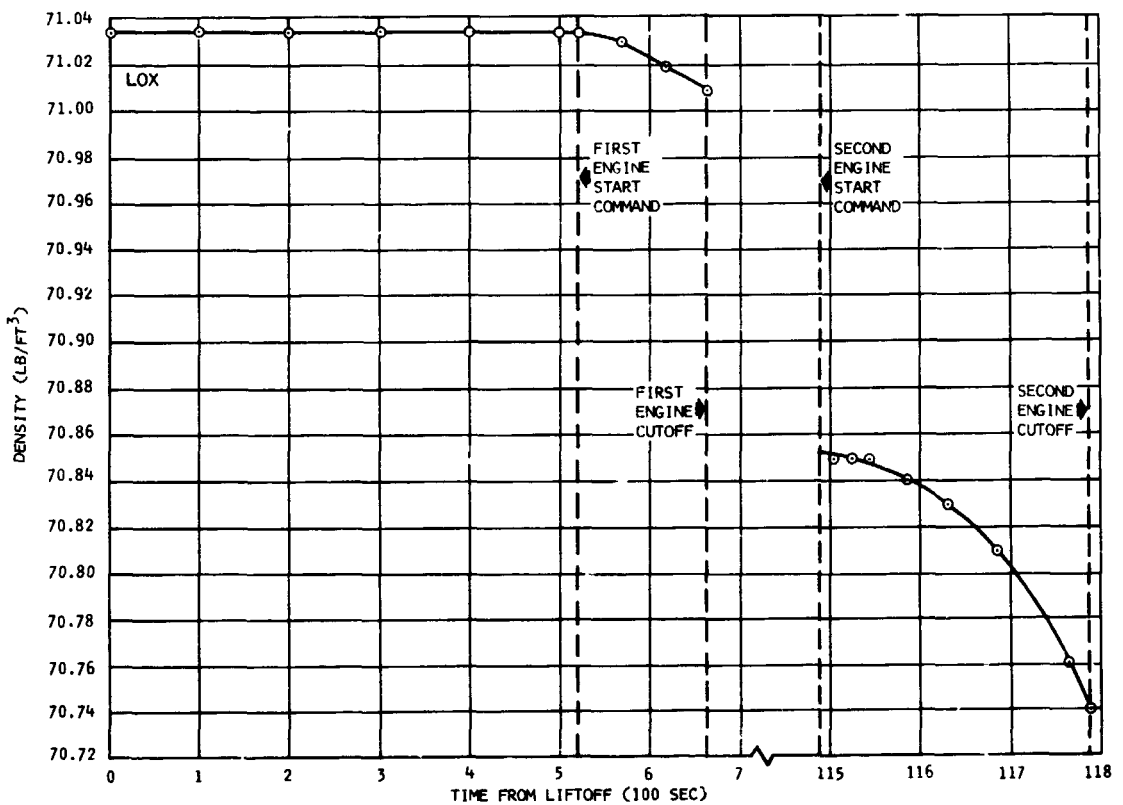
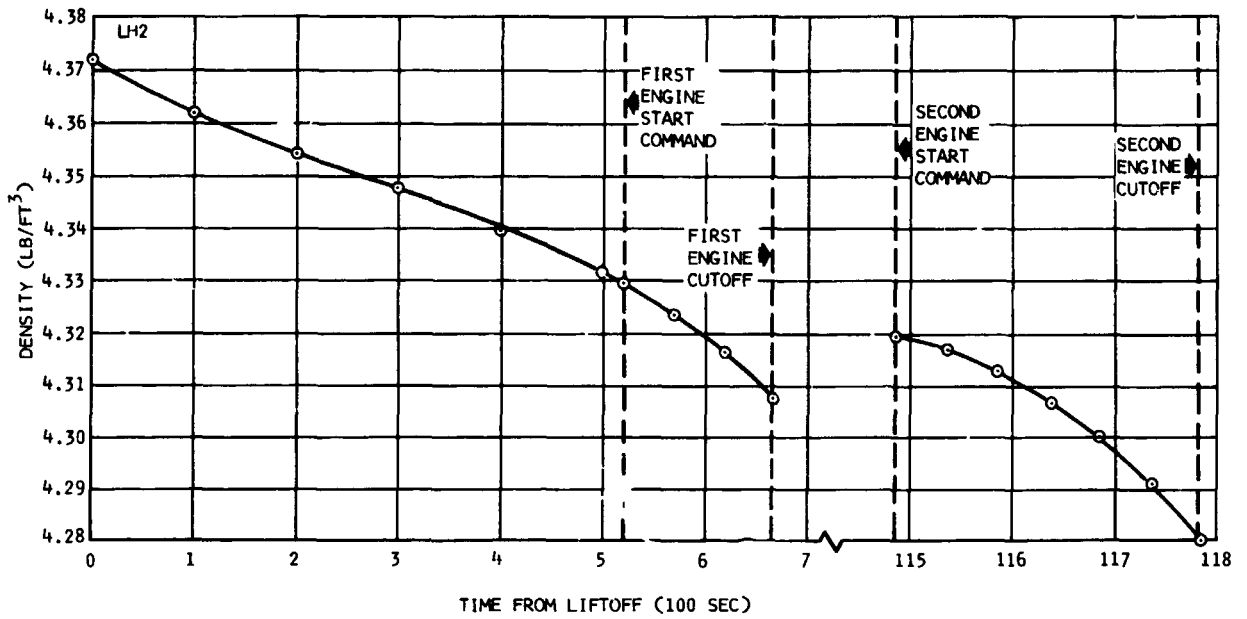


Figure 15-5. Propellant Intank Bulk Density Histories

Section 15
Propellant Utilization

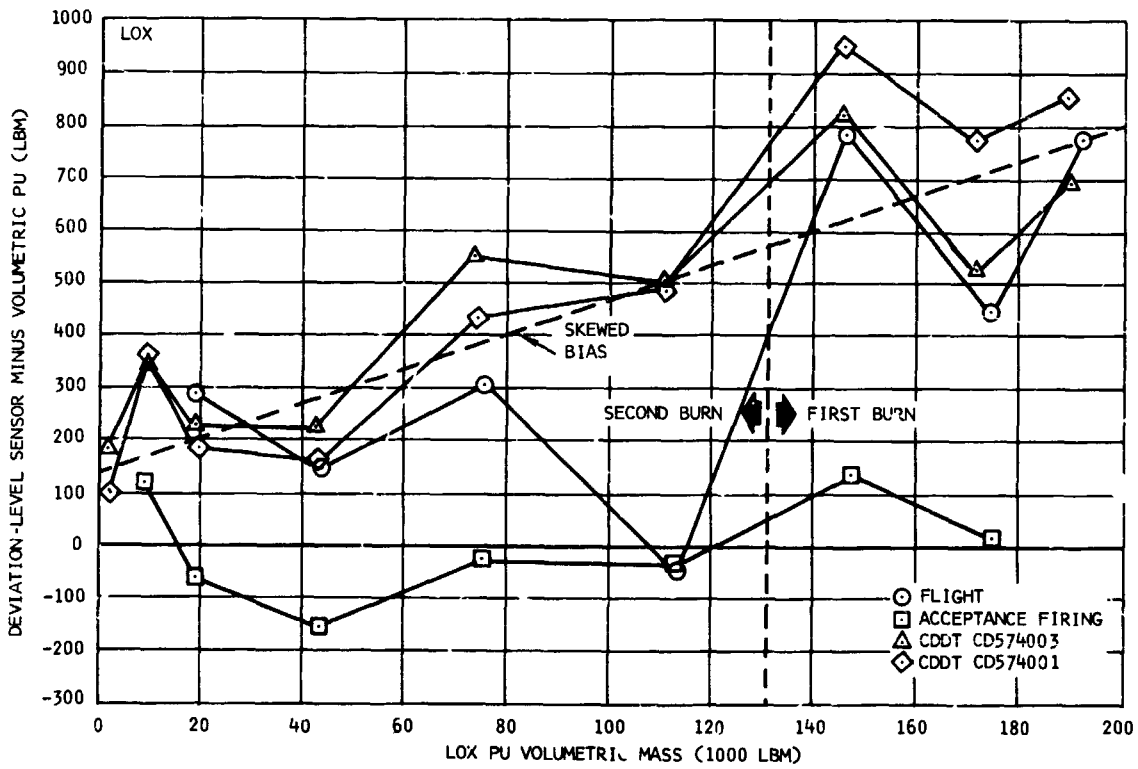
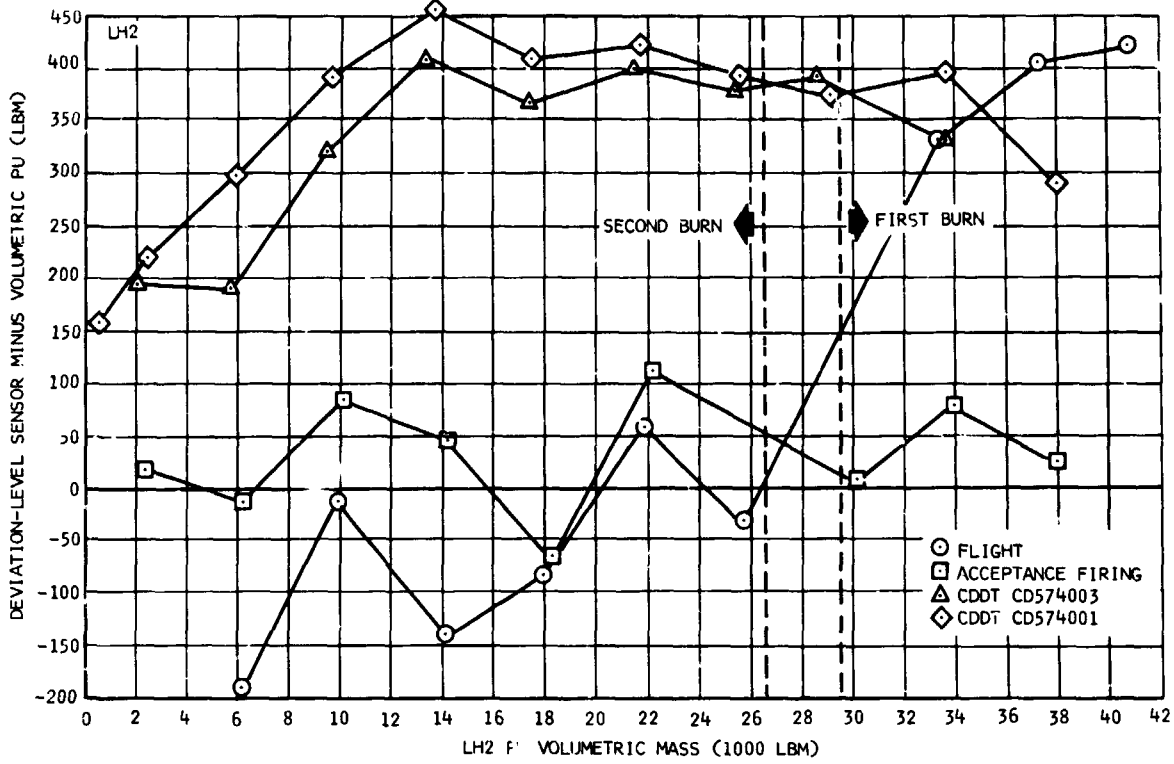


Figure 15-6. Comparison of Level Sensor and Volumetric PU Mass at Level Sensor Activation

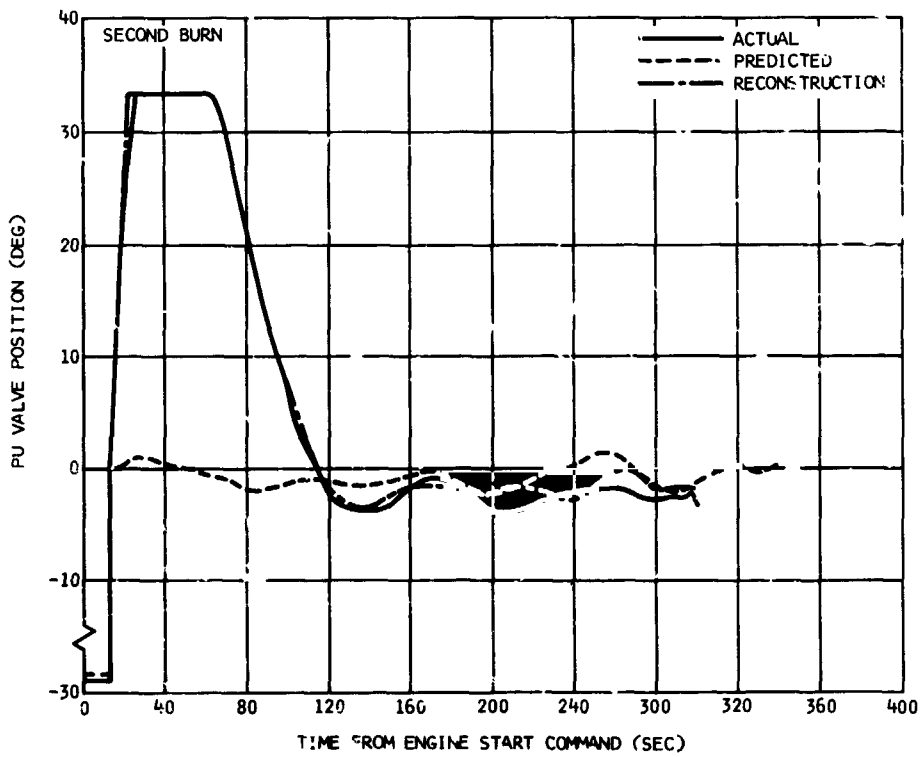
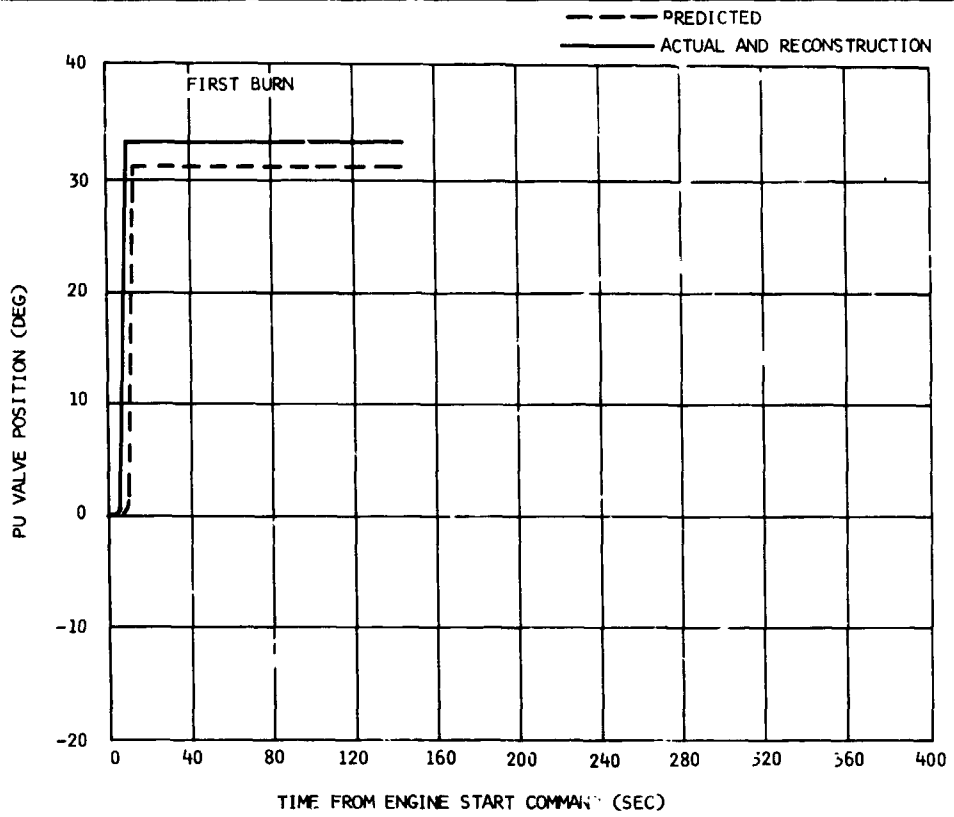
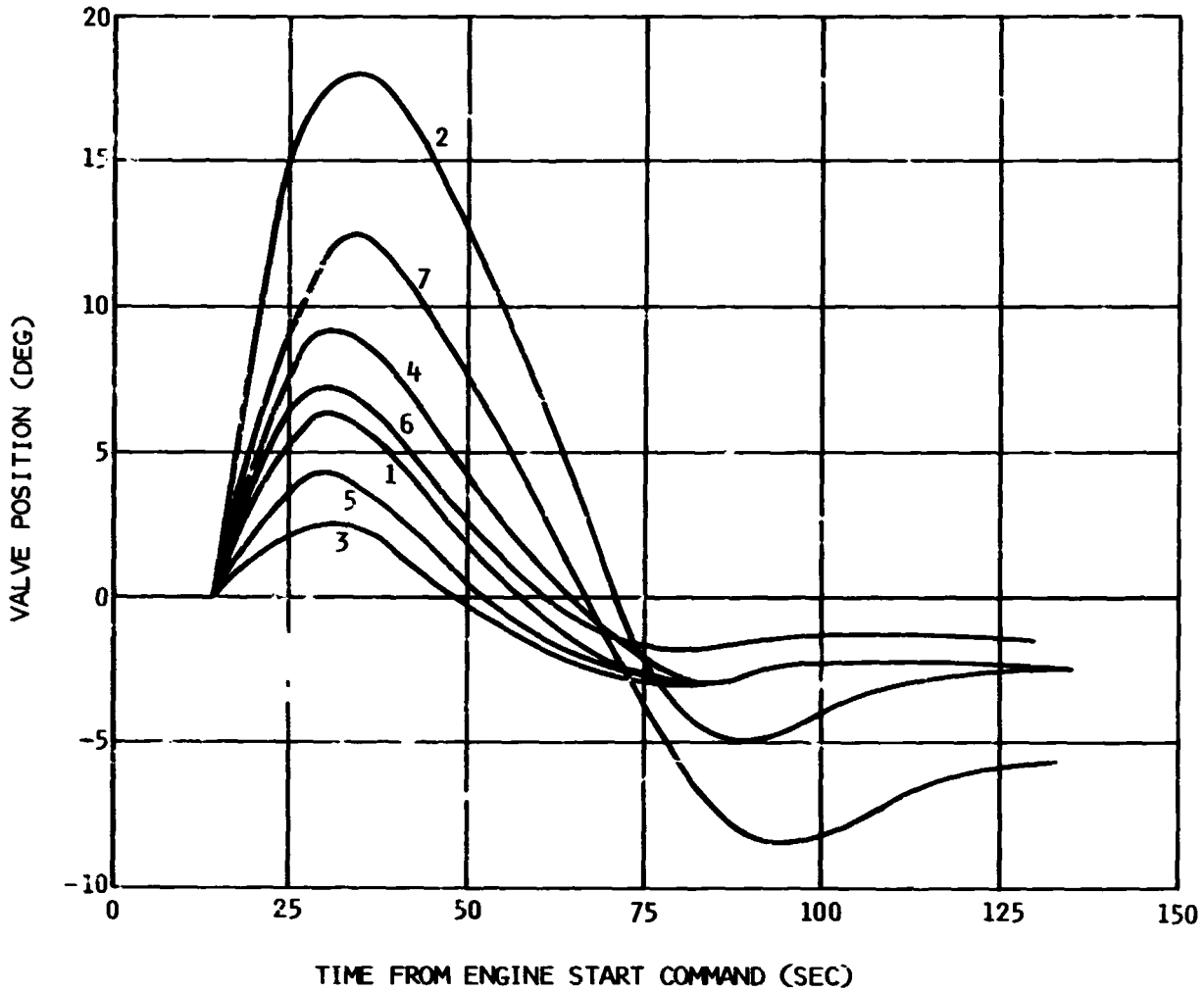


Figure 15-7. PU Valve Position History

Section 15
Propellant Utilization



CURVE NO.	DEVIATION
1	LOADING COMPUTER
2	LH2 ORBITAL BOILOFF
3	LOX ORBITAL BOILOFF
4	ENGINE PERFORMANCE
5	PU SYSTEM NONLINEARITIES
6	CALIBRATION
7	BRIDGE GAIN RATIO

Figure 15-8. PU System Deviation Effects on Second Burn PU Valve History

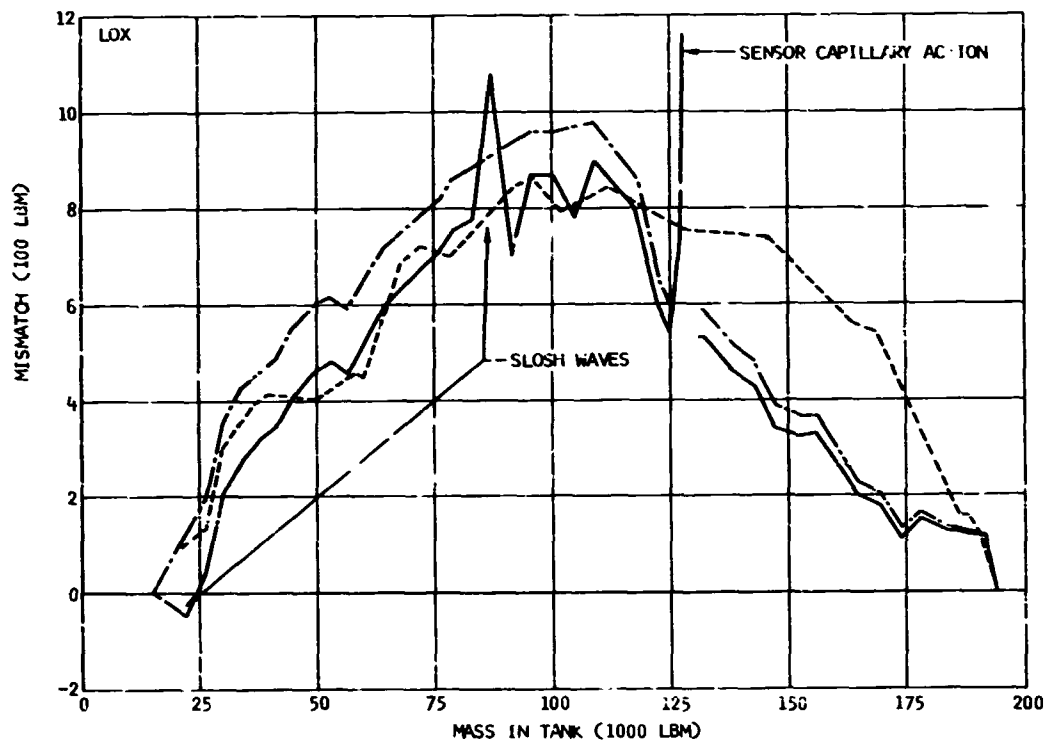
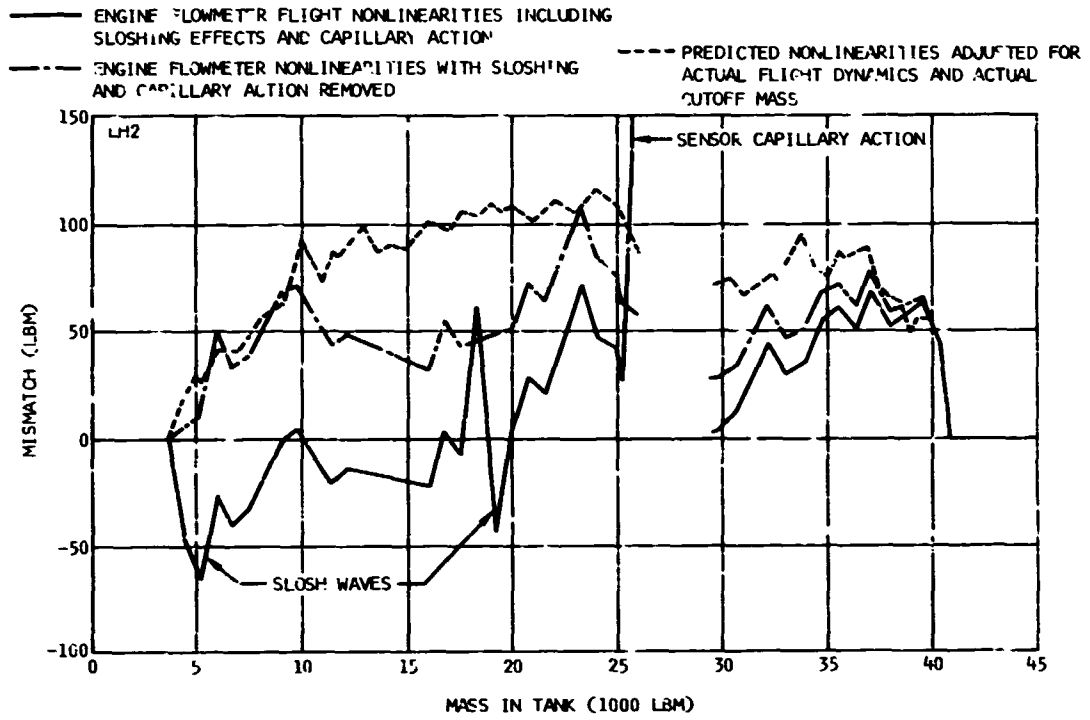


Figure 15-9. Total PU System Tank-to-Sensor Nonlinearities Normalized to Flight Consumed Mass

Section 15
Propellant Utilization

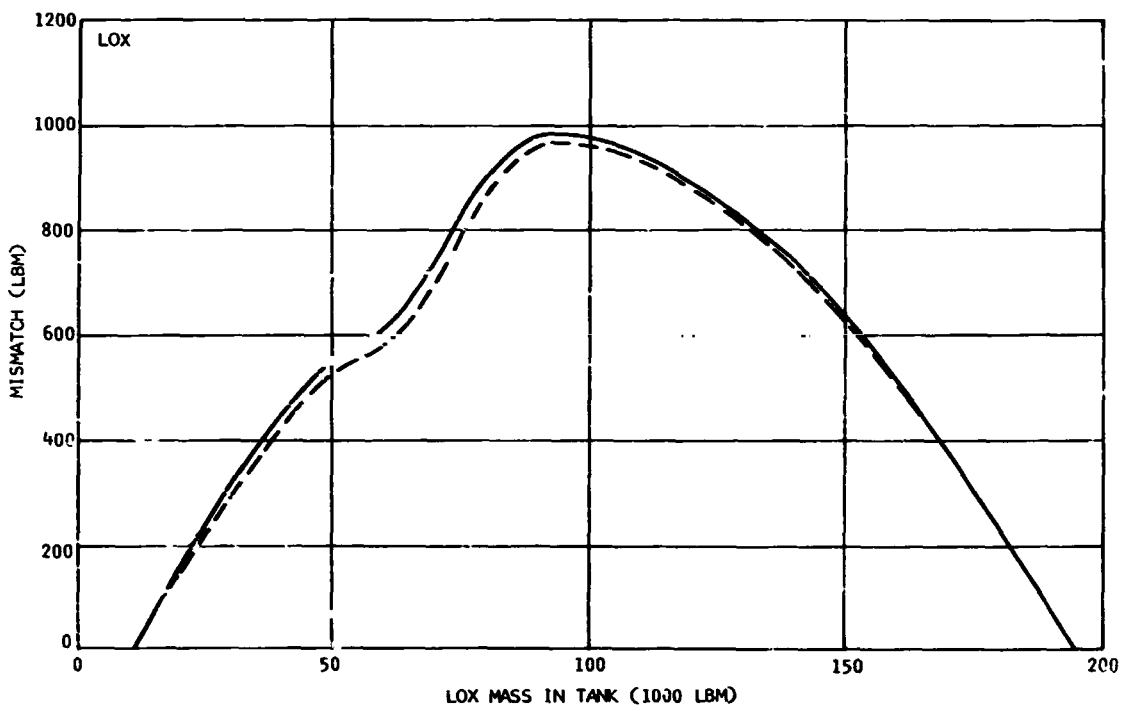
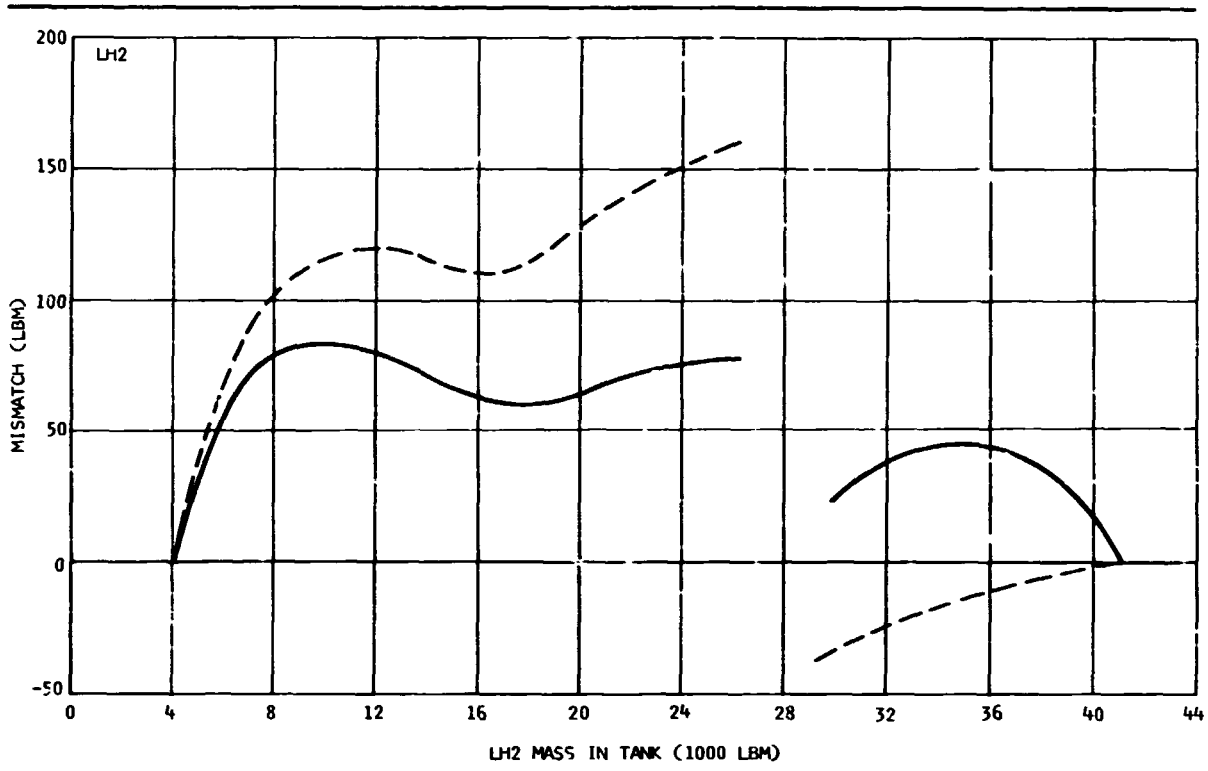


Figure 15-10. Volumetric Tank-to-Sensor Nonlinearities Normalized to Flight Consumed Mass

Section 15
Propellant Utilization

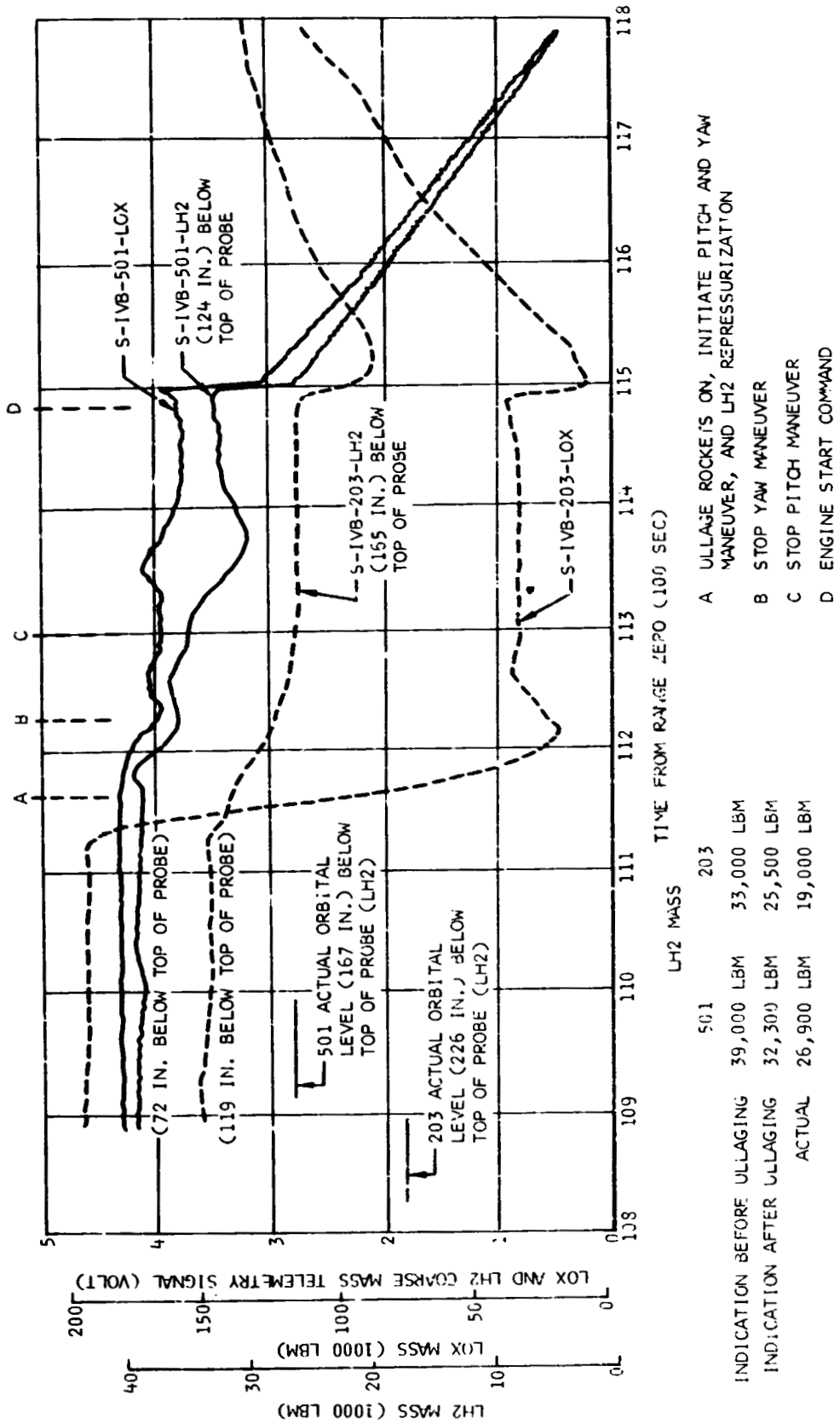


Figure i5-11. Capillary Effects on Mass Sensor Signal Prior to Second Burn

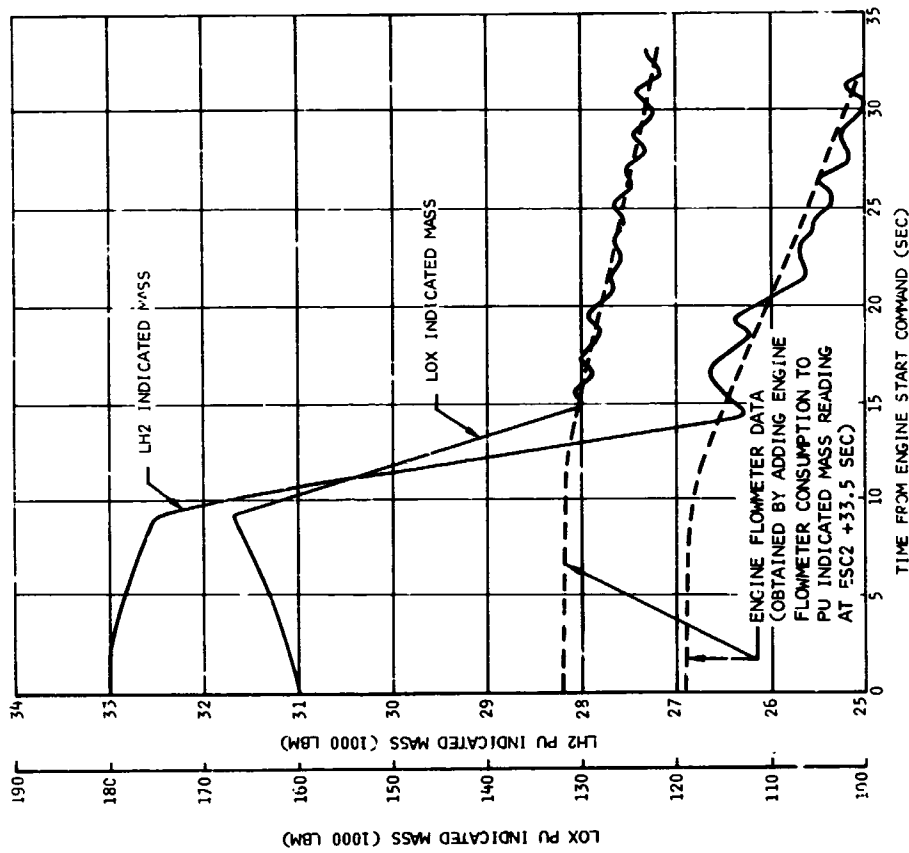


Figure 15-12. PU Indicated Fine Mass Data Following
Second Engine Start Command

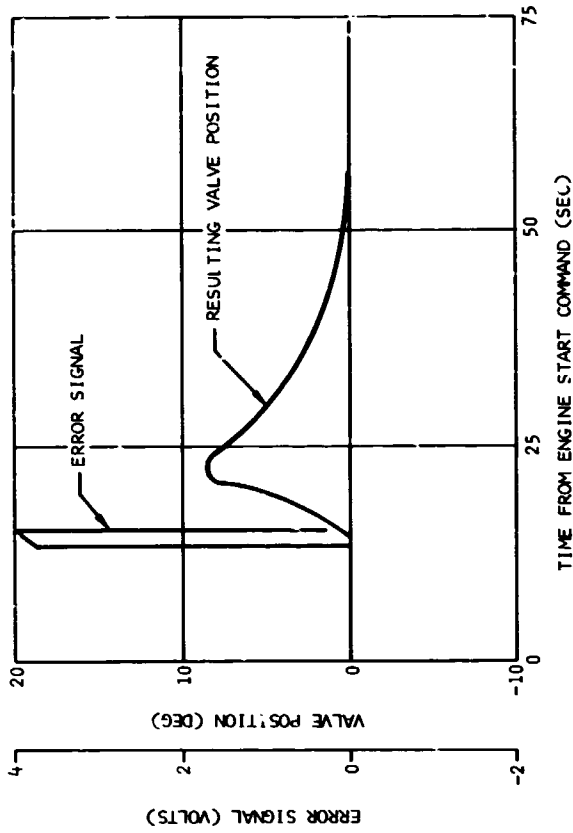


Figure 15-13. Effect of Capillary Action on PU Valve Position History

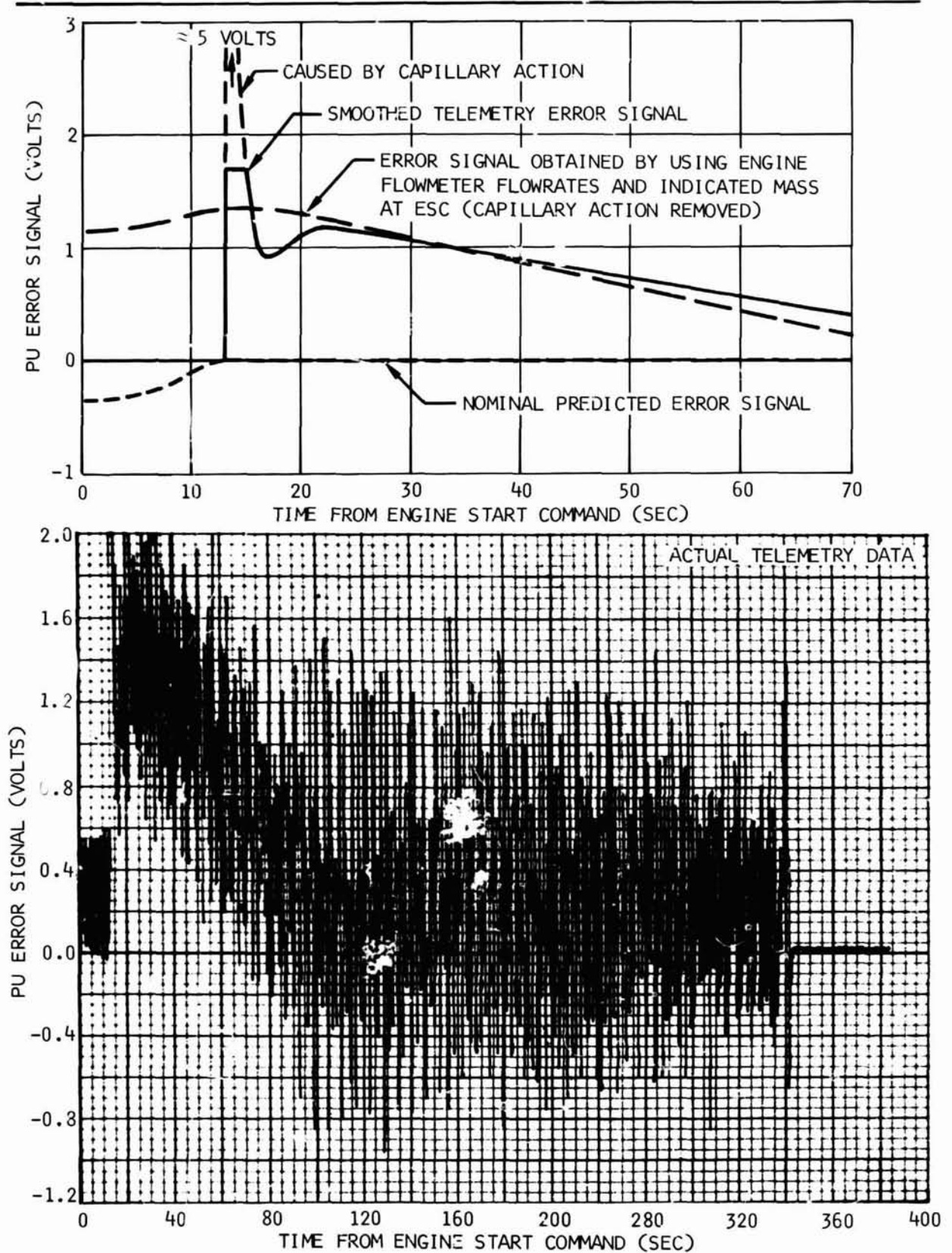


Figure 15-14. Propellant Utilization System Error Signal

Section 15
Propellant Utilization

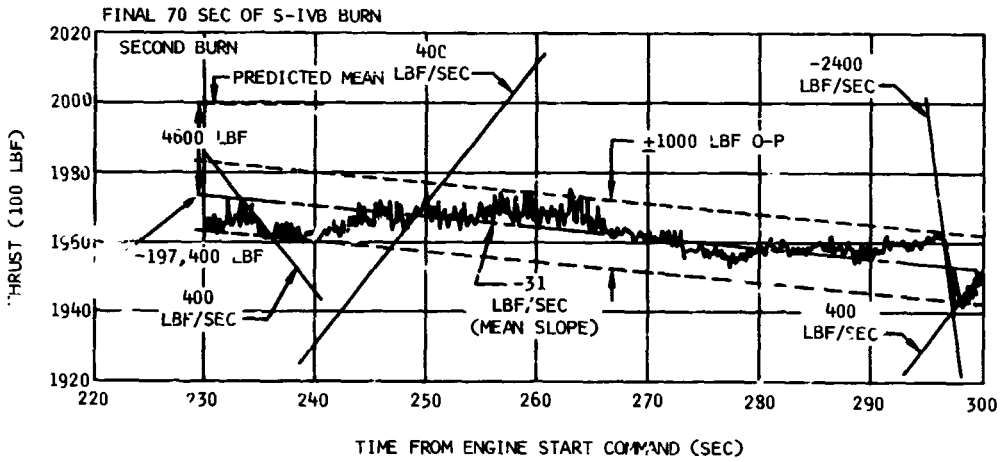
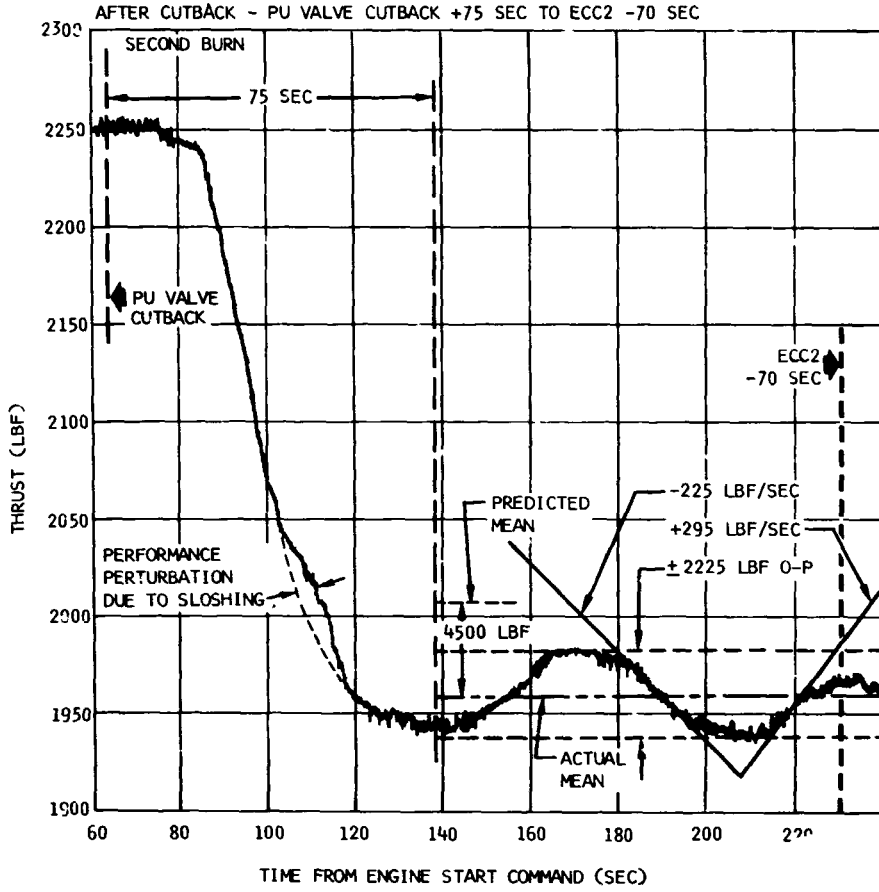


Figure 15-15. Thrust Variations

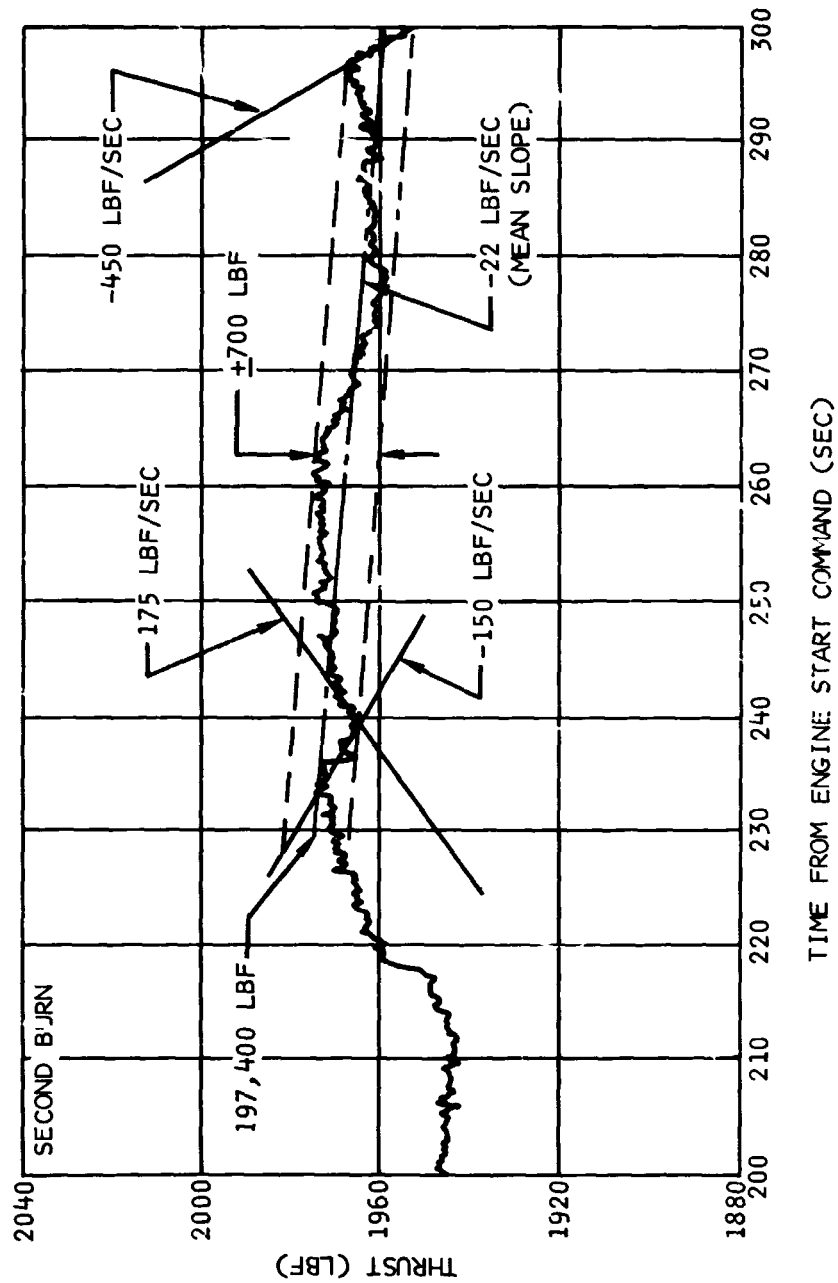


Figure 15-16. Engine Response to PU Valve Positions